Oxidative Medicine and Cellular Longevity

Nanoparticle-Induced Toxicities: an Update on the Role of Oxidative Stress

Lead Guest Editor: Gvozden L. Rosić
Guest Editors: Dragica Selakovic, Igor Jakovcevski, Miodrag Stojkovic, Sergey Bolevich, and Vladimir Jakovljevic

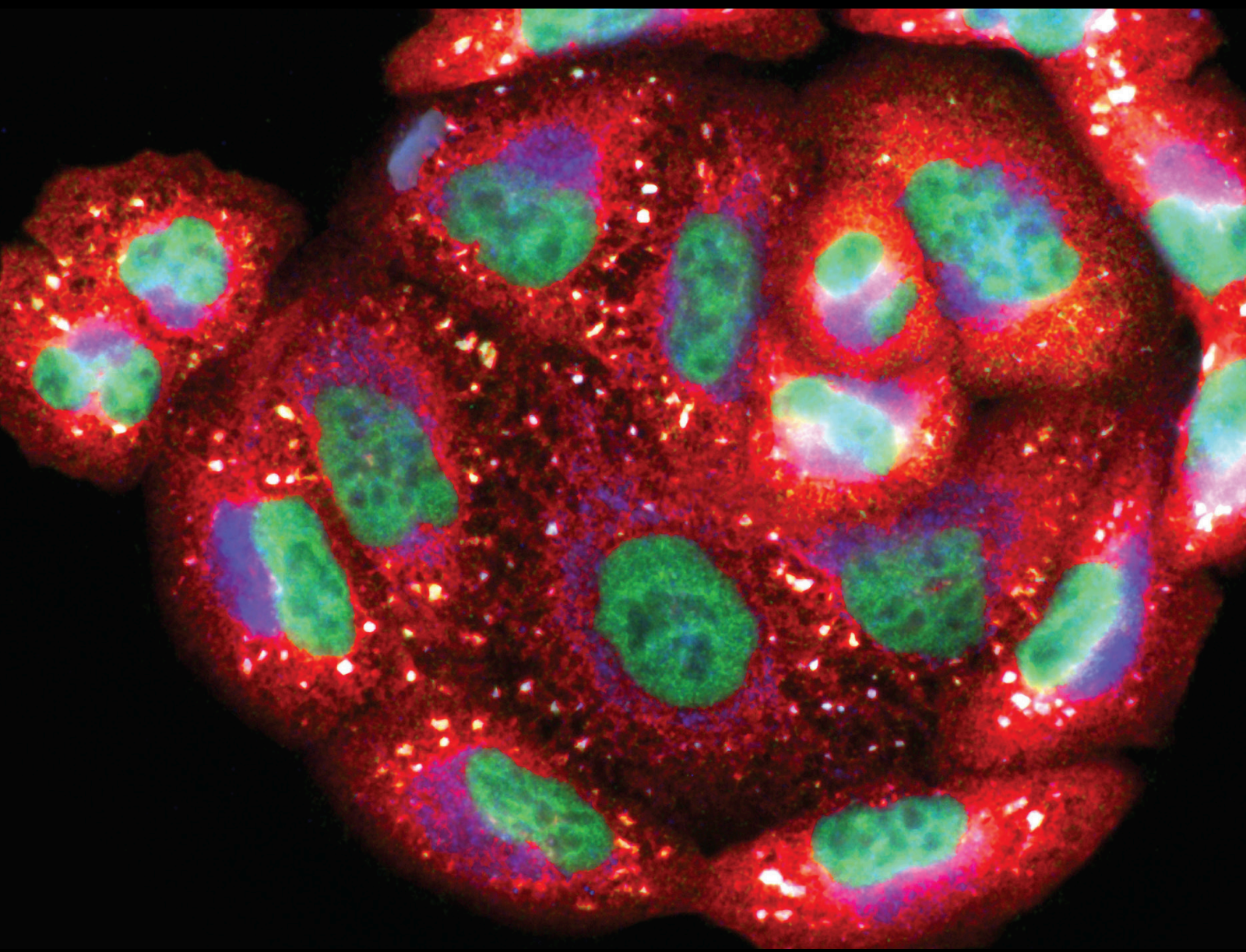

Nanoparticle-Induced Toxicities: an Update on the Role of Oxidative Stress

Oxidative Medicine and Cellular Longevity

Nanoparticle-Induced Toxicities: an Update on the Role of Oxidative Stress

Lead Guest Editor: Gvozden L. Rosić
Guest Editors: Dragica Selakovic, Igor Jakovcevski, Miodrag Stojkovic, Sergey Bolevich, and Vladimir Jakovljevic

Contents

Nanoparticle-Induced Toxicities: An Update on the Role of Oxidative Stress
Gvozden Rosic and Dragica Selakovic
Editorial (2 pages), Article ID 9895061, Volume 2022 (2022)

Comparative In Vitro Cytotoxicity Study of Carbon Dot-Based Organometallic Nanoconjugates: Exploration of Their Cell Proliferation, Uptake, and Localization in Cancerous and Normal Cells
Eepsita Priyadarshini, Ramovatar Meena, Himadri B. Bohidar, Saurabh Kumar Sharma, Magda H. Abdellattif, Muthupandian Saravanan, and Paulraj Rajamani
Research Article (11 pages), Article ID 3483073, Volume 2022 (2022)

Exploring Dose-Dependent Cytotoxicity Profile of Gracilaria edulis-Mediated Green Synthesized Silver Nanoparticles against MDA-MB-231 Breast Carcinoma
Yugal Kishore Mohanta, Awdhesh Kumar Mishra, Debasis Nayak, Biswajit Patra, Amra Bratovcic, Satya Kumar Avula, Tapan Kumar Mohanta, Kadarkarai Murugan, and Muthupandian Saravanan
Research Article (15 pages), Article ID 3863138, Volume 2022 (2022)

Effects of Metal Oxide Nanoparticles in Zebrafish
Marta d'Amora, Tiziana Julia Nadjeschda Schmidt, Soultana Konstantinidou, Vittoria Raffa, Francesco De Angelis, and Francesco Tantussi
Review Article (37 pages), Article ID 3313016, Volume 2022 (2022)

Evaluation of Zebrafish Toxicology and Biomedical Potential of Aeromonas hydrophila Mediated Copper Sulfide Nanoparticles
S. Rajeshkumar, J. Santhoshkumar, M. Vanaja, P. Sivaperumal, M. Ponnanikajamideen, Daoud Ali, and Kalirajan Arunachalam
Research Article (12 pages), Article ID 7969825, Volume 2022 (2022)

Exacerbation of Thrombotic Responses to Silver Nanoparticles in Hypertensive Mouse Model
Zannatul Ferdous, Sumaya Beegam, Nur E. Zaaba, Ozaz Elzaki, Saeed Tariq, Yaser E. Greish, Badreldin H. Ali, and Abderrahim Nemmar
Research Article (10 pages), Article ID 2079630, Volume 2022 (2022)

An Overview of the Beneficial Role of Antioxidants in the Treatment of Nanoparticle-Induced Toxicities
Vladimir Mihailovic, Jelena S. Katanic Stankovic, Dragica Selakovic, and Gvozden Rosic
Review Article (21 pages), Article ID 7244677, Volume 2021 (2021)

Combining Nanotechnology and Gas Plasma as an Emerging Platform for Cancer Therapy: Mechanism and Therapeutic Implication
Milad Rasouli, Nadia Fallah, and Sander Bekeschus
Review Article (20 pages), Article ID 2990326, Volume 2021 (2021)

Phytoantioxidant Functionalized Nanoparticles: A Green Approach to Combat Nanoparticle-Induced Oxidative Stress
Acharya Balkrishna, Ashwani Kumar, Vedpriya Arya, Akansha Rohela, Rachna Verma, Eugenie Nepovimova, Ondrej Krejcar, Dinesh Kumar, Naveen Thakur, and Kamil Kuca
Review Article (20 pages), Article ID 3155962, Volume 2021 (2021)

Anticancer, Enhanced Antibacterial, and Free Radical Scavenging Potential of Fucoidan- (Fucus vesiculosus Source) Mediated Silver Nanoparticles
S. Rajeshkumar, Eman F. Aboelfetoh, Sri Renukadevi Balusamy, Daoud Ali, Mohammed H. A. Almarzoug, Jule Leta Tesfaye, and Ramaswamy Krishnaraj
Research Article (11 pages), Article ID 8511576, Volume 2021 (2021)

An Update Report on the Biosafety and Potential Toxicity of Fullerene-Based Nanomaterials toward Aquatic Animals
Nemi Malhotra, Gilbert Audira, Agnes L. Castillo, Petrus Siregar, Johnsy Margotte S. Ruallo, Marri Jmelou Roldan, Jung-Ren Chen, Jiann-Shing Lee, Tzong-Rong Ger, and Chung-Der Hsiao
Review Article (14 pages), Article ID 7995223, Volume 2021 (2021)

Hindawi
Oxidative Medicine and Cellular Longevity
Volume 2022, Article ID 9895061, 2 pages
https://doi.org/10.1155/2022/9895061

Editorial

Nanoparticle-Induced Toxicities: An Update on the Role of Oxidative Stress

Gvozden Rosic and Dragica Selakovic

Department of Physiology, Faculty of Medical Sciences, University of Kragujevac, Serbia

Correspondence should be addressed to Gvozden Rosic; grosic@medf.kg.ac.rs

Received 22 April 2022; Accepted 22 April 2022; Published 19 May 2022

The variety of nanoparticles has, unfortunately, become common constituents of the growing pollution problem. Since there is a significant presence of nanoparticles in the food industry, cosmetics, and other unavoidable products, better knowledge of their properties and undesirable effects seems necessary to reduce their adverse effects. Although nanoparticles induce numerous toxicities, some common pathways are harmful to human health, including oxidative damage. Significant impact of nanoparticles has previously been documented in clinical trials and preclinical investigations. Therefore, the objective of this special issue is to allow a comprehensive insight based on both original research and review articles that focus on the estimation of oxidative stress as the key point mechanism in many toxicities induced by nanoparticles. At the same time, numerous investigations confirmed the beneficial role of nanoparticles administration for many medical indications, with the final effects strongly depending on the applied methodology. Thus, to enlighten the complex impact of nanoparticles on targeting species, in this special issue, we are now offering an update to the existing information that can help to reveal our current knowledge from competent and reliable sources.

This special issue covers 10 articles focusing on nanoparticle-induced toxicities, highlighting the role of oxidative stress. The guest editors are pleased to present a compendium of these updates on nanoparticles' effects in the published articles as follows:

Potential benefits of nanotechnology in the field of cancer treatment were presented by Priyadarshini and coworkers in the article "Comparative in vitro Cytotoxicity Study of Carbon Dot-Based Organometallic Nanoconjugates: Exploration of Their Cell Proliferation, Uptake, and Localization in Cancerous and Normal Cells". The results obtained in this *in vitro* study confirmed that carbon dot-based nanoconjugates with Ag had potent therapeutic potential, signifying the effect of silver in cancer cell lines. At the same time, those nanoconjugates potentiated the nontoxic nature of human health cell line.

On the other hand, the adverse effects of specific nanoparticles were elaborated in the article "Exacerbation of thrombotic responses to silver nanoparticles in a hypertensive mouse model" by Ferdous and coworkers. Based on the results of this original research, the population with hypertension is at higher risk of the toxicity of polyethylene glycol-AgNPs. This conclusion appeared following the results that confirm that polyethylene glycol-AgNPs can potentially exacerbate the *in vivo* and *in vitro* procoagulatory and oxidative stress effect in hypertensive mice.

Although there is a lot of evidence considering nanoparticle-induced toxicities, potential benefits of their clinical usage highlight the necessity for treatment of their adverse effects, primarily by attenuation of this specific kind of iatrogenic oxidative damage. Therefore, the extensive overview of literature data presented in the article "An overview of the beneficial role of antioxidants in the treatment of nanoparticle-induced toxicities" by Mihailovic and colleagues offers the confirmation that nanoparticles-induced oxidative stress may be attenuated by different antioxidant substances. It is worth noting that naturally occurring antioxidants have an important role in the enhancement of the antioxidant defense systems in the prevention and mitigation of organism damage caused by

nanoparticle-induced oxidative stress. Naturally occurring antioxidant protection was also elaborated in detail in the insightful review article "Phyto-antioxidant functionalized nanoparticles: A green approach to combat nanoparticles-induced oxidative stress" by Balkrishna and colleagues. This review article, in turn, offers convincing evidence that nanoparticles may be useful in combating the oxidative damage of other origins. Namely, the majority of silver, gold, iron, zinc oxide, and copper nanoparticles produced utilizing various plant extracts were active free radical scavengers. According to the authors, this potential is linked to several surface-fabricated phytoconstituents, such as flavonoids and phenols, which accentuated the potential of phyto-antioxidant functionalized nanoparticles to be a better alternative to nanoparticles prepared by other existing approaches.

Interestingly, one of the most promising and state-of-the-art methodological approaches in the field of nanotechnology, the green synthesis of nanoparticles, had been the subject of several papers in this Issue. Mohanta and collaborators in the original article "Exploring dose dependent cytotoxicityprofile of *Gracilaria edulis* mediated green synthesized silver nanoparticles against MDA-MB-231 breast carcinoma" showed that silver nanoparticles synthesized through the extensively elaborated green method expressed potential anticancer and antimicrobial activity. This finding allows potential utility in the food preservative film industry, as well as biomedical and pharmaceutical industries. Another intervention performed on silver nanoparticles was presented in the original article "Anticancer, enhanced antibacterial and free radical scavenging potential of Fucoidan (*Fucus vesiculosus* Source) mediated silver nanoparticles" by Rajeshkumar and coworkers. Based on the results presented in this study, the activities of commercial antibiotics were enhanced by impregnation with the synthesized silver nanoparticles, which led to the conclusion that the utilization of environmentally synthesized silver nanoparticles offers numerous benefits of eco-friendliness and compatibility for biomedical applications. Even more beneficial impact of green methods in nanotechnology was presented in the original research "Evaluation of zebra fish toxicology and biomedical potential of *Aeromonas hydrophila* mediated copper sulfide nanoparticles" by Shanmugam and colleagues. The applied methodology resulted in the confirmation that *Aeromonashydrophila*-mediated copper sulfide nanoparticles can be considered as a potential candidate with therapeutic proficiencies as antibacterial, antioxidant, and anti-inflammatory agents. Innovative approaches in the application of nanotechnology were also the subject of the review by Rasouli and colleagues. The overview of data obtained in clinical studies presented in the article "Combining nanotechnology and gas plasma as an emerging platform for cancer therapy: mechanism and therapeutic implication" had been summarized in the way that concluded that the convergence of plasma and nanotechnology provided a suitable strategy that may lead to the required therapeutic outcomes in oncology research, and traditional methods remained improvable for many types of tumor entities.

A significant impact of different nanomaterials manifested with a variety of toxicities (including oxidative stress) that occurs in the aquatics was also presented in this Issue. Malhotra and colleagues in the review article "An Update Report on the Biosafety and Potential Toxicity of Fullerene-Based Nanomaterials toward Aquatic Animals" presented a lot of evidence that waterborne exposure to fullerene-based nanomaterials triggers toxicities at the cellular, organic, and molecular, as well as neurobehavioral levels. Analyzing numerous original studies, the authors explained that the effects of fullerene-based nanomaterials strongly depend on their chemical structure. Likewise, for the organic nanoparticles, the inorganic nanosized particles also induced numerous toxicities in aquatic species, as presented by d'Amora and collaborators. In their comprehensive review article entitled "Effects of metal oxide nanoparticles in zebrafish", they offered a plethora of data that the use of metallic oxide nanoparticles leads to the possible toxicity in zebrafish (during both adulthood and growth stages). Thus, the unavoidable human exposure to this kind of pollution may also have an adverse effect, emphasizing the role of oxidative stress.

Conflicts of Interest

The editors declare that they have no conflicts of interest regarding the publication of this special issue.

Acknowledgments

We would like to thank the authors of the published articles in this special issue. Their inspiring original research, as well as the insightful critical update in review articles, made a significant improvement in the knowledge of these rather current research topics. We also emphasize the reviewers' extremely professional attitude that allowed the authors to achieve the highest standards of the journal. We are particularly expressing our deep and sincere gratitude to guest editors Igor Jakovcevski, Miodrag Stojkovic, Sergey Bolevich, and Vladimir Jakovljevic for their excellent expert contribution at all stages of the published papers mentoring. Finally, we highly appreciate the effort of the journal editorial and management that accurately and competently supported the whole process and significantly improved the quality of this issue.

Gvozden Rosic
Dragica Selakovic

Hindawi
Oxidative Medicine and Cellular Longevity
Volume 2022, Article ID 3483073, 11 pages
https://doi.org/10.1155/2022/3483073

Research Article

Comparative In Vitro Cytotoxicity Study of Carbon Dot-Based Organometallic Nanoconjugates: Exploration of Their Cell Proliferation, Uptake, and Localization in Cancerous and Normal Cells

Eepsita Priyadarshini,[1] Ramovatar Meena,[1] Himadri B. Bohidar,[2] Saurabh Kumar Sharma,[3] Magda H. Abdellattif,[4] Muthupandian Saravanan,[5,6] and Paulraj Rajamani[1]

[1]*School of Environmental Sciences, Jawaharlal Nehru University, New Delhi 110067, India*
[2]*School of Physical Sciences, Jawaharlal Nehru University, New Delhi 110067, India*
[3]*School of Computational and Integrative Sciences, Jawaharlal Nehru University, New Delhi 110067, India*
[4]*Department of Chemistry, College of Science, Taif University, Al-Haweiah, P. O. Box 11099, Taif 21944, Saudi Arabia*
[5]*Department of Medical Microbiology and Immunology, Division of Biomedical Sciences, School of Medicine, College of Health Sciences, Mekelle University, Tigray, Ethiopia*
[6]*AMR and Nanomedicine Laboratory, Department of Pharmacology, Saveetha Dental College, Saveetha Institute of Medical and Technical Sciences (SIMATS), Chennai 600 077, Chennai, India*

Correspondence should be addressed to Muthupandian Saravanan; bioinfosaran@gmail.com
and Paulraj Rajamani; paulrajr@yahoo.com

Received 15 October 2021; Revised 3 February 2022; Accepted 10 February 2022; Published 15 March 2022

Academic Editor: Dragica Selakovic

Organometallic nanoconjugates have raised great interest due to their bimodal properties and high stability. In the present study, we analyzed the cytotoxicity property of carbon dots (CDs) and a series of organometallic nanoconjugates including gold@carbon dots (Au@CDs) and silver@carbon dots (Ag@CDs) synthesized via an aqueous mode. We aimed to divulge a comparative analysis of cell proliferation, uptake, and localization of the particles in HeLa and HEK293 cell lines. Our results showed dose-dependent cytotoxicity of Au@CDs, Ag@CDs, and CDs. However, Ag@CDs showed the highest inhibition through HeLa cells with an IC_{50} value of around $50 \pm 1.0\,\mu g/mL$. Confocal imaging signified the uptake of the particles suggested by blue fluorescence in the interior region of HeLa cells. Furthermore, the TEM micrographs depicted that the particles are entrapped by endocytosis assisted through the cell microvilli. The CDs and Au@CDs were thus observed to be relatively safe up to a concentration of $100\,\mu g/mL$ and did not induce any morphological changes in the cells. Moreover, the cell proliferation assay of these nanoconjugates against HEK 293 cells signified the nontoxic nature of the nanoconjugates. The results thus revealed two major facts: firstly, the Ag@CDs had potent therapeutic potential, signifying their potential as a promising anticancer drug, and secondly, the CDs and Au@CDs at a defined dose could be used as probes for detection and also bioimaging agents.

1. Introduction

Engineered nanomaterials with multimodal properties have been of much focus recently, with particular emphasis on applications related to the domain of biomedicine including imaging, drug delivery, and biosensing probes [1–4]. The small size of nanoparticles (NPs) allows their easy penetration into the cells and interaction with the cellular systems [5]. Additionally, the intriguing physicochemical properties of NPs such as the size, shape, surface chemistry, and surface charge play a pivotal role in their uptake by the cells [6–9]. Due to these properties, NPs have been widely analyzed for

their potential in gene delivery, target-specific drug delivery, therapeutics, and tumor targeting [10–12].

In specific, metal oxide NPs are reported for their significant biological applicability [13]. There is a plethora of reports that suggest the application of silver and gold NPs in biomedicines [14–17]. Endosome-entrapped gold NPs in the size ranging from 4 to 6 nm have been reported for their excellent uptake and bioimaging potential by HeLa and MCF-7 cell lines [15]. Carbon dots (CDs) are novel zero-dimensional carbon-based nanomaterials with relatively strong fluorescence characteristics. There has been a tremendous rise in the use of carbon dots (CDs) as fluorescent probes for bioimaging applications [18]. The synthesis methods for CD production include techniques such as laser irradiation, electrochemical oxidation, strong acid oxidation, and ultrasonic synthesis [19–22]. But, these methods suffer from disadvantages of aqueous dispersibility, expensiveness, hazardous precursors, and complex instrumentation, thereby limiting their usage in biomedicines. Therefore, researchers are now focusing on the synthesis of nanoconjugates that present the advantages of multifunctionality, targeted functionality, and superior physicochemical properties.

Regardless of the significant advances in the arena of nanotechnology, not much is understood about their cellular uptake and the subsequent mode of action. Furthermore, most of the studies nowhere suggest the toxicity assessment of these specific particles. A huge number of factors such as the dose, distribution, period of treatment, and interaction with specific biomolecule affect NP-based cellular response [23, 24]. In general, NPs are internalized by endocytic pathways wherein the uptake efficiency and resultant toxicity are correlated with the route of administration. In addition to the size and shape of the particles, charge density, cell type, stage of differentiation, and surface chemistry of NPs determine the uptake route [10, 25–27].

The uncertainties of a mode of action and compatibility before deciding its bioapplication are associated with the introduction of any new composite nanomaterial. To ensure the efficacious and harmless implementation of nanomaterials, it is essential to completely elucidate the cellular response to the nanomaterial. To eliminate the risk of toxicity and undesired *in vitro* cellular response, many parameters (cell viability, dose of particles, cell type, number of internalized particles, and degradation product) require investigation. Our prior studies report the synthesis of CDs from biocompatible precursors wherein the synthesized particles offer the advantages of aqueous solubility, stability, and high quantum yield. Additionally, we have synthesized dual-mode nanoconjugates (Au@CDs and Ag@CDs) with both well-defined optical and fluorescent properties, thereby presenting promising usage in bioimaging.

Therefore, in the present study, we coveted to investigate the toxic effects of the synthesized nanoconjugates (CDs, Ag@CDs, and Au@CDs) and understand the antiproliferation, cellular uptake, and internalization pathway. The cellular uptake and distribution of the Ag@CDs, Au@CDs, and CDs were analyzed in HeLa cell lines. Overall, our study established the cellular response of HeLa cells on exposure to CD-based nanoconjugates, fluorescence imaging potential, and intracellular uptake efficiency.

2. Materials and Methods

2.1. Synthesis of Carbon Dots (CDs). CDs were synthesized as per our previous study [28]. PEG and citric acid were used as the precursors, and synthesis was performed via microwave-assisted method.

2.2. Synthesis of Au@CD/Ag@CD Nanoconjugates. The synthesized CDs were appropriately diluted and used for gold@-carbon dots (Au@CDs) and silver@carbon dots (Ag@CDs) synthesis. Au@CDs were synthesized at $HAuCl_4$ concentration of 0.12 mg/mL as per the protocol adopted by [28, 29]. UV-visible and fluorescence spectral analysis was performed to ascertain the synthesis of the nanoconjugates. Average particle size and morphology were determined by dynamic light scattering (DLS) and JEOL 2100F transmission electron microscope (TEM) operating at a voltage of 200 kV. The hydrodynamic size (R_h) of particles was determined using the Stokes-Einstein equation [30] from the DLS data.

2.3. In Vitro Toxicity

2.3.1. Cell Culture. The human cervical cancer cell line (HeLa) and human healthy embryonic kidney cell line (HEK293) were procured from National Centre for Cell Science, Department of Biotechnology, Pune, India. The cells were cultured in RPMI-1640 medium supplemented with 10% (v/v) FBS and antibiotics (streptomycin 10 μg/mL and penicillin 100 U/mL).

2.3.2. Cytotoxicity Assay. The cytotoxicity of the nanoconjugates and CDs was determined by MTT assay against HeLa and HEK293 cell lines. Briefly, 5×10^3 cells/well were seeded in a 96-well plate and incubated for 24 h in an incubator maintained at 37°C and 5% CO_2. The old media were replaced with a fresh medium containing various concentrations of nanoconjugates and CDs and incubated further for another 24 hours. Thereafter, 30 μL of 1 mg/mL MTT (3-(4,5-dimethylthiazol-2-yl)-2,5-diphenyl tetrazolium bromide) and 70 μL of the media were added to each well. After 4 h of incubation, the media were replenished with 100 μL DMSO and incubated for 10 minutes. Absorbance was recorded in ELISA plate reader at 570 nm, and % viability was calculated as per the below-mentioned formula.

$$\text{Cell Viability } (\%) = \text{Mean of absorbance (Treated samples/Untreated samples)} * 100.$$

2.3.3. Determination of Reactive Oxygen Species (ROS). Intracellular ROS generated by incubating the cell lines with nanoconjugates was estimated by 2′,7′dichlorofluorescein-diacetate (DCFHDA) staining. The cell line was seeded at a density of 5×10^3 cells/well and incubated overnight at 37°C at 5% CO_2. The cells were then treated with varying concentrations of the nanoconjugates and carbon dots and left for exposure for 24 h. The cells were thereafter washed with phosphate-buffered saline (PBS), and 40 μM DCFHDA was added to each well and incubated for 30 min at 37°C.

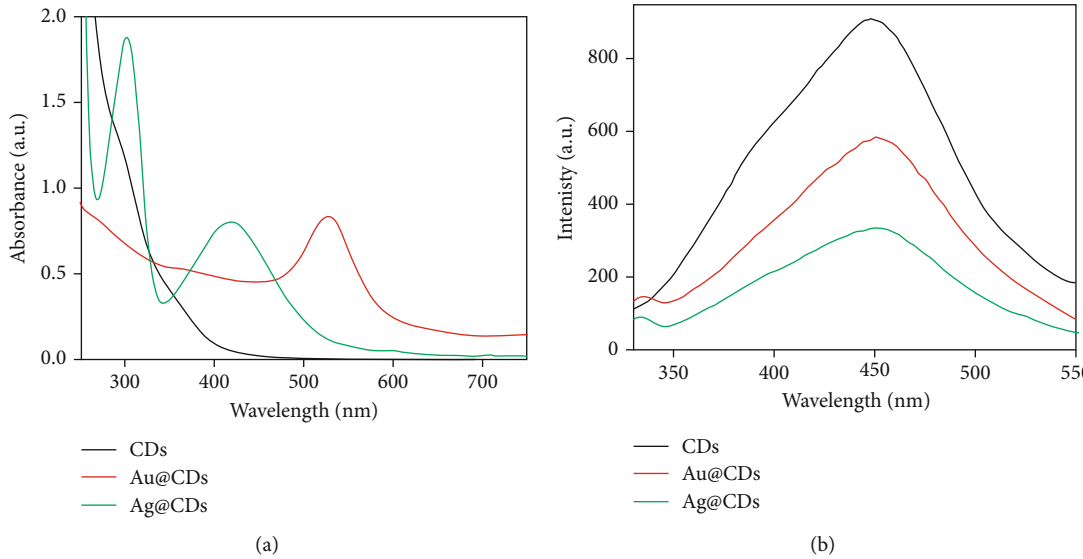

Figure 1: (a) UV-visible absorption spectra and (b) fluorescence spectra of synthesized CDs and nanoconjugates (Au@CDs and Ag@CDs).

The cells were then washed twice with PBS, and fluorescence intensity was measured using 485 excitation and 520 nm emission filters using a fluorimeter (RF-5301 PC Shimadzu spectrofluorometer Nakagyo-Ku, Kyoto, Japan).

Furthermore, the ROS generated on the treatment of HeLa cell line with nanoconjugates was determined by fluorescence imaging using DCFHDA dye. The HeLa cells at 5 $\times 10^5$ cells/well were seeded over coverslip in six-well plates. The plate was incubated overnight that allows growth and attachment of cells. The nanoconjugates at varying concentration was added to the wells and incubated overnight at 37°C and 5% CO_2. The cells were washed with PBS and 40 μM DCFHDA and incubated for 30 min. After incubation, DCFHDA was removed, and the coverslips were suspended in PBS. The coverslips were removed and visualized on a Nikon Eclipse Ti-E (Tokyo, Japan) fluorescence microscope at 20x magnification.

2.3.4. Analysis of Cell Morphology. The changes in cellular morphology of HeLa cells after treatment with nanoconjugates were analyzed using phase-contrast microscope. The cells were treated for 18 h, and any morphological variations were observed using a microscope (Nikon Eclipse Ti-S, Tokyo, Japan).

2.3.5. Cellular Uptake and Bioimaging. To analyze the uptake of the nanoconjugates by the HeLa cells, the cells were treated with 50 μg/mL of nanoconjugates and incubated for 6 h. After completion of the incubation period, the cells were trypsinized and centrifuged at 5000 rpm for 5 min. The pellet obtained was washed and dissolved in 1 mL of 0.1 M PBS. Imaging was performed using an Olympus FluoView TM FV1000 laser confocal microscope.

2.3.6. TEM Analysis. Subcellular localization of nanoconjugates in the HeLa cells was analyzed by treating the cells with nanoconjugates and subsequent incubation for 24 hours. The treated cells were trypsinized and fixed with 2.5% glutaraldehyde for 45 min, postfixed using 1% osmic acid, and 0.1 M PBS was added to it. The cells were then dehydrated in ethanol, embedded in Epon 812, and sectioning was done using an ultramicrotome (Leica Ultracut-UCT). The sections were observed under a JEOL-JEM-2100F transmission electron microscope at 200 kV after staining with uranyl acetate.

Table 1: Physical parameters of the synthesized nanoconjugates.

Sample	Maximum absorbance (nm)	Maximum emission (nm)	DLS R_h (nm)
CDs	305	454	13 ± 1
Au@CDs	520	454	47 ± 1
Ag@CDs	415	454	65 ± 2

3. Results

3.1. Characterization of Nanoconjugates. The CDs synthesized using PEG and citric acid were used as the reducing agent for subsequent synthesis of Au- and Ag-based nanoconjugates. A change in color from initial yellow to purple and reddish brown provided initial evidence of Au@CD and Ag@CD formation, respectively. An evident surface plasmon resonance (SPR) peak was observed at around 530 and 420 nm for Au@CDs and Ag@CDs, respectively, in the UV-visible absorption spectra. Additionally, quenching of fluorescence intensity confirmed the formation of nanoconjugates (Figures 1(a) and 1(b)).

The detailed physical characterization (TEM, HRTEM, and EDX spectra) and mechanism of CDs and Au@CD and Ag@CD synthesis have been already published, and the data is available there in our previous study with multimode sensing application [28, 29], and hence, in this study, we explored the cell proliferation, uptake, and localization in cancerous and normal cells. The crystalline nature of the

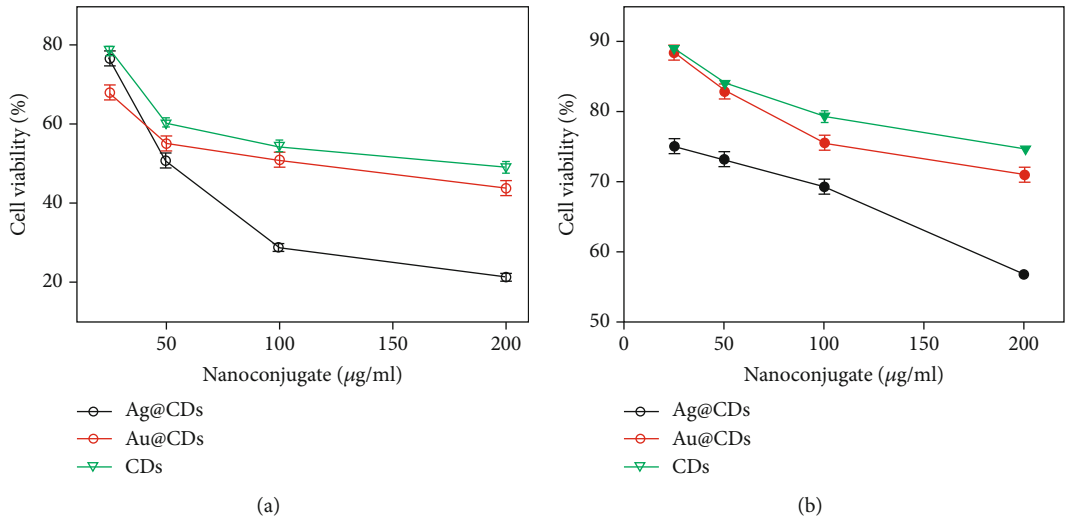

Figure 2: MTT assay: graph depicting the cell viability percentage as a function of varying nanoconjugate concentration: (a) HeLa and (b) HEK 293.

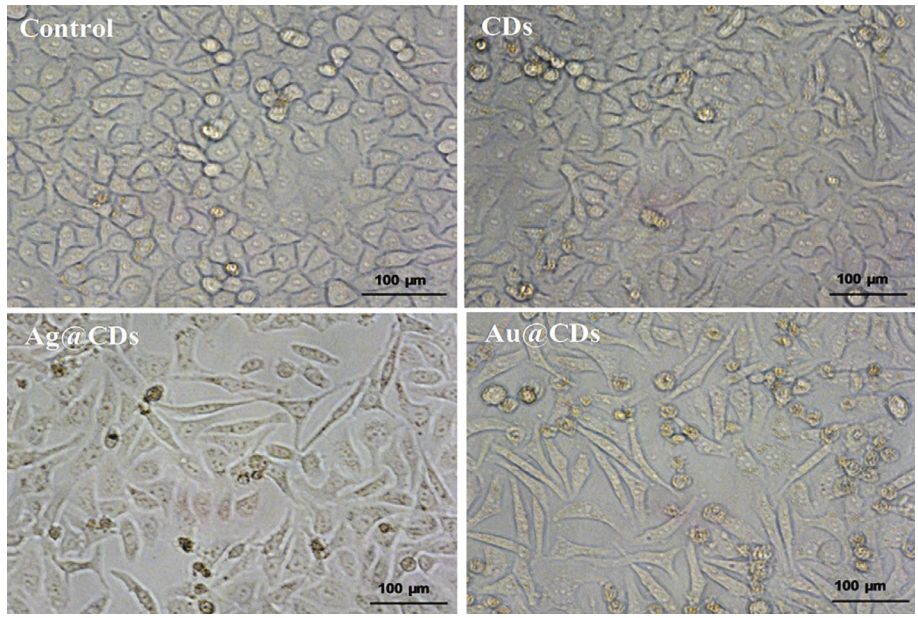

Figure 3: Morphological changes in HeLa cells after treatment with the nanoconjugates (100 μg/mL). No morphological alterations were found in cells treated with CDs and control set. Images were captured at 20x magnification.

particles was confirmed from XRD analysis. Table 1 summarizes the physical parameters of the synthesized nanoconjugates and CDs.

3.2. Assessment of In Vitro Toxicity of Synthesized Nanoconjugates. The antiproliferative effect of the synthesized nanoconjugates and CDs was investigated against HeLa cells via MTT assay. The cells were treated with the nanoconjugates in the concentration range of 25 to 200 μg/mL for 24 hours (Figure 2). Among the particles, Ag@CDs showed the highest inhibition of HeLa cells with an IC_{50} value (concentration where 50% cell death is observed) of around 50 ± 1.0 μg/mL, while CDs showed the least toxicity with an IC_{50} value of around 180 ± 0.5 μg/mL. Au@CDs showed an IC_{50} value of 150 ± 0.08 μg/mL, thus signifying minimal toxicity of Au@CDs. The cytotoxicity studies indicated the antiproliferative effect of the Ag@CDs in a dose-dependent manner. The literature suggests the superior toxicity of silver NPs, with an almost 60% decrease in cell viability at a mere concentration of 65 μg/mL in L929 cells [31]. In the present case, the highest inactivation of cell proliferation was observed in Ag@CDs, which can be attributed to the Ag^+ ions that form the integral core of the particles. In a similar instance, gold NPs have been reported to inhibit the proliferation of dalton lymphoma cells, with around 40-50% viability at a concentration range of 80–100 μg

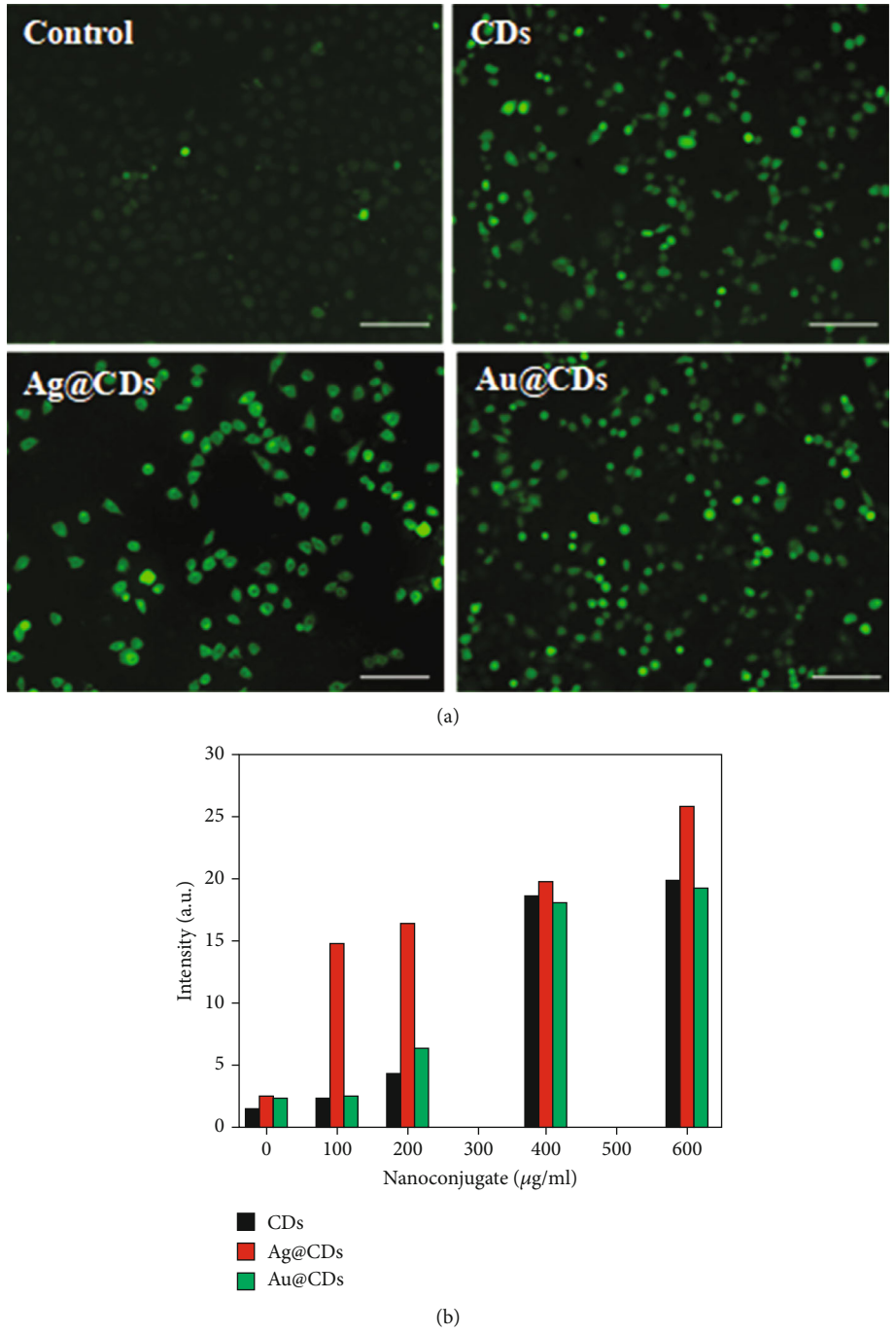

Figure 4: (a) Fluorescence microscopic images of DCFDA-stained cells including control cells, CD-treated cells, Ag@CD-treated cells, and Au@CD-treated cells. (b) ROS level in treated cells after incubation with the nanoconjugates as estimated by DCFDA.

[32]. In this study, the least toxicity of Au@CDs was observed which might be due to the CD shell over the gold particles that renders them nontoxic. Comparatively, slightly higher toxicity of Au@CDs compared to CDs can be postulated to be the formation of efficient bonding between the Au ions and the cellular surface that allows superior interaction and penetration into the cells.

To observe the morphological changes induced by the nanoconjugates, images of the treated cells were taken under a microscope. The HeLa cells were treated with the nanoconjugates at 100 μg/mL concentration. Distinct changes in the morphology as well as in the cell density were found compared to the control cells (Figure 3). While the control set (untreated HeLa cells) showed intact morphological features, the cells treated with Ag@CDs showed disrupted cell organization, cell shrinkage, and round cells. The cells appeared to shrink, were irregular in shape, and became round in shape. The dead cells or cells under stress showed a round morphology and get detached from the surface. Additionally, marked reductions in the number of surviving

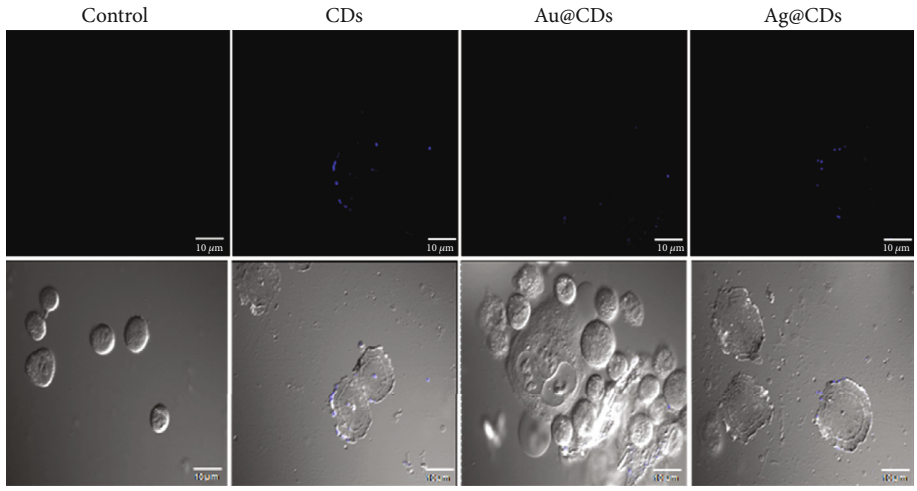

Figure 5: Representative confocal images of nanoconjugates treated HeLa cells after 6 h of incubation. The first set represents the scattering images, and the second set is the corresponding merged images, after incubation with CDs, Au@CDs, and Ag@CDs.

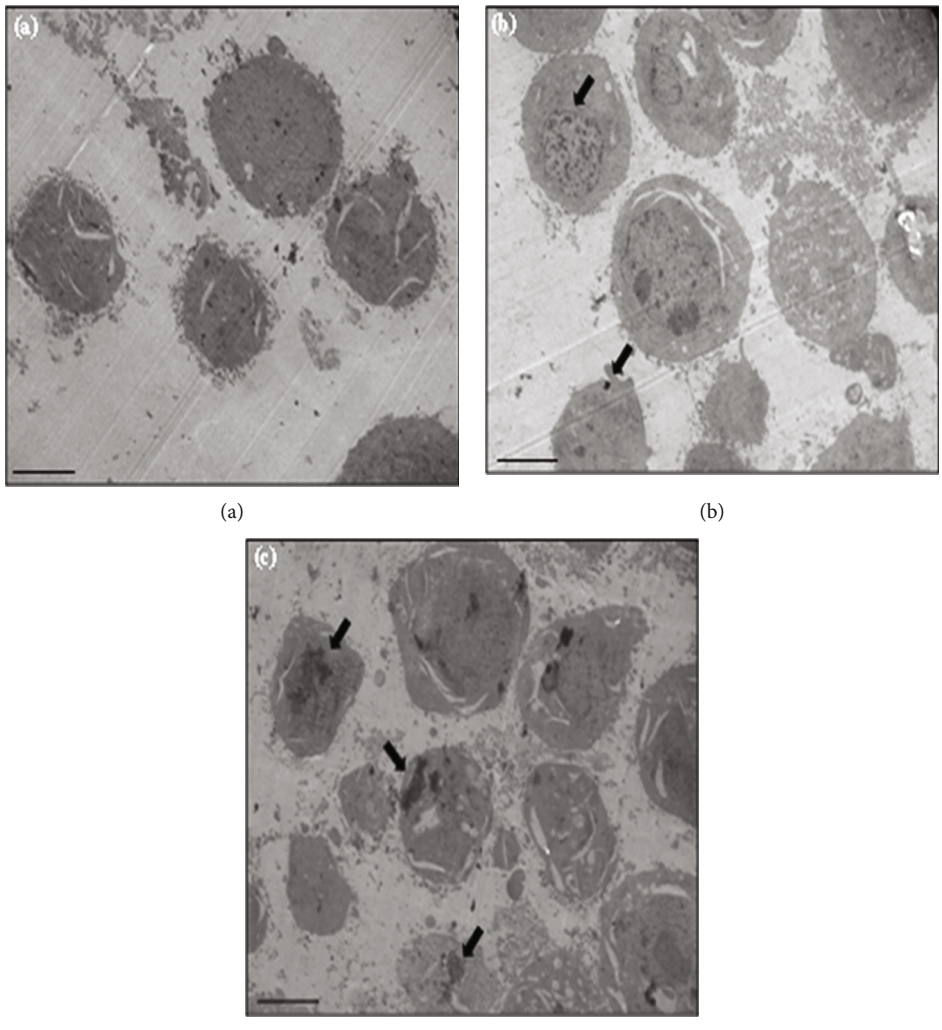

Figure 6: Low magnification TEM images showing intracellular localization of particles in HeLa cells. (a) untreated cells, (b) CD-treated cells, and (c) Au@CD-treated cells. The arrows in (c) and (b) show electron-dense particles corresponding to CDs and Au@CDs, respectively. Scale bar corresponds to 2 μm.

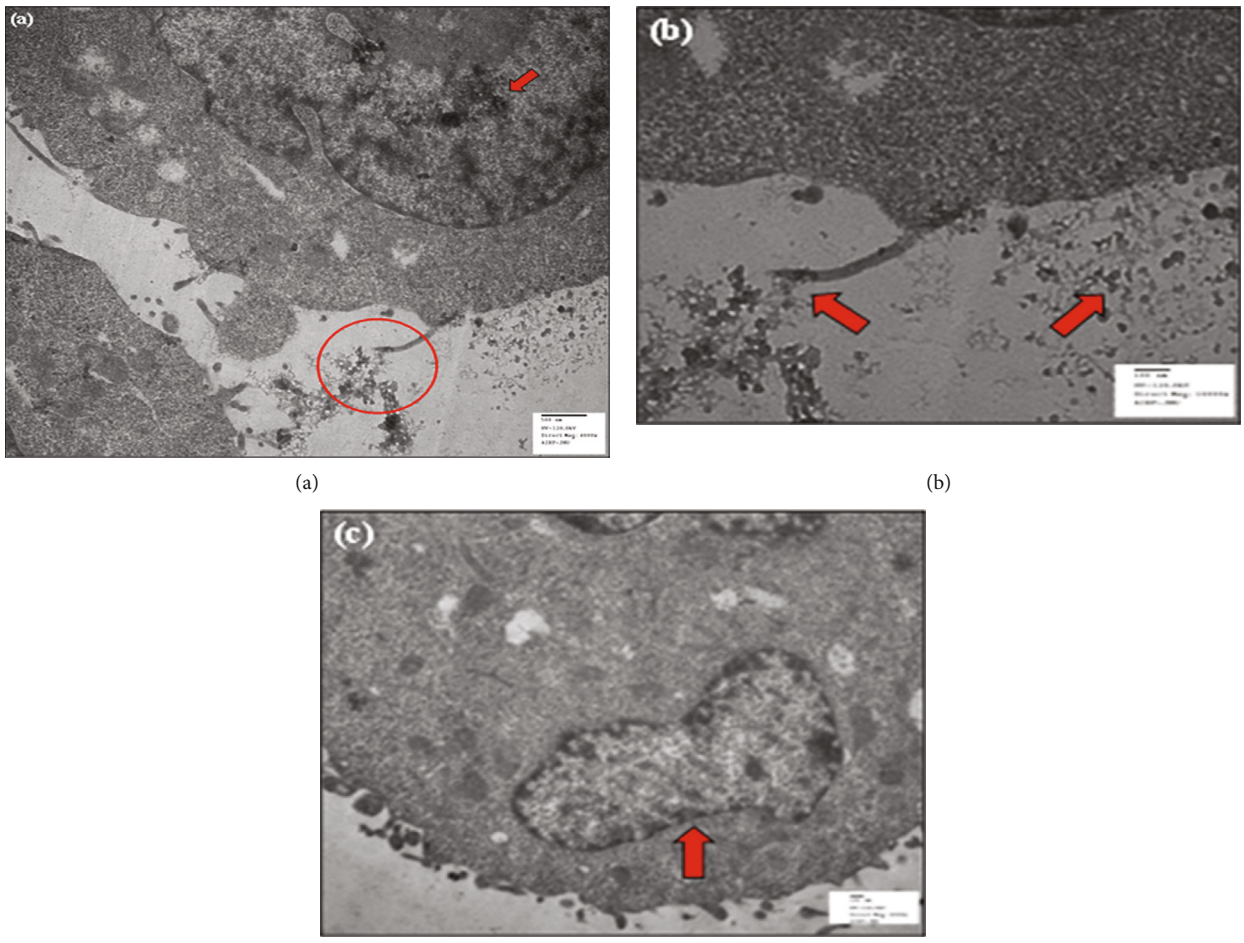

Figure 7: TEM images of HeLa cells treated with CDs. Images (a) and (b) correspond to the different magnification of the same cell showing the interaction of CDs with the cell microvilli. Image (c) represents the internalization of particles within cytoplasmic vesicles.

cells suggested the high toxicity and induction of apoptosis and necrosis at 100 μg/mL Ag@CD concentrations. Furthermore, cells treated with CDs appeared similar in morphology to that of the control cells suggesting the nontoxicity of CDs towards HeLa cells. Likewise, the cells treated with Au@CDs showed few round cells with intact morphology signifying their lesser toxicity in comparison to Ag@CDs.

The literature suggests that the induction of toxicity by NPs is generally mediated by apoptosis, mitochondrial damage, metabolic inactivity, and oxidative stress [33–36]. These processes are assisted by the production of ROS. In this study, we investigated ROS production in the HeLa cells after treatment with nanoconjugates. We used the fluorescent dye DCFHDA for analysis of ROS generation, wherein a direct correlation between the ROS amount and green fluorescence intensity is found. We did not observe any fluorescence in the control cells, while the HeLa cells treated with CDs showed weakly and diffused green fluorescence. However, the HeLa cells treated with Ag@CDs showed a high intensity of green fluorescence. Simultaneously, a decrease in the number of cells was found which suggested cell death due to high toxicity. ROS analysis thus stated that Au@CDs were less toxic compared to Ag@CDs, signified by comparatively lower fluorescence intensity (Figure 4(a)). Likewise, quantitative analysis of ROS estimation showed a relatively high intensity of DCF in Ag@CD-treated cells compared to CDs and Au@CDs (Figure 4(b)).

3.3. Cellular Uptake and Internalization of Nanoconjugates. The uptake of nanoconjugates is important for analyzing the internalization of particles in cells. To analyze the potential of the synthesized nanoconjugates in live cell imaging studies and other biomedical applications, the uptake of CDs, Ag@CDs, and Au@CDs was assessed by treating the cells with 50 μg/mL nanoconjugate concentrations, which was almost half the concentration that was observed to be toxic to cells. Figure 5 shows the confocal imaging data signifying the cellular uptake of the nanoconjugates. The blue florescence signified the internalization of nanoconjugates inside the HeLa cells. The cells without any nanoconjugates treatment were taken as control for adjusting the detector gain and baseline correction. The images (Figure 5) suggest that the scattering intensity is highest for Au@CD-treated particles. All the three particles were internalized in the cells, signifying the ability of the particles to attach and be taken up by the cells. The

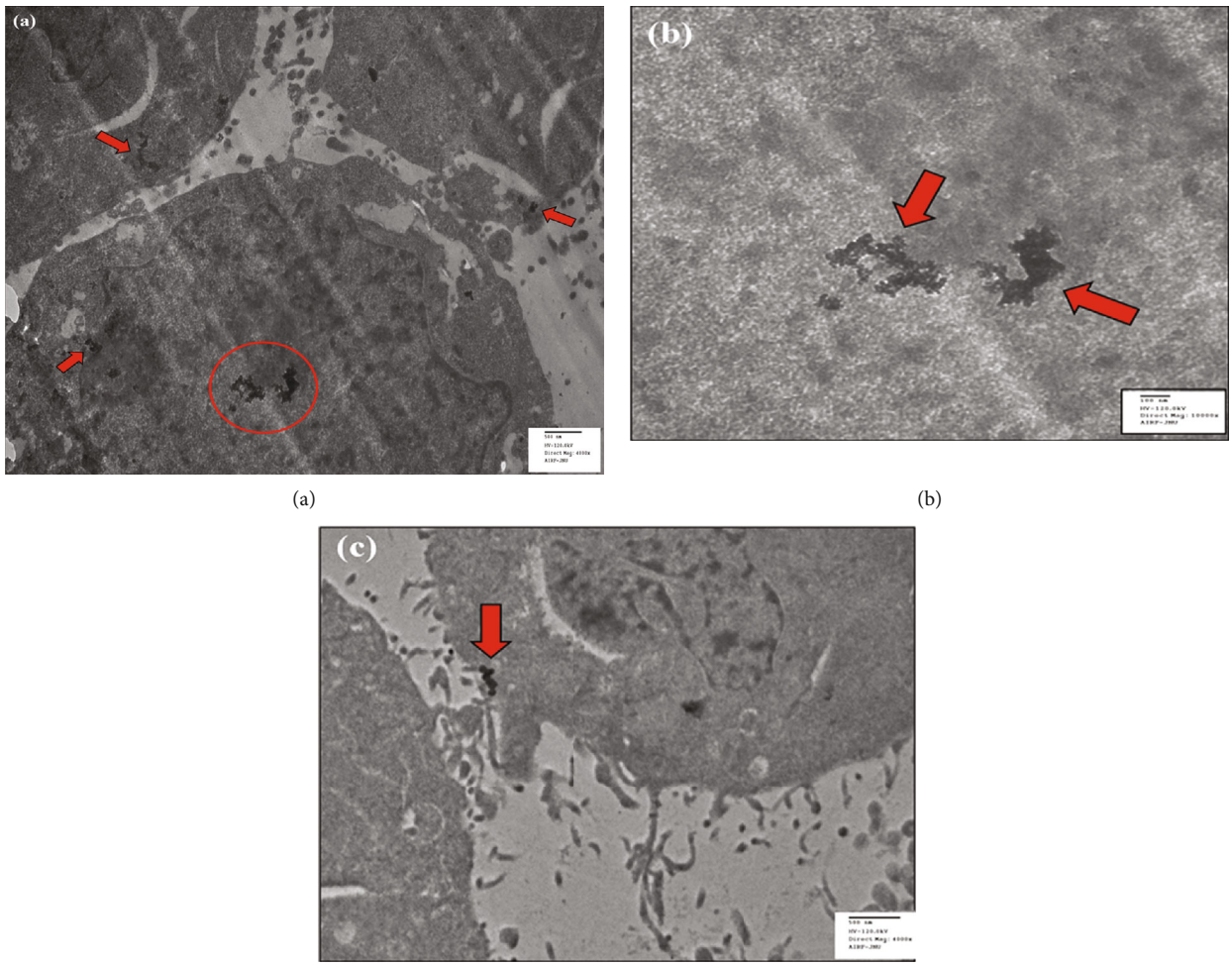

FIGURE 8: TEM images of HeLa cells treated with Au@CDs. Image (a) shows the localization of nanoconjugates within the cells. The arrows indicate the localization of Au@CDs, while image (b) corresponds to the magnified section of the same cell. Image (c) shows the interaction of particle at cell surface.

fluorescence intensity was maximum for Au@CDs followed by Ag@CDs and CDs, respectively.

The TEM further confirmed the cellular internalization of particles. The uptake of CDs and Au@CDs was studied by TEM. Due to the high toxicity of Ag@CDs, it was not possible to perform the TEM study. Due to the rapid death and subsequent detachment of cells from the adhered surface, the cell pellet could not be obtained. Figure 6(a) shows the representative TEM images of control, CD-treated, and Au@CD-treated HeLa cells. In untreated HeLa cells, no vivid morphological changes were found, and the cell membrane was intact with an almost homogeneous cytoplasm and uniform vesicles. However, in the treated group of cells, dense aggregates were observed within the vesicles that correspond to the internalized particles (Figures 6(b) and 6(c)).

In specific, both the particles are internalized by the HeLa cells, signified by the electron-dense aggregates, shown by the red arrows in Figures 7 and 8. In the HeLa cells treated with CDs, the vesicles were quite large and were filled with ample CD aggregates. Simultaneously, the endocytotic vesicles were small and restricted to the cytoplasm, as indicated by the red arrows in Figures 7(a) and 7(c).

Additionally, as encircled in Figure 8(a), we observed the attachment of CDs to cell microvilli. The CD attachment to the microvilli has been shown by an enlarged image in Figure 7(b). A large number of aggregated particles were observed attached to the external cell surface or the plasma membrane. On the other hand, the red-encircled site in Figure 8(a) represents the localization of Au@CDs in HeLa cells. The magnified image has been shown in Figure 8(b). Notably, Figure 8(c) shows the interaction of particles on cell surface interlacing between the microvilli and cytoplasm. The images thus suggested that the particles enter the cells via endocytosis assisted by the cell microvilli. Comparative analysis suggested significantly more internalization of CDs into the cellular vesicles compared to Au@CDs, which was because of the minute size of CDs that favor its uptake both by endocytosis and diffusion through the cell surface. However, both the particle type (CDs and Au@CDs) did not induce any change in cell morphology which was consistent with the cell viability data.

4. Discussion

In this study, a new series of organometallic nanoconjugates including Au@CDs, Ag@CDs, and CDs were characterized by UV-visible spectroscopy, fluorescence spectroscopy, TEM, SEM, and DLS and assessed for their antiproliferative action on the HeLa cells. Fluorescence analysis signified the high quantum yield of CDs. Additionally, the synthesized Ag@CDs and Au@CDs exhibited the dual properties of optical as well as fluorescence detection [28]. Recently, quantum dots (QDs) specifically Cd-based QDs are reported for their use as *in vivo* contrast agents; however, the high toxicity offered by leaching of Cd^{2+} ions into the solution limits their applications. With regard to this, the in-house synthesized nanoconjugates have superior properties (solubility, stability, and surface accessibility) that make them promising candidates for *in vivo* applications. Cytotoxicity, in particular for Ag, Au, and CD has already been described in different cell types [37, 38]. In contrast, we analyzed the toxicity of novel dual property nanomaterials (optical and fluorescence). The aqueous solubility, easy accessibility, high stability, and quantum yield efficiency make such dual-mode nanoconjugates of superior interest in biomedical applications. Therefore, assessing the biocompatibility of these nanoconjugates is essential for determining the subsequent applications. The toxicity of nanomaterials depends on many factors such as rate of cellular uptake, particle size, and cell type [39, 40]. Cell viability assay suggested that of the three particles, Ag@CDs significantly inhibited the growth of the HeLa cells via dose-dependent manner. Most of the mechanisms postulate the production of ROS to be one of the major factors contributing towards nanomaterial-induced cell toxicity. The substrate used for synthesis as well as the nature of surface modification plays an integral role in the uptake of particles and corresponding toxicity. Consequently, we studied the generation of intracellular ROS in the HeLa cells as a response to internalized particles, using the fluorescent probe DCFDA. Indeed, DCFDA in general measures the hydroxyl, peroxyl, and other reactive oxygen species within the cell. The Ag@CD-treated HeLa cells showed relatively high ROS intensity and vivid changes in cellular morphology; apoptotic and necrotic cells were observed. The probable leaching of Ag^{+} ions into the solution and subsequent binding to the thiol groups of the inner mitochondrial membrane results in the weakening of the antioxidant defense mechanism leading to ROS formation. Accumulation of ROS results in mitochondrial disruption and release of Cyt C that in turn activates caspases ultimately resulting in cell death or DNA fragmentation [37, 38, 41]. On the other hand, CDs and Au@CDs were found to be relatively nontoxic up to a high concentration of 100 μg/mL and did not induce any morphological changes. The cellular uptake and internalization of CD and Au@CDs were studied by confocal imaging and TEM. The analysis suggested that both the particles had a similar internalization process assisted by cell microvilli; however, the intracellular distribution was different. Due to the small size of CDs, they easily penetrated the cells by diffusion and were extensively accumulated within the cytosolic vesicles, while Au@CDs were mostly localized in the cytoplasmic space. It thus implies that the cellular uptake of NPs depends on the nature of material, size, shape, and surface charge [42]. Bioimaging studies demand the synthesis of nanomaterials that can easily penetrate the cells, without affecting their morphology and inducing cell death. The particles that are easily internalized and evenly distributed within the cell serve as suitable drug delivery and fluorescent markers. The results thus signify that the CDs and Au@CDs synthesized by the current protocol may serve as superior probes for biomedical and theranostic applications.

5. Conclusion

The Ag@CDs (50 μg/mL) were found to be toxic to the HeLa cells compared to CDs and Au@CDs, thus signifying particle-type-specific toxicity. While the CD and Au@CD particles did not exhibit acute toxicity even at a high dose (100 μg/mL), distinct interaction with the HeLa cells was observed. Both confocal and TEM analysis demonstrated the uptake and subsequent internalization of these particles within the cytoplasmic space and vesicles. This thus suggested that CDs and Au@CDs could be taken up by cells without any toxic effect or induction of morphological changes. Furthermore, Ag@CDs induced apoptosis in HeLa cells probably through ROS-mediated apoptotic pathway. In summary, the study divulges that cytotoxicity depends on particle composition as well as surface modification. Simultaneously, CDs and Au@CDs due to their aqueous solubility, nontoxicity, and fluorescence efficiency are suggested to be used for bioapplications, however with well-controlled concentration as cytotoxicity varies with particle dose.

Data Availability

The data associated with the manuscript are available from the first and corresponding authors.

Conflicts of Interest

The authors declare that they have no conflict of interest.

Acknowledgments

EP is thankful to DST-SERB, Government of India, for the fellowship under the National Postdoctoral Fellowship Scheme (Grant number PDF/2017/000024), and the work was funded by UPE-II (project ID 357). The authors thank the Advanced Instrument Research Facility of Jawaharlal Nehru University for the instrumental analysis. M.H.A thanks the Taif University research, Saudi Arabia, supporting project TURSP2020/91.

References

[1] D. Medina-Cruz, E. Mostafavi, A. Vernet-Crua et al., "Green nanotechnology-based drug delivery systems for osteogenic disorders," *Drug Delivery*, vol. 17, no. 3, pp. 341–356, 2020.

[2] D.-E. Lee, H. Koo, I.-C. Sun, J. H. Ryu, K. Kim, and I. C. Kwon, "Multifunctional nanoparticles for multimodal imaging and

theragnosis," *Chemical Society Reviews*, vol. 41, no. 7, pp. 2656–2672, 2012.

[3] T. L. Doane and C. Burda, "The unique role of nanoparticles in nanomedicine: imaging, drug delivery and therapy," *Chemical Society Reviews*, vol. 41, no. 7, pp. 2885–2911, 2012.

[4] K. Saha, S. S. Agasti, C. Kim, X. Li, and V. M. Rotello, "Gold nanoparticles in chemical and biological sensing," *Chemical Reviews*, vol. 112, no. 5, pp. 2739–2779, 2012.

[5] A. Salvati, C. Åberg, T. dos Santos et al., "Experimental and theoretical comparison of intracellular import of polymeric nanoparticles and small molecules: toward models of uptake kinetics," *Nanomedicine: Nanotechnology, Biology and Medicine*, vol. 7, no. 6, pp. 818–826, 2011.

[6] L. Treuel, X. Jiang, and G. U. Nienhaus, "New views on cellular uptake and trafficking of manufactured nanoparticles," *Journal of the Royal Society Interface*, vol. 10, article 20120939, 2013.

[7] S. Salatin, S. Maleki Dizaj, and A. Yari Khosroushahi, "Effect of the surface modification, size, and shape on cellular uptake of nanoparticles," *Cell Biology International*, vol. 39, no. 8, pp. 881–890, 2015.

[8] J. A. Kim, C. Åberg, A. Salvati, and K. A. Dawson, "Role of cell cycle on the cellular uptake and dilution of nanoparticles in a cell population," *Nature Nanotechnology*, vol. 7, no. 1, pp. 62–68, 2012.

[9] E. Mostafavi, P. Soltantabar, and T. J. Webster, "Nanotechnology and picotechnology: a new arena for translational medicine," in *Biomaterials in Translational Medicine*, pp. 191–212, Elsevier, 2019.

[10] C. A. Mirkin, T. J. Meade, S. H. Petrosko, and A. H. Stegh, "Nanotechnology-based precision tools for the detection and treatment of cancer," *Springer*, vol. 166, 2015.

[11] M. Pentenero, "Nanotechnology: a novel adjunctive aid to fight cancer," *Oral Diseases*, vol. 23, no. 3, pp. 273–275, 2017.

[12] H. Maeda, H. Nakamura, and J. Fang, "The EPR effect for macromolecular drug delivery to solid tumors: improvement of tumor uptake, lowering of systemic toxicity, and distinct tumor imaging in vivo," *Advanced Drug Delivery Reviews*, vol. 65, no. 1, pp. 71–79, 2013.

[13] J. W. Rasmussen, E. Martinez, P. Louka, and D. G. Wingett, "Zinc oxide nanoparticles for selective destruction of tumor cells and potential for drug delivery applications," *Drug Delivery*, vol. 7, no. 9, pp. 1063–1077, 2010.

[14] A. Haider and I.-K. Kang, "Preparation of silver nanoparticles and their industrial and biomedical applications: a comprehensive review," *Advances in Materials Science and Engineering*, vol. 2015, 16 pages, 2015.

[15] C. S. Kim, X. Li, Y. Jiang et al., "Cellular imaging of endosome entrapped small gold nanoparticles," *MethodsX*, vol. 2, pp. 306–315, 2015.

[16] H. Amani, E. Mostafavi, M. R. Alebouyeh et al., "Would colloidal gold nanocarriers present an effective diagnosis or treatment for ischemic stroke?," *International Journal of Nanomedicine*, vol. 14, pp. 8013–8031, 2019.

[17] K. Kalantari, E. Mostafavi, A. M. Afifi et al., "Wound dressings functionalized with silver nanoparticles: promises and pitfalls," *Nanoscale*, vol. 12, no. 4, pp. 2268–2291, 2020.

[18] Z. L. Wu, Z. X. Liu, and Y. H. Yuan, "Carbon dots: materials, synthesis, properties and approaches to long-wavelength and multicolor emission," *Journal of Materials Chemistry*, vol. 5, no. 21, pp. 3794–3809, 2017.

[19] S.-L. Hu, K.-Y. Niu, J. Sun, J. Yang, N.-Q. Zhao, and X.-W. Du, "One-step synthesis of fluorescent carbon nanoparticles by laser irradiation," *Journal of Materials Chemistry*, vol. 19, no. 4, pp. 484–488, 2009.

[20] S. Yang, H. Zeng, H. Zhao, H. Zhang, and W. Cai, "Luminescent hollow carbon shells and fullerene-like carbon spheres produced by laser ablation with toluene," *Journal of Materials Chemistry*, vol. 21, no. 12, pp. 4432–4436, 2011.

[21] L. Zheng, Y. Chi, Y. Dong, J. Lin, and B. Wang, "Electrochemiluminescence of water-soluble carbon nanocrystals released electrochemically from graphite," *Journal of the American Chemical Society*, vol. 131, no. 13, pp. 4564-4565, 2009.

[22] H. Li, X. He, Y. Liu et al., "One-step ultrasonic synthesis of water-soluble carbon nanoparticles with excellent photoluminescent properties," *Carbon*, vol. 49, no. 2, pp. 605–609, 2011.

[23] S. Zhang, H. Gao, and G. Bao, "Physical principles of nanoparticle cellular endocytosis," *ACS Nano*, vol. 9, no. 9, pp. 8655–8671, 2015.

[24] C. S. Paulo, R. P. das Neves, and L. S. Ferreira, "Nanoparticles for intracellular-targeted drug delivery," *Nanotechnology*, vol. 22, no. 49, article 494002, 2011.

[25] G. Sahay, D. Y. Alakhova, and A. V. Kabanov, "Endocytosis of nanomedicines," *Journal of Controlled Release*, vol. 145, no. 3, pp. 182–195, 2010.

[26] E. Fröhlich, "The role of surface charge in cellular uptake and cytotoxicity of medical nanoparticles," *International Journal of Nanomedicine*, vol. 7, p. 5577, 2012.

[27] A. E. Nel, L. Mädler, D. Velegol et al., "Understanding biophysicochemical interactions at the nano-bio interface," *Nature Materials*, vol. 8, no. 7, pp. 543–557, 2009.

[28] E. Priyadarshini and K. Rawat, "Au@ carbon dot nanoconjugates as a dual mode enzyme-free sensing platform for cholesterol," *Journal of Materials Chemistry B*, vol. 5, no. 27, pp. 5425–5432, 2017.

[29] E. Priyadarshini, K. Rawat, and H. B. Bohidar, "Multimode sensing of riboflavin via ag@ carbon dot conjugates," *Applied Nanoscience*, vol. 10, no. 1, pp. 281–291, 2020.

[30] I. A. Mir, K. Das, K. Rawat, and H. B. Bohidar, "Hot injection versus room temperature synthesis of CdSe quantum dots: a differential spectroscopic and bioanalyte sensing efficacy evaluation, colloids surf," *Colloids and Surfaces A: Physicochemical and Engineering Aspects*, vol. 494, pp. 162–169, 2016.

[31] S. Barua, R. Konwarh, S. S. Bhattacharya et al., "Non-hazardous anticancerous and antibacterial colloidal 'green'silver nanoparticles, colloids surf," *Colloids and Surfaces B: Biointerfaces*, vol. 105, pp. 37–42, 2013.

[32] P. Gautam, S. Kumar, M. Tomar, R. Singh, and A. Acharya, "Biologically synthesized gold nanoparticles using Ocimum sanctum (Tulsi leaf extract) induced anti-tumor response in a T cell daltons lymphoma," *Journal of Cell Science & Therapy*, vol. 8, p. 2, 2017.

[33] J. J. Li, D. Hartono, C.-N. Ong, B.-H. Bay, and L.-Y. L. Yung, "Autophagy and oxidative stress associated with gold nanoparticles," *Biomaterials*, vol. 31, no. 23, pp. 5996–6003, 2010.

[34] K. A. Clark, C. O'Driscoll, C. A. Cooke et al., "Evaluation of the interactions between multiwalled carbon nanotubes and Caco-2 cells," *Journal of Toxicology and Environmental Health, Part A: Current Issues*, vol. 75, no. 1, pp. 25–35, 2012.

[35] J. S. Kim, K. S. Song, H. J. Joo, J. H. Lee, and I. J. Yu, "Determination of cytotoxicity attributed to multiwall carbon nanotubes (MWCNT) in normal human embryonic lung cell

(WI-38) line," *Journal of Toxicology and Environmental Health, Part A: Current Issues*, vol. 73, no. 21-22, pp. 1521–1529, 2010.

[36] Y. Pan, A. Leifert, D. Ruau et al., "Gold nanoparticles of diameter 1.4 nm trigger necrosis by oxidative stress and mitochondrial damage," *Small*, vol. 5, no. 18, pp. 2067–2076, 2009.

[37] H.-U. Simon, A. Haj-Yehia, and F. Levi-Schaffer, "Role of reactive oxygen species (ROS) in apoptosis induction," *Apoptosis*, vol. 5, no. 5, pp. 415–418, 2000.

[38] J. Firdhouse and P. Lalitha, "Apoptotic efficacy of biogenic silver nanoparticles on human breast cancer MCF-7 cell lines," *Progress in Biomaterials*, vol. 4, no. 2-4, pp. 113–121, 2015.

[39] J. Zhu, L. Liao, L. Zhu et al., "Size-dependent cellular uptake efficiency, mechanism, and cytotoxicity of silica nanoparticles toward HeLa cells," *Talanta*, vol. 107, pp. 408–415, 2013.

[40] K. Shapero, F. Fenaroli, I. Lynch, D. C. Cottell, A. Salvati, and K. A. Dawson, "Time and space resolved uptake study of silica nanoparticles by human cells," *Molecular BioSystems*, vol. 7, no. 2, pp. 371–378, 2011.

[41] I. I. Hejazi, R. Khanam, S. H. Mehdi et al., "New insights into the antioxidant and apoptotic potential of _Glycyrrhiza glabra_ L. during hydrogen peroxide mediated oxidative stress: An _in vitro_ and _in silico_ evaluation," *Biomedicine & Pharmacotherapy*, vol. 94, pp. 265–279, 2017.

[42] L. Damalakiene, V. Karabanovas, S. Bagdonas, M. Valius, and R. Rotomskis, "Intracellular distribution of nontargeted quantum dots after natural uptake and microinjection," *International Journal of Nanomedicine*, vol. 8, p. 555, 2013.

Hindawi
Oxidative Medicine and Cellular Longevity
Volume 2022, Article ID 3863138, 15 pages
https://doi.org/10.1155/2022/3863138

Research Article

Exploring Dose-Dependent Cytotoxicity Profile of *Gracilaria edulis*-Mediated Green Synthesized Silver Nanoparticles against MDA-MB-231 Breast Carcinoma

Yugal Kishore Mohanta,[1] **Awdhesh Kumar Mishra**,[2] **Debasis Nayak**,[3] **Biswajit Patra**,[4] **Amra Bratovcic**,[5] **Satya Kumar Avula**,[6] **Tapan Kumar Mohanta**,[6] **Kadarkarai Murugan**,[7] **and Muthupandian Saravanan**[8,9]

[1]*Department of Applied Biology, School of Biological Sciences, University of Science and Technology Meghalaya, Ri-Bhoi-793101, Meghalaya, India*
[2]*Department of Biotechnology, Yeungnam University, Gyeongsan-38541, Gyeongsangbuk-do, Republic of Korea*
[3]*Department of Wild Life and Biodiversity Conservation, Maharaja Sriram Chandra Bhanjadeo University, Baripada 757003, India*
[4]*School of Life Sciences, Sambalpur University, Odisha, India*
[5]*Department of Physical Chemistry and Electrochemistry, Faculty of Technology, University of Tuzla, Univerzitetska 8, 75000 Tuzla, Bosnia and Herzegovina*
[6]*Natural and Medical Sciences Research Centre, University of Nizwa, Nizwa 616, Oman*
[7]*School of Biological Sciences, University of Science and Technology Meghalaya, Ri-Bhoi-793101, India*
[8]*Department of Microbiology, Division of Biomedical Sciences, Mekelle University, Ethiopia*
[9]*AMR and Nanotherapeutics Laboratory, Department of Pharmacology, Saveetha Dental College, Saveetha Institute of Medical and Technical Sciences (SIMATS), Chennai, 600077 Chennai, India*

Correspondence should be addressed to Yugal Kishore Mohanta; ykmohanta@gmail.com
and Muthupandian Saravanan; bioinfosaran@gmail.com

Received 24 November 2021; Revised 18 January 2022; Accepted 5 February 2022; Published 24 February 2022

Academic Editor: Dragica Selakovic

Green-based synthesis of metal nanoparticles using marine seaweeds is a rapidly growing technology that is finding a variety of new applications. In the present study, the aqueous extract of a marine seaweed, *Gracilaria edulis*, was employed for the synthesis of metallic nanoparticles without using any reducing and stabilizing chemical agents. The visual color change and validation through UV-Vis spectroscopy provided an initial confirmation regarding the *Gracilaria edulis*-mediated green synthesized silver nanoparticles. The dynamic light scattering studies and high-resolution transmission electron microscopy pictographs exhibited that the synthesized *Gracilaria edulis*-derived silver nanoparticles were roughly spherical in shape having an average size of 62.72 ± 0.25 nm and surface zeta potential of -15.6 ± 6.73 mV. The structural motifs and chemically functional groups associated with the *Gracilaria edulis*-derived silver nanoparticles were observed through X-ray diffraction and attenuated total reflectance Fourier transform infrared spectroscopy. Further, the synthesized nanoparticles were further screened for their antioxidant properties through DPPH, hydroxyl radical, ABTS, and nitric oxide radical scavenging assays. The phycosynthesized nanoparticles exhibited dose-dependent cytotoxicity against MDA-MB-231 breast carcinoma cells having IC_{50} value of 344.27 ± 2.56 μg/mL. Additionally, the nanoparticles also exhibited zone of inhibition against pathogenic strains of *Bacillus licheniformis* (MTCC 7425), *Salmonella typhimurium* (MTCC 3216), *Vibrio cholerae* (MTCC 3904), *Escherichia coli* (MTCC 1098), *Staphylococcus epidermidis* (MTCC 3615), and *Shigella dysenteriae* (*MTCC*9543). Hence, this investigation explores the reducing and stabilizing capabilities of marine sea weed *Gracilaria edulis* for synthesizing silver nanoparticles in a cost-effective approach with potential anticancer and antimicrobial activity. The nanoparticles synthesized through green method may be explored for their potential utility in food preservative film industry, biomedical, and pharmaceutical industries.

1. Introduction

Nanotechnology is a rapidly growing, dynamic, multidisciplinary research area with potential health, environmental, and socioeconomic applications [1–4]. Natural, engineered, or chemically derived nanoparticles (NPs) are typically ≤100 nm in size and possess unique biophysicochemical properties, such as surface functionalization, an abundant surface-to-volume ratio, target specificity, and controlled release in relative to similar bulk materials. The unique properties of nanoparticles make them suitable for potential applications in cosmetics, biomedicines, and agriculture [5, 6]. Notably, the synthesis of both metal and nonmetal nanoparticles by the use of extracts from both plants and microorganisms has become more prevalent than previous chemical and physical synthesis technologies. The major advantages of green-based synthesis of nanoparticles are (i) lower health and environmental toxicity due to the utilization of natural products during the synthesis of the nanoparticles; (ii) the superior attributes of the green-based nanoparticles that are based on their shape, size, composition, and stability, all of which impact their bioactive properties; (iii) the cost-effectiveness and eco-friendly nature of green-based synthesis; and (iv) and the potential application and acceptability of green-based nanoparticles in food, cosmetics, and textile industries [1–4, 7].

Biofabricated metallic nanoparticles have recently been recognized as a valuable nanomaterial due to their wide range of antimicrobial, antioxidant, and anticancer properties. Metallic nanoparticles (e.g., silver, gold, and platinum) have been utilized in bioelectronics, biosensors, medicine, and pharmaceuticals [8–10]. In particular, silver nanoparticles (AgNPs) have become one of the most commercially important nanoparticles due to their numerous potential applications [9, 11, 12]. Nanoparticles have been explored in the pharmaceutical field for drug delivery, as antibacterial and anticancer drugs, wound dressing, and other applications [13, 14]. Biological synthesis has been researched as a potential platform for the utilization of living organisms, such as plants, microbes, and their primary and secondary metabolites to synthesize nanoparticles [15, 16]. Higher plants, algae, bacteria, fungi, and yeast have been used to synthesize gold (Au), silver (Ag), Palladium (Pd), Platinum (Pt), and selenium (Se) nanoparticles. The derived nanoparticles have been shown to have antimicrobial, anticancer, anthelmintic, and larvicidal activities [11, 17]. The foremost asset of biological synthesis is that it only requires the use of an extract from the host organism that contains chemically active functional groups, a reducing agent, and a capping agent, for the synthesis of nanoparticles, while in chemical synthesis, there is a need for extramural reducing and capping agents [17].

The current trend in the "green synthesis" of nanoparticles is the utilization of algal species, including members of the Chlorophyceae, Phaeophyceae, Cyanophyceae, Rhodophyceae, and Diatoms [18]. This approach to the synthesis of metallic nanoparticles is growing rapidly because (i) it is easy to handle and utilize algae, (ii) algae have a strong ability to accumulate and/or absorb inorganic metallic ions, and (iii) utilization of algae to synthesize nanoparticles represents a natural, ecofriendly, fast, and cost-effective method that has low toxicity [18].

Algae are autotrophic and polyphyletic groups of photosynthetic eukaryotic organisms that are classified as microalgae (unicellular in nature, including diatoms) and multicellular or macroalgae (such as seaweeds). These classifications are generally based on morphological features of algae residing in marine or freshwater habitats, or on the surface of moist rocks [19]. Algae play a key role in aquatic ecosystems; however, some species can form toxic blooms. While nanoparticles have been used to control algal blooms, it should be noted that these blooms represent a valuable biomass source for various deriving compounds that can be utilized in agriculture, pharmaceuticals, cosmetics, bioenergy, etc. [20, 21].

A broad spectrum of natural compounds have been identified in green, red, and brown algae that have a variety of bioactive properties, including antimicrobial, antioxidant, antiviral, anti-inflammatory, cytotoxic, antimitotic, antineoplastic, and antifouling activity [22]. Extracts from marine algae also have the potential to synthesize inorganic metallic nanoparticles [23, 24]. *Gracilaria edulis* is an edible marine alga belonging to the class Gracilariaceae, found exclusively in India. It is a potential warehouse of docosahexaenoic acid (DHA) which is renowned as a vital n-3 polyunsaturated fatty acid (PUFA) [25]. Along with it, the marine alga contains functionally significant amino acids such as aspartic acid, alanine, glutamic acid, and glutamine and chemically important phytochemicals such as polyphenols, phenols, terpenes, steroids, halogenated ketones, fucoxanthin, polyphloroglucinol, and bromophenols [26]. However, the edible marine alga *Gracilaria edulis* has not been explored for their potential in the synthesis of metallic AgNPs. Hence, taking into account the rich phytochemical profile, anticancer efficacy of the crude extract, the current study was designed to explore the efficacy and prospective effect of the green synthesized *Gracilaria edulis*-derived silver nanoparticles (GE-AgNPs) against MDA-MB 231 breast carcinoma cells along with their antibacterial and antioxidant properties.

2. Results and Discussion

2.1. UV–Vis Spectrum of GE-AgNPs. The color change inference is considered the preliminary optical inference for the synthesis of AgNPs. Figure 1(a) shows the color change inference of the primary transparent extract mixture with $AgNO_3$ to a reddish-brown solution upon incubation. To confirm the color change inference, the reddish-brown solution obtained was scanned through a UV-Vis spectrophotometer, exhibiting a surface plasmon resonance (SPR) vibration band at 431 nm confirming the synthesis of AgNPs (Figure 1(b)). The results obtained in our study are similar to the previously reported absorption of AgNPs between 410 and 450 nm and accredited to the SPR of AgNPs [27–29]. Notably, use of a UV-Vis spectrophotometer is readily applicable for use in nanoparticle research.

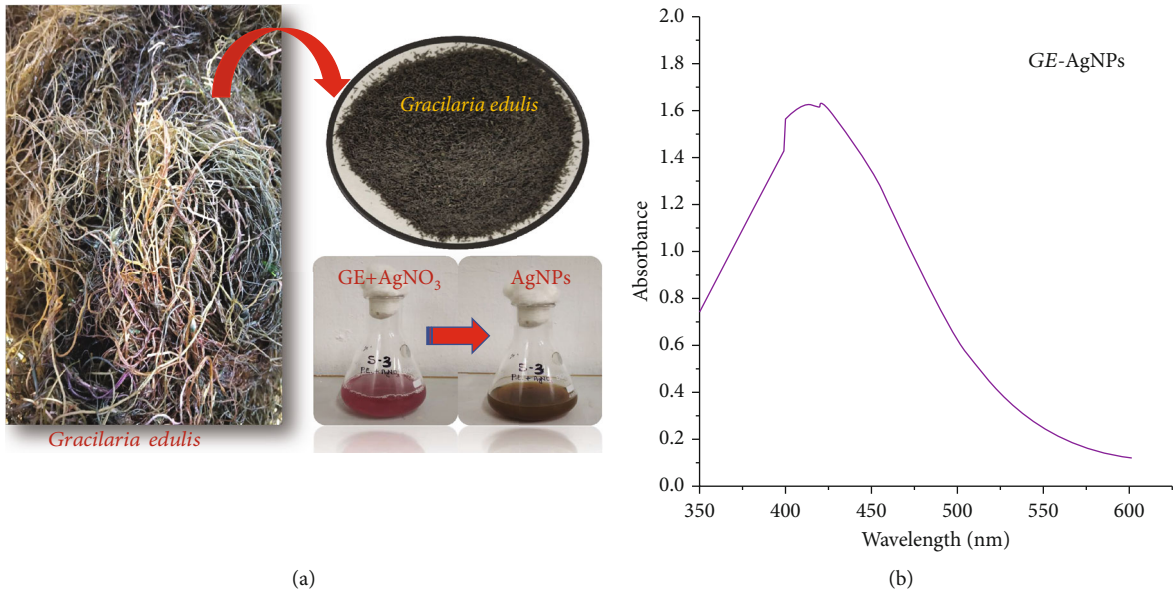

Figure 1: (a) Synthesis of AgNPs from *G. edulis* aqueous extract. (b) UV–Vis spectrophotometric analysis of AgNPs.

2.2. Dynamic Light Scattering (DLS) Analysis of GE-AgNPs. The size and charge are highly related to the potential suitability of a particle in any application. Therefore, it is essential to know the size and charge of a nanoparticle. The size distribution and surface charge of the synthesized GE-AgNPs in an aqueous solution were determined using DLS. The average size of the synthesized GE-AgNPs was calculated to be 62.72 ± 0.25 nm (Figure 2(a)) and the charge was -15.6 ± 6.73 mV (Figure 2(b)). Nanoparticle size plays crucial role in cell transport and communication. Small-sized nanoparticles allow for easier movement of the particles through the plasma membrane of the cell. Therefore, nanosize particles ≤ 100 nm are useful for applications such as drug delivery and construction of biosensors [30–32]. Similarly, the surface charge of GE-AgNPs is also an important attribute as it will affect the ability of the nanoparticles to interact with macromolecules that function in different biochemical pathways [5, 33].

2.3. Attenuated Total Reflectance–Fourier Transform Infrared Spectroscopy (ATR-FTIR) Analysis of GE-AgNPs. The ATR-FTIR spectra of the GE-AgNPs was assessed to determine the functional groups of biomolecules present in the aqueous extract of *G. edulis* that participated in the synthesis and stabilization of the derived AgNPs. Phytochemicals present in the *G. edulis* extract interacted with the nanoparticles during the synthesis process and exhibited sharp peaks at 3228.56, 2933.69, 2625.83, 1714.23, 1393.38, 1278.43, 1034.54, and 661.70 cm^{-1} (Figure 3). It could be seen from Figure 3 that upon interaction with the GE-AgNP extracts, the native vibrational peaks of the inherent AgNPs get interacted with the phenolic groups (-OH) present in the extracts of the biological machinery of the algal species. Such interactions are spectroscopically altered and exhibited an inverse Fourier spectrum at ~3228 cm^{-1}. Moreover, besides the –OH functional groups interaction system, there is interionic exchanges taking place at the C-H vibrational forms, where the carbon groups in the biological systems of marine algae extracts gets influenced by the formation of AgNPs formed in the culture at ~2933 cm^{-1}. Similarly, the vibrational spectra interactions at the C=O (~1714 cm^{-1}), C-O-C, and C-OH (~1278 cm^{-1}) indicating the presence of ether-, alcohol-, and sugar-based bond interactions could be easily noticed in the FTIR plots of the *G. edulis* extracts and its out product of *GE*-AgNPs at its corresponding transmittance value. The presence of mild vibration bands at around 660-800 cm^{-1} exhibits the specific fingerprint regions associated with the *G. edulis* extract which signifies the presence of trace elements such as C-I, C-Br which emerges due to the marine nature of the plant extract, and the synthesized GE-AgNPs. Similar results have been reported by various groups for synthesis of AgNPs [34, 35]. It is expected that during the synthesis process of AgNPs from its marine algal source, the biological metabolic groups existing in the algal species like carbon, nitrogen, and oxygen are getting interacted with the differential redox state of the AgNPs produced from its native ionic state to zero valence states of nanoscale particles. Such transformations at the nanoscale phenomenon uncover the explanation of quantum mechanical and redox energetic exchanges taking place at the subatomic stage leading to conversion from ionic state of Ag to its zero state of AgNPs. The biological extracts play hereby a crucial role in the intercalated mechanisms for the lesser toxic product of AgNPs from its ionic precursors, which is much safer and more comprised of lesser defects in its systems as compared to the production of AgNPs from chemical mediated routes.

The overall ATR-FTIR analysis revealed that the proteins and halogenated biomolecules present in the seaweed extract were functioning as both reducing and stabilizing agents during the synthesis of AgNPs, a feature that may be characteristic of all macroalgae extracts. Marine macroalgae are rich sources of both proteins and halogenated compounds that have beneficial applications in many different

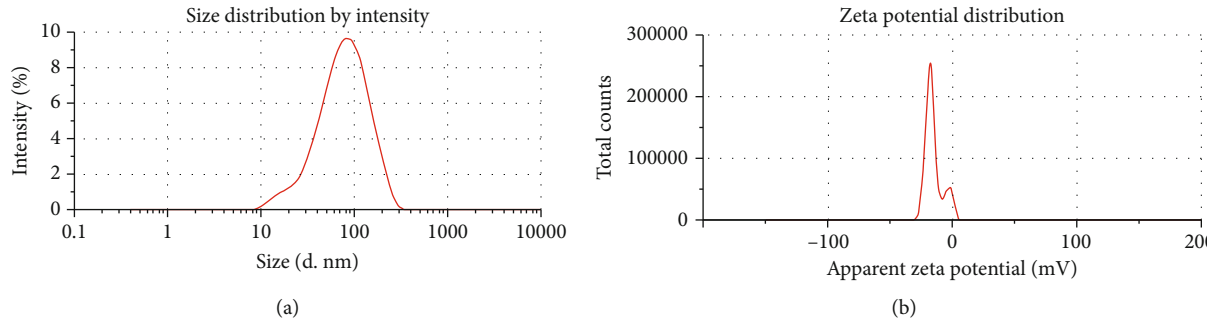

Figure 2: DLS analysis of AgNPs synthesized using *GE* extracts. (a) Average size distribution. (b) Surface charge.

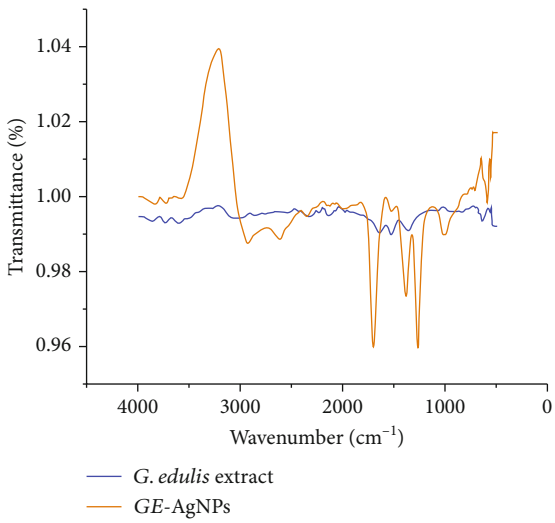

Figure 3: ATR-FTIR analysis of *G. edulis* extract and GE-AgNPs.

processes [36, 37]. Notably, the proteins present in the seaweed could bind to the AgNPs via free amine groups, stabilizing clustered nanoparticles through surface-bound proteins [38]. The present results are also strongly supported by the findings presented in previous studies [6, 16, 39].

2.4. X-Ray Diffraction (XRD) Analysis of GE-AgNPs. XRD is a rapid analytical technique primarily utilized for phase identification of a crystalline material and provides information on unit cell dimensions. Therefore, the analyzed material needs to be finely ground and homogenized to determine its average bulk composition. The results of the XRD analysis of GE-AgNPs are presented in Figure 4. The figure represents a typical XRD diffractogram revealing Bragg peaks predominantly at (angle 2θ) at 28.5, 33, 42, and 48.5 (in degree) for the AgNPs synthesized from *G. edulis* seaweed extract which corresponds to (100), (010), (200), and (002), respectively. Miller indices confirm the formation of crystalline elemental AgNPs with a face-centered cubic (FCC) lattice [40, 41]. Thus, the XRD pattern provides strong evidence supporting the UV–Vis spectra and HR-TEM images of the GE-AgNPs.

2.5. HR-TEM Analysis of GE-AgNPs. HR-TEM micrographs confirmed the spherical shape and polydisperse nature of the GE-AgNPs and their attached biomoieties (Figure 5). The HR-TEM pictographs exhibited that the GE-AgNPs were regular and roughly spherical in shape, with blunt margins. The TEM images also revealed that the nanoparticles were nonagglomerated and freely scattered, making them a strong candidate for biosensor development and drug delivery. The DLS studies also support the properties of the GE-AgNPs revealed in the TEM images, with approximately 80% of the DLS-scanned samples of the GE-AgNPs displaying a size of ~62 nm. Collectively, the dynamic light scattering studies and HR-TEM micrographs confirm that the size of the GE-AgNPs is in the nanorange and that they possess a roughly spherical morphology. This morphological shape and size indicate the potential efficiency of nanoparticles for drug conjugation and drug delivery [42–44].

2.6. Qualitative and Quantitative Phytochemical Analyses of the Seaweed Extract. The results of the qualitative and quantitative phytochemical analyses of the aqueous *G. edulis* seaweed extracts are summarized in Tables 1 and 2. The analysis revealed the presence of alkaloids, tannins, phenolic, flavonoids, and saponins, while glycosides, steroids, and sterols were absent. The identified compounds may represent the principal chemical ingredients that are involved in the biosynthesis of AgNPs and define the potential of the nanoparticles for different bioapplications [45–47]. Polyols, terpenoids, phenols, flavones, and polysaccharides have been previously reported to be the principle components in the bio reduction of silver and chloroaurate ions [48]. Importantly, the potential absence of glycosides, steroids, and sterols in the *G. edulis* extracts in our study may be due to the selective qualitative tests that were conducted and/or the extraction procedures. The hypothetical mechanism of the synthesis of AgNPs may involve a cascade of complex antioxidant enzymes [49].

2.7. Antibacterial Activity of GE-AgNPs. Preliminary evaluation of the antibacterial activity of GE-AgNPs against six pathogenic bacteria was conducted in an agar well diffusion assay (Table 1). Results of this assay indicated that the largest zone of inhibition was observed against *Bacillus licheniformis* and the smallest against *Salmonella typhimurium* (Figure 6). Overall, significant antibacterial activity was observed against *V. cholerae*, *E. coli*, *S. epidermidis*, and *S. dysenteriae*. GE-AgNPs exhibited good bactericidal activity against both Gram-positive and Gram-negative bacteria. A

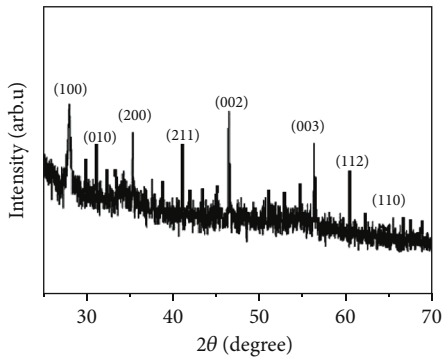

Figure 4: XRD analysis of GE-AgNPs.

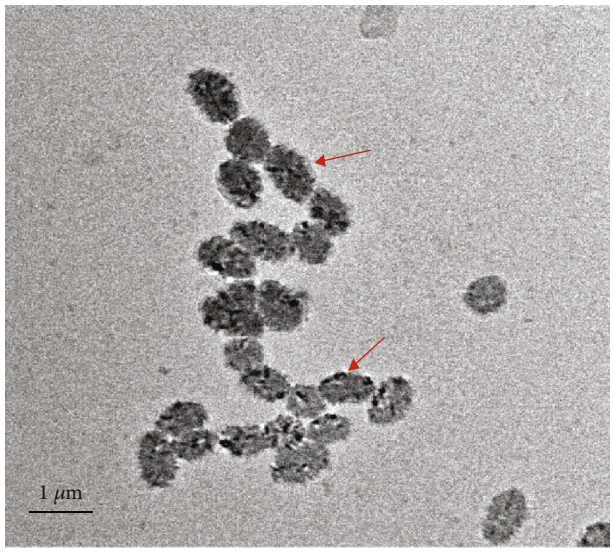

Figure 5: HR-TEM micrograph of GE-AgNPs (indicated by arrows).

Table 1: Qualitative phytochemical analysis of an aqueous extract of *G. edulis* seaweed.

Phytoconstituent	Observation
Alkaloids	+
Tannins and phenolic compounds	+
Glycoside	-
Flavonoids	+
Steroids and sterols	-
Triterpenoids	+
Saponins	+

Notes: +: present; -: absent.

Table 2: Quantitative analysis of total phenolics and carbohydrates in an aqueous extract of *G. edulis* seaweed.

Phytochemical constituent	mg/g dry weight (mean ± SD)
TPC	7.27 ± 1.10
TFC	4.70 ± 0.63

microbroth dilution assay was also used to verify the antibacterial activity of GE-AgNPs and percent to determine percent inhibition and the MICs for each of the pathogenic species of bacteria (Figure 7). The MICs was calculated of six pathogenic bacteria undertaken for the investigation such as *B. licheniformis* (72.84 ± 1.54 μg/mL), *S. dysenteriae* (130.67 ± 2.93 μg/mL), *E. coli* (132.42 ± 3.08 μg/mL), *S. typhimurium* (132.42 ± 3.08 μg/mL), *V. cholerae* (65.58 ± 1.52 μg/mL), and *S. epidermidis* (127.57 ± 3.08 μg/mL). Significant growth inhibition (>94%) was observed in all six pathogenic bacterial species. Although the specific mechanism by which nanoparticles exhibit antibacterial activity is not fully understood, different mechanisms of action have been reported in the literature. Structural changes in the bacterial membrane and ultimate cell death as a result of penetration of nanoparticles into the cell wall due to their anchoring ability have been reported [39, 50, 51]. Enzyme degradation, inactivation of structural proteins, and breakage of genetic materials by AgNPs have also been proposed as mechanisms of action [38, 52, 53]. It has also been suggested that several bacterial cellular enzymes are inactivated by the substantial attachment of Ag ions to –SH groups, a major chemical component of enzyme structure present in the structure [42, 54, 55]. The intermittent interaction of AgNPs with phosphorus and sulfur groups, interfering with the DNA replication processes and dismantling the microbial nuclear system, has also been proposed [56–59]. In our study, the antibacterial results obtained with GE-AgNPs suggests that the seaweed extract-derived AgNPs possess an excellent antimicrobial with widespread potential applications.

2.8. Antioxidant Activity of GE-AgNPs. Abiotic stress induces an overabundance of reactive oxygen species (ROS) that are highly toxic at high levels due to their strong oxidative properties. ROS can damage DNA and RNA, carbohydrates, lipids, and proteins. Chronic oxidative stress can also result in the induction of a variety of different diseases [60], and pharmaceuticals with antioxidant properties have been developed as an option to help minimize oxidative stress in humans. Notably, organisms have evolved an antioxidant system that can scavenge ROS and other free radicals. Delayed and poor absorption potential of exogenous antioxidants, difficulty in passing through cell membranes, and rapid degradation of antioxidants after their delivery, however, represent major challenges to the use of both natural and synthetic antioxidant molecules. Unfortunately, the utilization of nanoparticles as an antioxidant has not been widely recognized and investigated and has been limited to only a few types of nanomaterials [61]. Importantly, functional antioxidant AgNPs derived from the use of various natural extracts obtained from plant species appear to represent a pivotal alternative due to their high stability, biocompatibility, and targeted delivery [6]. Plants, algae, bacteria, and fungi possess a wide array of diverse phenolic compounds and other secondary metabolites that are highly useful as reducing and stabilizing agents. In addition, they also possess excellent antioxidant properties. Therefore, the GE-AgNPs fabricated in the current study were extensively

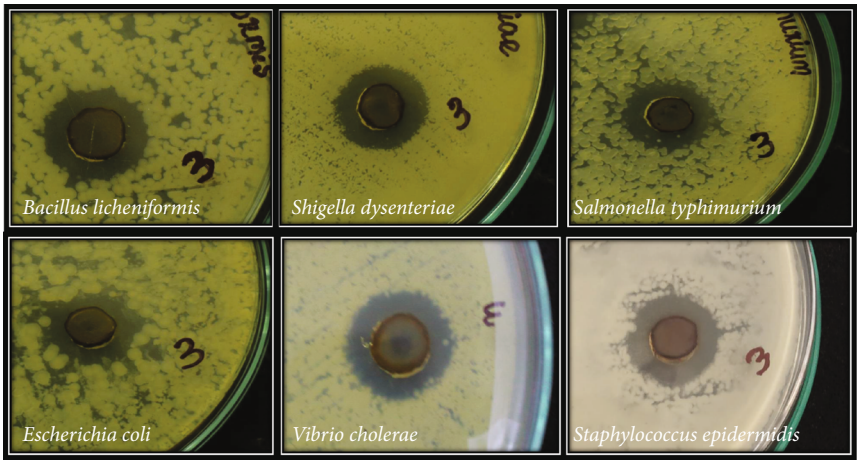

Figure 6: Antibacterial activity (Agar well method) of GE-AgNPs.

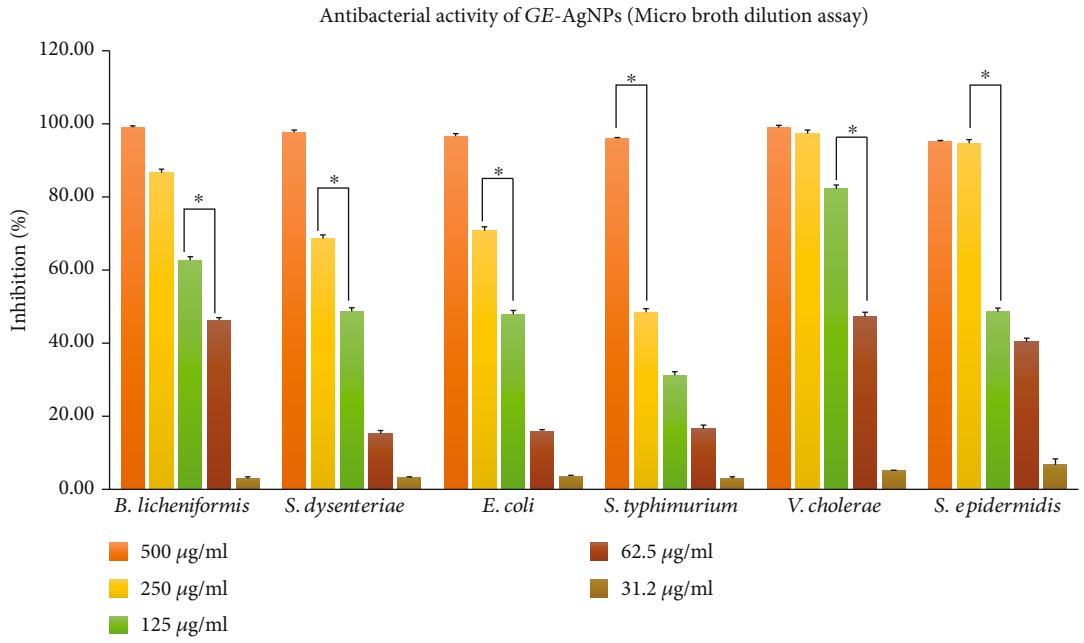

Figure 7: Antibacterial activity (microbroth dilution method) and MICs of GE-AgNPs. Error bar represents standard deviation of mean. $^{*}p \leq 0.05$. Significant difference ($p \leq 0.05$) within a parameter between two lines is denoted by asterisk.

analyzed for their antioxidant properties (Figure 8). The antioxidant activity of *GE*-AgNPs was evaluated using a variety of radical-scavenging assays against different types of reactive radicals, including DPPH, hydroxyl ions, ABTS, and nitric oxide radicals (Figure 8). The DPPH radical-scavenging activity of GE-AgNPs was found to be dose dependent, displaying a maximum inhibition of 86.83% at a concentration of 50 μg/mL. An IC_{50} value of 30.71 ± 0.22 μg/mL was found to be significant, compared to the positive control, ascorbic acid (IC_{50} value 10.33 ± 0.16 μg/mL), thus demonstrating the strong antioxidant property of GE-AgNPs. DPPH is commonly used to evaluate the antioxidant properties of a compound. The radical scavenging activity of GE-AgNPs was also tested against hydroxyl ion (OH^{-}) radicals, exhibiting a 94.20% scavenging capacity at 100 μg/mL and an IC_{50} value of 43.85 ± 0.36 μg/mL, compared to the ascorbic acid standard which had an IC_{50} value of 20.43 ± 0.03 μg/mL. Hydroxyl ions readily disrupt disulfide bonds in proteins, resulting in unfolding and refolding into atypical protein structures [62]. Therefore, the current study provides strong evidence for the potential use of GE-AgNPs as antioxidants in biological systems without adverse side effects.

ABTS is another free radical that is generally involved in oxidative damage to cells and polyphenols are capable of minimizing the generation of ABTS. In the present study, the FT-IR analysis of the *G. edulis* extract identified the presence of polyphenols in the synthesized GE-AgNPs. The

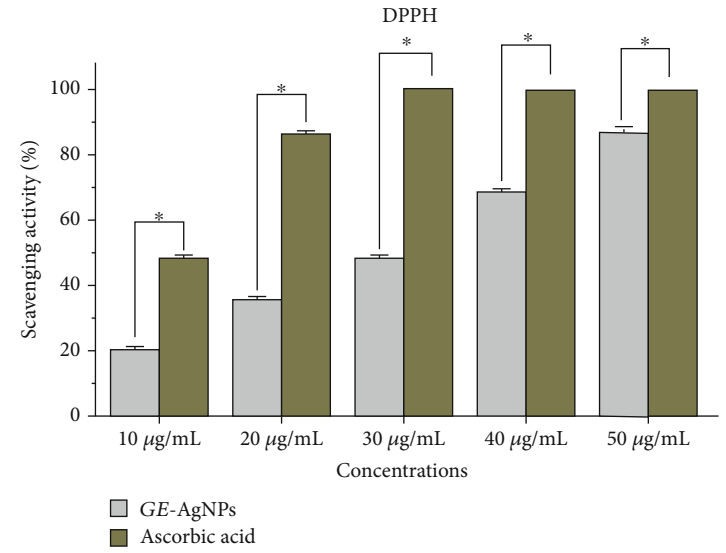

(a)

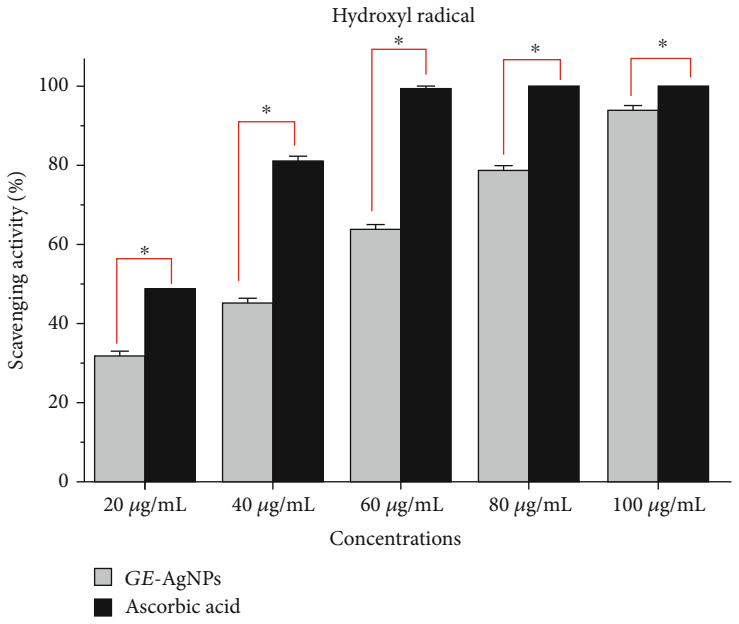

(b)

Figure 8: Continued.

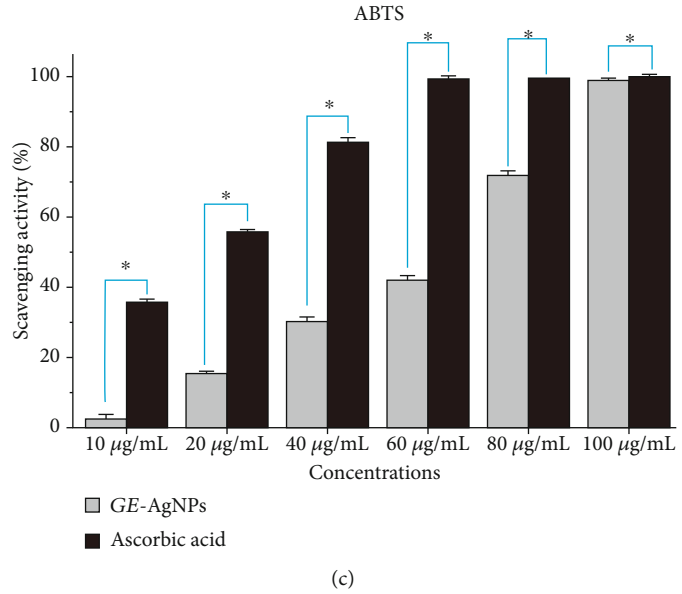

(c)

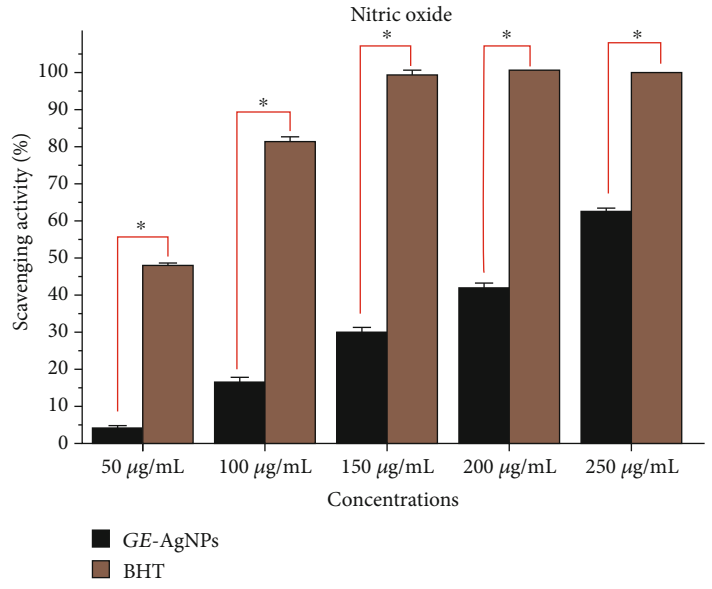

(d)

Figure 8: Antioxidant activity of GE-AgNPs in terms of radical scavenging activity: (a) DPPH, (b) hydroxyl ions, (c) ABTS, and (d) nitric oxide radicals. Error bar represents standard deviation of mean. $^{*}p \leq 0.05$. Significant difference ($p \leq 0.05$) within a parameter between two lines is denoted by asterisk.

ABTS scavenging assay indicated 99.16% maximum scavenging activity at 100 μg/mL of GE-AgNPs and an IC_{50} value of 64.77 ± 0.16 μg/mL compared to an IC_{50} value of 16.31 ± 0.11 μg/mL for ascorbic acid. Nitrite has harmful effects on human health due to its reaction with secondary amines in cells, which forms toxic byproducts in human digestive systems [62]. Thus, the activity of GE-AgNPs against nitric oxide radicals was evaluated. A maximum scavenging activity of 62.43% was observed at 250 μg/mL, and the IC_{50} value was determined to be 217.96 ± 1.42 μg/mL; a value that is representative of a moderately active antioxidant compound against nitric oxide radicals. BHT was used as a positive standard in the nitric oxide radical scavenging assay and was determined to have an IC_{50} value of 51.74 ± 0.13 μg/mL. Oxidative stress is believed to play a crucial role in degenerative senescence. As a result, AgNPs with antioxidant capacity could provide a promising therapeutic for the prevention of oxidative stress. *G. edulis* extracts have been previously reported to have antioxidant activity [63]. The present results are also in good accordance to the results obtained from previous studies (Das et al., 2019; Kumar et al., 2020; Otunola and Afolayan, 2018; Ramamurthy et al., 2013b).

2.9. Biocompatibility and Cytotoxicity Analyses of GE-AgNPs. A methylthiazolyldiphenyl-tetrazolium bromide (MTT) assay was used to determine cell viability when evaluating the biocompatibility and cytotoxicity of GE-AgNPs. Normal

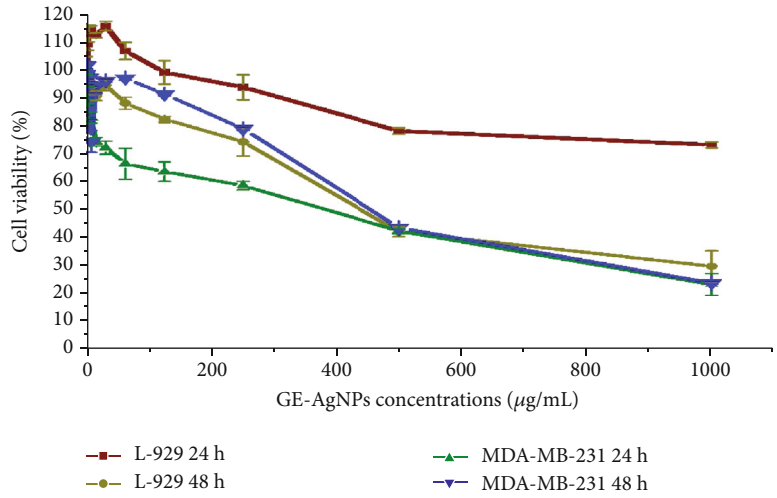

Figure 9: Cell viability of MDA-MB-231 and L-929 after treatment with different concentrations of GE-AgNPs after 24 and 48 h.

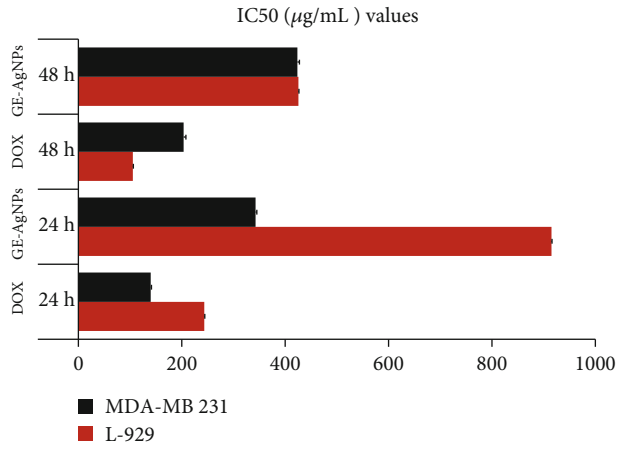

Figure 10: Cell viability (IC_{50} value) of MDA-MB-231, L-929, after treatment with different nanoformulations (Dox: doxorubicin (control), GE-AgNPs) after 24 and 48 h. Error bar represents standard deviation of mean. $^{*}p \leq 0.05$. Significant difference ($p \leq 0.05$) within a parameter between two lines is denoted by asterisk.

fibroblast cells (L-929) were treated with GE-AgNPs in culture for 24 hour (h) at 37°C and cell viability was subsequently assessed (Figure 9). Results indicated a dose-dependent effect of GE-AgNPs on L-929 cell viability. L-929 cells exposed to a 125 μg/mL concentration of GE-AgNPs exhibited a 99.50% level of cell viability. However, the percent viability gradually reduced as the concentration of GE-AgNPs increased with L-929 cell viability being74.38% when exposed to 1000 μg/mL concentration of GE-AgNPs. These results indicate that GE-AgNPs are relatively nontoxic to normal cells, even at a high concentration. Consequently, these data demonstrate that GE-AgNPs can be potentially used for different biological applications without detrimental effects on the health of cells. The biocompatibility of GE-AgNPs with L-929 cells has been previously reported [64–67].

In contrast to the biocompatibility of GE-AgNPs with normal fibroblast cells, the viability assay of breast cancer cells (MDA-MB-231) exposed to GE-AgNPs revealed significantly higher levels of cytotoxicity (Figure 10). The breast cancer cells were exposed to ~1000 μg/mL solution of GE-AgNPs for 24 h, which reduced the cell viability to ~21.23%. A time- and dose-dependent cytotoxicity for AgNPs derived from different biological sources against MDA-MB-231 cells has been previously reported [68].

The percentage of viable cancer cells decreased as the concentration of GE-AgNPs increased. A cell viability of 63.81% and 94.06% was observed after exposure to a 125 μg/mL and 1.95 μg/mL solution of GE-AgNPs, respectively. The MIC of *GE*-AgNPs was calculated as 344.27 ± 2.56 μg/mL against MDA-MB-231. These results indicate that the MDA-MB-231 cell lines exhibit a concentration-dependent response with response to viability. The level of cytotoxicity, however, did not appear to be time dependent as an identical percentage of viable cells was observed after both 24 and 48 h exposure to the same concentration of GE-AgNPs. The IC_{50} values for doxorubicin (used as a positive control) were higher in MDA-MB-231 cells than in L-929 cells after 24 hr or 48 hr of exposure. In contrast, the IC_{50} values for GE-AgNP treatment were significantly lower in MDA-MB-231 cells than in L-929 cells after exposure for 24 or 48 h (Figure 10).

AgNPs induce cytotoxic effect due to their impact on different metabolic pathways. Another study reported that the cytotoxicity of AgNPs results from an increase in ROS production [69]. Previous studies stated that the introduction of AgNPs into target cells could promote the overproduction of intracellular ROS, which activates apoptosis-associated metabolic pathways including p53, MAPK, and AKT apoptotic signaling pathways [70, 71]. Similar to other metal nanoparticles, AgNPs also promote oxidative stress in cells by inducing the overproduction of ROS [70]. Mitochondria are vital sources of apoptosis signals and the effect of AgNPs on mitochondrial membrane permeability results in the loss of mitochondrial membrane integrity, leading to caspase-dependent apoptotic cell death [72]. In addition to

AgNPs stimulating apoptosis in cells, it is more than likely that future studies will reveal other mechanisms by which AgNPs establish their cytotoxicity.

3. Materials and Methods

3.1. Collection and Preparation of Seaweed Extract. The red seaweed, *G. edulis* (Linnaeus), was collected from Chilika Lake, Odisha, India (19° 43′ 0″ N, 85° 19′ 0″ E) and transported to a laboratory in a portable ice cooler. The harvested seaweed was then thoroughly cleaned in running tap water followed by distilled water to remove extraneous materials and to substantially reduce the salt content, after which the seaweed was dried in a shady, open-air environment for 3–5 days. The dried seaweed was subsequently ground to a fine powder using a commercial-grade mixer grinder. Then, 5.0 g of the *G. edulis* seaweed powder was boiled in 50 mL of sterilized Milli Q water for 20-30 min and subsequently filtered through Whatman No. 1 filter paper. The filtered extract was stored at -4°C until further use.

3.2. Synthesis of GE-AgNPs. A total of 10 mL of seaweed extract was mixed with 90 mL of a 1.0 mM aqueous solution of $AgNO_3$ [45, 73] and incubated at room temperature on a rotary shaker for 1 hr. A color change in the reaction solution from light brick red to deep brown was noted by visual observation and was used to confirm the completion of the AgNP synthesis. The synthesized AgNPs were pelleted by centrifugation at 8000 rpm for 15 min at 10°C. The obtained AgNPs were dried and stored at 4°C for characterization and assessment of their bioactive properties.

3.3. Characterization of GE-AgNPs. The synthesis of the AgNPs using an aqueous extract of *G. edulis* was periodically monitored by UV-Vis spectrophotometer (Lambda 35R PerkinElmer, USA) in the range of 350-600 nm. The UV-visible spectra of the synthesis reaction solution were recorded as a function of reaction time at a resolution of 1 nm at 25°C. The surface charge and average size of the AgNPs were analyzed using a Zetasizer (ZS 90, Malvern, UK). The purified nanoparticle samples were diluted tenfold in PBS (0.15 M, pH 7.2). Aliquots were sampled and placed in dynamic light scattering (DLS) cuvettes and then evaluated for equivalent size distribution, diameters, and zeta potential. Particle diameters were assessed at a scattering angle of 90° at 25°C. ATR-FTIR spectroscopy analysis of the, *G. edulis* aqueous extract and the synthesized *GE*-AgNPs was conducted to substantiate the potential role of the various functional chemical groups present in the seaweed extracts on the modification of the surface of the synthesized nanoparticles. ATR-FTIR was conducted on a Bruker ALPHA spectrophotometer (Ettlinger, Germany) at a resolution of 4 cm^{-1}. The samples were evaluated in the spectral region of 4000 to 500 cm^{-1} by taking an average of 25 scans per sample. For continuous observations, one drop of the sample was kept on the sample holder and the samples were scanned and the obtained results were analyzed using OPUS software. The crystalline properties of the AgNPs were assessed using an X-ray diffractometer (PANalytical X'Pert, Almelo, The Netherlands) equipped with a Ni filter and a CuK ($l = 1.54056$ Å) radiation source. The scanning rate was 0.05°, while the diffraction angle varied from 20–80°. High-resolution transmission electron microscopy (Technai™ F30 G2 STWIN, FEI, Lincoln, NE, USA) was used to observe the nanomorphology of the AgNPs. The synthesized AgNPs were placed on a coated copper grid with a 300 mesh size and observed at an accelerating voltage of 300 kV.

3.4. Qualitative and Quantitative Analyses of the Seaweed Extract. The qualitative phytochemical analysis of the *G. edulis* extract was performed following standard methods [63]. The obtained results were qualitatively expressed as positive (+ve) or negative (-ve). The chemicals and reagents used for the study were purchased from Sigma–Aldrich (India).

3.4.1. Total Phenol Content. Total phenol content (TPC) in the seaweed extract was estimated using the Folin–Ciocalteu method with slight modifications as described by Lim et al. (2007). The analysis was performed in triplicate. TPC was expressed as gallic acid equivalents (GAE) in mg/g sample.

The concentration of total phenolic compounds in the extract was determined using the following formula:

$$T = C * \frac{V}{M}, \tag{1}$$

where T is the total phenolic content mg/gm of seaweeds extract in GAE, C is the concentration of Gallic acid from the calibration curve in mg/mL, V is the volume of the extract in mL, and M is the Wt of the seaweeds extracts in g.

3.4.2. Total Flavonoid Content. Total flavonoid content (TFC) of the *G. edulis* extract was determined using an aluminum chloride ($AlCl_3$) colorimetric assay and expressed as milligrams of quercetin equivalents per gram dry mass (mg·Q/g dw) [74]. The analysis was performed in triplicate.

3.5. Antibacterial Activity of the GE-AgNPs

3.5.1. Bacterial Strains. The six species of human pathogenic bacteria, *Bacillus licheniformis* (MTCC 7425), *Salmonella typhimurium* (MTCC 3216), *Vibrio cholerae* (MTCC 3904), *Escherichia coli* (MTCC 1098), *Staphylococcus epidermidis* (MTCC 3615), and *Shigella dysenteriae* (MTCC-9543) were used in the antibacterial assay. The bacterial strains were purchased from MTCC, Pune.

3.5.2. Agar Well Diffusion and Microbroth Dilution Methods. A small colony of each targeted bacterial strain was inoculated from a stock agar slant into 2 mL Muller Hinton (MH) broth medium (0.015% soluble starch, 0.2% beef extract, and 1.75% casamino acids) under proper aseptic conditions. The inoculated tubes were incubated overnight at 37°C on a rotary shaker at 200 rpm.

The assessment of the antibacterial activity of the synthesized GE-AgNPs against the selected pathogenic bacteria was conducted using a well diffusion assay with Muller Hinton Agar (MHA). Briefly, 100 μL of each bacterium was seeded over the prepared MHA plates. Test wells (5 mm

diameter and 3 mm deep) were then made in the inoculated agar medium using a sterile cork borer. Each well was then filled with 50 μL of GE-AgNPs. Wells filled with 50 μL of silver nitrate ($AgNO_3$) solution served as the control while wells filled with the antibiotic, gentamicin, were used as a positive control. The inoculated plates were kept in an incubator at 37°C for 24 h. Following the period of incubation, the diameter of inhibition zones was measured and a zone diameter ≥ 8 mm was recorded as a positive antibacterial activity.

Antibacterial assessment was carried out using the microbroth dilution method. The minimum inhibitory concentration (MIC) of the GE-AgNPs on bacterial strains was also assessed [75]. Inhibition ≥ 90% in the microbroth dilution assay was used as an indication of good antibacterial activity, and additional experiments were carried out for MIC estimation. The test inoculum (190 μL; $A_{600} = 0.1$) were incubated in 10 μL of different concentrations (500-31.25 mg/mL; twofold dilution) of the GE-AgNPs until the level of inhibition was found to be <50%. The assays were conducted in 96-well plates, and microbial growth was determined in a microplate reader (Bio-Rad, USA) at 600 nm. The numerical MIC values were calculated using IC_{50}/IC_{90} Laboratory Excel Calculation formulas and expressed as IC_{50}. All of the assays were conducted in triplicate, and zones of inhibition were expressed in a mean ± SD.

3.6. Antioxidant Activity of the GE-AgNPs. The antioxidant activity of the GE-AgNPs was assessed by its radical scavenging ability.

3.6.1. DPPH Radical Scavenging Activity. The radical scavenging activity of GE-AgNPs was determined using the 1,1-diphenyl-2-picryl-hydrazil (DPPH) assay with slight modification (Arul Kumar et al., 2018; Lim et al., 2007). Different concentrations (10, 20, 30, 40, and 50 μg/mL) of GE-AgNPs were used in the assay. Ascorbic acid in equivalent concentrations was used as a positive control, and results were expressed as percentage (%) radical scavenging activity. The MIC for DPPH radical scavenging activity was also calculated and expressed as an IC_{50}.

3.6.2. Hydroxyl Radical Scavenging Activity. Hydroxyl (OH^-) radical scavenging activity of GE-AgNPs was evaluated as previously described [76] using different concentrations (20, 40, 60, 80, and 100 μg/mL) of GE-AgNPs. Ascorbic acid at equivalent concentrations was used as a positive control. The MIC for hydroxyl radical scavenging activity was also calculated and expressed as an IC_{50}.

3.6.3. 2,2-Azino-bis(3-ethylbenzothiozoline-6-sulfonic acid) Diammonium Salt (ABTS) Radical Scavenging Activity. ABTS radical scavenging activity of the GE-AgNPs was also determined using a radical cation decolorization assay as previously described [77] using different concentrations (20, 40, 60, and 80 μg/mL) of GE-AgNPs. Ascorbic acid at equivalent concentrations was used as a positive control. The MIC for ABTS radical scavenging activity was also calculated and expressed as an IC_{50}.

3.6.4. Nitric Oxide Radical (NO^*) Scavenging Activity. Nitric oxide radical scavenging activity of the GE-AgNPs was evaluated using the method described by Garrat (1964) with slight modification. Briefly, sodium nitroprusside (Na_2[**Fe**(**CN**)$_5$NO]$2H_2O$) in aqueous solution generates nitric oxide spontaneously at physiological pH, which immediately interacts with oxygen to produce nitrite ions (NO^{2-}), which can be determined by the Griess-Ilosvay reaction. A standard method [63] to evaluate the NO^* scavenging activity was also used. Different concentrations (50, 100, 150, 200, and 250 μg/mL) of GE-AgNPs were used in the assay, and BHT was used as a positive control. The MIC for NO^{2-} radical scavenging activity was also calculated and expressed as an IC_{50}.

3.7. Biocompatibility and Cytotoxicity Analysis of GE-AgNPs

3.7.1. Cell Culture. A normal fibroblast cell line (L-929) and a breast cancer cell line (MDA-MB 231) were used in the biocompatibility and cytotoxicity assays. Both cell lines were seeded on Dulbecco's modified Eagle's medium and M-199 medium supplemented with 10% fetal bovine serum (FBS), as well as streptomycin sulfate and benzyl antibiotics at a final concentration of 100 μg/mL and 100 U/mL, respectively. Cell cultures were incubated at 37°C (5% CO_2) for 24 h, for the duration of the assays. The cells were trypsinized using 0.25% Trypsin-EDTA at a 70 to 80% confluence. Cells were counted and then placed in a 96-well enzyme-linked immunosorbent assay (ELISA) plate at a density of 5×10^3 cells/well to conduct MTT assay. All cell culture chemicals are purchased from Sigma–Aldrich (India).

3.7.2. MTT Assay. Biocompatibility and cytotoxicity were evaluated using a MTT colorimetric assay after 24 and 48 h. incubation of the cell lines with the GE-AgNPs. When the cells were at 90% confluency, the media was removed and the cells were exposed with fresh medium containing different concentrations of GE-AgNPs (viz., 100, 200, 400, 600, 800, and 1000 μg/mL) and was further incubated for 24 h. Doxorubicin was employed as a positive control. Similar to the GE-AgNPs, various concentrations of DOX was used to see its efficacy along with the synthesized GE-AgNPs. A stock solution of MTT (1 mg/mL) in PBS was prepared immediately prior to use. A 500 μL volume of the MTT solution (50 μg/mL MTT in the culture medium) was added to each culture dish and left uncovered. Cells were incubated for 3 hr, after which the reduced formazan was extracted with 500 μL of DMSO and absorbance was measured at 595 nm in a microtiter plate reader (Bio-Rad, USA). Cell viability was assessed as the percentage absorption of treated cells relative to the untreated and control cells.

3.8. Statistical Analysis. All assays in this study were performed in triplicate. The results of the antioxidant assays are presented as a percentage inhibition, while the cytotoxicity results are presented as % viability, relative to the control. The antioxidant and cytotoxicity assay data for the different treatment groups vs. the controls were statistically evaluated using Student's t-test ($p \leq 0.05$).

4. Conclusion

Marine macroalgae or sea weed *G. edulis* has momentous attributes in the green synthesis process of metal nanoparticles, like other biological resources such as plant, bacteria, fungi, macrofungi or mushrooms, and yeast. Due to the encouraging involvement of algae in the nanotechnology advancement, the separate branch known as phyconanotechnology is growing enormously to substantiate the different biomedical, agriculture, and environmental issues. Various studies on the biosynthesis of nanoparticles using seaweed extracts have been conducted. In the current investigations, the physiochemical characterization of the synthesized AgNPs demonstrated the stable synthesis of AgNPs that can potentially be used in different applications. The antibacterial, antioxidant, biocompatibility, and cytotoxicity of the AgNPs indicate their potential commercial utility in biomedical and pharmaceutical industries. The use of seaweed extract in nanoparticle biosynthesis is highly advantageous due to the presence of a variety of secondary metabolites in the extract that affect the properties of the synthesized nanoparticles and exhibit low cytotoxicity to healthy cells. The use of "green-based" synthesis of nanoparticles is compatible with large-scale production and smooth downstream processing. Further studies are warranted and necessary to explore the use of seaweed extracts in nanotechnological applications and to fully understand the properties of seaweed-fabricated metal nanoparticles, their mechanism of action, and their potential applications in food, health, and environmental industries. Comprehensively, the nanobiotechnology that utilizes the sources from algae and blue-green algae to synthesize nanomaterials is in the budding stage, and further research and development are necessary.

Data Availability

The data supporting the reported results are available upon request from the first and corresponding author.

Additional Points

Research Highlights: (1) Green synthesis of silver nanoparticles from marine sea weed *Gracilaria edulis* for efficient use in biomedical industry sector is highly demanding for its ecofriendly and less toxic byproduct production, (2) The use of marine sea weed for such green synthesis is highly attractive to a combinatorial approach in addition of natural compounds with nanoparticles, (3) Silver nanoparticles also exhibited potential antibacterial activity against *Bacillus licheniformis*, *Shigella dysenteriae*, *Escherichia coli*, *Salmonella typhimurium*, *Vibrio cholerae*, and *Staphylococcus epidermidis,* (4) AgNPs performed high efficacy of DPPH, hydroxyl radical, ABTS, and nitric oxide radical scavenging activity, (5) AgNPs are highly biocompatible to normal fibroblast cell line L-929 and cytotoxic against breast cancer (MDA-MB-231) cells

Ethical Approval

Experimental research/field studies on plants comply with relevant institutional, national, and international guidelines and legislation.

Conflicts of Interest

The authors declare that they have no conflicts of interest.

Authors' Contributions

Y.K.M and A.K.M have conceptualized, designed, and perform experiments and wrote the manuscript. D.N and T.K.M characterized the samples and wrote the manuscript. S.K.A and B.P. analyzed the characterization data and revised the manuscript. A.B, K.M, and S.M. helped in the review and editing of the manuscript. All the authors read and approved the final manuscript. Yugal Kishore Mohanta and Awdhesh Kumar Mishra contributed equally to this work.

Acknowledgments

The authors are thankful to the University of Science and Technology Meghalaya, India, University of Nizwa, Oman, and Saveetha Institute of Medical and Technical Sciences (SIMATS), Chennai, for providing necessary support to conduct the research.

References

[1] A. Batool, F. Menaa, K. B. Ali, B. Uzair, and B. Menaa, "Progress and prospects in translating nanobiotechnology in medical theranostics," *Current Nanoscience*, vol. 15, pp. 1–23, 2019.

[2] A. Sharma, S. Sharma, K. Sharma et al., "Algae as crucial organisms in advancing nanotechnology: a systematic review," *Journal of Applied Phycology*, vol. 28, no. 3, pp. 1759–1774, 2016.

[3] F. Menaa, "When pharma meets nano or the emerging era of nanopharmaceuticals," *Pharm. Anal. Acta.*, vol. 4, p. 223, 2013.

[4] B. Menaa, "The importance of nanotechnology in biomedical sciences," *J. Biotechnol. Biomater*, vol. 1, p. 105e, 2011.

[5] D. Nayak, A. P. Minz, S. Ashe et al., "Synergistic combination of antioxidants, silver nanoparticles and chitosan in a nanoparticle based formulation: characterization and cytotoxic effect on MCF-7 breast cancer cell lines," *Journal of Colloid and Interface Science*, vol. 470, pp. 142–152, 2016.

[6] P. Jakinala, N. Lingampally, B. H. Id, and R. Z. Sayyed, "Silver nanoparticles from insect wing extract: biosynthesis and evaluation for antioxidant and antimicrobial potential," *PLoS One*, vol. 16, no. 3, pp. 1–15, 2021.

[7] B. Uzair, A. Liaqat, H. Iqbal et al., "Green and cost-effective synthesis of metallic nanoparticles by algae: safe methods for translational medicine," *Bioengineering*, vol. 7, no. 4, 2020.

[8] C. R. Patra, R. Bhattacharya, D. Mukhopadhyay, and P. Mukherjee, "Fabrication of gold nanoparticles for targeted therapy in pancreatic cancer," *Advanced Drug Delivery Reviews*, vol. 62, no. 3, pp. 346–361, 2010.

[9] P. D. Shankar, S. Shobana, I. Karuppusamy et al., "A review on the biosynthesis of metallic nanoparticles (gold and silver)

using bio-components of microalgae: formation mechanism and applications," *Enzyme and Microbial Technology*, vol. 95, pp. 28–44, 2016.

[10] Y. Wang, X. Dong, L. Zhao et al., "Facile and green fabrication of carrageenan-silver nanoparticles for colorimetric determination of Cu 2 + and S2−," *Nanomaterials*, vol. 10, pp. 1–12, 2020.

[11] S. R. Vijayan, P. Santhiyagu, R. Ramasamy et al., "Seaweeds: a resource for marine bionanotechnology," *Enzyme and Microbial Technology*, vol. 95, pp. 45–57, 2016.

[12] S. Pugazhendhi, P. Sathya, P. K. Palanisamy, and R. Gopalakrishnan, "Synthesis of silver nanoparticles through green approach using _Dioscorea alata_ and their characterization on antibacterial activities and optical limiting behavior," *Journal of Photochemistry and Photobiology. B*, vol. 159, pp. 155–160, 2016.

[13] S. Pugazhendhi, E. Kirubha, P. K. Palanisamy, and R. Gopalakrishnan, "Synthesis and characterization of silver nanoparticles from _Alpinia calcarata_ by Green approach and its applications in bactericidal and nonlinear optics," *Applied Surface Science*, vol. 357, pp. 1801–1808, 2015.

[14] P. Singh, H. Singh, Y. J. Kim, R. Mathiyalagan, C. Wang, and D. C. Yang, "Extracellular synthesis of silver and gold nanoparticles by _Sporosarcina koreensis_ DC4 and their biological applications," *Enzyme and Microbial Technology*, vol. 86, pp. 75–83, 2016.

[15] S. Iravani, "Green synthesis of metal nanoparticles using plants," *Green Chemistry*, vol. 13, no. 10, pp. 2638–2650, 2011.

[16] C. Vanlalveni, S. Lallianrawna, A. Biswas, M. Selvaraj, B. Changmai, and S. L. Rokhum, "Green synthesis of silver nanoparticles using plant extracts and their antimicrobial activities: a review of recent literature," *RSC Advances*, vol. 11, no. 5, pp. 2804–2837, 2021.

[17] K. B. Narayanan and N. Sakthivel, "Biological synthesis of metal nanoparticles by microbes," *Adv Colloid Interface Sci*, vol. 156, no. 1-2, pp. 1–13, 2010.

[18] D. K. Tripathi, P. Ahmad, S. Sharma, D. K. Chauhan, and N. K. Dubey, *Nanomaterials in Plants, Algae, and Microorganisms: Concepts and Controversies*, Academic Press, Cambridge, MA, USA, 2017.

[19] D. Sharma, S. Kanchi, and K. Bisetty, "Biogenic synthesis of nanoparticles: a review," *Arabian Journal of Chemistry*, vol. 12, no. 8, pp. 3576–3600, 2019.

[20] H.-M. D. Wang, X.-C. Li, D.-J. Lee, and J.-S. Chang, "Potential biomedical applications of marine algae," *Bioresource Technology*, vol. 244, pp. 1407–1415, 2017.

[21] M. I. Khan, J. H. Shin, and J. Kim, "The promising future of microalgae: current status, challenges, and optimization of a sustainable and renewable industry for biofuels, feed, and other products," *Microbial Cell Factories*, vol. 17, no. 1, p. 36, 2018.

[22] E. M. Cabral, M. Oliveira, J. R. M. Mondala, J. Curtin, B. K. Tiwari, and M. Garcia-Vaquero, "Antimicrobials from seaweeds for food applications," *Marine Drugs*, vol. 19, no. 4, p. 211, 2021.

[23] N. Asmathunisha and K. Kathiresan, "A review on biosynthesis of nanoparticles by marine organisms," *Colloids Surfaces B Biointerfaces.*, vol. 103, pp. 283–287, 2013.

[24] S. R. Vijayan, P. Santhiyagu, M. Singamuthu, N. Kumari Ahila, R. Jayaraman, and K. Ethiraj, "Synthesis and characterization of silver and gold nanoparticles using aqueous extract of seaweed, Turbinaria conoides, and their antimicrofouling activity," *Sci. World J*, vol. 2014, article ???, pp. 1–10, 2014.

[25] E. Sokoła-Wysoczańska, T. Wysoczański, J. Wagner et al., "Polyunsaturated fatty acids and their potential therapeutic role in cardiovascular system disorders—a review," *Nutrients*, vol. 10, no. 10, pp. 1–21, 2018.

[26] T. Rosemary, A. Arulkumar, S. Paramasivam, A. Mondragon-Portocarrero, and J. M. Miranda, "Biochemical, micronutrient and physicochemical properties of the dried red seaweeds < i>Gracilaria edulis and Gracilaria corticata," *Molecules*, vol. 24, no. 12, pp. 1–14, 2019.

[27] J. Ashraf, M. Ansari, H. Khan, M. Alzohairy, and I. Choi, "Green synthesis of silver nanoparticles and characterization of their inhibitory effects on AGEs formation using biophysical techniques," *Scientific Reports*, vol. 6, no. 1, p. 20414, 2016.

[28] Y. K. Mohanta, D. Nayak, K. Biswas et al., "Silver nanoparticles synthesized using wild mushroom show potential antimicrobial activities against food borne pathogens," *Molecules*, vol. 23, pp. 1–18, 2018.

[29] Y. K. Mohanta, S. K. Panda, R. Jayabalan, N. Sharma, A. K. Bastia, and T. K. Mohanta, "Antimicrobial, antioxidant and cytotoxic activity of silver nanoparticles synthesized by leaf extract of Erythrina suberosa (Roxb)," *Frontiers in Molecular Biosciences*, vol. 4, pp. 1–9, 2017.

[30] S. Mukherjee, D. Chowdhury, R. Kotcherlakota, S. Patra, and B. Vinothkumar, "Potential theranostics application of biosynthesized silver nanoparticles (4-in-1 system)," *Theranostics*, vol. 4, no. 3, pp. 316–335, 2014.

[31] P. Tan, H. Li, J. Wang, and S. C. B. Gopinath, "Silver nanoparticle in biosensor and bioimaging : clinical perspectives," *Biotechnology and Applied Biochemistry*, vol. 68, no. 6, pp. 1236–1242, 2021.

[32] K. V. Alex, P. T. Pavai, R. Rugmini, M. S. Prasad, K. Kamakshi, and K. C. Sekhar, "Green synthesized ag nanoparticles for biosensing and photocatalytic applications," *ACS Omega*, vol. 5, no. 22, pp. 13123–13129, 2020.

[33] S. H. Lee and B. Jun, "Silver nanoparticles : synthesis and application for nanomedicine," *International Journal of Molecular Sciences*, vol. 20, no. 4, pp. 1–24, 2019.

[34] S. P. Vinay, N. Chandrasekhar, and C. P. Chandrappa, "Eco-friendly approach for the green synthesis of silver nanoparticles using flower extracts of Sphagneticola trilobata and study of antibacterial activity," *Int. J. Pharm. Biol. Sci.*, vol. 7, pp. 145–152, 2017.

[35] P. Devaraj, P. Kumari, C. Aarti, and A. Renganathan, "Synthesis and characterization of silver nanoparticles using cannonball leaves and their cytotoxic activity against MCF-7 cell line," *J. Nanotechnol.*, vol. 2013, pp. 1–5, 2013.

[36] A. Jesus, M. Correia-da-Silva, C. Afonso, M. Pinto, and H. Cidade, "Isolation and potential biological applications of haloaryl secondary metabolites from macroalgae," *Marine Drugs*, vol. 17, no. 2, pp. 1–19, 2019.

[37] M. T. Cabrita, C. Vale, and A. P. Rauter, "Halogenated compounds from marine algae," *Marine Drugs*, vol. 8, no. 8, pp. 2301–2317, 2010.

[38] G. Das, J. K. Patra, T. Debnath, A. Ansari, and H. S. Shin, "Investigation of antioxidant, antibacterial, antidiabetic, and cytotoxicity potential of silver nanoparticles synthesized using the outer peel extract of Ananas comosus (L.)," *PLoS One*, vol. 14, pp. 1–19, 2019.

[39] D. H. Nguyen, T. N. N. Vo, N. T. Nguyen, Y. C. Ching, and T. T. H. Thi, "Comparison of biogenic silver nanoparticles formed by Momordica charantia and Psidium guajava leaf extract and antifungal evaluation," *PLoS One*, vol. 15, no. 9, p. e0239360, 2020.

[40] K. D. Arunachalam, S. Suhashani, and K. A. Sathesh, "Wound healing and Antigenotoxic activities of Aegle marmelos with relation to its antioxidant properties," *Journal of Pharmacy Research*, vol. 5, pp. 1492–1502, 2012.

[41] C. Dipankar and S. Murugan, "The green synthesis, characterization and evaluation of the biological activities of silver nanoparticles synthesized from _Iresine herbstii_ leaf aqueous extracts," *Colloids Surfaces B Biointerfaces.*, vol. 98, pp. 112–119, 2012.

[42] M. Yousefzadi, Z. Rahimi, and V. Ghafori, "The green synthesis, characterization and antimicrobial activities of silver nanoparticles synthesized from green alga Enteromorpha flexuosa (wulfen)," *J. Agardh, Mater. Lett*, vol. 137, pp. 1–4, 2014.

[43] K. Biswas, Y. K. Mohanta, V. B. Kumar et al., "Nutritional assessment study and role of green silver nanoparticles in shelf- life of coconut endosperm to develop as functional food," *Saudi J. Biol. Sci*, vol. 27, no. 5, pp. 1280–1288, 2020.

[44] Y. Mohanta, K. Biswas, S. Jena, A. Hashem, E. A. Allah, and T. Mohanta, "Anti-biofilm and antibacterial activities of silver nanoparticles synthesized by the reducing activity of phytoconstituents present in the Indian medicinal plants," *Frontiers in Microbiology*, vol. 11, pp. 1–15, 2020.

[45] V. Sri, A. Pugazhendhi, and K. Gopalakrishnan, "Biofabrication and characterization of silver nanoparticles using aqueous extract of seaweed _Enteromorpha compressa_ and its biomedical properties," *Biotechnol. Reports*, vol. 14, pp. 1–7, 2017.

[46] P. Khanna, A. Kaur, and D. Goyal, "Algae-based metallic nanoparticles: Synthesis, characterization and applications," *Journal of Microbiological Methods*, vol. 163, p. 105656, 2019.

[47] R. I. Priyadharshini, G. Prasannaraj, N. Geetha, and P. Venkatachalam, "Microwave-mediated extracellular synthesis of metallic silver and zinc oxide nanoparticles using macro-algae (Gracilaria edulis) extracts and its anticancer activity against human PC3 cell lines," *Applied Biochemistry and Biotechnology*, vol. 174, no. 8, pp. 2777–2790, 2014.

[48] J. Huang, Q. Li, D. Sun et al., "Biosynthesis of silver and gold nanoparticles by novel sundried Cinnamomum camphora leaf," *Nanotechnology*, vol. 18, no. 10, p. 105104, 2007.

[49] E. O. Mikhailova, "Silver nanoparticles: mechanism of action and probable bio-application," *J. Funct. Biomater.*, vol. 11, no. 4, p. 84, 2020.

[50] I. Sondi and B. Salopek-Sondi, "Silver nanoparticles as antimicrobial agent: a case study on E. coli as a model for Gram-negative bacteria," *J Colloid Interface Sci*, vol. 275, 2004.

[51] M. S. Jabir, A. A. Hussien, G. M. Sulaiman et al., "Green synthesis of silver nanoparticles from Eriobotrya japonica extract: a promising approach against cancer cells proliferation, inflammation, allergic disorders and phagocytosis induction," *Artif. Cells, Nanomedicine Biotechnol*, vol. 49, pp. 48–60, 2021.

[52] M. Guzman, J. Dille, and S. Godet, "Synthesis and antibacterial activity of silver nanoparticles against gram- positive and gram-negative bacteria," *Nanomedicine: Nanotechnology, Biology and Medicine*, vol. 8, no. 1, pp. 37–45, 2012.

[53] J. K. Patra and K.-H. Baek, "Antibacterial activity and synergistic antibacterial potential of biosynthesized silver nanoparticles against foodborne pathogenic bacteria along with its anticandidal and antioxidant effects," *Frontiers in Microbiology*, vol. 8, pp. 1–14, 2017.

[54] Y. Mohanta, S. Panda, K. Biswas et al., "Biogenic synthesis of silver nanoparticles from Cassia fistula (Linn.): In vitro assessment of their antioxidant, antimicrobial and cytotoxic activities," *IET Nanobiotechnology.*, vol. 10, no. 6, pp. 438–444, 2016.

[55] R. A. Ismail, G. M. Sulaiman, M. H. Mohsin, and A. H. Saadoon, "Preparation of silver iodide nanoparticles using laser ablation in liquid for antibacterial applications," *IET Nanobiotechnology.*, vol. 12, no. 6, pp. 781–786, 2018.

[56] B. Singh, C. Prateeksha, A. Rao, D. Rawat, and B. Upreti, "Agricultural nanotechnologies: what are the current possibilities?," *Current Science*, vol. 10, no. 2, pp. 124–127, 2015.

[57] P. Ramesh, T. Kokila, and D. Geetha, "Plant mediated green synthesis and antibacterial activity of silver nanoparticles using _Emblica officinalis_ fruit extract," *Spectrochimica Acta. Part A, Molecular and Biomolecular Spectroscopy*, vol. 142, pp. 339–343, 2015.

[58] Y. Dong, H. Zhu, Y. Shen, W. Zhang, and L. Zhang, "Antibacterial activity of silver nanoparticles of different particle size against Vibrio natriegens," *PLoS One*, vol. 14, no. 9, pp. 1–12, 2019.

[59] M. Wypij, T. Jedrzejewski, J. Trzcin'ska-Wencel, M. Ostrowski, M. Rai, and P. Golinska, "Green synthesized silver nanoparticles : antibacterial and anticancer activities , biocompatibility, and analyses of surface-attached proteins," *Front. Microbiol*, vol. 12, pp. 1–17, 2021.

[60] C. Ramamurthy, M. Padma, I. M. Samadanam et al., "The extra cellular synthesis of gold and silver nanoparticles and their free radical scavenging and antibacterial properties," *Colloids and Surfaces. B, Biointerfaces*, vol. 102, pp. 808–815, 2013.

[61] H. Kumar, K. Bhardwaj, E. Nepovimova et al., "Antioxidant functionalized nanoparticles: a combat against oxidative stress," *Nanomaterials*, vol. 10, no. 7, pp. 1–31, 2020.

[62] A. Phaniendra, D. B. Jestadi, and L. Periyasamy, "Free radicals: properties, sources, targets, and their implication in various diseases," *Indian Journal of Clinical Biochemistry*, vol. 30, no. 1, pp. 11–26, 2015.

[63] A. Arulkumar, T. Rosemary, S. Paramasivam, and R. Rajendran, "Phytochemical composition, _in vitro_ antioxidant, antibacterial potential and GC-MS analysis of red seaweeds (_Gracilaria corticata_ and _Gracilaria edulis_) from Palk Bay, India," *Biocatalysis and Agricultural Biotechnology*, vol. 15, pp. 63–71, 2018.

[64] M. Składanowski, P. Golinska, K. Rudnicka, H. Dahm, and M. Rai, "Evaluation of cytotoxicity, immune compatibility and antibacterial activity of biogenic silver nanoparticles," *Medical Microbiology and Immunology*, vol. 205, no. 6, pp. 603–613, 2016.

[65] M. Adabi, M. Naghibzadeh, M. Adabi et al., "Biocompatibility and nanostructured materials: applications in nanomedicine," *Artif. Cells, Nanomedicine Biotechnol*, vol. 45, pp. 833–842, 2017.

[66] P. Mathur, S. Jha, S. Ramteke, and N. K. Jain, "Pharmaceutical aspects of silver nanoparticles," *Artif. Cells, Nanomedicine Biotechnol*, vol. 46, pp. 115–126, 2018.

[67] Y. K. Mohanta, S. K. Panda, A. K. Bastia, and T. K. Mohanta, "Biosynthesis of silver nanoparticles from Protium serratum and investigation of their potential impacts on food safety and control," vol. 8, pp. 1–10, 2017.

[68] M. Akter, M. T. Sikder, M. M. Rahman et al., "A systematic review on silver nanoparticles-induced cytotoxicity: physicochemical properties and perspectives," *Journal of Advanced Research*, vol. 9, pp. 1–16, 2018.

[69] R. Foldbjerg, P. Olesen, M. Hougaard, D. Dang, H. Hoffmann, and H. Autrup, "PVP-coated silver nanoparticles and silver ions induce reactive oxygen species, apoptosis and necrosis in THP-1 monocytes," *Toxicology Letters*, vol. 190, no. 2, pp. 156–162, 2009.

[70] Y. Li, M. Guo, Z. Lin, T. Chen, and B. Zhu, "Polyethylenimine-functionalized silver nanoparticle-based co-delivery of paclitaxel to induce HepG2 cell apoptosis," *International Journal of Nanomedicine*, vol. Volume 11, pp. 6693–6702, 2016.

[71] M. S. Jabir, Y. M. Saleh, G. M. Sulaiman et al., "Green synthesis of silver nanoparticles using Annona muricata extract as an inducer of apoptosis in cancer cells and inhibitor for NLRP3 inflammasome via enhanced autophagy," *Nanomaterials*, vol. 11, no. 2, pp. 1–22, 2021.

[72] M. Jing, K. Ah, I. Kyung et al., "Silver nanoparticles induce oxidative cell damage in human liver cells through inhibition of reduced glutathione and induction of mitochondria-involved apoptosis," *Toxicology Letters*, vol. 201, no. 1, pp. 92–100, 2011.

[73] P. K. S. Senthamil and S. M. Govindaraju, "Seaweed-mediated biosynthesis of silver nanoparticles using Gracilaria corticata for its antifungal activity against Candida spp," *Applied Nanoscience*, vol. 3, no. 6, pp. 495–500, 2013.

[74] D. Marinova, F. Ribarova, and M. Atanasova, "Total phenolics and flavonoids in Bulgarian fruits and vegetables," *J. Univ. Chem. Technol. Metall.*, vol. 40, pp. 255–260, 2005.

[75] S. K. Panda, Y. K. Mohanta, L. Padhi, and W. Luyten, "Antimicrobial activity of select edible plants from Odisha, India against food-borne pathogens," *LWT*, vol. 113, p. 108246, 2019.

[76] P. Tanamatayarat, "Antityrosinase, antioxidative activities, and brine shrimp lethality of ethanolic extracts from _Protium serratum_ (Wall. ex Colebr.) Engl.," *Asian Pacific Journal of Tropical Biomedicine*, vol. 6, no. 12, pp. 1050–1055, 2016.

[77] P. Vijayabaskar and V. Shiyamala, "Antioxidant properties of seaweed polyphenol from _Turbinaria ornata_ (Turner) J. Agardh, 1848," *Asian Pac J Trop Biomed*, vol. 2, no. 1, pp. S90–S98, 2012.

Hindawi
Oxidative Medicine and Cellular Longevity
Volume 2022, Article ID 3313016, 37 pages
https://doi.org/10.1155/2022/3313016

Review Article

Effects of Metal Oxide Nanoparticles in Zebrafish

Marta d'Amora,[1,2] **Tiziana Julia Nadjeschda Schmidt**,[2] **Soultana Konstantinidou**,[2] **Vittoria Raffa**,[2] **Francesco De Angelis**,[1] **and Francesco Tantussi**[1]

[1]*Istituto Italiano di Tecnologia, Via Morego 30, 16163 Genova, Italy*
[2]*Department of Biology, University of Pisa, S.S. 12 Abetone e Brennero 4, 56127 Pisa, Italy*

Correspondence should be addressed to Marta d'Amora; marta.damora@iit.it

Received 17 December 2021; Accepted 18 January 2022; Published 4 February 2022

Academic Editor: Dragica Selakovic

Metal oxide nanoparticles (MO NPs) are increasingly employed in many fields with a wide range of applications from industries to drug delivery. Due to their semiconducting properties, metal oxide nanoparticles are commonly used in the manufacturing of several commercial products available in the market, including cosmetics, food additives, textile, paint, and antibacterial ointments. The use of metallic oxide nanoparticles for medical and cosmetic purposes leads to unavoidable human exposure, requiring a proper knowledge of their potentially harmful effects. This review offers a comprehensive overview of the possible toxicity of metallic oxide nanoparticles in zebrafish during both adulthood and growth stages, with an emphasis on the role of oxidative stress.

1. Introduction

The field of engineered nanomaterials has gained increasing attention over the last years in human health science, optoelectronics, agriculture, food science, and in everyday use products [1]. Metal oxide nanoparticles (MO NPs) have shown fascinating physical and chemical properties, such as good sensitivity, catalytic and selective activity, unusual adsorptive behavior, and superparamagnetic state (Table 1) [2, 3]. Different studies focused on easy and efficient synthesis methods, a few of which implementing "green chemistry approaches," providing thus a variety of different strategies to efficiently achieve the desired size, shape, structure, morphology, stabilization, and nonagglomeration. One of the most important advantages of MO NPs is the ease of their surface modification allowing for the functionalization of numerous molecules to improve their stability and biocompatibility [4]. Hence, MO NPs serve as a promising tool for biomedical applications. Metal oxide nanoparticles are known for their antimicrobial properties [5, 6] and cytotoxic effects [2]. The synthesis method of the nanoparticles plays a critical role in determining their properties, i.e., their biological and optical characteristics. For instance, it seems that the smaller the nanoparticles are, the higher is the antibacterial activity they exert [2, 7]. Moreover, due to their metallic core, MO NPs can be used as plasmon resonance agents, in cancer therapeutics and theranostics (Table 1) [3, 8].

Different classes of MO NPs are exploited in commercially available daily life products and biomedical applications (Table 1). The most commonly applied ones correspond to three types of MO NPs, the titanium dioxide (TiO_2), iron oxide (IO), and zinc oxide (ZnO) nanoparticles. The TiO_2 and ZnO nanoparticles are extensively used in sunscreens due to their ability to attenuate UV radiation and as antimicrobial reagents given their antibacterial properties. On the other hand, IO NPs are employed in several medical applications, such as hyperthermia-based anticancer therapy and iron-deficient anemia treatment, as well as in magnetic resonance imaging (MRI).

The rising demand and use of nanotechnologies inevitably questions their impact on the environment. In this framework, TiO_2, IO NPs, and ZnO nanoparticles could be released i.e., via bathing and cause any toxic effects in the aquatic habitats [9]. Since metal oxide nanoparticles are exposed to humans and are extensively used in daily life and industrial content, their ecotoxicological profile should

Table 1: Properties and applications of the most used metal oxide nanoparticles.

Metal oxide nanoparticles	Physical, chemical properties	Potential applications in medicine (tested *in vitro*/*in vivo*)	Biomedical and life science applications (in use and commercial products)	References
Aluminium oxide (Al_2O_3)	Catalyst, high thermal and mechanical stability, high corrosion resistance, and high melting point.	Drug delivery.	—	[18]
Copper oxide (CuO)	Catalyst, high-temperature superconductors.	Anticancer treatment.	Antimicrobial coating agents.	[2, 11]
Iron oxide (α-Fe_2O_3, γ-Fe_2O_3, and Fe_3O_4)	Superparamagnetic and magnetic hyperthermia properties, catalyst.	Antibacterial agent, drug delivery, anticancer treatment (photothermal therapy, chemotherapy, and magnetic hyperthermia therapy), and theragnostic (near-infrared imaging, positron emission tomography, single-photon emission computed tomography, and ultrasound imaging).	Iron-deficient anemia treatment (Venofer®, Feraheme®, and Rienso®). Solid tumor treatment (NanoTherm®). Magnetic resonance imaging (in liver: Feridex I.V.®, Endorem®, and Resovist®; in gastrointestinal: Gastromark™ and Lumirem®; and in blood pooling: Supravist®).	[2, 19]
Magnesium oxide (MgO)	High ionic character, catalyst, and semiconductor.	Antibacterial agent, anticancer treatment (hyperthermia therapy), and tissue engineering.	Antimicrobial agents (in food industry).	[2, 18]
Nickel oxide (NiO)	Catalyst, magnetic properties, and high electrochemical stability.	Anticancer treatment (cytotoxic properties).	—	[11]
Silica dioxide (SiO_2)	Low density.	Antibacterial agent, drug and gene delivery, anticancer treatment, and biosensor.	Additive in drugs, cosmetics.	[2, 11, 13, 20]
Titanium oxide (TiO_2)	Semiconductor, photocatalyst, and high chemical stability.	Anticancer treatment (photodynamic, photothermal, sonodynamic therapy, chemodynamic therapy, and radiotherapy), theragnostic (bioimaging), drug delivery, and tissue engineering.	UV-A, UV-B radiation filter (in sunscreens, cosmetics). Antimicrobial agents (in food packaging, biomedical devices, and dentistry & orthopedic implants).	[2, 8, 11, 19, 20]
Zinc oxide (ZnO)	Semiconductor, photocatalyst, high chemical stability, large exciton binding energy, and high isoelectric point.	Anticancer treatment (photodynamic, photothermal, and sonodynamic therapy), theragnostic (bioimaging), drug delivery, and tissue engineering.	UV-A, UV-B radiation filter (in sunscreens, cosmetics). Antimicrobial agents (in toothpaste, dentistry implants, food packaging, and as food additive).	[2, 4, 9, 11]

be evaluated [1]. Metal oxide nanoparticles present some toxic defects as they [10] internalize in the cells and interact with the DNA, proteins, and organelles. Here, they can induce the formation of reactive oxidative species (ROS) and interfere with the antioxidant mechanisms. The excessive production of ROS, and accumulation in cells and tissues, leads to oxidative stress and subsequently to lipid peroxidation, DNA damage, inflammation, and cell death [11]. Undoubtedly, this along with the penetration abilities of the nanoparticles enhances their toxic effects in the cells [2]. The ROS usually include singlet oxygen ($^1O_2$), hydroxyl radical ($\cdot OH$), and superoxide radical ($O_2\cdot^-$) [12]. The excess of ROS can be detected by missregulation of antioxidant enzymes, either of their genes or of their activity. In this context, the expression and activity of superoxide dismutase (SOD), catalase (CAT), glutathione peroxidase (GP), and glutathione S-transferase (GST) are most commonly evaluated. SOD catalyses the disproportionation of superoxide anions (O_2^-) into oxygen (O_2) and hydrogen peroxide (H_2O_2), and CAT and GP reduce the hydrogen peroxide levels. GST instead plays a role in detoxification by removing glutathione. Their normal regulation is critical for the survival of the cells. On the other hand, to prevent the imbalance between production and catalysis of ROS, various cytoprotective genes might be influenced. Nuclear factor erythroid 2-related factor 2 (Nrf2) is a transcription factor with such a protective antioxidative role, targeting numerous redox cycling enzymes, including the ones named before

[13]. Upon transcription of Nfr2 target genes, the ROS level is normalized, leading to detoxification and the reestablishment of homeostasis.

One of the main factors believed to be responsible of the MO NP-induced toxicity is the release of their appropriate metal ions and the ions' inherent toxic effects in the cells [11].

Hence, there is a not only a great need to fully understand the mechanisms underlying nanotoxicity but also to develop innovative strategies allowing to mitigate this effect in order to fully exploit their potential [9] for our purposes. Most of the toxicological profiles of metal oxide nanoparticles have been studied *in vitro*, in suspensions of MO NPs, in several cell types, and *in vivo* in different invertebrates and vertebrate animal models. Zebrafish (*Danio rerio*) represent a link between the *in vitro* cell culture studies and *in vivo* animal models. The zebrafish embryo toxicity test (ZET) known also as the early life stage test (ELS) is widely accepted as a valid model system for the evaluation of ecotoxicological effects and as a preclinical *in vivo* model [14, 15]. Zebrafish emerged as a model for *in vivo* toxicity screening of nanoparticles due to several characteristics [16]. First of all, zebrafish and humans are highly genetically conserved. Additionally, zebrafish grow rapidly and are transparent during early life stages, two very important characteristics that allow studying easily the development. A variety of developmental endpoints have been already described to evaluate toxicity during the embryonic stages, including the hatching timing, pericardial and yolk sac edema, spinal curvatures, tail malformations, swim bladder abnormalities, and mortality rates [4, 17, 18]. These phenotypes, together with other characteristic ones, are visible and detectable up to the first five days after fertilization of the embryos, allowing thus zebrafish serve for fast screenings. Due to the small size of these fish, and the high number of embryos that they produce, different parameters can be tested simultaneously. The standardization of tests using zebrafish to assess adverse effects induced by nanomaterials allows gathering reproducible and reliable results. Doing so would allow counteracting contradictory results obtained in the past, implementing other model systems while introducing a controllable amount of bias in the experimental setups. For instance, as it is evident in this review, it is critical to test not only the metal oxide nanoparticles but also the appropriate metal ions they release. This is necessary to estimate the direct contribution of the dissolved ions in the establishment of toxicity and to identify the potentially involved mechanisms [9].

In this framework, we focus on the toxicity studies performed on zebrafish embryos and adult zebrafish, stating the effects of three different types of metal oxide nanoparticles: titanium dioxide (TiO_2), iron oxide (IO), and zinc oxide (ZnO) nanoparticles. Different studies using either one type or a combination of these analyzed the toxicokinetic behavior of the particles on the development of zebrafish and/or adult zebrafish. This review will provide thus an extended overview of the impact of metal oxide nanoparticle exposure on zebrafish while conferring a better understanding of the potentially underlying toxicity mechanisms, such as the induction of oxidative stress and apoptosis in *Danio rerio (*Figure 1).

2. Titanium Dioxide Nanoparticles

Titanium dioxide nanoparticles are one of the most commonly employed manufactured nanoparticles in a wide range of applications, including building materials [21], medical treatments [22], and personal care and food products [23]. Titanium oxide and zinc oxide are considered as "GRAS" (generally recognized as safe) by the US Food and Drug Administration (FDA) and by the International Agency for Research on Cancer [24]. TiO_2 is highly stable, biocompatible, and a semiconductor material. This increasing interest and use of TiO_2 in our daily life and several applications are due to their fascinating properties, such as good optical performance, electrical characteristics, durability, and corrosion resistance [25] [26–28]. In addition, since TiO_2 NPs are excellent photocatalysts, they can produce peroxide under ultraviolet (UV) illumination. Indeed, they are extensively used in photocatalytic applications [24]. TiO_2 NPs are nontoxic, and due to their optical and UV absorption properties, they are used in sunscreens, though there are more restrictions in the EU than in the United States (EUR-Lex -32020R0217 - EN - EUR-Lex). One of the main biomedical applications of metal oxide nanoparticles is their use as drug carriers [24]. For instance, TiO_2 NPs were functionalized with daunorubicin (DNR), an anticancer drug, for controllable release of the drug by lowering the pH from 7.4 to 5. In this way, the side effects of DNR could be reduced, and the cytotoxicity of cancer cells augmented due to the improved penetration of the drug in the cell [29]. Another example showing the anticancer activities of TiO_2 NPs comes from the work of Masoudi et al. who prepared TiO_2 NPs with doxorubicin hydrochloride (DOX) to induce cytotoxicity [30]. In addition, as other MO NPs, TiO_2 NPs are used in tissue engineering and in antibacterial applications [31]. TiO_2 are also used as biosensors, such as in nanowires, to recognize bacteria *Listeria monocytogenes i*n food with high specificity [32]. Metal oxide nanoparticles can induce the production of reactive oxidative stress, an important characteristic employed for cancer cytotoxicity. Considering all the above-mentioned applications in medicine, it was critical to validate that the produced reactive oxygen species levels are nontoxic [33]. Anyway, the wide use of TiO_2 NPs led to their inevitable release in the aquatic environments, arising harmful threats for ecosystems and living organisms. For this reason, the adverse effects of TiO_2 NPs need to be considered and evaluated. In the past years, different toxicity studies have elucidated the in vitro and in vivo behavior of TiO_2 NPs and their biointeractions with several cell lines and animal models. In particular, several works have assessed the potential harmful effects of TiO_2 NPs both in embryos and in adults (Table 2).

2.1. Effects of TiO_2 NPs during the Development. The first research studies of titanium dioxide biointeraction with zebrafish have reported their nontoxicity [34–36]. Zhu et al. have assessed the impact of titanium dioxide nanoparticles

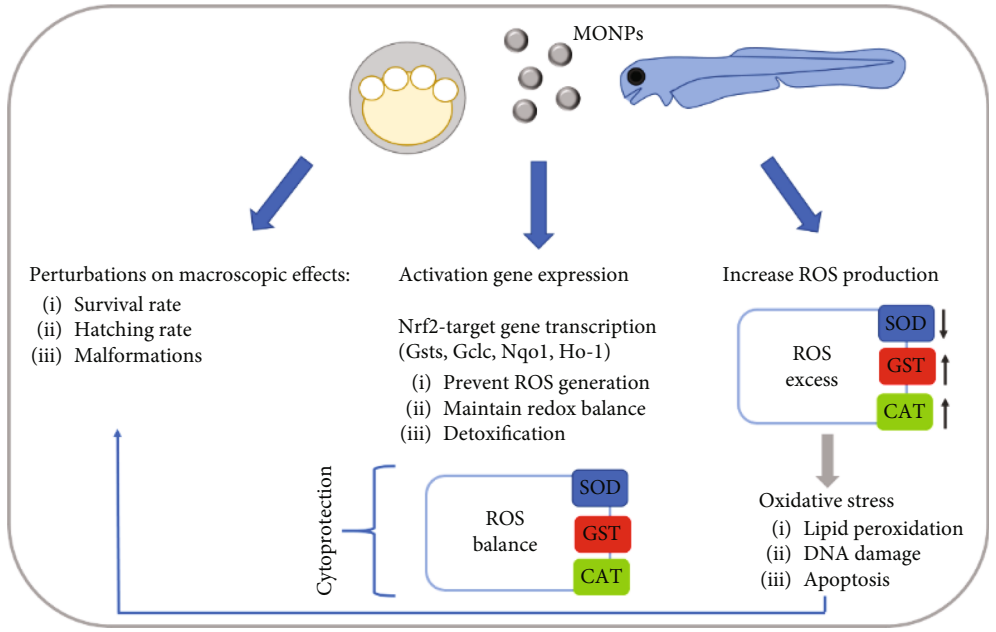

Figure 1: Overview of the MO NP effects of in zebrafish, with an emphasis on oxidative stress.

on zebrafish growth, reporting that the treatment of embryos with high doses (up to 500 mg/L) of TiO_2 NPs did not lead to a significant decrease of the survival rate or delay in the hatching rate or presence of morphological abnormalities [34, 37]. However, larvae treated with low doses of nanoparticles presented behavioral alterations at 120 hours post fertilization (hpf). At doses of 0.1, 0.5, and 1 mg/L TiO_2 NPs, larvae had a significantly lower velocity and higher activity level compared to the samples of control, while higher concentrations of 5 and 10 mg/L did not show any changes. These perturbations can be attributed to physiological injuries or neurotoxicity induced by TiO_2 NP treatment [37]. Moreover, this type of nonlinear concentration-reaction relationship was already previously shown [38, 39]. This nonmonotonic behavior could be related to superimposition of linear concentration interaction of constituent biological counterbalances. Previous works in different aquatic species have shown that rainbow trout [40] and carp [41] treated with TiO_2 NPs had gill injuries, including fusion and hyperplasia in filaments and lamellae and edema. These damages can implicate a reduction of oxygen assumption ability and alter the activity. On the other hand, both treated fish species presented oxidative stress in the brain [40, 41] that could cause neurotoxic effects [42]. To evaluate the potential implication of oxidative stress in the perturbations noted in TiO_2 NP-exposed zebrafish, the embryos were cotreated with an antioxidant compound, NAC, and/or an antioxidant suppressor, the inhibitor of GSH synthesis, the buthionine sulfoximine (BSO) [37]. The used doses of BSO and NAC were 5 and 50 μM, respectively, while the selected concentration of TiO_2 was one of those implicated in behavioral changes (1 mg/L). The cotreatment did not lead to perturbations on the hatching or survival rate or malformations. Moreover, NAC or BSO did not modify the behavioral perturbations induced by titanium dioxide nanoparticles. This observation indicated that, as well as oxidative stress, other processes can be implicated. The mentioned research studies indicated the nontoxicity of the tested TiO_2 NPs. Nevertheless, the potential of titanium dioxide nanoparticles to generate reactive oxygen species under illumination indicates that they can induce adverse effects in a photo-dependent manner. Moreover, the consequent oxidative stress can lead to lipids, proteins, or DNA injuries and ultimately to cell death [43, 44]. To verify this assumption, Bar-Ilan et al. treated the zebrafish embryos with different doses of TiO_2 NPs under a metal halide light [45]. First, a solution of TiO_2 NPs illuminated under this source generates an important amount of ROS. The survival rate of treated and illuminated zebrafish with TiO_2 NPs showed a lethal dose of 300 μg/mL, while the embryos that were exposed to nanoparticles but not illuminated had a value superior to 1000 μg/mL. By increasing the exposure time to 8 days, all the illuminated larvae died at a dose of 100 μg/mL. The combined exposure of light and nanoparticles led also to different malformations, affecting prevalently the head, tail, yolk, and heart [45]. Moreover, the ROS generation led by TiO_2 NPs in the treated embryos and larvae was demonstrated by using the dihydroethidium (DHE), an *in vivo* fluorescent superoxide indicator. Samples treated with TiO_2 NPs and illuminated presented fluorescence, reporting the presence of ROS. Moreover, the use of a transgenic zebrafish, Tg (are: eGFP), enables the observation of the oxidative stress response directly in the zebrafish. In particular, a dose of TiO_2 NPs $\leq$ 1000 μg/mL under illumination generates DNA damage. The same authors treated the zebrafish embryos with different concentrations (0.01 to 10 000 ng/mL) of two different batches of titanium dioxide nanoparticles for a longer temporal window (over 23 days post fertilization, dpf) to detect subsequent and increasing effects due to ROS generation, such as damages to macromolecules [46]. A significant

Table 2: Impact of TiO_2 NPs on zebrafish.

Stage	NPs diameter	Treatment duration	Tested concentrations	General toxicity response	Specific ROS responses	Reference
Embryos	30 nm	48 h	Up to 10 mg/L	No toxic effects.	—	[35]
Embryos	≤20 nm	96 h	1, 10, 50, 100, and 500 mg/L	No significant differences in survival, hatching, and malformation rates.	—	[34]
Embryos	27.7 nm	120 hpf	0.1, 0.5, 1, 5, and 10 mg/L	No significant differences in survival and hatching rates; reduction in average swimming speed at 120 hpf at low concentration; and no changes after the coexposure with NAC or BSO.	—	[37]
Embryos	86 and 409 nm	96 hpf	170 ng/mL +40 μg/mL hydroxylated fullerenes/ C60(OH) 24)	—	Downregulation of genes associated with circadian rhythm, transport and vesicular trafficking, and immune response.	[48]
Embryos	23.3 nm	120 hpf	1, 10, 100, 500, and 1000 μg/mL	LC50 = 300 μg/mL with no light; LC50<1000 μg/mL with light; at 8 days all illuminated larvae died at 100 μg/mL; and different malformations (head, tail, yolk, and heart).	ROS generation in presence of light; oxidative stress response in transgenic line; and DNA damage with TiO_2 NPs ≤1000 μg/mL under illumination.	[45]
Embryos	5, 10, and 21 nm	Over 23 days	0.01-10 000 ng/ mL	Significant mortality rate (speed up with light); reduction in size, deformations of craniofacial structures and absence or abnormal organization in the pigmentation; and swim bladder with a single lobe.	Significant oxidative stress and intracellular damages.	[46]
Embryos	4, 10, 30, 50, and 134 nm	48 h	50, 500, 5000, 25000, and 50000 μg/L	No effects on zebrafish with 4 and 30 nm NPs; low impact on the mortality rate at 5000 and 250000 μg/L with 10 nm and 134 nm NPs.	No necrotic cells or a low amount of them for all the different size and doses tested; normal expression of Mt2.	[59]
Embryos	21 nm	72 hpf	1 mg/L	No effects on mortality rate; no significant incidence of malformations; expression of *atho7* in the retina similar to controls; all the components of the retina well differentiated; and no effects on the neurogenesis.	—	[51]
Embryos	7.04 nm	7 dpf	0.1 mg/L+BDE (0.08 and 0.38 mg/L)	Similar survival and hatching rates of the sample treated with BDE or BDE plus NPs; important increase in T4 values in cotreated samples; no difference in T3; important upregulation in the expression of the *tg*, *tshβ*, and *dio2* genes; downregulations of *α1-tubulin* and *mbd* genes; perturbations in the expression of the *mbd* protein; and reduction in the swimming speed.	—	[50]

Table 2: Continued.

Stage	NPs diameter	Treatment duration	Tested concentrations	General toxicity response	Specific ROS responses	Reference
Embryos	≤25 nm	96 hpf	10 and 50 mg/L +5 and 10 mg/L of BPA	TiO_2 NPs: normal survival rate; no important malformations; and decreased hatching rate at the highest dose tested TiO_2 NPs+BPA: significant decrease dose-dependent of survival rate, different abnormalities (spine deformation, weak pigmentation, and pericardial edema).	—	[52]
Embryos	NM-103/104: 20 nm; P25: 21 nm; and micro-TiO_2: 200 nm	8 dpf	0.01, 0.1, and 1 mg/mL	No effects on survival, hatching, or deformities rates; decrease in the length of larvae at one dose of microsized TiO_2.	Decrease in SOD activity; perturbation in GSH levels; and highest levels of ROS in embryos treated with P25 NPs.	[54]
Embryos	25 nm	6 dpf	0.1 mg/L+PCP (3, 10, and 30 μg/L)	Similar survival and hatching rates in samples treated with PCP and PCP plus nanoparticles; incidence of malformations higher in coexposed larvae.	Alterations in GSH content, SOD activity and MDA in sample treated with only NPs; decrease in the SOD activity and GSH content and important levels of MDA and ROS in cotreated samples; and an important upregulation *sod1* and *nrf2* in cotreated samples.	[49]
Embryos	6, 12, and 15 nm	120 hpf	0–1000 μg/mL	LC50 6 nm: 23 μg/mL; LC50 for 12 nm: 610 μg/mL LC50 for 15 nm: not detectable; several phenotypic abnormalities (opaque yolk, axial curvatures, craniofacial defects, yolk sac, and pericardial edema).	High levels of hydroxyl radical ($^{\cdot}OH$) and ROS; higher values for 6 nm NPs in comparison to 12 and 15 nm NPs.	[47]
Embryos	Anatase, TA <25 nm; anatase/rutile mixture, TM, form, 25 nm	96 h	1, 10, and 100 mg/L	5% of mortality only after 96 hpf in the group treated with 100 mg/L of TA under UV light; lower hatching rate in zebrafish treated with TA and under UV illuminations; egg coagulation and perturbations in equilibrium in zebrafish treated with TM; and significant decrease of survival and hatching rates under UV light.	Under UV illumination decrease in the enzymatic activity of AP, GST, and CAT; state of oxidative stress.	[68]

Table 2: Continued.

Stage	NPs diameter	Treatment duration	Tested concentrations	General toxicity response	Specific ROS responses	Reference
Embryos	7.02 nm	6 dpf	0.1 mg/L+Pb (0, 5, 10, 20, and 30 μg/mL)	Effects on organogenesis in coexposed larvae; decrease in T3 and T4 levels in zebrafish treated with 30 μg/mL of Pb alone or to all the doses of Pb plus TiO_2 NPs; downregulation of *tg* and TTR *shha*, *gfap*, α-tubulin, and *mbp* genes; upregulation in *tsβ* gene; and significant decreased in the swimming speed.	—	[61]
Embryos	50-70 nm	96 hpf	0.1, 1, and 10 μg mL	No alteration in survival rate; decrease in hatching rate; significant incidence of abnormalities (tail flexure and pericardial edema); decrease in total distance of swimming; and TiO_2 NPs able to cross the BBB, localized in the larvae brain.	High ROS production with consequent oxidative stress; high apoptosis in the hypothalamus region; upregulations of the genes *α-syn*, *parkin*, *uchl1*, and *pink1*; and decrease in the dopaminergic neurons.	[60]
Embryos	Bulk TiO_2: ~110 nm; 5 h TiO_2 NPs: 85 nm; 10 h TiO_2 NPs: 62 nm; 15 h TiO_2 NPs: 46	96 h	10-250 μg/mL	Significant decreased or increased, respectively, in a dose-dependent manner of survival rates and hatching rates; strongest effect for embryos/larvae treated with TiO_2 NPs milled for the longer time (15 h).	ROS quenching; steatosis, lipid accumulation in dose-dependent manner in different areas of the animal (tail, head, and notochord); high number of apoptotic cells in tail and head; perturbation of *sod1* protein activity; and perturbation of protein *tp53*.	[56]
Adults	<150 nm	5 days	1, 2, and 4 mg/L	Structural changes and degeneration of the follicles.	Several vacuolizations in the cytoplasm; evident forms of paraptosis; mitochondrial vesiculation and chromatin condensation; and swelling and mitotic catastrophe.	[69]
Embryos	5–25 nm	72 hpf	500 and 1000 mg/L	No changes in the survival rate for all the treated samples.	Perturbation of *SOD2* mRNA level both under illumination and in dark condition; normal level of *Pxmp2*; and significant difference in *IF1* mRNA level under illumination.	[65]
Embryos	20 and 30 nm	96 h	1, 10, 50, and 100 μg/mL +10 μg/mL	TiO_2 NPs: survival rate of 85%: TiO_2 NPs+HA: 95%. HA decrease harmful effects of TiO_2 NPs.	—	[53]
Embryos	40 nm	96 h	10, 25, 50, 100, 250, and 500 μg/L	LC50 = 90 μg/mL; enhancement of hatching rate of embryos; and some abnormalities (both body and organs).	Lower ROS production for the TiO_2 NPs produced by HEBM method, compared to the bulk one.	[56]

Table 2: Continued.

Stage	NPs diameter	Treatment duration	Tested concentrations	General toxicity response	Specific ROS responses	Reference
Embryos	1-3 nm		10, 100, and 1000 mg/L	100% mortality at the highest concentrations; delay in hatching rate at the middle and highest doses tested; several malformations (aneurysm and pericardial edema) in embryos injected with TiO_2 USNPs; any perturbations or vascular toxicity in the ones injected in the circulatory systems at 48 hpf; length reduction of the ISVs in eggs treated by soaking or injection with 100 mg/L of TiO_2 USNPs; and perturbation in *Myo1c* expression.	—	[58]
Embryos	21 nm	34, 58, 82, 106, and 130 h	0.01, 10, and 1000 mg/mL	73% of embryos exposed to highest dose hatched prematurely between 34 and 58 hours post exposure.	—	[57]
Embryos	5 nm	2 days	100 μg/L) TiO_2 NPs+Pb (0, 10, 20, and 40 μg/L); a subsequent depuration (144 h)	Survival and hatching rates up to 85% for all the investigated cases; significant perturbation in these biological parameters observed only in at 40 μg/L Pb plus TiO_2 NPs; and reduction in the larvae swimming speed.	—	[62]
Embryos	Micro-TiO_2 1–2 μm Nano-TiO_2 21 nm	6 dpf	0.01, 0.1, and 1.0 mg/L nano-TiO_2 and 1.0 mg/L micro-TiO_2	No effects on survival and hatching rates; body weight and length of larvae decreased as well as rotation times and the swimming speed; perturbation in the neurogenesis and in the motor neuron axon length; and perturbation in the expression of genes *α1-tubulin*, *mbp*, and *gap43*.	—	[63]
Adults	20.5	48 h	1000 μg/L	No significant alterations in gill histopathology; important changes in the expression of 171 genes (111 genes downregulated and 60 upregulated).	—	[36]
Adults	21 nm	14 days	0.1 or 1.0 mg/L	No behavioral abnormalities and no mortality; changes in the number of white blood cells at the last day of exposure (14) for all the tested doses of TiO_2 NPs.	Normal Na^+K^+-ATPase activities in the liver, gill, and brain; values of GSH in the liver, gill, and brain higher in comparison to controls; histology of all these tissues normal; and absence of intracellular oxidative damage.	[67]

Table 2: Continued.

Stage	NPs diameter	Treatment duration	Tested concentrations	General toxicity response	Specific ROS responses	Reference
Adults	9.7 nm	90 days	100 μg/L+0, 2 and 20 μg/L BPA	Change in the intestinal microbial community after cotreatment of TiO_2 NPs and BPA.	Oxidative stress and inflammation dose-dependent and sex-dependent; oxidative responses due to the cotreatment linked to a different amount of *Lawsonia* and *Hyphomicrobium*.	[72]
Adults	<150 nm	5 days	1, 2, and 4 mg/L	Swelling and loss of cristae and degenerated mitochondria in spermatocytes and Sertoli cells; high amount of necrotic cells; and damages in the testicular morphology and negative impact on the fertility.	—	[70]
Adults	23.8 nm	5, 7, 14, 21, and 28 days	1 and 10 μg/L	—	Significant percentage of DNA fragmentation with maximum injuries after 14 days; significant number of apoptotic cells; and important decrease of genome stability (GTS%) at 14 days, and then recovered in part at 28 days.	[71]
Adults	240–360 nm	91 days	0.1, 1.0 mg/L	After 9 weeks, decreased number of embryos; increase in mortality rate at 2 dpf of embryos produced by the exposed female; perturbation in the follicular stages, with a block in the development; and important alteration of genes involved in the development of oocytes.	—	[66]
Embryos and adults	25 nm	Embryos: 96 hpf Adults: 7 days	Embryos: 10, 50, and 100 mg/L Adults: 10, 50, and 100 mg/L	—	Embryos: no effects on hatching rate, no sign of deformity. Adults: significant decrease of activities of GSTs, CAT, and SOD in the gills and liver; oxidative stress condition.	[64]
Adults	21 nm	21 days,	5 and 40 mg/L	Increase of both bacteria (gut) in the water and animal motility; *Actinobacteria*, *Bacteroidetes*, and *Proteobacteria* main component of the flora of the gut.	—	[73]

Abbreviations: AP: acid phosphatase; *atho7*: atonal homolog; BDE: polybrominated diphenyl ethers; BBB: blood-brain barrier; BPA: bisphenol A; BSO: buthionine sulfoximine; CAT: catalase; *dio2*: iodothyronine deiodinase 2; *gap-43*: growth-associated protein 43; *gfap*: glial fibrillary acidic protein; GSH: glutathione; GST: glutathione S-transferase; HEBM: high-energy ball milling; *HIF1*: hypoxia-inducible factor 1; HA: humic acid; hpf: hours post fertilization; ISVs: growing intersegmental vessels; LC50: 50% of lethal concentration; MDA: malondialdehyde; *mbd*: methyl-CpG-binding domain; Mt2: metalloprotein 2; *Myo1c*: Myosin IC; NAC: N-acetylcysteine (NAC); *Nrf2*: nuclear factor erythroid 2-related factor 2; PCP: pentachlorophenol; *Pxmp2*: peroxisomal membrane protein 2; ROS: reactive oxygen species; *shha*: hedgehog protein A precursor; SOD: superoxide dismutase; TA: anatase; *tg*: thyroglobulin; T3: triiodothyroxine; T4: thyroxine; TM: anatase/rutile mixture; *tp53*: tumor protein 53; *tshβ*: thyroid-stimulating hormone β; *uchl1m*: ubiquitin C-terminal hydrolase L1; USNPs: ultrasmall nanoparticles.

mortality rate was observed for all the tested doses in comparison to control samples. In normal conditions, a certain number of zebrafish do not survive during the metamorphosis period, when they are especially vulnerable. Exposure to light and TiO_2 NPs speeded up the death of fish in this life stage. In addition, the nanoparticles induced distinctive abnormalities and perturbations in the growth. The embryos and larvae showed reduced size, not developed fin rays, deformations of craniofacial structures, and absence or abnormal organization in the pigmentation. The larvae treated with 1000 μg/mL presented a swim bladder with only a single lobe. Moreover, an important increase of 8-hydroxy-2′-deoxyguanosine (8-OHdG) detected by ELISA revealed an indication of oxidative stress and intracellular damages. Another study explored the effects of size on the biointeractions of citrate-functionalized TiO_2 NPs on zebrafish during the development under illumination [47]. Zebrafish were exposed to 6, 12, or 15 nm sizes to citrate-TiO_2 NPs for 120 hpf. The smallest NPs (6 nm) were the ones that presented the highest dose-dependent harmful effects, with a LC50 value of 23 μg/mL; the LC50 for 12 and 15 nm NPs were 610 μg/mL and not detectable, respectively. Moreover, the exposed larvae showed several phenotypic abnormalities, including the opaque yolk, axial curvatures, craniofacial defects, yolk sac, and pericardial edema. On the other hand, high levels of hydroxyl radical ($^{\cdot}OH$) and ROS were detected by using specific indicators, the 3′-(*p*-aminophenyl) fluorescein (APF) and the acetyl ester of 5-(and 6-) chloromethyl-2′,7′-dichlorodihydrofuorescein diacetate (CM-H2DCFDA). The detected values were higher for 6 nm NPs than those for the 12 and 15 nm NPs [47].

Jovanovic et al. evaluated the potential neuroimmunological effects of TiO_2 NPs injected together with hydroxylated fullerenes in the otic vesicle of zebrafish [48]. To this end, the expression of different genes linked to the immune and nervous systems was analyzed. The coinjection caused the downregulation of three clusters of genes, associated with the circadian rhythm, transport, vesicular trafficking, and immune response.

Due to the concomitant presence in the aquatic environment of toxicants and nanoparticles, their combined effects were tested in zebrafish. In particular, three different studies evaluated the combined effects of pentachlorophenol (PCP), or deca-BDE (BDE-209), or bisphenol A with titanium dioxide nanoparticles, assessing a possible effect impacting on *Danio rerio* growth [49, 50]. The study on the effects of PCP and TiO_2 NPs focused mainly on the genotoxicity and oxidative stress evaluation [49]. The values of survival and hatching rates in samples treated with both PCP and PCP plus nanoparticles were similar, while the incidence of malformations was higher in the coexposed zebrafish larvae exposed. Regarding oxidative stress, zebrafish treated only with nanoparticles presented an alteration in glutathione content, SOD activity, and malondialdehyde, while no increase in ROS production was revealed in comparison to the control groups. However, coexposure to PCP and nanoparticles to fish led to a decrease in the SOD activity and GSH content when compared to the sample treated with PCP alone. Moreover, coexposure led to an increase in ROS production and important levels of MDA in comparison to the single treatment. Similarly, the coexposure caused an important upregulation of two genes, implicated in the glutathione metabolism and oxidative damage, *sod1* and *nrf2* [49]. These findings indicate that titanium oxide nanoparticles enhance the PCP metabolism, causing genotoxicity and oxidative stress in zebrafish during their development. In another study, the effects of BDE or BDE plus nanoparticles were investigated in the embryos for 7 dpf [50] with emphasis on the neurodevelopment and thyroid tissues. The survival and hatching rates of the samples treated with BDE or BDE plus nanoparticles had similar values over 90% for both the biological parameters. Since a previous work reported a thyroid endocrine disruption led by BDE-209 [50], the values of TH were noted. Samples cotreated with BDE and nanoparticles led to an important increase in the thyroxine (T4) values in comparison to the ones exposed only to the toxicant. No difference in the triiodothyroxine (T3) levels was found. The analysis of different genes implicated in TH regulation, and metabolism reported an important upregulation in the expression of the thyroglobulin (*tg*), thyroid-stimulating hormoneβ (*tshβ*), and iodothyronine deiodinase 2 (*dio2)* genes, in the cotreated larvae. The same control was performed on genes implicated in zebrafish neurodevelopment. Downregulations of *α1-tubulin* and methyl-CpG-binding domain (*mbd)* genes were detected, while the expression of the growth-associated protein 43 (*gap-43)* genes was normal in cotreated fish. In accordance with these results, also the expression of the *mbd* protein was perturbed, while the one of *α1-tubulin* was not affected. Coexposed larvae presented also a reduction in the swimming speed [50]. These findings reported that TiO_2 NPs enhance the metabolism of BDE. In addition, the exposure of zebrafish to BDE plus nanoparticles led to neurodevelopmental toxicity and thyroid endocrine perturbation. This study together with the one performed by Fang et al. demonstrated that TiO_2 NPs can absorb toxicants, suggesting that toxicity assessments on contaminates should take into account also the copresence of titanium dioxide nanoparticles. The same research groups investigated the impact of TiO_2 NPs on neurogenesis with emphasis on the retina in a parallel study [51]. The embryos treated with 1 mg/L of TiO_2 NPs until 72 hpf showed a normal phenotype, with no increase in the mortality rate or significant incidence of malformations. In addition, the expression of the atonal homolog 7 (*atho7*) in the retina of treated fish was found to be similar to the control by using the *in situ* hybridization. Moreover, the expression of different cell types was investigated through immunostaining (Zn12, Zpr1, and Zpr3 antibodies), which allowed to further investigate neuronal differentiation. At 3 dpf, all the components of the retina (cones, ganglion cells, and rods) were well-differentiated in all the samples, demonstrating the absence of TiO_2 NP-induced effects on the neurogenesis [51]. Finally, the analysis of microglia migration revealed the absence of perturbations in macrophage migration in the retina and the brain of the treated larvae. Another work evaluated the toxicological profile of bisphenol A (4,4′-isopropylidenediphenol, BPA) and TiO_2 NPs [52]. Fish treated with only TiO_2 NPs showed a normal survival rate and

presented no important malformations compared to the controls. On the other hand, after treatment with up to 40 mg/L of TiO_2 NPs, the hatching rate was importantly decreased. The combined exposure to BPA and TiO_2 NPs led to a significant dose-dependent decrease of the survival rate and induced different malformations in the larvae, such as spine deformation, weak pigmentation, and pericardial edema. These abnormalities were much more intense in the cotreated zebrafish compared to ones treated only with BPA. These findings, as in the case of the previously analyzed toxicants, demonstrated that the effect of a chemical is enhanced by the presence of TiO_2 NPs. The combined impact, in all three cases (PCP, BDE, and BPA), caused a potentiation of the harmful effects.

Another study evaluated the toxicity of TiO_2 NPs in combination with humic acid (HA) [53]. The presence of HA led to a change in the survival rate of embryos. Indeed, the survival rate of eggs treated only with TiO_2 NPs was 85% and increased to 95% in the presence of HA. This indicated that the presence of HA mitigates the harmful effects exerted by TiO_2 NPs.

In the same year, Faria et al. evaluated the oxidative effects of three different titanium dioxide nanoparticle aggregates (NM TiO_2) in the presence or absence of solar irradiation [54]. These aggregates were different in terms of crystal structure or coating: NM-103 and NM-104 (89% TiO_2, primary crystal size of 20 nm), P25 (99.5% TiO_2 and a primary size of 21 nm), and microsized TiO_2 (98.5% TiO_2 nontreated surface). The three aggregates did not affect the survival and hatching rates of the treated larvae nor induce significant abnormalities in the embryos/larvae. Only one dose of microsized TiO_2 caused a shortening of the length of the larvae. In addition to a general decrease in SOD activity, glutathione levels were perturbed. However, the analysis of photo-oxidative stress indicated that the P25 NPs produced aggregates that led to the highest levels of reactive oxygen species in comparison to the other NM TiO_2. Taken together, titanium dioxide nanoparticle aggregates did not cause strong toxicity or mortality to zebrafish during the development.

Another study assessed the potential toxicity of TiO_2 NPs produced with a particular technique, using the high-energy ball milling (HEBM) for 15 h, in comparison to the bulk particles [55]. The determined value of LC50 was 90 μg/mL similar to the one of bulk NPs (95 μg/mL). Surprisingly, the TiO_2 NP exposure enhanced the hatching rate of embryos. The embryos and larvae presented some abnormalities (both body and organs). Finally, the analysis of ROS showed lower levels for the TiO_2 NPs produced by the HEBM method, compared to the bulk one. The same research group focused their attention again on TiO_2 NPs produced using the HEBM method by milling bulk TiO_2 particles for different times (5, 10, and 15 h). The survival rates and hatching rates of exposed embryos significantly decreased or increased, respectively, in a dose-dependent manner. In both cases, the strongest effect was found for embryos/larvae treated with TiO_2 NPs milled for the longest period (15 h). As varying the milling times allows modifying the size and the charge of NPs, it was possible to assess potential effects induced by these alterations. In particular, the evaluated biological parameter was found to be dependent on the NP milling time. Moreover, by using an *in vivo* and *in silico* computational approach, steatosis, apoptosis, and oxidative stress were assessed. Surprisingly, 5 h, 10 h, and 15 h milled TiO_2 NPs led to ROS quenching. This particular behavior of industrial TiO_2 NPs could be probably due to the production of oxygen vacancies during the HEBM approach. In addition, the analysis of perturbations in neutral lipids allows determining the TiO_2 NP-induced steatosis. Zebrafish treated with TiO_2 NPs showed a concentration-dependent accumulation of lipid in different areas of the animal, including the tail, the head, and the notochord. Moreover, acridine orange staining revealed a high number of apoptotic cells in the tail and head of samples treated with TiO_2 NPs. Different computational investigations were performed to reveal the interaction of NPs with the *sod1* gene, implicated in the ROS production, or the *apoa1a61* (apo-lipoprotein), or docking the tumor protein 53 (*tp53)* protein (apoptotic factor) with TiO_2 NPs. These analyses allow understanding the key role of lipid accumulation and ROS quenching in the TiO_2 NPs toxicity in zebrafish during the development. In particular, the production of TiO_2 NPs via the HEBM approach led to a change not only in the zeta potential and size of the synthetized nanoparticles but importantly in the oxygen vacancies, causing harmful effects. Moreover, the alteration of the activity of *sod1* causes a perturbation of *tp53*. The final pathway caused lipid alterations, apoptosis, and oxidative stress [56].

Even if different studies have already analyzed the effects of TiO_2 NPs on the most common toxicological endpoints (hatching, survival rates, and abnormalities), a deeper study was performed to evaluate the hatching rate at different time points (34, 58, 82, 106, and 130 hpf) by exposure of embryos to different TiO_2 NPs doses (0.01,10, and 1000 mg/mL) [57]. The 73% of embryos exposed to the highest dose of TiO_2 NPs hatched prematurely between 34 and 58 hours post exposure (hpe) in comparison to the control group, exposed only to normal medium (58-82 hpe). This indicates that the presence of TiO_2 NPs can induce premature hatching of the embryos.

The impact of ultrasmall TiO_2 NPs (USNPs) (1-3 nm, 10, 100, and 1000 mg/L) with a focus on vascular toxicity was studied in zebrafish during development [58]. Simple soaking exposure to the highest concentration of TiO_2 USNPs (1000 mg/L) induced 100% mortality and together with the intermediate dose (100 mg/L) delayed hatching. No vascular effects were noted at 120 hpf. On the other hand, embryos injected a 0 hpf with TiO_2 USNPs (1 ng/embryo) presented several malformations such as aneurysm and pericardial edema, while the ones injected in the circulatory systems at 48 hpf did not present any perturbations or vascular toxicity. To assess the specific impact on angiogenesis, eggs were treated by soaking or injected with 100 mg/L of TiO_2 USNPs. In both cases, nanoparticles led to a reduction in length of the growing intersegmental vessels (ISVs). To comprehend the mechanism related to the impact on angiogenesis, the expression of genes involved in vascular toxicity was evaluated. Only the expression of Myosin IC

(*Myo1c*), involved in glomerular development, was affected by TiO_2 USNPs. These data demonstrated for the first time the vascular effects of ultrasmall TiO_2 on zebrafish during development.

The effects of coating and size on the toxicity of TiO_2 NPs were evaluated by exposure of embryos to nanoparticles with different sizes (4, 10, 30, and 134 nm) prepared at 6 different concentrations (50, 500, 5000, 50000, and 250000 μg/L) [59]. TiO_2 NPs of 4 and 30 nm did not exert toxicity on zebrafish, while the 10 nm and 134 nm had a low impact on the mortality rate at 5000 and 250000 μg/L, respectively. Moreover, embryos treated with different sized NPs, and the respective doses presented no necrotic cells or only a low amount of them. The expression of metalloprotein 2 (Mt2) by *in situ* hybridization was found to be comparable to the control samples. These findings were in line with previous studies, reporting the absence or low toxicity of TiO_2 NPs.

Also, the specific possible neurotoxicity of TiO_2 NPs was evaluated in zebrafish during the development [60]. The treated embryos/larva did not present an alteration in the survival rate in comparison to the control samples. Contrarily, the hatching rate was decreased, and a significant incidence of abnormalities (tail flexure and pericardial edema) at 96 hpf was observed. In addition, the behavior of larvae was affected by the treatment with nanoparticles, with a decrease in the total distance of swimming of the larvae at 96 hpf compared to the controls. This indicates a toxic effect of TiO_2 NPs, but without consequent mortality. TEM images showed that once internalized in the embryos, TiO_2 NPs can cross the blood-brain barrier (BBB) and localize in the larvae brain. A high ROS production with consequent oxidative stress was detected in the treated larvae. On the other hand, histological analysis showed high apoptosis levels in the hypothalamus. Moreover, the analysis of the genes alpha-synuclein (*α-syn*), *parkin*, ubiquitin C-terminal hydrolase L1 (*uchl1m*), and *pink1*, implicated in the Lewy body formations, revealed their upregulation [60]. Finally, zebrafish larvae presented a decrease in the dopaminergic neurons. All these findings underline that TiO_2 NPs induced effects that are similar to symptoms of Parkinson's disease (PD).

Since TiO_2 NP can interface with heavy metals in the aquatic environment, few studies have assessed the effects on zebrafish of TiO_2 NPs and Pb cotreatments [61, 62]. To this end, zebrafish embryos were coexposed to TiO_2 NPs (0.1 mg/L) and several doses of Pb (0, 5, 10, 20, and 30 μg/mL) [61]. The hatching and survival rates were similar in the samples that were cotreated or exposed only to one of the two compounds. However, adverse effects on organogenesis were revealed only in the coexposed larvae. To evaluate the potential impact of the cotreatment on the thyroid endocrine system, the levels of T3 and T4 were determined. A decrease in the T3 and T4 levels was observed when zebrafish were treated with 30 μg/mL of Pb alone or with all the doses of Pb plus TiO_2 NPs. On the other hand, no changes were found in the embryos exposed only to NPs. In addition, the expressions of *tg* gene and transthyretin (*TTR*) gene were found to be downregulated, while the one of the thyroid-stimulating hormone (*tsβ*) resulted to be upregulated, in treatments relying on both the compounds. Moreover, the genes sonic hedgehog protein A precursor (*shha*), *gfap*, *α-tubulin*, and *mbp*, implicated in the development of the central nervous system (CNS), were downregulated in comparison to the samples exposed only to different doses of Pb. Finally, larvae coexposed presented a significant decrease in the swimming speed. All these perturbations indicated that TiO_2 NPs could induce toxicity in the thyroid endocrine system and the development of the zebrafish CNS [61]. In a similar study, embryos were treated with Pb or Pb plus TiO_2 NP for 2 days with a subsequent depuration (144 h) [62]. The uptake and complex formation between TiO_2 NPs and Pb were assessed by transmission electron microscopy-energy dispersive spectrometry (TEM-EDS). The survival and hatching rates of treated embryos/larvae were up to 85% for all the investigated cases. A significant perturbation in the two biological parameters was observed only in the case of 40 μg/L Pb plus TiO_2 NPs when compared to the samples treated with Pb alone. Moreover, the coexposure led also to a reduction in the larval swimming speed. This perturbation in the locomotor behavior is in line with the previous finding of Miao et al. Further, the expressions of genes implicated in brain formation and development and, specifically, those encoding for glial fibrillary acidic protein (*gfap*), HuC (*elavl3*), and synapsin IIa (*syn2a*) were evaluated. A downregulation was observed in the expression of all three genes. These results indicated that the presence of TiO_2 NPs could enhance the neurotoxicity effects of Pb in zebrafish during the development [62].

A recent study has deeply assessed the specific and potential neurotoxic effects of TiO_2 NPs on *Danio rerio* [63]. Zebrafish were treated until 6 dpf with 4 different doses of nanoparticles (0.01, 0.1, and 1.0 mg/L nano-TiO_2 and 1.0 mg/L micro-TiO_2). The survival and hatching rates were not affected by any exposure, while the body weight and length of larvae were decreased at 1.0 mg/L nano-TiO_2 as well as rotation times and the swimming speed. The treatment of the transgenic line Tg (HuC-GFP) and Tg (hb9-GFP) with nano-TiO_2 caused, respectively, perturbation in the neurogenesis and the motor neuron axon length. Similarly, the expression of genes *α1-tubulin*, *mbp*, and *gap43* implicated in the axonal growth, and the genes *nrd* and *elavl3*, involved in the neurogenesis, were perturbed. It can be thus concluded that nano-TiO_2 induce neurotoxic effects in zebrafish, particularly in the motor neuron axonal growth and neuronal development.

Tang et al. assessed the toxicity in embryos treated chronically with high doses of TiO_2 NPs (100 mg/L) [64]. However, no significant changes were observed in the hatching, survival, or deformity rates.

Only one work evaluated the effects of a coating of the TiO_2 NPs on zebrafish during development [65]. Eggs were exposed to bare TiO_2 NPs or TiO_2 NPs with polyelectrolyte on the surface under illumination or darkness. In particular, nanoparticles were coated with poly(sodium 4-styrene sulfonate) sodium salt (PSS, anionic) (TiO_2 NPs/PSS,) and polyallylamine hydrochloride (cationic, PAH) (TiO_2 NPs/PSS/PAH). No changes in the survival rate were observed for all the treated samples under both conditions. In addition,

the gene expression of peroxisomal membrane protein 2 (*Pxmp2*), a marker of hypoxia, hypoxia-inducible factor 1 (*HIF1)*, a marker for membrane function, and *SOD2*, a marker of oxidative stress, of samples exposed to bare TiO_2 NPs, TiO_2 NPs/PSS, and TiO_2 NPs/PSS/PAH were measured. The level of *SOD2* mRNA resulted to be perturbed, under both illumination and dark conditions for all the different treatments. *Pxmp2* expression was normal in all the cases. The mRNA level of *HIF1* presented a significant alteration only when the experiments were performed under illumination. These findings demonstrated that the toxicity of TiO_2 NPs can be influenced by several factors, including the presence/absence of illumination and surface coating.

2.2. Effects of Titanium Dioxide Nanoparticles on Adults. Studies on the effects of titanium dioxide nanoparticles on adult zebrafish are limited. Griffit et al. treated adult zebrafish females with titanium dioxide nanoparticles and analyzed their possible effect on gills in terms of both morphological changes and perturbations in gene patterns. Titanium dioxide NPs did not alter significantly the gill histopathology after 24 and 48 h of treatment [35]. Moreover, the investigation of transcriptional activity revealed important changes in the expression of 171 genes after 48 h of treatment, with 111 genes downregulated and 60 upregulated. Interestingly, some of these genes are implicated in the function of ribosomes [35].

In 2011, Wang et al. performed a prolonged (91 days) and chronic treatment of zebrafish with titanium oxide nanoparticles, focusing on the potential impact on reproduction [66]. After 9 weeks, females treated with TiO_2 NPs started to produce a decreased number of eggs. In addition, the mortality rate of embryos produced by exposed females presented an increase in the mortality rate at 2 dpf. This observation indicates that prolonged treatment with TiO_2 NPs impairs the survival and reproduction of zebrafish. Since the decreased number of eggs generated by females can be linked to a problem in folliculogenesis, histological analysis of the ovaries was performed. TiO_2 NPs caused a perturbation in the follicular stages, reporting a block in the development probably due to nanoparticles interacting with the follicles (Figure 2). The gene expression implicated in the development of oocytes was evaluated by a microarray of ovarian tissues. 0.1 and 1 mg/mL of TiO_2 NPs led to an important alteration of several genes (1043 downregulated/2383 and 471 upregulated/2069), demonstrating a perturbation in the functionality and maturation of the ovary [66].

Ramsden and his research group investigated the biointeractions of TiO_2 NPs on zebrafish of 14 dpf, focusing on the reproduction and different physiological parameters, such as organ anatomy, hematology, and osmoregulation [67]. The treated adult did not present behavioral abnormalities or mortality. As the number of white blood cells changed only on the last day of exposure (14) for all the tested doses of TiO_2 NPs, this observation can be neglected. The amounts of trace metals and whole electrolytes were normal for all the temporal windows of investigation. Also, Na^+K^+-ATPase activities in the liver, gills, and brain were found similar to the control, demonstrating good osmoregulation. However, the values of GSH in the same tissues were higher in the treated adults in comparison with the control ones. The histological analysis of all these tissues did not reveal any significant changes. Indeed, no aneurisms or edema were detected in the gills, together with no parenchymatic changes in the liver. The morphological structures of the brain and the gonads resulted to be normal. The lack of damage revealed via the histological analysis in the investigated tissues suggested the absence of intracellular oxidative damage [67]. These results are in agreement with the previous study conducted by Chen et al. [37].

The toxicological profile of two different formulations of TiO_2 NPs (anatase, TA or an anatase/rutile mixture, TM, form) on zebrafish was assessed under different illumination settings (visible light or visible and ultraviolet light) [68]. No mortality was detected in embryos treated with TA between 4 and 72 hpf in all the investigated samples. Five percent mortality was present only after 96 hpf in the group treated with 100 mg/L of TA under UV light. On the other hand, zebrafish treated with TA under UV illumination showed a lower hatching rate as well as shortening in terms of larval body length. Treatment with TM led to egg coagulation and perturbation of the larval equilibrium in all the samples, while the survival and hatching rates were significantly decreased and increased, respectively, only under UV light. Under UV illumination, the analysis of biochemical markers revealed a decrease in the enzymatic activity of acid phosphatase, GST, and CAT [68]. These changes indicated a state of oxidative stress.

Akbulut et al. focused their research on the potential and specific effects of TiO_2 NPs on ovaries. To this end, adults were treated for 5 days with different doses of nanoparticles (1, 2, and 4 mg/L). The analysis was performed by using both histological staining (hematoxylin and eosin on paraffin sections) and TEM [69]. Several toxic effects of TiO_2 NPs were observed in the ovaries. Treated samples presented structural changes and degeneration of the follicles. In particular, several vacuolizations in the cytoplasm indicated evident forms of specific cell death (paraptosis, type III). Further, the tissue showed mitochondrial vesiculation and chromatin condensation (Figure 2). In addition to this, mitochondria presented swelling and mitotic catastrophe. Hence, TiO_2 NPs led to paraptosis in adult zebrafish and inhibited oogenesis. These findings are in line with the previous work of Wang et al. related to zebrafish development [66] in which they reported perturbations in the female reproduction, with evident defects in folliculogenesis.

The impact of TiO_2 NPs on testis was further investigated by treatment of zebrafish with 1 mg/L, 2 mg/L, and 4 mg/L of nanoparticles, subsequent dissection, and fixation of the testis, and final analysis of sections by TEM [70]. TiO_2 NPs affected the testis in a dose-dependent manner, causing swelling and loss of cristae and degenerated mitochondria in spermatocytes and Sertoli cells (Figure 2). Zebrafish exposed to TiO_2 NPs presented a high amount of necrotic cells. As the TiO_2 NP-induced alterations in the Sertoli cells caused damage in the testicular morphology, a concomitant possible negative impact on fertility cannot be excluded.

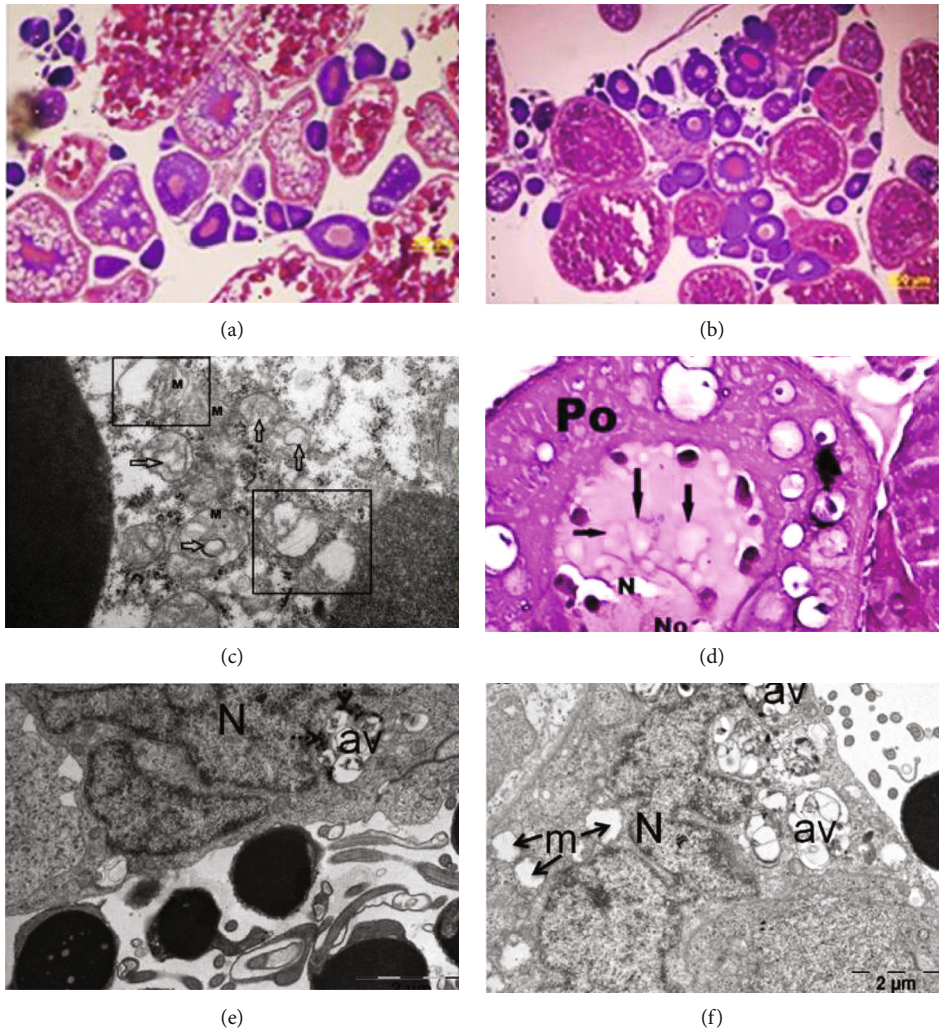

Figure 2: Images of (a–d) ovaries and (e–f) testis tissues of adult zebrafish treated with TiO_2 NPs. Reproduced with permissions from [66, 69, 70].

To assess potential genotoxic effects induced by TiO_2 NPs, adult zebrafish were exposed to NP doses similar to the one present in the aquatic environment (1 and 10 μg/L) for different time points (5, 7, 14, 21, and 28 days) [71]. The genotoxicity was investigated by using three different and complementary approaches. First, the level of DNA damage was evaluated using the comet assay. A significant percentage of DNA fragmentation in treated zebrafish was detected at a dose of 10 μg/L of TiO_2 NPs at 5 days while reaching a maximum after 14 days in comparison to controls. In addition, the number of apoptotic cells in zebrafish exposed to the same dose of nanoparticles detected by diffusion assay was found to be significantly reduced after 10 days of treatment, supporting the results obtained with the comet assay. Moreover, the DNA injuries were further analyzed by the RAPD-PCR technique. This analysis showed a clear deviation from the control in terms of DNA band pattern of adults exposed to TiO_2 NPs for 14 and 21 days, even if after 28 days this observation was partially mitigated. The same technique showed that the genome stability (GTS%) decreased notably at 14 days but then recovered partially after 28 days. These data demonstrate clearly that the highest tested concentration (10 μg/L) of TiO_2 NPs caused genotoxic effects in adult zebrafish after 14 and 21 days of exposure [71].

Tang et al. assessed the toxicity of TiO_2 NPs both in embryos and adults. Here, they focused their attention on the potential impact of NPs on the liver, gills, and intestine with emphasis on oxidative stress [64]. The activities of GSTs, CAT, and SOD were investigated in adults treated with different doses of nanoparticles. The enzymatic activity of all three investigated proteins was shown to be significantly decreased when compared to controls. Especially in the gills and liver, these alterations are associated with the induction of a condition of oxidative stress. Moreover, no important perturbations of their activities were detected in the intestine. This observation could be attributed to the low absorption of TiO_2 NPs in the small intestine after ingestion. On the other hand, the expression of CAT, SOD, and GST genes was upregulated in all the investigated organs. It can be concluded that although TiO_2 NPs induce upregulation of genes involved in the antioxidant

machinery, the corresponding level of traduced proteins was not sufficient to counteract the production of ROS, causing thus oxidative stress in the liver and gill of adult zebrafish.

As in the case of zebrafish during the development, also adult fish were exposed both to TiO_2 NPs (100 μg/L) and BPA (0, 2, and 20 μg/L) or their mixture for 90 days, to understand the possible effects on the gut microbiota [72]. The cotreatment of TiO_2 NPs and BPA caused a change in the intestinal microbial community. In addition, the impact of TiO_2 NPs on zebrafish development and in particular on the intestine (oxidative stress and inflammation) was found to be dose- and sex-dependent. The oxidative responses due to the cotreatment were linked to a different amount of *Lawsonia* and *Hyphomicrobium*. The treatment with a mixture of TiO_2 NPs and BPA had an impact on the gut microbiota, with consequent effects on the *Danio rerio* as a host organism.

A subsequent work evaluated the mortality and injury induced by TiO_2 NPs (5 and 40 mg/L) [73]. The TiO_2 NP exposure was connected with an increase of both bacteria in the water and animal motility. Moreover, the increase in bacteria was found in the gut and not in the caudal and dorsal fins. *Actinobacteria*, *Bacteroidetes*, and *Proteobacteria* were found to be the main component of the flora of the gut, containing a high amount of bacteria present in zebrafish treated with TiO_2 NPs. These findings suggest a correlation between the zebrafish mortality caused by TiO_2 NPs and bacterial infections.

3. Iron Oxide Nanoparticles (IO NPs)

Iron oxide nanoparticles (IO NPs) can be designed with a wide range of physicochemical and biological properties, making them a useful platform for biological and medical applications. Due to their versatile characteristics, colloidal stability, and increased biocompatibility and degradability, they have been intensively studied and implemented in clinics over the past decades. As iron oxide is a naturally occurring mineral, it allows for ecofriendly nanoparticle (NPs) synthesis, without the need to rely on potentially toxic chemical procedures and costly reagents. Moreover, it is responsible for the inherent magnetic properties that characterize these kinds of nanoparticles [74]. While IO NPs come in different shapes and sizes, generally, they share a basic design, composed of a magnetic iron core (mostly magnetite, maghemite, or γ-Fe_2O_3 for biological and environmental applications) comprised of one or multiple crystals [15, 75]. Based on this crystalline core, IO NPs can be grouped into three main categories: micron-sized magnetic iron oxide particles (MP IO), superparamagnetic particles (SP IO) displaying a hydrodynamic diameter larger than 50 nm, and ultrasmall ones (USP IO), with less than 50 nm [76]. It follows that the response of IO NPs to an external magnetic field (MF) is influenced by their composition, as well as by their dimension [5]. Indeed, the coating does not only prevent the IO NPs from aggregating and protects them from environmental influences but importantly confers the basis for the attachment of other biomolecules creating a plethora of opportunities for possible applications [77]. Notably, IO NPs are so far the only class of metallic nanoparticles that have been approved for clinical use, i.e., in cancer bioimaging, hyperthermia-based therapy, and the treatment of iron deficiency [78]. As the particles' size and surface coating influence strongly its biodistribution, several medical applications have been developed accordingly [79]. Polymeric coated-IO NPs are clinically proven and widely approved as magnetic resonance agents, where they can be further implemented to display dysfunctional processes [76, 79, 80]. Iron oxide-based nanoparticles hold thus great promise in theranostic applications and are extensively exploited as targeted drug delivery systems due to their capability to undergo versatile functionalization processes [80, 81]. As IO NPs are generally of hydrophobic nature, a coating of hydrophilic layers does not only improve their biocompatibility but allows further for subsequent attachment of biological molecules of interest [81, 82]. Here, a prominent example is given by anemia therapy where IO NPs have been successfully used as a remedy for many years [80, 82]. In contrast, in cancer treatment, IO NPs have been implemented as in vivo cytotoxicity and apoptosis inducers, leading to a significant reduction of the number of malignant cells [74, 78]. Indeed, IO NPs are the only nanoparticles approved for hyperthermia-based therapy in humans, an approach that exploits their magnetic properties for the generation of heat when exposed to an alternating magnetic field (AMF) [78, 83]. A completely different approach is instead based on a similar concept: it has been shown that the application of an MF to IO NP-labeled neuronal cells allows to stimulate them mechanically, inducing consequently a cellular response, transduced, e.g., in neurite outgrowth [84–86]. Achieving controllable magnetic guidance of neurons could contribute importantly to the understanding of neurodegenerative diseases and their treatment as knowledge in this field of research is scarce. Indeed, recently several studies tried to take advantage of the unique properties of IO NPs for tissue engineering and regenerative medicine [82]. In addition, IO NPs can act as potent catalysts, due to their particular physiochemical properties that cannot be found in their bulk counterparts, and as a consequence, they have been implemented successfully to address plenty of different economic and environmental issues [87].

As demonstrated by their wide range of clinical applications, IO NPs display without any doubt a high degree of safety in living organisms. However, most studies assessing the cytotoxicity of IO NPs are performed in cell culture model systems and lack in whole animal systems [86]. While *in vitro* studies generally revealed an absence of toxicity, it must be kept in mind that nanoparticles can be still identified as invading non-self-components by the immune system of living organisms. Here, they could trigger immunogenetic responses, such as an allergic reaction, hypersensitivity, localized or systemic inflammation, immunosuppression, or a combination of all [75, 78]. The size, shape, and surface coating, but also the administration method, the exposure condition, and the host itself, play a role in the induction of a potentially unexpected health effect to the IO NPs [15, 88, 89]. The type of interaction the IO NPs establish with the immune system depends highly on their

Table 3: Impact of IO NPs on zebrafish.

Stage	NP diameter	Treatment time	Tested concentrations	General toxicity response	Specific ROS responses	Reference
Embryos	22 nm	144 h	0.3; 0.6; 1.25; 2.5; 5; and 10 mg/L	High mortality rate; cardiotoxicity (reduction of heart beat rate); and morphological alterations.	—	[3]
Embryos	6-12 nm	120 hpf	SP IONs, S PION-DX, SP ION-CS, SP ION-T, SPI ON-T-PEG, SP ION@SiO_2: 0.125 mM, 0.5 mM, 2.0 mM, and 8.0 mM	SP ION-CS: reduced survival rate, SPI ON-CS, and SP ION@SiO_2 delay in hatching rate; SP ION-DX, SP ION-T-PEG and SP ION-T: slightly premature hatching; SP ION-CS and SPI ON@SiO_2: reduction in locomotor activity; and SP ION-CS, SP ION-T-PEG SP ION@SiO_2 reduction in escape behavior.	—	[15]
Embryos		168 hpf	0.1, 0.5, 1, 5, 10, 50, and 100 mg/L	Mortality concentration and exposure time dependent; LC50 = 53.35 mg/L; delay in hatching rate, LC50 = 36.06 mg/L; and different malformations (pericardial edema, tissue ulceration, and body arcuation).	—	]76]
Embryos	40 nm	96 h	Fe_3O_4 NPs: 100-800 μg/mL bare Cr@Fe_3O_4: 5, 150, 300, and 600 mg/mL	Fe_3O_4 NPs: dose- and time-dependent delay in hatching rate; slight decrease in embryo viability; Cr@Fe_3O_4: NPs high mortality in 2-week-old larvae; dose-dependent accumulation in digestive tract.	—	[93]
Embryos	100-250 nm	168 hpf	1, 5, 10, 50, and 100 mg/L	LC50 = 10 mg/L; delay in the hatching rate.	—	[97]
Embryos	22-45 nm	96 hpf	10, 20, 40, 60, 80, 110, 120, and 140 ppm	LC50 =60.17 ppm; delay in hatching rate; reduction in heart beat rate; and increased teratogenicity.	Dose-dependent decrease of $Na+K^+$-ATPase activity; dose-dependent increase of AChE; increased levels of lipid peroxidation ROS, PC, and NO; increase of apoptotic bodies; and decrease of antioxidant enzymes, CAT, SOD, and Gpx.	[98]
Embryos/adults	15 nm	Embryos: 96 hpf Adults: 2 weeks	Embryos: 1, 10, 100, and 1000 ppm Adults: 1, 10 ppm	Embryos: no adverse effect observed Adults: reduced locomotor and exploration activity, increased anxiety, reduced social interaction, tightened shoaling behavior; dysregulation of circadian rhythm locomotor activity, reduction of short-term memory retention, and reduction of serotonin and dopamine.	Increased CAT, cortisol level in the brain; reduction of AChE activity.	[92]

Table 3: Continued.

Stage	NP diameter	Treatment time	Tested concentrations	General toxicity response	Specific ROS responses	Reference
Adults	21 nm	7 days	100 mg/L	Bare IO NPs accumulate mainly in the gills, coated IO NPs in the liver.	Altered expression of genes involved in inflammation, immune response, oxidative stress, antioxidant response, and mitochondria in the gills of Fe_3O_4-treated fish. Upregulation in the liver of genes involved in immune and inflammation responses, and downregulation of genes involved in DNA damage and repair in both exposures; different expression of genes involved in DNA damage/repair and apoptosis (*tp53*) for starch-coated NPs; upregulation of *cyp1a*; and dysregulation of genes involved in the mitochondrial dysfunction pathway.	[111]
Adults	Fe_2O_3: 80-90 nm Fe_3O_4: 140-160 nm	28 days	4 and 10 mg/L	Shift in coloration, extravasated blood, and chronic toxicity in the gut.	—	[95]
Adults	23 nm	48 h	20, 50, 100. 140, and 200 mg/kg	Reduction of AChE activity; impaired swimming.	Increased expression of transcriptional *jun*, *caspase-8*, *caspase-9*, *gclc*, *Gpx1a*, *CAT*, *gstp1*, and *sod2*.	[110]

Abbreviations: AChE: acetylcholinesterase; ATP: adenosine-5′-triphosphate; CAT: catalase; *cyp1a*: cytochrome P450 1 A; *gclc*: glutamate-cysteine ligase, catalytic subunit; *Gpx:* glutathione peroxidase; *GST:* glutathione transferase; *HIF1*: hypoxia-inducible factor 1; IO NPs: iron oxide nanoparticles; LC50: 50% of lethal concentration; NO: nitric oxygen; PC: pyruvate carboxylase; ROS: reactivity oxygen species; SOD: superoxide dismutase; *tp53*: tumor protein 53.

characteristics as these govern ultimately their biodistribution in the organisms. Indeed, several IO NP-based contrast agents have been withdrawn from the market in several countries after causing adverse side effects [72]. In this context, it is particularly noteworthy that several studies revealed the immune reaction to IO NPs being either immune-stimulating or immune-suppressive [78, 89]. Especially when present in a high concentration, IO NPs can favor the outcome of toxic side effects [90].

Over the past years, IO NPs have further gained growing attention in commercial and industrial applications while increasing consequently also their release in the environment [15, 91]. Here, a particular concern is given to the aquatic environment, as alarming estimations regarding extensive sedimentary depositions of these nanopollutants demand an accurate evaluation of their ecotoxicological impact on this niche, and thus ultimately on human health [15]. As a consequence of the globally increasing implementation of IO NPs in several branches, the deposition of these particles in various life domains is inevitable. Several studies have thus focused on the adverse effects induced by IO NPs on aquatic organisms [14], with particular focus on zebrafish. Different studies have elucidated the possible harmful effects of IO NPs both during the development and in adult organisms (Table 3).

3.1. Effects of IO NPs on Zebrafish during Development. Although IO NPs have been widely accepted as nontoxic, care must be taken as different studies reveal contradictory results [92]. In general, it must be distinguished between primary and secondary IO NP-dependent induced toxicity. The latter one is given, e.g., by the induction of an inflammatory status in response to the entry of NPs in the organism with subsequent activation of several downstream responses, such as an increase in systemic levels of reactive oxygen species (ROS). A primary response instead requires the intracellular localization of the NPs and involves the responses that take place at a cellular level [88]. Several studies showed that NPs can interfere with the chorion by blocking its pores, limiting thus the exchange of nutrients and oxygen. However, especially this factor is strongly influenced by the size of the IO NPs and their concentration [15, 89]. Usually, small IO NPs can pass the chorion without any disturbance and do not induce any embryo toxicity if not exceeding in concentration. In addition, the thickness of the chorion can be altered due to NPs sticking to it and accumulating on its inner/outer surface, especially when present in high concentrations [15]. Together with the accumulation of NPs on its surface, this could lead to a retard of embryo growth and/or altered hatching due to hypoxia and the establishment of ROS [15, 89]. In the study performed by Pereira and colleagues, no deviation from normal hatching behavior was observed for any of the investigated doses, exposure conditions, and iron forms, indicating that the treatments did not exhibit any adverse effect during the early stages of development and presumably did not interfere negatively with the embryonic gene expression and/or chorionic surface [15]. Being hatching the transition point from the developing embryo to the free-living larvae, it is often evaluated in toxicity tests, as it allows to assess the overall developmental status [75]. However, a deviation of the hatching time point cannot be strictly associated with toxicity, as the hatched larvae might not display signs of underdevelopment during later life stages. Nevertheless, the absence of an alteration of hatching behavior can be indicative of the fact that the IO NPs that have surpassed the chorion accumulate in the organs, displaying their potential toxic effects only at later time points of the zebrafish development. Indeed, IO NPs functionalized with citrate and their dissolved counterpart revealed a mild embryo toxic effect after an exposure period of 144 h [15]. Nevertheless, the absence of an alteration of hatching behavior can be indicative of the fact. However, this effect was shown to be dose- and exposure-type dependent. While the treatment of the larvae with γ-Fe_2O_3 NPs resulted in a high mortality rate after 144 h when surpassing a certain concentration, the lethal dose was diverse according to the exposure type. In this context, static exposure (0.6-10 mg/L) appeared to be less toxic, as higher concentrations were needed for the induction of death when compared to the semistatic setup (0.3-10 mg/L) [15]. Regarding the iron ions, no difference was observed in terms of the type of exposure but resulted in a high mortality rate in all groups treated with doses >0.3 mg/L. These observations hint towards the fact that the exposure conditions of the IO NPs need to be considered in the establishment of nanotoxicity and that the induced effect is partially independent of the presence of iron ions themselves. This comes as static exposure of IO NPs enables for treatment with a higher dose without an increase in mortality when compared to the same concentration of free iron. A slightly different trend was observed with regard to neurotoxicity, assessed by the SCF, a common marker for the potential neurotoxicity of substances. While the SCF of embryos treated with IO NPs under static and semistatic conditions did not reveal any neurotoxicity, this was not true for their dissolved counterpart. Here, only semistatic exposure to iron ions (5 mg/L) led to a reduction in the spontaneous embryo contraction, when compared to lower doses (0.3, 0.6 mg/L) and the control group. The increase of toxic effects caused by the free iron ions when compared to the same concentration of IO NPs strengthens the assumption that proper surface coating can reduce the potentially adverse effects of IO NPs. This hypothesis is in line with the finding that the coated γ-Fe_2O_3 NPs induced a low frequency of morphological alterations on zebrafish larvae and embryos in comparison to their dissolved counterpart under static conditions [15]. However, this was not true for semistatic exposure, where a large number of malformations were observed for both iron forms. In addition, the investigated concentrations of IO NPs did not alter the morphometric parameters of zebrafish exposed for 144 under static and semistatic conditions. Higher doses of free iron ions (1.25 and 2.5 mg/L) induced instead notable physiological alterations (i.e., reduction of the area of the swim bladder, yolk sac, head height, and body length) under semistatic exposure. Nevertheless, by implementing uncoated γ-Fe_2O_3 NPs, this effect was reversed, with the embryos displaying pericardial edema, tissue ulceration, and spinal curvature [15]. Taken together, the degree

of toxicity induced by IO NPs is not only strongly influenced by the physicochemical composition of the surface of the NPs but also by the exposure condition itself that could potentiate the adverse effect notably.

Another recent study revealed a dose-dependent delay of embryo hatching after incubation of 96 h with Congo red-labeled Fe_3O_4 ($Cr@Fe_3O_4$). The observed effect was both dose- (>200 μg/mL) and time-dependent. In particular, the highest dose of 800 μg/mL induced a reduction of around 70% in the overall hatching behavior. However, as no adverse effect in terms of hatching was revealed for the bare NPs at any investigated concentration, it might be concluded that the toxic impact is due to the presence of the dye [93]. Indeed, another possibly cytotoxic effect to take into consideration for IO NPs is the one given by their surface structure. This is further demonstrated by the fact that proper surface coating of the IO NPs could ameliorate the observed adverse effects to a certain degree underlying again the importance of the physicochemical composition of nanoparticles in the induction of toxicity and teratogenicity [89]. Indeed, it has been shown that specific coatings, such as dextran or polyethylene, can significantly reduce the toxicity of IO NPs for a wide range of concentrations [77, 94].

To investigate further this aspect, Oliveira et al. reported the effect of different coatings in the elicitation of SP ION-induced toxicity [77]. In addition to the classic sublethal endpoints, they assessed also behavioral patterns after 5 days of exposure (locomotion, thigmotaxis, and escape response). They evaluated the impact of different coatings: dextran (SP ION-DX), chitosan (SP ION-CS), carboxy-silane (SP ION-T), polyethylene glycol (SP ION-T-PEG), and silica (SP $ION@SiO_2$). The animals were evaluated daily for mortality, hatching rate, and malformations using a stereomicroscope. Interestingly, only SP ION-CS led to a reduction in the survival of zebrafish embryos when administered in concentrations of >2 mM. More in detail, the deadly effect was dose-dependent and was accentuated continuously after 2 days of exposure, leading to a 100% mortality rate after 5 days. As reported in other studies, precipitation of high concentrated NPs might be at the basis of this adverse effect [14, 77, 95].

Next, the hatching behavior was evaluated between 48 and 72 hpf. According to the specific surface coating, slight differences were revealed. In line with the increased mortality rate, animals treated with 8 mM of SP ION-CS died even before hatching. While 2 mM of SP ION-CS and SP $ION@SiO_2$ delayed the hatching, all other groups led to mild premature hatching at all investigated concentrations. The fact that none of the investigated IO NPs induced any morphological malformations after 5 days of incubation, even at the highest investigated dose, supports the idea that appropriate surface coating can favor the biocompatibility of IO NPs when compared to the same dose of bare NPs [14]. However, as the animals treated with high concentrations of SP ION-CS deceased before analysis could take place, no conclusion about teratogenicity in this context could be given. With regard to the behavioral evaluation, similar to what has been observed for the hatching rate, only SP ION-CS (0.125 mM) and SP $ION@SiO_2$ 82 mM) revealed a deviation in their locomotor activity in comparison to the controls—although these results were not completely convincing. For all investigated particles, an anxiogenic effect could be excluded. However, in terms of the escape response, zebrafish treated with SP ION-CS, SP ION-T-PEG, and SP $ION@SiO_2$ showed a significant decrease in their performance [77]. The study performed by Oliveira et al. strongly affirms that surface coatings do mitigate potentially toxic effects of IO NPs by reducing their reactivity while increasing their colloidal stability. Nevertheless, this effect might be bilateral. Indeed, as demonstrated by Jurewicz et al., while IO NPs functionalized with a certain compound did not impact negatively the zebrafish development, the same compound induced toxicity when administered alone at the corresponding concentration [93]. In this context, a previous study evaluated the effect of pure chitosan nanoparticles on zebrafish embryos [96]. Here, the authors showed that chitosan induced mortality and hatching delay in a dose-dependent manner, together with the induction of morphological alterations. At the basis of this toxicity were increased levels of ROS, apoptosis, and physiological stress [96]. These findings could corroborate the hypothesis that together with the characteristics of the nanoparticle, the surface coating must be evaluated carefully in the assessment of potential toxicity, generated probably by a combination of both components.

To further increase the biocompatibility, Hafiz et al. synthetized IO NPs based on a green chemistry approach based on spinach. Zebrafish embryos and larvae were exposed to these 150-200 nm sized crystalline Fe_2O_3 particles at different concentrations for several time points, from 8 to 168 hpf. While concentrations ranging from 1 to 5 mg/L did not reveal any toxicity, higher doses of 50 and 100 mg/L had a deleterious effect on the embryos (100% mortality), with an LC50 of 10 mg/L, concomitant with a delay in hatching. The most sensitive stadium of development was identified to be 24 hpf, corresponding to the time point of organogenesis [97]. Indeed, as reported in previous studies, probably also in this case, high concentrations of IO NPs favor their aggregation, especially in the case of pristine particles due to their intrinsic reduced stability [77]. The identified toxic effects are probably a consequence of the obstruction of the pores of the chorion by the presence of IO NPs. However, the observed toxicity in the early stages of the development is mostly attributable to altered gas exchange between the embryo and its environment rather than to the IO NP composition itself [97]. Usually, IO NPs of smaller dimensions are considered more toxic than their bigger counterparts [98]. This is because smaller NPs present a bigger reactive surface area and thus could generate theoretically more ROS. In addition, smaller NPs are generally degraded more rapidly, leading to fast iron accumulation [94].

Zhu et al. evaluated the effect of the exposure of different doses of uncoated Fe_2O_3 NPs (0.1, 0.5, 1, 5, 10, 50, and 100 mg/L) on the early development of zebrafish [14]. For this purpose, they analyzed the embryos and larvae at different time points (6, 12, 24, 36, 48, 60, 72, 84, 96, 120, 144, and 168 h) via microscopy, emphasizing the survival, hatching rate, and morphological malformations.

First, they demonstrated a correlation between IO NP concentration and hatching rate, where doses >10 mg/L induced hatching retardation and severe toxicity [14]. Indeed, the high concentration-induced increased adherence of IO NPs to the chorion is known to alter not only its thickness but also its physiological functions, as reported by other studies. The disturbance of the homeostasis of this important barrier, and especially the alteration of gas exchanges, could lead to ROS accumulation and thus ultimately to the observed developmental toxicity [14]. In particular, the establishment of hypoxia is tightly associated with the onset of oxidative stress [98]. Moreover, Zhu et al. showed that similar concentrations to the ones investigated by Hafiz et al. (0.1-10 mg/L) of naked Fe_2O_3 NPs did not exhibit any toxicity to embryos or larvae, while again higher concentrations reduced significantly viability (75% 50 mg/L and 45% 100 mg/L) after 168 hpf, with an LC50 corresponding to 53.35 mg/L. The survival of the embryos dropped importantly after 48 hpf, from 90% to 25% at 168 hpf, indicating that also here the embryo toxic effect exerted by the NPs is not only depending on the dose but also on the exposure time itself [14, 15, 97]. Indeed, treatment period is a crucial point in the establishment of toxicity of metal oxide nanoparticles in aquatic organisms [95] Moreover, serious malformations, such as pericardial edema, tissue ulceration, and body deformation, were observed for doses >50 mg/L. These effects were even more accentuated for the group treated with 100 mg/L [14]. In extreme cases, the treated embryos were unable to hatch and died consequently. It must be kept in mind that the observed aggregate formation and precipitation of the naked IO NPs after adding them to the maintenance medium, and which is due to their colloidal instability (especially observed for doses >10 mg/L), possibly affects the effective concentration at which the embryos/larvae have been exposed [14, 94]. However, as zebrafish embryos/larvae are demersal, this effect might be less important than previously stated, and the observed severe toxicity might be due to the IO NPs strong adherence to the organisms surface concomitant with a localized increase of released iron [14, 77, 97, 98]. Another important factor that contributes importantly to IO NPs' toxicity is the state of the iron of the NP itself; Fe^{3+} present in Fe3O4 NPs revealed a greater toxicity than Fe^{2+} stemming from Fe_2O_3 NPs [94]. For example, in the lung cancer cell line A549, bare Fe_2O_3 NPs (20-60 nm) did not reveal any toxicity for concentrations under 200 μg/mL [99]. Interestingly, while bare Fe_2O_3 have been shown to be completely cleared by zebrafish after a prolonged exposure time, Fe_3O_4 particles are still retained in the organism after the same time span [95]. This observation might indicate that while the first ones are excreted through the digestive system, the latter ones may reach other organs where they then accumulate.

Once internalized by an organism, many studies have described the capture of IO NPs by cells belonging to the immune system, and their subsequent degradation concomitant with the release of iron ions [78, 88]. However, under physiological conditions, tissue macrophages are the ones in charge of replenishing the organisms' iron needs by clearance of senescent erythrocytes [100]. Under physiological conditions, free iron ions are sequestered under the form of the redox-inactive Fe^{3+}, while only a small fraction used in the cellular metabolism is available as the redox-active Fe^{2+} [94]. Upon cell absorption, IO NPs accumulate usually inside lysosomes or endosomes where they are metabolized, causing the release of iron ions [94]. Although iron is involved in important biochemical processes, its intracellular levels must be monitored carefully [100, 101]. It is thus clear that any disturbance of the iron homeostasis might affect cellular functions adversely. Importantly, it has been shown that the accumulation of iron in living organisms is associated with the establishment of oxidative stress and pathological conditions [75, 102]. This is because when the iron storing ability is exceeded, the free ions lead to the production of reactive oxygen species and/or reactive nitrogen species (RNS) [15, 103]. Interestingly, while 2.5 mg/L of pure iron ions induced a 100% mortality rate, this could not be observed for the same concentration of investigated IO NPs. Generally speaking, the γ-Fe_2O_3 NPs showed low toxicity when compared to their dissolved counterpart [15]. In biological systems, the Fenton or the Haber-Weiss reaction is at the basis of the generation of ROS molecules [100, 104]. Iron is a transition metal and consequently it can change easily its valence, providing or accepting an electron [98]. Fe^{2+} reacts with hydrogen peroxide under the release of radical OH [94]. It follows that the accumulation of iron, and thus Fe^{2+}, leads to the production of ROS inside the cytoplasm, which then could cause oxidative injury in cells. This would be true especially for uncoated IO NPs, which once endocytosed would release ions easily and thus elevate the intracellular iron concentration disturbing redox homeostasis [105]. Indeed, Pereira et al. showed that semistatic exposure to iron induced neurotoxicity in zebrafish embryos after 24 hours of incubation, while intact IO NPs corresponding to the same concentration did not induce this effect [15]. This comes as "increased free iron" favors the production of the highly reactive hydroxyl radicle, promoting lipid peroxidation, which in turn is further amplified in a self-sustained loop of cytotoxic events as it reacts directly with iron ions [101]. However, ROS is a normal byproduct of cellular metabolism, and as it carries a key role as an intracellular signaling molecule, its concentration is usually regulated by the antioxidative machinery of the cell [106]. Specific enzymes involved in this process ensure the maintenance of intracellular redox homeostasis [87]. It is known that exposure to xenobiotics increases the production of ROS. Under certain conditions, such as IO NP-induced reduction of the mRNA levels of genes involved in the antioxidant defense system or the direct inhibition of their activity [89], ROS can though accumulate and exert its toxicity, damaging biomolecules and the DNA, leading eventually to cell death [87, 100]. Moreover, in this context, a concomitant iron accumulation inside cells has been associated with cellular death due to oxidative injury [94]. As programmed cell death is induced in response to adverse stimuli occurring during embryogenic development, the onset of malformations is a clear indication of toxicity. It has been reported that the increase of intracellular iron levels is correlated

with the dose of administered IO NPs [94], explaining thus the aggravation of the toxic effects in the cited studies implementing higher concentrations.

Several studies revealed that increasing concentrations of IO NPs induce in zebrafish larvae mainly cardiotoxic effects, such as pericardial edema, bradycardia, and cardiac blood accumulation [14, 15, 98]. IO NPs and iron accumulate preferentially in the heart as they display a high affinity for this organ, where they are known to induce several myocardial deficits as shown in mammalian model systems [15]. The cardiotoxic effects, observable in zebrafish embryos and/or larvae after incubation with IO NPs starting from a few hours post-fertilization, could be associated with the failure of the exposed cells to maintain normal physiological functions [15, 104]. Pereira et al. showed that citrate-coated γ-Fe_2O_3 NPs and iron ions reduced significantly the heartbeat rate after 48 h of semistatic exposure, with the latter ones inducing mortality when present at the highest dose (10 mg/L). Static exposure to γ-Fe_2O_3 instead did not induce any effect when compared to the control groups. However, both exposure conditions to γ-Fe_2O_3 and iron induced an increase of embryos displaying bradycardia. Higher concentrations of free iron ions (5 and 10 mg/L) resulted to be toxic for the embryos under both exposure conditions. Interestingly the semistatic exposure had an overall negative effect nearly for all investigated conditions, highlighting the importance of the surrounding circumstances in the establishment of toxicity [15, 75]. The cardiotoxic effects observed by Pereira et al. and induced by these treatments should be related to the accumulation of iron ions in this organ, known to be able to induce inflammation, lipid peroxidation (LPO), and oxidative stress, associated with tissue degeneration and cell death. More in detail, iron accumulation in cardiomyocytes induces the production of the highly toxic hydroxyl radicals [15]. Consequently, it is not surprising that the administration of free iron ions induced a much more severe effect on the treated embryos when compared to the IO NPs, although both iron forms display cardiotoxicity.

In addition, two recent studies focused on the sublethal effects induced by low concentrations of maghemite NPs [77, 98]. Similar to what has been reported previously, higher amounts of IO NPs correlate directly with hatching delay and the induction of cardiac dysfunction [98]. The heart is the first organ to function during embryogenesis, and cardiogenesis itself is one of the most sensitive processes taking place during development. In addition, after uptake, IO NPs are rapidly targeted to this organ thanks to blood circulation. It follows that environmental pollutants to which an organism might be exposed during early life stages would reveal their potentially hazardous effect, especially on this organ, leading to cardiac defects in later life. In zebrafish, cardiogenesis initiates 5 hpf [107], the time point at which most of the conducted experiments regarding IO NP exposure start. The most common targets implemented for the assessment of cardiotoxicity induced by a compound in zebrafish are usually pericardial edema and altered heart rate, the first indicating a general status of dysfunction, the latter instead pointing towards a defective cardiac function [107].

A comparable observation, which could be in line with this, was made by another research group [103]. Most of the research coping with IO NP-associated toxicity identified ROS as the main player involved [81]. However, contrary to what has been previously thought, the production of free radicals is rather attributable to reactions that take place at the surface of the IO NPs than to the dissolved iron oxide ions. Voinov et al. demonstrated that the catalytic centers present on the surface of uncoated γ-Fe_2O_3 nanoparticles are strongly responsible for the production of hydroxyl radicals [105].

Thirumurthi and colleagues described in a recent study that increased amounts of Fe_3O_4 nanoparticles induced malformations by triggering several pathways that are activated by the accumulation of ROS in tissues and organs [98]. To understand better the underlying phenomena, they first treated zebrafish embryos statically with several concentrations of bare IO NPs (10, 20, 40, 60, 80, 100, 120, and 140 ppm) for 96 h. After individuating the LC50 = 60.17 ppm, they choose to assess only the sublethal doses of 40 and 60 ppm in further experiments. However, the obtained results are in sharp contrast with another study performed by Malhotra et al., in which concentrations up to 1000 ppm of bare Fe_2O_3 NPs did not induce any mortality in exposed embryos after 96 h exposure [92]. Thirumurthi et al. monitored the animals throughout the experimental setup for survival, hatching rate, and signs of teratogenicity via microscopy. To evaluate the potential impact of iron levels in the establishment of adverse effects, they further measured the iron content in the groups using inductively coupled plasma mass spectrometry (ICP-MS) and SEM and assessed the number of dissolved iron ions in the medium and animals with atomic absorption spectroscopy (AAS). As the authors were interested in the potential underlying mechanisms triggered by the naked IO NPs, they focused their attention on important biomarkers involved in oxidative stress. Among these, alteration of the activities of acetylcholinesterase (AChE), responsible for cholinergic transmission, and Na^+K^+-ATPase, involved in osmoregulation, are warning bells for xenobiotic toxicity. In addition, apoptosis, ROS, and NO levels, along with LPO and protein carbonyls, hallmarks for protein oxidation were assessed among the groups. As other studies showed that IO NPs could have an impact on the antioxidative response of the cell, the authors investigated further the status of important antioxidant markers. As described in previous studies, the authors revealed a dose- and time-dependent lethality and delay in hatching (10% 40 ppm and 38% 60 ppm), concomitant with colloidal instability of the bare IO NPs associable to high doses. Precipitation of aggregates of IO NPs to the bottom of the plate leads to an immediately increased interaction with the embryos, while adhesion to the chorion and interference with the pores is known to limit oxygenation. Regarding later life stages, it was shown that 40 and 60 ppm led to a 20% and 40% augmentation in teratogenicity, respectively. In line with other studies, both investigated doses induced a reduction in the heartbeat rate (24% 40 ppm and 36% 60 ppm). As Na^+K^+-ATPase in combination with ROS is known to be involved in cardiotoxicity, they now

focused on the activity of this enzyme. They revealed a significant dose-dependent decrease in the activity of the Na^+K^+-ATPase. The opposite effect was obtained for AChE, in which protein levels were increased in the treated groups. The altered activity of this enzyme is associated with developmental neurotoxicity. In line with these alterations, Thirumurthi et al. showed that upon treatment with increasing doses of Fe_3O_4, the animals displayed a concomitant increase of ROS, LPO, PC, and NO levels. Consequent to the augmentation of oxidants, larvae treated with 40 and 60 ppm revealed an elevated number of apoptotic bodies when compared to the control group. Due to these first results, the group focused subsequently on the antioxidant machinery, whose IO NP-induced alteration could be connected to the observed effects. Strikingly, a substantial decrease of SOD, CAT, and glutathione peroxidase (Gpx) activity was assessed in a dose-dependent manner, explaining thus the failure of the cell to counteract the oxidative stress. As described earlier, the accumulation of iron ions is thought to be involved in the establishment of oxidative stress. For this reason, the authors evaluated the amount of iron in the treated larvae. Indeed, it was shown that the exposed animals presented a concentration-dependent increase in iron. Taken together, the authors showed clearly that static exposure of zebrafish larvae for 96 hpf with Fe_2O_3 NPs leads to a significant increase of oxidative stress concomitant with a downregulation of the antioxidant machinery [98].

This observation was partially supported by a study conducted in another aquatic organism, the microalgae *Coelastrella terrestris* [108]. Here, they demonstrated that prolonged incubation of uncoated iron oxide NPs did reduce in a dose-dependent manner (up to 50 mg/L) viability and growth. They identified oxidative stress as a key element responsible for inducing the observed phenotype. It has been suggested that in response to the temporary increase of intracellular ROS levels induced by IO NPs, the cellular antioxidative machinery is activated, including SOD, to reduce its harmful production [106]. In line with this, SOD levels were augmented in cells of *Coelastrella terrestris* accumulating IO NPs.

Jurewicz et al. investigated further the effect of different concentrations of naked and fluorescently labeled Fe_3O_4 nanoparticles ($Cr@Fe_3O_4$) on two-week-old zebrafish larvae [93]. A significantly toxic effect (up to 40%) was revealed for all investigated concentrations above 200 μg/mL after 72 h of exposure, with the establishment of a saturation limit of toxicity for doses >600 μg/mL. One possible explanation of this observation is that higher doses did not lead to a higher metabolization rate of the IO NPs. On the other hand, a high concentration-favored increase in agglomeration and precipitation of the IO NPs could cause a reduction of the interaction of the particles with the larvae, ameliorating thus toxicity. In line with this idea, and keeping in mind a potential effect induced by the presence of the conjugated dye, naked NPs showed an effect only at the highest investigated dose of 800 μg/mL. Indeed, administration of Congo red alone reduced the viability starting from concentrations of 50 μg/mL. The revealed highly life stage-dependent toxicity of the investigated IO NPs can be explained by an increased oral uptake by the zebrafish larvae concomitant with an accumulation of the IO NPs in the digestive tract. Indeed, larvae exposed to 100-800 μg/mL of Cr@Fe3O4 revealed a dose-dependent accumulation of particles mainly in the intestine [93]. Indeed, the digestive system is one of the primary sites of iron absorption under physiological conditions and, together with the liver, usually one of the first organs to be affected by IO NP exposure in zebrafish [97, 100]. In this context, the intestinal barrier is known to play a crucial role in the establishment of NP-induced toxicity [85]. According to the size of the implemented IO NPs, the biodistribution can be limited to these organs, as crossing the intestinal barriers can be hampered by the necessity to rely on active transport mechanisms [91].

3.2. Effects of IO NPs on Adult Zebrafish. Although much less research concerns the toxicological effect of substances on adult zebrafish, this model system proved important especially in the evaluation of cardiotoxicity [107]. In a study performed by Chemello and colleagues, γ-Fe_2O_3 IO NPs were exploited as a drug carrier, to facilitate the absorption of antibiotics in adult zebrafish. After 28 days of incubation with oxytetracycline (OTC), tissue accumulation and toxicology markers were assessed for functionalized and naked NPs [109]. In detail, relative quantification of the expression of genes involved in fish stress response (*hnf4a*, *hsp70.1*, *sod1*, *sod2*, and *gsta1*) and growth (*igf1*, *igf2a*, and *mstnb*) was performed in addition to histological analysis of the liver and intestine to elucidate a potential effect. The results showed that uncoated NPs did not induce any alteration in the gene expression pattern concerning the control group. On the contrary, the presence of OCT, alone or on the surface of the IO NPs, led in some cases to a deviation of normal gene expression. In addition, OCT-coated IO NPs showed a reduction of *hsp70* and *sod1* expression concomitant with an increased expression of *gsta1* in the liver of treated fish. These observations are in line with previous studies, revealing a potentially toxic effect of OCT [109]. The authors reported further that the test group receiving the nanocarrier showed a significant increase in drug accumulation, especially in the digestive system. This is in line with previous studies conducted in zebrafish embryos, evidencing the strong ability of IO NPs to be internalized via oral routes and to be then targeted to the intestine tract. They did not reveal any morphological alterations for all analyzed tissues, not for the conjugated nor for the uncoated IO NPs [109], indicating the importance of the status of the organism itself at the moment of administration in the development of teratogenicity. In addition, the fact that no increase in stress response markers was detectable in the presence of the IO NPs is indicative of the absence of any stress response in adults upon IO NP incubation.

A study conducted in 2015 analyzed the effect of static exposure of Fe_2O_3 and Fe_3O_4 on adult fish in terms of iron accumulation and elimination [95]. For this purpose, adult zebrafish were exposed to the IO NPs at two different concentrations for 28 days and afterward moved to IO NP-free water for 24 days. Interestingly, adult fish exposed to Fe_2O_3 NPs displayed a shift in their coloration, probably

due to the direct accumulation of IO NPs onto the fish skin, or underlying [95]. In line with what has been described earlier for uncoated IO NPs, both types aggregated in the exposure medium. Since Fe_2O_3 precipitated less intensively, their actual exposure to the fish was greater, potentially explaining why the researchers did not observe a shift in the color of the fish treated with Fe_3O_4. Independent of the two investigated concentrations (4 and 10 mg/L), a similar amount of internalized iron was revealed in the fish body after 28 days of incubation. However, the amount of body iron did not reach a steady state but declined after reaching a maximum level, indicating that the chronic gut toxicity established as a consequence of the NP exposure induced a reduction of food intake. Given that NPs are taken up by adult zebrafish mostly via ingestion, this led to a decrease in IO NP uptake and thus whole-body iron levels [95].

Another study evaluated the toxicity of IO NPs in the adult zebrafish brain. For this purpose, different doses of cross-linked aminated dextran-coated IO NPs were injected intraperitoneally. Particular emphasis was given on the activity of acetylcholinesterase at different time points after exposure. Only at the highest investigated concentration (200 mg/kg), the enzymatic activity was strongly reduced 24 h posttreatment, concomitant with impaired swimming behavior, indicative of brain toxicity [110]. Although this effect was given only at this time point, no transcriptional regulation seemed to be at its basis. In addition, under the same condition, a significant accumulation of iron in the brain, as well as the increased expression of genes involved in oxidative stress (transcriptional factor AP-1), inflammation (caspase-9), and apoptosis (caspase-8), was observed. Moreover, the oxidative stress markers gclc, *Gpx1a*, *cat*, *gstb1*, and *sod2* were differentially expressed when compared to the control groups. The obtained results are in line with previous findings, where a localized accumulation of IO NPs and thus iron induces oxidative stress, apoptosis, and proinflammatory signaling. In addition, it has been shown several times that mostly high concentrations of IO NPs develop toxicity, underlying the importance to establish carefully the upper limit for each use.

In 2018, Zheng et al. evaluated the effect of 100 mg/L naked and starch-coated Fe_3O_4 nanoparticle exposure of 7 days on two different organs, the liver and the gills, known to be a common target for IO NP accumulation [111]. As this concentration of bare IO NPs is known to induce cytotoxic effects in a relatively short exposure time, the authors chose it to discern a possible effect of the coating. To prevent particle aggregation and improve biocompatibility, bare IO NPs are often stabilized or coated with various solvents or chemicals. However, it is widely accepted that the nature of these coatings has an impact on the potential toxicity of IO NPs [111]. Among these, starch coatings are widely implemented in different applications, but especially in the environmental remediation sector. To elucidate this potential effect of the coating on the IO NP-induced toxicity, Zheng and colleagues relied on the transcriptome sequencing (RNA-seq) technique. It was shown that naked NPs accumulated preferentially in the gills where they exerted their toxicity when compared to the coated ones, probably due to higher aggregation and negative surface charge. Indeed, a total of 17 genes involved in immune response, inflammation, oxidative stress, antioxidant response, and endoplasmic reticulum (ER = stress) were differentially expressed upon the treatment. Strikingly, only 3 of these genes were altered in the gills of fish exposed to starch-coated particles, strongly suggesting that the presence of the coated ameliorated notably the toxic effects of the IO NPs on this organ. Bare particles displayed generally higher bioaccumulation in the whole zebrafish when compared to the coated IO NPs. As the gills are one of the first external targets for MO NPs upon exposure, their accumulation in this organ seems logical. However, after surpassing this first entry point, especially the starch-coated IO NPs reach the liver, as their increased biocompatibility renders them more transportable. This is in line with previous findings and further supported by the fact that the liver acts as a reservoir for excess iron and is involved in its excretion [111]. While Zheng and colleagues did not reveal any mortality upon treatment, they noted a noteworthy alteration of gene expression profiles in the investigated organs. More in detail, especially in the case of bare IO NPs, an increase in the gene expression of genes involved in stress response and inflammation was observed. This finding is supported by a wide body of evidence, showing that exposure to IO NPs triggers stress responses and associated toxicity in several in vitro and in vivo model systems [99, 106, 111]. However, the affected sets of genes identified to be altered by IO NPs were only barely overlapping. This difference could be explained by the fact that according to the surface composition of the IO NPs, the interaction with the target organ and thus the activation/inactivation of downstream signaling might be of a different entity. While the presence of the starch coating mitigated the toxic effects at the level of the gills, an increase was observed instead in the liver. This observation is in line with the fact that the coated IO NPs accumulated mainly in the latter one. Indeed, in the liver, both exposures led to an upregulation of genes involved in immune and inflammation responses, concomitant with a downregulation of genes involved in DNA damage and repair. Genes involved in DNA damage/repair and apoptosis (i.e., *tp53*) were differentially expressed especially in the case of starch-coated NPs, indicating the possibility that the nature of the coating is involved in determining mainly this alteration. Interestingly, in the same organ, both forms induced a notable upregulation of the stress gene indicator, cytochrome P450 1 A (*cyp1a*), involved in the antioxidant defense system. In addition, also *tsc22d3*, a marker for an inflammation stress condition, was significantly overexpressed. In line with previous findings, several genes involved in the mitochondrial dysfunction pathway were differentially expressed after exposure to bare particles, further suggesting the production of ROS. Despite the chemophysical properties of the IO NPs, the properties of the main target tissue must be evaluated to assess properly a potentially toxic effect. However, in the study conducted by Zheng et al., both types of IO NPs increased the expression of biomarkers involved in the pathways governing DNA damage, apoptosis, and oxidative stress, in both tissues, indicating that the treated zebrafish were exposed to constant stress.

To assess further the potential ecotoxicity induced by IO NPs accumulating in the environment, another recent study instead investigated the effect of Fe_3O_4 MNPs in terms of behavioral and biochemical alterations in zebrafish adults [92]. More in detail, several tests that indicate potential neurotoxicity, such as novel tank, mirror biting, social interaction, shoaling, circadian rhythm, and short-term memory, were performed after 96 h exposure. In particular, the authors assessed two different concentrations, 1 and 10 ppm, with the latter corresponding to the maximal concentration of iron allowed to be present in the Taiwanese industrial waste effluents.

Diverse to what has been described in other studies, Malhotra et al. did not reveal a difference of iron content in ROS levels of the brain, the liver, and the gills of treated and control fish for the investigated concentrations, hinting towards the fact that these kinds of IO NPs are either readily excreted from the adult fish or their uptake from the surrounding environment is reduced [95]. Consequently, it could be hypothesized that potentially associated hazardous effects should be absent for the investigated concentrations. For this purpose, the expression patterns of biomarkers involved in oxidative stress induction and defense were assessed. In line with the absence of IO NP accumulation in this organ, no increase of local ROS levels was observed in the brain of treated fish. In addition, mRNA levels of the enzyme CAT, importantly involved in the antioxidative stress response [106], were significantly increased for the 10 ppm treated groups, indicating a state of stress. It followed that cortisol and catecholamine levels were evaluated, and indeed, an increase of cortisol was revealed again for the highest dose. In addition, hypoxia-inducible factor-1α (*HIF-1α*), adenosine-5′-triphosphate (ATP), and creatine kinase (CK) together with markers of DNA damage (ssDNA) were evaluated. Interestingly, only the DNA damage marker revealed a significant upregulation in fish treated with 10 ppm. Exposure to a high dose could thus be associated with the induction of stress response in zebrafish concomitant with elevated brain cortisol levels. Further, the authors showed that an especially high dosage of MNPs could induce several alterations in neurological behavior. For example, a significant correlation was observed in terms of reduced novel tank exploration as well as a reduction in social behavior. Zebrafish are highly social animals, and especially under threat, they tend to swim tightly together. This comportment is known also as shoaling behavior and indicates the anxiety status of the animals. Malhotra and colleagues were able to demonstrate that group formation was tightened in an IO NP dose-dependent manner, indicating increased anxiety in the treated fish. This is in line with the fact that IO NP-exposed fish showed reduced locomotion and exploratory activity for both investigated doses and tended to spend less time at the top of the tank. Furthermore, IO NP exposure led to a considerable reduction in social interaction among the treated fish in comparison to the control group. As no difference was revealed during the mirror biting assay, treated fish did not seem to be more aggressive, although swimming speed was notably increased in the group that has been treated with 10 ppm of IO NPs, underlying a dose-dependent impact on the behavioral patterns. Interestingly, a high concentration of Fe_3O_4 NPs affected the circadian rhythm locomotor activity in both light and dark cycles, while 1 ppm induced an alteration only in the light cycle.

These observations were further supported by the fact that exposed fish showed a reduction in the neurotransmitter levels of serotonin, known to be associated with anxiety and depression-like behavior. In addition, the same groups revealed decreased dopamine levels, responsible for stress response, explaining the observed reduction in locomotor activity and aggressiveness. An interesting point in this study is that a high dosage of Fe_3O_4 MNPs is correlated to memory deficiency and changes in the levels of the cholinergic neurotransmitter. Indeed, the results revealed that a high dosage of IO NPs had an adverse effect on short-term memory. As reported previously, alteration of AChE is strongly related to neurotoxicity. In line with the behavioral observations made by Malhotra et al., fish treated with both doses of IO NPs showed a significant decrease in AChE when compared to controls. This finding is in line with the study performed by de Oliveira et al. [110], where treatment with high doses of MNP induced a reduction in the enzymatic activity.

4. Zinc Oxide Nanoparticles

Zinc oxide is considered a safe material and is approved by the Food and Drug Administration [112]. It is one of the most used metal oxides due to its unique physical and chemical properties, including semiconducting, photo- and sonocatalytic, and piezo- and pyroelectric properties [112, 113]. For all these reasons, zinc oxide nanoparticles have gained scientific interest and present a wide range of applications [114], including cosmetics, optoelectronics [115], ceramics, and pigments; they are implemented as catalysts as well as pain killers and for itch relief.

ZnO nanoparticles present strong antimicrobial properties [5, 6, 116–118]. The antibacterial toxicity of ZnO NPs has been tested against different gram-positive and gram-negative bacteria, such as *Vibrio fischeri*, *Staphylococcus aureus*, *E. coli*, *Salmonella typhimurium*, and *Klebsiella pneumoniae*, showing that higher concentrations of NPs are more toxic [117]. Moreover, in the latest years, ZnO NPs have emerged in the cancer nanomedicine field. As mentioned before, iron oxide nanoparticles are already in clinical use for the hyperthermia treatment of cancer cells. Also, ZnO NPs are implemented in cancer diagnosis and therapeutics due to their unique physicochemical properties and low toxicity impact under certain circumstances [119]. For instance, an immunosensor was developed using ZnO NPs for the early and accurate diagnosis of patients with hepatocellular carcinoma detecting des-carboxy-prothrombin (DCP), which is a highly specific and sensitive biomarker for liver cancer [119, 120]. Taking advantage of their photodynamic and sonodynamic properties, ZnO NPs could be used for exerting remotely cancer cytotoxicity upon an external stimulus, such as light [121], or a mechanical one, like ultrasound [122]. ZnO nanoparticles are also used as targeted and pH-triggered drug delivery systems, as other MO NPs. Indeed, different sizes and shapes of ZnO NPs have been

Table 4: Impact of ZnO NPs on zebrafish.

Stage	NPs diameter	Treatment time	Tested concentrations	General toxicity response	Specific ROS responses	Reference
Embryos	20 nm	96 h	0.1, 0.5, 1, 5, 10, and 50 mg/L	Significant decrease of survival rate; delay in hatching rate dose-dependent; 96 h LC50 = 1.793 mg/L; and several abnormalities (body accusation and pericardial edema).	—	[34]
Embryos	20 nm	96 hpf	0.1, 0.5, 1, 5, 10, 50, and 100 mg/L	Decrease of survival rate; delay in hatching rate; and incidence of pericardial edema dose-dependent.	Increase in ROS production; low levels of *Gstp2* and *Nqo1* expressions; and downfall in counteracting the ROS by oxidative stress responses.	[138]
Embryos	<100 nm	144 hpf	1, 5, 10, 20, 50, and 100 mg/L	No effect bin the survival rate; important decrease in the hatching rate; and different malformations (spinal curvature and hyperemia).	Important elevation in the SOD activity and MDA levels in a dose-dependent way; decrease in CAT activity; high levels of ROS; DNA damage only at the highest concentration tested; and important downregulation in *Bcl-2*, *Nqo1,* and *Gstp2* transcriptions and upregulation in *Ucp-2* level.	[18]
Embryos	30 nm	96 hpf	1, 5, 10, 25, 50, and 100 mg/L	Decrease in survival rate and increase in hatching rate dose-dependent; severe decrease in body length.	—	[18]
Embryos	<100 nm	96 hpf	1, 5, 10, 20, 50, and 100 mg/L	—	Increase in the lipid peroxidation and SOD activity; upregulation in the expression of the *ppaα* and *sod1*; downregulation of *cat*; altered expression of antiapoptotic genes (*bcl-2*) and proapoptotic (*bax*, *puma*, and *apaf-1*; upregulation of *p53* gene, with overexpression of its protein; and increase in the activity of caspase-3 and caspase-9.	[116]
Embryos	9.4 nm	96 hpf	0.2, 1, and 5 mg/L/	Dramatic delay in hatching.	Upregulation of the cat and Cu/Zn-sod transcripts in embryos and downregulation in eleuthero; important upregulation of Mt2<; different expression of mRNA of *IL-1β*, *TNFα*, and proinflammatory cytokines in eleuthero-embryos in comparison to embryos; alteration in the jun proto-oncogene (*c-jun*) embryos treated with high concentration; and perturbation in antiviral and immune-related gene Myxovirus resistance A.	[131]
Embryos	50–70 nm	144 hpf	0.1, 0.5, 1, 5, and 10 mg/L	Significant delay in hatching for ZnO NPs and Zn ions; no significant difference in cotreatment with	ROS generation; cotreatment with BSO: lower production of GSH.	[132]

Table 4: Continued.

Stage	NPs diameter	Treatment time	Tested concentrations	General toxicity response	Specific ROS responses	Reference
				ZnO NPs and NAC; and increased rates of delay in hatching in cotreatment with BSO. LC50 for Zn^{2+} =7.9 mg Zn/L, LC50 ZnO SMPs =10.0 mg Zn/L LC50 nanosticks =7.1 Zn/L		
Embryos	Nanospheres: 27 nm; nanosticks: 32×81 nmM; and SMPs: 202 nm	120 hpf	2, 4, 8, 16, and 32 mg Zn/L	LC50 nanospheres =11.9 mg Zn/L, respectively; higher toxicity of Zn ions in comparison to the different shaped NPs; and decrease of hatching rate dose-dependent in the embryos treated with all the different kind of nanoparticles and sulfate, strongest delay in samples exposed to nanosticks. Decrease dose-dependent of swimming activity; nanosticks more toxic than the other NPs.	—	[133]
Embryos	5, 10, 15, 26, 34, 62, and 70 nm	120 hpf	0.016 to 250 mg/L	Significant mortality at 24 hpf for all the coated NPs; no alteration in mortality with bare nanoparticles.	—	[134]
Embryos	20-30 nm	96 hpf	0.01, 0.1, 1, and 10 mg/L	Higher mortality rate by ZnO NPs than $ZnSO_4$; LC25 for ZnO NPs =2.64 mg/L; LC25 for $ZnSO_4$ = 7.75 mg/L; and significant embryonic malformations after both treatments (tail malformation, pericardial edema, and yolk sac edema).	Downregulation of *ogfrl2* and *intl2* transcripts; upregulation of *cyb5d1*.	[17]
Embryos	<100 nm	48 h	10, 30, 60, 90, or 120 mg/L	Delay in hatching, increased heart rate, pericardial edema, hyperemia, yolk sac edema, spinal curvature, tail deformities, and swim bladder abnormalities.	SOD increased activity; *sod1* upregulation; CAT downregulation; increased MDA levels; and increased production of ROS.	[116]
Embryos	40 nm	96 hpf	12.5, 25, 50 mg/L; PFOS (0, 0.4, 0.8, and 1.6 mg/L); and PFOS plus ZnO-NPs (0.4 + 12.5, 0.8 + 25, and 1.6 +50 mg/L	—	Significant increase of SOD activity as well as the activity of glutathione peroxidase; decrease dose-dependent of CAT activity: excess of ROD; increase of MDA level; upregulation of Bax; downregulation of *Bcl-2*; and no changes in the activities of the caspase-3 and caspase-9 (apart at 50 mg/L).	[124]
Embryos	300 nm	72 h, 96 h	10-100 ppm	Mitigate effects on the toxicity of ZnO NPs induced organic matter.	—	[4]

Table 4: Continued.

Stage	NPs diameter	Treatment time	Tested concentrations	General toxicity response	Specific ROS responses	Reference
Embryos, adults	PEG =2588 nm PVA =58 nm PVP =60 Bare =69 nm	Embryos: 72 h Adults: 96 h	Embryos: 0.001-100 mg/L	Embryos: morphological defects (yolk sac edema, notochord bending, and egg coagulation) for bare and the capped NPs; rates of toxicity after treatment with 10 mg/L were 38.67%, 28.49%, 95.46%, and 89.32% for PEG-, PVA-, and PVP-capped and bare ZnO NPs, respectively; toxicity of bulk ZnO < ZnO-PVA < ZnO-PEG < ZnO NPs < ZnO-PVP. Adults: LC50 of bulk ZnO =3239 mg/L; LC50 ZnO-PEG =6.44 mg/L; LC50 ZnO-PVA =9.40 mg/L; LC50 ZnO-PVP =3.77 mg/L; LC50 ZnO NPs =20.72 mg/L; and different morphological alterations; severe damages to the gill tissues (secondary lamellar structure alterations, necrosis, desquamation, acute cellular swelling, aneurysm, and lamellar disorganization).	—	[16]
Adults	30 nm	96 h	2, 5, 10, 30, and 50 mg/L	Toxicity dose-dependent; 100% of mortality at 30 mg/mL of ZnO NPs and bulk ZnO; and LC50 = 4.92 mg/L and 3.31 mg/L, for the ZnO NPs and bulk ZnO, respectively.	Increase of SOD activity SOD in the gut; reduction of CAT activity in the liver; increase of CAT activity in gut and gills (only slightly); decrease of GSH in the liver; MDA levels higher in the case of liver; and injuries in the gill tissues with shrinkage of the cells, loss of the cytoplasm, and abnormalities in the nuclei shapes.	[9]

Abbreviations: *Bax*: BCL2-associated X, apoptosis regulator; *bcl2*: B-cell lymphoma 2; BSO: buthionine sulfoximine; CAT: catalase; *cyb5d1*: cytochrome b5 domain containing 1; GSH: glutathione; Gstp2: glutathione S-transferase P 2; hpf: hours post fertilization; *IL-1β*: interleukin-1*β*; *intl2*: Intelectin 2; LC50: 50% of lethal concentration; MDA: malondialdehyde; Mt2: metalloprotein 2; NAC: N-acetyl cysteine; *Nqo1*: NAD(P)H:quinone oxidoreductase; *ogfrl2*: opioid growth factor receptor-like; PEG: polyethylene glycol; PVA: polyvinyl alcohol; PVP: polyvinylpyrrolidone; PFOS: perfluoro octane sulfonate; ROS: reactive oxygen species; SMPs: submicron particles; *TNFα*: tumor necrosis factor-*α*; *Ucp-2*: uncoupling protein 2.

used for this reason, including mesoporous nanospheres and dandelion-like or hexagonal structures [112]. A lot of nanomaterials have been employed in tissue engineering, which is possible due to the easy functionalization methods of their surface with peptides, proteins, and other molecules [112]. As mentioned previously for IO NPs, the biocompatibility of ZnO NPs makes them a good candidate for several biomedical purposes.

Since they can absorb UV radiation, they are commercially used in sunscreens and other products of personal care. In addition to their increasing employment in theragnostic and therapeutics, a lot of questions have been raised on their impact on the aquatic systems [123] and the potentially negative and toxic effects in different organisms. To address the toxicity of these nanoparticles, a lot of studies have been performed on bacteria, plants [124, 125], cells [8, 126], and vertebrates [4, 127].

Understanding the toxicity induced by ZnO NPs turned out to be a quite challenging task for the scientific community. This comes as a large number of parameters contribute to this, such as high experimental condition variability, NP formulation, size, and surface coating [128]. Each of them results in diverse NP physicochemical characteristics that eventually affect the release of Zn^{2+} ions, the reactive oxygen species and photocatalytic ROS production, the pharmacokinetics and biodistribution, and the dynamic interactions with cells [128, 129]. Nevertheless, given the huge potential and advantages of the ZnO NP supersize, researchers focus intensively on approaches allowing to mitigate possible negative aspects while investigating at the same time the optimal working conditions [4, 130]. For this reason, several works have evaluated the potential interactions of ZnO NPs with zebrafish (Table 4).

4.1. Effects of ZnO NPs during the Development. Different studies have revealed a dose-dependent toxicity of ZnO NPs in zebrafish during the development [16, 18, 55, 131]. The first work on the toxicological profile of ZnO NPs in zebrafish reported a significant decrease in the survival rate and a delay in the hatching rate, both concentration-dependent, with a value of the LC50 at 96 h of 1.793 mg/L. In addition, larvae presented several abnormalities typical of metal oxide nanoparticle-induced toxicity, including body accusation and pericardial edema [34]. One year later, the same research group demonstrated that the concentration-dependent toxicity of zinc oxide nanoparticles was due to the sedimentation and formation of nanoparticle aggregates (micron-sized) in the experimental plate during the ZnO NP exposure time. Moreover, by using a fluorogenic ROS indicator, an increase in ROS production was detected in treated embryos and larvae. Concomitant with this expression analysis of genes encoding for the oxidant metabolism enzymes, glutathione S-transferase P 2 (*Gstp2*) and NAD(P)H:quinone oxidoreductase (*Nqo1*) revealed a downregulation, hinting thus towards a downfall in the oxidative stress response counteracting normally ROS. Indeed, the impairment of the antioxidant system is known to be associated with the establishment of oxidative stress and injuries. Similar behavior of the previously investigated biological markers was also shown by a subsequent work performed by Bai et al., even if the treated larvae displayed only one malformation, characterized by a severe reduction in the larvae body length [18]. In 2013, Zhao et al. investigated deeply the toxicological profile of ZnO NPs during zebrafish development, focusing also on the DNA damage and oxidative stress. The survival rate did not present any important changes for all the tested groups, while the hatching rate was importantly decreased. In addition, they revealed different morphological malformations, such as tail deformity, spinal curvature, and hyperemia. The study of the antioxidant defense system showed an important elevation in the SOD activity in a ZnO NP concentration-dependent way. In line with this, also the MDA levels were significantly increased in embryos treated with ZnO NPs. CTA activity was instead found to be lower in treated samples in comparison with control ones. Importantly, the level of reactive oxygen species in exposed zebrafish was significantly increased for all the treatments, while the DNA damage level was augmented only at a ZnO NP dose of 100 mg/L [129]. Positive correlations were detected between ROS and DNA damage levels, as well as between ROS and MDA. Moreover, the gene expression analysis of several genes of antioxidant proteins (*Bcl-2*, *Nqo1*, and *Gstp2*) revealed an important downregulation, as previously reported also by Bai et al. [18]. On the contrary, the transcriptome level of uncoupling protein 2 (*Ucp-2*) was importantly upregulated in all the treated groups. These findings underline the fact that ZnO NPs cause adverse effects in zebrafish during the development, leading to an alteration in the expression of genes involved in the oxidation concomitant with oxidative stress [129].

A perturbation in the different toxicological endpoints of zebrafish embryos/larvae treated with ZnO NPs was noted also in other studies [4, 131]. Since Zn^{2+} ions can be released from the ZnO and subsequently transported and uptaken from the embryos, the effects of ZnO NPs and Zn^{2+} were evaluated separately [131]. Zebrafish embryos treated both with ZnO NPs and Zn^{2+} presented a dramatic delay in hatching [131]. The expression analysis by RT-qPCR of specific genes involved in oxidative stress in embryos treated with ZnO NPs and Zn^{2+} showed an upregulation of the cat and Cu/Zn-sod transcripts at 2 dpf, and a downregulation at 3 dpf, respectively, at the highest investigated doses. Instead, eleuthero-embryos showed a downregulation at 5 dpf. On the other hand, the expression of Mt2 was strongly upregulated at 2 dpf and 4 dpf in all the tested doses of both ZnO NPs and Zn^{2+}. Moreover, mRNA levels of interleukin-1β (*IL-1β*), *TNFα*, and proinflammatory cytokines presented a different expression pattern in eleuthero-embryos in comparison to normal embryos. In eleuthero-embryos treated with Zn^{2+} or ZnO NPs, the *TNF-α* and the *IL-1β* were upregulated, while they were downregulated in treated embryos. Furthermore, an alteration of the jun proto-oncogene (*c-jun*) was detected only in the case of embryos treated with a high concentration of Zn^{2+} and ZnO NPs. In addition, also the antiviral and immune-related gene Myxovirus resistance A (*MxA*) was perturbed in the treatment, both with Zn^{2+} and ZnO NPs. These results indicated that the perturbations

induced by Zn^{2+} and ZnO NPs were stronger in the treated embryos in comparison to eleuthero-embryo, indicating that early-stage embryos are more sensitive to nanoparticle exposure [131]. The effects of Zn^{2+} in comparison to ZnO NPs were evaluated also in other studies. Ultrafiltration and ICP-OES allow to calculate the dissolved Zn ions [16]. The concentration of Zn ions keeps increasing over time and is transduced in an increase of pH [16, 18]. The presence of released Zn^{2+} ions derived from the ZnO NPs could explain the low hatching rates [4]. However, this is not yet clarified and there are different contradictory studies, some of which support the same conclusion, while others claim that ions contribute only partially to the low hatching rate. Chen et al. compared the adverse effects of ZnO NPs in zebrafish during the development in comparison to Zn ions. Both treatments induced a hatching delay that was more severe in the groups of embryos treated with ZnO NPs, rather than in those exposed to Zn ions alone. However, as Zn ions did cause a delay in hatching, it can be concluded that the toxicity on hatching is probably caused by a combination of different factors. Indeed, the presence of released Zn^{2+} ions contributes to this. The induced ROS generation and, consequently, the oxidative stress could be another reason [132]. To understand better the cause that leads to the hatching delay, Chen et al. coexposed the embryos to ZnO NPs and NAC or buthionine BSO. In the groups cotreated with ZnO NPs and NAC, no significant difference was observed. However, treatment with BSO further increased the rates of delay in hatching. Moreover, when GSH was no longer synthetized due to the presence of BSO, further hatching delay was observed, suggesting that oxidative stress could be related to the hatching delay along with Zn^{2+} ion release [132].

In the same year, another study evaluated the effects of zinc oxide nanoparticles with different shapes, including submicron particles, nanosticks, and nanospheres [133] and $Zn(NO_3)_2$. The LC50 values for $Zn(NO_3)_2$, ZnO SMPs, nanosticks, and nanospheres at 120 hpf were 7.9 (7.1–8.8) mg Zn/L, 10.0 (8.9–11.1) mg Zn/L, 7.1 (6.8–7.5) mg Zn/L, and 11.9 (10.3–13.7) mg Zn/L, respectively, reporting higher toxicity of Zn ions in comparison to the differently shaped NPs. The hatching rate showed a dose-dependent decrease in the embryos treated with all the different kinds of nanoparticles and sulfate, with the strongest delay in samples exposed to nanosticks. Besides this, the swimming activity displayed a dose-dependent decrease. The ZnO nanosticks were found to be more toxic in comparison to nanoparticles with other shapes [133].

To determine the contribution of Zn^{2+} ions in the toxicity of ZnO NPs, $ZnCl_2$ or $ZnSO_4$ exposure is used to compare experimentally the toxic effects [16, 17]. Choi et al. performed toxicity experiments exposing the embryos to ZnO NPs and $ZnSO_4$ to compare eventual effects on zebrafish development. As it is also shown in other studies, exposure to nanoparticles leads to a higher rate of mortality than exposure to only $ZnSO_4$. The LC25 values for ZnO NPs were 2.64 mg/L and 7.75 mg/L for $ZnSO_4$ [17]. However, embryos showed significant embryonic malformations after both treatments, including tail malformation, pericardial edema, and yolk sac edema, indicating an adverse impact given by the presence of nanoparticles and Zn ions (Figure 3) [17]. In particular, embryos exposed to all the tested doses of ZnO NPs presented a yolk sac edema. After an extended analysis of differentially expressed genes (DEGs) in larvae zebrafish, it was shown that exposure to ZnO NPs and $ZnSO_4$ affects different molecular mechanisms and subsequently causes distinct toxic effects. In particular, the treatment with ZnO NPs altered genes involved in the immune system inflammation. Indeed, the expression of *ogfrl2* (opioid growth factor receptor-like 2 [ogfrl2]) and Intelectin (2*intl*2) was upregulated after treatment with ZnO NPs, while cytochrome b5 domain containing 1 (*cyb5d1*) was upregulated. Together with *cyb5d1*, *Ogfr12* and *intl2* play an important role in developmental and transcriptional regulation, and both genes were upregulated after treatment with Zn nanoparticles [17].

Wehmas et al. instead found that Zn ions caused the same mortality rate and affected zebrafish development in the same way as ZnO NPs. This result suggests that the toxicity is mainly due to the presence of dissolved zinc ions [16]. But again, also in this case, not all the reported studies arrive at the same conclusion. Indeed, Xiong et al. observed that all the zebrafish embryos died at a concentration of 30 mg/L ZnO NPs or their bulk counterpart after 96 h of exposure [9]. In addition, a high toxicity rate was observed in the group of embryos treated with Zn^{2+} ions. The LC50 values were 4.92 mg/L, 3.31 mg/L, and 8.062 mg/L for ZnO NPs, ZnO bulk, and Zn^{2+} ions, respectively. As a result, the released $Zn2^{+}$ ions could not be the main cause of toxicity, but it is rather the combination of nanoparticles with ZnO [9], as in the case of other metallic oxide NPs.

As for other metal oxide nanoparticles, the influence of coating and size on the toxicity of zinc oxide nanoparticles was evaluated [116]. To this end, zebrafish embryos were treated with 17 different types of ZnO NPs, and they were investigated in terms of 19 different toxicological endpoints, including morphological and behavioral tests. The biological parameters that resulted to be more affected in all the tested nanoparticles were the mortality/survival rate. In particular, all tested and differentially coated nanoparticles induced significant mortality at 24 hpf, while the bare nanoparticles did not lead to important alterations until 5 dpf. These findings indicate that the surface coating, as in the case of other families of nanoparticles, is a key factor influencing the adverse effects in biological systems [134]. Next, the effects of ZnO NPs functionalized with polymeric surface-modifying agents including polyvinyl alcohol (PVA), polyethylene glycol (PEG), and polyvinylpyrrolidone (PVP) were evaluated in zebrafish during the development [130]. The treatment with the bare or the capped nanoparticles caused morphological defects, such as yolk sac edema, notochord bending, and egg coagulation. Indeed, the rates of toxicity reported after treatment with 10 mg/L were 38.67%, 28.49%, 95.46%, and 89.32% for PEG-, PVA-, and PVP-capped and bare ZnO NPs, respectively [130]. It was demonstrated that the NP toxicity is a combination of the toxicity caused by dissolved Zn ions and aggregation of nanoparticles on the eggs, shown by the increased toxicity caused by capped or bare ZnO NPs in comparison to bulk

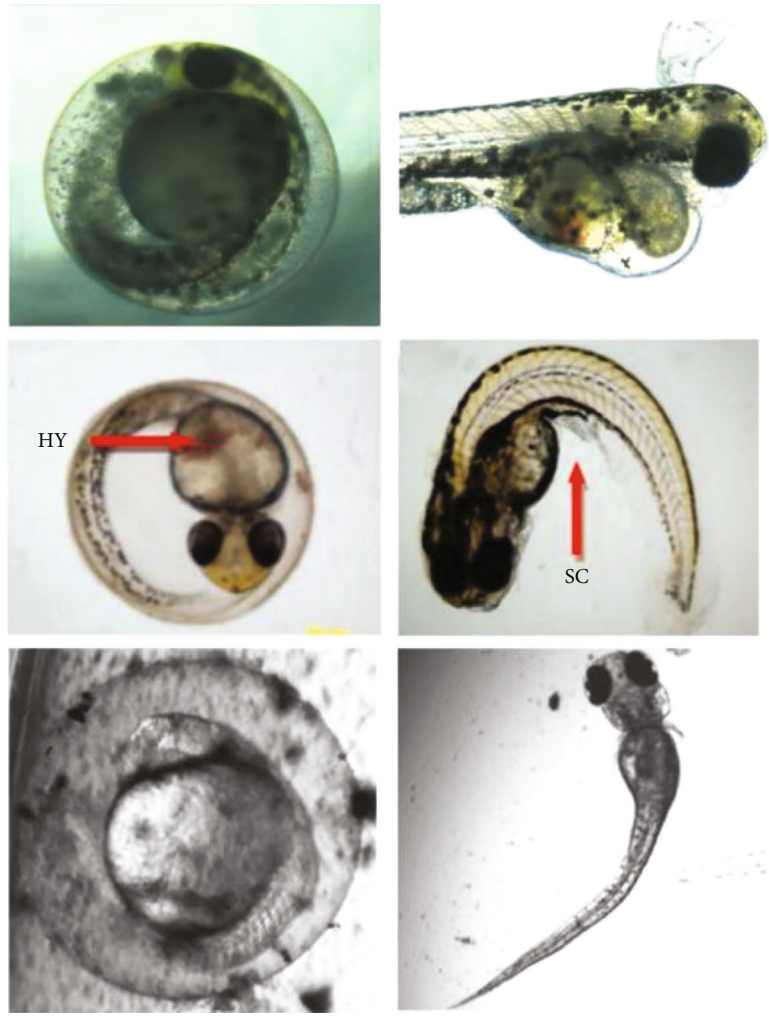

Figure 3: Malformations induced by ZnO NPs in zebrafish during the development. Reproduced with permissions from [17, 135, 137].

ZnO (bulk ZnO < ZnO − PVA < ZnO − PEG < ZnO NPs < ZnO − PVP) [130].

The effects of size and surface charge were deeply investigated by Verma et al. [135]. Here, they evaluated a potential impact on the zebrafish development of different ZnO nanoparticles produced by the HEBM technique relying on a variety of milling times [55, 56]. They showed that decreasing the size and the charge influenced proportionally both the survival and hatching rates of treated embryos. This observation was confirmed also in the case of the heartbeat rate and incidence of malformations (Figure 3). In addition, ZnO NPs induced an increase in ROS production in zebrafish larvae and embryos, as already observed in previous works [134, 136].

Several studies have also reported that treatment with ZnO NPs affects the expression of different genes which play a crucial role in oxidative stress and inflammation [116]. The expression and activity of CAT and SOD and the levels of MDA were evaluated in zebrafish embryos exposed to different concentrations of ZnO NPs [116, 136]. Embryos treated with ZnO NPs in a concentration range of 30-120 mg/L showed an increase in lipid peroxidation and in SOD activity and revealed perturbations of genes involved in the antioxidant defense mechanism. In particular, an upregulation was found in the expression of *ppaα* and *sod1*, while *cat* was downregulated. To understand if such an increase in SOD activity was caused by the released Zn^{2+} ions, Zhao et al. treated zebrafish embryos with dissolved ions. They concluded that dissolved Zn^{2+} ions in concentrations below 60 mg/L do not lead to increased SOD activity. This means that the upregulation of SOD cannot be caused only by the release of Zn^{2+} ions from the nanoparticles, but other factors contribute to it [116]. Furthermore, the production of ROS, the basis of oxidative stress, was confirmed by an altered expression of antiapoptotic genes (*Bcl-2,* B-cell lymphoma 2) and proapoptotic (*bax, puma*, and *apaf-1*) genes. In addition, the transcription of the *p53* gene was upregulated causing an augmentation of p53 and cytochrome C protein levels. To determine the effect of ZnO NPs on apoptosis, also the expression levels of genes related to apoptosis (antiapoptotic and proapoptotic genes) were evaluated. Augmenting the concentration of nanoparticles, a higher apoptotic ratio was observed in a dose-dependent manner (10-120 mg/L), corresponding to a significant increase in the activity of

caspase-3 and caspase-9. As the expression of ROS is involved in the mitochondrial pathway responsible for the induction of apoptosis, it is plausible that its accumulation leads to a concomitant increase in MDA levels. In this framework, Du et al. treated zebrafish embryos with different doses of ZnO NPs and measured the activity of antioxidant enzymes at 96 hpf [136]. In agreement with the previous results, the SOD activity was significantly increased even in embryos treated with the lowest concentration of nanoparticles, as well as the activity of glutathione peroxidase. In contrast, the CAT activity was decreased in a dose-dependent manner. However, despite this reduction, the expression of *cat* was not different from the control. The levels of intracellular ROS were analyzed by the cell-permeable dye DCFH-DA. ROS levels were highly increased in a dose-dependent manner in the groups of zebrafish exposed to ZnO NPs [136]. Moreover, the cellular content was evaluated. As for the ROS, the MDA levels were significantly increased after treatment with 25 and 50 mg/L of ZnO. While the expression of BCL2-associated X apoptosis regulator (*Bax*) was significantly upregulated, *Bcl-2* resulted to be downregulated after treatment with 50 mg/L for both conditions. These findings are in agreement with the study conducted by Zhao et al. [116]. The only difference was related to the caspase activity. In fact, Du et al. did not find any changes in the activities of the caspase-3 and caspase-9 after exposure with ZnO NPs for 96 h [136]. However, the expression of caspase-3 was upregulated in the groups treated with 25 and 50 mg/L of ZnO NPs, with caspase-9 resulting to be upregulated in the group treated with 50 mg/L. Both studies, as well as others, conclude that apoptotic cell death is mediated by oxidative stress [116, 136].

4.2. Effects of ZnO NPs on Adults. The first work performed on ZnO NPs and adult zebrafish has deeply investigated the adverse and oxidative effects of this class of nanoparticles in comparison to the titanium nanoparticles and their bulk counterparts [9]. To this end, adult zebrafish were exposed to different concentrations of NPs and bulk materials for 96 h. It was shown that the toxicity of ZnO NPs and bulk ZnO was dose-dependent. Treatment with 30 mg/mL of ZnO NPs and bulk ZnO led to a 100% of mortality. The values of LC50 at 96 hpf were found to be 4.92 mg/L and 3.31 mg/L, for the ZnO NPs and bulk ZnO, respectively. Zebrafish treated under light or dark conditions with the highest dose of ZnO NPs and bulk ZnO presented a temporary increase in liver activity of SOD in the gut, compared to the controls. Interestingly, in the groups of zebrafish treated with bulk ZnO, the SOD activity was less than the control in both tissues [9]. The CAT activity instead was reduced in the liver, whereas in the gut and gill (but only slightly), it was shown to be increased. Glutathione was decreased in the liver tissue after 96 h of exposure, probably due to ROS that neutralized it. However, in the gut tissue, an increase in GSH content was detected after exposure to the ZnO NPs, but not to bulk ZnO. Moreover, the MDA levels were two or three times higher in the case of the liver, while they were similar to the control in the case of gut and gills. As reported before, ZnO NPs can impair the maturation of gills and cause developmental defects [16, 130]. In addition, histological analysis performed by using transmission electron microscopy (TEM) revealed injuries in the gill tissue after treatment with the lowest doses tested of ZnO NPs and bulk ZnO. Here, cells displayed shrinkage, loss of the cytoplasm, and abnormalities in the nuclei shapes. It is worth mentioning that as for TiO_2 NPs, ZnO NPs in suspension can generate OH ions after illumination with fluorescent light. Interestingly, the bulk ZnO or ZnO did not generate any OH in a dark environment. Moreover, at the concentration of 5 mg/L, the amount of produced OH^- was quite low. Due to this low concentration of·OH^-, and the lack of significantly increased levels of oxidative indicators in the gills, the damage of the gill cells could not be caused by the induction of ROS and oxidative stress. Hence, Xiong et al. stated that a different mechanism had to be at the basis of the gill tissue damage. Since zebrafish ingested the NPs mainly with the diet, the liver was the tissue mostly exposed to the nanoparticles and consequently mainly affected [9].

As mentioned in the case of zebrafish embryos/larvae, different studies have been focused their attention on the impact of surface modifications on the toxicity of ZnO NPs. Kizhakkumpat et al. investigated these factors not only in embryos and larvae but also in adult zebrafish. Adult fish were treated with ZnO-PEG, ZnO-PVA, and ZnO-PVP NPs. In embryos, the LC50 of bulk ZnO, ZnO-PEG, ZnO-PVA, ZnO-PVP, and ZnO NPs were found to be 520.9, 17.21, 131, 0.6823, and 0.7579 mg/L, respectively. However, the LC50 values in adults were 3239, 6.44, 9.40, 3.77, and 20.72 mg/L. In addition, capped ZnO nanoparticles were taken up by the embryos at higher rates than bare ZnO NPs, resulting in increased toxicity in later life stages. Moreover, as ZnO-PVP NPs showed the highest uptake level, adult zebrafish had a lower survival rate when exposed to this form of nanoparticles [130]. Furthermore, adult zebrafish treated with these different kinds of nanoparticles showed different morphological alterations. In particular, the histopathological study revealed severe damage in the gill tissue. More specifically, secondary lamellar structure alterations, necrosis, desquamation, acute cellular swelling, aneurysm, and lamellar disorganization were observed [130]. This specific effect was already noticed in the previous studies elucidating the toxicity of ZnO NPs in zebrafish embryos. Larvae treated with ZnO NPs and Zn^{2+} presented specifically tissue ulcerations and gill primordia. These findings are in agreement with work of Kizhakkumpat et al. and clearly indicate that ZnO NPs cause diverse toxic effects relevant to the stages of zebrafish life, with later life stages being more sensitive than the embryonic ones [16].

5. Conclusions

Current research suggests that exposure to metallic nanoparticles, especially when administered in high concentrations, causes adverse effects in zebrafish. Although TiO_2 NPs, IO NPs, and ZnO NPs are widely approved and considered nontoxic, they can indeed present some harmful properties. All the three nanoparticles types have in common that the contribution given by their size (core and hydrodinamic),

coating, as well as by the experimental conditions themselves, need to be considered in the establishment of their toxicity. Importantly, several studies showed that the accumulation of highly concentrated metallic oxide nanoparticles, concomitant with the release of their appropriate ions, is at the basis of the observed nanotoxicity. Especially in combination with longer exposure times, this seems to play a crucial role in the induction of ROS and the activation of related inflammatory and/or immunogenetic mechanisms for all classes of investigated NPs. Particularly the exposure to the highly investigated TiO_2 NPs has been revealed to affect these pathways. It has been shown that alteration of *sod1* activity with consequent perturbation of *tp53* impacts lipid homeostasis while promoting genotoxicity and apoptosis. Given their particular optical properties, these effects can even deteriorate under illumination, demanding for an accurate evaluation of their potential toxicokinetics prior to their implementation. Similarly, ZnO NPs can cause an increase in reactive oxygen species in response to fluorescent light. Furthermore, the ZnO NP-induced steep increase of ROS stimulates the apoptotic pathways regulated by caspases and mitochondria (*Gstp2, Nqo1, Bcl-2*, *caspase-3*, and *caspase*-9) causing extensive cellular dysfunction even at lower concentrations. Regarding IO NPs, which are associated with oxidative stress and the induction of redox-sensitive signal transduction pathways (AP), nanoparticle size and coating seem to be the factors mostly contributing to the observed cellular dysfunction. As iron ions are important components of many biochemical reactions, its concentration must be tightly controlled although when administered as IO NPs. Despite the increasing implementations of MO NPs, and the constant development of new variants, the obtained results regarding nanotoxicity are often contradictory. Taken as a whole, caution must be thus advised in the usage of all the indicated nanoparticles. This is even more important as MO NPs are widely used in several daily life applications, leading inevitable to environmental and human exposure. It is clear that further research is needed to fully unravel the mechanisms underlying nanotoxicity in organisms upon MO NP exposure to mitigate as much as possible potentially occurring adverse effects. In addition, proper evaluation of their ecotoxicological profile demands strongly for the standardization of the experimental conditions.

Data Availability

All data are included in the manuscript.

Conflicts of Interest

The authors declare no conflict of interest.

Authors' Contributions

M.d.A., T.J.N.S., S.K., V.R., F.D.A., and F.T. conceptualized the study; M.d.A., T.J.N.S., and S.K. wrote the original draft preparation; V.R., F.D.A., and F.T. wrote, reviewed, and edited the manuscript; V.R., F.D.A, and F.T carried out funding acquisition. All authors have read and agreed to the published version of the manuscript.

Acknowledgments

The European Union's Horizon 2020 research and innovation program under grant agreement 862714—I-GENE (In vivo Gene Editing by Nanotransducers) is greatly acknowledged for funding.

References

[1] E. Lombi, E. Donner, M. Dusinska, and F. Wickson, "A One Health approach to managing the applications and implications of nanotechnologies in agriculture," *Nature Nanotechnology*, vol. 14, no. 6, pp. 523–531, 2019.

[2] S. Stankic, S. Suman, F. Haque, and J. Vidic, "Pure and multi metal oxide nanoparticles: synthesis, antibacterial and cytotoxic properties," *Journal of Nanobiotechnology*, vol. 14, no. 1, pp. 1–20, 2016.

[3] E. V. Soares and H. M. V. M. Soares, "Harmful effects of metal (loid) oxide nanoparticles," *Applied Microbiology and Biotechnology*, vol. 105, no. 4, pp. 1379–1394, 2021.

[4] S. M. Kteeba, H. I. El-Adawi, O. A. El-Rayis et al., "Zinc oxide nanoparticle toxicity in embryonic zebrafish: mitigation with different natural organic matter," *Environmental Pollution*, vol. 230, pp. 1125–1140, 2017.

[5] Q. Li, S. Mahendra, D. Y. Lyon et al., "Antimicrobial nanomaterials for water disinfection and microbial control: potential applications and implications," *Water Research*, vol. 42, no. 18, pp. 4591–4602, 2008.

[6] Y. Li, C. Liao, and S. C. Tjong, "Recent advances in zinc oxide nanostructures with antimicrobial activities," *International Journal of Molecular Sciences*, vol. 21, no. 22, p. 8836, 2020.

[7] T. Ohira, O. Yamamoto, Y. Iida, and Z. E. Nakagawa, "Antibacterial activity of ZnO powder with crystallographic orientation," *Journal of Materials Science: Materials in Medicine*, vol. 19, no. 3, pp. 1407–1412, 2008.

[8] C. Liao, Y. Jin, Y. Li, and S. C. Tjong, "Interactions of zinc oxide nanostructures with mammalian cells: cytotoxicity and photocatalytic toxicity," *International Journal of Molecular Sciences*, vol. 21, no. 17, p. 6305, 2020.

[9] D. Xiong, T. Fang, L. Yu, X. Sima, and W. Zhu, "Effects of nano-scale TiO_2, ZnO and their bulk counterparts on zebrafish: acute toxicity, oxidative stress and oxidative damage," *Science of the Total Environment*, vol. 409, no. 8, pp. 1444–1452, 2011.

[10] S. Attarilar, J. Yang, M. Ebrahimi et al., "The toxicity phenomenon and the related occurrence in metal and metal oxide nanoparticles: a brief review from the biomedical perspective," *Frontiers in Bioengineering and Biotechnology*, vol. 8, 2020.

[11] M. Horie, K. Fujita, H. Kato et al., "Association of the physical and chemical properties and the cytotoxicity of metal oxide nanoparticles: metal ion release, adsorption ability and specific surface area," *Metallomics*, vol. 4, no. 4, pp. 350–360, 2012.

[12] C. Peng, W. Zhang, H. Gao et al., "Behavior and potential impacts of metal-based engineered nanoparticles in aquatic environments," *Nanomaterials*, vol. 7, no. 1, p. 21, 2017.

[13] F. He, X. Ru, and T. Wen, "NRF2, a transcription factor for stress response and beyond," *International Journal of Molecular Sciences*, vol. 21, no. 13, p. 4777, 2020.

[14] X. Zhu, S. Tian, and Z. Cai, "Toxicity assessment of iron oxide nanoparticles in zebrafish (Danio rerio) early life stages," *PLoS One*, vol. 7, no. 9, article e46286, 2012.

[15] A. C. Pereira, B. B. Gonçalves, R. . S. Brito, L. G. Vieira, E. C. . O. Lima, and T. L. Rocha, "Comparative developmental toxicity of iron oxide nanoparticles and ferric chloride to zebrafish (*Danio rerio*) after static and semi-static exposure," *Chemosphere*, vol. 254, article 126792, 2020.

[16] L. C. Wehmas, C. Anders, J. Chess et al., "Comparative metal oxide nanoparticle toxicity using embryonic zebrafish," *Toxicology Reports*, vol. 2, pp. 702–715, 2015.

[17] J. S. Choi, R.-O. Kim, S. Yoon, and W.-K. Kim, "Developmental toxicity of zinc oxide nanoparticles to zebrafish (Danio rerio): a transcriptomic analysis," *PLoS One*, vol. 11, no. 8, article e0160763, 2016.

[18] W. Bai, Z. Zhang, W. Tian et al., "Toxicity of zinc oxide nanoparticles to zebrafish embryo: a physicochemical study of toxicity mechanism," *Journal of Nanoparticle Research*, vol. 12, no. 5, pp. 1645–1654, 2010.

[19] R. K. Kawassaki, M. Romano, N. Dietrich, and K. Araki, "Titanium and iron oxide nanoparticles for cancer therapy: surface chemistry and biological implications," *Frontiers in Nanotechnology*, vol. 3, p. 68, 2021.

[20] S. Jafari, B. Mahyad, H. Hashemzadeh, S. Janfaza, T. Gholikhani, and L. Tayebi, "Biomedical applications of TiO2 nanostructures: recent advances," *International Journal of Nanomedicine*, vol. 15, pp. 3447–3470, 2020.

[21] L. Bergamonti, I. Alfieri, M. Franzò et al., "Synthesis and characterization of nanocrystalline TiO_2 with application as photoactive coating on stones," *Environmental Science and Pollution Research*, vol. 21, no. 23, pp. 13264–13277, 2014.

[22] R. Y. Pelgrift and A. J. Friedman, "Nanotechnology as a therapeutic tool to combat microbial resistance," *Advanced Drug Delivery Reviews*, vol. 65, no. 13-14, pp. 1803–1815, 2013.

[23] A. Weir, P. Westerhoff, L. Fabricius, K. Hristovski, and N. Von Goetz, "Titanium dioxide nanoparticles in food and personal care products," *Environmental Science & Technology*, vol. 46, no. 4, pp. 2242–2250, 2012.

[24] O. Długosz, K. Szostak, A. Staroń, J. Pulit-Prociak, and M. Banach, "Methods for reducing the toxicity of metal and metal oxide NPs as biomedicine," *Materials*, vol. 13, no. 2, p. 279, 2020.

[25] S. Kalathil, M. M. Khan, S. A. Ansari, J. Lee, and M. H. Cho, "Band gap narrowing of titanium dioxide (TiO 2) nanocrystals by electrochemically active biofilms and their visible light activity," *Nanoscale*, vol. 5, no. 14, pp. 6323–6326, 2013.

[26] M. M. Khan, S. A. Ansari, M. I. Amal, J. Lee, and M. H. Cho, "Highly visible light active Ag@ TiO 2 nanocomposites synthesized using an electrochemically active biofilm: a novel biogenic approach," *Nanoscale*, vol. 5, no. 10, pp. 4427–4435, 2013.

[27] M. A Shaheed and F. H Hussein, "Preparation and applications of titanium dioxide and zinc oxide nanoparticles," *Journal of Environmental Analytical Chemistry*, vol. 2, no. 1, 2014.

[28] M. Khan, S. F. Adil, and A. al-Mayouf, "Metal oxides as photocatalysts," *Journal of Saudi Chemical Society*, vol. 19, no. 5, pp. 462–464, 2015.

[29] B. Chen and H. Zhang, "Daunorubicin-TiO2 nanocomposites as a "smart" pH-responsive drug delivery system," *International Journal of Nanomedicine*, vol. 7, p. 235, 2012.

[30] M. Masoudi, M. Mashreghi, E. Goharshadi, and A. Meshkini, "Multifunctional fluorescent titania nanoparticles: green preparation and applications as antibacterial and cancer theranostic agents," *Artificial Cells, Nanomedicine, and Biotechnology*, vol. 46, Supplement 2, pp. 248–259, 2018.

[31] M. P. Nikolova and M. S. Chavali, "Metal oxide nanoparticles as biomedical materials," *Biomimetics*, vol. 5, no. 2, p. 27, 2020.

[32] R. Wang, C. Ruan, D. Kanayeva, K. Lassiter, and Y. Li, "TiO2 nanowire bundle microelectrode based impedance immunosensor for rapid and sensitive detection of Listeria monocytogenes," *Nano Letters*, vol. 8, no. 9, pp. 2625–2631, 2008.

[33] T. Xia, M. Kovochich, J. Brant et al., "Comparison of the abilities of ambient and manufactured nanoparticles to induce cellular toxicity according to an oxidative stress paradigm," *Nano Letters*, vol. 6, no. 8, pp. 1794–1807, 2006.

[34] X. Zhu, L. Zhu, Z. Duan, R. Qi, Y. Li, and Y. Lang, "Comparative toxicity of several metal oxide nanoparticle aqueous suspensions to zebrafish (Danio rerio) early developmental stage," *Journal of Environmental Science and Health Part A, Toxic/Hazardous Substances & Environmental Engineering*, vol. 43, no. 3, pp. 278–284, 2008.

[35] R. J. Griffitt, J. Luo, J. Gao, J. C. Bonzongo, and D. S. Barber, "Effects of particle composition and species on toxicity of metallic nanomaterials in aquatic organisms," *Environmental Toxicology and Chemistry*, vol. 27, no. 9, pp. 1972–1978, 2008.

[36] R. J. Griffitt, K. Hyndman, N. D. Denslow, and D. S. Barber, "Comparison of molecular and histological changes in zebrafish gills exposed to metallic nanoparticles," *Toxicological Sciences*, vol. 107, no. 2, pp. 404–415, 2009.

[37] T. H. Chen, C. Y. Lin, and M. C. Tseng, "Behavioral effects of titanium dioxide nanoparticles on larval zebrafish (Danio rerio)," *Marine Pollution Bulletin*, vol. 63, no. 5-12, pp. 303–308, 2011.

[38] E. Calabrese and R. Blain, "The occurrence of hormetic dose responses in the toxicological literature, the hormesis database: an overview," *Toxicology and Applied Pharmacology*, vol. 202, no. 3, pp. 289–301, 2005.

[39] R. B. Conolly and W. K. Lutz, "Nonmonotonic dose-response relationships: mechanistic basis, kinetic modeling, and implications for risk assessment," *Toxicological Sciences*, vol. 77, no. 1, pp. 151–157, 2004.

[40] G. Federici, B. Shaw, and R. Handy, "Toxicity of titanium dioxide nanoparticles to rainbow trout (*Oncorhynchus mykiss*): Gill injury, oxidative stress, and other physiological effects," *Aquatic Toxicology*, vol. 84, no. 4, pp. 415–430, 2007.

[41] L. Hao, Z. Wang, and B. Xing, "Effect of sub-acute exposure to TiO2 nanoparticles on oxidative stress and histopathological changes in juvenile carp (Cyprinus carpio)," *Journal of Environmental Sciences (China)*, vol. 21, no. 10, pp. 1459–1466, 2009.

[42] Y.-L. Hu and J.-Q. Gao, "Potential neurotoxicity of nanoparticles," *International Journal of Pharmaceutics*, vol. 394, no. 1-2, pp. 115–121, 2010.

[43] I. M. Copple, C. E. Goldring, N. R. Kitteringham, and B. K. Park, "The Nrf2-Keap1 defence pathway: role in protection

against drug-induced toxicity," *Toxicology*, vol. 246, no. 1, pp. 24–33, 2008.

[44] T. W. Kensler, N. Wakabayashi, and S. Biswal, "Cell survival responses to environmental stresses via the Keap1-Nrf2-ARE pathway," *Annual Review of Pharmacology and Toxicology*, vol. 47, no. 1, pp. 89–116, 2007.

[45] O. Bar-Ilan, K. M. Louis, S. P. Yang et al., "Titanium dioxide nanoparticles produce phototoxicity in the developing zebrafish," *Nanotoxicology*, vol. 6, no. 6, pp. 670–679, 2012.

[46] O. Bar-Ilan, C. C. Chuang, D. J. Schwahn et al., "TiO2 nanoparticle exposure and illumination during zebrafish development: mortality at parts per billion concentrations," *Environmental Science & Technology*, vol. 47, no. 9, pp. 4726–4733, 2013.

[47] M.-S. Kim, K. M. Louis, J. A. Pedersen, R. J. Hamers, R. E. Peterson, and W. Heideman, "Using citrate-functionalized TiO 2 nanoparticles to study the effect of particle size on zebrafish embryo toxicity," *Analyst*, vol. 139, no. 5, pp. 964–972, 2014.

[48] B. Jovanović, T. Ji, and D. Palić, "Gene expression of zebrafish embryos exposed to titanium dioxide nanoparticles and hydroxylated fullerenes," *Ecotoxicology and Environmental Safety*, vol. 74, no. 6, pp. 1518–1525, 2011.

[49] Q. Fang, X. Shi, L. Zhang et al., "Effect of titanium dioxide nanoparticles on the bioavailability, metabolism, and toxicity of pentachlorophenol in zebrafish larvae," *Journal of Hazardous Materials*, vol. 283, pp. 897–904, 2015.

[50] Q. Wang, Q. Chen, P. Zhou et al., "Bioconcentration and metabolism of BDE-209 in the presence of titanium dioxide nanoparticles and impact on the thyroid endocrine system and neuronal development in zebrafish larvae," *Nanotoxicology*, vol. 8, no. sup1, pp. 196–207, 2014.

[51] Y.-J. Wang, Z.-Z. He, Y.-W. Fang et al., "Effect of titanium dioxide nanoparticles on zebrafish embryos and developing retina," *International Journal of Ophthalmology*, vol. 7, p. 917, 2014.

[52] J. Yan, B. Lin, C. Hu, H. Zhang, Z. Lin, and Z. Xi, "The combined toxicological effects of titanium dioxide nanoparticles and bisphenol A on zebrafish embryos," *Nanoscale Research Letters*, vol. 9, no. 1, pp. 1–9, 2014.

[53] G. S. Gupta, K. Kansara, H. Shah et al., "Impact of humic acid on the fate and toxicity of titanium dioxide nanoparticles in Tetrahymena pyriformis and zebrafish embryos," *Nanoscale Advances*, vol. 1, no. 1, pp. 219–227, 2019.

[54] M. Faria, J. M. Navas, A. M. V. M. Soares, and C. Barata, "Oxidative stress effects of titanium dioxide nanoparticle aggregates in zebrafish embryos," *Science of the Total Environment*, vol. 470-471, pp. 379–389, 2014.

[55] S. K. Verma, A. K. Mishra, M. Suar, and S. Parashar, "In vivo assessment of impact of titanium oxide nanoparticle on zebrafish embryo," in *Proceedings of the AIP Conference Proceedings*, p. 040030, Bhubaneswar, Odisha, India, 2017.

[56] S. K. Verma, E. Jha, P. K. Panda et al., "Mechanistic insight into ROS and neutral lipid alteration induced toxicity in the human model with fins (Danio rerio) by industrially synthesized titanium dioxide nanoparticles," *Toxicology Research*, vol. 7, no. 2, pp. 244–257, 2018.

[57] S.-M. Samaee, S. Rabbani, B. Jovanović, M. R. Mohajeri-Tehrani, and V. Haghpanah, "Efficacy of the hatching event in assessing the embryo toxicity of the nano-sized TiO2 particles in zebrafish: a comparison between two different classes of hatching-derived variables," *Ecotoxicology and Environmental Safety*, vol. 116, pp. 121–128, 2015.

[58] N. Bayat, V. R. Lopes, J. Schölermann, L. D. Jensen, and S. Cristobal, "Vascular toxicity of ultra-small TiO_2 nanoparticles and single walled carbon nanotubes *in vitro* and *in vivo*," *Biomaterials*, vol. 63, pp. 1–13, 2015.

[59] O. J. Osborne, B. D. Johnston, J. Moger et al., "Effects of particle size and coating on nanoscale Ag and TiO2 exposure in zebrafish (Danio rerio) embryos," *Nanotoxicology*, vol. 7, no. 8, pp. 1315–1324, 2013.

[60] Q. Hu, F. Guo, F. Zhao, and Z. Fu, "Effects of titanium dioxide nanoparticles exposure on parkinsonism in zebrafish larvae and PC12," *Chemosphere*, vol. 173, pp. 373–379, 2017.

[61] W. Miao, B. Zhu, X. Xiao et al., "Effects of titanium dioxide nanoparticles on lead bioconcentration and toxicity on thyroid endocrine system and neuronal development in zebrafish larvae," *Aquatic Toxicology*, vol. 161, pp. 117–126, 2015.

[62] S. Hu, J. Han, L. Yang et al., "Impact of co-exposure to titanium dioxide nanoparticles and Pb on zebrafish embryos," *Chemosphere*, vol. 233, pp. 579–589, 2019.

[63] J. Gu, M. Guo, C. Huang et al., "Titanium dioxide nanoparticle affects motor behavior, neurodevelopment and axonal growth in zebrafish (*Danio rerio*) larvae," *Science of the Total Environment*, vol. 754, article 142315, 2021.

[64] T. Tang, Z. Zhang, and X. Zhu, "Toxic effects of TiO2 NPs on zebrafish," *International Journal of Environmental Research and Public Health*, vol. 16, no. 4, p. 523, 2019.

[65] Z. H. Arabeyyat, M. J. Al-Awady, G. M. Greenway, V. N. Paunov, and J. M. Rotchell, "Toxicity of polyelectrolyte-functionalized titania nanoparticles in zebrafish (Danio rerio) embryos," *SN Applied Sciences*, vol. 2, pp. 1–12, 2020.

[66] J. Wang, X. Zhu, X. Zhang et al., "Disruption of zebrafish (*Danio rerio*) reproduction upon chronic exposure to TiO_2 nanoparticles," *Chemosphere*, vol. 83, no. 4, pp. 461–467, 2011.

[67] C. Ramsden, T. B. Henry, and R. D. Handy, "Sub-lethal effects of titanium dioxide nanoparticles on the physiology and reproduction of zebrafish," *Aquatic Toxicology*, vol. 126, pp. 404–413, 2013.

[68] Z. Clemente, V. L. S. S. Castro, M. A. M. Moura, C. M. Jonsson, and L. F. Fraceto, "Toxicity assessment of TiO_2 nanoparticles in zebrafish embryos under different exposure conditions," *Aquatic Toxicology*, vol. 147, pp. 129–139, 2014.

[69] C. Akbulut, T. Kotil, B. Öztürk, and N. D. Yön, "Exposure of zebrafish (Danio rerio) to titanium dioxide nanoparticle causes paraptosis: evaluation of ovarian follicle ultrastructure," *Pakistan Journal of Zoology*, vol. 49, no. 3, pp. 1077–1083, 2017.

[70] T. Kotil, C. Akbulut, and N. D. Yön, "The effects of titanium dioxide nanoparticles on ultrastructure of zebrafish testis (Danio rerio)," *Micron*, vol. 100, pp. 38–44, 2017.

[71] L. Rocco, M. Santonastaso, F. Mottola et al., "Genotoxicity assessment of TiO2 nanoparticles in the teleost Danio rerio," *Ecotoxicology and Environmental Safety*, vol. 113, pp. 223–230, 2015.

[72] L. Chen, Y. Guo, C. Hu, P. K. S. Lam, J. C. W. Lam, and B. Zhou, "Dysbiosis of gut microbiota by chronic coexposure to titanium dioxide nanoparticles and bisphenol A: implications for host health in zebrafish," *Environmental Pollution*, vol. 234, pp. 307–317, 2018.

[73] C.-Y. Huang, W. S. Yu, G. C. Liu et al., "Opportunistic gill infection is associated with TiO2 nanoparticle-induced mortality in zebrafish," *PLoS One*, vol. 16, no. 7, article e0247859, 2021.

[74] M. Jacinto, V. C. Silva, D. M. S. Valladão, and R. S. Souto, "Biosynthesis of magnetic iron oxide nanoparticles: a review," *Biotechnology Letters*, vol. 43, no. 1, pp. 1–12, 2021.

[75] M. Geppert and M. Himly, "Iron oxide nanoparticles in bioimaging–an immune perspective," *Frontiers in Immunology*, vol. 12, 2021.

[76] S. Laurent, D. Forge, M. Port et al., "Magnetic iron oxide nanoparticles: synthesis, stabilization, vectorization, physicochemical characterizations, and biological applications," *Chemical Reviews*, vol. 108, no. 6, pp. 2064–2110, 2008.

[77] E. Oliveira, G. I. Selli, A. von Schmude et al., "Developmental toxicity of iron oxide nanoparticles with different coatings in zebrafish larvae," *Journal of Nanoparticle Research*, vol. 22, no. 4, pp. 1–16, 2020.

[78] F. Soetaert, P. Korangath, D. Serantes, S. Fiering, and R. Ivkov, "Cancer therapy with iron oxide nanoparticles: agents of thermal and immune therapies," *Advanced Drug Delivery Reviews*, vol. 163-164, pp. 65–83, 2020.

[79] S. M. Dadfar, K. Roemhild, N. I. Drude et al., "Iron oxide nanoparticles: diagnostic, therapeutic and theranostic applications," *Advanced Drug Delivery Reviews*, vol. 138, pp. 302–325, 2019.

[80] S. Laurent, J.-L. Bridot, L. V. Elst, and R. N. Muller, "Magnetic iron oxide nanoparticles for biomedical applications," *Future Medicinal Chemistry*, vol. 2, no. 3, pp. 427–449, 2010.

[81] U. S. Patil, S. Adireddy, A. Jaiswal, S. Mandava, B. Lee, and D. Chrisey, "In vitro/in vivo toxicity evaluation and quantification of iron oxide nanoparticles," *International Journal of Molecular Sciences*, vol. 16, no. 10, pp. 24417–24450, 2015.

[82] N. Elahi and M. Rizwan, "Progress and prospects of magnetic iron oxide nanoparticles in biomedical applications: a review," *Artificial Organs*, vol. 45, no. 11, pp. 1272–1299, 2021.

[83] C. S. Kumar and F. Mohammad, "Magnetic nanomaterials for hyperthermia-based therapy and controlled drug delivery," *Advanced Drug Delivery Reviews*, vol. 63, no. 9, pp. 789–808, 2011.

[84] S. de Vincentiis, A. Falconieri, M. Mainardi et al., "Extremely low forces induce extreme axon growth," *Journal of Neuroscience*, vol. 40, no. 26, pp. 4997–5007, 2020.

[85] Y. Hu, D. Li, H. Wei et al., "Neurite extension and orientation of spiral ganglion neurons can be directed by superparamagnetic iron oxide nanoparticles in a magnetic field," *International Journal of Nanomedicine*, vol. 16, pp. 4515–4526, 2021.

[86] H. Schöneborn, F. Raudzus, E. Secret et al., "Novel tools towards magnetic guidance of neurite growth:(I) Guidance of magnetic nanoparticles into neurite extensions of induced human neurons and in vitro functionalization with RAS regulating proteins," *Journal of Functional Biomaterials*, vol. 10, no. 3, p. 32, 2019.

[87] V. Parlak, "Evaluation of apoptosis, oxidative stress responses, AChE activity and body malformations in zebrafish (*Danio rerio*) embryos exposed to deltamethrin," *Chemosphere*, vol. 207, pp. 397–403, 2018.

[88] V. Valdiglesias, N. Fernández-Bertólez, G. Kiliç et al., "Are iron oxide nanoparticles safe? Current knowledge and future perspectives," *Journal of Trace Elements in Medicine and Biology*, vol. 38, pp. 53–63, 2016.

[89] Z. Wang and Z. Wang, "Nanoparticles induced embryo–fetal toxicity," *Toxicology and Industrial Health*, vol. 36, no. 3, pp. 181–213, 2020.

[90] N. Lewinski, V. Colvin, and R. Drezek, "Cytotoxicity of nanoparticles," *Small*, vol. 4, no. 1, pp. 26–49, 2008.

[91] A. Ali, H. Zafar, M. Zia et al., "Synthesis, characterization, applications, and challenges of iron oxide nanoparticles," *Nanotechnology, Science and Applications*, vol. 9, pp. 49–67, 2016.

[92] N. Malhotra, J.-R. Chen, S. Sarasamma et al., "Ecotoxicity assessment of fe3o4 magnetic nanoparticle exposure in adult zebrafish at an environmental pertinent concentration by behavioral and biochemical testing," *Nanomaterials*, vol. 9, no. 6, p. 873, 2019.

[93] A. Jurewicz, S. Ilyas, J. K. Uppal, I. Ivandic, S. Korsching, and S. Mathur, "Evaluation of magnetite nanoparticle-based toxicity on embryo–larvae stages of zebrafish (Danio rerio)," *ACS Applied Nano Materials*, vol. 3, no. 2, pp. 1621–1629, 2020.

[94] Z. Yarjanli, K. Ghaedi, A. Esmaeili, S. Rahgozar, and A. Zarrabi, "Iron oxide nanoparticles may damage to the neural tissue through iron accumulation, oxidative stress, and protein aggregation," *BMC Neuroscience*, vol. 18, no. 1, pp. 1–12, 2017.

[95] Y. Zhang, L. Zhu, Y. Zhou, and J. Chen, "Accumulation and elimination of iron oxide nanomaterials in zebrafish (Danio rerio) upon chronic aqueous exposure," *Journal of Environmental Sciences*, vol. 30, pp. 223–230, 2015.

[96] Y.-L. Hu, W. Qi, F. Han, J. Z. Shao, and J. Q. Gao, "Toxicity evaluation of biodegradable chitosan nanoparticles using a zebrafish embryo model," *International Journal of Nanomedicine*, vol. 6, pp. 3351–3359, 2011.

[97] S. Mohiuddin Hafiz, S. Sameer Kulkarni, and M. Kapil Thakur, "In-vivo toxicity assessment of biologically synthesized iron oxide nanoparticles in zebrafish (Danio rerio)," *Biosciences Biotechnology Research Asia*, vol. 15, no. 2, pp. 419–425, 2018.

[98] N. A. Thirumurthi, A. Raghunath, S. Balasubramanian, and E. Perumal, "Evaluation of maghemite nanoparticles–induced developmental toxicity and oxidative stress in zebrafish embryos/larvae," *Biological Trace Element Research*, pp. 1–16, 2021.

[99] A. Miri, H. Najafzadeh, M. Darroudi, M. J. Miri, M. A. J. Kouhbanani, and M. Sarani, "Iron oxide nanoparticles: biosynthesis, magnetic behavior, cytotoxic effect," *ChemistryOpen*, vol. 10, no. 3, pp. 327–333, 2021.

[100] D. Galaris, A. Barbouti, and K. Pantopoulos, "Iron homeostasis and oxidative stress: an intimate relationship," *Biochimica et Biophysica Acta (BBA)-Molecular Cell Research*, vol. 1866, no. 12, article 118535, 2019.

[101] J. Emerit, C. Beaumont, and F. Trivin, "Iron metabolism, free radicals, and oxidative injury," *Biomedicine & Pharmacotherapy*, vol. 55, no. 6, pp. 333–339, 2001.

[102] I. B. Afanas'ev, "Superoxide and nitric oxide in pathological conditions associated with iron overload. The effects of antioxidants and chelators," *Current Medicinal Chemistry*, vol. 12, no. 23, pp. 2731–2739, 2005.

[103] R. E. Özel, R. S. J. Alkasir, K. Ray, K. N. Wallace, and S. Andreescu, "Comparative evaluation of intestinal nitric

oxide in embryonic zebrafish exposed to metal oxide nanoparticles," *Small*, vol. 9, no. 24, pp. 4250–4261, 2013.

[104] P. P. Fu, Q. Xia, H.-M. Hwang, P. C. Ray, and H. Yu, "Mechanisms of nanotoxicity: generation of reactive oxygen species," *Journal of Food and Drug Analysis*, vol. 22, no. 1, pp. 64–75, 2014.

[105] M. A. Voinov, J. O. S. Pagán, E. Morrison, T. I. Smirnova, and A. I. Smirnov, "Surface-mediated production of hydroxyl radicals as a mechanism of iron oxide nanoparticle biotoxicity," *Journal of the American Chemical Society*, vol. 133, no. 1, pp. 35–41, 2011.

[106] H. Wei, Y. Hu, J. Wang, X. Gao, X. Qian, and M. Tang, "Superparamagnetic iron oxide nanoparticles: cytotoxicity, metabolism, and cellular behavior in biomedicine applications," *International Journal of Nanomedicine*, vol. 16, pp. 6097–6113, 2021.

[107] R. K. Sharma, S. Dutta, S. Sharma, R. Zboril, R. S. Varma, and M. B. Gawande, "Fe 3 O 4 (iron oxide)-supported nanocatalysts: synthesis, characterization and applications in coupling reactions," *Green Chemistry*, vol. 18, no. 11, pp. 3184–3209, 2016.

[108] P. Saxena, V. Sangela, and Harish, "Toxicity evaluation of iron oxide nanoparticles and accumulation by microalgae Coelastrella terrestris," *Environmental Science and Pollution Research*, vol. 27, no. 16, pp. 19650–19660, 2020.

[109] G. Chemello, C. Piccinetti, B. Randazzo et al., "Oxytetracycline delivery in adult female zebrafish by iron oxide nanoparticles," *Zebrafish*, vol. 13, no. 6, pp. 495–503, 2016.

[110] G. M. T. de Oliveira, L. W. Kist, T. C. B. Pereira et al., "Transient modulation of acetylcholinesterase activity caused by exposure to dextran-coated iron oxide nanoparticles in brain of adult zebrafish," *Comparative Biochemistry and Physiology Part C: Toxicology & Pharmacology*, vol. 162, pp. 77–84, 2014.

[111] M. Zheng, J. Lu, and D. Zhao, "Effects of starch-coating of magnetite nanoparticles on cellular uptake, toxicity and gene expression profiles in adult zebrafish," *Science of the Total Environment*, vol. 622-623, pp. 930–941, 2018.

[112] M. Carofiglio, S. Barui, V. Cauda, and M. Laurenti, "Doped zinc oxide nanoparticles: synthesis, characterization and potential use in nanomedicine," *Applied Sciences*, vol. 10, no. 15, p. 5194, 2020.

[113] M. Laurenti and V. Cauda, "ZnO nanostructures for tissue engineering applications," *Nanomaterials*, vol. 7, no. 11, p. 374, 2017.

[114] F. Piccinno, F. Gottschalk, S. Seeger, and B. Nowack, "Industrial production quantities and uses of ten engineered nanomaterials in Europe and the world," *Journal of Nanoparticle Research*, vol. 14, no. 9, pp. 1–11, 2012.

[115] S. Singh, P. Thiyagarajan, K. Mohan Kant et al., "Structure, microstructure and physical properties of ZnO based materials in various forms: bulk, thin film and nano," *Journal of Physics D: Applied Physics*, vol. 40, no. 20, pp. 6312–6327, 2007.

[116] X. Zhao, X. Ren, R. Zhu, Z. Luo, and B. Ren, "Zinc oxide nanoparticles induce oxidative DNA damage and ROS-triggered mitochondria-mediated apoptosis in zebrafish embryos," *Aquatic Toxicology*, vol. 180, pp. 56–70, 2016.

[117] K. S. Siddiqi, A. ur Rahman, and A. Husen, "Properties of zinc oxide nanoparticles and their activity against microbes," *Nanoscale Research Letters*, vol. 13, pp. 1–13, 2018.

[118] S.-E. Jin, J. E. Jin, W. Hwang, and S. W. Hong, "Photocatalytic antibacterial application of zinc oxide nanoparticles and self-assembled networks under dual UV irradiation for enhanced disinfection," *International Journal of Nanomedicine*, vol. 14, pp. 1737–1751, 2019.

[119] S. Anjum, M. Hashim, S. A. Malik et al., "Recent advances in zinc oxide nanoparticles (ZnO NPs) for cancer diagnosis, target drug delivery, and treatment," *Cancers*, vol. 13, no. 18, p. 4570, 2021.

[120] Y. Mita, Y. Aoyagi, M. Yanagi, T. Suda, Y. Suzuki, and H. Asakura, "The usefulness of determining des-γ-carboxy prothrombin by sensitive enzyme immunoassay in the early diagnosis of patients with hepatocellular carcinoma," *Cancer: Interdisciplinary International Journal of the American Cancer Society*, vol. 82, no. 9, pp. 1643–1648, 1998.

[121] A. Ancona, B. Dumontel, N. Garino et al., "Lipid-coated zinc oxide nanoparticles as innovative ROS-generators for photodynamic therapy in cancer cells," *Nanomaterials*, vol. 8, no. 3, p. 143, 2018.

[122] L. Racca, T. Limongi, V. Vighetto et al., "Zinc oxide nanocrystals and high-energy shock waves: a new synergy for the treatment of cancer cells," *Frontiers in Bioengineering and Biotechnology*, vol. 8, p. 577, 2020.

[123] J. Tokarský, K. Mamulová Kutláková, R. Podlipná, and T. Vaněk, "Phytotoxicity of ZnO/kaolinite nanocomposite—is anchoring the right way to lower environmental risk?," *Environmental Science and Pollution Research*, vol. 26, no. 21, pp. 22069–22081, 2019.

[124] C. García-Gómez, A. Obrador, D. González, M. Babín, and M. D. Fernández, "Comparative study of the phytotoxicity of ZnO nanoparticles and Zn accumulation in nine crops grown in a calcareous soil and an acidic soil," *Science of the Total Environment*, vol. 644, pp. 770–780, 2018.

[125] N. Ruiz-Torres, A. Flores-Naveda, E. D. Barriga-Castro et al., "Zinc oxide nanoparticles and zinc sulfate impact physiological parameters and boosts lipid peroxidation in soil grown coriander plants (Coriandrum sativum)," *Molecules*, vol. 26, no. 7, p. 1998, 2021.

[126] D. Cao, X. Shu, D. Zhu, S. Liang, M. Hasan, and S. Gong, "Lipid-coated ZnO nanoparticles synthesis, characterization and cytotoxicity studies in cancer cell," *Nano Convergence*, vol. 7, no. 1, pp. 1–18, 2020.

[127] H. M. el-Shorbagy, S. M. Eissa, S. Sabet, and A. A. el-Ghor, "Apoptosis and oxidative stress as relevant mechanisms of antitumor activity and genotoxicity of ZnO-NPs alone and in combination with N-acetyl cysteine in tumor-bearing mice," *International Journal of Nanomedicine*, vol. 14, pp. 3911–3928, 2019.

[128] M. Canta and V. Cauda, "The investigation of the parameters affecting the ZnO nanoparticle cytotoxicity behaviour: a tutorial review," *Biomaterials Science*, vol. 8, no. 22, pp. 6157–6174, 2020.

[129] X. Zhao, S. Wang, Y. Wu, H. You, and L. Lv, "Acute ZnO nanoparticles exposure induces developmental toxicity, oxidative stress and DNA damage in embryo-larval zebrafish," *Aquatic Toxicology*, vol. 136-137, pp. 49–59, 2013.

[130] A. Kizhakkumpat, A. Syed, A. M. Elgorban, A. H. Bahkali, and S. S. Khan, "The toxicity analysis of PVP, PVA and PEG surface functionalized ZnO nanoparticles on embryonic as well as adult Danio rerio," *Environmental Monitoring and Assessment*, vol. 193, no. 12, pp. 1–11, 2021.

[131] N. R. Brun, M. Lenz, B. Wehrli, and K. Fent, "Comparative effects of zinc oxide nanoparticles and dissolved zinc on zebrafish embryos and eleuthero-embryos: importance of zinc ions," *Science of the Total Environment*, vol. 476, pp. 657–666, 2014.

[132] T.-H. Chen, C.-C. Lin, and P.-J. Meng, "Zinc oxide nanoparticles alter hatching and larval locomotor activity in zebrafish (Danio rerio)," *Journal of Hazardous Materials*, vol. 277, pp. 134–140, 2014.

[133] J. Hua, M. G. Vijver, M. K. Richardson, F. Ahmad, and W. J. G. M. Peijnenburg, "Particle-specific toxic effects of differently shaped zinc oxide nanoparticles to zebrafish embryos (Danio rerio)," *Environmental Toxicology and Chemistry*, vol. 33, no. 12, pp. 2859–2868, 2014.

[134] Z. Zhou, J. Son, B. Harper, Z. Zhou, and S. Harper, "Influence of surface chemical properties on the toxicity of engineered zinc oxide nanoparticles to embryonic zebrafish," *Beilstein Journal of Nanotechnology*, vol. 6, pp. 1568–1579, 2015.

[135] S. K. Verma, P. K. Panda, E. Jha, M. Suar, and S. K. S. Parashar, "Altered physiochemical properties in industrially synthesized ZnO nanoparticles regulate oxidative stress; induce *in vivo* cytotoxicity in embryonic zebrafish by apoptosis," *Scientific Reports*, vol. 7, no. 1, p. 13909, 2017.

[136] J. Du, J. Cai, S. Wang, and H. You, "Oxidative stress and apotosis to zebrafish (Danio rerio) embryos exposed to perfluorooctane sulfonate (PFOS) and ZnO nanoparticles," *International Journal of Occupational Medicine and Environmental Health*, vol. 30, no. 2, pp. 213–229, 2017.

[137] D. M. Fasil, H. Hamdi, A. al-Barty, A. A. Zaid, S. K. S. Parashar, and B. Das, "Selenium and zinc oxide multinutrient supplementation enhanced growth performance in zebra fish by modulating oxidative stress and growth-related gene expression," *Frontiers in Bioengineering and Biotechnology*, vol. 9, 2021.

[138] X. Zhu, J. Wang, X. Zhang, Y. Chang, and Y. Chen, "The impact of ZnO nanoparticle aggregates on the embryonic development of zebrafish (Danio rerio)," *Nanotechnology*, vol. 20, no. 19, article 195103, 2009.

Hindawi
Oxidative Medicine and Cellular Longevity
Volume 2022, Article ID 7969825, 12 pages
https://doi.org/10.1155/2022/7969825

Research Article

Evaluation of Zebrafish Toxicology and Biomedical Potential of *Aeromonas hydrophila* Mediated Copper Sulfide Nanoparticles

S. Rajeshkumar,[1] **J. Santhoshkumar**,[2] **M. Vanaja**,[3] **P. Sivaperumal**,[1] **M. Ponnanikajamideen**,[4] **Daoud Ali**,[5] **and Kalirajan Arunachalam**[6]

[1]*Centre for Transdisciplinary Research, Nanobiomedicine Lab, Department of Pharmacology, Saveetha Dental College and Hospital, SIMATS, Chennai 600077, India*
[2]*Department of Biotechnology, Saveetha School of Engineering, Saveetha Institute of Medical and Technical Science (SIMATS), 602105, Chennai, India*
[3]*SPKCES, Manonmaniam Sundaranar University, Alwarkurichi, 627410 Tamil Nadu, India*
[4]*Department of Pharmacology and Toxicology, University of Mississippi Medical Centre, Jackson, Mississippi, USA*
[5]*Department of Zoology, College of Science, King Saud University, PO Box 2455, Riyadh 11451, Saudi Arabia*
[6]*Department of Science and Mathematics, School of Science, Engineering and Technology, Mulungushi University, Kabwe 80415, Zambia*

Correspondence should be addressed to Kalirajan Arunachalam; akalirajan@mu.edu.zm

Received 9 September 2021; Revised 27 December 2021; Accepted 7 January 2022; Published 28 January 2022

Academic Editor: Dragica Selakovic

The present study deals with extracellular synthesis and characterization of copper sulfide (CuS) nanoparticles using *Aeromonas hydrophila*, and the biological applications of the synthesized CuS like antibacterial, anti-inflammatory, and antioxidant activity were reported. Further, the toxicological effects of the CuS were evaluated using zebrafish as an animal model. The primary step of the synthesis was carried out by adding the precursor copper sulfates to the culture supernatant of *Aeromonas hydrophila*. The UV-visible spectrophotometer was used to characterize the synthesized nanoparticles, and the peak was obtained at 307 nm through the reduction process. Fourier transform infrared spectroscopy (FTIR) was involved to find out the functional groups (carboxylic acid, alcohols, alkanes, and nitro compounds) associated with copper sulfide nanoparticles (CuS-NPs). Atomic force microscopy (AFM) was used to characterize the CuS topographically, and a scanning electron microscope (SEM) revealed about 200 nm sized CuS nanoparticles with agglomerated structures. Overall, the characterized nanoparticles can be considered as a potential candidate with therapeutic proficiencies as antibacterial, antioxidant, and anti-inflammatory mediator/agents.

1. Introduction

Copper is a common element that exists naturally in the environment and distributes through anthropogenic activities. It is soft, flexible metal with high thermal and electrical conductivity. Like iron, copper is a trace element required for the formation of body tissues and red blood cells. The economic value of combining crystalline copper and semiconductor nanoparticles is used in various fields including catalysis, material science, solar cells, the environment aspects, and medicine, owing to their unique properties [1, 2]. The size of semiconductor nanoparticles reduced into nanometer scale is due to quantum effects. As a result, size, shape, and quantum effects of such reduction play a critical role in determining the properties of semiconductor nanoparticles. Copper sulfide nanoparticles have tremendous applications, such as in solar cells [3–5], wastewater treatment, and sensors [6, 7], and also used in the manufacturing of other electronic components [8]. Different techniques, like physical, chemical, and biological methods, are used to synthesize copper sulfide nanoparticles [9, 10]. The biological method has several advantages such as environmentally

friendly, cost-effective, and usage of less toxic chemicals in the synthesis process [11]. The described biological method used the biological sources such as bacteria [12], fungi [13–15], algae, plants [16, 17], and other biological materials. Here, the bacteria is used for nanoparticle synthesis, as it produces metal resistance and participates in effectively reducing the ions into nanoparticles. When bacteria were exposed to low metal ion concentrations, they develop resistance and induce nanoparticle synthesis [18]. Bacterial synthesis of nanoparticles can be done either (i) intracellular or extracellular. Both methods are used to obtain the controlled size and shape of the nanoparticle during synthesis process. Bacterial culture supernatant was used for the extracellular synthesis of nanoparticles, and this method can be reproduced for the better size and shape with controllable synthesis of nanoparticles than the intracellular one [19]. There are plenty of reports on the synthesis of copper nanoparticles using bacteria such as acidophilic sulfate-reducing bacteria [20], *Escherichia coli* [21], *Pseudomonas* sp. [22], *Pseudomonas stutzeri* [23, 24], *Serratia sp.* [25], *Streptomyces sp.* [26], *Morganella* bacteria [27], *Pseudomonas fluorescens* [28], and *Shewanella oneidensis* MR-1 [12]; among them, extracellular synthesis of copper sulfide nanoparticles (CuS-NPs) using the bacteria *Aeromonas hydrophila* has rarely been reported. The synthesized nanoparticles were characterized using UV-vis spectra, XRD, FTIR, AFM, SEM, and EDX analyses; biological applications such as antibacterial, antioxidant, and anti-inflammatory properties of the CuS-NPs were assessed to determine their biological role. In addition, characterized nanoparticles and their biological roles were assessed by antibacterial, anti-inflammatory, and antioxidant activities. Furthermore, a toxicological assay of CuS-NPs was performed in zebrafish embryos as an animal model.

2. Materials and Methods

2.1. Materials Used. The bacterial strain *Aeromonas hydrophila* (7966) was purchased from the American Type Culture Collection, Tamil Nadu, India. Nutrient broth, Mueller-Hinton agar, DPPH, and media were purchased from Sigma-Aldrich, India, and the standard antibiotics were purchased from Hi-Media Laboratories, Mumbai, India. In addition, zebrafish (*Danio rerio*) embryos were purchased from Tarun fish farm, Manimangalam, Chennai.

2.2. Culturing Aeromonas hydrophila and Synthesis of CuS Nanoparticles. Aeromonas hydrophila is a rod-shaped, gram-negative bacterium commonly found in brackish water and causes disease in fish. It is used in this experiment for the synthesis of copper sulfide nanoparticles. The bacterial culture was grown in the nutrient broth with the pH 7.2 and incubated at 30°C for 24 hours in a shaking incubator at 120 rpm. The culture was centrifuged at 10000 rpm for 10 min and collected the cell-free supernatant. The nanoparticle synthesis was attempted by following slightly modified protocol [29] and related applications as well. The bacterial supernatant was used for the extracellular synthesis of copper sulfide nanoparticles by adding the precursor material, 1 mM copper sulfates thoroughly mixed and incubated for reduction process. After the addition of copper sulfate, the reaction mixture turns into greenish-blue from greenish-brown color. The color change indicates the synthesis of CuS-NPs.

2.3. Characterization of Synthesized Copper Sulfide Nanoparticles. The crystalline character of the synthesized copper sulfide nanoparticles was investigated with the help of powder XRD (XRD D8 ADVANCE BRUKER) analysis. The X-ray patterns were obtained in the 2 theta configurations in the range of 20°–80°. After drying off the purified CuS nanoparticles, the sample's elemental composition was analyzed with energy dispersive analysis of X-ray spectroscopy (scanning electron microscope predicted ZEISS (EVD18)) and the morphology and size. Absorption spectra were determined by a UV-vis spectrophotometer (SHIMADZU UV-1280) with a frequency range from 300 nm to 320 nm.

3. Biomedical Applications

3.1. Antibacterial Activity of Copper Sulfide (CuS) Nanoparticles. Antibacterial activity was done by the agar well diffusion method using various pathogenic bacteria such as *Vibrio parahaemolyticus*, *Serratia marcescens*, *Proteus sp*, *E. coli*, and *Bacillus* sp. Fresh bacterial inoculum of pathogens was spread on sterile Mueller-Hinton agar plate using sterile cotton swabs, respectively. About four wells were made in each plate using a sterile gel puncture for adding different concentrations of CuS nanoparticles. Various concentrations (25 and 100 μg/mL) of copper sulfide nanoparticles were incorporated into each well, and negative control was kept; a standard antibiotic (chloramphenicol) (25 μg/mL) was used as positive control. All the plates were incubated at 35°C for 24 hours and observed zone formation around the well.

3.2. Antioxidant Activity. Antioxidant activity of biosynthesized CuS nanoparticles was performed by assaying the free radical scavenging effect on DPPH (2-diphenyl-2-picrylhydrazyl). For the present activity, 1 mL of different concentrations of CuS nanoparticles (25, 50, 75, and 100 μg/mL) was mixed with 1 mL of 1 mM DPPH prepared using methanol. DPPH solution prepared in methanol without sample was considered as control. Then, the reaction solutions were mixed thoroughly by vortexing and incubated at room temperature under dark conditions for up to 30 min. After incubation, the discolorations of DPPH from purple to yellow were observed and the absorbance of the DPPH scavenging by nanoparticles was recorded at 517 nm using a UV-vis spectrophotometer.

The percentage of inhibition was calculated using the following formula:

$$\text{Inhibition \%} = \text{OD of control} - \text{OD of test sample/OD of control} * 100. \quad (1)$$

3.3. Anti-Inflammatory Activity. The inflammation inhibitory effects of CuS nanoparticles were performed by membrane stabilizing activity in human red blood cells (RBCs). Fresh human blood (10 mL) was collected and mixed with 10 mL of saline (pH 7.2) solution. The mixed saline blood was centrifuged at 3000 rpm for 10 mins and washed with saline solution. This process was repeated three times. Presently, 2 mL of CuS nanoparticles was taken in different concentrations (25, 50, 75, and 100 μg/mL) and mixed with 1 mL of RBCs (10%v/v), respectively. The standard drug was prepared by mixing 2 mL of diclofenac sodium (25 mg) with 1 mL of RBCs in saline. Distilled water instead of saline is considered as a control. All the mixtures were incubated at 56°C for 30 mins. After incubation, all the tubes were cooled and centrifuged at 2500 rpm for 5 mins. The absorbance of the supernatants was read at 560 nm.

The percentage of inhibition was calculated using the following formula:

$$\text{Inhibition \%} = \text{OD of control} - \text{OD of test sample/OD of control} * 100. \quad (2)$$

3.4. Toxicology Analysis of Synthesized Copper Nanoparticles using Zebrafish. The embryos of Zebrafish were incubated at 26°C in culture water. Randomly selected embryos at 4 hours postfertilization (sphere stage) were maintained with 10 mL of zebrafish culture water. Healthy embryos were selected and placed in 96-well culture plates containing 0.2 mL of culture water. To each well, 0.1 mL of different concentrations of CuS nanoparticles (0 to 150 μg/mL) was added, respectively. Three replicates were included, and the embryos in the culture medium were considered as control. Then, the plates were incubated at 26°C and observed the developmental status of the embryos and zebrafish larvae at different fertilizing periods. Hatching and mortality rates in percentages were calculated at every 12 h from the total number of survival embryos. Malfunction in embryos caused by nanoparticles was observed using a microscope.

3.5. Statistical Analyses. All the experiments were performed in triplicate, and the obtained data were expressed as mean values ± standard error (SE). Data were interpreted using GraphPad 6.1 software. Two-way ANOVA was performed using the Bonferroni post hoc test to evaluate the significant differences between groups (standard drug and nanomaterial sample). The significant level for different concentrations of standard drug and test samples was set top ≤ 0.05.

4. Results and Discussion

4.1. UV-Visible Spectroscopy. The optical properties and the bioreduction of nanoparticles have been studied using the UV-vis absorption spectrum. A color change from pale yellow to green was primarily observed when the $CuSO_4$ was added to the cell-free supernatant. After incubation, the color of the reaction mixture changed into greenish-brown (Figure 1). Several strong peaks for copper sulfide nanoparticles were observed between 300 and 320 nm. As the size of the $CuSO_4$ to the bulk decreases the absorption shifts to shorter wavelengths (blue shift), which were observed in the nanoregion, the maximum absorption spectrum that produced blue shift during synthesis was observed at 307 nm, which implies the presence of copper synthesized in high amounts.

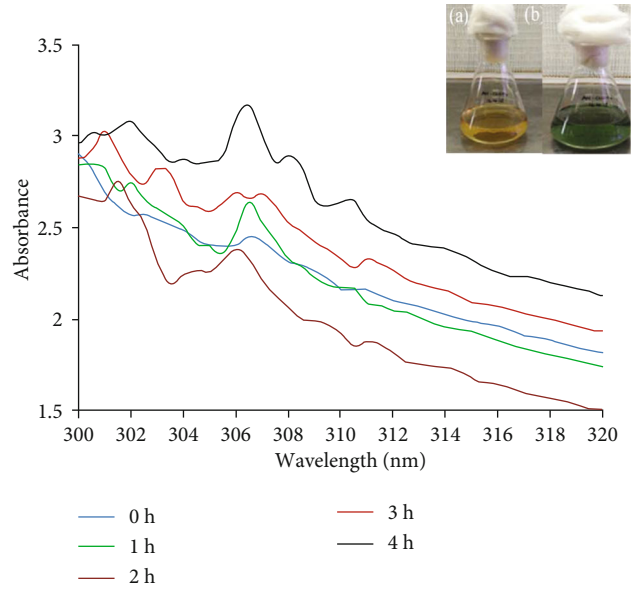

Figure 1: UV spectra of extracellularly synthesized copper sulfide nanoparticles recorded at various time intervals. Insert figure ("a" and "b") shows color change of culture supernatant from yellow to green indicates synthesis of copper sulfide nanoparticles by extracellularly.

4.2. Nature and Functional Group of CuS Nanoparticles. XRD result revealed the crystalline nature of the synthesized copper sulfide nanoparticles. The peaks obtained represent the presence of copper sulfide, and it is confirmed by the planes (110) and (111), which are corresponding to the 2θ degree 31.18° and 43.81°, respectively (Figure 2). The average size of nanoparticles was found to be 20 nm which was calculated using the formula Debye-Scherrer equations $D = K\lambda/(\beta \text{Cos}\theta)$. Here, D is the particle size, K is the Blanks constant, λ is the X-ray wavelength, β is the FWHM intensity, and θ is the Bragg angle.

The functional groups present in the supernatant of *A. hydrophila* were revealed through the frequency peaks at the wavenumber of 3350.35 cm^{-1} pointed to the O-H stretching vibration of carboxylic acid. Likely, two small peaks were found at 3215.34 and 2856.58 cm^{-1} signifying the C-H stretching vibration of alkanes and represented to be asymmetric. Similarly, two peaks at 1627.92 and 1408.04 cm^{-1} were assigned to N–O asymmetric stretch nitro compounds. The two wavenumbers at 1301.95 and 1037.70 cm^{-1} were corresponding to the presence of C-O stretching alcohols, respectively. A frequency band at 736.81 cm^{-1} was due to the vibrations of the CH_3, and the peak implies the weak bond with C-C skeleton vibration (Figure 3).

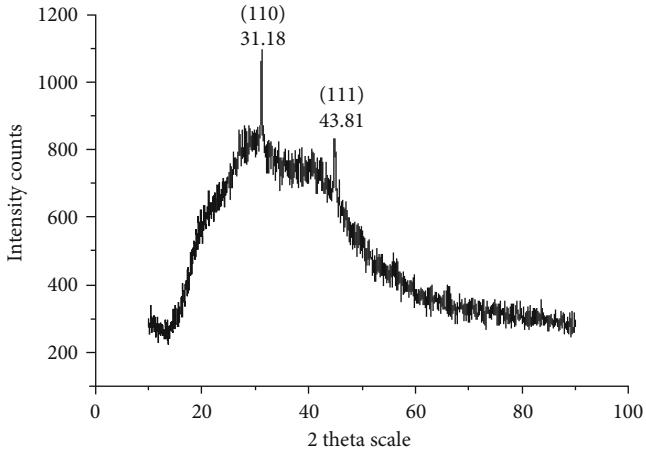

Figure 2: XRD shows crystalline nature of copper sulfide nanoparticles.

4.3. Surface and Shape of the CuS Nanoparticles. The AFM analysis confirmed the characteristic surface smoothness and also portrayed the 3-dimensional structure of the nanoparticles. Figure 4 shows the average size of 20.65 nm of copper sulfide nanoparticles. The smooth-surfaced and spherical-shaped nanoparticles were observed from AFM. Scanning electron microscopy analyzed the size and shape of the synthesized CuS nanoparticles, which are shown in Figure 5. It reveals that the copper sulfide nanoparticles were in spherical and rod shaped with the size range of 20 to 200 nm. EDX graph shows the elemental composition of biosynthesized CuS nanoparticles (Figure 6). A strong signal was received at 1 keV assigned to elemental copper, and a weak signal at 2.3 keV displays the sulfur component. Other peaks like carbon, oxygen, and sodium are associated with CuS nanoparticles.

4.4. Biomedical Applications

4.4.1. Antibacterial Activity. Antibacterial activity of copper sulfide nanoparticles was performed against gram-positive and gram-negative bacteria. The bacterial pathogens, namely, *E. coli*, *Vibrio harveyi*, *Vibrio parahaemolyticus*, *Bacillus* sp., and *Proteus* sp., were used in this study. From the antibacterial assay, CuS nanoparticles exhibited the highest zone of inhibition in *E. coli* with 9.00 ± 0.35 mm at the highest concentration.

The results obtained for the other three concentrations are 5.31 ± 0.20 mm, 5.99 ± 0.34 mm, and 7.99 ± 0.34 mm for 25, 50, and 75 μg/mL, respectively. Copper sulfide NPs are more active against *Proteus* sp. recorded a maximum zone of inhibition with the size 12.11 ± 0.25 mm in the concentration of 100 μg/mL, which confirmed potential antibacterial activity against *Proteus sp.* than on other tested pathogens. Activity against *Vibrio harveyi* obtained 7.08 ± 0.43 mm, 7.32 ± 0.48 mm, 10.77 ± 0.16 mm, and 11.11 ± 0.28 mm for the tested concentrations. Similarly, activity against *Vibrio parahaemolyticus* was measured as 5.35 ± 0.32 mm, 7.48 ± 0.41 mm, 9.43 ± 0.10 mm, and 12.03 ± 0.07 mm for the tested concentrations, respectively. For *Bacillus* sp., the zone of inhibition was recorded as 5.08 ± 0.37 mm, 5.39 ± 0.21 mm, 9.41 ± 0.32 mm, and 10.58 ± 0.09 mm. The concentration of nanoparticles increases in the treatment against pathogenic bacteria; consequently, the zone of inhibition was increased (Figure 7).

4.4.2. Antioxidant Activity. Antioxidant activity of synthesized copper sulfide nanoparticles by DPPH free radical scavenging assay showed increased activity, while increasing the concentrations. The highest inhibition was exhibited by CuS nanoparticles at the maximum concentrations (100 μg/mL). The result observed that increasing the concentration of CuS nanoparticles increases the percentage of antioxidant activity (Figure 8). Statistically, from the two-way ANOVA test, the experimental p value recorded here is less than 0.05. In this connection, copper sulfide nanoparticles caused a significant increase in the antioxidant activity at the concentrations of 75 μg/mL and 100 μg/mL, when compared to the standard drug, ascorbic acid. DPPH reduction activity of nanoparticles showed the percentage of inhibition as $64.37 \pm 1.11\%$, which is higher than the standard drug ($55.16 \pm 1.28\%$) at the concentration of 75 μg/mL ($p < 0.01$). Whereas at 100 μg/mL concentration, copper sulfide nanoparticles exhibited the most significant ($p < 0.001$) increase in the antioxidant activity ($88.71 \pm 0.98\%$) than the standard drug ($72.50 \pm 2.21\%$). Other concentrations (25 μg/mL and 50 μg/mL) did not show any significant differences between CuS nanoparticles and standard drugs. IC_{50} values of nanoparticles and commercial drug that required for 50% reduction of DPPH radical were found to be 55.43 ± 0.33 and 67.25 ± 1.62 μg/mL, respectively.

4.4.3. Anti-Inflammatory Activity. Anti-inflammatory activity was carried out by the membrane-stabilizing method, and the OD value of inhibition was recorded at 565 nm. The percentage of anti-inflammatory activity was calculated, and the graph of copper sulfide nanoparticles shows the maximum inhibition at 100 μg/mL concentration when compared to the other concentrations. The results have shown that CuS nanoparticles actively inhibited the heat-induced hemolysis. Statistically, the two-way ANOVA shows the experimental p value is less than 0.05. Therefore, it was clear that the copper sulfide nanoparticles shows a significant increase in the anti-inflammatory activity at the increasing concentrations compared to the standard drug. The percentage of inhibition produced by CuS nanoparticles was found to be $68.68 \pm 1.29\%$, which is highly significant than standard drug ($56.25 \pm 2.34\%$) at the concentration of 75 μg/mL ($p < 0.001$). At 100 μg/mL concentration, the nanoparticles exhibited the most significant increase ($p < 0.001$) in the activity ($93.87 \pm 0.80\%$) than standard drug ($79.55 \pm 1.32\%$). Other concentrations did not show any significant differences between nanoparticles and standard drug. The inhibition of hemolysis by the nanoparticles at 50% inhibition concentration (IC_{50}) was calculated and compared with the standard drug. The IC_{50} values for the CuS nanoparticles and standard drugs were recorded as 47.23 ± 0.33 and 62.72 ± 0.45 μg/mL, respectively (Figure 9).

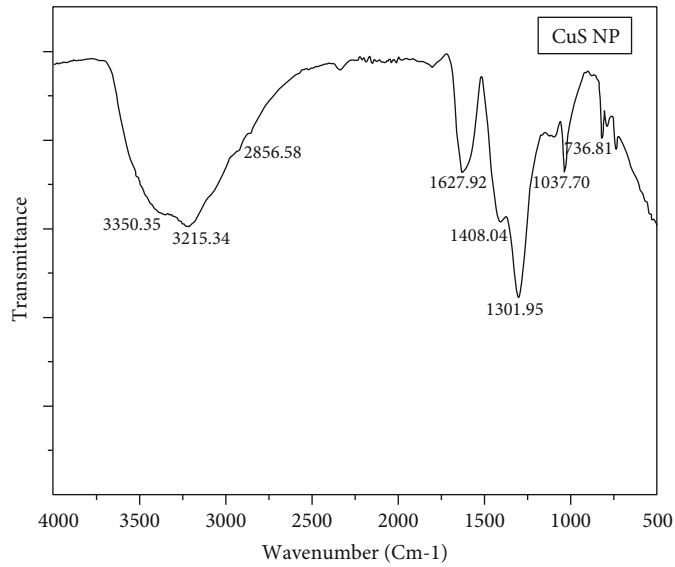

Figure 3: FTIR spectrum shows the functional molecules present in copper sulfide nanoparticles.

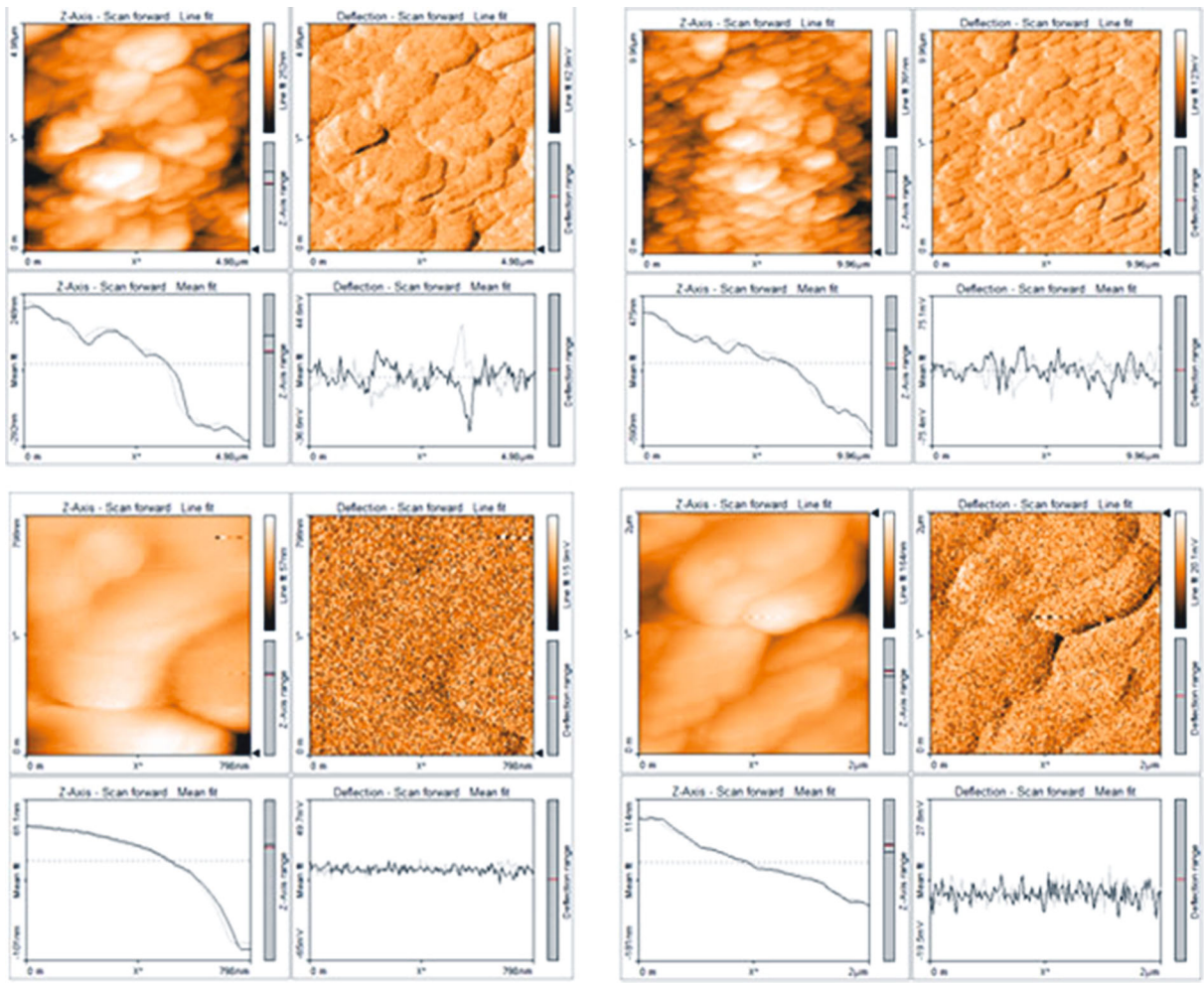

Figure 4: AFM image shows surface morphology of copper sulfide nanoparticles.

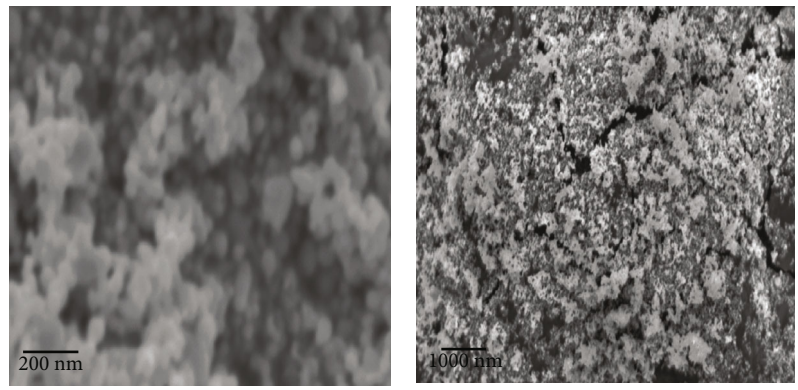

(a) (b)

Figure 5: SEM analysis of copper sulfide nanoparticle synthesized by *Aeromonas hydrophila* scanned at different magnification ranges: (a) scale bar: 2 μm; (b) scale bar: 200 nm.

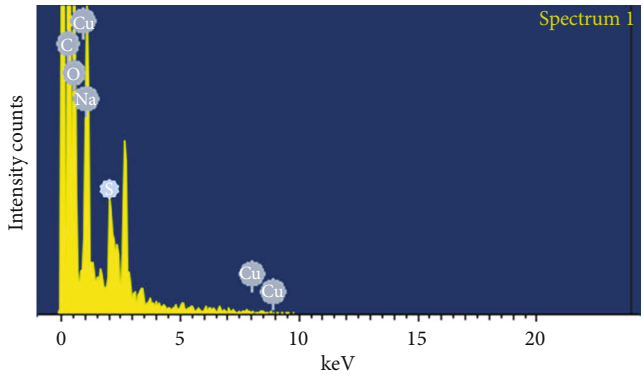

Figure 6: EDX spectrum of CuS nanoparticles.

4.5. Toxicology Study of Copper Nanoparticles on the Zebrafish Model. Embryos prior to 4 hpf (sphere stage) were treated with different concentrations of copper sulfide nanoparticles, and developmental abnormalities were observed in embryos treated at different concentrations (20-150 μg/mL). Figure 10 represents the toxicity of untreated and nanoparticle-treated groups, which shows no significant ($p > 0.05$) effects at the concentrations of 20 and 60 μg/mL, respectively, at all the exposure times. The increased concentrations of 80 and 150 μg/mL of CuS nanoparticles caused highly significant effects ($p < 0.001$) on mortality in embryos. The mortality rate of the fish was gradually and significantly ($p < 0.05$) increased up to 96 hpf while increasing the concentration of nanoparticles. Both 100 and 150 μg/mL of CuS nanoparticles caused 80 and 100% mortality off the embryos, respectively, at the period of 96 hpf. There is a significant effect noticed in 150 μg/mL at the exposure time of 72 and 96 hpf of the embryos. Noticeably, the 50% of lethal concentration (LC_{50}) of CuS nanoparticles was found to be 60 μg/mL.

Likewise, the hatching rate of zebrafish embryos is also affected by the increasing concentration of CuS nanoparticles. The untreated embryos have shown an $80 \pm 2.9\%$ hatching rate, whereas 60 μg/mL CuS nanoparticle-treated embryos showed $95 \pm 1.7\%$ hatching rates, respectively. There are no significant differences observed in the hatching percentage at 20 and 40 μg/mL copper sulfide nanoparticle-treated groups. The concentration of 40 and 60 μg/mL exhibits p value as less than 0.01 ($p < 0.01$). This hatching rate was found to be moderately significant ($p < 0.05$) and decreased while increasing the concentration of nanoparticles up to 150 μg/mL. Figure 11 shows significantly delayed hatching ability while increasing the concentration of CuS-NPs. Profoundly, the higher concentration of CuS nanoparticles caused developmental toxicity and growth retardation in zebrafish.

The untreated control zebrafish shows average growth without any delayed activity. The 60 μg/mL concentration did not show any significant malfunctions or developmental toxicity up to 96 hpf. Above 80 μg/mL of CuS nanoparticles caused tail and spinal cord flexure and truncation, yolk sac edema, and fin abnormalities. Axial bent and tail bend, pericardial edema was identified through a microscope, which was indicated by arrows, head and eye hypoplasia, and no swim bladder and reduced digestive gut were observed in CuS-NP-exposed embryos (Figure 12). The abnormality was observed in 80 μg/mL CuS-NP-treated groups at 24 hpf, 48 hpf, and 96 hpf.

5. Discussion

The formation of greenish-brown indicates the reduction of Cu^{2+} to zerovalent copper (Cu^0) in the reaction mixture. The mechanism behind this reduction is copper sulfate which is dissociating into Cu^{2+} and sulfate initially. Further, the Cu^{2+} is reduced into zerovalent copper sulfide nanoparticles (Cu^0) through the biomolecules present in the culture supernatant [30]. Similarly, Pradhan et al. [31] have observed blue color, and later, it could be changed into brown by the involvement of lemon extract.

UV-vis spectrum showed the highest peak at 307 nm, which could be due to surface plasmon resonance effects of copper sulfide nanoparticles [32]. The peak intensity was increased by increasing the time of incubation of reaction mixture. The present results were in good accordance with Rawat et al. [17] who observed the range from 220 to 380 nm for copper nanoparticles during UV-vis spectrum

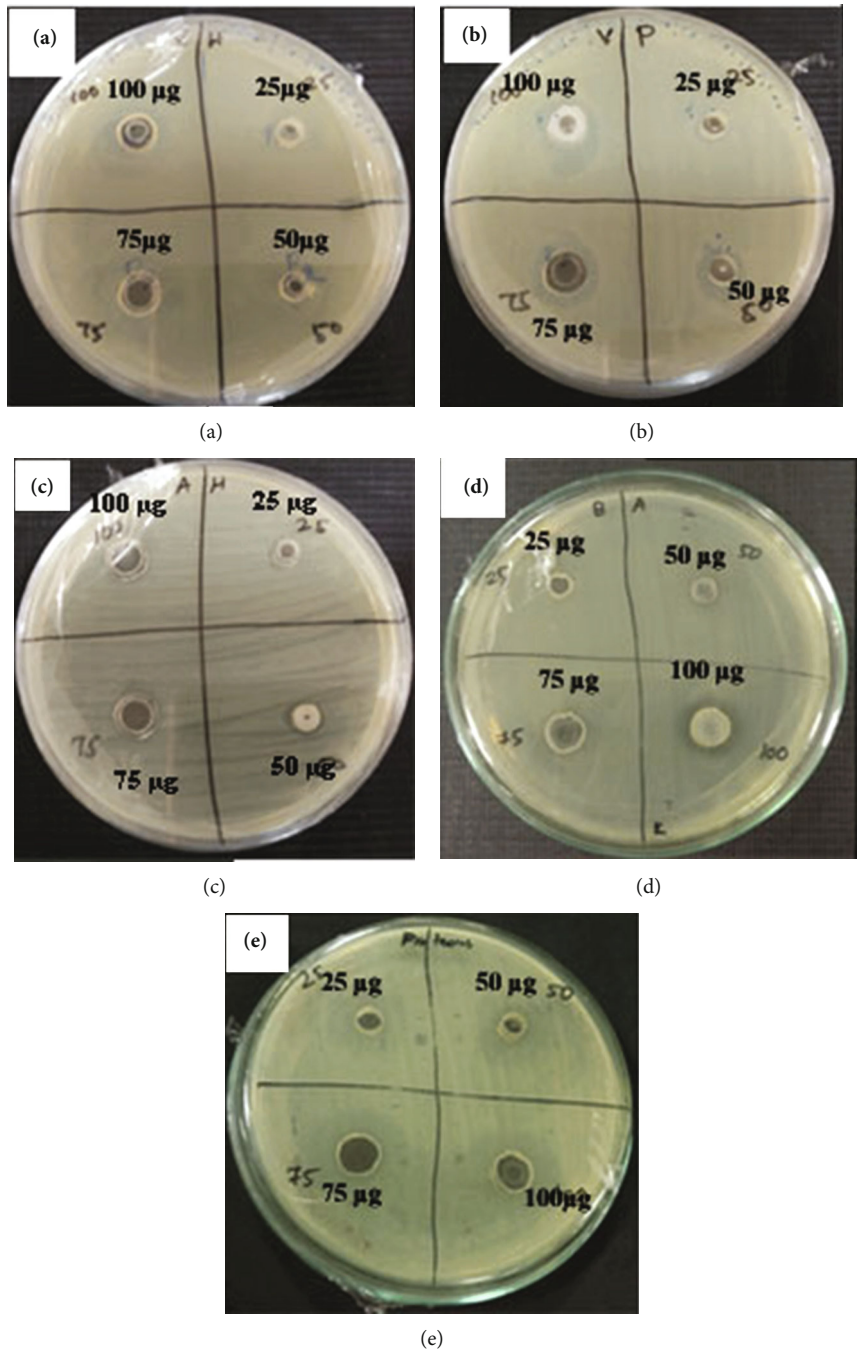

Figure 7: Antibacterial activity of CuS nanoparticles against pathogenic bacteria: (a) *V. harveyi*; (b) *V. parahaemolyticus*; (c) *E. coli*; (d) *Bacillus sp*; (e) *Proteus* sp.

analysis. Presently, some minor peaks were observed as fluctuations, which corresponded to the biomolecules associated with cell-free supernatant that may not be actively involved in the synthesis [33].

XRD spectrum shows two distinct peaks at the 2θ values, 31.18° and 44.81°, which are corresponding to the respective (hkl) planes of (110) and (111). These diffraction peaks are well-matched with the pattern of the FCC (face-centred cubic) phase of copper sulfide nanoparticles (JCPDS 04-0836). The average size of nanoparticles observed in this present study (20 nm) using the Debye-Scherrer equation was found to be proficient due to its size which implies more surface area to volume ratio might act as a good candidate to target drug delivery. Also, the present findings are in line with Rosy et al. [34] who have synthesized that the copper nanoparticles in 56 ± 8 nm sized from *Cissus arnotiana* proved significant biological properties.

The functional groups associated with the biosynthesized copper sulfide nanoparticles using cell-free supernatant of *A. hydrophila* were characterized. It was clear that the functional groups, N-O asymmetric stretch nitro compounds, and alcohols involved in the synthesis have been confirmed

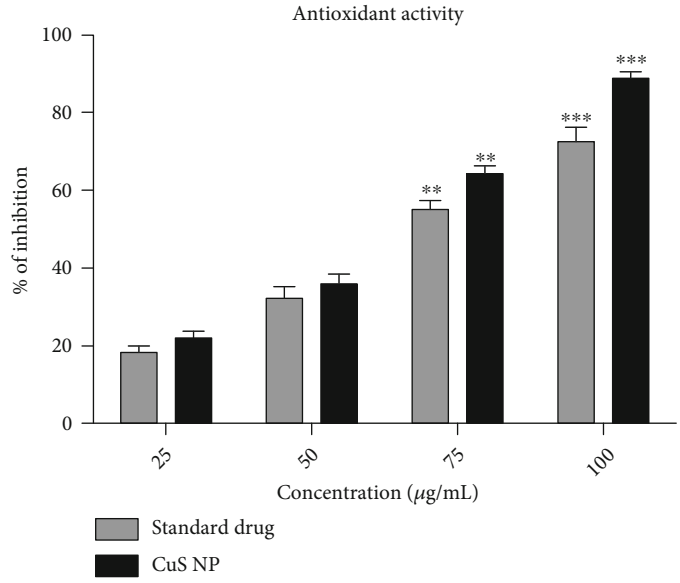

Figure 8: Antioxidant activity of copper sulfide nanoparticles. The error bar values are expressed as mean ± SE. Significant differences were expressed as $p < 0.001$ (***), $p < 0.01$ (**), and $p < 0.05$ (*), and all the experiments were performed in triplicate.

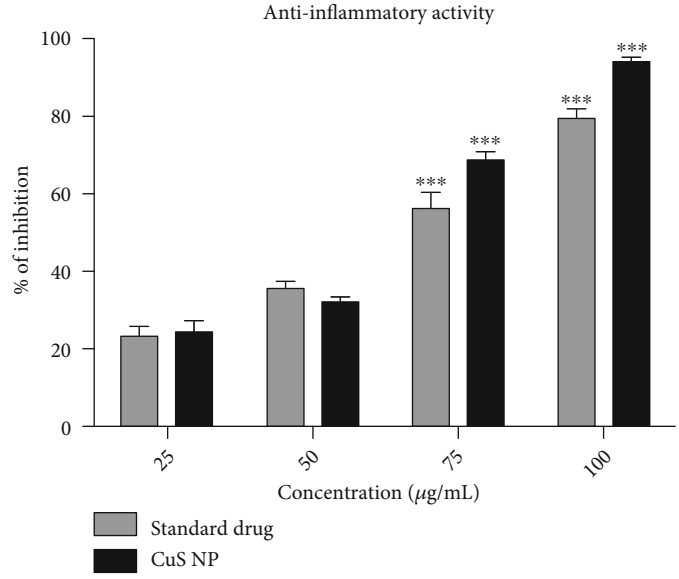

Figure 9: Anti-inflammatory activity of synthesized copper sulfide nanoparticles. The error bar values are expressed as mean ± SE. Significant differences were expressed as $p < 0.001$ (***), $p < 0.01$ (**), and $p < 0.05$ (*), and all the experiments were performed in triplicate.

in the dried and purified copper nanoparticles by comparing the earlier results of Rasouli et al. [35] who have stated that carboxylic acid from protein molecules in supernatant might be responsible for the synthesized nanoparticles. The absorption peak at 1627 cm^{-1} corresponds to protein linkages that interact with nanoparticles and reduce copper ions (Cu^{2+}) to copper nanoparticles (Cu^{0}) which have been well coincided with Patel et al. [36], who reported the exact wavenumber in their copper nanoparticle biosynthesis.

AFM study revealed the surface characters of synthesized nanoparticles which are showing the rough and smooth surfaces. The average size of CuS nanoparticles is 20.65 nm, which is approximately equal to the XRD size calculation. The presently obtained sizes of the nanoparticles are in accordance with the earlier findings of Karthik and Singh [37] who reported the average size of nanocopper from AFM images as 6.45 nm.

The morphological characters like size and shape of nanoparticles were determined using SEM. The biosynthesized copper sulfide nanoparticles are homogenous and uniformly dispersed. Some are observed as rod and spherical with the size ranging from 20 to 200 nm. Copper and sulfide were bonded to each other, and it appears clustered. Similarly, Ghidan et al. [38] and Khani et al. [39] reported the

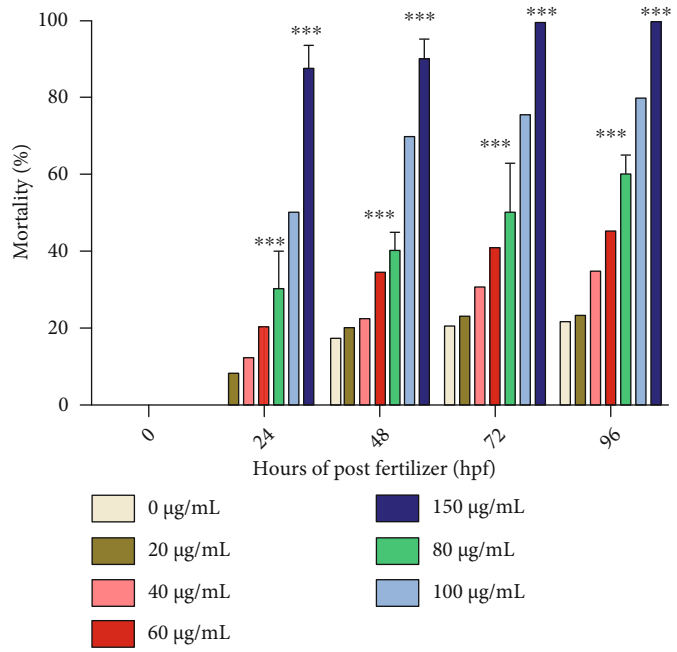

Figure 10: Mortality rate of zebrafish embryos treated with copper sulfide nanoparticles. The error bar values are expressed as mean ± SE. Significant differences were expressed as $p < 0.001$ (***), $p < 0.01$ (**), and $p < 0.05$ (*), and all the experiments were performed in triplicate.

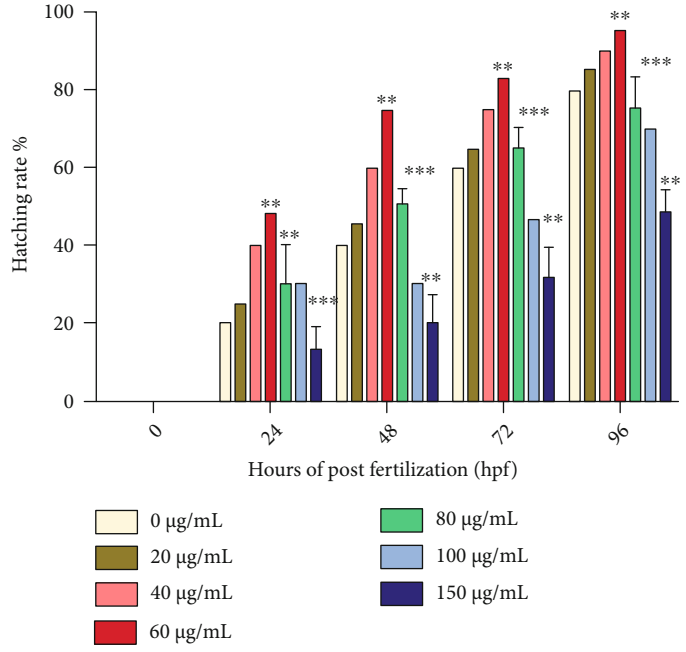

Figure 11: Hatching rate of zebrafish embryos using copper sulfide nanoparticles. The error bar values are expressed as mean ± SE. Significant differences were expressed as $p < 0.001$ (***), $p < 0.01$ (**), and $p < 0.05$ (*), and all the experiments were performed in triplicate.

average size observed between 10 and 100 nm using *Punica granatum* and 5–20 nm using *Z. spina-christi* supernatants', respectively. Inspiringly, the CuS-NPs may elicit a good biological activity due to their different morphological characteristics.

EDX analysis showed the presence of different elemental composition of biosynthesized CuS nanoparticles. The EDAX pattern confirmed respective peaks for copper and the sulfur component as well as the other peaks called

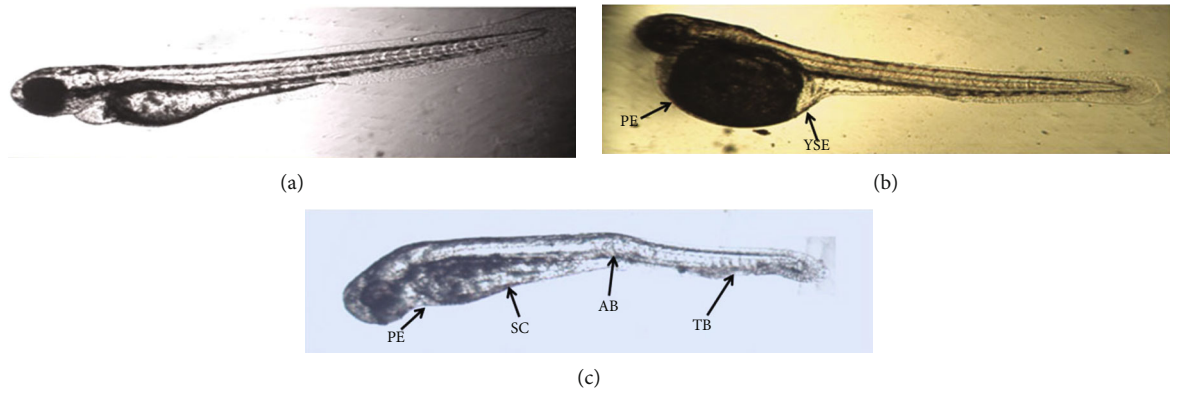

FIGURE 12: Microscopic image of the zebrafish embryo recorded 80 μg/mL of CuS nanoparticles at different time periods: (a) 24 hpf: not shown toxicity; (b) 48 hpf: shows PE (precardial edema) and YSE (yolk sac edema); (c) 96 hpf: shows SC (spinal cord curvature), AB (axial bent), and TB (tail bent).

biomoities, which may be evolved from the culture supernatant of *A. hydrophila* [40].

Copper sulfide nanoparticles exhibited the preponderant inhibition activity against gram-negative pathogenic bacteria like *E. coli*, *Vibrio harveyi*, *Vibrio parahaemolyticus*, and *Proteus* sp. The gram-positive *Bacillus* sp. resulted in a low inhibition activity that might be due to integrity of cell wall where evasion of the nanoparticles is quite difficult, as they have thick and strong cell wall composition, and made up of complex peptidoglycan [41]. Whereas in the gram-negative bacteria, the nanoparticles may easily penetrate the cell and cause leakage of cell components. Sometimes, nanoparticles were altering either DNA or RNA and even thus lead to cell death [41, 42].

Free radicals are highly uncharged and unstable molecules that contain one or more unpaired electrons which are highly reactive to produce any toxic components. *In vitro* radical scavenging activity of biosynthesized copper sulfide nanoparticles has been evaluated against DPPH. Biosynthesized CuS nanoparticles exhibited significant scavenging activity when compared to the standard drug, ascorbic acid. This difference could be achieved by NPs due to the presence of carboxylic acid, alkanes, and alcohol. *In vitro* anti-inflammatory activity (inflammation inhibition) of biosynthesized CuS nanoparticles was determined by the membrane stabilizing method. The nanoparticles exhibited excellent percentage of inhibition around 93.71%, when compared to a standard drug (79.43%). Comparably, the presently recorded inhibition is prominent as like the previous reports of Tiwari et al. [43] who obtained 92% of inflammation inhibition from the biosynthesized copper nanoparticles.

Toxicity assay of CuS nanoparticles carried out on zebrafish embryos at different concentrations and exposure time. The mortality rate and hatching rate were affected with the increased concentration of nanoparticles. Biosynthesized CuS nanoparticles were found to be toxic to the zebrafish that resulted above 80 μg/mL. Diplomatically to the above biological activity, though the CuS-NPs are potential enough, presently, the nontargeted toxic potentials have not been favored in the acceptable dose of copper nanoparticles in various biomedical applications, i.e., below 80 μg/mL. On contrary to this, various abnormalities like axial bent, spinal cord curvature, tail bent, and yolk sac edema were observed at 80 μg/mL concentration of CuS-NPs. Similarly, Rajendran et al. [44] reported the toxic effect of zirconium nanoparticles on zebrafish. They obtained LC_{50} values for Zr nanoparticles to be 1 μg/mL. Then, 2 to 5 μg/mL shows delayed hatching ability and increased concentration caused malfunctions and developmental retardation in zebrafish.

6. Conclusion

One of the affordable and reproducible sources for biosynthesis, the bacteria (*A. hydrophila*), a very perceptible method compared to physical- or chemical-based ones for synthesizing metal nanoparticles was successfully achieved. Bacteria-mediated synthesis can also save time, can be a cost-effective one, and can be grown large scale at an optimum condition. Hence, bacteria will be a best choice as an impending source for the improvement in nanotechnology to synthesize nanoparticles for large-scale production. Extracellular synthesis using *Aeromonas hydrophila* and its biomedical applications have been extensively studied in this present research. Nanoparticle synthesis was characterized and confirmed by XRD, FTIR, UV, SEM, and AFM analyses. Applications such as antibacterial, anti-inflammatory, and antioxidant activity and the nontargeted toxicology effects of copper nanoparticles using zebrafish were also been evaluated. Future studies are warranted with further characterization and field applications.

Data Availability

The data used to support the findings of this study are included within the article.

Conflicts of Interest

The authors declare that there is no conflict of interest.

Authors' Contributions

SR designed the research; SR, SJ, and VM carried out research; and SP, PM, DA, SR, and KA carried out statistical analysis and wrote and corrected the manuscript.

Acknowledgments

The authors did this research with their researcher fund provided by their institutions. The authors would like to acknowledge Saveetha Dental College and Hospital, SIMATS, and this work was funded by Researchers Supporting Project number (RSP-2021/165), King Saud University, Riyadh, Saudi Arabia.

References

[1] K. Iwahori, R. Takagi, N. Kishimoto, and I. Yamashita, "A size controlled synthesis of CuS nano-particles in the protein cage, apoferritin," *Materials Letters*, vol. 65, no. 21-22, pp. 3245–3247, 2011.

[2] Y. Lu, X. Meng, G. Yi, and J. Jia, "In situ growth of CuS thin films on functionalized self-assembled monolayers using chemical bath deposition," *Journal of Colloid and Interface Science*, vol. 356, no. 2, pp. 726–733, 2011.

[3] L. Isac, A. Duta, A. Kriza, S. Manolache, and M. Nanu, "Copper sulfides obtained by spray pyrolysis – Possible absorbers in solid- state solar cells," *Thin Solid Films*, vol. 515, no. 15, pp. 5755–5758, 2007.

[4] U. K. Gautam and B. Mukherjee, "A simple synthesis and characterization of CuS nanocrystals," *Bulletin of Materials Science*, vol. 29, no. 1, pp. 1–5, 2006.

[5] C. Jiang, W. Zhang, G. Zou, L. Xu, W. Yu, and Y. Qian, "Hydrothermal fabrication of copper sulfide nanocones and nanobelts," *Materials Letters*, vol. 59, no. 8-9, pp. 1008–1011, 2005.

[6] A. A. Sagade and R. Sharma, "Copper sulphide (Cu $_{x}$ S) as an ammonia gas sensor working at room temperature," *Sensors and Actuators B: Chemical*, vol. 133, no. 1, pp. 135–143, 2008.

[7] D. Manoj, R. Saravanan, J. Santhanalakshmi, S. Agarwal, V. K. Gupta, and R. Boukherroub, "Towards green synthesis of monodisperse Cu nanoparticles: an efficient and high sensitive electrochemical nitrite sensor," *Sensors and Actuators B: Chemical*, vol. 266, pp. 873–882, 2018.

[8] Y. Wu, C. Wadia, W. Ma, B. Sadtler, and A. P. Alivisatos, "Synthesis and photovoltaic application of copper (I) sulfide nanocrystals," *Nano Letters*, vol. 8, no. 8, pp. 2551–2555, 2008.

[9] T.-Y. Ding, M.-S. Wang, S.-P. Guo, G.-C. Guo, and J.-S. Huang, "CuS nanoflowers prepared by a polyol route and their photocatalytic property," *Materials Letters*, vol. 62, no. 30, pp. 4529–4531, 2008.

[10] J. Santhoshkumar, S. Rajeshkumar, and S. Venkat Kumar, "Phyto-assisted synthesis, characterization and applications of gold nanoparticles - A review," *Biochemistry and Biophysics Reports*, vol. 11, pp. 46–57, 2017.

[11] M. Schaffie and M. Hosseini, "Biological process for synthesis of semiconductor copper sulfide nanoparticle from mine wastewaters," *Journal of Environmental Chemical Engineering*, vol. 2, no. 1, pp. 386–391, 2014.

[12] N.-Q. Zhou, L. J. Tian, Y. C. Wang et al., "Extracellular biosynthesis of copper sulfide nanoparticles by *Shewanella oneidensis* MR-1 as a photothermal agent," *Enzyme and Microbial Technology*, vol. 95, pp. 230–235, 2016.

[13] M. Hosseini, M. Schaffie, M. Pazouki, E. Darezereshki, and M. Ranjbar, "Biologically synthesized copper sulfide nanoparticles: production and characterization," *Materials Science in Semiconductor Processing*, vol. 15, no. 2, pp. 222–225, 2012.

[14] M. Hosseini, M. Schaffie, M. Pazouki, A. Schippers, and M. Ranjbar, "A novel electrically enhanced biosynthesis of copper sulfide nanoparticles," *Materials Science in Semiconductor Processing*, vol. 16, no. 2, pp. 250–255, 2013.

[15] R. Sanghi and P. Verma, "A facile green extracellular biosynthesis of CdS nanoparticles by immobilized fungus," *Chemical Engineering Journal*, vol. 155, no. 3, pp. 886–891, 2009.

[16] P. Ananthi and S. M. J. Kala, "Plant extract mediated synthesis and characterization of copper nanoparticles and their pharmacological activities," *International Journal of Innovative Science Engineering and Technology*, vol. 6, pp. 13455–13465, 2017.

[17] P. Rawat, A. Nigam, and S. Kala, "Green synthesis of copper and copper sulfide nanoparticles," *AIP Conference Proceedings*, vol. 2220, no. 1, article 020102, 2020.

[18] D. H. Nies, "Microbial heavy-metal resistance," *Applied Microbiology and Biotechnology*, vol. 51, no. 6, pp. 730–750, 1999.

[19] P. Mohanpuria, N. K. Rana, and S. K. Yadav, "Biosynthesis of nanoparticles: technological concepts and future applications," *Journal of Nanoparticle Research*, vol. 10, no. 3, pp. 507–517, 2008.

[20] C. Colipai, G. Southam, P. Oyarzún et al., "Synthesis of copper sulfide nanoparticles using biogenic H_2S produced by a low-pH sulfidogenic bioreactor," *Minerals*, vol. 8, no. 2, p. 35, 2018.

[21] A. V. Singh, R. Patil, A. Anand, P. Milani, and W. Gade, "Biological synthesis of copper oxide nano particles using Escherichia coli," *Current Nanoscience*, vol. 6, no. 4, pp. 365–369, 2010.

[22] D. Majumder, "Bioremediation: copper nanoparticles from electronic-waste," *International Journal of Engineering Science and Technology*, vol. 4, no. 10, 2012.

[23] R. Varshney, S. Bhadauria, M. S. Gaur, and R. Pasricha, "Characterization of copper nanoparticles synthesized by a novel microbiological method," *Jom*, vol. 62, no. 12, pp. 102–104, 2010.

[24] G. Shobha, V. Moses, and S. Ananda, "Biological synthesis of copper nanoparticles and its impact," *International Journal of Pharmaceutical Science Invention*, vol. 3, no. 8, pp. 6–28, 2014.

[25] S. Saif Hasan, S. Singh, R. Y. Parikh et al., "Bacterial synthesis of copper/copper oxide nanoparticles," *Journal of Nanoscience and Nanotechnology*, vol. 8, no. 6, pp. 3191–3196, 2008.

[26] R. Usha, E. Prabu, M. Palaniswamy, C. K. Venil, and R. Rajendran, "Synthesis of metal oxide nano particles by Streptomyces sp. for development of antimicrobial textiles," *Global Journal of Biochemistry and Biotechnology*, vol. 5, no. 3, pp. 153–160, 2010.

[27] R. Ramanathan, S. K. Bhargava, and V. Bansal, "Biological synthesis of copper/copper oxide nanoparticles," *Chemeca*, pp. 1–8, 2011.

[28] S. Shantkriti and P. Rani, "Biological synthesis of copper nanoparticles using Pseudomonas fluorescens," *International*

Journal of Current Microbiology and Applied Sciences, vol. 3, no. 9, pp. 374–383, 2014.

[29] S. Jayakodi and V. K. Shanmugam, "Green synthesis of CuO nanoparticles and its application on toxicology evaluation," *Biointerface Research in Applied Chemistry*, vol. 10, no. 5, pp. 6343–6353, 2020.

[30] S. Rajeshkumar, M. Tharani, M. Jeevitha, and J. Santhoshkumar, "Anticariogenic activity of FreshAloe Vera-Gel mediated copper oxide nanoparticles," *Indian Journal of Public Health Research & Development*, vol. 10, no. 11, p. 3664, 2019.

[31] S. Pradhan, R. Shrestha, and K. Bhandari, "Effect of various parameters on bio-synthesis of copper nanoparticles using Citrus medica Linn (lemon) extract and its antibacterial activity," *Amrit Research Journal*, vol. 1, no. 1, pp. 51–58, 2020.

[32] K. B. Ayaz Ahmed and V. Anbazhagan, "Synthesis of copper sulfide nanoparticles and evaluation of in vitro antibacterial activity and in vivo therapeutic effect in bacteria-infected zebrafish," *RSC Advances*, vol. 7, no. 58, pp. 36644–36652, 2017.

[33] M. T. el-Saadony, M. E. Abd el-Hack, A. E. Taha et al., "Eco-friendly synthesis and insecticidal application of copper nanoparticles against the storage pest Tribolium castaneum," *Nanomaterials*, vol. 10, no. 3, p. 587, 2020.

[34] J. P. Rosy, V. Shanmugam, J. S. Jas, and S. Jayakodi, "Biomimetic copper oxide nanoparticles and its validation through in-silico approach on cardiac enzymes," *Current Nanoscience*, vol. 17, no. 3, 2021.

[35] E. Rasouli, W. J. Basirun, M. R. Johan et al., "Facile and greener hydrothermal honey-based synthesis of Fe_3O_4/Au core/shell nanoparticles for drug delivery applications," *Journal of Cellular Biochemistry*, vol. 120, no. 4, pp. 6624–6631, 2019.

[36] B. Patel, M. Channiwala, S. Chaudhari, and A. Mandot, "Biosynthesis of copper nanoparticles; its characterization and efficacy against human pathogenic bacterium," *Journal of Environmental Chemical Engineering*, vol. 4, no. 2, pp. 2163–2169, 2016.

[37] P. Karthik and S. P. Singh, "Copper conductive inks: synthesis and utilization in flexible electronics," *RSC Advances*, vol. 5, no. 79, pp. 63985–64030, 2015.

[38] A. Y. Ghidan, T. M. Al-Antary, and A. M. Awwad, "Green synthesis of copper oxide nanoparticles using _Punica granatum_ peels extract: Effect on green peach Aphid," *Environmental Nanotechnology, Monitoring & Management*, vol. 6, pp. 95–98, 2016.

[39] R. Khani, B. Roostaei, G. Bagherzade, and M. Moudi, "Green synthesis of copper nanoparticles by fruit extract of _Ziziphus spina- christi_ (L.) Willd.: Application for adsorption of triphenylmethane dye and antibacterial assay," *Journal of Molecular Liquids*, vol. 255, pp. 541–549, 2018.

[40] S. Jayakodi and V. K. Shanmugam, "Statistical optimization of copper oxide nanoparticles using response surface methodology and Box–Behnken design towards in vitro and in vivo toxicity assessment," *Biointerface Research in Applied Chemistry*, vol. 11, no. 3, pp. 10027–10039, 2021.

[41] P. Dibrov, J. Dzioba, K. K. Gosink, and C. C. Häse, "Chemiosmotic mechanism of antimicrobial activity of Ag+inVibrio cholerae," *Antimicrobial Agents and Chemotherapy*, vol. 46, no. 8, pp. 2668–2670, 2002.

[42] S. Shrivastava, T. Bera, A. Roy, G. Singh, P. Ramachandrarao, and D. Dash, "Characterization of enhanced antibacterial effects of novel silver nanoparticles," *Nanotechnology*, vol. 18, no. 22, article 225103, 2007.

[43] M. Tiwari, K. Narayanan, M. B. Thakar, H. V. Jagani, and J. Venkata Rao, "Biosynthesis and wound healing activity of copper nanoparticles," *IET Nanobiotechnology*, vol. 8, no. 4, pp. 230–237, 2014.

[44] S. Rajendran, G. Annadurai, and S. Rajeshkumar, "Characterization and toxicology evaluation of zirconium oxide nanoparticles on the embryonic development of zebrafish, Danio rerio," *Drug and Chemical Toxicology*, vol. 42, no. 1, pp. 104–111, 2019.

Hindawi
Oxidative Medicine and Cellular Longevity
Volume 2022, Article ID 2079630, 10 pages
https://doi.org/10.1155/2022/2079630

Research Article

Exacerbation of Thrombotic Responses to Silver Nanoparticles in Hypertensive Mouse Model

Zannatul Ferdous,[1] Sumaya Beegam,[1] Nur E. Zaaba,[1] Ozaz Elzaki,[1] Saeed Tariq,[2] Yaser E. Greish,[3] Badreldin H. Ali,[4] and Abderrahim Nemmar [1,5]

[1]*Department of Physiology, College of Medicine and Health Sciences, United Arab Emirates University, P.O. Box 17666, Al Ain, UAE*
[2]*Department of Anatomy, College of Medicine and Health Science, United Arab Emirates University, P.O. Box 17666, Al Ain, UAE*
[3]*Department of Chemistry, College of Sciences, United Arab Emirates University, P.O. Box 17666, Al Ain, UAE*
[4]*Department of Pharmacology and Clinical Pharmacy, Sultan Qaboos University, P.O. Box 35, Muscat 123, Al-Khod, Oman*
[5]*Zayed Center for Health Sciences, United Arab Emirates University, UAE*

Correspondence should be addressed to Abderrahim Nemmar; anemmar@uaeu.ac.ae

Received 31 August 2021; Accepted 30 November 2021; Published 15 January 2022

Academic Editor: Vladimir Jakovljevic

With advent of nanotechnology, silver nanoparticles, AgNPs owing majorly to their antibacterial properties, are used widely in food industry and biomedical applications implying human exposure by various routes including inhalation. Several reports have suggested AgNPs induced pathophysiological effects in a cardiovascular system. However, cardiovascular diseases such as hypertension may interfere with AgNPs-induced response, yet majority of them are understudied. The aim of this work was to evaluate the thrombotic complications in response to polyethylene glycol- (PEG-) coated AgNPs using an experimental hypertensive (HT) mouse model. Saline (control) or PEG-AgNPs (0.5 mg/kg) were intratracheally (i.t.) instilled four times, i.e., on days 7, 14, 21, and 28 post-angiotensin II-induced HT, or vehicle (saline) infusion. On day 29, various parameters were assessed including thrombosis in pial arterioles and venules, platelet aggregation in whole blood in vitro, plasma markers of coagulation, and fibrinolysis and systemic oxidative stress. Pulmonary exposure to PEG-AgNPs in HT mice induced an aggravation of *in vivo* thrombosis in pial arterioles and venules compared to normotensive (NT) mice exposed to PEG-AgNPs or HT mice given saline. The prothrombin time, activated partial thromboplastin time, and platelet aggregation in vitro were exacerbated after exposure to PEG-AgNPs in HT mice compared with either NT mice exposed to nanoparticles or HT mice exposed to saline. Elevated concentrations of fibrinogen, plasminogen activator inhibitor-1, and von Willebrand factor were seen after the exposure to PEG-AgNPs in HT mice compared with either PEG-AgNPs exposed NT mice or HT mice given with saline. Likewise, the plasma levels of superoxide dismutase and nitric oxide were augmented by PEG-AgNPs in HT mice compared with either NT mice exposed to nanoparticles or HT mice exposed to saline. Collectively, these results demonstrate that PEG-AgNPs can potentially exacerbate the in vivo and in vitro procoagulatory and oxidative stress effect in HT mice and suggest that population with hypertension are at higher risk of the toxicity of PEG-AgNPs.

1. Introduction

Silver nanoparticles (AgNPs) became one of the most investigated engineered nanomaterials during the past few years, given the fact that these nanomaterials proved to have interesting, challenging, and promising characteristics suitable for various household and biomedical applications [1–3]. The widespread application in turn results in environmental contamination and human exposure raising serious concern about their potential adverse effects and toxicity on human health [2, 4]. Of all the various routes of exposure of nanoparticles reported so far, pulmonary exposure provides a major a potential route to aerosolized AgNPs used in health sprays, nebulizers, deodorants, and disinfectants [5].

Moreover, inhalation exposure to these particles is inescapable to workers in nanosilver-manufacturing industries, particularly during particle synthesis and handling of dry powders, as well as during the manufacture of AgNPs-containing products [6].

A collection of studies have previously addressed the effects and applications of different kinds of AgNPs (shaped, sized, coated and functionalized) in several components of the cardiovascular system, such as endothelial cells, isolated vessels, and organs as well as integrative animal models, trying to elucidate the underlying mechanisms involved in their pathophysiological effect and hence to understand their implication in the field of biomedicine [7–11]. For instance, Sun et al. [12] demonstrated that AgNPs exposure significantly and dose-dependently decreased the cell viability, induced NADPH oxidase 4 and nuclear factor erythroid 2-related factor 2 (Nrf2) mediated oxidative stress, and led to early apoptosis in human umbilical vein endothelial cells. Using Langendorff rat heart preparation, Ramirez-Lee and colleagues evaluated direct actions of AgNPs (15 ± 4 nm) on coronary vascular tone and cardiac contractility [13]. Similarly, we have recently demonstrated significant pathophysiological effect to pulmonary-exposed polyvinylpyrrolidone and citrate-coated AgNPs (10 nm) on a cardiovascular system particularly on the thrombotic events, oxidative stress, inflammatory markers, DNA damage, and apoptosis [14]. Our *in vitro* study further revealed the potential of these same nanoparticles to cause significant erythrocytic oxidative damage and eryptosis [10].

Although the number of evidence about the toxic effects and mechanisms induced by AgNPs on heart is limited, there are much fewer investigations on the impeding effects of these nanoparticles on populations with cardiovascular pathologies such as hypertension. In this regard, previous studies have demonstrated that pulmonary exposure to engineered nanomaterials is capable of aggravating cardiovascular dysfunction via mechanisms including systemic inflammation, coronary artery dysfunction, metabolic derangement, autonomic dysregulation, and oxidative stress [15–18]. Oxidative stress contributed by increased reactive oxygen species level generates an imbalance between reactive oxygen species generation and antioxidant defence mechanism such as catalase and superoxide dismutase [19]. This process also contributes to the development of a common cardiovascular disorder, namely, hypertension [20]. In addition, evidence for the prothrombotic and hypercoagulable state in hypertension has been extensively reviewed [20–22]. In fact, some studies have reported abnormalities in the coagulation and fibrinolytic pathways, as well as in platelets and the endothelium, among hypertensive experimental models and patients [23–25]. In this context, we have recently shown significant oxidative stress and prothrombotic and inflammatory effects in mice exposed to 10 nm AgNPs via intratracheal instillation [14]. Nevertheless, influence of hypertension on the latter effects has not been studied so far.

AgNPs are coated with various natural or synthetic polymers in order to preserve their bioavailability, increase stability, and reduce toxicity [2, 3, 26]. In this regard, polyethylene glycol (PEG) has been widely applied as an effective stabilizing agent in the fabrication of AgNPs and other metal nanoparticles. Consequently, the aim of this study is to assess the effect of PEG-AgNPs, in a mouse model of angiotensin (ANG) II-induced hypertension, on thrombotic events, coagulation profile, and oxidative stress by measuring thrombotic occlusion time in pial arterioles and venules, prothrombin time (PT), activated partial thromboplastin time (aPTT), fibrinogen, plasminogen activator inhibitor-1 (PAI-1), von Willebrand factor (vWF), superoxide dismutase, and total nitric oxide.

2. Materials and Methods

2.1. Nanoparticles. Suspensions of polyethylene glycol-(PEG-) coated silver nanoparticles (PEG-AgNPs) of 40.6 ± 3.8 nm (BioPure™) were purchased from NanoComposix (San Diego, CA, USA). The provided stock concentrations were 1.0 mg/ml with silver purity of 99.99% and endotoxin level < 2.5 EU/ml. The nanoparticle surface area was 13.8 m2/g. PEG-AgNPs were suspended in sterile 0.9% NaCl. Silver acetate (AgAc), as the source of Ag^+ ions, purchased from Sigma-Aldrich (#216674, St. Louis, MO, USA), was dissolved in sterile water to yield a stock concentration of 1 mg/ml. In order to reduce nanoparticle aggregation, the suspensions of PEG-AgNPs were constantly sonicated (Clifton Ultrasonic Bath, Clifton, NJ, USA) for 10 min and vortexed prior their dilution and intratracheal (i.t.) instillation.

2.2. Animal, Experimental Hypertensive Model, and Dosing. Both male and female BALB/C mice of age 8–10 weeks, weighing 20 to 25 g (Animal House of the College of Medicine and Health Sciences, United Arab Emirates University), were housed in light- (12 h light : 12 h dark cycle) and temperature-controlled ($22 \pm 1^{\circ}$C) rooms. They had free access to commercial laboratory chow and were provided tap water *ad libitum*.

A well-validated murine model of hypertension (HT mice) was utilized [21, 27, 28]. BALB/c (8-10 weeks old) mice were administered angiotensin II (ANG II, 0.75 mg/kg/day in 0.15 mol/l NaCl and 0.01 N acetic acid) or vehicle (normotensive (NT), i.e., control mice) for the entire duration of the experiments using an osmotic pump (Alzet osmotic pump model 2006, Durect Corporation, Cupertino, CA, USA). This treatment delivers ANG II plasma concentration equivalent to that observed in patients with renovascular hypertension [28, 29]. The systolic blood pressure (SBP) was measured using computerized noninvasive tail cuff manometry system (ADInstruments, Colorado Springs, USA). SBP was recorded prior to the measurement of thrombosis or animal sacrifice for blood collection and analysis.

Pulmonary exposure was achieved by intratracheal (i.t.) instillation [30, 31]. Mice were anesthetized with isoflurane and positioned supine with an extended neck on an angled board. A Becton Dickinson 24 Gauge cannula was introduced via the mouth into the trachea. The PEG-AgNPs (0.5 mg/kg) or saline (control) was instilled (100 μl) via a

sterile syringe, followed by an equal volume of air bolus. The nanoparticles or saline were i.t. instilled four times, i.e., on days 7, 14, 21, and 28 post-ANG II or vehicle (control) infusion. Another similar group of NT and HT mice received AgAc as a source of Ag^+. On day 29, mice weights were taken, and various cardiovascular parameters were assessed.

This study was reviewed and approved (approval # ERA_2019_5876) by the United Arab Emirates University Animal Ethics Committee, and experiments were performed in accordance with protocols approved by the committee.

2.3. Characterization of PEG-AgNPs. Transmission electron microscopy (TEM) of AgNPs was performed by a method described in our previous paper [10]. Briefly, the suspensions were subjected to sonication at room temperature for 15 min prior to processing for TEM. A drop of PEG-AgNPs suspensions was deposited on a 200-mesh Formvar/Carbon coated copper grid and allowed to dry for 1 h at room temperature. Then, the grids were examined and photographed at different magnifications using Tecnai™ G^2 Spirit transmission microscope (FEI Company, Hillsboro, OR, USA).

Regarding zeta potential analysis, the PEG-AgNPs suspensions were diluted to 10% by volume in absolute ethanol, vortexed for 10 minutes, and then were subjected to the size distribution and zeta potential measurements using Malvern zetasizer instrument (Malvern Panalytical, UK) and Zetasizer 7.11 software for the measurement and data processing. All measurements were carried out at room temperature and were done in triplicate.

2.4. Experimental Pial Arteriole and Venule Thrombosis Model. In separate animals, *in vivo* thrombogenesis in the pial arterioles and venules was assessed in NT and HT mice after saline or PEG-AgNPs or Ag^+ ion exposure, according to a previously described technique [32]. Briefly, the animal was anesthetized with urethane (1 mg/g BW, i.p.), the trachea was intubated, and the right jugular vein was cannulated with a 2F venous catheter (Portex, Hythe, UK) for the administration of fluorescein (Sigma-Aldrich, St. Louis, MO, USA). Thereafter, craniotomy was first performed on the right temporoparietal cortex with a hand-held microdrill, and the dura was stripped open. Only untraumatized preparations were used, and those showing trauma to either microvessels or underlying brain tissue were discarded. Cerebral microcirculation was directly visualized using a fluorescence microscope (Olympus, Melville, NY, USA) connected to a camera and DVD recorder. A heating pad was used, and body temperature was raised to 37°C, as monitored by a rectal thermoprobe connected to a temperature reader (Physitemp Instruments, NJ, USA). A field containing arterioles and venules (15-20 μm) in diameter was chosen. Such a field was taped prior to and during the photochemical insult, which was carried out by injecting fluorescein (0.1 ml/mouse of 5% solution) via the jugular vein, which was allowed to circulate for 30-40 sec. The cranial preparation was then exposed to stabilized mercury light. The photochemically induced injury to arterioles and venules, in turn, causes platelets to adhere at the site of endothelial damage and aggregate. Platelet aggregates and thrombus formation grow in size until complete vascular occlusion. The time from the injury until complete vascular occlusion (time to flow stop) in arterioles and venules was measured in seconds. At the end of the experiments, the animals were euthanized by an overdose of urethane.

2.5. Prothrombin Time (PT) and Activated Partial Thromboplastin Time (aPTT) Measurements in Plasma. The PT and aPTT were measured in plasma collected from treated mice by using TEClot PT-S and TEClot aPTT-S kits (TECO GmbH, Dieselstr. 1, 84088, Neufahrn, NB, Germany), according to the manufacturer's instruction. Briefly, the PT and aPTT were measured in platelet poor plasma (PPP), preincubated at 37°C for 3 minutes, followed by addition of PT and aPTT reagent, using a Merlin coagulometer (MC 1 VET, Merlin, Lemgo, Germany).

2.6. In Vitro Platelet Aggregation in Mouse Whole Blood. In vitro platelet aggregation in whole blood collected from NT or HT mice after i.t. instillation of saline or PEG-AgNPs or Ag^+ ions was performed with slight modifications as previously described [32]. After anesthesia, blood from untreated mice was withdrawn from the inferior vena cava, placed in citrate (3.2%), and 0.1 ml aliquots were added to the well of a Merlin coagulometer (MC 1 VET; Merlin, Lemgo, Germany). Blood samples were incubated at 37.2°C with ADP (0.1 μM) for 3 min and then stirred for another 3 min. At the end of this period, 25 μl samples were removed and fixed on ice in 225 ml cellFix (Becton Dickinson, Franklin Lakes, NJ). After fixation, single platelets were counted in a VET ABX Micros with a mouse card (ABX). The occurrence of platelet aggregation induced by ADP caused a decrease in the counted single platelets in the blood (fall in the number of single platelets counted) obtained from the four studied groups compared with each other and with untreated (without ADP) whole blood obtained from control (unexposed) mice.

2.7. Measurement of Systemic Markers of Coagulation, Fibrinolysis, and vWF. The concentrations of fibrinogen (Molecular Innovation, Southfield, MI, USA) and plasminogen activation inhibitor (PAI-1, Molecular Innovation, Southfield, USA) were determined using an ELISA Kit. The plasma concentration of vWF (Molecular Innovation, Southfield, MI, USA) was measured using an ELISA kit.

2.8. Oxidative Stress Evaluation: Total NO_2 and Superoxide Dismutase (SOD). The determination of NO was performed with a total NO assay kit from R&D Systems (Minneapolis, MN, USA) which measures the more stable NO metabolites NO_2^- and NO_3^- [33]. SOD activity was measured as the conversion of nitroblue tetrazolium (NBT) to NBT-diformazan according to the vendor's protocol (Chemical Cayman, MI, USA). The extent of reduction in the appearance of NBT-formazan was used as a measure of SOD activity present in the plasma.

2.9. Statistics. All data are presented as the mean ± standard error of the mean, and the statistical significance was determined by one-way analysis of variance (ANOVA-1) followed by the Holm-Sidak post hoc test. P values less

than 0.05 were regarded as significant using GraphPad Prism Ver. 5.01 (GraphPad Software Inc., La Jolla, CA, USA).

3. Results

3.1. Characterization of PEG-AgNPs and Establishment of Hypertension. The morphology and particle size of PEG-AgNPs were determined by TEM are shown in Figure 1. TEM analysis of PEG-AgNPs revealed a homogenous particle size of approximately 40 nm in diameter, and this corroborates the size provided by the manufacturer. The nanoparticles were spherical in shape. The zeta potential assessments of PEG-AgNPs revealed that they were electroneutral (0.160 mV).

Mice infused with Angiotensin II exhibited a significant increase in SBP ($P < 0.0001$) compared with normotensive mice as shown in supplementary Figure S1.

3.2. Effect of PEG-AgNPs on Photochemically Induced Thrombosis in Pial Arterioles and Venules of Mice In Vivo. The effect of PEG-AgNPs on thrombotic occlusion time is illustrated in Figure 2. PEG-AgNPs induced significant shortening of the thrombotic occlusion time ($P < 0.0001$) in both the arterioles (Figure 2(a)) and venules (Figure 2(b)) of HT mice compared to NT mice. Moreover, thrombotic occlusion time was significantly reduced in HT mice exposed to PEG-AgNPs ($P < 0.0001$) compared to HT mice exposed to saline.

Ag ions also caused significant shortening of thrombotic occlusion time ($P < 0.0001$) in NT and HT mice compared to controls receiving saline (data shown in supplementary Figure S2).

3.3. Effect of PEG-AgNPs on PT and aPTT. Figure 3 represents the PT and aPTT in PPP collected from NT and HT mice treated with either saline or PEG-AgNPs. Compared to NT mice treated with PEG-AgNPs, a significant decrease in PT was observed in HT mice ($P < 0.0001$) exposed to PEG-AgNPs. Similar significant decrease was also observed with aPTT in HT mice exposed to PEG-AgNPs compared to NT mice given PEG-AgNPs. In addition, significant decreases in PT and aPTT were observed in HT mice exposed to PEG-AgNPs ($P < 0.0001$) compared to saline exposed HT mice. Likewise, there was a significant shortening of PT and aPTT in NT mice exposed to PEG-AgNPs ($P < 0.0001$) compared to NT mice treated with saline (Figure 3).

Similar significant reduction ($P < 0.0001$) in PT and aPTT was also observed in Ag^+ ion-exposed NT and HT mice compared to their respective controls. Significant reduction ($P < 0.0001$) was also observed in Ag^+ ion-exposed HT mice compared to NT mice (data shown in supplementary Figure S3).

3.4. Effect of PEG-AgNPs on Platelet Aggregation in Whole Blood In Vitro. Figure 4 illustrates the effect of e PEG-AgNPs on platelet aggregation in whole blood. The *in vitro* ADP incubation of whole blood collected from HT mice exposed to PEG-AgNPs caused a significant platelet aggregation compared with HT mice exposed to saline ($P < 0.0001$) and NT mice exposed to nanoparticles ($P < 0.0001$).

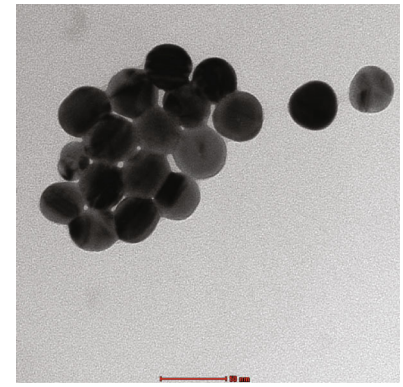

Figure 1: Transmission electron microscope (TEM) image of polyethylene glycol silver nanoparticles (PEG-AgNPs).

Ag^+ ions also caused significant platelet aggregation in HT mice compared to the saline-treated HT group ($P < 0.0001$) and also NT mice exposed to Ag^+ ions ($P < 0.0001$) (data shown in supplementary Figure S4).

3.5. Effect of PEG-AgNPs on Fibrinogen, PAI-1, and vWF. After exposure to PEG-AgNPs, the concentrations of fibrinogen were significantly increased in HT mice compared to either saline-exposed HT mice ($P < 0.05$) or PEG-AgNPs-exposed NT mice ($P < 0.05$) as represented in Figure 5(a).

The concentration of PAI-1 was significantly increased in PEG-AgNPs-exposed HT mice compared to either saline-exposed HT mice ($P < 0.01$) or PEG-AgNPs-exposed NT mice ($P < 0.01$) as represented in Figure 5(b).

A significant increase in the concentration of vWF was also seen in PEG-AgNPs-exposed HT mice compared to either saline-exposed HT mice ($P < 0.0001$) or PEG-AgNPs-exposed NT mice ($P < 0.05$) as represented in Figure 5(c).

In the Ag^+ ions-exposed group, there was significant reduction in fibrinogen level in HT mice compared to either saline-exposed HT mice ($P < 0.0001$) and Ag^+ ion-exposed NT mice ($P < 0.0001$). A significant reduction was also observed in concentration of PAI-1 in Ag^+ ion-exposed HT mice compared to either saline-exposed HT mice ($P < 0.05$) and Ag^+ ion-exposed NT mice ($P < 0.01$) (data shown in supplementary Figure S5).

3.6. Effect of PEG-AgNPs on SOD and NO. Figure 6 illustrates the effect of PEG-AgNPs on plasma levels of SOD and NO. The activity of SOD in plasma was significantly elevated in PEG-AgNPs-exposed HT mice compared to saline-exposed HT mice ($P < 0.05$) and PEG-AgNPs-exposed NT mice ($P < 0.01$) as shown in Figure 6(a).

Likewise, the level of NO was significantly increased in PEG-AgNPs-exposed HT mice compared to either saline-exposed HT mice ($P < 0.05$) or PEG-AgNPs-exposed NT mice ($P < 0.001$) as shown in Figure 6(b).

Ag^+ ions caused significant elevation of SOD ($P < 0.05$) in HT mice compared to NT mice. A significant increase

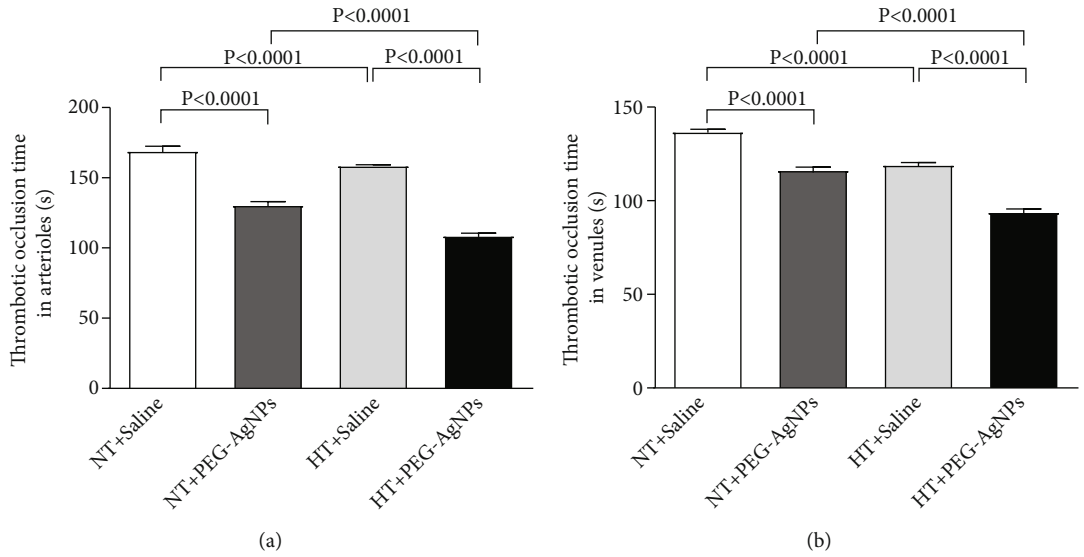

Figure 2: Thrombotic occlusion time in pial arterioles (a) or venules (b) following intratracheal instillation of saline or polyethylene glycol silver nanoparticles (PEG-AgNPs) in normotensive (NT) or hypertensive (HT) mice. Data are the mean ± SEM ($n = 6$–8 in each group). Statistical analysis by one-way ANOVA followed by Holm-Sidak's multiple comparison test.

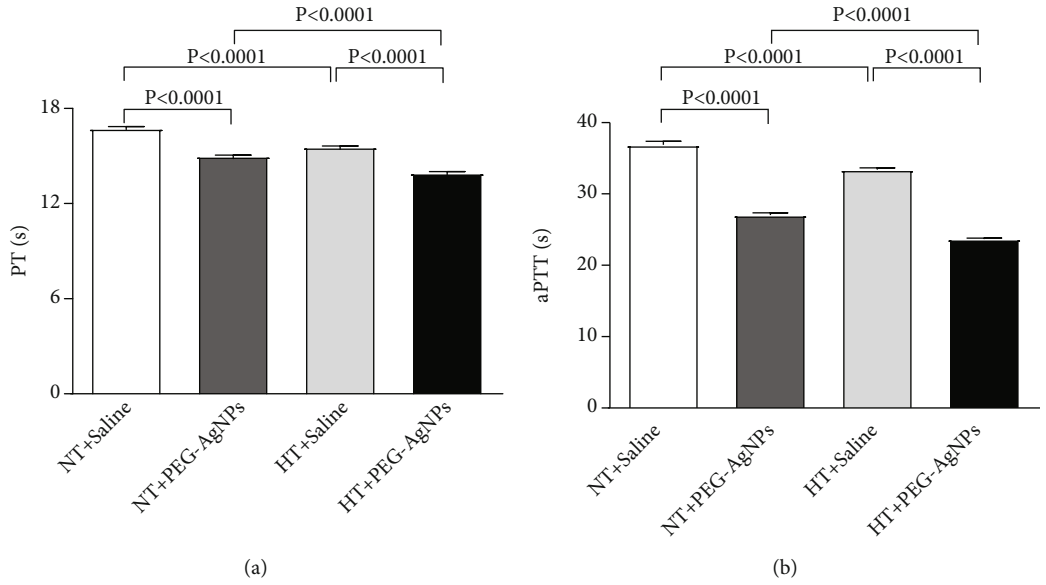

Figure 3: Prothrombin time (PT (a)) and activated partial thromboplastin time (aPTT (b)) measured following intratracheal instillation of saline or polyethylene glycol silver nanoparticles (PEG-AgNPs) in normotensive (NT) or hypertensive (HT) mice. Data are the mean ± SEM ($n = 6$–8 in each group). Statistical analysis by one-way ANOVA followed by Holm-Sidak's multiple comparison test.

of NO was also observed in this group in Ag^+ ions-exposed HT mice compared to either saline-exposed HT mice ($P < 0.0001$) or Ag^+ ions-exposed NT mice ($P < 0.0001$) (data shown in supplementary Figure S6).

4. Discussion

Application of AgNPs has been increasing immensely over the last few years in various industries, given their strong antimicrobial properties [26, 34, 35]. Consequently, their potential exposure to environment and human health via various routes including respiratory, oral, and dermal also soared, warranting intensive studies in order to understand the safe application and effect of AgNPs on human health [36]. A considerable amount of studies has reported Ag accumulation and toxicity to local as well as distant organs following AgNPs exposure [37–39]. To this regard, several data revealed the toxic effects of different kinds of AgNPs (shaped, sized, coated, and functionalized) on the cardiovascular system including systemic inflammatory response, oxidative stress, DNA damage, apoptosis, and thrombosis [14, 15]. An aspect that has been overlooked is the nanotoxicity

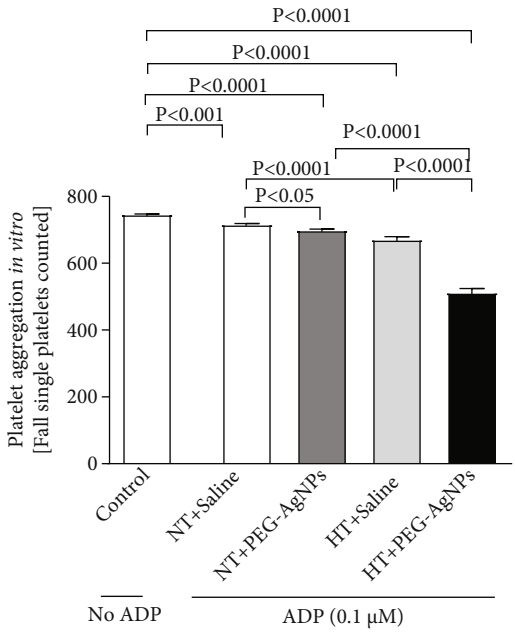

Figure 4: In vitro platelet aggregation in whole blood collected from normotensive (NT) or hypertensive (HT) mice after intratracheal (i.t.) instillation of saline or polyethylene glycol silver nanoparticles (PEG-AgNPs). Blood samples obtained from the aforementioned groups were incubated at 37°C with ADP (0.1 μM) for 3 min and stirred for another 3 min, and single platelets were then counted. The degree of platelet aggregation in HT or NT mice exposed to PEG-AgNPs or saline was compared with each other and with that obtained in untreated (without ADP) whole blood obtained from control (unexposed) mice. Data are the mean ± SEM ($n = 4$). Statistical analysis by one-way ANOVA followed by Holm-Sidak's multiple comparison test.

effects on susceptible populations as majority of the studies mainly focused on the risks to healthy adult population. Susceptible populations, due to alterations in physiological structure and functions, may suffer more damage and toxicity from the same exposure. A study by Holland et al. [16] revealed that pulmonary exposure to different size and coated AgNPs (size 20 nm and 110 nm, coating: polyvinylpyrrolidone and citrate) can induce exacerbation of cardiovascular injury such as expansion of cardiac/ischemic reperfusion injury. Recently, another investigation of cardiovascular responses to AgNPs (15 ± 4 nm) in spontaneously hypertensive rats suggested that hypertension intensified AgNPs cardiotoxicity [40].

Despite collection of studies reporting into how pulmonary exposure to AgNPs may impact cardiovascular toxicity, there are far fewer investigations on the impact of respiratory exposures on populations with preexisting cardiovascular conditions such as hypertension. In an effort to address these influences, we evaluated the effects of pulmonary-exposed AgNPs in healthy BALB/C mice and compared the same in a HT model. Our findings showed that PEG-AgNPs can induce acute dose-dependent cardiovascular effects including thrombosis, oxidative stress, and coagulation, and these effects were significantly aggravated in the animal model of hypertension. Due to potential of AgNPs to dissociate to Ag^+ ions, we further studied the latter effects in NT and HT mice exposed to Ag^+ ions.

In our present study, we used PEG-AgNPs and characterized them using TEM which revealed a homogenous particle size of 40 nm, correlating with the size of the manufacturer. Similar to our previous studies, intratracheal instillation was chosen to simulate pulmonary exposure which gave better control of the dose administered, given the fact that mice are obligate nose breathers and filter most inhaled particles. The dose selected was comparable to those in previous animal models of AgNPs exposure [41].

We have recently shown that single i.t. administration of AgNPs induced a significant dose-dependent shortening of the thrombotic occlusion time in pial arterioles and venules, 1 and 7 days after exposure, indicating that AgNPs possess prothrombotic effects [14]. Also, it is well known that thrombogenesis is the basic pathophysiological process underlying the major complications of hypertension [23, 42]. Interestingly, our current data reveals a marked shortening of thrombotic occlusion time in the HT mice compared to NT mice, confirming the prothrombotic effect of PEG-AgNPs. To gain further insights, into the mechanism underlying the latter effects of PEG-AgNPs, we investigated *in vitro* platelet aggregation in whole blood and the coagulation pathways. In agreement with our previous study [14], the addition of ADP into the whole blood of PEG-AgNPs-exposed NT mice caused significant platelet aggregation *in vitro*, and much stronger effect was observed in the whole blood of HT mice exposed to PEG-AgNPs. Furthermore, we demonstrated enhanced activation of PT and aPTT in HT mice compared to NT mice in response to AgNPs exposure. These effects reflect aggravated hypercoagulability caused by PEG-AgNPs in the HT model. We further studied the effects of PEG-AgNPs on haemostatic markers including fibrinogen, PAI-1, and vWF. Fibrinogen is an acute-phase protein that increases blood viscosity and promotes thrombus formation. Our data shows significant increase in fibrinogen levels in NT mice exposed to PEG-AgNPs, and the effect is aggravated in the HT mice. Likewise, an exacerbated effect was also observed with PAI-1, a potent endogenous inhibitor of fibrinolysis in HT mice comparted to NT mice receiving AgNPs. vWF is a biomarker for endothelial damage, and an increase in its level is associated with hypertension and cardiovascular disease [43]. Interestingly, our data reveals that this increase is further accelerated in PEG-AgNPs-exposed HT mice. Our results are in corroboration with previous *in vitro* and *in vivo* studies demonstrating AgNPs increase platelet aggregation, procoagulant activity, and consequently enhance thrombus formation [8, 14, 44, 45]. In line with our data, a recent study evaluating effect of titanium oxide nanoparticles exhibited significant deterioration of hemodynamic performance, demonstrated by an increase in the left ventricular end-diastolic pressure, decrement in the maximal rate of left ventricular pressure rise and decline, and marked prolongation of isovolumic contraction time in spontaneously hypertensive rats [46]. Further, our results corroborate findings that showed that exposure to particulate matter air pollution and nanoparticles is associated with

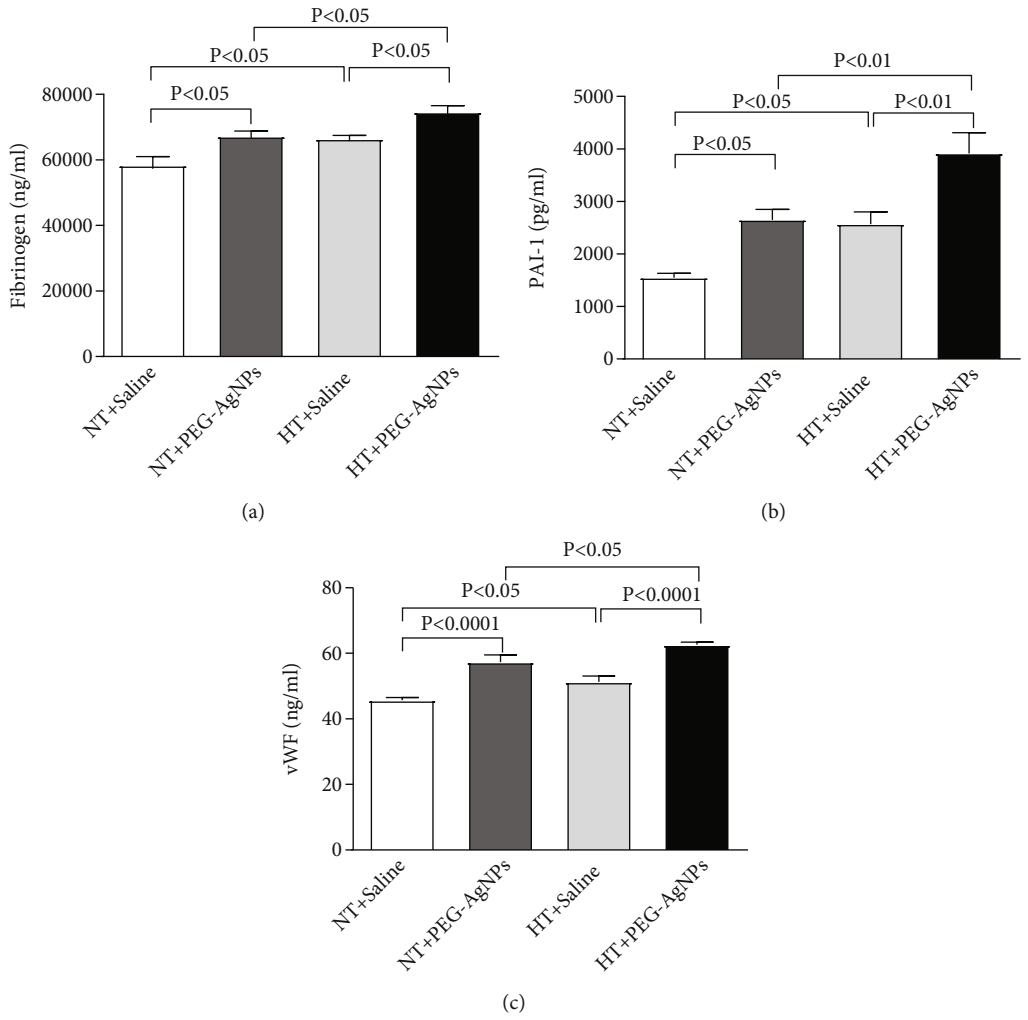

Figure 5: Fibrinogen (a), plasminogen activator inhibitor-1 (PAI-1 (b)), and von Willebrand factor (vWF (c)) concentrations in plasma, following intratracheal instillation of saline or polyethylene glycol silver nanoparticles (PEG-AgNPs) in normotensive (NT) or hypertensive (HT) mice. Data are the mean ± SEM ($n = 6–8$ in each group). Statistical analysis by one-way ANOVA followed by Holm-Sidak's multiple comparison test.

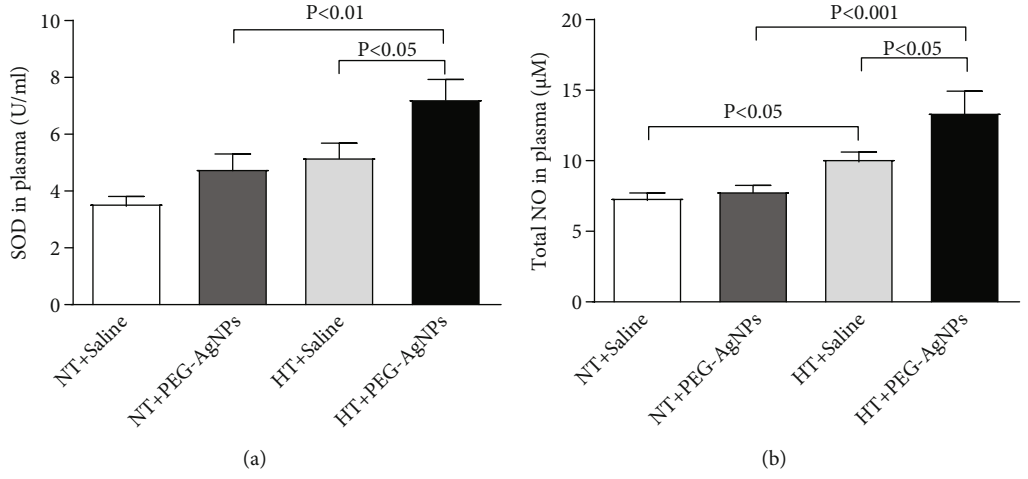

Figure 6: Superoxide dismutase (SOD (a)), total nitric oxide (NO (b)) levels in plasma, following intratracheal instillation of saline or polyethylene glycol silver nanoparticles (PEG-AgNPs) in normotensive (NT) or hypertensive (HT) mice. Data are the mean ± SEM ($n = 6–8$ in each group). Statistical analysis by one-way ANOVA followed by Holm-Sidak's multiple comparison test.

changes in the global coagulation function suggesting a tendency toward hypercoagulability [21, 22, 47].

Similar to many nanoparticles, dissolution of PEG-AgNPs to Ag^+ ions in vivo may also contribute to the cause of the observed effect discussed above. Hence, we repeated the identical tests on the Ag^+ ion-exposed group. Interestingly, we found similar significant effects with regard to thrombotic occlusion time, PT, aPTT, and *in vitro* platelet aggregation. However, distinct results were obtained with the level of fibrinogen and PAI-1 and no effects were observed on the level of vWF. This dissimilar pattern of data observed corroborates with our previous study indicating Ag^+ ions may induce different pathophysiological effect compared to the nanoparticle form [14, 48].

A central phenomenon associated with vascular structural and functional changes in hypertension, leading to cardiovascular disease, stroke, and renal failure, is oxidative stress, generating an imbalance between the levels of reactive oxygen species and antioxidants such as superoxide dismutase [20]. This condition also plays a key role in AgNPs-induced toxicity in living organisms [49–51]. In fact, the data in our present study shows an increase of superoxide dismutase in AgNPs-exposed NT mice compared to saline-exposed NT mice, and this effect was significantly aggravated in HT mice exposed to AgNPs or Ag^+. Likewise, similar results were also obtained with the level of total NO. The increase of SOD and NO in our study indicates the development of counterbalance system that in turn prevents the potentially damaging activity of reactive oxygen species by antioxidant defence mechanisms [52, 53].

The limitations of the present work include the fact that we did not differentiate the observed effects in male and female mice separately. Given the fact that gender is an important biological variable in biomedical research and hormonal variations can potentially influence vascular function and circulating factors [54], additional studies are required to clarify this point. We evaluated the impact of pulmonary-exposed PEG-AgNPs on the model of hypertension. Nevertheless, it is equally important to understand the impact of AgNPs on other susceptible populations, for instance, diabetes, cancer, and pregnancy, before their wider use. Hence, additional research is warranted to assess AgNPs toxicity among other populations of increased susceptibility or disease model.

In conclusion, our present study provides a number of assertions regarding the correlation of the biological impact of AgNPs on models of hypertension and their possible mechanism. Our data reveals that pulmonary-exposed AgNPs can exacerbate procoagulatory and systemic oxidative stress in animals with preexisting hypertension. The findings of the present work have potential clinical significance. Actually, silver nanoparticles are widely used for therapeutic interventions and diagnosis in medical practice (e.g., drug carriers, nanoprobes, bioimaging, and labeling agents). In this regard, susceptible populations, due to alterations in physiological structure and functions, may suffer more damage and toxicity from the same exposure. Our data revealed that the impact of pulmonary exposure to silver nanoparticles is more severe in hypertensive animals compared to normotensive mice, indicating the importance of assessing the toxicity of nanoparticles not only in healthy people but also in populations with high risk factors or disease.

Data Availability

The data that support the findings of this study are available from the corresponding author (Abderrahim Nemmar), upon reasonable request.

Conflicts of Interest

The authors declare that they have no conflicts of interest.

Acknowledgments

This work was supported by funds of the Sheikh Hamdan Foundation for Medical Research (grant #MRG-157/2017-2018) and the College of Medicine and Health Sciences, United Arab Emirates University (grant #12M022).

Supplementary Materials

Supplementary 1. Figure S1: systolic blood pressure, measured prior to sacrifice and analysis. Data are the mean ± SEM ($n = 8$ in each group). Statistical analysis by unpaired Student's *t*-test.

Supplementary 2. Figure S2: thrombotic occlusion time in pial arterioles (A) or venules (B) following intratracheal instillation of saline or silver acetate (AgAc) in normotensive (NT) or hypertensive (HT) mice. Data are the mean ± SEM ($n = 6$–8 in each group). Statistical analysis by one-way ANOVA followed by Holm-Sidak's multiple comparison test.

Supplementary 3. Figure S3: prothrombin time (PT, A) and activated partial thromboplastin time (aPTT, B) measured following intratracheal instillation of saline or silver acetate (AgAc) in normotensive (NT) or hypertensive (HT) mice. Data are the mean ± SEM ($n = 6$–8 in each group). Statistical analysis by one-way ANOVA followed by Holm-Sidak's multiple comparison test.

Supplementary 4. Figure S4: in vitro platelet aggregation in whole blood collected from normotensive (NT) or hypertensive (HT) mice after intratracheal (i.t.) instillation of saline or silver acetate (AgAc). Blood samples obtained from the aforementioned groups were incubated at 37°C with ADP (0.1 μM) for 3 min and stirred for another 3 min, and single platelets were then counted. The degree of platelet aggregation in HT or NT mice exposed to AgAc or saline was compared with each other and with that obtained in untreated (without ADP) whole blood obtained from control (unexposed) mice. Data are the mean ± SEM ($n = 4$). Statistical analysis by one-way ANOVA followed by Holm-Sidak's multiple comparison test.

Supplementary 5. Figure S5: fibrinogen (A), plasminogen activator inhibitor-1 (PAI-1, B), and von-Willebrand factor (vWF, C) concentrations in plasma, following intratracheal instillation of saline or silver acetate (AgAc) in normotensive

(NT) or hypertensive (HT) mice. Data are the mean ± SEM ($n = 6–8$ in each group). Statistical analysis by one-way ANOVA followed by Holm-Sidak's multiple comparison test.

Supplementary 6. Figure S6: superoxide dismutase (SOD, A) and total nitric oxide (NO, B) levels in plasma, following intratracheal instillation of saline or silver acetate (AgAc) in normotensive (NT) or hypertensive (HT) mice. Data are the mean ± SEM ($n = 6–8$ in each group). Statistical analysis by one-way ANOVA followed by Holm-Sidak's multiple comparison test.

References

[1] Q. H. Tran, V. Q. Nguyen, and A. T. le, "Silver nanoparticles: synthesis, properties, toxicology, applications and perspectives," *Advances in Natural Sciences: Nanoscience and Nanotechnology*, vol. 4, no. 3, 2013.

[2] J. Natsuki, T. Natsuki, and Y. Hashimoto, "A review of silver nanoparticles: synthesis methods, properties and applications," *International Journal of Materials Science and Applications*, vol. 4, no. 5, pp. 325–332, 2015.

[3] A.-C. Burduşel, O. Gherasim, A. Grumezescu, L. Mogoantă, A. Ficai, and E. Andronescu, "Biomedical applications of silver nanoparticles: an up-to-date overview," *Nanomaterials*, vol. 8, no. 9, p. 681, 2018.

[4] A. Nemmar, M. F. Hoylaerts, and B. Nemery, "Effects of particulate air pollution on hemostasis," *Clinics in Occupational and Environmental Medicine*, vol. 5, no. 4, pp. 865–881, 2006.

[5] I. G. Theodorou, M. P. Ryan, T. D. Tetley, and A. E. Porter, "Inhalation of silver nanomaterials—seeing the risks," *International Journal of Molecular Sciences*, vol. 15, no. 12, pp. 23936–23974, 2014.

[6] J. H. Lee, J. Mun, J. D. Park, and I. J. Yu, "A health surveillance case study on workers who manufacture silver nanomaterials," *Nanotoxicology*, vol. 6, no. 6, pp. 667–669, 2012.

[7] P. V. Asharani, S. Sethu, S. Vadukumpully et al., "Investigations on the structural damage in human erythrocytes exposed to silver, gold, and platinum nanoparticles," *Advanced Functional Materials*, vol. 20, no. 8, pp. 1233–1242, 2010.

[8] Y. Bian, K. Kim, T. Ngo et al., "Silver nanoparticles promote procoagulant activity of red blood cells: a potential risk of thrombosis in susceptible population," *Particle and Fibre Toxicology*, vol. 16, no. 1, p. 9, 2019.

[9] L. Q. Chen, L. Fang, J. Ling, C. Z. Ding, B. Kang, and C. Z. Huang, "Nanotoxicity of silver nanoparticles to red blood cells: size dependent adsorption, uptake, and hemolytic activity," *Chemical Research in Toxicology*, vol. 28, no. 3, pp. 501–509, 2015.

[10] Z. Ferdous, S. Beegam, S. Tariq, B. H. Ali, and A. Nemmar, "The in vitro effect of polyvinylpyrrolidone and citrate coated silver nanoparticles on erythrocytic oxidative damage and eryptosis," *Cellular Physiology and Biochemistry*, vol. 49, no. 4, pp. 1577–1588, 2018.

[11] N. A. Holland, *Intratracheal instillation of silver nanoparticles exacerbates cardiac ischemia/reperfusion injury in male Sprague-Dawley rats*, ProQuest Dissertations Publishing, 2014.

[12] X. Sun, Y. Yang, J. Shi, C. Wang, Z. Yu, and H. Zhang, "NOX4- and Nrf2-mediated oxidative stress induced by silver nanoparticles in vascular endothelial cells," *Journal of Applied Toxicology*, vol. 37, no. 12, pp. 1428–1437, 2017.

[13] A. Ramirez-Lee Manuel, P. P. Martinez-Cuevas, H. Rosas-Hernandez et al., "Evaluation of vascular tone and cardiac contractility in response to silver nanoparticles, using Langendorff rat heart preparation," *Nanomedicine: Nanotechnology, Biology and Medicine*, vol. 13, no. 4, pp. 1507–1518, 2017.

[14] Z. Ferdous, S. Al-Salam, Y. E. Greish, B. H. Ali, and A. Nemmar, "Pulmonary exposure to silver nanoparticles impairs cardiovascular homeostasis: effects of coating, dose and time," *Toxicology and Applied Pharmacology*, vol. 367, pp. 36–50, 2019.

[15] N. A. Holland, L. C. Thompson, A. K. Vidanapathirana et al., "Impact of pulmonary exposure to gold core silver nanoparticles of different size and capping agents on cardiovascular injury," *Particle and Fibre Toxicology*, vol. 13, no. 1, p. 48, 2016.

[16] H. N. A. Becak DP and J. H. Shannahan, "Cardiac ischemia reperfusion injury following instillation of 20 nm citrate-capped nanosilver," *Journal of Nanomedicine & Nanotechnology*, vol. s6, Suppl 6, 2015.

[17] V. C. Minarchick, P. A. Stapleton, D. W. Porter et al., "Pulmonary cerium dioxide nanoparticle exposure differentially impairs coronary and mesenteric arteriolar reactivity," *Cardiovascular Toxicology*, vol. 13, no. 4, pp. 323–337, 2013.

[18] P. A. Stapleton, A. B. Abukabda, S. L. Hardy, and T. R. Nurkiewicz, "xenobiotic pulmonary exposure and systemic cardiovascular response via neurological links," *American Journal of Physiology Heart and Circulatory Physiology*, vol. 309, no. 10, pp. H1609–H1620, 2015.

[19] R. Shrivastava, P. Kushwaha, Y. C. Bhutia, and S. J. S. Flora, "Oxidative stress following exposure to silver and gold nanoparticles in mice," *Toxicology and Industrial Health*, vol. 32, no. 8, pp. 1391–1404, 2016.

[20] H. N. Siti, Y. Kamisah, and J. Kamsiah, "The role of oxidative stress, antioxidants and vascular inflammation in cardiovascular disease (a review)," *Vascular Pharmacology*, vol. 71, pp. 40–56, 2015.

[21] A. Nemmar, S. Zia, D. Subramaniyan, M. A. Fahim, and B. H. Ali, "Exacerbation of thrombotic events by diesel exhaust particle in mouse model of hypertension," *Toxicology*, vol. 285, no. 1-2, pp. 39–45, 2011.

[22] J. Duan, Y. Yu, Y. Li, Y. Wang, and Z. Sun, "Inflammatory response and blood hypercoagulable state induced by low level co- exposure with silica nanoparticles and benzo[a]pyrene in zebrafish (*Danio rerio*) embryos," *Chemosphere*, vol. 151, pp. 152–162, 2016.

[23] C. Savoia, L. Sada, L. Zezza et al., "Vascular inflammation and endothelial dysfunction in experimental hypertension," *International Journal of Hypertension*, vol. 2011, 8 pages, 2011.

[24] C. Catena, G. Colussi, M. Novello, V. Fagotto, and L. A. Sechi, "Intrarenal vascular resistance is associated with a prothrombotic state in hypertensive patients," *Kidney and Blood Pressure Research*, vol. 41, no. 6, pp. 929–936, 2016.

[25] C. Catena, G. Colussi, G. Brosolo, and L. A. Sechi, "A prothrombotic state is associated with early arterial damage in hypertensive patients," *Journal of Atherosclerosis and Thrombosis*, vol. 19, no. 5, pp. 471–478, 2012.

[26] A. Abbaszadegan, Y. Ghahramani, A. Gholami et al., "The effect of charge at the surface of silver nanoparticles on antimicrobial activity against gram-positive and gram-negative bacteria: a preliminary study," *Journal of Nanomaterials*, vol. 2015, no. 1, pp. 1–8, 2015.

[27] D. Weiss, J. J. Kools, and W. R. Taylor, "Angiotensin II-induced hypertension accelerates the development of atherosclerosis in apoE-deficient mice," *Circulation*, vol. 103, no. 3, pp. 448–454, 2001.

[28] Z. Ying, P. Yue, X. Xu et al., "Air pollution and cardiac remodeling: a role for RhoA/Rho-kinase," *American Journal of Physiology. Heart and Circulatory Physiology*, vol. 296, no. 5, pp. H1540–H1550, 2009.

[29] Y. Higashi, S. Sasaki, K. Nakagawa, H. Matsuura, T. Oshima, and K. Chayama, "Endothelial function and oxidative stress in renovascular hypertension," *The New England Journal of Medicine*, vol. 346, no. 25, pp. 1954–1962, 2002.

[30] A. Nemmar, K. Melghit, S. al-Salam et al., "Acute respiratory and systemic toxicity of pulmonary exposure to rutile Fe-doped TiO_2 nanorods," *Toxicology*, vol. 279, no. 1-3, pp. 167–175, 2011.

[31] A. Nemmar, S. Al-Salam, P. Yuvaraju, S. Beegam, and B. H. Ali, "Emodin mitigates diesel exhaust particles-induced increase in airway resistance, inflammation and oxidative stress in mice," *Respiratory Physiology & Neurobiology*, vol. 215, pp. 51–57, 2015.

[32] A. Nemmar, S. Al-Salam, S. Beegam, P. Yuvaraju, and B. H. Ali, "The acute pulmonary and thrombotic effects of cerium oxide nanoparticles after intratracheal instillation in mice," *International Journal of Nanomedicine*, vol. Volume 12, pp. 2913–2922, 2017.

[33] A. Nemmar, S. Beegam, P. Yuvaraju, J. Yasin, A. Shahin, and B. H. Ali, "Interaction of amorphous silica nanoparticles with erythrocytes in vitro: role of oxidative stress," *Cellular Physiology and Biochemistry*, vol. 34, no. 2, pp. 255–265, 2014.

[34] S. Ahmed, M. Ahmad, B. L. Swami, and S. Ikram, "A review on plants extract mediated synthesis of silver nanoparticles for antimicrobial applications: a green expertise," *Journal of Advanced Research*, vol. 7, no. 1, pp. 17–28, 2016.

[35] S. K. Kailasa, T.-J. Park, J. V. Rohit, and J. R. Koduru, "Antimicrobial activity of silver nanoparticles," in *Nanoparticles in Pharmacotherapy*, pp. 461–484, Elsevier, 2019.

[36] Z. Ferdous and A. Nemmar, "Health impact of silver nanoparticles: a review of the biodistribution and toxicity following various routes of exposure," *International Journal of Molecular Sciences*, vol. 21, no. 7, p. 2375, 2020.

[37] C. Recordati, M. de Maglie, S. Bianchessi et al., "Tissue distribution and acute toxicity of silver after single intravenous administration in mice: nano-specific and size-dependent effects," *Particle and Fibre Toxicology*, vol. 13, no. 1, p. 12, 2015.

[38] C. A. Austin, G. K. Hinkley, A. R. Mishra et al., "Distribution and accumulation of 10 nm silver nanoparticles in maternal tissues and visceral yolk sac of pregnant mice, and a potential effect on embryo growth," *Nanotoxicology*, vol. 10, no. 6, pp. 654–661, 2016.

[39] M. D. Boudreau, M. S. Imam, A. M. Paredes et al., "Differential effects of silver nanoparticles and silver ions on tissue accumulation, distribution, and toxicity in the Sprague Dawley rat following daily oral gavage administration for 13 weeks," *Toxicological Sciences*, vol. 150, no. 1, pp. 131–160, 2016.

[40] M. A. Ramirez-Lee, P. Aguirre-Bañuelos, P. P. Martinez-Cuevas et al., "Evaluation of cardiovascular responses to silver nanoparticles (AgNPs) in spontaneously hypertensive rats," *Nanomedicine: Nanotechnology, Biology and Medicine*, vol. 14, no. 2, pp. 385–395, 2018.

[41] Y. Morimoto, H. Izumi, Y. Yoshiura et al., "Comparison of pulmonary inflammatory responses following intratracheal instillation and inhalation of nanoparticles," *Nanotoxicology*, vol. 10, no. 5, pp. 607–618, 2016.

[42] W.-L. Song, E. Ricciotti, X. Liang, T. Grosser, G. R. Grant, and G. A. FitzGerald, "Lipocalin-Like Prostaglandin D Synthase but not Hemopoietic Prostaglandin D Synthase deletion causes hypertension and accelerates thrombogenesis in mice," *Journal of Pharmacology and Experimental Therapeutics*, vol. 367, no. 3, pp. 425–432, 2018.

[43] M. C. Van Schie, J. E. Van Loon, M. P. M. De Maat, and F. W. G. Leebeek, "Genetic determinants of von Willebrand factor levels and activity in relation to the risk of cardiovascular disease: a review," *Journal of Thrombosis and Haemostasis*, vol. 9, no. 5, pp. 899–908, 2011.

[44] E.-A. Jun, K. M. Lim, K. Y. Kim et al., "Silver nanoparticles enhance thrombus formation through increased platelet aggregation and procoagulant activity," *Nanotoxicology*, vol. 5, no. 2, pp. 157–167, 2011.

[45] J. Laloy, V. Minet, L. Alpan et al., "Impact of silver nanoparticles on haemolysis, platelet function and coagulation," *Nano*, vol. 1, p. 4, 2014.

[46] S. Rossi, M. Savi, M. Mazzola et al., "Subchronic exposure to titanium dioxide nanoparticles modifies cardiac structure and performance in spontaneously hypertensive rats," *Particle and Fibre Toxicology*, vol. 16, no. 1, p. 25, 2019.

[47] P. M. Mannucci, S. Harari, I. Martinelli, and M. Franchini, "Effects on health of air pollution: a narrative review," *Internal and Emergency Medicine*, vol. 10, no. 6, pp. 657–662, 2015.

[48] Z. Ferdous, S. Al-Salam, P. Yuvaraju, B. H. Ali, and A. Nemmar, "Remote effects and biodistribution of pulmonary instilled silver nanoparticles in mice," *NanoImpact*, vol. 22, article 100310, 2021.

[49] M. Ahamed, R. Posgai, T. J. Gorey, M. Nielsen, S. M. Hussain, and J. J. Rowe, "Silver nanoparticles induced heat shock protein 70, oxidative stress and apoptosis in *Drosophila melanogaster*," *Toxicology and Applied Pharmacology*, vol. 242, no. 3, pp. 263–269, 2010.

[50] J. Blanco, S. Tomás-Hernández, T. García et al., "Oral exposure to silver nanoparticles increases oxidative stress markers in the liver of male rats and deregulates the insulin signalling pathway and p53 and cleaved caspase 3 protein expression," *Food and Chemical Toxicology*, vol. 115, pp. 398–404, 2018.

[51] H. Guo, J. Zhang, M. Boudreau et al., "Intravenous administration of silver nanoparticles causes organ toxicity through intracellular ROS-related loss of inter-endothelial junction," *Particle and Fibre Toxicology*, vol. 13, no. 1, p. 21, 2015.

[52] A. Nemmar, P. Yuvaraju, S. Beegam, J. Pathan, E. E. Kazzam, and B. H. Ali, "Oxidative stress, inflammation, and DNA damage in multiple organs of mice acutely exposed to amorphous silica nanoparticles," *International Journal of Nanomedicine*, vol. 11, p. 919, 2016.

[53] A. Nemmar, P. Yuvaraju, S. Beegam, M. A. Fahim, and B. H. Ali, "Cerium oxide nanoparticles in lung acutely induce oxidative stress, inflammation, and DNA damage in various organs of mice," *Oxidative Medicine and Cellular Longevity*, vol. 2017, 12 pages, 2017.

[54] P. A. Stapleton, C. R. McBride, J. Yi, A. B. Abukabda, and T. R. Nurkiewicz, "Estrous cycle-dependent modulation of *in vivo* microvascular dysfunction after nanomaterial inhalation," *Reproductive Toxicology*, vol. 78, pp. 20–28, 2018.

Hindawi
Oxidative Medicine and Cellular Longevity
Volume 2021, Article ID 7244677, 21 pages
https://doi.org/10.1155/2021/7244677

Review Article

An Overview of the Beneficial Role of Antioxidants in the Treatment of Nanoparticle-Induced Toxicities

Vladimir Mihailovic,[1] **Jelena S. Katanic Stankovic**,[2] **Dragica Selakovic**,[3] **and Gvozden Rosic**[3]

[1]*University of Kragujevac, Faculty of Science, Department of Chemistry, Radoja Domanovica 12, 34000 Kragujevac, Serbia*
[2]*University of Kragujevac, Institute for Information Technologies Kragujevac, Department of Science, Jovana Cvijica bb, 34000 Kragujevac, Serbia*
[3]*University of Kragujevac, Faculty of Medical Sciences, Department of Physiology, Svetozara Markovica 69, 34000 Kragujevac, Serbia*

Correspondence should be addressed to Dragica Selakovic; dragica984@gmail.com and Gvozden Rosic; grosic@medf.kg.ac.rs

Received 13 September 2021; Accepted 26 October 2021; Published 15 November 2021

Academic Editor: Alessandra Durazzo

Nanoparticles (NPs) are used in many products and materials for humans such as electronics, in medicine for drug delivery, as biosensors, in biotechnology, and in agriculture, as ingredients in cosmetics and food supplements. Besides that, NPs may display potentially hazardous properties on human health and the environment as a consequence of their abundant use in life nowadays. Hence, there is increased interest of researchers to provide possible therapeutic agents or dietary supplements for the amelioration of NP-induced toxicity. This review summarizes the new findings in the research of the use of antioxidants as supplements for the prevention and alleviation of harmful effects caused by exposure of organisms to NPs. Also, mechanisms involved in the formation of NP-induced oxidative stress and protective mechanisms using different antioxidant substances have also been elaborated. This review also highlights the potential of naturally occurring antioxidants for the enhancement of the antioxidant defense systems in the prevention and mitigation of organism damage caused by NP-induced oxidative stress. Based on the presented results of the most recent studies, it may be concluded that the role of antioxidants in the prevention and treatment of nanoparticle-induced toxicity is unimpeachable. This is particularly important in terms of oxidative stress suppression.

1. Introduction

The "nano era" has emerged latterly in many different fields of science and industry. Nanotechnology refers to the development and use of small nanometer-sized objects based on their various properties. The European Commission defines nanomaterials (NM) as "Natural, incidental and manufactured materials that contain particles of which 50% or more have one or more external dimensions in the size range 1–100 nm and/or their volume-specific surface area is larger than 60 m^2/cm^3" [1]. There are three main classes of nanomaterials (NPs): nanoparticles, nanofibers, and nanoplates [2]. All of them have valuable and diverse use, e.g., in the electronics industry, in medicine for drug delivery, as biosensors, in biotechnology, and in agriculture, as ingredients in cosmetics and food supplements [3, 4]. They are used in paints, fillers, and filters for water purification, as catalysts, semiconductors, and opacifiers. Besides that, many nanomaterials find their purpose in material science, for making clothes, as well as in aerospace engineering [5–7]. The distinctive physical, chemical, and optical properties of nanomaterials enabled their use for a variety of purposes, but the most prominent is the progressive application in the field of medicine.

Because of their particularly interesting and unique properties, like solubility, specific surface area, aggregation

state, conductivity, and high tensile strength, the metal-based nanoparticles (NP) and carbon nanotubes (CNT) have gained most of the attention of science and industry [3]. The fields of immense interest in different types of nanomaterials, e.g., lipid- or polymer-based NM, metal, metal oxide, or carbon-based NM, are medicinal and biological sciences. Regarding their small size and potential to enter the body easily, NPs have been used as drug delivery systems where they are capable to reach targeted organs or sites by cellular pathways [5]; thus, they are also used in cancer therapy, bioimaging, and diagnostics [4, 6].

As a consequence of the abundant use of nanomaterials in life nowadays, a new question has arisen concerning their potentially hazardous nature on human health and the environment in general [2, 3, 6]. In their interaction with cell membranes, many key signaling pathways may be disrupted [8]. Numerous nanotoxicological studies reported that autophagy, the main cellular process in the human organism, is affected by NMs. The disruption in autophagy can lead to many ailments such as cancer and neurodegenerative diseases [6]. By entering the cell, NPs cause the excessive formation of reactive oxygen species (ROS) which can lead to oxidative stress. The process of oxidative stress lies in the background of NP-induced cell damage and destruction, cytotoxicity, and genotoxicity [3, 9].

In recent years, there are several review papers regarding the nanoparticle-induced toxicities and their harmful mechanism of action [6, 7, 10–13] but also the positive effects of NPs synthesized using antioxidant compounds such as vitamins, minerals, natural compounds, or plant extracts [14–16]. Nevertheless, there are no comprehensive studies about the effects of antioxidants on the prevention and mitigation of severe toxicities induced by the application of nanoparticles in therapies and everyday life. In that sense, in this review, our focus was to present the recent knowledge in the field of indicative application of antioxidants to combat the deleterious effects of nanoparticles in living organisms.

2. The Mechanism of Nanoparticle Toxicity

Nanoparticles may enter the human body via three main pathways. The most common cause is the NP entrance by inhalation, then via the skin, and last and the most infrequent though the digestion process that depends mostly on their physicochemical characteristics. These include their hydrophilic and hydrophobic properties, particle size, shape, surface charge, and dispersity. The inhalation of NPs will transfer them into the lungs and respiratory tract, and as a result of the lower size of particles, there is an increasing concern of NPs to get deeper into the respiratory system quickly. In the dermal system, the nanoparticles will penetrate through the process of absorption but only if the skin is deeply damaged or the size of particles is below 5 nm. Ingestion of NPs rarely happens [17, 18]. After entering the body, NPs can be transferred via the bloodstream throughout the body and then accumulate and interact with various systems affecting many vital organs, such as the lungs, liver, kidneys, and reproductive organs [5, 18–21]. Additionally, the NPs can be transferred into the brain by affecting the cells and disrupting the blood-brain barrier. They can cause severe neurotoxicity; nevertheless, the way they pass through the membrane is still not sufficiently elucidated [8, 18, 22–25].

The interactions of NPs with cells lead to the disruption of many cell barriers, NPs entering the cell and causing mitochondrial damage, affecting DNA via DNA methylation and histone modifications, the development of the state of oxidative stress, and aftermost cell apoptosis. The high levels of reactive oxygen species (ROS) produced in the cell generally introduce the cell into the state of oxidative stress where proteins, DNA, and lipid structures are damaged, leading to the malfunction of the cells and severe toxicity. The oxidative stress is usually accompanied by increased expression of proinflammatory genes and activation of neutrophils and macrophages [17, 26, 27]. Nanoparticles may produce various concentrations of ROS depending on their physicochemical properties. The main properties of NPs that cause increased production of ROS are the presence of prooxidant functional groups on the NP surface, particle-cell interactions, and the existence of active redox cycling on the surface of NPs (in transition metal-based NPs) [3]. Nevertheless, the claims that oxidative stress is the most prominent factor in NP-induced toxicity have not been proven in all cases since various NPs, which have an inactive surface or low solubility, may induce toxicity without causing oxidative stress [2].

2.1. Nanoparticle-Induced Oxidative Stress. In most circumstances, the excess production of ROS caused by the interaction with nanoparticles underlays the formation of oxidative stress [27–29]. Oxidative stress, by its definition, represents "an imbalance between ROS production and their elimination in reaction with antioxidant defensive systems" [30]. This imbalance in the prooxidant/antioxidant relation may induce severe damage of various biomolecules like proteins, lipids, and nucleic acids, thereby causing damage to the cells and the whole organism. Although the synthesis of ROS in the organism during mitochondrial respiration or phagocytosis is a normal process, the excess in their production can be caused by various elements. If antioxidant defense systems of the organism, containing catalase (CAT), superoxide dismutase (SOD), glutathione (GSH), etc., are not capable to neutralize the increased concentration of ROS, this condition may lead to the development of severe diseases [31].

The physicochemical properties of nanoparticles significantly affect their interaction with the cell. The entrance of NPs into the cell can occur via diffusion and endocytosis or interacting with phospholipids in the cell membrane. In the physicochemical interaction with the cell membrane surface, NPs can disrupt the membrane affecting the transport mechanisms as well as induce oxidative stress by generating ions. NPs can also affect the function of cell organelles, primarily mitochondria and peroxisome, influencing the intracellular transport and therefore inducing oxidative stress [2, 18].

In general, there are two types of NP-induced oxidative stress: (i) primary or direct and (ii) secondary or indirect oxidative stress (Figure 1). The first one refers to a direct

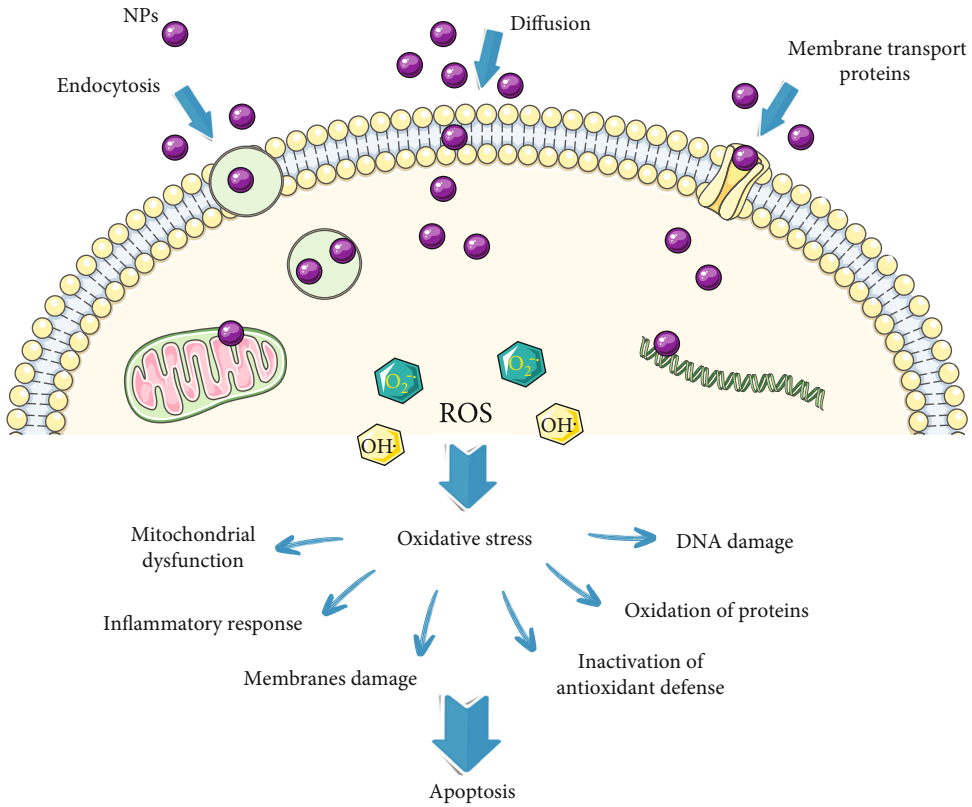

Figure 1: Nanoparticle-induced oxidative stress in the cell—an outline of main events.

reaction of the NP surface with cells inducing ROS generation. Metal-based NPs are able to release the metal ion into the cells that may also trigger an increase in ROS formation. The secondary oxidative stress may arise via indirect pathways, mainly due to NPS-induced disruption in mitochondrial function or the inability of the antioxidant defense to reinstate the redox balance. In this case, NPs are not directly responsible for the oxidative stress but affect mitochondria and phagocytes, indirectly increasing the ROS level in the cell. For instance, NPs are interacting with phagocytes (macrophages and neutrophils) whose goal is to digest them, but since NPs have often an inorganic part, the phagocytes become damaged due to their inability to neutralize the inorganic molecules. This ultimately results in an increase of the ROS level in the cell and therefore the generation of oxidative stress. NPs may affect the levels of inflammatory factors like TNF-α and interleukins causing mitochondrial disruption and thereafter ER stress and DNA damage. All this can finally induce the activation of apoptotic response and cell death [2, 18]. When the level of oxidative stress surpasses the ability of the organism to neutralize it, many severe conditions may occur, like inflammation, fibrosis, genotoxicity, and cancer formation [3].

The cell disturbance caused by NPs was characterized by the direct destruction of cell and organelle membranes, as well as binding to biomacromolecules with an impact on their structure and function. In addition, the NP-induced intracellular generation of ROS, also, modulates the structure and function of lipids, DNA, proteins, and carbohydrates, as main cell constituents, leading to cellular organelles and membrane damage. NP-induced toxicity involves complex mechanisms with the important role of mitochondria, lysosomes, and endoplasmic reticulum (ER) in that process [32, 33]. The intensive ROS generation has also a role in several signal pathways causing cell apoptosis, inflammation, and autophagy process. The main consequences of these processes are mitochondrial dysfunction, lysosomal, and ER damage [32]. It has been shown that the increased ROS production provoked by exposure to NPs, as well as some toxic xenobiotics, leads to mitochondrial respiration disturbance and damage of mitochondrial membrane phospholipid bilayer. The lower adenosine triphosphate (ATP) production and increased mitochondrial membrane permeability initiate apoptotic cascade and cell death [34–36]. It was also shown that the toxic concentration of different NPs accompanied by oxidative stress may disrupt the structure of the lysosomal membrane. The liberation of the lysosomal inner content to the cytosol, due to its membrane damage, could induce further damage of other organelles (especially the mitochondrial outer membrane) and further activate apoptosis [34, 37, 38]. In this regard, the use of antioxidants regulating ROS production seems a promising therapeutic strategy for NP-induced toxicity.

2.2. Toxicological Effects of Various Nanoparticles. In the global market of NPs, the alumina nanoparticles (Al_2O_3-NPs) are represented around 20% [17]. The purpose of their use is diverse, from application in medicine (for site-specific

drug delivery), orthopedic implants, cosmetics, food industry, chemical engineering, catalysis, resistant coatings, lithium batteries, and all the way to jet and rocket fuels [22, 39, 40]. They also have been used in weapons, munitions, and explosives; in propeller shafts as surface coatings; also as scratch and abrasive-resistant coatings on sunglasses; and in the car industry [41]. However, their potential adverse effects on humans, animals, and the environment increase due to many ways of exposure. The most common modus of Al_2O_3-NPs entering into the organism is via inhalation, dermal exposure, food, and water. The small size of Al_2O_3-NPs and high reactivity allow easier penetration into the cells, transport via circulation, and thus the accumulation in multiple organs and tissues, e.g., the lungs, heart, spleen, testes, bone marrow, lymph nodes, and brain [22, 39]. They can also easily cross the blood-brain barrier and enter the CNS causing severe neurotoxicity. Al_2O_3-NP accumulation in different parts of the brain may generate memory dysfunction, depressive behavior, and neurodegenerative disorders such as Alzheimer's and Parkinson's diseases [22, 42]. Oxidative stress plays a key role in Al_2O_3-NP-induced toxicity in many organ systems. Recent findings showed that Al_2O_3-NPs provoke high production of ROS, the elevation of the MnSOD level, high levels of markers of oxidative damage (CAT, SOD, and GSH), activation of caspases, expression of endothelial cell adhesion molecules (VCAM-1, ICAM-1, and ELAM-1), and high levels of interleukins in serum. Based on published data, it can be concluded that they are triggering many adverse reactions causing an inflammatory response, mitochondrial dysfunction, cytotoxicity, genotoxicity, carcinogenicity, and apoptosis [22, 39, 42–44]. For instance, Park et al. [44] in their study related to the toxicity of aluminum NPs showed that their daily administration to mice for 28 days lead to the significant platelet increase; decrease in white blood cells, neutrophils, lymphocytes, and monocytes; and high accumulation of Al in the lung, brain, and thymus in the group treated with the highest dose. Besides, neurotoxicological effects have been observed leading to the formation of neurodegenerative and immunosuppressive effects. Another *in vivo* study by Shrivastava et al. [39] suggested that Al_2O_3-NPs induce a high level of oxidative stress followed by high ROS concentration, reduced levels of GSH, and low CAT and SOD activities, in mice during 7 days of an oral application. The hepatorenal toxicity of Al_2O_3-NPs and ZnO-NPs was monitored by Yousef et al. [43], showing that both NPs exerted significant toxicity but also synergistic toxicological effect on the liver and kidneys accompanied by systemic inflammation. Al_2O_3-NPs affected mitochondrial membrane potential, activation of caspases, and red blood cell dysfunction and increased ROS formation. Neurotoxicity and brain damage have been primary adverse effects in the Al_2O_3-NP *in vivo* application. Abou-Zeid et al. [22] reported that Al_2O_3-NPs caused disrupted levels of oxidative stress markers, such as MDA, 8-OHdG, GSH, CAT, and SOD; the expression of GST, TNF-α, and caspase-3 genes in the brain; and IL-1β and IL-6 levels in serum of treated animals, pointing to severe oxidative stress, inflammatory reactions, and neurotoxicity. Since NPs can also be transferred through the placental barrier, Zhang et al. [42] studied the effects of aluminum NP exposure to pregnant female mice that will influence the CNS development in the offspring. The concentration of Al in a newborn's hippocampus was significantly increased, and they showed stunted neurodevelopmental behaviors with high anxiety and impaired learning and memory performance. Taking into consideration that aluminum has many questionable deleterious effects [45], the concern of the scientific community regarding the further application of Al nanoparticles is justified.

Various calcium-containing nanoparticles (CaNPs), frequently used in composites, may also be the cause of developing serious conditions in the organism. CaNPs such as hydroxyapatite, mono-, di-, tri-, and tetracalcium phosphates as well as amorphous calcium phosphate were reported to provoke many adverse reactions in the organism. Accumulation of ROS, oxidative stress development, and cytotoxicity are just some of the consequences of CaNP use. They can affect the structure and function of various organs, like the liver, kidneys, and testes [46] and influence prodepressant behavior and cognitive impairment [23].

Cerium nanoparticles (CeO_2-NPs or nanoceria) are widely used metal oxide nanoparticles. They are mostly applied as a diesel fuel additive to enhance combustion, as abrasive agents, in solar cells, sunscreens as UV absorbent, and contact lenses [20, 47]. Their biomedical and pharmacological application is based on their outstanding antioxidant properties. Since CeO_2-NPs contain a small amount of Ce^{3+} ions, the redox reactions between the Ce^{3+} and Ce^{4+} open the possibility of nanoceria to react with free radicals like $O_2^{-\bullet}$ and $^{\bullet}OH$, therefore establishing a function similar to CAT and SOD. Based on these criteria, they can be used to combat oxidative stress in the organism so their yearly production of around 10 000 t is not surprising [47–49]. The CeO_2-NP dermal and intestinal absorption is unlikely; therefore, the main route of entering the organism is by inhalation into the respiratory tract [47]. Although it could be concluded that the antioxidant effects of CeO_2-NPs can only bring benefits, the *in vivo* studies showed that inhalation of CeO_2-NPs can induce severe damages in the respiratory system, pulmonary tissues, and systematic toxicity. The investigation of Ma et al. [20] showed that due to the exposure of rats with CeO_2-NPs, the NO production was reduced but IL-12 production in alveolar macrophages increased leading to the activation of caspases 3 and 9 and alveolar macrophage apoptosis. Arginase-1 and osteopontin were elevated in lung cells. CeO_2-NPs induced significant lung inflammation and damage of tissue that may cause fibrosis [20]. Another *in vivo* research reported tissue distribution of inhaled CeO_2-NPs in rats after a 28-day exposure [50]. Geraets et al. came up with astonishing results that nanoceria particles were distributed in every monitored tissue (lung, liver, kidney, spleen, brain, testis, and epididymis) after a single 6 h exposure. Moreover, repeated exposures lead to a significant accumulation of CeO_2-NPs in tissues. Besides severe toxicity in the respiratory tract, hepatic, neural, and dermal toxicities of CeO_2-NPs were also reported [47].

Titanium dioxide nanoparticles (TiO_2-NPs) are in high use in medicine, cosmetics, and industry. They are added to sunscreen, toothpaste, food, and various paints and are

also used for drug delivery and in wastewater treatment, due to their photocatalytic, UV-protective, antibacterial, and self-cleaning properties [29, 51]. TiO_2-NPs have the ability to absorb photons after exposure to UV light, but photoexcited TiO_2-NPs can also induce high production of ROS, thus triggering a state of oxidative stress in live organisms [52]. The rising concern regarding human exposure to TiO_2-NPs is more than justified. There are two crystalline forms of TiO_2, anatase, and rutile. Anatase is a frequently used form in sunscreens (regulated by the United States Food and Drug Administration); thus, dermal exposure to TiO_2-NPs can be quite high leading to possible keratinocyte toxicity and skin allergy responses [53]. TiO_2-NP accumulation may cause severe problems in heart function, developing oxidative stress, inflammation, and atherosclerosis. The study of Hong et al. [51] showed significant TiO_2-NP-induced cardiac lesions and pulmonary inflammation in mice, with high levels of oxidative stress parameters. Besides the skin and hearth tissue, TiO_2-NPs were reported to accumulate in other vital organs, like the kidney, liver, lung, spleen, and brain, leading to apoptosis and organ failure [19, 29]. One of the most serious toxicities of TiO_2-NPs was observed in the reproductive system. Because of their physicochemical properties and small size, TiO_2-NPs can easily go through the blood-testis barrier, accumulate and damage testes tissue, and disrupt all vital functions [54]. Gao and coworkers [19] reported that the application of a low dose of TiO_2-NPs during a long period caused severe testicular tissue damage accompanied by sperm lesions and reduced spermatogenesis in mice. The expression of the genes included in the process of spermatogenesis was also disrupted. Many similar results should raise awareness of the TiO_2-NP negative effects on human health [19].

The iron oxide nanoparticles (IONPs) can be of various types of oxides depending on the ferrous valence, such as magnetite (Fe_3O_4), hematite (α-Fe_2O_3), and maghemite (γ-Fe_2O_3). The bioavailability of IONPs is very high, and they can be located in certain tissues by the influence of an external magnetic field. In that sense, they find their application mostly in medicine (magnetite and maghemite), for various purposes like drug delivery, therapy of cancer and thermal ablation, and magnetic resonance imaging (MRI). Even FDA approved some of the IONPs, ferumoxytol and ferumoxides, for use in MRI. Since IONPs are superparamagnetic, they can be used for medical imaging or magnetic drug targeting (MDT) [55, 56]. Various studies have been reporting the discrepant results on IONP toxicological effects, some claiming that there is no significant toxicity while others reported severe consequences. A recent study dealt with *in vivo* toxicity induced by ultrafine IONPs in rats [56]. The results of 4 weeks of exposure to IONPs showed to be decreasing in bone marrow-mononuclear cell proliferation, with high ROS levels, increased inflammatory response, and DNA changes leading to an apoptotic outcome. Although structural spleen tissue damage had not been noticed, the level of oxidative stress markers in tissue was extremely high, suggesting that high doses of IONPs may cause significant toxicity in the organism [56, 57]. One can be exposed to IONPs also via inhalation, and by entering the respiratory tract, these nanoparticles may become extremely deleterious, thereby causing pulmonary inflammation, tissue fibrosis, changes in pulmonary function, and immunological response. Zhang and coworkers [58] showed that the treatment with Fe_3O_4-NPs can induce high toxicity in the human bronchial epithelial cells by cumulative oxidative stress, whereby low GST, SOD, and CAT activities were detected.

The application of copper oxide nanoparticles (CuO-NPs) is quite versatile, from industrial use as additives in inks, medical devices, and metallic coatings, up to medicinal purposes due to their antibacterial, antifungal, and anti-inflammatory properties [59, 60]. Although the use of CuO-NPs in nanomedicine showed many benefits, for drug delivery, as a contrast agent, and in diagnostics, their overaccumulation in the human body may lead to pronounced consequences, mainly via inducing oxidative stress [61]. Like the abovementioned NPs, because of their size, CuO-NPs can easily cross biological barriers, therefore reacting with biomolecules, inducing ROS synthesis and accumulation, which further evokes oxidative stress and damage on various levels [60]. They interact with biological membranes, DNA, and proteins, causing severe damage and inactivation, liver and kidney toxicities, brain dysfunction, and metabolic alkalosis [62].

One of the most important and the most used nanoparticles is zinc oxide nanoparticles (ZnO-NPs). ZnO-NPs have been listed as safe substances by the US FDA so that their use increased sharply in recent years [63]. They can be synthesized by various methods and used in different fields, such as the rubber, textile, electronics, electrotechnology, and food packaging industries, in concrete production, in photocatalysis, and as pigments and coatings. ZnO-NPs are quite used in the cosmetic industry, in sunscreens, based on their valuable UV absorption effects, but also in many other products because of their remarkable antimicrobial properties [63, 64]. Although these NPs are generally considered to be safe, some aspects of their potential to induce toxicity should be mentioned. ZnO-NPs can induce various toxicities accumulating in the human organism, but the exact mechanisms of their toxicity are still quite unknown [28, 65]. Pandurangan and Kim [64] explained the most likely mechanisms of ZnO-NP action in the cells causing severe damage based on their high solubility. One is that the high extracellular concentration of these NPs may lead to an increase of the Zn^{2+} level inside the cells cutting down the activity of the Zn-dependent enzymes and transcription factors. Another mechanism of ZnO-NP toxicity can arise when they enter the cell where they can affect the structure of enzymes and transcription factors, and the last mechanism is via disrupting the pH level caused by dissolution of ZnO-NPs in the lysosomes. Cytotoxicity of ZnO-NPs was demonstrated in a study designed by Yu et al. [28] where normal skin cells were exposed to ZnO-NPs. It was shown that ZnO-NPs induced the formation of ROS in high concentrations, leading to oxidative stress development, autophagic vacuole accumulation, and mitochondria dysfunction. Cytotoxic effects and genotoxicity of ZnO-NPs were also demonstrated on human SHSY5Y neuronal cells [24].

Although zinc NPs did not enter the neuronal cells, they caused cell death via various damages of the cell cycle, DNA, and cell structure. *In vivo* studies on ZnO-NPs reported similar findings and the possibility of developing serious disorders. ZnO-NPs, at concentrations of 200 or 400 mg/kg/day (for 90 days), induced a state of high oxidative stress in mice [65]. The level of liver injury was enormous, including tissue disruption, reduced concentration of GSH, high levels of transaminases in serum, and endoplasmic reticulum stress which lead to apoptosis. Similar results were obtained by Yousef et al. [43] in the study on male Wistar rats treated, not just with ZnO-NPs, but also with Al_2O_3-NPs. It was shown that the oral administration of those NPs, alone and together, induced high toxicity in the liver and kidneys with the loss of function, oxidative stress, tissue damage, and systemic inflammation, with highly synergistic action.

Gold nanoparticles (AuNPs) are recognized and FDA approved for their biomedical application, drug delivery, biosensing, cell imaging, gene therapy, and radiotherapy but also find use in the food industry, water purification, and alleviation of pollution [13]. Nevertheless, certain studies revealed potential harmful effects of AuNPs on humans and the environment. After entering the organism, via previously mentioned routes, AuNPs can induce inflammation and cytotoxicity, increasing levels of oxidative stress. Abdelhalim et al. [66] conducted an *in vivo* study in which male Wistar-Kyoto rats were intraperitoneally treated with AuNPs for 7 days. AuNPs significantly elevated the oxidative stress markers, but also the parameters of liver function, causing hepatotoxicity. Gold NPs also may affect the red blood cells (RBCs), causing hemoglobin deoxygenation [4]. The same study reported similar activity of silver nanoparticles (AgNPs) on RBCs, additionally producing ROS and therefore high oxidative stress levels and cell damage. The conclusion was derived that changes in the structure of hemoglobin were mainly due to pH shifting in the cytoplasm [4].

Silver nanosized particles are used, to the greatest extent, for their immense antimicrobial properties, like silver itself. AgNPs proved their effects as antibacterial, antifungal, and antiviral agents [17] so their usage in biomedical purposes relies on these properties. Since they are FDA approved for antibactericidal purposes, over four hundred products on the market contain these NPs [67]. They are applied in wound dressings, but also as the coating of medical appliances, like surgical instruments or prosthetics [5]. AgNPs have also been applied, as many previously mentioned NPs, for drug delivery, molecular imaging, and even cancer therapy, but in the food and textile industry too [10, 17]. Due to the widespread use of AgNPs, there is, again, reasonable concern whether these NPs can harm live organisms. The route of uptake of AgNPs does not differ much from the above stated. In the cells, AgNPs can accumulate and release Ag^+ ions, therefore affecting the cell function by provoking oxidative stress, damage of the mitochondria and genetic material, and, ultimately, apoptosis [3, 10, 67]. They are also able to readily transfer the blood-brain barrier, reach the brain tissue, and provoke severe consequences [17]. Thus, AgNP-induced neurotoxicity was investigated by Yin et al. [25] on neonatal Sprague-Dawley rats and it was shown that AgNPs induced significant alterations in neuronal tissue. Hepatic tissue can also be affected by AgNPs [5], where they induce high levels of oxidative stress (observed through CAT, SOD, MDA, and GSH levels) and increase serum markers of liver function (transaminases, alkaline phosphatase, and proteins), accompanied with tissue changes and DNA damage. Besides the accumulation in organs, AgNPs have extensive toxicity on the human sperm. Wang et al. [27] reported a dose- and time-dependent change in sperm viability and motility after treatment with AgNPs with high levels of ROS and DNA damage. Treatment of freshwater snail (*Lymnaea luteola* L.) with silver NPs lowered the levels of GSH, glutathione-S-transferase, and glutathione peroxidase while lipid peroxidation was significantly elevated as well as DNA damage in digestive gland cells [68].

3. Antioxidants

The antioxidants can be defined in different ways, but one of the most simple definitions is that they are molecules able to protect the various section of biological systems against oxidative damage [69]. They are able to act in the prevention of the damage, to scavenge and neutralize free radicals and reactive oxygen and nitrogen species, and to repair new antioxidants, thus counteracting their action, inhibiting the oxidation of biologically important molecules [70]. In that sense, antioxidants possess an important role in aerobic living organisms. Essentially, this group of different components in organisms possesses a high ability to prevent oxidative stress (preventing reactions of free radicals with biomolecules), terminate radical oxidation reactions, and repair the damage induced by free radical reactions [71]. The intensive production of free radical and reactive species in humans leads to an imbalance between the rate of their formation and the antioxidant defense of the organism leading to pathological processes called "oxidative stress." This imbalance may be provoked by intense exposure of the organism to exogenous harmful factors such as UV and radioactive irradiation, pollutants, xenobiotics, smoking, heavy metals, and extreme physical exertion. This may be a cause of different tissue and organ damage, as well as different disease promotions [72]. The exogenous nonenzymatic antioxidants such as mineral elements, vitamins, dietary supplements, or plant antioxidants represent an important source of compounds for support of the human antioxidant defense system in the prevention and mitigation of organism damage caused by oxidative stress [70, 73].

The most used antioxidants among the human population are vitamins, such as vitamin A, vitamin C, and vitamin E and, then, β-carotene, minerals (like Se), and plant polyphenols. Regardless of their importance for human halt and vitality, they can cause adverse effects if consumed in much higher doses than those found in foodstuffs. Scientists have reported that long-term consumption of high dosages of antioxidant supplements (vitamins A, C, and E and β-carotene) may be associated with an increased risk of some disorders in humans. Researchers reported that the most

beneficial use of antioxidant supplements may be in the case of their deficit for normalization of their levels [74, 75].

Despite the high efficacy and a high number of currently known natural or synthetic antioxidants, there are some limitations in their specific applications in biomedicine, food industry, pharmaceutical, and cosmetic products. Sometimes, the main problem for their application is possible toxic effects, self-retention in the desired location, and sensitivity to atmospheric oxygen or enzyme degradation. Antioxidants in the form of nanoparticles have been recently proposed as an innovative solution for the improvement of their characteristics. Advancement in nanotechnology has revealed several nanoparticles consisting of biologically originated molecules with antioxidant activities, such as lignin, melanin, coenzyme Q10, or polyphenol nanoparticles [38, 76, 77]. Many antioxidant compounds are developed as nanoparticles functionalized with antioxidants. This type of nanoparticle antioxidants may possess a core with a surface consisting of covalently bound antioxidants (magnetic nanoantioxidants) or nanoparticles as passive carriers able to deliver and release antioxidants (e.g., nanoencapsulated, nanotubes, or mesoporous materials). There is a number of functionalized nanoparticles, e.g., Fe_3O_4 or graphite-coated cobalt magnetic NPs functionalized with different natural or synthetic antioxidants, as well as nanoencapsulated antioxidants [76, 78, 79].

Considering the wide use of different NPs in many products and materials for human use, as well as due to the people exposure risk workplaces and their existence in the environment [29, 80], there is increased interest of researchers to provide possible therapeutic agents or dietary supplements for the amelioration of nanoparticle-induced toxicity. In this context, the authors focused in this review, to summarize the knowledge about the use of antioxidants as supplements for prevention and alleviation of harmful effects caused by exposure of organisms to NPs. The studies in this field were searched using Scopus, Google Scholar, Science Direct, and PubMed. The most relevant publications were selected based on the following keywords: "nanoparticle-induced toxicity," "prevention of nanoparticle-induced toxicity," "effects of antioxidants on nanoparticle-induced toxicity," "antioxidants and nanoparticles," "plants and nanoparticle-induced toxicity," "plant extracts and nanoparticle-induced toxicity," and "bioactive compounds in nanoparticle-induced toxicity." The references from 2010 until 2021 are included in this review.

3.1. Vitamins and Dietary Supplements. Vitamin E (α-tocopherol) is one of the most important carotenoids with remarkable antioxidant properties. It is able to neutralize ROS and decrease the lipid peroxidation reactions in the organism [81]. Therefore, the idea of its application to counteract the NP-induced oxidative stress is not surprising. Most of the recent *in vivo* studies used silver nanoparticles for inducing toxicity. For example, Hedayati et al. [82] used the zebrafish (*Danio rerio*) model for the evaluation of vitamin E protective effects towards AgNP-induced toxicity. Vitamin E was applied as a food supplement in three different doses. The results showed that AgNPs induced significant immunological impairments with inhibition of lysozyme and ACH50 (alternative complement pathway) activity, cellular damage with increased LDH activity and cortisol levels, and high levels of oxidative and metabolic stress by lowering of inhibiting CAT and SOD activities. Higher doses of vitamin E were able to significantly protect the organism from AgNP action, restoring all vital parameters [82]. The lipophilic nature of vitamin E grants its use as a neuroprotective agent, but the studies of its effect against neurological impairment induced by NPs are rare. One of these is the study of Yin et al. [25] dealing with the AgNP-induced neurological toxicity in neonatal Sprague Dawley rats. A series of deleterious neurotoxic effects of nasal administration of AgNPs were reported, including structural disorders in the cerebellum, stress, and body weight loss. Vitamin E oral supplementation exerted strong neuroprotective effects and was able to improve the bodyweight of animals and reduce the level of astrocyte activation or proliferation, but it was unable to significantly ameliorate AgNP-induced neurohistological changes [25]. Recently, another *in vivo* study showed valuable effects of vitamin E on AgNP-induced degeneration of filiform and circumvallate tongue papillae [83]. The albino rats were exposed to AgNPs and vitamin E for 28 days. The immunohistochemical and histological examinations showed valuable protective effects of vitamin E administration in terms of protecting both tongue papillae of AgNP toxic effects and apoptotic changes. The combination of lipophilic vitamin E and hydrophilic vitamin C proved to be efficient against toxicity induced by zinc oxide nanoparticles (ZnO-NPs) in fish species Nile tilapia (*Oreochromis niloticus*) [84]. The oxidative stress parameters, such as glutathione reductase (GR), glutathione peroxidase (GPx), and glutathione-S-transferase (GST) activities and gene expression, the levels of glutathione (GSH) and lipid peroxidation, in the liver and gill of Nile tilapia were monitored. It was shown that ZnO-NPs significantly altered all parameters, but the mixture of vitamins E and C was able to reduce the levels of oxidative stress in Nile tilapia by upgrading all parameters within normal limits. The synergistic effects of tocopherols with vitamin C, where vitamin C is able to regenerate tocopherol activity, seem to be a crucial factor for their use as a mixture [72].

Another lipophilic vitamin used as an antioxidant is vitamin A (retinol) which showed significant activity in different cellular processes, and it is essential for the vision and reproductive system. Its activity, in mixture with vitamin E, regarding TiO_2-NP-induced toxicity was monitored by several recent studies. Khanvirdiloo et al. [85] evaluated testicular changes induced by titanium dioxide nanoparticles (TiO_2-NPs) and how vitamin A, vitamin E, and their combination can alter those changes in male Wistar rats. TiO_2-NPs caused severe damage to the spermatogenesis process; it decreased sperm count, motility, and viability, sperm chromatin integrity was disturbed, and inflammation in testicular tissue was observed. Nevertheless, the administration of vitamins A and E, particularly their mixture, had profound effects on reducing the testicular toxicity of TiO_2-NPs. Besides testicles, TiO_2-NPs can be accumulated in many other organs where they may provoke severe implications. The spleen is very susceptible to TiO_2-NP

accumulation and deleterious action. Afshari-Kaveh et al. [86] reported severe changes in the oxidative status of spleen tissue of Wistar rats treated with TiO_2-NPs. Nanoparticles induced significantly increased total oxidant status and lipid peroxidation levels. The total antioxidant capacity in spleen tissue was decreased likewise SOD and GPx activities and their gene expression. Nevertheless, the treatment with vitamins A and E, separately and as a mixture, showed outstanding antioxidant properties in terms of reinstating the levels of antioxidant parameters back to normal as well as protecting spleen tissue from histological changes induced by TiO_2-NPs.

Vitamin D, also called "the sunshine vitamin," has a crucial role in promoting bone health in children and adults as well as lowering the potential formation of chronic diseases, including cancer and cardiovascular disorders. It serves as a membrane antioxidant but also as a regulator of endogenous antioxidant defense systems. Generally, vitamin D exists in its inactive form, whether made in the skin or ingested, but becomes activated by hydroxylation in the liver and kidneys [87]. Its protective role towards the liver and kidneys was studied in the state of oxidative stress induced by manganese oxide-nanoparticles (MnO_2-NPs) [88]. Although MnO_2-NPs can affect environmental conditions, their possibility of entering into the human organism, via previously mentioned routes, is of great concern. They can be toxic on different levels, wherever they accumulate, including the possibility to penetrate the blood-brain barrier. In the BALB c mice, significant toxicity was developed after exposing them to MnO_2-NPs and the levels of liver and kidney functions were substantially lowered while serum bilirubin and glucose concentrations were much higher compared with the control group. The intraperitoneal administration of vitamin D for 50 consecutive days showed improvement in liver and kidney functions with a reduction of disrupted serum parameters. Taking that into account, vitamin D exerted significant hepato- and nephroprotective effects against MnO_2-NP-induced toxicity [88].

Hydrophilic vitamin C (L-ascorbic acid) is known as a very potent antioxidant compound. Since it is easily soluble in water, it can react directly with free radicals or its action may be indirect via reinstating the antioxidant activity of liposoluble vitamin E, as mentioned previously [89]. Besides its activity as a radical scavenger, it may also react as a chelator of heavy metals. Vitamin C has many beneficial effects on human health, it prevents heart disease; improves the function of cartilage, joints, and skin; has profound effects on the immune system; increases nutrition absorption; and has antigenotoxic and anticarcinogenic potential [90]. In *in vitro* assays, in human lung carcinoma, A549 cells showed significant toxicity of ZnO-NPs. Exposure to vitamin C leads to a decrease in intracellular ROS production which lowered the inflammation level [91]. The proposed mechanism of vitamin C action was based on its antioxidant activity and chelating reaction with Zn leading to the formation of a stable complex. The *in vivo* fish model, common carp (*Cyprinus carpio*), was used for the evaluation of vitamin C protective activity against TiO_2-NP-induced toxicity [92]. It was reported that TiO_2-NPs significantly increased the level of oxidative stress in the organism, which can be seen through increased levels of glucose and cortisol; higher activity of ALT, AST, and ALP; and decreased immune parameters. Liver tissue damage was also observed in the group treated only with TiO_2-NPs. Supplementation with vitamin C, at a concentration of 500 to 1000 mg/kg of feed, decreased the level of tissue damage and mainly restored oxidative stress parameters preventing severe consequences which may have arisen due to exposure with TiO_2-NPs. Vitamin C has also proven itself in the protection of rats against reproductive toxicities and oxidative stress induced by nickel nanoparticles (NiNPs) as reported by Kong et al. [93]. NiNPs induced severe consequences in rats' testicular tissue function; the levels of CAT, SOD, and gonad-stimulating hormone (GSH) were disrupted, with increased levels of ROS, nitric oxide, and lipid peroxidation. Also, NiNPs affected caspases 9, 8, and 3 and expression of Bcl-2-associated X protein (Bax) and apoptosis-inducing factor (AIF). Vitamin C upregulated all parameters and ameliorated NiNP-induced reproductive toxicity mostly due to its antioxidant properties [93].

Besides vitamins, many other compounds used as dietary supplements can serve as natural antioxidant supplementation to help combat NP-induced oxidative stress. One of those is selenium (Se), an essential trace element with valuable antioxidant and anticancer activities [94]. In the *in vivo* study by Ansar et al. [95], sodium selenite was used in the treatment of rats exposed to silver nanoparticles (AgNPs). AgNPs applied at a concentration of 5 mg/kg/b.w. induced substantial oxidative stress in animal testes, by reducing GSH levels, GPx, SOD, and CAT activities and, on the other hand, increasing the levels of lipid peroxidation and expression of interleukins (IL-1β and IL-6) and tumor necrosis factor-alpha (TNF-α). Moreover, the testes tissue damage induced by AgNPs was prominent and spermatogenesis was affected. Sodium selenite (0.2 mg/kg/b.w.) was able to improve all parameters of oxidative stress defense and inflammatory markers, including testicular tissue morphology. Although the exact mechanism of Se antioxidant effects against AgNP-induced toxicity is not known, its beneficial role in reestablishing endogenous antioxidant defense mechanisms should be acknowledged.

A sulfur-containing amino acid N-acetylcysteine (NAC) is known as an impressive free radical scavenger and antioxidant. It serves as a contributor to L-cysteine, in relation to which it has a more stable structure, as a precursor in glutathione synthesis, thus regulating the intracellular levels of GSH. Antioxidant effects of NAC are realized through releasing of sulfhydryl groups to reduce ROS levels. NAC can react with various free radicals such as hydrogen peroxide, superoxide, and peroxynitrite. It can also act on the reduction of the NF-κB pathway and secretion of inflammatory cytokines. In the state of oxidative stress, NAC plays a crucial role in preventing and reducing the damage that may arise [96, 97]. The effects of NAC on cobalt nanoparticle- (CoNP-) induced cytotoxicity in a mouse renal tubular epithelial cell model (TCMK-1 cell line) were monitored *in vitro* [98]. The application of CoNPs induced a higher rate of cell apoptosis; increased the p-ERK, p-p38, and p-JNK expression; and activated the MAPK pathway. NAC was able

to reverse the cell death process and inhibited ROS-induced p-ERK, p-p38, and p-JNK MAPK pathways. These findings support the fact that NAC has an exceptional antioxidant potential which can find its application in NP-induced oxidative stress [98]. In that sense, an *in vivo* study conducted in male albino rats used titanium dioxide nanoparticles (TiO_2-NPs) for inducing the testicular toxicity [97]. As expected, TiO_2-NPs caused severe histological changes in testes tissue accompanied by positive TNF-α immunoreaction and DNA damage. Lipid peroxidation in serum was highly elevated while GSH and testosterone levels were reduced. The treatment with NAC had an impact on all parameters and lead to their restoration, with minor antigenotoxic effects. Therefore, its antioxidant potential was significantly expressed in this state of TiO_2-NP-induced oxidative stress.

Another amino acid, L-arginine (Arg), defined as a conditionally essential amino acid, can be implemented in the treatment of NP-induced toxicities. Recently, Abdelhalim et al. [66] conducted an *in vivo* study using rats as a model organism. They were treated with gold nanoparticles (AuNPs), and the level of oxidative stress was monitored via estimation of crucial markers (ALP, ALT, GGT, total protein, MDA, and GSH). The AuNP administration induced significant hepatotoxicity and increased oxidative stress levels. The use of arginine proved to be very successful in terms of alleviation of all oxidative stress parameters thus acting protectively against the influence of AuNPs.

α-Lipoic acid, also known as thioctic acid, is a naturally occurring organosulfur compound that can be synthesized by plants, animals, and humans. It is often used as a dietary supplement due to its remarkable bioactive properties, particularly the antioxidant potential. α-Lipoic acid can act as a direct antioxidant by scavenging reactive oxygen and nitrogen species, or it may activate various antioxidants and regulate other signaling pathways [99]. This supplement has been used as additional therapy in the state of mesoporous silica nanoparticle- (MSiNP-) induced oxidative stress [100]. Primarily, Sun et al. designed *in vitro* experiment on the human neuroblastoma SH-SY5Y cell line which showed that MSiNPs were able to inhibit cellular proliferation via ROS generation that further entails impaired mitochondrial function and apoptosis activation. The *in vivo* part of the study was conducted on mice and showed high levels of oxidative stress and disrupted the brain function due to the easy transition of MSiNPs through the blood-brain barrier. α-Lipoic acid was used for modification of MSiNPs and showed a reduction in the oxidative stress level, alleviation of the cytotoxicity both *in vitro* and *in vivo*, and reduction of NP toxicity due to its significant antioxidant effects [100]. The combination of α-lipoic acid and vitamin E turned out to be great in the treatment of AuNP-induced nephrotoxicity in rats [101]. Since AuNPs caused severe changes in renal tissue and, again, high levels of oxidative stress, α-lipoic acid and vitamin E were able to reduce lipid peroxidation, inflammation, and toxicity by increasing antioxidant defense in the organism.

3.2. Plant-Based Antioxidants. The use of medicinal and edible plants is intensively studied in the prevention and treatment of oxidative stress ailments [73, 102, 103]. The potential use of plant extracts as antioxidant supplements for the mitigation of nanoparticle-induced toxicity has intensively been researched in recent years.

The most extensive research about the ameliorated effects of plant extracts or essential oils has been conducted on TiO_2-NP- and AgNP-induced oxidative stress using different model organisms (Table 1). The use of *Tinospora cordifolia* ethanol extract in experiments with Nile tilapia (*Oreochromis niloticus*) fish showed that a standard fish diet supplemented with this plan extracts can regulate antioxidant parameters in fish gill, liver, and kidney, as well as inflammation in the liver induced by TiO_2-NPs [104]. *Rosmarinus officinalis* is reported as a plant that successfully ameliorated plasma antioxidant markers (CAT, SOD, MDA, and total antioxidant status (TAS)), the IL-6 level, and DNA damage in rats treated with TiO_2-NPs [105]. The modulation of hepatotoxicity induced by TiO_2-NPs in rats showed grape seed standardized (based on proanthocyanidins (95%)) extract [106] and cinnamon bark extract [107] enhancing oxidative parameters in liver tissue. Besides the hepatoprotective activity of cinnamon bark extract, an encapsulated cinnamon essential oil also possesses protective properties of TiO_2-NP-induced oxidative stress. It is observed that the treatment of mice with maltodextrin-encapsulated cinnamon essential oil significantly reduced oxidative markers in the liver and kidney caused by TiO_2-NPs. In the same study, cinnamon essential oil reduced serum cytokines levels, DNA fragmentation in the hepatocytes, chromosomal aberrations in bone marrow cells, and sperm shape abnormalities of male mice treated with TiO_2-NPs [108]. Abdou et al. [109] demonstrated that *Moringa oleifera* leaf extract possesses nephroprotective potential in rats treated with TiO_2-NPs. This plant extract decreased oxidative stress in the kidneys induced by TiO_2-NPs, as well as modulated expression of NF-κB, Nrf2, and HSP-70 attributed to increased oxidative stress. Another study also showed that *M. oleifera* seed extract displayed a similar effect on TiO_2-NP-induced cerebral oxidative damage in rats [110]. *Moringa oleifera* seed extract was also applied in the prevention of copper nanoparticle- (CuNP-) induced toxicity in *Cyprinus carpio* fish, suggesting that this extract may successfully normalized lipid peroxidation, GSH level, and CAT activity in gill and liver tissues of fish [60].

In vitro studies published about AgNP-induced toxicity showed that studied NPs induced ROS formation leading to DNA damage of human embryonic kidney (HEK 293) cells. Pretreatment of these cells with *G. asclepiadea* extracts showed prevention of AgNP-induced DNA damage determined in comet assay and reduction of oxidized base lesions (8-oxoG) compared with cells that were not pretreated with the extracts [114, 115]. Experiments performed on Nile tilapia fish demonstrated the beneficial role of diet supplemented with pomegranate (*Punica granatum*) peel when the fish were exposed to sublethal levels of AgNPs (up to 2.0 mg/L) for six weeks. In this study, pomegranate peel supplementation significantly improved biochemical parameters in blood related with liver and kidney function, antioxidant markers in liver and kidney tissues, and

Table 1: Plant extracts, essential oils, and phytocompounds used in antioxidant supplementation of NP-induced toxicity.

Extract/compound	Nanoparticles	Action	Reference
Extracts and essential oils			
Basil essential oil (nanoencapsulated)	IONPs	Hepatoprotection in rats	El-Nekeety et al. [111]
Beta vulgaris (beetroot) juice	AgNPs	Hepatoprotection in rats	Albrahim and Alonazi [5]
Cinnamomum cassia extract	TiO_2-NPs	Hepatoprotection in rats	Shakeel et al. [107]
Cinnamomum cassia oil encapsulated with maltodextrin	TiO_2-NPs	Increase antioxidant capacity in the liver and kidney and prevent genotoxicity and reproductive disturbances in male mice	Salman et al. [108]
Eruca sativa seeds	Hydroxyapatite NPs	Cardioprotection in rats	Alotaibi et al. [112]
Filipendula ulmaria	CaNPs	Reduce oxidative stress in brain tissue of rats as well as in liver, kidney, and testes tissues	Arsenijevic et al. [23] Scepanovic et al. [46]
Foeniculum vulgare (fennel) and *Pimpinella anisum* (anise) seeds	ZnO-NPs	Hepatoprotection in rats	Barakat [113]
Gentiana asclepiadea	AgNPs	*In vitro* DNA protection	Hudecová et al. [114, 115]
Ginkgo biloba	AgNPs	Hepatoprotection in rats	Abd El-Maksoud et al. [116]
		Improved neurotoxic side effects in rats	Lebda et al. [117]
Ginseng	SiO_2-NPs	Reduce oxidative stress and apoptotic and inflammatory processes in rat lung	El-Sayed et al. [118]
Grape seed extract	TiO_2-NPs	Hepatoprotection in rats	Mohammed and Safwat, [106]
Green tea extract	CuNPs	Hepatoprotection in rats	Ibrahim et al. [59]
Moringa oleifera leaf extract	TiO_2-NPs	Nephroprotection in rats	Abdou et al. [109]
Moringa oleifera seed extract	TiO_2-NPs	Cerebroprotective effect	Kandeil et al. [110]
	CuNPs	Enhance gill and liver oxidative damage in *Cyprinus carpio*	Noureen et al. [60]
Pistacia lentiscus essential oil	NiO-NPs	Decrease ROS generation in human lung epithelial (A549) cells	Mohamed et al. [119]
Pomegranate peel	AgNPs	Enhance liver and kidney damage, oxidative stress, and immunity biomarkers in Nile tilapia fish	Hamed et al. [120]
Pomegranate juice	CuO-NPs	Reduce oxidative stress manifestations in the brain through regulation of HO-1 and Nrf2 gens	Hassanen et al. [121]
		Antioxidant, anti-inflammatory, and antiapoptotic effects in the liver and kidney of rats	Hassanen et al. [122]
	AgNPs	Hepatoprotection in mice	Sallam et al. [123]
Zataria multiflora essential oil	IONPs	Hepatoprotection in rats	Attaran et al. [124]
Pumpkin seed oil	Al_2O_3-NPs	Antioxidant protection of rats' maternal and fetal hepatic and brain tissues	Hamdi et al. [125]
Rosmarinus officinalis extract	TiO_2-NPs	Ameliorated plasma antioxidant markers in rets	Grissa et al. [105]
Tinospora cordifolia extract	TiO_2-NPs	Enhance gill, liver and kidney oxidative damage and immunity biomarkers in Nile tilapia fish	Vineetha et al. [104]
Zataria multiflora essential oil	IONPs	Hepatoprotection in rats	Attaran et al. [124]
Phytocompounds			
Apigenin	NiO-NPs	Hepatorenal protection in rats	Ali et al. [126]
	Mesoporous silica nanoparticles (MSNs)	Nephroprotection in mice	Wang et al. [127]
β-Carotene	TiO_2-NPs	Cerebroprotective effect	

Table 1: Continued.

Extract/compound	Nanoparticles	Action	Reference
			Abdel-kareem and Ayat Domouky [128]
Crocetin	CuO-NPs	Oxidative stress protection in HT22 cells	Niska et al. [129]
	NiO-NPs	Reduce oxidative stress in human HEp-2 and MCF-7 cells	Siddiqui et al. [130]
Curcumin	TiO_2-NPs	Reduction of ROS generation in *Caenorhabditis elegans* worms	Sonane et al. [131]
		In vitro DNA protection in lymphocytes	Ryu et al. [132]
	ZnO-NPs	Reduction of ROS generation in *Caenorhabditis elegans* worms	Sonane et al. [131]
Curcumin nanoparticles	Hydroxyapatite nanoparticles	Cardioprotection in rats	Mosa et al. [133]
Ellagic acid	IONPs	Nephroprotection in rats	Mohammed et al. [57]
Eugenol	TiO_2-NPs	Reduce oxidative stress in different organs of rats	Wani et al. [134]
Epigallocatechin-3-gallate	NiNPs	Reduce intracellular ROS generation and cell apoptosis in the JB6 cell line	Gu et al. [135]
Geraniol	ZnO-NPs	Neuroprotective effect in rats	Farokhcheh et al. [136]
Glycyrrhizic acid	TiO_2-NPs	Hepatoprotection in rats	Orazizadeh et al. [137]
Hesperidin	ZnO-NPs	Hepatoprotection in rats	Ansar et al. [138]
Lycopene	TiO_2-NPs	Reduce oxidative stress in testicular tissue of rats	Meng et al. [139]
	ZnO-NPs	Enhance gill, liver, and kidney oxidative damage in Nile tilapia fish	Abdel-Daim et al. [140]
Morin	TiO_2-NPs	Reduce oxidative stress in testicular tissue of rats	Hussein et al. [141]
Pterostilbene	AgNPs	Prevent oxidative stress in zebrafish embryos	Chen et al. [142]
Resveratrol	CuO-NPs	Hepatorenal protection in rats	Khalid et al. [62]
	TiO_2-NPs	Prevent testicular damage	Solaiman et al. [143]
		In vitro DNA protection in lymphocytes	Ryu et al. [132]
	ZnO-NPs	Prevent prooxidant mitochondrial damage and apoptotic and necrotic effects in zebrafish embryos	Giordo et al. [144]
		Enhance gill, liver, and kidney oxidative damage in Nile tilapia fish	Abdel-Daim et al. [140]
Rutin	TiO_2-NPs	Reduce oxidative stress in testicular tissue of rats	Hussein et al. [141]
Sesamol	Al_2O_3-NPs	Neuroprotective effect in rats	Abou-Zeid et al. [22]
Silymarin	AgNPs	Hepatoprotection in Nile tilapia fish	Veisi et al. [145]
Sulforaphane	CuO-NPs	Reduce oxidative stress in BALB C3T cells	Akhtar et al. [146]
	TiO_2-NPs	*In vitro* DNA protection in lymphocytes	Ryu et al. [132]
Tannic acid	AgNPs	Hepatorenal protection in rats	Mosa et al. [147]
Thymol	TiO_2-NPs	Protection of testicular damage	Jafari et al. [54]
		Hepatoprotection in rats	Jafari et al. [148]
Quercetin	AuNPs	Hepatoprotection in rats	Abdelhalim et al. [66]
		Hepatoprotection in rats	Abdelhalim et al. [149]
	CuO-NPs	Reduce oxidative stress in the liver and antiapoptotic action in rats' liver	Abdelazeim et al. [150]
		Hepatoprotection in rats	Arafa et al. [151]

Table 1: Continued.

Extract/compound	Nanoparticles	Action	Reference
	TiO_2-NPs	Hepatoprotection in rats	Fadda et al. [152]
		Nephroprotection in rats	Alidadi et al. [153]
		Protection of testicular damage	Khorsandi et al. [154]
	ZnO-NPs	Hepatoprotection in rats	Lotfy et al. [155]

immunity biomarkers of the fish exposed to sublethal levels of AgNPs [120]. The hepatoprotective properties of several plant species were also studied *in vivo* against AgNP-induced hepatotoxicity. *Ginkgo biloba* aqueous extract showed an important influence on liver function and the antioxidative status of rats treated with AgNPs (50 mg/kg b.w.) upregulating PGC-1α, mtTFA, and Nrf2 mRNA mitochondrial transcription factors [116]. In another study, standardized *G. biloba* extract to 24% ginkgo flavonoids improved oxidative damage in the brain of rats treated with AgNPs, as well as significantly regulated proinflammatory cytokine gene expression in brain tissue [117]. Pomegranate [123] and beetroot [5] juices also provided significant hepatoprotective activities against AgNP-induced toxicity in animal experiments. Albrahim and Alonazi [5] showed that beetroot juice posttreatment has the potential to regulate apoptotic proteins p53 and Bcl-2 in liver tissue of rats treated with AgNPs. Pomegranate juice also displayed the decrease of the MDA level and the increase of the GSH level in the liver and kidney of rats intoxicated with CuO-NPs, regulating caspase-3, Bcl-2 levels, and NF-κB disturbed expression caused by overproduction of ROS [122]. In another publication, Hassanen et al. [121] showed that pomegranate juice can reduce oxidative stress manifestations in the brain of rats treated with CuO-NPs through regulation of HO-1 and Nrf2 expression, important for cellular redox balance. Green tea extract also showed significant improvement of hepatotoxic manifestation caused by CuO-NP application in rats, improving the oxidative status of the liver and regulating the expression of the caspase-3 and Bax proteins [59].

Essential oils of *Ocimum basilicum* L. (basil) and *Zataria multiflora* Boiss. were studied for hepatoprotective activity against IONP-induced toxicity. Both essential oils had the ability to prevent hepatotoxicity of IONPs in rats regulating antioxidant parameters in liver tissue of experimental animals [111, 124]. A few published studies examined the application of plant extract or oils for the prevention of toxic effects of lesser-extent-investigated NPs. Pumpkin seed oil was applied in the study for the determination of its protective effects against Al_2O_3-NP-induced toxicity in pregnant rats. The oil possessed the ability to enhance antioxidant parameters in maternal and fetal hepatic and brain tissues of pregnant rats with developed Al_2O_3-NP-toxicity [125]. Alotaibi et al. [112] used *Eruca sativa* L. seed extract for the treatment of hydroxyapatite nanoparticle-induced toxicity concluding that this extract improved antioxidant parameters (SOD, CAT, GSH, and TBARS) in heart tissues of hydroxyapatite NP-treated rats. *Filipendula ulmaria* extract also showed a positive influence on CaNP- and hydroxyapatite NP-induced oxidative stress in brain tissue of rats [23], but also in liver, kidney, and testes tissues [46]. The essential oil of *Pistacia lentiscus* L. lowered ROS generation and stimulated SOD and CAT activities in human lung epithelial cells (A549) exposed to NiO-NPs [119]. SiO_2-NPs-induced toxicity in rats described by El-Sayed et al. [118] was ameliorated using ginseng dried plant which could reduce oxidative stress, as well as apoptotic and inflammatory processes in rat lung. The mixture of *Foeniculum vulgare* (fennel) and *Pimpinella anisum* (anise) seed extracts showed hepatoprotective potential significantly lowering oxidative stress in liver tissue of rats exposed to ZnO-NPs [113].

In terms of reducing NP toxicity, many plant extracts are frequently used in the eco-friendly synthesis of NPs with lower toxic effects. NPs obtained in these processes usually display additional pharmacological properties compared with conventionally synthesized NPs. Besides, plants represent a renewable, environment-friendly, and widely available material for NP synthesis. This relatively new approach in NP synthesis is in the research focus in recent years [14, 156, 157]. Hence, plants are also important for the development of new methods for the synthesis of less-toxic NPs as well as for the suppression of NP toxicity. Analyzed literature data about the use of plant extracts or essential oils in the prevention and reduction of NP-induced oxidative stress showed that some plants may be utilized as effective supplements in this type of oxidative damage. Most studies deal with research about the use of aromatic and edible plants in NP-induced oxidative stress that emphasizes and encourages the consumption of these plant species in the prevention and fight against oxidative stress. The highest number of analyzed studies reported that examined plant products exert hepatorenal protection in experimental animals reporting essential results about the oxidative status of organ tissues. The significantly lower number of studies deals with a profound analysis of protection mechanisms of NP-induced oxidative stress using plants. Hence, there is a need for more research with comprehensive results about the application of plants in the suppression of NP-induced oxidative stress. All these results open the possibility for further research of plants in this field.

3.3. Phytochemicals. Different plant constituents are well known for their excellent antioxidant properties; among them, phenolic compounds and some components of essential oils possess the most pronounced antioxidant properties [70, 157]. In this regard, phytochemicals with high

antioxidant potential are frequently used in studies for NP-induced toxicity as protection agents. The most studied phytocompounds in such studies are phenolic compounds and flavonoids such as quercetin, resveratrol, or curcumin (Table 1).

Quercetin (Figure 2) is one of the most studied dietary flavonoids present in many fruits, vegetables, and medicinal plants. Its antioxidant, anti-inflammatory, neuroprotective, chemopreventive, and cardioprotective properties are well documented. The bioactivity of quercetin is related to its high antioxidant and free radical scavenging activities [152, 158]. The antioxidant potential of quercetin in the suppression of NP-induced oxidative stress was examined using different models exposed to TiO_2-NPs, AuNPs, CuO-NPs, and ZnO-NPs. Quercetin showed antioxidant protection of liver [152], kidney [153], and testicular [154] tissues in rats exposed to an overdose of TiO_2-NPs. The concentration of TiO_2-NPs used in these studies was in the range of 50 to 1000 mg/kg of body weight (b.w.) daily or once during the experiment, while the dose of quercetin was 75 or 200 mg/kg b.w. of tested animals daily. Quercetin displayed oxidative protection of liver, kidney, and testicular tissues lowering lipid peroxidation and improving antioxidant parameters of kidney and testicular tissues. Also, quercetin (75 mg/kg b.w. daily) significantly reduced the apoptotic index in kidneys [153] and testes [154], while mitigation of apoptotic marker caspase 3 and DNA fragmentation in liver tissue using 200 mg/kg b.w. daily for 21 days was observed [152]. The hepatoprotective activity of quercetin was also proven in AuNP-intoxicated rats reducing oxidative stress parameters in the liver [66, 149]. Quercetin was effective against CuO-NP-induced hepatotoxicity in rats. It is repented that coadministration of 150 μg/kg b.w. quercetin daily for 3 weeks reduced significantly oxidative stress in liver tissue, serum levels of TNF-α, caspase-3 activity, and mRNA of Bax, while the significant elevation of the Bcl2 level was observed [150]. This research suggests that quercetin has the properties to inhibit some critical points of apoptosis. Similar antioxidant protection of quercetin against CuO-NP-induced hepatotoxicity in rats was observed in the study published by Arafa et al. [151], as well as against ZnO-NP-induced hepatotoxicity in rats [155].

Resveratrol (Figure 2), a stilbene, is also one of the commonly used plant antioxidants in the prevention of NP-induced toxicity. It can be found in different fruits, berries and medicinal and edible plants. Its antioxidant properties are the subject of many scientific publications, and results suggest that it possesses better antioxidant properties compared with vitamin E and C [143]. An *in vitro* study conducted by Ryu et al. [132] showed antioxidant effects of resveratrol on DNA damage induced by TiO2-NPs in lymphocytes. Resveratrol provoked significant decreases of ZnO-NP-induced prooxidant effects measured using DCFDA fluorescence intensity, mitochondrial damage, and apoptotic and necrotic effects in zebrafish embryos [144]. Pterostilbene, a stilbene chemically related to resveratrol, showed similar protection effects against AgNP-induced oxidative stress in zebrafish embryos [142]. The experiments with Nile tilapia fish showed that a fish diet supplemented with resveratrol enhances antioxidant protection parameters in fish gill, liver, and kidney disturbed by ZnO-NP application [140]. Resveratrol also displayed antioxidant protection of CuO-NP-induced oxidative stress in rats increasing total antioxidant capacity (TAC) and decreasing the total oxidant status (TOS) in serum [62]. Solaiman et al. [143] reported that resveratrol also has the ability to mitigate the increase of the serum MDA level induced by TiO2-NPs in an experiment with rats.

Curcumin (Figure 2), the main phenolic compound in spice turmeric, is reported as a natural antioxidant supplement against NiO-NPs, TiO_2-NPs, and ZnO-NPs. Siddiqui et al. [130] reported that curcumin reduces ROS and lipid peroxidation levels, as well as increases the GSH level in NiO-NP-induced toxicity in human airway epithelial (HEp-2) and breast cancer (MCF-7) cells. Another *in vitro* study showed antioxidant protective effects of curcumin on DNA damage induced by TiO_2-NPs in lymphocytes [132]. Curcumin also displayed a reduction in ROS generation measured using H_2DCF-D dye on *Caenorhabditis elegans* worms exposed for 24 h to the LC_{50} concentration of TiO_2-NPs and ZnO-NPs [131]. *In vivo* experiment on rats showed that coadministration of curcumin nanoparticles improved antioxidant parameters (TBARS, NO, GST, GPx, GSH, CAR, SOD, and total antioxidant capacity) and suppressed increased levels of tumor suppressor P53, TNF-α, and interleukin-6 in heart tissue of rats exposed to hydroxyapatite nanoparticles [133]. Apigenin is also one of the dietary flavonoids that showed hepato- and nephroprotective activities in animal models with NP-induced toxicity. Apigenin can protect the liver and kidneys against NiO-NP-induced toxicity [126] and kidneys against mesoporous silica nanoparticle- (MSN-) induced toxicity [127]. Apigenin in both mentioned studies significantly upregulated antioxidant parameters in analyzed tissues, while reducing the expression of TNF-α and IL-6 in the kidney of mice with MSN-induced toxicity. Similar protection activity of ellagic acid, as described for apigenin nephroprotection of MSN-induced toxicity in mice, was observed in a study conducted by Mohammed et al. [57] for IONP-induced nephrotoxicity in Wistar rats.

Among examined phenolic compounds in the protection of NP-induced oxidative stress, epigallocatechin-3-gallate was proved to be effective in the inhibition of oxidative stress developed with NiNPs in a mouse epidermal (JB6) cell line [135]. Epigallocatechin-3-gallate reduced intracellular ROS generation and cell apoptosis, significantly regulating the expression levels of AP-1 and NF-κB and the MAPK signaling pathways disturbed by NiNP application. Nanoencapsulated silymarin and tannic acid showed potential to ameliorate hepatotoxicity in Nile tilapia fish [145] and hepatonephrotoxicity induced in rats [147] with AgNP-induced toxicity, respectively. These phenolic components modulated disturbed antioxidant parameters in the liver or renal tissues. Also, similar effects, with the regulation of antioxidant parameters GSH, CAT, GPx, SOD, and MDA in liver tissue, demonstrated coadministration of hesperidin parallel with ZnO-NP-induced oxidative stress in rats [138]. Flavonoids morin and rutin showed the same effects on testicular

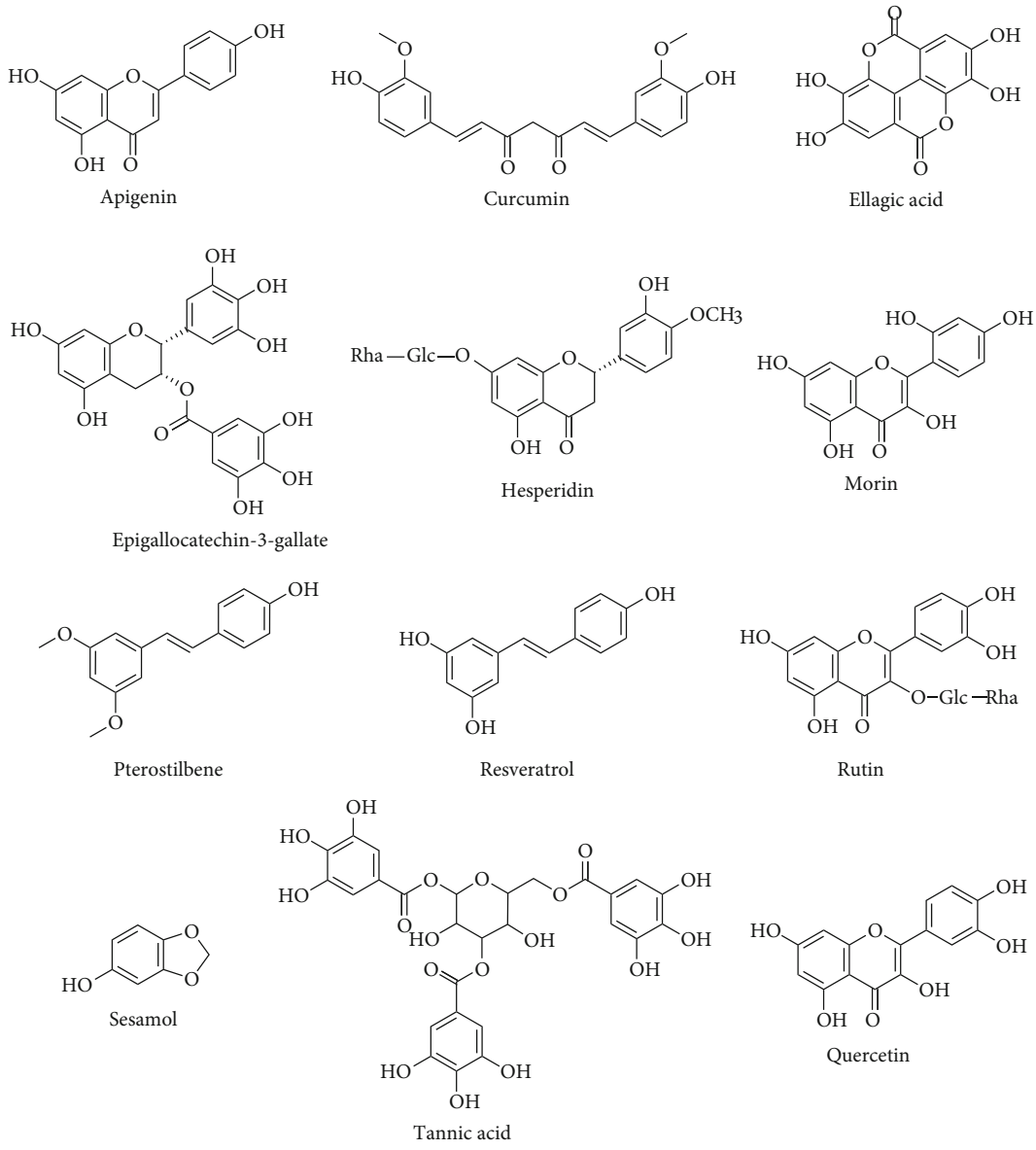

Figure 2: Plant phenolic compounds used in supplementation of nanoparticle-induced oxidative stress.

tissue of rats treated with TiO2-NPs [141]. Sesamol, a phenolic lignan from sesame oil, exhibited significant antioxidant protection effects of brain tissue in Al_2O_3-NP-treated rats [22].

Sulforaphane, an isothiocyanate compound found in cruciferous vegetables, also manifested antioxidant protection of CuO-NP-induced oxidative stress in BALB C3T cells [146], as well as DNA damage induced by TiO_2-NPs in lymphocytes [132]. Glycyrrhizic acid, a natural sweetener isolated from the root of *Glycyrrhiza glabra*, showed the potential to reduce oxidative stress and the apoptotic process in the liver of rats treated with TiO_2-NPs [137].

In addition to phenolic compounds, terpenoids and components of plant essential oils are often the subjects of NP-induced oxidative stress protection (Figure 3). β-Carotene showed potential to reduce the apoptotic index and increase CAT and GPx activities in the cerebral tissues of TiO_2-NP-intoxicated rats [128]. A fish diet supplemented with lycopene manifested an increase of antioxidant protection parameters in Nile tilapia fish gill, liver, and kidney disturbed by ZnO-NP application [140]. Lycopene also enhances antioxidant protection and decreases cell apoptosis in testes of mice treated with TiO_2-NPs [139]. CuO-NP-induced oxidative stress in the mouse hippocampal HT22 cell was effectively protected with coadministration of crocetin, a compound found in gardenia fruits and saffron [129]. It is found that crocetin increases the activity of antioxidant enzymes SOD and CAT, as well as GSH, SOD mRNA, CAT mRNA, and Bcl-2 mRNA levels in CuO-NP-intoxicated HT22 cell. The same study described the crocetin potential to reduce intracellular ROS and proapoptotic Bax mRNA levels in HT22 cells treated with CuO-NPs. The common constituents of essential oils eugenol, thymol, and geraniol are proven as antioxidant compounds in the prevention of

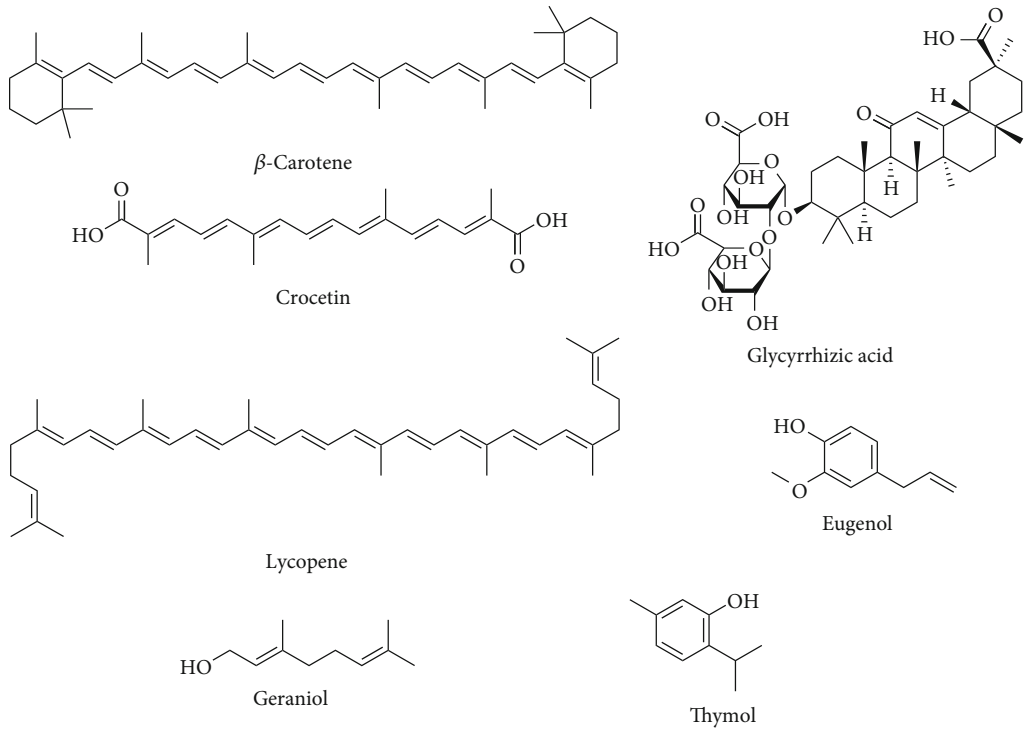

Figure 3: Plant terpenoids used in supplementation of nanoparticle-induced oxidative stress.

oxidative stress in different organs induced by various NPs in experiments performed on rats [54, 134, 136, 148].

Available literature data about the use of phytochemicals as supplements in NP-induced oxidative stress showed the high potential of these compounds for application and development of new plant-based dietary supplements. The investigated phytochemicals are common constituents of aromatic, medicinal, and edible plants, and obtained results indicate a beneficial effect of the use of these plants or plant-based supplements in oxidative stress-related disorders. Also, these results are very useful for further research in this field suggesting that most of the known antioxidant phytocompounds have not been investigated yet as potential supplements in the treatment of oxidative stress induced by NPs.

4. Conclusion

Considering the many benefits of antioxidants, including vitamins, dietary supplements, plant products, and phytochemicals and their great potential in suppression of NP-induced oxidative stress, there is no doubt that the research that deals with the application of antioxidants in this field will continue with more attention in the forthcoming years. Different natural occurring antioxidants have been comprehensively reviewed in this paper. Although vitamins, plant extracts, and phytochemicals have shown great potential in NP-induced oxidative stress protection, understanding the mechanisms involved in the modulation of NP-induced oxidative stress of these natural products is still not fully understood. Hence, it seems that achieved results in this field present a good base for further research on protection mechanisms of NP-induced oxidative stress using naturally occurring antioxidants, as well as for more research including some earlier not tested plants and their bioactive compounds. The overall goals of future studies are dominantly focused to give an insight into new perspectives of NP usage with an imperative to decrease their toxicity using verified, safe, and validated antioxidant supplementary therapy that may be also beneficial for the living organism as a whole. Based on the analyzed results, one of the greatest potentials for further research is antioxidants of plant origin. A further strategy for the advancement of this area of research could be the related investigation for the use of new plant-based antioxidants as dietary supplements in the prevention or alleviation of oxidative stress symptoms associated with long-term exposure to NPs or their high concentration.

Data Availability

All data are available upon request.

Conflicts of Interest

The authors declare no conflict of interest.

Authors' Contributions

Vladimir Mihailovic and Jelena S. Katanic Stankovic contributed equally to this paper.

Acknowledgments

This work was supported by the Faculty of Medical Sciences, University of Kragujevac (JP 01/19). VM and JKS thank the Ministry of Education, Science, and Technological Development of the Republic of Serbia for the research support (contract nos: 451-03-68/2021-14/200122 and 451-03-68/2021-14/200378).

References

[1] H. Rauscher, B. Sokull-Klüttgen, and H. Stamm, "The European Commission's recommendation on the definition of nanomaterial makes an impact," *Nanotoxicology*, vol. 7, no. 7, pp. 1195–1197, 2013.

[2] M. Horie and Y. Tabei, "Role of oxidative stress in nanoparticles toxicity," *Free Radical Research*, vol. 55, no. 4, pp. 331–342, 2021.

[3] A. Manke, L. Wang, and Y. Rojanasakul, "Mechanisms of nanoparticle-induced oxidative stress and toxicity," *BioMed Research International*, vol. 2013, 15 pages, 2013.

[4] S. Barkur, J. Lukose, and S. Chidangil, "Probing nanoparticle–cell interaction using micro-Raman spectroscopy: silver and gold nanoparticle-induced stress effects on optically trapped live red blood cells," *ACS Omega*, vol. 5, no. 3, pp. 1439–1447, 2013.

[5] T. Albrahim and M. A. Alonazi, "Role of beetroot (Beta vulgaris) juice on chronic nanotoxicity of silver nanoparticle-induced hepatotoxicity in male Rats," *International Journal of Nanomedicine*, vol. Volume 15, pp. 3471–3482, 2020.

[6] K. Peynshaert, B. B. Manshian, F. Joris et al., "Exploiting intrinsic nanoparticle toxicity: the pros and cons of nanoparticle-induced autophagy in biomedical research," *Chemical Reviews*, vol. 114, no. 15, pp. 7581–7609, 2014.

[7] V. Srivastava, D. Gusain, and Y. C. Sharma, "critical review on the toxicity of some widely used engineered nanoparticles," *Industrial & Engineering Chemistry Research*, vol. 54, no. 24, pp. 6209–6233, 2015.

[8] S. J. Hawkins, L. A. Crompton, A. Sood et al., "Nanoparticle-induced neuronal toxicity across placental barriers is mediated by autophagy and dependent on astrocytes," *Nature Nanotechnology*, vol. 13, no. 5, pp. 427–433, 2018.

[9] M. Mishra and M. Panda, "Reactive oxygen species: the root cause of nanoparticle-induced toxicity inDrosophila melanogaster," *Free Radical Research, ahead-of-print*, vol. 55, no. 8, pp. 919–935, 2021.

[10] S. Kim and D. Y. Ryu, "Silver nanoparticle-induced oxidative stress, genotoxicity and apoptosis in cultured cells and animal tissues," *Journal of Applied Toxicology*, vol. 33, no. 2, pp. 78–89, 2013.

[11] T. Sun, Y. Kang, J. Liu et al., "Nanomaterials and hepatic disease: toxicokinetics, disease types, intrinsic mechanisms, liver susceptibility, and influencing factors," *Journal of Nanobiotechnology*, vol. 19, no. 1, p. 108, 2021.

[12] A. Scherzad, T. Meyer, N. Kleinsasser, and S. Hackenberg, "Molecular mechanisms of zinc oxide nanoparticle-induced genotoxicity," *Materials*, vol. 10, no. 12, p. 1427, 2017.

[13] A. Sani, C. Cao, and D. Cui, "Toxicity of gold nanoparticles (AuNPs): a review," *Biochem Biophys Reports*, vol. 26, p. 100991, 2021.

[14] C. Vanlalveni, S. Lallianrawna, A. Biswas, M. Selvaraj, B. Changmai, and S. L. Rokhum, "Green synthesis of silver nanoparticles using plant extracts and their antimicrobial activities: a review of recent literature," *RSC Advances*, vol. 11, no. 5, pp. 2804–2837, 2021.

[15] A. Eftekhari, S. M. Dizaj, L. Chodari et al., "The promising future of nano-antioxidant therapy against environmental pollutants induced-toxicities," *Biomedicine Pharmacotherapy*, vol. 103, pp. 1018–1027, 2018.

[16] C. W. Li, L. L. Li, S. Chen, J. X. Zhang, and W. L. Lu, "Antioxidant nanotherapies for the treatment of inflammatory diseases," *Frontiers in Bioengineering and Biotechnology*, vol. 8, 2020.

[17] A. B. Sengul and E. Asmatulu, "Toxicity of metal and metal oxide nanoparticles: a review," *Environmental Chemistry Letters*, vol. 18, no. 5, pp. 1659–1683, 2020.

[18] M. Ajdary, M. A. Moosavi, M. Rahmati et al., "Health concerns of various nanoparticles: a review of their in vitro and in vivo toxicity," *Nanomaterials*, vol. 8, no. 9, p. 634, 2018.

[19] G. Gao, Y. Ze, X. Zhao et al., "Titanium dioxide nanoparticle-induced testicular damage, spermatogenesis suppression, and gene expression alterations in male mice," *Journal of Hazardous Materials*, vol. 258-259, pp. 133–143, 2013.

[20] J. Y. Ma, H. Zhao, R. R. Mercer et al., "Cerium oxide nanoparticle-induced pulmonary inflammation and alveolar macrophage functional change in rats," *Nanotoxicology*, vol. 5, no. 3, pp. 312–325, 2011.

[21] F. Ravish, A. Kafil, H. M. Mobarak, and A. Riaz, "Chromium oxide nanoparticle–induced biochemical and histopathological alterations in the kidneys and brain of Wistar rats," *Toxicology and Industrial Health*, vol. 33, no. 12, pp. 911–921, 2017.

[22] S. M. Abou-Zeid, B. A. Elkhadrawey, A. Anis et al., "Neuroprotective Effect of Sesamol against Aluminum Nanoparticle-Induced Toxicity in Rats," *Environmental Science and Pollution Research*, vol. 28, no. 38, pp. 53767–53780, 2021.

[23] N. Arsenijevic, D. Selakovic, J. S. K. Stankovic et al., "The beneficial role of Filipendula ulmaria extract in prevention of Prodepressant effect and cognitive impairment induced by nanoparticles of calcium phosphates in rats," *Oxidative Medicine and Cellular Longevity*, vol. 2021, 12 pages, 2021.

[24] V. Valdiglesias, C. Costa, G. Kiliç et al., "Neuronal cytotoxicity and genotoxicity induced by zinc oxide nanoparticles," *Environment International*, vol. 55, pp. 92–100, 2013.

[25] N. Yin, X. Yao, Q. Zhou, F. Faiola, and G. Jiang, "Vitamin E attenuates silver nanoparticle-induced effects on body weight and neurotoxicity in rats," *Biochemical and Biophysical Research Communications*, vol. 458, no. 2, pp. 405–410, 2015.

[26] M. Pogribna and G. Hammons, "Epigenetic effects of nanomaterials and nanoparticles," *Journal of Nanobiotechnology*, vol. 19, no. 1, p. 2, 2021.

[27] E. Wang, Y. Huang, Q. Du, and Y. Sun, "Silver nanoparticle induced toxicity to human sperm by increasing ROS(reactive oxygen species) production and DNA damage," *Environmental Toxicology and Pharmacology*, vol. 52, pp. 193–199, 2017.

[28] K.-N. Yu, T.-J. Yoon, A. Minai-Tehrani et al., "Zinc oxide nanoparticle induced autophagic cell death and mitochondrial damage via reactive oxygen species generation," *Toxicology In Vitro*, vol. 27, no. 4, pp. 1187–1195, 2013.

[29] B. Song, T. Zhou, W. Yang, J. Liu, and L. Shao, "Contribution of oxidative stress to TiO_2 nanoparticle- induced toxicity,"

Environmental Toxicology and Pharmacology, vol. 48, pp. 130–140, 2016.

[30] S. Reuter, S. C. Gupta, M. M. Chaturvedi, and B. B. Aggarwal, "Oxidative stress, inflammation, and cancer: how are they linked?," *Free Radical Biology & Medicine*, vol. 49, no. 11, pp. 1603–1616, 2010.

[31] A. Rahal, A. Kumar, V. Singh et al., "Oxidative stress, prooxidants, and antioxidants: the interplay," *BioMed Research International*, vol. 2014, 19 pages, 2014.

[32] N. Liu and M. Tang, "Toxic effects and involved molecular pathways of nanoparticles on cells and subcellular organelles," *Journal of Applied Toxicology*, vol. 40, no. 1, pp. 16–36, 2020.

[33] P. R. Suma, R. A. Padmanabhan, S. R. Telukutla et al., "Vanadium pentoxide nanoparticle mediated perturbations in cellular redox balance and the paradigm of autophagy to apoptosis," *Free Radical Biology & Medicine*, vol. 161, pp. 198–211, 2020.

[34] J. K. Fard, H. Hamzeiy, M. Sattari, A. Eftekhari, E. Ahmadian, and M. A. Eghbal, "Triazole rizatriptan induces liver toxicity through lysosomal/mitochondrial dysfunction," *Drug Research*, vol. 66, no. 9, pp. 470–478, 2016.

[35] S. Yan, L. Qiao, X. Dou et al., "Biogenic selenium nanoparticles byLactobacillus caseiATCC 393 alleviate the intestinal permeability, mitochondrial dysfunction and mitophagy induced by oxidative stress," *Food & Function*, vol. 12, no. 15, pp. 7068–7080, 2021.

[36] D. Bou-Teen, N. Kaludercic, D. Weissman et al., "Mitochondrial ROS and mitochondria-targeted antioxidants in the aged heart," *Free Radical Biology & Medicine*, vol. 167, pp. 109–124, 2021.

[37] R. Jahangirnejad, M. Goudarzi, H. Kalantari, H. Najafzadeh, and M. Rezaei, "Subcellular organelle toxicity caused by arsenic nanoparticles in isolated rat hepatocytes," *International Journal of Occupational and Environmental Medicine*, vol. 11, no. 1, pp. 41–52, 2020.

[38] A. Eftekhari, E. Ahmadian, A. Azami, M. Johari-Ahar, and M. A. Eghbalgerc, "Protective effects of coenzyme Q10 nanoparticles on dichlorvos-induced hepatotoxicity and mitochondrial/lysosomal injury," *Environmental Toxicology*, vol. 33, no. 2, pp. 167–177, 2018.

[39] R. Shrivastava, R. Bhargava, and S. J. S. Flora, "Antioxidant activity and free radical scavenging potential of alpha lipoic acid and quercetin against Al2O3 nanoparticle-induced toxicity in mice," *Free Radicals and Antioxidants*, vol. 4, no. 1, pp. 8–14, 2014.

[40] L. K. Braydich-Stolle, J. L. Speshock, A. Castle, M. Smith, R. C. Murdock, and S. M. Hussain, "Nanosized aluminum altered immune function," *ACS Nano*, vol. 4, no. 7, pp. 3661–3670, 2010.

[41] N. A. Monteiro-Riviere, S. J. Oldenburg, and A. O. Inman, "Interactions of aluminum nanoparticles with human epidermal keratinocytes," *Journal of Applied Toxicology*, vol. 30, no. 3, pp. 276–285, 2010.

[42] Q. Zhang, Y. Ding, K. He et al., "Exposure to alumina nanoparticles in female mice during pregnancy induces neurodevelopmental toxicity in the offspring," *Frontiers in Pharmacology*, vol. 9, 2018.

[43] M. I. Yousef, T. F. Mutar, and M. A. E. N. Kamel, "Hepatorenal toxicity of oral sub-chronic exposure to aluminum oxide and/or zinc oxide nanoparticles in rats," *Toxicology Reports*, vol. 6, pp. 336–346, 2019.

[44] E. J. Park, H. Kim, Y. Kim, and K. Choi, "Repeated-dose toxicity attributed to aluminum nanoparticles following 28-day oral administration, particularly on gene expression in mouse brain," *Toxicological & Environmental Chemistry*, vol. 93, no. 1, pp. 120–133, 2011.

[45] C. A. Shaw and L. Tomljenovic, "Aluminum in the central nervous system (CNS): toxicity in humans and animals, vaccine adjuvants, and autoimmunity," *Immunologic Research*, vol. 56, no. 2-3, pp. 304–316, 2013.

[46] R. Scepanovic, D. Selakovic, J. S. K. Stankovic et al., "The antioxidant supplementation with Filipendula ulmaria extract attenuates the systemic adverse effects of nanosized calcium phosphates in rats," *Oxidative Medicine and Cellular Longevity*, vol. 2021, 16 pages, 2021.

[47] Z. M. Milani, F. Charbgoo, and M. Darroudi, "Impact of physicochemical properties of cerium oxide nanoparticles on their toxicity effects," *Ceramics International*, vol. 43, no. 17, pp. 14572–14581, 2017.

[48] I. Celardo, J. Z. Pedersen, E. Traversa, and L. Ghibelli, "Pharmacological potential of cerium oxide nanoparticles," *Nanoscale*, vol. 3, no. 4, pp. 1411–1420, 2011.

[49] E. Casals, M. Zeng, M. Parra-Robert et al., "Cerium oxide nanoparticles: advances in biodistribution, toxicity, and preclinical exploration," *Small*, vol. 16, no. 20, p. 1907322, 2020.

[50] L. Geraets, A. G. Oomen, J. D. Schroeter, V. A. Coleman, and F. R. Cassee, "Tissue distribution of inhaled micro- and nano-sized cerium oxide particles in rats: results from a 28-day exposure study," *Toxicological Sciences*, vol. 127, no. 2, pp. 463–473, 2012.

[51] F. Hong, L. Wang, X. Yu, Y. Zhou, J. Hong, and L. Sheng, "Toxicological effect of TiO2 nanoparticle-induced myocarditis in mice," *Nanoscale Research Letters*, vol. 10, no. 1, p. 1029, 2015.

[52] M. Li, J.-J. Yin, W. G. Wamer, and Y. M. Lo, "Mechanistic characterization of titanium dioxide nanoparticle-induced toxicity using electron spin resonance," *Journal of Food and Drug Analysis*, vol. 22, no. 1, pp. 76–85, 2014.

[53] B. C. Palmer and L. A. DeLouise, "Morphology-dependent titanium dioxide nanoparticle-induced keratinocyte toxicity and exacerbation of allergic contact dermatitis," *Current Research in Toxicology*, vol. 4, no. 1, pp. 1–7, 2020.

[54] A. Jafari, M. Karimipour, M. R. Khaksar, and M. Ghasemnejad-Berenji, "Protective effects of orally administered thymol against titanium dioxide nanoparticle–induced testicular damage," *Environmental Science and Pollution Research*, vol. 27, no. 2, pp. 2353–2360, 2020.

[55] B. B. Gonçalves, F. C. Dias, N. S. de Souza Trigueiro et al., "Chronic exposure to iron oxide nanoparticles (γ-Fe_2O_3) induces gonadal histopathology on male guppies (_Poecilia reticulata_)," *Environmental Nanotechnology, Monitoring & Management*, vol. 16, p. 100522, 2021.

[56] U. S. Gaharwar, S. Kumar, and P. Rajamani, "Iron oxide nanoparticle-induced hematopoietic and immunological response in rats," *RSC Advances*, vol. 10, no. 59, pp. 35753–35764, 2020.

[57] E. T. Mohammed, K. S. Hashem, A. Z. Abdelazem, and F. A. M. A. Foda, "Prospective protective effect of ellagic acid as a SIRT1 activator in iron oxide nanoparticle-induced renal damage in rats," *Biological Trace Element Research*, vol. 198, no. 1, pp. 177–188, 2020.

[58] W. Zhang, J. Gao, L. Lu et al., "Intracellular GSH/GST antioxidants system change as an earlier biomarker for toxicity evaluation of iron oxide nanoparticles," *NanoImpact*, vol. 23, p. 100338, 2021.

[59] M. A. Ibrahim, A. A. Khalaf, M. K. Galal, H. A. Ogaly, and A. H. M. Hassan, "Ameliorative influence of green tea extract on copper nanoparticle-induced hepatotoxicity in rats," *Nanoscale Research Letters*, vol. 10, no. 1, p. 363, 2015.

[60] A. Noureen, F. Jabeen, T. A. Tabish et al., "Ameliorative effects of Moringa oleifera on copper nanoparticle induced toxicity in Cyprinus carpio assessed by histology and oxidative stress markers," *Nanotechnology*, vol. 29, no. 46, p. 464003, 2018.

[61] S. Hu, J. Yang, M. Rao et al., "Copper nanoparticle-induced uterine injury in female rats," *Environmental Toxicology*, vol. 34, 2018.

[62] S. Khalid, N. Afzal, J. A. Khan et al., "Antioxidant resveratrol protects against copper oxide nanoparticle toxicity in vivo," *Naunyn-Schmiedeberg's Archives of Pharmacology*, vol. 391, no. 10, pp. 1053–1062, 2018.

[63] J. Jiang, J. Pi, and J. Cai, "The advancing of zinc oxide nanoparticles for biomedical applications," *Bioinorganic Chemistry and Applications*, vol. 2018, Article ID 1062562, 18 pages, 2018.

[64] M. Pandurangan and D. H. Kim, "In vitro toxicity of zinc oxide nanoparticles: a review," *Journal of Nanoparticle Research*, vol. 17, no. 3, 2015.

[65] X. Yang, H. Shao, W. Liu et al., "Endoplasmic reticulum stress and oxidative stress are involved in ZnO nanoparticle-induced hepatotoxicity," *Toxicology Letters*, vol. 234, no. 1, pp. 40–49, 2015.

[66] M. Abdelhalim, S. Moussa, and H. Qaid, "The protective role of quercetin and arginine on gold nanoparticles induced hepatotoxicity in rats," *International Journal of Nanomedicine*, vol. 13, pp. 2821–2825, 2018.

[67] B.-H. Mao, J.-C. Tsai, C.-W. Chen, S.-J. Yan, and Y.-J. Wang, "Mechanisms of silver nanoparticle-induced toxicity and important role of autophagy," *Nanotoxicology*, vol. 10, no. 8, pp. 1021–1040, 2016.

[68] D. Ali, P. G. Yadav, S. Kumar, H. Ali, S. Alarifi, and A. H. Harrath, "Sensitivity of freshwater pulmonate snail *Lymnaea luteola* L., to silver nanoparticles," *Chemosphere*, vol. 104, pp. 134–140, 2014.

[69] B. Halliwell, "Free radicals and antioxidants - *quo vadis*?," *Trends in Pharmacological Sciences*, vol. 32, no. 3, pp. 125–130, 2011.

[70] J. S. K. Stankovic, D. Selakovic, V. Mihailovic, and G. Rosic, "Antioxidant supplementation in the treatment of neurotoxicity induced by platinum-based chemotherapeutics—a review," *International Journal of Molecular Sciences*, vol. 21, no. 20, 2020.

[71] I. Mirończuk-Chodakowska, A. M. Witkowska, and M. E. Zujko, "Endogenous non-enzymatic antioxidants in the human body," *Advances in Medical Sciences*, vol. 63, no. 1, pp. 68–78, 2018.

[72] M. Carocho, P. Morales, and I. C. F. R. Ferreira, "Antioxidants: reviewing the chemistry, food applications, legislation and role as preservatives," *Trends in Food Science & Technology*, vol. 71, pp. 107–120, 2018.

[73] A. M. Pisoschi, A. Pop, F. Iordache, L. Stanca, G. Predoi, and A. I. Serban, "Oxidative stress mitigation by antioxidants - An overview on their chemistry and influences on health status," *European Journal of Medicinal Chemistry*, vol. 209, p. 112891, 2021.

[74] B. Salehi, M. Martorell, J. L. Arbiser et al., "Antioxidants: positive or negative actors?," *Biomolecules*, vol. 8, no. 4, 2018.

[75] A. Bast and G. R. M. M. Haenen, "The toxicity of antioxidants and their metabolites," *Environmental Toxicology and Pharmacology*, vol. 11, no. 3-4, pp. 251–258, 2002.

[76] A. Baschieri and R. Amorati, "Methods to determine chain-breaking antioxidant activity of nanomaterials beyond DPPH•. A review," *Antioxidants*, vol. 10, no. 10, p. 1551, 2021.

[77] T. Wang, Q. Fan, J. Hong et al., "Therapeutic nanoparticles from grape seed for modulating oxidative stress," *Small*, no. - article 2102485, 2021.

[78] L. Valgimigli, A. Baschieri, and R. Amorati, "Antioxidant activity of nanomaterials," *Journal of Materials Chemistry B*, vol. 6, no. 14, pp. 2036–2051, 2018.

[79] I. Khalil, W. A. Yehye, A. E. Etxeberria et al., "Nanoantioxidants: recent trends in antioxidant delivery applications," *Antioxidants*, vol. 9, no. 1, p. 24, 2020.

[80] M. R. Wani and G. G. H. A. Shadab, "Coenzyme Q10 protects isolated human blood cells from TiO2 nanoparticles induced oxidative/antioxidative imbalance, hemolysis, cytotoxicity, DNA damage and mitochondrial impairment," *Molecular Biology Reports*, vol. 48, no. 4, pp. 3367–3377, 2021.

[81] M. S. Brewer, "Natural antioxidants: sources, compounds, mechanisms of action, and potential applications," *Comprehensive Reviews in Food Science and Food Safety*, vol. 10, no. 4, pp. 221–247, 2011.

[82] S. A. Hedayati, H. G. Farsani, S. S. Naserabad, S. H. Hoseinifar, and H. Van Doan, "Protective effect of dietary vitamin E on immunological and biochemical induction through silver nanoparticles (AgNPs) inclusion in diet and silver salt ($AgNO_3$) exposure on Zebrafish (*Danio rerio*)," *Comparative Biochemistry and Physiology - Part C*, vol. 222, pp. 100–107, 2019.

[83] N. T. Zaki, M. M. A. Al, R. M. Amin, and A. M. Halawa, "The possible protective role of vitamin e on the induced silver nanoparticles toxicity on filiform and circumvallate tongue papillae of albino rats histological and immunohistochemical study," *Journal of Chemical Health Risks*, vol. 11, no. 1, pp. 63–74, 2020.

[84] A. Alkaladi, "Vitamins E and C ameliorate the oxidative stresses induced by zinc oxide nanoparticles on liver and gills of _Oreochromis niloticus_," *Saudi Journal of Biological Sciences*, vol. 26, no. 2, pp. 357–362, 2019.

[85] S. Khanvirdiloo, N. Ziamajidi, A. Moradi et al., "Effects of vitamins A and E on TiO2 nanoparticles-induced spermatogenesis defects in male Wistar rats," *Iranian Journal of Science and Technology, Transactions A*, vol. 45, no. 4, pp. 1191–1200, 2021.

[86] M. Afshari-Kaveh, R. Abbasalipourkabir, A. Nourian, and N. Ziamajidi, "The protective effects of vitamins A and E on titanium dioxide nanoparticles (nTiO2)-induced oxidative stress in the spleen tissues of male Wistar rats," *Biological Trace Element Research*, vol. 199, no. 10, pp. 3677–3687, 2021.

[87] M. F. Holick, "Vitamin D status: measurement, interpretation, and clinical application," *Annals of Epidemiology*, vol. 19, no. 2, pp. 73–78, 2009.

[88] A. A. Hafez, P. Naserzadeh, K. Ashtari, A. M. Mortazavian, and A. Salimi, "Protection of manganese oxide nanoparticles-induced liver and kidney damage by vitamin D," *Regulatory Toxicology and Pharmacology*, vol. 98, pp. 240–244, 2018.

[89] A. Bendich, L. J. Machlin, O. Scandurra, G. W. Burton, and D. D. M. Wayner, "The antioxidant role of vitamin C," *Advances in Free Radical Biology & Medicine*, vol. 2, no. 2, pp. 419–444, 1986.

[90] P. Rajendran, N. Nandakumar, T. Rengarajan et al., "Antioxidants and human diseases," *Clinica Chimica Acta*, vol. 436, pp. 332–347, 2014.

[91] H. Fukui, H. Iwahashi, K. Nishio, Y. Hagihara, Y. Yoshida, and M. Horie, "Ascorbic acid prevents zinc oxide nanoparticle–induced intracellular oxidative stress and inflammatory responses," *Toxicology and Industrial Health*, vol. 33, no. 9, pp. 687–695, 2017.

[92] S. Hajirezaee, G. Mohammadi, and S. S. Naserabad, "The protective effects of vitamin C on common carp (*Cyprinus carpio*) exposed to titanium oxide nanoparticles (TiO_2-NPs)," *Aquaculture*, vol. 518, article 734734, 2020.

[93] L. Kong, W. Hu, C. Lu, K. Cheng, and M. Tang, "Mechanisms underlying nickel nanoparticle induced reproductive toxicity and chemo-protective effects of vitamin C in male rats," *Chemosphere*, vol. 218, pp. 259–265, 2019.

[94] U. Tinggi, "Selenium: its role as antioxidant in human health," *Environmental Health and Preventive Medicine*, vol. 13, no. 2, pp. 102–108, 2008.

[95] S. Ansar, M. Abudawood, S. S. Hamed, and M. M. Aleem, "Sodium selenite protects against silver nanoparticle-induced testicular toxicity and inflammation," *Biological Trace Element Research*, vol. 175, no. 1, pp. 161–168, 2017.

[96] R. Vukovic, I. Kumburovic, J. Joksimovic Jovic et al., "N-acetylcysteine protects against the anxiogenic response to cisplatin in rats," *Biomolecules*, vol. 9, no. 12, 2019.

[97] A. M. B. Elnagar, A. Ibrahim, and A. M. Soliman, "Histopathological effects of titanium dioxide nanoparticles and the possible protective role of N-acetylcysteine on the testes of male albino rats," *International Journal of Fertility and Sterility*, vol. 12, no. 3, pp. 249–256, 2018.

[98] Y. Liu, H. Yang, M. Wang, W. Wang, F. Liu, and H. Yang, "N-acetylcysteine attenuates cobalt nanoparticle-induced cytotoxic effects through inhibition of cell death, reactive oxygen species-related signaling and cytokines expression," *Orthopaedic Surgery*, vol. 8, no. 4, pp. 496–502, 2016.

[99] B. Salehi, Y. Berkay Yılmaz, G. Antika et al., "Insights on the Use of α-Lipoic Acid for Therapeutic Purposes," *Biomolecules*, vol. 9, no. 8, p. 356, 2019.

[100] A. Sun, D. Qian, Z. Wang et al., "Protective effect of lipoic acid modification on brain dysfunctions of mice induced by mesoporous silica nanoparticles," *Chemical Engineering Journal*, vol. 415, article 128957, 2021.

[101] M. A. K. Abdelhalim, H. A. Y. Qaid, Y. H. Al-Mohy, and M. M. Ghannam, "The protective roles of vitamin E and α-lipoic acid against nephrotoxicity, lipid peroxidation, and inflammatory damage induced by gold Nanoparticles," *International Journal of Nanomedicine*, vol. 15, pp. 729–734, 2020.

[102] A. P. A. de Carvalho and C. A. Conte-Junior, "Health benefits of phytochemicals from Brazilian native foods and plants: antioxidant, antimicrobial, anti-cancer, and risk factors of metabolic/endocrine disorders control," *Trends in Food Science & Technology*, vol. 111, pp. 534–548, 2021.

[103] N. Pap, M. Fidelis, L. Azevedo et al., "Berry polyphenols and human health: evidence of antioxidant, anti- inflammatory, microbiota modulation, and cell-protecting effects," *Current Opinion in Food Science*, vol. 42, pp. 167–186, 2021.

[104] V. P. Vineetha, P. Devika, K. Prasitha, and T. V. Anilkumar, "Tinospora cordifolia ameliorated titanium dioxide nanoparticle-induced toxicity via regulating oxidative stress-activated MAPK and NRF2/Keap1 signaling pathways in Nile tilapia (Oreochromis niloticus)," *Comparative Biochemistry and Physiology Part C: Toxicology & Pharmacology*, vol. 240, article 108908, 2021.

[105] I. Grissa, L. Ezzi, S. Chakroun et al., "Rosmarinus officinalis L. ameliorates titanium dioxide nanoparticles and induced some toxic effects in rats' blood," *Environmental Science and Pollution Research*, vol. 24, no. 13, pp. 12474–12483, 2017.

[106] E. T. Mohammed and G. M. Safwat, "Grape seed proanthocyanidin extract mitigates titanium dioxide nanoparticle (TiO2-NPs)–induced hepatotoxicity through TLR-4/NF-κB signaling pathway," *Biological Trace Element Research*, vol. 196, no. 2, pp. 579–589, 2020.

[107] M. Shakeel, F. Jabeen, R. Iqbal et al., "Assessment of titanium dioxide nanoparticles (TiO2-NPs) induced hepatotoxicity and ameliorative effects of Cinnamomum cassia in Sprague-Dawley rats," *Biological Trace Element Research*, vol. 182, no. 1, pp. 57–69, 2018.

[108] A. S. Salman, T. M. Al-Shaikh, Z. K. Hamza et al., "Matlodextrin-cinnamon essential oil nanoformulation as a potent protective against titanium nanoparticles-induced oxidative stress, genotoxicity, and reproductive disturbances in male mice," *Environmental Science and Pollution Research*, vol. 28, no. 29, pp. 39035–39051, 2021.

[109] K. H. Abdou, W. A. Moselhy, H. M. Mohamed, E. S. El-Nahass, and A. G. Khalifa, "Moringa oleifera leaves extract protects titanium dioxide nanoparticles-induced nephrotoxicity via Nrf2/HO-1 signaling and amelioration of oxidative stress," *Biological Trace Element Research*, vol. 187, no. 1, pp. 181–191, 2019.

[110] M. A. Kandeil, E. T. Mohammed, K. S. Hashem, L. Aleya, and M. M. Abdel-Daim, "Moringa seed extract alleviates titanium oxide nanoparticles (TiO2-NPs)-induced cerebral oxidative damage, and increases cerebral mitochondrial viability," *Environmental Science and Pollution Research*, vol. 27, no. 16, pp. 19169–19184, 2020.

[111] A. A. El-Nekeety, M. E. Hassan, R. R. Hassan et al.Nanoencapsulation of basil essential oil alleviates the oxidative stress, genotoxicity and DNA damage in rats exposed to biosynthesized iron nanoparticles," *Heliyon*, vol. 7, no. 7, article 07537, 2021.

[112] B. Alotaibi, T. A. El-Masry, E. Tousson, S. J. Alarfaj, and A. Saleh, "Therapeutic effect of rocket seeds (*Eruca sativa* L.) against hydroxyapatite nanoparticles injection induced cardiac toxicity in rats," *Pakistan Journal of Pharmaceutical Sciences*, vol. 33, no. 4, pp. 1839–1845, 2020.

[113] A. Barakat, "Ameliorating role of Foeniculum vulgare (fennel) and Pimpinella anisum (anise) against zinc oxide nanoparticles induced hepatotoxicity in male albino rats," *Journal of Bioscience and Applied Research*, vol. 5, no. 3, pp. 262–277, 2019.

[114] A. Hudecová, B. Kusznierewicz, K. Hašplová et al., "*Gentiana asclepiadea* exerts antioxidant activity and enhances DNA

repair of hydrogen peroxide- and silver nanoparticles-induced DNA damage," *Food and Chemical Toxicology*, vol. 50, no. 9, pp. 3352–3359, 2012.

[115] A. Hudecová, B. Kusznierewicz, E. Rundén-Pran et al., "Silver nanoparticles induce premutagenic DNA oxidation that can be prevented by phytochemicals from Gentiana asclepiadea," *Mutagenesis*, vol. 27, no. 6, pp. 759–769, 2012.

[116] E. M. Abd el-Maksoud, M. A. Lebda, A. E. Hashem, N. M. Taha, and M. A. Kamel, "Ginkgo biloba mitigates silver nanoparticles-induced hepatotoxicity in Wistar rats via improvement of mitochondrial biogenesis and antioxidant status," *Environmental Science and Pollution Research*, vol. 26, no. 25, pp. 25844–25854, 2019.

[117] M. A. Lebda, K. M. Sadek, H. G. Tohamy et al., "Potential role of *α*-lipoic acid and *Ginkgo biloba* against silver nanoparticles-induced neuronal apoptosis and blood-brain barrier impairments in rats," *Life Sciences*, vol. 212, pp. 251–260, 2018.

[118] R. El-Sayed, F. El-Demerdash, and M. El-Magd, "Ginseng ameliorates pulmonary toxicity induced by silicon dioxide nanoparticles in rats," *Asian Pacific Journal of Tropical Biomedicine*, vol. 11, no. 6, pp. 254–262, 2021.

[119] K. Mohamed, K. Zine, K. Fahima, E. Abdelfattah, S. M. Sharifudin, and K. Duduku, "NiO nanoparticles induce cytotoxicity mediated through ROS generation and impairing the antioxidant defense in the human lung epithelial cells (A549): Preventive effect of *Pistacia lentiscus* essential oil," *Toxicology Reports*, vol. 5, pp. 480–488, 2018.

[120] H. S. Hamed and M. Abdel-Tawwab, "Dietary pomegranate (*Punica granatum*) peel mitigated the adverse effects of silver nanoparticles on the performance, haemato-biochemical, antioxidant, and immune responses of Nile tilapia fingerlings," *Aquaculture*, vol. 540, article 736742, 2021.

[121] E. I. Hassanen, M. A. Ibrahim, A. M. Hassan, S. Mehanna, S. H. Aljuaydi, and M. Y. Issa, "Neuropathological and cognitive effects induced by CuO-NPs in rats and trials for prevention using pomegranate juice," *Neurochemical Research*, vol. 46, no. 5, pp. 1264–1279, 2021.

[122] E. I. Hassanen, A. F. Tohamy, M. Y. Issa, M. A. Ibrahim, K. Y. Farroh, and A. M. Hassan, "Pomegranate juice diminishes the mitochondria-dependent cell death and Nf-kB signaling pathway induced by copper oxide nanoparticles on liver and kidneys of Rats," *International Journal of Nanomedicine*, vol. 14, pp. 8905–8922, 2019.

[123] A. A. Sallam, M. M. Ahmed, A. H. Abou Hadeed, and M. F. Abou el-Fotoh, "The protective effect of pomegranate juice in silver nanoparticles induced hepatotoxicity in mature male albino mice," *Zagazig Veterinary Journal*, vol. 45, pp. 289–295, 2017.

[124] H. R. Attaran, F. Fatemi, A. Rasooli et al., "Zataria multiflora essential oil prevent iron oxide nanoparticles-induced liver toxicity in rat model," *Journal of Medicinal plants and By-product*, vol. 1, pp. 15–24, 2018.

[125] H. Hamdi and M. M. Hassan, "Maternal and developmental toxicity induced by nanoalumina administration in albino rats and the potential preventive role of the pumpkin seed oil," *Saudi Journal of Biological Sciences*, vol. 28, no. 8, pp. 4778–4785, 2021.

[126] A. A. M. Ali, A. B. Mansour, and S. A. Attia, "The potential protective role of apigenin against oxidative damage induced by nickel oxide nanoparticles in liver and kidney of male Wistar rat, Rattus norvegicus," *Environmental Science and Pollution Research*, vol. 28, no. 22, pp. 27577–27592, 2021.

[127] T. Wang, Z. Zhang, M. Xie, S. Li, J. Zhang, and J. Zhou, "Apigenin Attenuates Mesoporous Silica Nanoparticles-Induced Nephrotoxicity by Activating FOXO3a," *Biological Trace Element Research*, 2021.

[128] R. H. Abdel-kareem and A. M. Domouky, "Role of *B*-carotene against toxic effect of titanium dioxide nanoparticles on cerebral cortex of adult albino rat: histological and biochemical approach," *Egyptian Journal of Histology*, vol. 43, no. 2, pp. 441–454, 2019.

[129] K. Niska, M. J. Santos-Martinez, M. W. Radomski, and I. Inkielewicz-Stepniak, "CuO nanoparticles induce apoptosis by impairing the antioxidant defense and detoxification systems in the mouse hippocampal HT22 cell line: protective effect of crocetin," *Toxicology In Vitro*, vol. 29, no. 4, pp. 663–671, 2015.

[130] M. A. Siddiqui, M. Ahamed, J. Ahmad et al., "Nickel oxide nanoparticles induce cytotoxicity, oxidative stress and apoptosis in cultured human cells that is abrogated by the dietary antioxidant curcumin," *Food and Chemical Toxicology*, vol. 50, no. 3-4, pp. 641–647, 2012.

[131] M. Sonane, N. Moin, and A. Satish, "The role of antioxidants in attenuation of *Caenorhabditis elegans* lethality on exposure to TiO_2 and ZnO nanoparticles," *Chemosphere*, vol. 187, pp. 240–247, 2017.

[132] J. H. Ryu and D. Kang, "Physicochemical properties, biological activity, health benefits, and general limitations of aged black garlic: a review," *Molecules*, vol. 22, no. 6, p. 919, 2017.

[133] I. F. Mosa, H. H. Abd, A. Abuzreda, A. B. Yousif, and N. Assaf, "Chitosan and curcumin nanoformulations against potential cardiac risks associated with hydroxyapatite nanoparticles in Wistar male rats," *International Journal of Biomaterials*, vol. 2021, Article ID 3394348, 19 pages, 2021.

[134] M. R. Wani, N. Maheshwari, and G. Shadab, "Eugenol attenuates TiO_2 nanoparticles-induced oxidative damage, biochemical toxicity and DNA damage in Wistar rats: an In Vivo study," *Environmental Science and Pollution Research*, vol. 28, no. 18, pp. 22664–22678, 2021.

[135] Y. Gu, Y. Wang, Q. Zhou et al., "Inhibition of nickel nanoparticles-induced toxicity by epigallocatechin-3-gallate in JB6 cells may be through down-regulation of the MAPK signaling pathways," *PLoS One*, vol. 11, no. 3, article e0150954, 2016.

[136] M. Farokhcheh, L. Hejazian, Z. Akbarnejad et al., "Geraniol improved memory impairment and neurotoxicity induced by zinc oxide nanoparticles in male wistar rats through its antioxidant effect," *Life Sciences*, vol. 282, article 119823, 2021.

[137] M. Orazizadeh, F. Fakhredini, E. Mansouri, and L. Khorsandi, "Effect of glycyrrhizic acid on titanium dioxide nanoparticles-induced hepatotoxicity in rats," *Chemico-Biological Interactions*, vol. 220, pp. 214–221, 2014.

[138] S. Ansar, M. Abudawood, A. S. A. Alaraj, and S. S. Hamed, "Hesperidin alleviates zinc oxide nanoparticle induced hepatotoxicity and oxidative stress," *BMC Pharmacology and Toxicology*, vol. 19, no. 1, pp. 1–6, 2018.

[139] X. Meng, L. Li, H. An et al., "Lycopene Alleviates Titanium Dioxide Nanoparticle-Induced Testicular Toxicity by Inhibiting Oxidative Stress and Apoptosis in Mice," *Biological Trace Element Research*, 2021.

[140] M. M. Abdel-Daim, I. A. M. Eissa, A. Abdeen et al., "Lycopene and resveratrol ameliorate zinc oxide nanoparticles-induced oxidative stress in Nile tilapia, *Oreochromis niloticus*," *Environmental Toxicology and Pharmacology*, vol. 69, pp. 44–50, 2019.

[141] M. M. A. Hussein, E. Gad, M. M. Ahmed et al., "Amelioration of titanium dioxide nanoparticle reprotoxicity by the antioxidants morin and rutin," *Environmental Science and Pollution Research*, vol. 26, no. 28, pp. 29074–29084, 2019.

[142] R. J. Chen, C. C. Huang, R. Pranata et al., "Modulation of innate immune toxicity by silver nanoparticle exposure and the preventive effects of pterostilbene," *International Journal of Molecular Sciences*, vol. 22, no. 5, 2021.

[143] A. A. Solaiman, I. Nabil, H. S. Ramadan, and A. A. Eid, "Histologic study of the possible protective effect of resveratrol versus resveratrol-loaded niosomes against titanium dioxide nanoparticles-induced toxicity on adult rat seminiferous tubules," *Egyptian Journal of Histology*, vol. 43, no. 4, pp. 1143–1161, 2020.

[144] R. Giordo, G. K. Nasrallah, O. Al-Jamal, P. Paliogiannis, and G. Pintus, "Resveratrol inhibits oxidative stress and prevents mitochondrial damage induced by zinc oxide nanoparticles in zebrafish (Danio rerio)," *International Journal of Molecular Sciences*, vol. 21, no. 11, p. 3838, 2020.

[145] S. Veisi, S. A. Johari, C. R. Tyler, B. Mansouri, and M. Esmaeilbeigi, "Antioxidant properties of dietary supplements of free and nanoencapsulated silymarin and their ameliorative effects on silver nanoparticles induced oxidative stress in Nile tilapia (Oreochromis niloticus)," *Environmental Science and Pollution Research*, vol. 28, no. 20, pp. 26055–26063, 2021.

[146] M. J. Akhtar, M. Ahamed, M. Fareed, S. A. Alrokayan, and S. Kumar, "Protective effect of sulphoraphane against oxidative stress mediated toxicity induced by CuO nanoparticles in mouse embryonic fibroblasts BALB 3T3," *The Journal of Toxicological Sciences*, vol. 37, no. 1, pp. 139–148, 2012.

[147] I. F. Mosa, M. Youssef, T. Shalaby, and O. F. Mosa, "The protective role of tannic acid against possible hepatonephrotoxicity induced by silver nanoparticles on male rats," *Sanamed*, vol. 14, no. 2, pp. 131–145, 2019.

[148] A. Jafari, Y. Rasmi, M. Hajaghazadeh, and M. Karimipour, "Hepatoprotective effect of thymol against subchronic toxicity of titanium dioxide nanoparticles: biochemical and histological evidences," *Environmental Toxicology and Pharmacology*, vol. 58, pp. 29–36, 2018.

[149] M. A. K. Abdelhalim, S. A. A. Moussa, H. A. Y. Qaid, and M. al-Ayed, "Potential effects of different natural antioxidants on inflammatory damage and oxidative-mediated hepatotoxicity induced by gold nanoparticles," *International Journal of Nanomedicine*, vol. 13, pp. 7931–7938, 2018.

[150] S. A. Abdelazeim, N. I. Shehata, H. F. Aly, and S. G. E. Shams, "Amelioration of oxidative stress-mediated apoptosis in copper oxide nanoparticles-induced liver injury in rats by potent antioxidants," *Scientific Repprts*, vol. 10, no. 1, pp. 1–14, 2020.

[151] A. Arafa, H. Ghanem, M. Soliman, and E. EL-Meligy, "Modulation effects of quercetin against copper oxide nanoparticles-induced liver toxicity in rats," *Egyptian Pharmaceutical Journal*, vol. 16, no. 2, p. 78, 2017.

[152] L. M. Fadda, H. Hagar, A. M. Mohamed, and H. M. Ali, "Quercetin and idebenone ameliorate oxidative stress, inflammation, DNA damage, and apoptosis induced by titanium dioxide nanoparticles in rat liver," *Dose-Response*, vol. 16, no. 4, 2018.

[153] H. Alidadi, L. Khorsandi, and M. Shirani, "Effects of quercetin on tubular cell apoptosis and kidney damage in rats induced by titanium dioxide nanoparticles," *Malaysian Journal of Medical Sciences*, vol. 25, no. 2, pp. 72–81, 2018.

[154] L. Khorsandi, M. Orazizadeh, N. Moradi-Gharibvand, M. Hemadi, and E. Mansouri, "Beneficial effects of quercetin on titanium dioxide nanoparticles induced spermatogenesis defects in mice," *Environmental Science and Pollution Research*, vol. 24, no. 6, pp. 5595–5606, 2017.

[155] M. M. Lotfy, I. A. Ibrahim, S. Y. Saleh, M. A. Elbeltagy, and H. A. Ali, "Protective role of qurecitin against zinc oxide nanoparticles induced hepatotoxicity," *Biochemistry Letters*, vol. 12, no. 1, pp. 30–39, 2017.

[156] Y. Kong, B. A. Paray, M. K. al-Sadoon, and M. Fahad Albeshr, "Novel green synthesis, chemical characterization, toxicity, colorectal carcinoma, antioxidant, anti-diabetic, and anticholinergic properties of silver nanoparticles: a chemopharmacological study," *Arabian Journal of Chemistry*, vol. 14, no. 6, article 103193, 2021.

[157] M. Z. M. Salem, M. EL-Hefny, H. M. Ali et al., "Plants-derived bioactives: novel utilization as antimicrobial, antioxidant and phytoreducing agents for the biosynthesis of metallic nanoparticles," *Microbial Pathogenesis*, vol. 158, pp. 105107–105125, 2021.

[158] I. U. H. Bhat and R. Bhat, "Quercetin: A bioactive compound imparting cardiovascular and neuroprotective benefits: scope for exploring fresh produce, their wastes, and by-products," *Biology*, vol. 10, no. 7, 2021.

Hindawi
Oxidative Medicine and Cellular Longevity
Volume 2021, Article ID 2990326, 20 pages
https://doi.org/10.1155/2021/2990326

Review Article

Combining Nanotechnology and Gas Plasma as an Emerging Platform for Cancer Therapy: Mechanism and Therapeutic Implication

Milad Rasouli,[1,2] **Nadia Fallah**,[3] **and Sander Bekeschus**[4]

[1]*Plasma Medicine Group, Endocrinology and Metabolism Research Center, Endocrinology and Metabolism Clinical Sciences Institute, Tehran University of Medical Sciences, Jalale-Al-Ahmad Ave, 1411713137 Tehran, Iran*
[2]*Department of Physics and Institute for Plasma Research, Kharazmi University, 49 Dr. Mofatteh Ave, Tehran 15614, Iran*
[3]*Department of Cell and Molecular Biology, Faculty of Biological Sciences, Kharazmi University, 49 Dr. Mofatteh Ave, 31979-37551 Tehran, Iran*
[4]*ZIK Plasmatis, Leibniz Institute for Plasma Science and Technology (INP), Felix-Hausdorff-Str. 2, 17489 Greifswald, Germany*

Correspondence should be addressed to Sander Bekeschus; sander.bekeschus@inp-greifswald.de

Received 29 July 2021; Revised 28 September 2021; Accepted 30 September 2021; Published 27 October 2021

Academic Editor: Dragica Selakovic

Nanomedicine and plasma medicine are innovative and multidisciplinary research fields aiming to employ nanotechnology and gas plasma to improve health-related treatments. Especially cancer treatment has been in the focus of both approaches because clinical response rates with traditional methods that remain improvable for many types of tumor entities. Here, we discuss the recent progress of nanotechnology and gas plasma independently as well as in the concomitant modality of nanoplasma as multimodal platforms with unique capabilities for addressing various therapeutic issues in oncological research. The main features, delivery vehicles, and nexus between reactivity and therapeutic outcomes of nanoparticles and the processes, efficacy, and mechanisms of gas plasma are examined. Especially that the unique feature of gas plasma technology, the local and temporally controlled deposition of a plethora of reactive oxygen, and nitrogen species released simultaneously might be a suitable additive treatment to the use of systemic nanotechnology therapy approaches. Finally, we focus on the convergence of plasma and nanotechnology to provide a suitable strategy that may lead to the required therapeutic outcomes.

1. Introduction

Albeit progress continues, cancer remains a devastating disease in millions of patients worldwide. In 2020, over 19 million new cancer cases are projected to occur globally [1]. The standard treatments for cancer therapy include radiotherapy, chemotherapy, surgery, and immunotherapy. These therapeutic strategies yield inadequate therapeutic efficacy in some patients or have unfavorable safety profiles [2]. Another challenge of current treatment methods is the therapy resistance related to tumor cells' intrinsic or acquired exit strategies to circumvent cytotoxic therapy effects [3]. For instance, tumors consistently comprise a mixture of drug-sensitive cells and stem cells, which leads to adaption and drug resistance [4]. Hence, efforts have been dedicated to exploiting multimodal, flexible, and multifunctional therapeutic modalities. In combination with main treatment strategies, nanomedicine helps overcome numerous oncotherapy obstacles and might reduce side effects for enhancing treatment tolerability of conventional treatment [5].

Nanotechnology refers to different designs of matter in nanoscale. This technology has emerged as a multidisciplinary scientific field, including physics, chemistry, engineering, and biology. In recent years, nanotechnology has gained much attention, especially in medicine, known as nanomedicine [6]. Nanoparticles (NPs) are utilized to treat, diagnose, image, and prevent disease spread in cancer. Different types of NPs with several properties, such as drug delivery, have been created to complement current treatments. Organic NPs (e.g., lipid-based and polymeric NPs) and inorganic

NPs (e.g., silica NPs and quantum dots), or the combination of them, indicate an efficient oncotherapy by targeting solid tumors [7]. Improved drug solubility, stability in the bloodstream, target delivery to tumors, control released, and reduction in toxicity are the outstanding features that distinguish this strategy from other therapies. Besides, enhancement in permeability and retention is accompanied by a high accumulation of NPs in tumors compared to normal tissues [8].

Gas plasma, produced at body temperature by applying an electric field to one or a set of electrodes, represents a multimodal environment of physical and chemical factors [9]. This technology has introduced an exciting application to modern medicine, ranging from wound healing, decontamination and antiviral action, and surface modification to recently also cancer therapy [10, 11]. Plasma cancer therapy is one of the most investigated applications of this technology today by engaging multiple disciplines, including engineering, physics, biology, and medicine, to achieve a novel oncotherapeutic approach. With effective targeting of multiple cancer hallmarks, gas plasmas provide a cocktail of physicochemical agents having great potential for translational cancer medicine separately or in combinatorial use with conventional therapeutic modalities [12]. Gas plasma treatment is performed directly by bringing the target tissue in immediate contact with the plasma plume or indirectly by exposing liquids suitable for clinical practice [13]. At the level of preclinical studies, gas plasma treatment showed a selective antitumor action to some extent [14], improves combination chemotherapy [15], and inhibits metastatic spread [16]. It is understood that these actions result from the multi-ROS/RNS (reactive oxygen species/reactive nitrogen species) generation by gas plasmas [17]. Apart from this, gas plasma can be combined with conventional therapies [18] due to its adjustable and flexible properties [19]. This introduces gas plasma as a promising modality in cancer treatment, separately or in combination with conventional methods and new technologies.

In pursuit of an innovative oncotherapeutic strategy, the combination of nanoparticles and gas plasma with their main features is presented. Moreover, therapeutic outcomes, efficacy, and implication of each technology are being discussed. To advance cancer treatment modality development, the convergence of plasma and nanotechnology in oncology, especially the nexus between reactivity and therapeutic implications of these therapeutic modalities, is summarized. The future horizons with opportunities and challenges also are presented.

2. Nanotechnology as a Platform for Oncotherapy: Types of Material and Targeting Systems

Playing a significant role in the COVID-19 vaccine development [20], nanotechnology was once again introduced as a multifunctional platform in resolving healthcare-related challenges. Cancer nanomedicine, which utilized nanotechnology for combating cancer, received significant attention owing to the promising results. Here, we present the NPs used to treat cancer based on their main features. Further, with a particular focus on NPs delivery vehicles, the therapeutic implications are described in detail.

2.1. Main Features of Appropriate Nanoparticles for Cancer Treatment. By their tunable capacity for loading agents and the facilitation and accuracy in drug delivery [21], nanocarriers are proper candidates for experiments at the level of in vitro and in vivo research and clinical trials [22]. In general, the use of NPs, due to their properties in various cancers, might play an essential role in the effectiveness of treatment across biological barriers. Charge, hydrophobicity, and surface cloaking are the surface properties of NPs, and shape, size, elasticity, and porosity are their physical features. Altering these physicochemical properties is the changes the subsequent penetration and toxicity profiles of NPs [23].

The surface coating, shapes, size, and elasticity of NPs play crucial roles in their biodistribution and pharmacokinetics in clinical and preclinical experiments [24–26]. Besides, the rate of internalization is linked to the shape and size of NPs [27]. Spherical NPs are very common and gained trust during these years. However, nonspherical properties with their unique characteristics gained attention in recent years [28]. It is interesting to note that the shape of the NPs is more important for the attraction of macrophages and phagocytosis than their size [29]. Evidence suggests the deviating hydrodynamic manner of nonspheroidal NPs; so ,their circulation time in the blood is more extended than spheroid NPs [30]. The aggregation of NPs at tumors sites is regulated by their shape, too [31]. The size of NPs is directly related to their effectiveness and biological function in experiments. Further, the formation of nanocarriers and agents is affected by the NP size [32]. Regarding elasticity, soft NPs represent higher permanence in blood circulation compared to hard NPs. On the contrary, hard NPs demonstrate higher cellular uptake rates. Accordingly, soft and hard NPs, according to the type of organ, display varying distributions [33].

NPs can have a positive or negative surface charge based on different components employed during their production. The surface charge has a significant effect on the stability, encapsulation capacity, and biodistribution of NPs. For instance, a slightly negative charge causes a better accumulation of NPs in tumor tissue [34]. Surface hydrophobicity has an essential role in immune processing and phagocytosis through opsonization and quicker blood clearance. Nowadays, using PEGylation (covalent or noncovalent attachment of amalgamation of polyethylene-glycol for masking an agent to reduce antigenicity) and hiding surface charge and hydrophobicity enhances the durability of NPs in blood circulation [31, 35]. In addition to PEG, some other factors for NP coating include peptides and biological membranes for concealing NPs and giving them unique properties [36, 37]. Hence, the active targeting decrements toxic effects in nonmalignant cells and enhances cellular uptake of NP-based drugs in tumors.

NPs in drug delivery systems for oncotherapy can be coated with different organic or inorganic substances

containing, for instance, metals, polymers, carbon, lipids, and proteins. These NPs, based on their hydrophilic or hydrophobic properties, also can encapsulate different agents. For example, liposomes with their hydrophilic core are suitable for hydrophobic therapeutic compounds [38]. Concerning polymeric NPs, different types of polymers (synthetic or natural) with biocompatible and biodegradable properties are used for drug delivery. Emulsion polymerization, emulsion evaporation, emulsion diffusion, nanoprecipitation, salting-out, dialysis, and supercritical fluids are used for synthesizing polymeric NPs [39]. In recent decades, metal-based (inorganic) NPs made of gold, silver, superparamagnetic iron oxide, and quantum dots have been utilized for experimental therapy and especially tumor diagnosis [40, 41].

2.2. Nanoparticle Delivery Vehicles. NPs should have specific properties for the successful delivery of therapeutic agents to tumor tissue. First, NPs require a particular marker or antibody targeted against tumor cells to reduce side effects to nonmalignant tissues. All types of NPs, including micelles, liposomes, and polymeric NPs, can load antibodies on their surface to increase efficacy and improve clinical trials' outcomes [42]. However, leakage of blood vessels and insufficient lymphatic drainage often result in drugs not reaching tumor cells sufficiently. Hence, targeted NP therapy is a suitable strategy to prevail these obstacles in tumor cells [8]. For instance, iron oxide NPs linked to anti-CD44 monoclonal antibodies are utilized for cancer cells with the high CD44 expression [43]. Polymeric and magnetic NPs coated with anti-HER2 antibodies are used for HER2-receptor-positive cancers, especially ovarian and breast cancer [44, 45]. Transferrin-coated liposomes are used against head and neck cancer [46] and glioblastoma [47].

At the same time, the immunological dimension of cancer therapy is increasingly being recognized, as evident by the advent and success of immunotherapies in the 21st century [48–50]. Therefore, NPs have been heavily investigated in the past decade for their effects of providing and stimulating antitumor immunity in several types of cancer. Notably, the versatility of NPs lies in their tunable composition and hence target penetration and delivery, as recently summarized for macrophage update [51]. As another example, NPs were shown to perform targeted delivery of miR-200c and a CXCR-4 antagonistic peptide that led to immunogenic cancer cell death (ICD), perpetuating antitumor immunity, decreasing immunosuppression, and abrogating the expression of immune checkpoints in the tumor microenvironment [52]. Primarily gold nanoparticles are envisioned to perform a dual role as immune regulators and drug delivery into the tumor tissue [53]. NPs were recently proposed as efficient vehicles for anticancer vaccines, owing to their unique properties in targeted delivery and tissue penetration [54]. Nevertheless, care must be taken that NPs do not overstimulate immunity, leading to multiple organ failures. Along those lines, other safety aspects need to be considered, including NP reactions with proteins in the blood, nonphysiological activation of platelets leading to coagulopathies, excessive cellular damage, and hemolysis [55]. By crossing biological barriers, some NPs can cause adverse effects on various organs kidney, liver, brain, and reproductive systems. For instance, aggregation of NPs in the reproductive system by toxicity inducing impair the cells related to reproductive function. Although the exact molecular mechanisms and signaling are not clear, apoptosis, stress oxidative, and inflammation are among the response of these organs to NP toxicity [56]. AgNPs are widely used for antimicrobial properties in medicine, but this kind of NP can cause alteration in neurobehavioral and organ development in offspring after long-term exposure. AgNPs passing the blood-brain barrier (BBB) and disrupting development in the fetal brain can induce oxidative stress causing sensitivity against infection [57].

The last factor for drug delivery in oncotherapy is controlled drug release, which some of the elements used for NP generation can regulate. The purpose of the controlled release of drugs from NPs is to preserve the drug coating during the NP journey in the bloodstream and increase its toxic effect once delivered to the purpose destination in the tumor microenvironment (TME) [58]. In general, it should be noted that the optimal concentrations are achieved after an appropriate dose is applied that allows maximum tumor toxicity while retaining acceptable levels of side effects [59]. Stimuli-responsive NPs for drug release are categorized into two groups responsive to either internal and external stimuli. For example, pH, temperature, electric field, magnetic fields, and glutathione levels are used as stimuli [60–62]. Moreover, polymeric NPs can release agents by a hydrolytic or enzymatic method called degradation-controlled release. In this strategy, bonds in the backbone of NPs are being destructed for triggering drug release [63]. The solvent-controlled release, which works based on osmosis or swelling, is another method for releasing drugs from NPs. The osmosis-controlled release is suitable for NPs with semipenetrable membranes [64], while swelling-controlled release occurs in polymeric NPs with a glassy hydrophilic membrane [65]. In the latter, water can quickly enter the NPs present in, for instance, hydrogels, and there is a direct relation between the rate of water diffusion and drug release.

2.3. Therapeutic Outcomes of NPs in Oncology. One of the essential applications of NPs is their targeted delivery of agents for oncotherapy engineered according to the type of cancer and the therapeutic agents, as well as the unique properties of the nanoparticles (Table 1). Overall, the use of NPs for the treatment or diagnosis of cancer is not limited to preclinical experiments. There have been many successes in clinical trials in several cancer entities; albeit, approval for medical use still is awaited in many instances. Colorectal cancer, breast cancer, melanoma, and head and neck cancer are examples of using NPs in clinical trials [66]. Gold nanoparticles (AuNPs) induce toxicity in tumor cells, and their size is directly associated with the rate of penetrance, leading to toxicity effect by increasing ROS/RNS levels and subsequently induce oxidative stress. AuNPs are also used for imaging and probing tumor tissues. This is facilitated by free electrons of gold atoms being exposed to light, which leads to collective oscillation, also known as localized surface plasmon resonance, and subsequent light

Table 1: Selected studies using nanoparticles in oncotherapy.

Tumor entity	Particle type	Main finding	Ref.
Preclinical studies			
Lung cancer	Polyurethane NPs, superparamagnetic iron oxide NPs coated with silica layers, mesoporous silica NPs, zinc oxide NPs, triphenylphosphonium-Pluronic F127 nanomicelles, cetuximab chitosan NPs, polymeric NPs, polyethyleneimine NPs coated with bovine serum albumin	Reduction in cancer cell survival, apoptosis induction (upregulating caspase-3, caspase-9, PARP, Bax), inhibition of lung tumor growth, pausing growth of cancerous cells, decrease in tumor size, induction of DNA leakage from nuclei by ROS/RNS, inhibition of metastasis, cell cycle arrest at G2/M phase, prevention of autophagy	[180–187]
Breast cancer	Porous silicon NPs, mesoporous maghemite NPs, PCE NPs, metal-organic frameworks, polymeric NPs (NVA-AA), porphyrin-based metal-organic framework carrier	Inhibition of metastasis; prevention of tumor growth; decrement of cell viability; suppression of cancer cell proliferation; reduction in tumor size; decrease in side effects; induction of apoptosis (downregulating Bcl-2 and upregulating caspase-3, UBA52, TIAL1, and PPP1C); suppression of cell motility and invasiveness; downregulating proteins involved in vesicular trafficking	[188–193]
Ovarian cancer	Selenium NPs, poly (lactic-co-glycolic) acid NPs with inorganic molybdenum octahedral cluster, Fe_2O_3 NPs, PEGL NPs, chitosan copolymer-magnetic NPs, poly-ε-caprolactone NPs	Inhibition of cancer cell growth, cytotoxic effect on cancer cells, reduction of metastasis, decrease of cancer cell viability and cytotoxicity, increased the intracellular ROS/RNS, diminution of tumor volume	[194–199]
Colon cancer	Albumin NPs, chitosan NPs, perfluorooctylbromide- porphyrin grafted lipid NPs, biosynthesized silver NPs, superparamagnetic iron oxide coated with mesenchymal stem cell, silver and gold NPs, mesoporous silica NPs coated with folic acid chitosan-glycine complex, hydroxyapatite NPs coated with gum Arabic, PLGA NPs co-loaded with 5-fluorouracil and perfluorocarbon	Enhancement of cancer cells killing; improved antitumor efficacy; prevention of tumor growth and metastasis; decrement of tumor volume; enhancement of photodynamic effects against cancer cells (by increasing oxidative stress); induction of apoptosis (overexpression of caspase-3, caspase-9, bid, and Bax); reduction of immune system response and systemic side effects; fragmentation of DNA in cancer cells; increase in antimitotic effects	[200–207]
Glioblastoma	Silver NPs, lanthanum oxide NPs, transferrin-conjugated porous silicon NPs, high-Z metal NPs, PEI surface-functionalized mesoporous silica NPs, PLGA NPs coated with polyvinyl alcohol and Poloxamer188, magnetic iron oxide NPs loaded trimethoxysilylpropyl-ethylenediamine triacetic acid, polymerized human serum albumin NPs, PEI-PEG-magnetic iron oxide NPs	Immense antitumor effect, increase in caspase activity, increase intrinsic and extrinsic apoptosis, diminution tumor cell viability, induce DNA damage and autophagic pathways, enhancing ROS/RNS, pausing cancer cell migration, causing a rupture of the lysosomal membranes, inhibition of cancer cell proliferation, downregulation of crucial enzymes for DNA repair and replication in cancer cells, upregulation of tumor suppressors	[208–214]
Pancreatic cancer	Magnetic NPs, nitric oxide donor S-nitroso-N-acetylpenicillamine loaded liposomes, PLGA NPs, polyanhydride NPs, solid lipid NPs, porous coordination network-Fe (III) NPs	Tumor growth inhibition, efficient tumor retention, enhancement of cytotoxicity; decrease of cell proliferation, reduction in cancer metastasis and progression, overexpression of proapoptotic genes, induction of ROS/RNS, improvement of anticancer treatment efficacy	[215–220]
Bone cancer	Superparamagnetic γ-Fe_2O_3 iron oxide with SiO2-CaO shell NPs, zinc oxide NPs; Fe ions-releasing mesoporous NPs, NPs with magnetic inner core and polymeric outer shell, alendronate-poly(amidoamine) NPs, metal-organic framework NPs	Increase of cytotoxicity in cancer cells, suppression of cancer cell growth, induction of apoptosis, exhibition of anticancer action, inhibition of the formation of osteoclasts, prevention of metastasis, induction of the polarization of tumor-resident macrophages to M1 phenotype	[221–226]
Prostate cancer	Selenium NPs, PLGA-PEG NPs, superparamagnetic iron oxide NPs, human serum albumin-coated NPs of (2) Ga, lipid-polymer hybrid NPs, manganese oxide–mesoporous silica, hexagonal boron nitride NPs	High anticancer activity, induction of tumor cell death via necrosis, increase of cytotoxicity, tumor regression, cell death induction, disruption of lysosomal structure in cancer cells, attenuation of lysosomal protease activity, modulator of autophagy	[227–232]

Table 1: Continued.

Tumor entity	Particle type	Main finding	Ref.
Liver cancer	Fe_3O_4-au nanoheterostructures, hydroxycamptothecin-based polyprodrug as the inner core, amphiphilic lipid-PEG as the outer shell NPs, exonanoRNA NPs, chondroitin-modified lipid NPs, glycogen NPs, rubber-like RNA NPs, $CoFe_2O_4$@$MnFe_2O_4$ magnetic NPs, mesoporous silica NPs	Significant cytotoxicity in cancerous cells, inhibition of tumor growth, induction of apoptosis, reduction in cell proliferation, increase of antitumor efficacy, inducing the enhanced permeability and retention effect, increment the release rate of the drug, reducing systemic side effects	[233–239]
Clinical trials			
Solid tumor in advanced stage	CYT-6091 (consist of AuNPs-PEG and tumor necrosis factor-α)	Treatment was well-tolerated, and one partial response was observed among 29 patients in this phase I study	[240, 241]
Colorectal cancer	CPX-1 (liposome-encapsulated formulation of irinotecan and floxuridine)	11 out of 13 patients showed disease control while 2 patients showed partial response	[242]
Breast cancer, lung cancer, colorectal cancer	FCE28068 (anthracycline doxorubicin linked to copolymers based on N-(2-hydroxypropyl) methacrylamide)	Response in breast and lung cancer patients, no response in colorectal cancer patients	[243]
Stomach cancer	MCC-465 (PEG immunoliposome-encapsulated doxorubicin)	Acute reactions related to infusion observed, no antitumor response observed, stable disease (SD) observed in 10 of 18 patients	[244]
Adenocarcinoma of the esophagus and gastroesophageal junction	SP1049C (doxorubicin in P-glycoprotein-targeting Pluronic)	9 out of 21 patients showed partial response, and 8 patients had either a minor response or stable disease	[245]
Advanced pancreatic cancer	Rexin-G (retroviral vector expressing a cytocidal cyclin G1 construct)	No antitumor activity observed	[246]
Pancreatic cancer	NK105 (a paclitaxel-incorporating micellar nanoparticle)	Partial response observed in 1 out of 11 patients, significant myelosuppression not observed up to 80 mg/m^{-2}, pain or local toxicity in the area of the injection not observed in any patient, and 10 patients did not experience any hypersensitivity during the study	[247]
Pancreatic cancer	Lipoplatin (liposomal cisplatin) and gemcitabine	Partial response in 2/24 patients, disease stability in 14 patients, clinical benefit in 8 patients	[248]

emission. Moreover, especially smaller AuNPs transmute light to heat and, as a result, are suitable for photothermal therapy [67, 68]. Due to their simple synthesis, suitable pharmacokinetics, and low toxicity profile, gold nanoparticles have drawn significant attention in the field of cancer therapy in recent years [69, 70].

Quantum dots are known as semiconductor NPs, and their characteristics originate from their ability to scatter fluorescent light from the visible to the infrared spectrum after excitation [71]. Quantum dots can help image small tumors in their initial stage that are otherwise difficult to diagnose [72]. Moreover, to better recognize tumor cells, they can be conjugate to different types of antibodies on their surface, which helps increase their utilization in clinical trials [73]. Polymeric-based NPs generally are made from naturally degradable materials such as polysaccharides, chitosan, hyaluronic acid, alginates, dextran, protein-based polymers, collagen, gelatin, and albumin, which do not cause toxic effects in the human body but can exert antitumor effects based on their cargo [39]. As an example of polymeric NPs, hyaluronic acid can affect tumor cell proliferation and angiogenesis, while albumin NPs can penetrate the blood-brain barrier. Chitosan NPs, by their unique features, have an essential role in tumor growth inhibition and apoptosis induction [74].

Lipid-based NPs consist of natural hydrocarbons or are being derived from plants and animal material. They can also be composed of synthetic phospholipids, cholesterol for membrane bilayer, and sphingolipids. For increasing therapy efficacy, lipid-based NPs can be conjugate with polymeric residues such as PEG and PEI (polyethyleneimine). Their form is usually spherical, and by active targeting, they enhance the drug's pharmacodynamics and pharmacokinetic properties [75, 76]. Lipid-based NPs can inhibit migration and invasion of tumor cells and improve the internalization of anticancer drugs loaded on lipid-based NPs compared to free drugs [77]. Mesoporous silica NPs are another widely used type of NPs, having a high capacity for encapsulating therapeutic agents and showing adjustable drug release. They are also utilized for optical imaging, ultrasound and magnetic resonance imaging, and positron emission tomography [78]. Furthermore, the alterable pore size of mesoporous silica NPs makes them a good option for proteins transfer [79]. Besides, they can easily be decorated with

different small molecules including folate, transferrin, VEGF, IGF, EGF, C-type lectin, mannose, asialoglycoprotein, and monoclonal antibodies targeting, for instance, HER2, CD44, TLR9, and integrins as a marker to improve the detection of cancer cells [80]. Ultimately, this can lead to decreased tumor volumes owing to enhanced cellular uptake of the NPs.

The mainstay of future clinical cancer treatment is combination therapy between novel technologies and conventional strategies. Nanomedicine and gas plasma as documented oncotherapeutic modalities have great potential to potentially improve cancer treatment due to the multifunctional capacity of NPs and the multimodal nature of gas plasmas.

3. Plasma Oncology: Processes, Efficacy, and Mechanisms of Action and Challenges

Medical gas plasma technology, also known as cold physical plasma, is a partially ionized gas generated at atmospheric pressure and operated at body temperature. It is distinguished for generating a complex physicochemical flux of agents, including ions, electrons, mild thermal radiation, UV light, electric fields, and ROS/RNS [81]. The latter has been identified as unique agents to deliver the biotherapeutic effects [82]. While plasmas generate a mixture of ROS/RNS simultaneously with defined spatiotemporal profiles [83, 84], the overall deposition of these redox agents can be controlled either via the treatment time or energy in put [85]. Once close to biological targets, the ROS/RNS react with different biomolecules and partially oxidize, for instance, proteins [86], peptides [87], amino acids [88], lipids [89], and nuclei acids [90]. Accordingly, gas plasma-treated cells are potentially challenged by multiple ways, including diffusion of long-lived ROS such as hydrogen peroxide into the cytosol via aquaporins [91], lipid peroxidation [92], uptake of proteins with oxidative posttranslational modifications (PTMs) [86], and stresses through damage-associated pattern (DAMPs) being released into the microenvironment [93]. Due to the apolar nature of cell membranes, it is unlikely that the majority of species will enter the cytosol, as most ROS/RNS will find plentiful reaction partners at cellular membranes and their immediate vicinity to react with [17].

3.1. Gas Plasma Generation and Delivery Technologies. Gas plasma is generated by electric discharges and represents a partly ionized gas, where all heavy particles except electrons remain cold. The collisions between surrounding air and gas plasma-derived species bring about a physicochemical environment, which comprises the reactive agents including ROS/RNS. Depending on the different device geometries (plasma jet, dielectric barrier discharge, and plasma torch) as well as device configurations and parameters along with individual treatment procedures, different amounts of reactive compounds are being produced, leading to different intensities of the effects observed [94].

Plasma treatment is the process of transferring a set of physical and chemical agents to the target. An important consideration, and perhaps downfall, of the field of plasma medicine is the polypragmasia in the use of plasma devices. Hundreds of different plasma sources for biomedical application have been published, and most work is not necessarily building on top of previous knowledge but is instead reproduced based on methods in physics, chemistry, and cell biology. A clear scheme on optimal plasma source design considerations and technical parameters is not present. However, several sources have been developed in Germany; among them, the first true (cold) medical gas plasma devices intended for medically accredited use in dermatology centers in Europe [95]. Notwithstanding, it is understood that despite different geometries and ROS/RNS profiles, gas plasma treatment overall produces similar effects, being stimulating at low doses, treatment times, or energy input, and toxic at higher doses, treatment times, or energy input as predicted by the concept of hormesis [82].

Direct plasma treatment and gas plasma-treated solution (PTS) are two very different plasma treatment procedures. Direct treatment transfers all physical and chemical agents concomitantly on target, especially the short-lived ROS/RNS unique to the gas plasma technology. When treating a liquid, some of the species can be retained in such liquid and stored for later therapeutic use. This concept is called plasma-oxidized liquids (POL) that can be used for clinical application if using solutions certified as medical products such as sodium chloride [13]. Alternative names for the concept are plasma-treated liquids (PTL), plasma-treated solution or saline (PTS), plasma-activated medium (PAM), and plasma-activated liquid (PAL), among others [96]. POS recently has received significant attention in widespread areas, especially where direct plasma treatment has faced challenges. Several animal models have shown the versatility of POL [97–99]. Current challenges include its large bulk liquid generation, storage, sterility, and the lack of animal studies showing a benefit of such liquids over concentration-matched hydrogen peroxide solutions.

3.2. Cocktail of Physical and Chemical Factors in Gas Plasmas. ROS/RNS are produced in several stages based on plasma interaction with air, liquid, and matter and appear to play a vital role in the plasma therapy process [94]. The most important aspect of plasma differentiation, along with the diversity of physical and chemical factors and their combination, is their controlled and adjustable transfer to the biological target. Thus, depending on the input factors (e.g., discharge voltage, external electric field, target capacitance above ground, gas flow rate, and quenching gas shielding), a specific concentration of ROS/RNS is generated, which is not achievable in any other conventional cancer treatment methods [17], including photodynamic therapy. At the same time, UV and microwave emissions', positive ions, and electrons as main output parameters are highly related to the input parameters; albeit, their individual contribution to anticancer effects has not been studied so far, primarily because of the lack of ability to separate such factors from the ubiquitous ROS/RNS being generated simultaneously. For more detail regarding the nexus between the inputs and output parameters, see [100].

Apart from identifying the chemistry being critical for biomedical gas plasma effects, the short half-life of generated

ROS/RNS [101] and the low penetration depth of species in cells and tissues [102] remain a practical challenge in some applications. For example, the half-life of hydrogen peroxide, nitrite, nitrate, and ozone is on minutes to hours scale, depending on the temperature, whereas for other species such as atomic oxygen, hydroxyl, and nitric oxide, it varies between nanoseconds to seconds [103–105]. Although it has been reported that gas plasma triggers tissues effects in cm ranges, it has to be kept in mind, however, that the penetration depth of the most reactive species is about a few micrometers only, which is not enough to penetrate the tissue and seems appropriate for superficial skin lesions treatment. Notwithstanding, the signaling function of these gas plasma-derived ROS/RNS seems to transport information deep into tissues, as demonstrated using hyperspectral imaging of murine gas plasma-treated skin and wounds [106–108]. Hence, the current model is that superficial layers are being oxidized by the gas plasma-generated ROS/RNS, subsequently leading to PTMs and oxPTMs (oxidative post-translational modifications) on biomolecules, ultimately being sensed by cells and translated into differential signaling responses [109]. OxPTMs are increasingly recognized as signaling agents in, for example, neurodegenerative and cardiovascular disease [110–112]. Oxidative distress occurs at supraphysiological ROS/RNS concentrations, and cell and tissue damage may be induced directly [113]. The biological responses can then affect neighboring cells via paracrine routes via soluble factors or communication via junctional proteins to deeper layers of the tissue [107, 114].

The other physiochemical parameters of gas plasma are thought to play a minor role. UV radiation is present but relatively weak [115]. Electric fields are moderate with dielectric barrier discharges [116] and helium plasma jets [117] and weak for the clinically relevant argon plasma jet kINPen, but the fields on their own cannot recapitulate the plasma effect.

3.3. Anticancer Effects and Mechanisms of Gas Plasma Therapy. Even though significant progress has been achieved in recent years, the exact dose definition and optimization of plasma devices remain a debate due to the variety of plasma devices, different therapeutic procedures, and input factors affecting the composition of the produced plasma. Primarily, the concentration of produced ROS/RNS is considered the plasma dose, and based on that, the effect of gas plasma on cancer cells is classified in the majority of cases as programmed cell death as evident in vitro [17], in vivo [93], in ovo [118], and ex vivo in human patient samples [119].

At low doses, gas plasma exposure causes autophagy, senescence, and cell cycle arrest. Concomitant modality of gas plasma and silymarin nanoemulsion (SN) resulted in autophagy activation in human melanoma cells (G-361) [120]. Besides, it was reported that the cell viability of AMEC and HEC50 cells, relevant to endometrial cancer, was decreased through POL treatment, and this was related to the induction of autophagic cell death [121]. Furthermore, short gas plasma exposure led to a senescence phenotype in the adipose-derived stromal cells (ASC) and dermal fibroblasts [122]. Senescence induction was also found in melanoma cells following gas plasma exposure [123]. This was found to be related to calcium influx [124]. Simultaneously, several studies showed that gas plasma treatment induces cell cycle arrest. Lung adenocarcinoma (A549 cells), epidermal papilloma (308 cells), glioblastoma (U87MG cells), epidermal carcinoma (PAM212 cells), and wild-type keratinocytes are among the reported cell line that gas plasma able to induce cell cycle arrest in them, especially at G2/M and G1/S and checkpoints [15, 125, 126].

Regardless of the various affected signaling, apoptosis is the most documented type of cell death that has been evaluated following gas plasma treatment. It can be claimed that the induction of apoptosis has been shown in the majority of cancer types that have been studied yet by gas plasma and POL. For example, we recently indicated that POL with high selectivity induces intrinsic apoptosis in chemotherapy-resistant ovarian cancer cells accompanied by high expression of p53, Bax, and caspase-3 [127]. Overall, in moderate concentrations of ROS/RNS, apoptosis is induced by gas plasma exposure.

Interestingly, gas plasma can induce ICD, a type of cell death eliciting an immune response that is highly important in progress on plasma oncology [128]. To overcome the penetrating depth challenges of gas plasmas-generated ROS/RNS into tumors, inducing ICD by gas plasma is the milestone of this multidisciplinary technology to introduce gas plasma as an emerging approach to complement traditional and novel oncotherapeutic modalities such as immunotherapies. This was previously shown in a vaccination model in mice [129] and in a model of elevating protein immunogenicity in a melanoma model [86]. The immune-stimulating effects of gas plasma were very recently shown to be dramatic, showing direct evidence of abscopal effects in a syngenic breast cancer tumor model in vivo [93]. Such effects are observed at high treatment energies or long exposure times, while low energy and short treatment times were also documented to be beneficial for tissue regeneration, including proangiogenic, and wound healing effects [130].

Further, nonprogrammed cell death might occur under a high dose of ROS/RNS so that both normal and cancer cells are affected and might cause undesirable hallmark effects and tissue damage. Therefore, the concentration of ROS/RNS should be adjusted for acquiring a unique environment for oncotherapy through gas plasma. Besides the abovementioned therapeutic efficacies, selectivity towards cancer and normal cells has been described in some reports [131–133]. The selectivity mechanism has been ascribed to the chemistry of gas plasma and the fundamental difference between cancer and healthy cells. Briefly, the high ROS/RNS baseline, more abundant aquaporins in cell membranes, and the lower cholesterol content in cancer cells versus healthy counterparts form the basis of selectivity [134–137].

It is important to note that several end-stage head and neck cancer patients have benefited from clinical gas plasma treatment using the medically accredited atmospheric pressure argon plasma jet kINPen MED [138]. Tissue analysis revealed induction of apoptosis but not severe side effects [139, 140]. Based on the results and responding vs. nonresponding patients, it was hypothesized that the immune

system might have contributed to the therapeutic effects observed [141].

4. Future Horizons: Convergence of Plasma and Nanotechnology in Oncology

Although the combination of nanotechnology and gas plasma is still in preclinical settings, the results show a new strategy that in the future might be able to advance the efficacy of conventional therapies. Here, we emphasize the complementary role of plasma and nanotechnology technologies in improving each other's performance and highlight their main features that led to promising results. In addition, the nexus between reactivity and their therapeutic implications and potential challenges for translating into clinical uses are presented as the basis for a future innovative trend in cancer treatment.

4.1. How Nanotechnology and Gas Plasma Complement Each Other. Considering the multifunctional and practical properties of nanotechnology platforms and gas plasmas in addressing various cancer hallmarks, the combination or concomitant modality of these technologies arises an emerging strategy towards personalized medicine for cancer patients [142]. Albeit advances in nanomedicine are more than plasma oncotherapy, gas plasmas with promising outcomes led to the emergence of multimodal, safe, and controllable therapy for cancer treatment. While the complexity of tumor morphology on the one hand and the toxicity of some NPs on the other are the biggest challenges of nanomedicine in cancer therapy, the low penetration of gas plasma-produced ROS/RNS and the complexity of controlling and determining gas plasmas' dose are the essential troubles in plasma cancer therapy [143, 144].

The proposed synergy of gas plasma and NPs is such that in addition to improving each other's strengths, they also cover each other's limitations (Figure 1). NPs have great potential to combine locally with gas plasma-generated ROS/RNS [145]. Moreover, the combinational use of gas plasma with NPs might reduce the minimum NPs concentration required, decreasing NPs toxicity as a novel strategy. Gas plasma improves the delivery of NPs and increases ROS/RNS in the target tissue. Such mechanisms have been previously shown in gas plasma-treated murine and human skin [107, 146–148]. Moreover, one of the most promising applications of these two technologies is the combination with chemotherapy drugs [149–151]. The potential combinatory routes are numerous and include, for instance, extrinsic and intrinsic apoptosis, enhanced drug transporter activity, DNA damage, oxidative stress, mitochondrial membrane collapse, growth factor deprival, and enhanced immune cell activity. Interestingly, in dermal applications, plasma appears to facilitate the penetration of NPs into the upper layers of the skin, and one hypothesis is that this is based on the plasma-generated electric fields [152]. In particular, transdermal delivery is an exciting field for combining plasma and nanotechnology, where the plasma-derived electric field is the most crucial factor for the efficient transfer of biological materials such as proteins, NPs, dextrans, and liposomes [153–155].

Due to the peroxynitrite production, gas plasma reduces the pH of tissue fluid or tissue in a rapid and reversible process and creates the acidic conditions required for the delivery of NPs [156, 157]. Another mechanism affecting the delivery NPs is the localized variation of temperature as adjuvant treatment in preclinical studies [158]. We have recently observed that the combination of hyperthermia with gas plasma leads to encouraging results for melanoma cancer treatment (unpublished observation). Therefore, the combination of hyperthermia, gas plasma, and nanomedicine seems to lead to an innovative combination therapy by increasing membrane fluidity, reducing tissue pH, and targeted transfer. Furthermore, the electric fields generated by the plasma possibly improve the magnetic NPs' performance for cancer therapy.

4.2. Relationship between Reactivity and Therapeutic Implications of These Therapeutic Modalities. Regardless of the types of cancer, NPs, and plasma devices, the combination of NPs and gas plasmas led to encouraging results. Regarding the mechanisms and effectiveness, current research is directed to the production of ROS/RNS and increase of NPs uptake. The currently available studies on combining NPs and gas plasma treatment in vitro and in vivo are summarized in Table 2.

Glioblastoma is the most studied tumor with a combination of gas plasmas and AuNPs, and numerous studies have emphasized the efficacy of concomitant treatments of these technologies compared to each of them. Increased cancer cell death, activation of tumor suppressors, inhibition of tumor growth, reduction of migration and invasion in cancer cells, increased induction of apoptosis, increased E-cadherin in treated tissues, and decreased tumor volume have been presented as a collection of the main findings. The action mechanisms were related to the production of ROS/RNS and enhancement of the uptake of NPs [154, 159–162].

Similar results for melanoma were obtained when gas plasmas and NPs were used together. The increase of ROS/RNS resulting from the combination of different configurations of gas plasma with FAK antibody conjugated-AuNPs, silica, silver, iron oxide, cerium oxide, titanium oxide, iron-doped titanium oxide NPs, and Anti-EGFR-AuNPs leads to a significant increase of early apoptosis and secondary necrosis, reduction in G2/M levels, increase in the sub-G1 fraction, FAS externalization, caspase-8 activation, increase of selective cancer cell death, inhibition the viability of cancer cells, and reduction of growth pattern [163–167].

In addition to the antiproliferative effects and induction of cytotoxic effects, decreased metastatic gene expression and increased cellular internalization of NPs have previously been revealed, where fluorouracil-loaded PLGA NPs and gas plasmas concomitantly are utilized as novel solutions for breast cancer oncotherapy [149]. Further, combined use of iron NPs and plasma jet exposure reduces cell proliferation and induces apoptosis and DNA fragmentation in breast cancer [168].

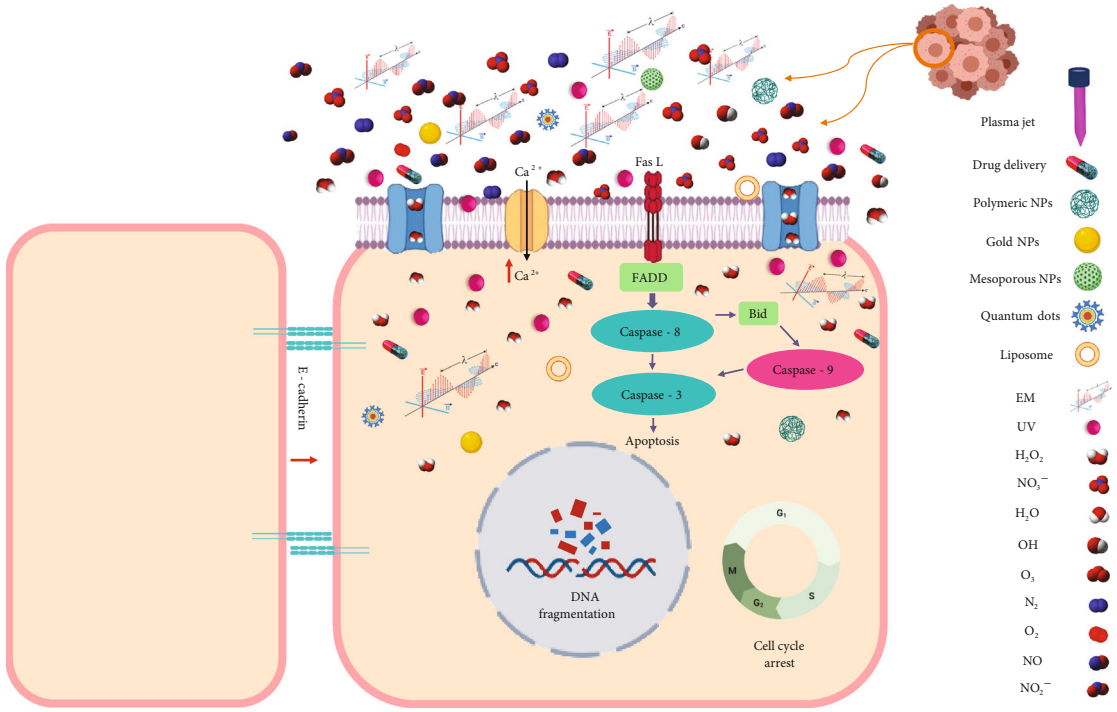

Figure 1: Combinational use of nanoparticles and gas plasma for cancer treatment, where reactive oxygen and nitrogen species along with the gas plasma-derived electromagnetic field and UV radiation affect tumor cells through the membrane. Reducing the pH acts as a complementary agent for improving nanoparticles efficacy and reducing toxicity. In addition, nanoparticles as carriers facilitate transferring gas plasma-generated reactive species to deep biological targets and may moderate the gas plasma irradiation time in highly selective ranges.

Iron oxide-based magnetic NPs and plasma jet treatment have previously been used to cause cell cycle arrest at the G0/G1 phase, apoptosis induction, condensation of nuclei, restraining tumor growth, intensive necrosis, and reduction of tumor size in lung cancer considering the high-level generation of ROS/RNS [169].

4.3. Challenges to Achieving Clinical Success and Future Needs. To avoid undesirable effects and target incurable tumors effectively, the mainstay strategy is combination therapies, which aims for cotreatments and integrating novel modalities with traditional methods. To this end, nanomedicine is combined with gas plasma as a multimodal and encouraging platform, as seen in the promising outcomes of preclinical studies. Based on these studies and the properties of gas plasma and NPs, the synergy of these two technologies can become an anticancer treatment strategy in the future. In particular, it is hoped that the synthesis of NPs with gas plasma or processing and subsequent plasma treatment will improve NPs in terms of preventing the degradation of conjugated drugs, delivery of optimum concentration and fluxes in desirable time, and improving the pharmacokinetics of the drug, which is consequently aimed to lead to enhanced cancer cell death and immunogenicity. Importantly, multifunctional and multimodal natures of NPs and gas plasma create a unique environment for cancer treatment.

Despite the increasing number of studies on cancer nanomedicine, there is a striking imbalance between preclinical and clinical applications, and the number of approved NPs, which are using for the clinical settings, is relatively limited [170]. Regarding plasma medicine, several devices have so far received accreditation as medical device class IIa in Europe [130]. However, plasma application in cancer patients has been mostly performed within exploratory studies [138, 171–175], and a guideline-based indication of plasma devices in cancer treatment is not given as of now. State-of-the-art NP synthesis methods, which can address some challenges of traditional bulk techniques, have not been considered in most clinical trials. Besides, a gap between preclinical and clinical studies indicates the need for additional clinical trials, especially given the acceptable safety profiles of some of the approaches (Table 1). As for the challenges facing plasma, since most research groups use self-made devices, the most critical issue is the lack of a specific framework for standardizing plasma devices. In addition, the multiplicity of factors involved in plasma processing and treatment causes obstacles to the definition of plasma dose. Therefore, more studies with the same treatment process and device are needed in addition to efforts to standardize and optimize these two technologies. An exciting option to combine both technologies would be to treat molecules or substances, including NPs, with gas plasma while the treated target has been modified to store the chemical energy of the short-lived plasma-derived ROS/RNS. At the delivery site in the TME, the highly reactive ROS/RNS modification can then perform the oxidative action to bring the gas plasma to the point of care via a detour.

Table 2: Studies on combining nanoparticle and gas plasma treatment in vitro and in vivo.

Particle and gas plasma type	Main finding	Tumor entity	Ref.
AuNPs and helium-based plasma jet	(i) Enhancement of the intracellular formation of superoxide andhydroxyl radical (ii) Decrease in intracellular glutathione (iii) Increase early apoptosis and secondary necrosis (iv) Caused a significant increase in the sub-G1 fraction (v) Reduction in G2/M levels (vi) FAS externalization and caspase-8 activation	Melanoma	[163]
AuNPs and plasma jet	(i) Increase of cell death (ii) Production of ROS/RNS (iii) decrease of cancer cells viability	Glioblastoma	[154]
Anti-NEU AuNPs and surface type air plasma	(i) Reduction of proliferation rate (ii) Increase of selective cancer cell death	Melanoma	[164]
PEG-coated AuNPs and surface DBD air plasma	(i) Decrease cancer cells viability (ii) Inhibiting tumor cell proliferation (iii) ROS/RNS-mediated apoptosis (iv) Activation of tumor suppressors (v) Inhibition of tumor growth (vi) Reduction of migration and invasion in cancer cells (vii) Decrease of tumor volume (viii) Increase of E-cadherin in treated tissues	Glioblastoma	[159]
AuNPs and DBD plasma	(i) Augmentation of anti-cancer cytotoxicity (ii) Increasing AuNP endocytosis and trafficking to lysosomes in cancer cells (iii) Enhancement of AuNP uptake	Glioblastoma	[160]
AuNPs and plasma jet	(i) Decrease of cell viability (ii) Improvement of NPs uptake rate into cells (iii) Increment of ROS/RNS intensity in the cancer cells	Glioblastoma	[161]
FAK antibody conjugated-AuNPs and DBD plasma	(i) Inhibition of the viability of cancer cells (ii) Induction of apoptosis (iii) Decrease of cell cycle phase in G1 (iv) Increase of the number of apoptotic cells	Melanoma	[165]
Fluorouracil loaded PLGA NPs and plasma jet	(i) Induction of cytotoxic effects (ii) Decrease of metastatic gene expression (iii) Enhancement of anti-cancer effects (iv) Exhibited anti-proliferative effects (v) Increase of cellular internalization of NPs	Breast cancer	[149]
Iron NPs and plasma jet	(i) Reduction in cell proliferation (ii) Induction apoptotic process (iii) Showed DNA fragmentation (iv) Increment of cancer cell death	Breast cancer	[168]
Epidermal growth factor conjugated AuNPs and DBD plasma	(i) Increase in cytotoxicity (ii) Enhancement of the apoptotic response	Lung cancer	[249]
Silica, silver, iron oxide, cerium oxide, titanium oxide, and iron-doped titanium oxide NPs, and plasma jet	(i) Reduction of growth pattern (ii) Increased cytotoxic effects (iii) ROS/RNS generation	Melanoma	[166]
AuNPs and plasma jet	(i) Increase of apoptotic cell death (ii) Induction of nuclear condensation and DNA fragmentation	Colorectal cancer	[250]

Table 2: Continued.

Particle and gas plasma type	Main finding	Tumor entity	Ref.
Iron oxide-based magnetic NPs and plasma jet	(i) Decrease of cell viability (ii) Indication of high levels of ROS/RNS (iii) G0/G1 Phase cell cycle arrest and condensation of nuclei (iv) Inhibitory effect on cell migration and invasion (v) Indicating intensive necrosis and apoptosis (vi) Inhibition of cancer cells proliferation (vii) Restraining tumor growth and reduction of tumor size	Lung cancer	[169]
PLGA-magnetic iron oxide NPs and plasma jet	(i) Inhibition of cancer cells proliferation (ii) Enhancement of cytotoxicity (iii) Induction of necrosis and apoptosis (iv) Increase of intracellular ROS/RNS levels	Lung cancer	[142]
Production of AuNPs by gas plasma	(i) Reduction of invasive cancer cell proliferation (ii) Induction of cancer cell apoptosis (iii) Impairment of cell migration	Breast cancer	[251]
Platinum NPs and plasma jet	(i) Decrease in the viability of cancer cells (ii) Enhancement the percentage of apoptosis cells (iii) Increment in the percentage of DNA fragmentation (iv) Decrease of cells in the G1 cell cycle phases (v) Induction of ROS/RNS production (vi) Augment of intracellular Ca^{2+} levels	Lymphoma	[252]
AuNPs and gas plasma	(i) Gas plasma-stimulated AuNP uptake (ii) Constant production of ROS/RNS (especially H_2O_2, NO_2^-, and NO_3^-) (iii) Gas plasma-induced lipid peroxidation (iv) Increase of AuNPs uptake through endocytosis	Glioblastoma	[162]
Anti-EGFR-AuNPs and air plasma	(i) Increment of death rate and proliferation (ii) Increase necrosis	Melanoma and oral cancer	[167]
PEG-AuNPs and plasma jet	(i) Production of singlet oxygen (ii) Hot electrons cause gold–PEG bond		[253]
Curcumin loaded on triphosphate chitosan NPs by plasma jet	(i) Decrease of cell viability (ii) Induction of sub-G1; arrest of G2/M (iii) Upregulation of TP53 mRNA expression as a tumor suppressor (iv) Increase in the percentage of apoptotic cells	Breast cancer	[254]

Finally, there are future challenges for NP drug discovery and development in oncology. First, standardized procedures in production for research and commercial applications will help accelerate results translated from bench to bedside [176]. Second, organo-typic 3D cultures much more resemble the clinical pathology of cancer tissues than 2D cultures while being faster and more ethical animal models, potentially allowing for screening many different types of functionalized NPs, which will eventually allow propelling the field to clinically relevant approaches at higher speeds [177, 178]. Third, novel functionalization techniques such as genetically engineered cell membranes may aid the targeted delivery of NPs' cargo [179]. Last, preclinical research would vastly benefit from adhering to standardized protocols on studying NPs and assessing their drug delivery and distribution, as proposed by the National Cancer Institute (NCI) [179].

5. Conclusions

Nanomedicine and gas plasmas have been considered appropriate options for future oncotherapy due to the

promising preliminary results. To improve nanomedicine's efficacy, combination with novel therapeutic modalities such as gas plasmas should be taken into account. Cocktail of ROS/RNS and electric fields of gas plasma and the NPs' ability to precisely targeting and penetrating tissues creates a putative oncotherapeutic platform for cancer treatment by enhancing selectivity and targeting chemotherapy resistance. Even though synergistic efficacy of NPs and gas plasmas are reported, more studies are essential to elucidate underlying mechanisms and impact on aggressive cancers.

Abbreviations

NPs: Nanoparticles
ROS: Reactive oxygen species
RNS: Reactive nitrogen species
ICD: Immunogenic cell death
TME: Tumor microenvironment
AuNPs: Gold nanoparticles
PTMs: Posttranslational modifications
PTS: Plasma-treated saline
TLR: Toll-like receptor
PEG: Polyethylenglycol
ASC: Adipose-derived stromal cells
PEI: Polyethyleneimine.

Conflicts of Interest

The authors declare no conflict of interest.

Authors' Contributions

Milad Rasouli and Nadia Fallah contributed equally to this paper as first authors.

Acknowledgments

SB has acquired and received funding from the German Federal Ministry of Education and Research (BMBF, grant number 03Z22DN11).

References

[1] H. Sung, J. Ferlay, R. L. Siegel et al., "Global cancer statistics 2020: Globocan estimates of incidence and mortality worldwide for 36 cancers in 185 countries," *CA: a Cancer Journal for Clinicians*, vol. 71, pp. 209–249, 2021.

[2] K. Fitzner, F. Oteng-Mensah, P. Donley, and E. A. F. Heckinger, "Safety of cancer therapies: at what cost?," *Population Health Management*, vol. 20, pp. 318–328, 2017.

[3] Y. Sun, "Tumor microenvironment and cancer therapy resistance," *Cancer Letters*, vol. 380, pp. 205–215, 2016.

[4] H. C. Zheng, "The molecular mechanisms of chemoresistance in cancers," *Oncotarget*, vol. 8, 2017.

[5] G. Housman, S. Byler, S. Heerboth et al., "Drug resistance in cancer: an overview," *Cancers (Basel)*, vol. 6, no. 3, pp. 1769–1792, 2014.

[6] S. E. McNeil, "Nanotechnology for the biologist," *Journal of Leukocyte Biology*, vol. 78, pp. 585–594, 2005.

[7] L. Salvioni, M. A. Rizzuto, J. A. Bertolini, L. Pandolfi, M. Colombo, and D. Prosperi, "Thirty years of cancer nanomedicine: success, frustration, and hope," *Cancers (Basel)*, vol. 11, 2019.

[8] D. Peer, J. M. Karp, S. Hong, O. C. Farokhzad, R. Margalit, and R. Langer, "Nanocarriers as an emerging platform for cancer therapy," *Nature Nanotechnology*, vol. 2, pp. 751–760, 2007.

[9] T. von Woedtke, S. Reuter, K. Masur, and K. D. Weltmann, "Plasmas for medicine," *Physics Reports*, vol. 530, pp. 291–320, 2013.

[10] D. B. Graves, "Low temperature plasma biomedicine: a tutorial review," *Physics of Plasmas*, vol. 21, 2014.

[11] S. Bekeschus, A. Kramer, E. Suffredini, T. von Woedtke, and V. Colombo, "Gas plasma technology-an asset to healthcare during viral pandemics such as the covid-19 crisis?," *IEEE Trans Radiat Plasma Med Sci*, vol. 4, pp. 391–399, 2020.

[12] X. Dai, K. Bazaka, E. W. Thompson, and K. K. Ostrikov, "Cold atmospheric plasma: a promising controller of cancer cell states," *Cancers (Basel)*, vol. 12, 2020.

[13] E. Freund and S. Bekeschus, "Gas plasma-oxidized liquids for cancer treatment: pre-clinical relevance, immuno-oncology, and clinical obstacles," *IEEE Transactions on Radiation and Plasma Medical Sciences*, pp. 1–1, 2020.

[14] S. Bekeschus, G. Liebelt, J. Menz et al., "Tumor cell metabolism correlates with resistance to gas plasma treatment: the evaluation of three dogmas," *Free Radical Biology & Medicine*, vol. 167, pp. 12–28, 2021.

[15] J. Koritzer, V. Boxhammer, A. Schafer et al., "Restoration of sensitivity in chemo-resistant glioma cells by cold atmospheric plasma," *PLoS One*, vol. 8, article e64498, 2013.

[16] S. Hasse, T. Meder, E. Freund, T. von Woedtke, and S. Bekeschus, "Plasma treatment limits human melanoma spheroid growth and metastasis independent of the ambient gas composition," *Cancers (Basel)*, vol. 12, p. 2570, 2020.

[17] A. Privat-Maldonado, A. Schmidt, A. Lin et al., "Ros from physical plasmas: redox chemistry for biomedical therapy," *Oxidative Medicine and Cellular Longevity*, vol. 2019, Article ID 9062098, 2019.

[18] G. Pasqual-Melo, R. K. Gandhirajan, I. Stoffels, and S. Bekeschus, "Targeting malignant melanoma with physical plasmas," *Clinical Plasma Medicine*, vol. 10, pp. 1–8, 2018.

[19] S. Bekeschus, A. Schmidt, F. Niessner, T. Gerling, K. D. Weltmann, and K. Wende, "Basic research in plasma medicine - a throughput approach from liquids to cells," *Journal of Visualized Experiments*, vol. e56331, 2017.

[20] A. Khurana, P. Allawadhi, I. Khurana et al., "Role of nanotechnology behind the success of mrna vaccines for covid-19," *Nano Today*, vol. 38, article 101142, 2021.

[21] S. Wilhelm, A. J. Tavares, Q. Dai et al., "Analysis of nanoparticle delivery to tumours," *Nature Reviews Materials*, vol. 1, 2016.

[22] V. Sanna and M. Sechi, "Therapeutic potential of targeted nanoparticles and perspective on nanotherapies," *ACS Medicinal Chemistry Letters*, vol. 11, pp. 1069–1073, 2020.

[23] Z. Zhao, A. Ukidve, V. Krishnan, and S. Mitragotri, "Effect of physicochemical and surface properties on in vivo fate of drug nanocarriers," *Advanced Drug Delivery Reviews*, vol. 143, pp. 3–21, 2019.

[24] J. A. Champion, Y. K. Katare, and S. Mitragotri, "Particle shape: a new design parameter for micro- and nanoscale drug

delivery carriers," *Journal of Controlled Release*, vol. 121, pp. 3–9, 2007.

[25] P. Aggarwal, J. B. Hall, C. B. McLeland, M. A. Dobrovolskaia, and S. E. McNeil, "Nanoparticle interaction with plasma proteins as it relates to particle biodistribution, biocompatibility and therapeutic efficacy," *Advanced Drug Delivery Reviews*, vol. 61, pp. 428–437, 2009.

[26] S. Mitragotri and J. Lahann, "Physical approaches to biomaterial design," *Nature Materials*, vol. 8, pp. 15–23, 2009.

[27] S. Muro, C. Garnacho, J. A. Champion et al., "Control of endothelial targeting and intracellular delivery of therapeutic enzymes by modulating the size and shape of icam-1-targeted carriers," *Molecular Therapy*, vol. 16, pp. 1450–1458, 2008.

[28] Y. Y. Khine and M. H. Stenzel, "Surface modified cellulose nanomaterials: a source of non-spherical nanoparticles for drug delivery," *Materials Horizons*, vol. 7, pp. 1727–1758, 2020.

[29] G. Sharma, D. T. Valenta, Y. Altman et al., "Polymer particle shape independently influences binding and internalization by macrophages," *Journal of Controlled Release*, vol. 147, pp. 408–412, 2010.

[30] Y. Geng, P. Dalhaimer, S. Cai et al., "Shape effects of filaments versus spherical particles in flow and drug delivery," *Nature Nanotechnology*, vol. 2, pp. 249–255, 2007.

[31] X. Duan and Y. Li, "Physicochemical characteristics of nanoparticles affect circulation, biodistribution, cellular internalization, and trafficking," *Small*, vol. 9, pp. 1521–1532, 2013.

[32] V. H. Nguyen and B. J. Lee, "Protein corona: a new approach for nanomedicine design," *International Journal of Nanomedicine*, vol. 12, pp. 3137–3151, 2017.

[33] A. C. Anselmo, M. Zhang, S. Kumar et al., "Elasticity of nanoparticles influences their blood circulation, phagocytosis, endocytosis, and targeting," *ACS Nano*, vol. 9, pp. 3169–3177, 2015.

[34] C. He, Y. Hu, L. Yin, C. Tang, and C. Yin, "Effects of particle size and surface charge on cellular uptake and biodistribution of polymeric nanoparticles," *Biomaterials*, vol. 31, pp. 3657–3666, 2010.

[35] J. V. Jokerst, T. Lobovkina, R. N. Zare, and S. S. Gambhir, "Nanoparticle pegylation for imaging and therapy," *Nanomedicine (London, England)*, vol. 6, pp. 715–728, 2011.

[36] Q. Zhang, D. Dehaini, Y. Zhang et al., "Neutrophil membrane-coated nanoparticles inhibit synovial inflammation and alleviate joint damage in inflammatory arthritis," *Nature Nanotechnology*, vol. 13, pp. 1182–1190, 2018.

[37] J. Y. Oh, H. S. Kim, L. Palanikumar et al., "Cloaking nanoparticles with protein corona shield for targeted drug delivery," *Nature Communications*, vol. 9, p. 4548, 2018.

[38] P. Y. Liyanage, S. D. Hettiarachchi, Y. Zhou et al., "Nanoparticle-mediated targeted drug delivery for breast cancer treatment," *Biochimica Et Biophysica Acta. Reviews on Cancer*, vol. 1871, pp. 419–433, 2019.

[39] P. Abasian, S. Ghanavati, S. Rahebi, S. Nouri Khorasani, and S. Khalili, "Polymeric nanocarriers in targeted drug delivery systems: a review," *Polymers for Advanced Technologies*, vol. 31, pp. 2939–2954, 2020.

[40] X. Huang, P. K. Jain, I. H. El-Sayed, and M. A. El-Sayed, "Gold nanoparticles: interesting optical properties and recent applications in cancer diagnostics and therapy," *Nanomedicine (London, England)*, vol. 2, pp. 681–693, 2007.

[41] X. Guo, Z. Wu, W. Li et al., "Appropriate size of magnetic nanoparticles for various bioapplications in cancer diagnostics and therapy," *ACS Applied Materials & Interfaces*, vol. 8, pp. 3092–3106, 2016.

[42] R. van der Meel, E. Sulheim, Y. Shi, F. Kiessling, W. J. M. Mulder, and T. Lammers, "Smart cancer nanomedicine," *Nature Nanotechnology*, vol. 14, pp. 1007–1017, 2019.

[43] A. Aires, S. M. Ocampo, B. M. Simoes et al., "Multifunctionalized iron oxide nanoparticles for selective drug delivery to cd44-positive cancer cells," *Nanotechnology*, vol. 27, article 065103, 2016.

[44] R. Dominguez-Rios, D. R. Sanchez-Ramirez, K. Ruiz-Saray et al., "Cisplatin-loaded plga nanoparticles for her2 targeted ovarian cancer therapy," *Colloids and Surfaces. B, Biointerfaces*, vol. 178, pp. 199–207, 2019.

[45] N. L. Adolphi, K. S. Butler, D. M. Lovato et al., "Imaging of her2-targeted magnetic nanoparticles for breast cancer detection: comparison of squid-detected magnetic relaxometry and mri," *Contrast Media & Molecular Imaging*, vol. 7, pp. 308–319, 2012.

[46] L. Xu, K. F. Pirollo, W. H. Tang, A. Rait, and E. H. Chang, "Transferrin-liposome-mediated systemic p53 gene therapy in combination with radiation results in regression of human head and neck cancer xenografts," *Human Gene Therapy*, vol. 10, pp. 2941–2952, 1999.

[47] L. Han, Y. Ren, L. Long et al., "Inhibition of c6 glioma in vivo by combination chemotherapy of implantation of polymer wafer and intracarotid perfusion of transferrin-decorated nanoparticles," *Oncology Reports*, vol. 27, pp. 121–128, 2012.

[48] S. A. Weiss, J. D. Wolchok, and M. Sznol, "Immunotherapy of melanoma: facts and hopes," *Clinical Cancer Research*, vol. 25, no. 17, pp. 5191–5201, 2019.

[49] K. Ganesh, Z. K. Stadler, A. Cercek et al., "Immunotherapy in colorectal cancer: rationale, challenges and potential," *Nature Reviews. Gastroenterology & Hepatology*, vol. 16, pp. 361–375, 2019.

[50] S. Y. Gun, S. W. L. Lee, J. L. Sieow, and S. C. Wong, "Targeting immune cells for cancer therapy," *Redox Biology*, vol. 25, article 101174, 2019.

[51] R. M. Pallares, P. Choo, L. E. Cole, C. A. Mirkin, A. Lee, and T. W. Odom, "Manipulating immune activation of macrophages by tuning the oligonucleotide composition of gold nanoparticles," *Bioconjugate Chemistry*, vol. 30, pp. 2032–2037, 2019.

[52] H. T. Nguyen, C. D. Phung, T. H. Tran et al., "Manipulating immune system using nanoparticles for an effective cancer treatment: combination of targeted therapy and checkpoint blockage mirna," *Journal of Controlled Release*, vol. 329, pp. 524–537, 2021.

[53] J. S. He, S. J. Liu, Y. R. Zhang et al., "The application of and strategy for gold nanoparticles in cancer immunotherapy," *Frontiers in Pharmacology*, vol. 12, article 687399, 2021.

[54] M. E. Aikins, C. Xu, and J. J. Moon, "Engineered nanoparticles for cancer vaccination and immunotherapy," *Accounts of Chemical Research*, vol. 53, pp. 2094–2105, 2020.

[55] M. A. Dobrovolskaia, M. Shurin, and A. A. Shvedova, "Current understanding of interactions between nanoparticles and the immune system," *Toxicology and Applied Pharmacology*, vol. 299, pp. 78–89, 2016.

[56] R. Wang, B. Song, J. Wu, Y. Zhang, A. Chen, and L. Shao, "Potential adverse effects of nanoparticles on the

reproductive system," *International Journal of Nanomedicine*, vol. Volume 13, pp. 8487–8506, 2018.

[57] Z. Lyu, S. Ghoshdastidar, K. R. Rekha et al., "Developmental exposure to silver nanoparticles leads to long term gut dysbiosis and neurobehavioral alterations," *Scientific Reports*, vol. 11, p. 6558, 2021.

[58] H. Mekaru, J. Lu, and F. Tamanoi, "Development of mesoporous silica-based nanoparticles with controlled release capability for cancer therapy," *Advanced Drug Delivery Reviews*, vol. 95, pp. 40–49, 2015.

[59] R. A. Siegel and M. J. Rathbone, *Overview of Controlled Release Mechanisms*, Springer, In Fundamentals and applications of controlled release drug delivery, 2012.

[60] C. W. Song, R. Griffin, and H. J. Park, *Influence of Tumor Ph on Therapeutic Response*, Springer, In Cancer drug resistance, 2006.

[61] D. C. Manatunga, R. M. de Silva, K. M. N. de Silva et al., "Ph responsive controlled release of anti-cancer hydrophobic drugs from sodium alginate and hydroxyapatite bicoated iron oxide nanoparticles," *European Journal of Pharmaceutics and Biopharmaceutics*, vol. 117, pp. 29–38, 2017.

[62] Z. Xu, S. Liu, Y. Kang, and M. Wang, "Glutathione- and ph-responsive nonporous silica prodrug nanoparticles for controlled release and cancer therapy," *Nanoscale*, vol. 7, pp. 5859–5868, 2015.

[63] H. J. Lee, S. E. Kim, I. K. Kwon et al., "Spatially mineralized self-assembled polymeric nanocarriers with enhanced robustness and controlled drug-releasing property," *Chem. Commun. (Camb.)*, vol. 46, pp. 377–379, 2010.

[64] S. Herrlich, S. Spieth, S. Messner, and R. Zengerle, "Osmotic micropumps for drug delivery," *Advanced Drug Delivery Reviews*, vol. 64, pp. 1617–1627, 2012.

[65] N. A. Peppas, P. Bures, W. Leobandung, and H. Ichikawa, "Hydrogels in pharmaceutical formulations," *European Journal of Pharmaceutics and Biopharmaceutics*, vol. 50, pp. 27–46, 2000.

[66] L. Cabeza, G. Perazzoli, C. Mesas et al., "Nanoparticles in colorectal cancer therapy: latest in vivo assays, clinical trials, and patents," *AAPS PharmSciTech*, vol. 21, p. 178, 2020.

[67] M. D'Acunto, P. Cioni, E. Gabellieri, and G. Presciuttini, "Exploiting gold nanoparticles for diagnosis and cancer treatments," *Nanotechnology*, vol. 32, article 192001, 2021.

[68] S. Siddique and J. C. L. Chow, "Gold nanoparticles for drug delivery and cancer therapy," *Applied Sciences-Basel*, vol. 10, p. 3824, 2020.

[69] B. Pang, X. Yang, and Y. Xia, "Putting gold nanocages to work for optical imaging, controlled release and cancer theranostics," *Nanomedicine (London, England)*, vol. 11, pp. 1715–1728, 2016.

[70] A. Shakeri-Zadeh, H. Zareyi, R. Sheervalilou, S. Laurent, H. Ghaznavi, and H. Samadian, "Gold nanoparticle-mediated bubbles in cancer nanotechnology," *Journal of Controlled Release*, vol. 330, pp. 49–60, 2021.

[71] L. J. Desmond, A. N. Phan, and P. Gentile, "Critical overview on the green synthesis of carbon quantum dots and their application for cancer therapy," *Environmental Science: Nano*, vol. 8, pp. 848–862, 2021.

[72] A. Alaghmandfard, O. Sedighi, N. Tabatabaei Rezaei et al., "Recent advances in the modification of carbon-based quantum dots for biomedical applications," *Materials Science & Engineering. C, Materials for Biological Applications*, vol. 120, article 111756, 2021.

[73] H. Zhang, D. Yee, and C. Wang, "Quantum dots for cancer diagnosis and therapy: biological and clinical perspectives," *Nanomedicine (London, England)*, vol. 3, pp. 83–91, 2008.

[74] K. H. Wong, A. Lu, X. Chen, and Z. Yang, "Natural ingredient-based polymeric nanoparticles for cancer treatment," *Molecules*, vol. 25, p. 3620, 2020.

[75] J. Meng, F. Q. Guo, H. Y. Xu, W. Liang, C. Wang, and X. D. Yang, "Combination therapy using co-encapsulated resveratrol and paclitaxel in liposomes for drug resistance reversal in breast cancer cells in vivo," *Scientific Reports*, vol. 6, pp. 1–11, 2016.

[76] P. Yingchoncharoen, D. S. Kalinowski, and D. R. Richardson, "Lipid-based drug delivery systems in cancer therapy: what is available and what is yet to come," *Pharmacological Reviews*, vol. 68, pp. 701–787, 2016.

[77] A. Rahiminejad, R. Dinarvand, B. Johari et al., "Preparation and investigation of indirubin-loaded sln nanoparticles and their anti-cancer effects on human glioblastoma u87mg cells," *Cell Biology International*, vol. 43, pp. 2–11, 2019.

[78] F. Dilnawaz, "Multifunctional mesoporous silica nanoparticles for cancer therapy and imaging," *Current Medicinal Chemistry*, vol. 26, pp. 5745–5763, 2019.

[79] C. Xu, C. Lei, and C. Yu, "Mesoporous silica nanoparticles for protein protection and delivery," *Frontiers in Chemistry*, vol. 7, p. 290, 2019.

[80] S. Barui and V. Cauda, "Multimodal decorations of mesoporous silica nanoparticles for improved cancer therapy," *Pharmaceutics*, vol. 12, p. 527, 2020.

[81] K. D. Weltmann and T. von Woedtke, "Plasma medicine-current state of research and medical application," *Plasma Physics and Controlled Fusion*, vol. 59, article 014031, 2017.

[82] T. von Woedtke, A. Schmidt, S. Bekeschus, K. Wende, and K. D. Weltmann, "Plasma medicine: a field of applied redox biology," *In Vivo*, vol. 33, no. 4, pp. 1011–1026, 2019.

[83] N. Y. Babaeva and M. J. Kushner, "Reactive fluxes delivered by dielectric barrier discharge filaments to slightly wounded skin," *Journal of Physics D: Applied Physics*, vol. 46, article 025401, 2013.

[84] A. Schmidt-Bleker, S. A. Norberg, J. Winter et al., "Propagation mechanisms of guided streamers in plasma jets: the influence of electronegativity of the surrounding gas," *Plasma Sources Sci. T.*, vol. 24, 2015.

[85] S. Bekeschus, A. Lin, A. Fridman, K. Wende, K.-D. Weltmann, and V. Miller, "A comparison of floating-electrode dbd and kinpen jet: plasma parameters to achieve similar growth reduction in colon cancer cells under standardized conditions," *Plasma Chemistry and Plasma Processing*, vol. 38, pp. 1–12, 2017.

[86] R. Clemen, E. Freund, D. Mrochen et al., "Gas plasma technology augments ovalbumin immunogenicity and ot-ii t cell activation conferring tumor protection in mice," *Adv Sci (Weinh)*, vol. 8, p. 2003395, 2021.

[87] S. Wenske, J. W. Lackmann, L. M. Busch, S. Bekeschus, T. von Woedtke, and K. Wende, "Reactive species driven oxidative modifications of peptides-tracing physical plasma liquid chemistry," *Journal of Applied Physics*, vol. 129, 2021.

[88] T. Heusler, G. Bruno, S. Bekeschus, J.-W. Lackmann, T. von Woedtke, and K. Wende, "Can the effect of cold physical

plasma-derived oxidants be transported via thiol group oxidation?," *Clinical Plasma Medicine*, vol. 14, 2019.

[89] J. Striesow, J. W. Lackmann, Z. Ni et al., "Oxidative modification of skin lipids by cold atmospheric plasma (cap): a standardizable approach using rp-lc/ms(2) and di-esi/ms(2)," *Chemistry and Physics of Lipids*, vol. 226, article 104786, 2020.

[90] L. Guo, Y. Zhao, D. Liu et al., "Cold atmospheric-pressure plasma induces DNA-protein crosslinks through protein oxidation," *Free Radical Research*, vol. 52, pp. 783–798, 2018.

[91] G. P. Bienert and F. Chaumont, "Aquaporin-facilitated transmembrane diffusion of hydrogen peroxide," *Biochimica et Biophysica Acta*, vol. 1840, pp. 1596–1604, 2014.

[92] C. M. Wolff, J. F. Kolb, K. D. Weltmann, T. von Woedtke, and S. Bekeschus, "Combination treatment with cold physical plasma and pulsed electric fields augments ros production and cytotoxicity in lymphoma," *Cancers (Basel)*, vol. 12, p. 845, 2020.

[93] H. Mahdikia, F. Saadati, E. Freund et al., "Gas plasma irradiation of breast cancers promotes immunogenicity, tumor reduction, and an abscopal effect in vivo," *Oncoimmunology*, vol. 10, p. 1859731, 2021.

[94] X. Lu, G. V. Naidis, M. Laroussi, S. Reuter, D. B. Graves, and K. Ostrikov, "Reactive species in non-equilibrium atmospheric-pressure plasmas: generation, transport, and biological effects," *Physics Reports-Review Section of Physics Letters*, vol. 630, pp. 1–84, 2016.

[95] S. Bekeschus, A. Schmidt, K.-D. Weltmann, and T. von Woedtke, "The plasma jet kinpen – a powerful tool for wound healing," *Clinical Plasma Medicine*, vol. 4, pp. 19–28, 2016.

[96] H. Tanaka, S. Bekeschus, D. Yan, M. Hori, M. Keidar, and M. Laroussi, "Plasma-treated solutions (pts) in cancer therapy," *Cancers (Basel)*, vol. 13, p. 1737, 2021.

[97] E. Freund, K. R. Liedtke, J. van der Linde et al., "Physical plasma-treated saline promotes an immunogenic phenotype in ct26 colon cancer cells in vitro and in vivo," *Scientific Reports*, vol. 9, p. 634, 2019.

[98] E. Freund, L. Miebach, R. Clemen et al., "Large volume spark discharge and plasma jet-technology for generating plasma-oxidized saline targeting colon cancer in vitro and in vivo," *Journal of Applied Physics*, vol. 129, 2021.

[99] S. Takeda, S. Yamada, N. Hattori et al., "Intraperitoneal administration of plasma-activated medium: proposal of a novel treatment option for peritoneal metastasis from gastric cancer," *Annals of Surgical Oncology*, vol. 24, pp. 1188–1194, 2017.

[100] L. Lin and M. Keidar, "A map of control for cold atmospheric plasma jets: from physical mechanisms to optimizations. Applied," *Physics Reviews*, vol. 8, 2021.

[101] K. Wende, T. von Woedtke, K. D. Weltmann, and S. Bekeschus, "Chemistry and biochemistry of cold physical plasma derived reactive species in liquids," *Biological Chemistry*, vol. 400, pp. 19–38, 2018.

[102] L. I. Partecke, K. Evert, J. Haugk et al., "Tissue tolerable plasma (ttp) induces apoptosis in pancreatic cancer cells in vitro and in vivo," *BMC Cancer*, vol. 12, 2012.

[103] D. B. Graves, "The emerging role of reactive oxygen and nitrogen species in redox biology and some implications for plasma applications to medicine and biology," *Journal of Physics D: Applied Physics*, vol. 45, article 263001, 2012.

[104] J. Benedikt, M. Mokhtar Hefny, A. Shaw et al., "The fate of plasma-generated oxygen atoms in aqueous solutions: non-equilibrium atmospheric pressure plasmas as an efficient source of atomic o(aq)," *Physical Chemistry Chemical Physics*, vol. 20, pp. 12037–12042, 2018.

[105] S. Mohades, N. Barekzi, H. Razavi, V. Maruthamuthu, and M. Laroussi, "Temporal evaluation of the anti-tumor efficiency of plasma-activated media," *Plasma Processes and Polymers*, vol. 13, pp. 1206–1211, 2016.

[106] A. Schmidt, G. Liebelt, F. Niessner, T. von Woedtke, and S. Bekeschus, "Gas plasma-spurred wound healing is accompanied by regulation of focal adhesion, matrix remodeling, and tissue oxygenation," *Redox Biology*, vol. 38, article 101809, 2021.

[107] A. Schmidt, G. Liebelt, J. Striesow et al., "The molecular and physiological consequences of cold plasma treatment in murine skin and its barrier function," *Free Radical Biology & Medicine*, vol. 161, pp. 32–49, 2020.

[108] A. Schmidt, F. Niesner, T. von Woedtke, and S. Bekeschus, "Hyperspectral imaging of wounds reveals augmented tissue oxygenation following cold physical plasma treatment in vivo," *IEEE Transactions on Radiation and Plasma Medical Sciences*, vol. 5, pp. 412–419, 2021.

[109] A. Schmidt, S. Dietrich, A. Steuer et al., "Non-thermal plasma activates human keratinocytes by stimulation of antioxidant and phase ii pathways," *The Journal of Biological Chemistry*, vol. 290, pp. 6731–6750, 2015.

[110] Y. M. Lee, W. He, and Y. C. Liou, "The redox language in neurodegenerative diseases: oxidative post-translational modifications by hydrogen peroxide," *Cell Death & Disease*, vol. 12, p. 58, 2021.

[111] S. I. Bibli and I. Fleming, "Oxidative post translational modifications: a focus on cysteine s-sulfhydration and the regulation of endothelial fitness," *Antioxidants & Redox Signaling*, 2021.

[112] A. Lermant and C. E. Murdoch, "Cysteine glutathionylation acts as a redox switch in endothelial cells," *Antioxidants (Basel)*, vol. 8, 2019.

[113] H. Sies, "On the history of oxidative stress: concept and some aspects of current development," *Current Opinion in Toxicology*, vol. 7, pp. 122–126, 2018.

[114] H. Y. Lee, J. H. Choi, J. W. Hong, G. C. Kim, and H. J. Lee, "Comparative study of the ar and he atmospheric pressure plasmas on e-cadherin protein regulation for plasma-mediated transdermal drug delivery," *Journal of Physics D: Applied Physics*, vol. 51, 2018.

[115] R. Bussiahn, N. Lembke, R. Gesche, T. von Woedtke, and K.-D. Weltmann, "Plasma sources for biomedical applications," *Hyg. Med.*, vol. 38, pp. 212–216, 2013.

[116] N. Y. Babaeva and M. J. Kushner, "Intracellular electric fields produced by dielectric barrier discharge treatment of skin," *Journal of Physics D: Applied Physics*, vol. 43, article 185206, 2010.

[117] T. Darny, J. M. Pouvesle, V. Puech, C. Douat, S. Dozias, and E. Robert, "Analysis of conductive target influence in plasma jet experiments through helium metastable and electric field measurements," *Plasma Sources Sci. T.*, vol. 26, article 045008, 2017.

[118] K. R. Liedtke, S. Diedrich, O. Pati et al., "Cold physical plasma selectively elicits apoptosis in murine pancreatic cancer CellsIn VitroandIn ovo," *Anticancer Research*, vol. 38, no. 10, pp. 5655–5663, 2018.

[119] S. Bekeschus, J. Moritz, I. Helfrich et al., "Ex vivo exposure of human melanoma tissue to cold physical plasma elicits apoptosis and modulates inflammation," *Applied Sciences*, vol. 10, 2020.

[120] M. Adhikari, N. Kaushik, B. Ghimire et al., "Cold atmospheric plasma and silymarin nanoemulsion synergistically inhibits human melanoma tumorigenesis via targeting hgf/c-met downstream pathway," *Cell Communication and Signaling: CCS*, vol. 17, p. 52, 2019.

[121] N. Yoshikawa, W. Liu, K. Nakamura et al., "Plasma-activated medium promotes autophagic cell death along with alteration of the mtor pathway," *Scientific Reports*, vol. 10, p. 1614, 2020.

[122] M. Bourdens, Y. Jeanson, M. Taurand et al., "Short exposure to cold atmospheric plasma induces senescence in human skin fibroblasts and adipose mesenchymal stromal cells," *Scientific Reports*, vol. 9, p. 8671, 2019.

[123] S. Arndt, E. Wacker, Y. F. Li et al., "Cold atmospheric plasma, a new strategy to induce senescence in melanoma cells," *Experimental Dermatology*, vol. 22, pp. 284–289, 2013.

[124] C. Schneider, L. Gebhardt, S. Arndt et al., "Cold atmospheric plasma causes a calcium influx in melanoma cells triggering cap-induced senescence," *Scientific Reports*, vol. 8, p. 10048, 2018.

[125] S. B. Karki, T. T. Gupta, E. Yildirim-Ayan, K. M. Eisenmann, and H. Ayan, "Miniature non-thermal plasma induced cell cycle arrest and apoptosis in lung carcinoma cells," *Plasma Chemistry and Plasma Processing*, vol. 40, pp. 99–117, 2019.

[126] D. Yan, A. Talbot, N. Nourmohammadi et al., "Principles of using cold atmospheric plasma stimulated media for cancer treatment," *Scientific Reports*, vol. 5, p. 18339, 2015.

[127] M. Rasouli, H. Mehdian, K. Hajisharifi, E. Amini, K. Ostrikov, and E. Robert, "Plasma-activated medium induces apoptosis in chemotherapy-resistant ovarian cancer cells: high selectivity and synergy with carboplatin," *Plasma Processes and Polymers*, vol. 18, no. 9, p. 2100074, 2021.

[128] M. Khalili, L. Daniels, A. Lin et al., "Non-thermal plasma-induced immunogenic cell death in cancer: a topical review," *Journal of Physics D: Applied Physics*, vol. 52, 2019.

[129] S. Bekeschus, R. Clemen, F. Niessner, S. K. Sagwal, E. Freund, and A. Schmidt, "Medical gas plasma jet technology targets murine melanoma in an immunogenic fashion," *Adv Sci (Weinh)*, vol. 7, p. 1903438, 2020.

[130] S. Bekeschus, T. von Woedtke, S. Emmert, and A. Schmidt, "Medical gas plasma-stimulated wound healing: evidence and mechanisms," *Redox Biology*, vol. 46, article 102116, 2021.

[131] A. Bisag, C. Bucci, S. Coluccelli et al., "Plasma-activated ringer's lactate solution displays a selective cytotoxic effect on ovarian cancer cells," *Cancers (Basel)*, vol. 12, 2020.

[132] C. Canal, R. Fontelo, I. Hamouda, J. Guillem-Marti, U. Cvelbar, and M. P. Ginebra, "Plasma-induced selectivity in bone cancer cells death," *Free Radical Biology & Medicine*, vol. 110, pp. 72–80, 2017.

[133] B. S. Kwon, E. H. Choi, B. Chang, J. H. Choi, K. S. Kim, and H. K. Park, "Selective cytotoxic effect of non-thermal micro-dbd plasma," *Physical Biology*, vol. 13, article 056001, 2016.

[134] D. Yan, H. Xiao, W. Zhu et al., "The role of aquaporins in the anti-glioblastoma capacity of the cold plasma-stimulated medium," *Journal of Physics D: Applied Physics*, vol. 50, 2017.

[135] M. Yusupov, D. Y. Yan, R. M. Cordeiro, and A. Bogaerts, "Atomic scale simulation of h2o2 permeation through aquaporin: toward the understanding of plasma cancer treatment," *Journal of Physics D: Applied Physics*, vol. 51, 2018.

[136] F. de Meyer and B. Smit, "Effect of cholesterol on the structure of a phospholipid bilayer," *Proceedings of the National Academy of Sciences of the United States of America*, vol. 106, pp. 3654–3658, 2009.

[137] D. Trachootham, J. Alexandre, and P. Huang, "Targeting cancer cells by ros-mediated mechanisms: a radical therapeutic approach?," *Nature Reviews Drug Discovery*, vol. 8, pp. 579–591, 2009.

[138] H.-R. Metelmann, C. Seebauer, V. Miller et al., "Clinical experience with cold plasma in the treatment of locally advanced head and neck cancer," *Clinical Plasma Medicine*, vol. 9, pp. 6–13, 2018.

[139] M. Schuster, R. Rutkowski, A. Hauschild et al., "Side effects in cold plasma treatment of advanced oral cancer—clinical data and biological interpretation," *Clinical Plasma Medicine*, vol. 10, pp. 9–15, 2018.

[140] M. Schuster, C. Seebauer, R. Rutkowski et al., "Visible tumor surface response to physical plasma and apoptotic cell kill in head and neck cancer," *Journal of Cranio-Maxillo-Facial Surgery*, vol. 44, pp. 1445–1452, 2016.

[141] K. Witzke, C. Seebauer, K. Jesse et al., "Plasma medical oncology: immunological interpretation of head and neck squamous cell carcinoma," *Plasma Processes and Polymers*, vol. 17, article e1900258, 2020.

[142] H. Yu, Y. Wang, S. Wang et al., "Paclitaxel-loaded core–shell magnetic nanoparticles and cold atmospheric plasma inhibit non-small cell lung cancer growth," *ACS Applied Materials & Interfaces*, vol. 10, pp. 43462–43471, 2018.

[143] X. Dai, Z. Zhang, J. Zhang, and K. Ostrikov, "Dosing: the key to precision plasma oncology," *Plasma Processes and Polymers*, vol. 17, no. 10, p. 1900178, 2020.

[144] A. Praetorius, R. Arvidsson, S. Molander, and M. Scheringer, "Facing complexity through informed simplifications: a research agenda for aquatic exposure assessment of nanoparticles," *Environmental Science-Processes & Impacts*, vol. 15, pp. 161–168, 2013.

[145] M. G. Kong, M. Keidar, and K. Ostrikov, "Plasmas meet nanoparticles-where synergies can advance the frontier of medicine," *Journal of Physics D: Applied Physics*, vol. 44, article 174018, 2011.

[146] J. Lademann, A. Patzelt, H. Richter et al., "Nanocapsules for drug delivery through the skin barrier by tissue-tolerable plasma," *Laser Physics Letters*, vol. 10, article 083001, 2013.

[147] O. Lademann, H. Richter, A. Kramer et al., "Stimulation of the penetration of particles into the skin by plasma tissue interaction," *Laser Physics Letters*, vol. 8, pp. 758–764, 2011.

[148] O. Lademann, H. Richter, M. C. Meinke et al., "Drug delivery through the skin barrier enhanced by treatment with tissue-tolerable plasma," *Experimental Dermatology*, vol. 20, pp. 488–490, 2011.

[149] W. Zhu, S. J. Lee, N. J. Castro, D. Yan, M. Keidar, and L. G. Zhang, "Synergistic effect of cold atmospheric plasma and drug loaded core-shell nanoparticles on inhibiting breast cancer cell growth," *Scientific Reports*, vol. 6, p. 21974, 2016.

[150] S. K. Sagwal, G. Pasqual-Melo, Y. Bodnar, R. K. Gandhirajan, and S. Bekeschus, "Combination of chemotherapy and

physical plasma elicits melanoma cell death via upregulation of slc22a16," *Cell Death & Disease*, vol. 9, p. 1179, 2018.

[151] K. R. Liedtke, E. Freund, M. Hermes et al., "Gas plasma-conditioned ringer's lactate enhances the cytotoxic activity of cisplatin and gemcitabine in pancreatic cancer in vitro and in ovo," *Cancers (Basel)*, vol. 12, p. 123, 2020.

[152] G. Busco, E. Robert, N. Chettouh-Hammas, J. M. Pouvesle, and C. Grillon, "The emerging potential of cold atmospheric plasma in skin biology," *Free Radical Biology & Medicine*, vol. 161, pp. 290–304, 2020.

[153] T. Kaneko, S. Sasaki, Y. Hokari, S. Horiuchi, R. Honda, and M. Kanzaki, "Improvement of cell membrane permeability using a cell-solution electrode for generating atmospheric-pressure plasma," *Biointerphases*, vol. 10, article 029521, 2015.

[154] X. Q. Cheng, W. Murphy, N. Recek et al., "Synergistic effect of gold nanoparticles and cold plasma on glioblastoma cancer therapy," *Journal of Physics D: Applied Physics*, vol. 47, article 335402, 2014.

[155] P. Shaw, N. Kumar, D. Hammerschmid, A. Privat-Maldonado, S. Dewilde, and A. Bogaerts, "Synergistic effects of melittin and plasma treatment: a promising approach for cancer therapy," *Cancers (Basel)*, vol. 11, 2019.

[156] P. Lukes, E. Dolezalova, I. Sisrova, and M. Clupek, "Aqueous-phase chemistry and bactericidal effects from an air discharge plasma in contact with water: evidence for the formation of peroxynitrite through a pseudo-second-order post-discharge reaction of h2o2and hno2," *Plasma Sources Sci. T.*, vol. 23, article 015019, 2014.

[157] Y. Dai, C. Xu, X. Sun, and X. Chen, "Nanoparticle design strategies for enhanced anticancer therapy by exploiting the tumour microenvironment," *Chemical Society Reviews*, vol. 46, pp. 3830–3852, 2017.

[158] G. Taneja, A. Sud, N. Pendse, B. Panigrahi, A. Kumar, and A. K. Sharma, "Nano-medicine and vascular endothelial dysfunction: options and delivery strategies," *Cardiovascular Toxicology*, vol. 19, pp. 1–12, 2019.

[159] N. K. Kaushik, N. Kaushik, K. C. Yoo et al., "Low doses of peg-coated gold nanoparticles sensitize solid tumors to cold plasma by blocking the pi3k/akt-driven signaling axis to suppress cellular transformation by inhibiting growth and emt," *Biomaterials*, vol. 87, pp. 118–130, 2016.

[160] Z. He, K. Liu, E. Manaloto et al., "Cold atmospheric plasma induces atp-dependent endocytosis of nanoparticles and synergistic u373mg cancer cell death," *Scientific Reports*, vol. 8, p. 5298, 2018.

[161] X. Q. Cheng, K. Rajjoub, J. Sherman et al., "Cold plasma accelerates the uptake of gold nanoparticles into glioblastoma cells," *Plasma Processes and Polymers*, vol. 12, pp. 1364–1369, 2015.

[162] G. C. Kim, G. J. Kim, S. R. Park et al., "Air plasma coupled with antibody-conjugated nanoparticles: a new weapon against cancer," *Journal of Physics D: Applied Physics*, vol. 42, article 032005, 2009.

[163] P. Jawaid, M. U. Rehman, Q. L. Zhao et al., "Small size gold nanoparticles enhance apoptosis-induced by cold atmospheric plasma via depletion of intracellular gsh and modification of oxidative stress," *Cell Death Discovery*, vol. 6, p. 83, 2020.

[164] B. B. Choi, M. S. Kim, U. K. Kim, J. W. Hong, H. J. Lee, and G. C. Kim, "Targeting neu protein in melanoma cells with non-thermal atmospheric pressure plasma and gold nanoparticles," *Journal of Biomedical Nanotechnology*, vol. 11, pp. 900–905, 2015.

[165] B. B. R. Choi, J. H. Choi, J. W. Hong et al., "Selective killing of melanoma cells with non-thermal atmospheric pressure plasma and p-fak antibody conjugated gold nanoparticles," *International Journal of Medical Sciences*, vol. 14, pp. 1101–1109, 2017.

[166] S. Bekeschus, "Combined toxicity of gas plasma treatment and nanoparticles exposure in melanoma cells in vitro," *Nanomaterials (Basel)*, vol. 11, 2021.

[167] Z. He, K. Liu, L. Scally et al., "Cold atmospheric plasma stimulates clathrin-dependent endocytosis to repair oxidised membrane and enhance uptake of nanomaterial in glioblastoma multiforme cells," *Scientific Reports*, vol. 10, p. 6985, 2020.

[168] A. Jalili, S. Irani, and R. Mirfakhraie, "Combination of cold atmospheric plasma and iron nanoparticles in breast cancer: gene expression and apoptosis study," *Oncotargets and Therapy*, vol. 9, pp. 5911–5917, 2016.

[169] W. Li, H. Yu, D. Ding et al., "Cold atmospheric plasma and iron oxide-based magnetic nanoparticles for synergetic lung cancer therapy," *Free Radical Biology & Medicine*, vol. 130, pp. 71–81, 2019.

[170] K. W. Witwer and J. Wolfram, "Extracellular vesicles versus synthetic nanoparticles for drug delivery," *Nature Reviews Materials*, vol. 6, pp. 103–106, 2021.

[171] J. Canady, S. Gordon, T. Zhuang et al., "Cold atmospheric plasma (cap) combined with chemo-radiation and cytoreductive surgery: the first clinical experience for stage iv metastatic colon cancer," in *Comprehensive Clinical Plasma Medicine: Cold Physical Plasma for Medical Application*, H.-R. Metelmann, T. Woedtke, and K.-D. Weltmann, Eds., pp. 163–183, Springer International Publishing, Cham, 2018.

[172] M. Arisi, S. Soglia, E. Guasco Pisani et al., "Cold atmospheric plasma (cap) for the treatment of actinic keratosis and skin field cancerization: clinical and high-frequency ultrasound evaluation," *Dermatology and Therapy*, vol. 11, pp. 855–866, 2021.

[173] G. Daeschlein, A. Arnold, S. Lutze et al., "Treatment of recalcitrant actinic keratosis (ak) of the scalp by cold atmospheric plasma," *Cogent Medicine*, vol. 4, p. 1412903, 2017.

[174] P. C. Friedman, V. Miller, G. Fridman, A. Lin, and A. Fridman, "Successful treatment of actinic keratoses using nonthermal atmospheric pressure plasma: a case series," *Journal of the American Academy of Dermatology*, vol. 76, pp. 349-350, 2017.

[175] M. Wirtz, I. Stoffels, J. Dissemond, D. Schadendorf, and A. Roesch, "Actinic keratoses treated with cold atmospheric plasma," *Journal of the European Academy of Dermatology and Venereology*, vol. 32, pp. e37–e39, 2018.

[176] J. Shi, P. W. Kantoff, R. Wooster, and O. C. Farokhzad, "Cancer nanomedicine: Progress, challenges and opportunities," *Nature Reviews. Cancer*, vol. 17, pp. 20–37, 2017.

[177] N. Bertrand, J. Wu, X. Xu, N. Kamaly, and O. C. Farokhzad, "Cancer nanotechnology: the impact of passive and active targeting in the era of modern cancer biology," *Advanced Drug Delivery Reviews*, vol. 66, pp. 2–25, 2014.

[178] A. Albanese, A. K. Lam, E. A. Sykes, J. V. Rocheleau, and W. C. Chan, "Tumour-on-a-chip provides an optical window

into nanoparticle tissue transport," *Nature Communications*, vol. 4, p. 2718, 2013.

[179] M. J. Mitchell, M. M. Billingsley, R. M. Haley, M. E. Wechsler, N. A. Peppas, and R. Langer, "Engineering precision nanoparticles for drug delivery," *Nature Reviews. Drug Discovery*, vol. 20, pp. 101–124, 2021.

[180] R. Iyer, T. Nguyen, D. Padanilam et al., "Glutathione-responsive biodegradable polyurethane nanoparticles for lung cancer treatment," *Journal of Controlled Release*, vol. 321, pp. 363–371, 2020.

[181] K. Reczynska, M. Marszalek, A. Zarzycki et al., "Superparamagnetic iron oxide nanoparticles modified with silica layers as potential agents for lung cancer treatment," *Nanomaterials (Basel)*, vol. 10, p. 1076, 2020.

[182] Y. Song, B. Zhou, X. Du et al., "Folic acid (fa)-conjugated mesoporous silica nanoparticles combined with mrp-1 sirna improves the suppressive effects of myricetin on non-small cell lung cancer (nsclc)," *Biomedicine & Pharmacotherapy*, vol. 125, article 109561, 2020.

[183] R. Tanino, Y. Amano, X. Tong et al., "Anticancer activity of zno nanoparticles against human small-cell lung cancer in an orthotopic mouse model," *Molecular Cancer Therapeutics*, vol. 19, pp. 502–512, 2020.

[184] H. Wang, F. K. Zhang, H. Y. Wen et al., "Tumor- and mitochondria-targeted nanoparticles eradicate drug resistant lung cancer through mitochondrial pathway of apoptosis," *Journal of Nanobiotechnology*, vol. 18, pp. 1–21, 2020.

[185] Y. Wang, H. Yu, S. Wang et al., "Targeted delivery of quercetin by nanoparticles based on chitosan sensitizing paclitaxel-resistant lung cancer cells to paclitaxel," *Materials Science & Engineering. C, Materials for Biological Applications*, vol. 119, article 111442, 2021.

[186] X. Wang, V. Parvathaneni, S. K. Shukla et al., "Inhalable resveratrol-cyclodextrin complex loaded biodegradable nanoparticles for enhanced efficacy against non-small cell lung cancer," *International Journal of Biological Macromolecules*, vol. 164, pp. 638–650, 2020.

[187] B. Vaidya, N. S. Kulkarni, S. K. Shukla et al., "Development of inhalable quinacrine loaded bovine serum albumin modified cationic nanoparticles: repurposing quinacrine for lung cancer therapeutics," *International Journal of Pharmaceutics*, vol. 577, article 118995, 2020.

[188] M. Landgraf, C. A. Lahr, I. Kaur et al., "Targeted camptothecin delivery via silicon nanoparticles reduces breast cancer metastasis," *Biomaterials*, vol. 240, article 119791, 2020.

[189] M. Sharifi, S. Jafari, A. Hasan et al., "Antimetastatic activity of lactoferrin-coated mesoporous maghemite nanoparticles in breast cancer enabled by combination therapy," *ACS Biomaterials Science & Engineering*, vol. 6, pp. 3574–3584, 2020.

[190] K. Xiong, Y. Zhang, Q. Wen et al., "Co-delivery of paclitaxel and curcumin by biodegradable polymeric nanoparticles for breast cancer chemotherapy," *International Journal of Pharmaceutics*, vol. 589, article 119875, 2020.

[191] J. Lei, H. Wang, D. Zhu, Y. Wan, and L. Yin, "Combined effects of avasimibe immunotherapy, doxorubicin chemotherapy, and metal-organic frameworks nanoparticles on breast cancer," *Journal of Cellular Physiology*, vol. 235, pp. 4814–4823, 2020.

[192] M. Mughees, S. Wajid, and M. Samim, "Cytotoxic potential of artemisia absinthium extract loaded polymeric nanoparticles against breast cancer cells: insight into the protein targets," *International Journal of Pharmaceutics*, vol. 586, article 119583, 2020.

[193] Q. Jiang, M. Zhang, Q. Sun, D. Yin, Z. Xuan, and Y. Yang, "Enhancing the antitumor effect of doxorubicin with photosensitive metal-organic framework nanoparticles against breast cancer," *Molecular Pharmaceutics*, vol. 18, no. 8, pp. 3026–3036, 2021.

[194] B. Toubhans, S. A. Gazze, C. Bissardon et al., "Selenium nanoparticles trigger alterations in ovarian cancer cell biomechanics," *Nanomedicine*, vol. 29, article 102258, 2020.

[195] N. Brandhonneur, Y. Boucaud, A. Verger et al., "Molybdenum cluster loaded plga nanoparticles as efficient tools against epithelial ovarian cancer," *International Journal of Pharmaceutics*, vol. 592, article 120079, 2021.

[196] V. Ramalingam, M. Harshavardhan, S. Dinesh Kumar, and S. Malathi devi, "Wet chemical mediated hematite α-fe2o3 nanoparticles synthesis: preparation, characterization and anticancer activity against human metastatic ovarian cancer," *Journal of Alloys and Compounds*, vol. 834, article 155118, 2020.

[197] A. I. Fraguas-Sanchez, A. I. Torres-Suarez, M. Cohen et al., "Plga nanoparticles for the intraperitoneal administration of cbd in the treatment of ovarian cancer: in vitro and in ovo assessment," *Pharmaceutics*, vol. 12, 2020.

[198] M. Fathi, J. Barar, H. Erfan-Niya, and Y. Omidi, "Methotrexate-conjugated chitosan-grafted ph- and thermo-responsive magnetic nanoparticles for targeted therapy of ovarian cancer," *International Journal of Biological Macromolecules*, vol. 154, pp. 1175–1184, 2020.

[199] Q. Pan, J. Tian, H. Zhu et al., "Tumor-targeting polycaprolactone nanoparticles with codelivery of paclitaxel and ir780 for combinational therapy of drug-resistant ovarian cancer," *ACS Biomaterials Science & Engineering*, vol. 6, pp. 2175–2185, 2020.

[200] Z. Yu, X. Li, J. Duan, and X. D. Yang, "Targeted treatment of colon cancer with aptamer-guided albumin nanoparticles loaded with docetaxel," *International Journal of Nanomedicine*, vol. 15, pp. 6737–6748, 2020.

[201] G. Chen, Y. Zhao, Y. Xu, C. Zhu, T. Liu, and K. Wang, "Chitosan nanoparticles for oral photothermally enhanced photodynamic therapy of colon cancer," *International Journal of Pharmaceutics*, vol. 589, article 119763, 2020.

[202] X. L. Liang, M. Chen, P. Bhattarai, S. Hameed, and Z. F. Dai, "Perfluorocarbon@porphyrin nanoparticles for tumor hypoxia relief to enhance photodynamic therapy against liver metastasis of colon cancer," *ACS Nano*, vol. 14, pp. 13569–13583, 2020.

[203] D. Acharya, S. Satapathy, P. Somu, U. K. Parida, and G. Mishra, "Apoptotic effect and anticancer activity of biosynthesized silver nanoparticles from marine algae chaetomorpha linum extract against human colon cancer cell hct-116," *Biological Trace Element Research*, vol. 199, pp. 1812–1822, 2021.

[204] Y. Liu, J. T. Zhao, J. L. Jiang, F. F. Chen, and X. D. Fang, "Doxorubicin delivered using nanoparticles camouflaged with mesenchymal stem cell membranes to treat colon cancer," *International Journal of Nanomedicine*, vol. 15, pp. 2873–2884, 2020.

[205] V. K. Chaturvedi, N. Yadav, N. K. Rai et al., "Pleurotus sajor-caju-mediated synthesis of silver and gold nanoparticles active against colon cancer cell lines: a new era of herbonanoceutics," *Molecules*, vol. 25, p. 3091, 2020.

[206] K. AbouAitah, A. Stefanek, I. M. Higazy et al., "Effective targeting of colon cancer cells with piperine natural anticancer prodrug using functionalized clusters of hydroxyapatite nanoparticles," *Pharmaceutics*, vol. 12, p. 70, 2020.

[207] P. P. Wu, Q. Zhou, H. Y. Zhu, Y. Zhuang, and J. Bao, "Enhanced antitumor efficacy in colon cancer using egf functionalized plga nanoparticles loaded with 5-fluorouracil and perfluorocarbon," *BMC Cancer*, vol. 20, pp. 1–10, 2020.

[208] I. Sur-Erdem, K. Muslu, N. Pinarbasi et al., "Trail-conjugated silver nanoparticles sensitize glioblastoma cells to trail by regulating chk1 in the DNA repair pathway," *Neurological Research*, vol. 42, pp. 1061–1069, 2020.

[209] V. M. Lu, T. R. Jue, and K. L. McDonald, "Cytotoxic lanthanum oxide nanoparticles sensitize glioblastoma cells to radiation therapy and temozolomide: an in vitro rationale for translational studies," *Scientific Reports*, vol. 10, p. 18156, 2020.

[210] S. Sheykhzadeh, M. Luo, B. Peng et al., "Transferrin-targeted porous silicon nanoparticles reduce glioblastoma cell migration across tight extracellular space," *Scientific Reports*, vol. 10, p. 2320, 2020.

[211] N. Prabhakar, J. Merisaari, V. Le Joncour et al., "Circumventing drug treatment? Intrinsic lethal effects of polyethyleneimine (pei)-functionalized nanoparticles on glioblastoma cells cultured in stem cell conditions," *Cancers (Basel)*, vol. 13, p. 2631, 2021.

[212] M. Norouzi, V. Yathindranath, J. A. Thliveris, B. M. Kopec, T. J. Siahaan, and D. W. Miller, "Doxorubicin-loaded iron oxide nanoparticles for glioblastoma therapy: a combinational approach for enhanced delivery of nanoparticles," *Scientific Reports*, vol. 10, p. 11292, 2020.

[213] J. V. Gregory, P. Kadiyala, R. Doherty et al., "Systemic brain tumor delivery of synthetic protein nanoparticles for glioblastoma therapy," *Nature Communications*, vol. 11, p. 5687, 2020.

[214] M. Norouzi, V. Yathindranath, J. A. Thliveris, and D. W. Miller, "Salinomycin-loaded iron oxide nanoparticles for glioblastoma therapy," *Nanomaterials (Basel)*, vol. 10, p. 477, 2020.

[215] H. Han, Y. Hou, X. Chen et al., "Metformin-induced stromal depletion to enhance the penetration of gemcitabine-loaded magnetic nanoparticles for pancreatic cancer targeted therapy," *Journal of the American Chemical Society*, vol. 142, pp. 4944–4954, 2020.

[216] X. Chen, F. Jia, Y. Li et al., "Nitric oxide-induced stromal depletion for improved nanoparticle penetration in pancreatic cancer treatment," *Biomaterials*, vol. 246, article 119999, 2020.

[217] S. Bao, H. Zheng, J. Ye et al., "Dual targeting egfr and stat3 with erlotinib and alantolactone co-loaded plga nanoparticles for pancreatic cancer treatment," *Frontiers in Pharmacology*, vol. 12, article 625084, 2021.

[218] L. Liu, P. Kshirsagar, J. Christiansen et al., "Polyanhydride nanoparticles stabilize pancreatic cancer antigen muc4beta," *Journal of Biomedical Materials Research. Part A*, vol. 109, pp. 893–902, 2021.

[219] K. O. Affram, T. Smith, E. Ofori et al., "Cytotoxic effects of gemcitabine-loaded solid lipid nanoparticles in pancreatic cancer cells," *Journal of Drug Delivery Science and Technology*, vol. 55, article 101374, 2020.

[220] T. Zhang, Z. Q. Jiang, L. B. Chen et al., "Pcn-fe(iii)-ptx nanoparticles for mri guided high efficiency chemo-photodynamic therapy in pancreatic cancer through alleviating tumor hypoxia," *Nano Research*, vol. 13, pp. 273–281, 2020.

[221] X. Kesse, A. Adam, S. Begin-Colin et al., "Elaboration of superparamagnetic and bioactive multicore-shell nanoparticles (gamma-fe2o3@sio2-cao): a promising material for bone cancer treatment," *ACS Applied Materials & Interfaces*, vol. 12, pp. 47820–47830, 2020.

[222] J. Cheng, X. Wang, L. Qiu et al., "Green synthesized zinc oxide nanoparticles regulates the apoptotic expression in bone cancer cells mg-63 cells," *Journal of Photochemistry and Photobiology. B*, vol. 202, article 111644, 2020.

[223] A. El-Fiqi and H. W. Kim, "Iron ions-releasing mesoporous bioactive glass ultrasmall nanoparticles designed as ferroptosis-based bone cancer nanotherapeutics: ultrasonic-coupled sol-gel synthesis, properties and iron ions release," *Materials Letters*, vol. 294, article 129759, 2021.

[224] D. Ahmadi, M. Zarei, M. Rahimi et al., "Preparation and in-vitro evaluation of ph-responsive cationic cyclodextrin coated magnetic nanoparticles for delivery of methotrexate to the saos-2 bone cancer cells," *Journal of Drug Delivery Science and Technology*, vol. 57, article 101584, 2020.

[225] S. B. Bai, Y. Cheng, D. Z. Liu et al., "Bone-targeted pamam nanoparticle to treat bone metastases of lung cancer," *Nanomedicine (London, England)*, vol. 15, pp. 833–849, 2020.

[226] Y. Pang, Y. Fu, C. Li et al., "Metal-organic framework nanoparticles for ameliorating breast cancer-associated osteolysis," *Nano Letters*, vol. 20, pp. 829–840, 2020.

[227] P. Sonkusre, "Specificity of biogenic selenium nanoparticles for prostate cancer therapy with reduced risk of toxicity: an in vitro and in vivo study," *Frontiers in Oncology*, vol. 9, p. 1541, 2019.

[228] Y. Q. Fang, S. X. Lin, F. Yang, J. Situ, S. D. Lin, and Y. Luo, "Aptamer-conjugated multifunctional polymeric nanoparticles as cancer-targeted, mri-ultrasensitive drug delivery systems for treatment of castration-resistant prostate cancer," *BioMed Research International*, vol. 2020, 2020.

[229] M. Soll, Q. C. Chen, B. Zhitomirsky et al., "Protein-coated corrole nanoparticles for the treatment of prostate cancer cells," *Cell Death Discovery*, vol. 6, p. 67, 2020.

[230] Y. Chen, Y. Deng, C. Zhu, and C. Xiang, "Anti prostate cancer therapy: aptamer-functionalized, curcumin and cabazitaxel co-delivered, tumor targeted lipid-polymer hybrid nanoparticles," *Biomedicine & Pharmacotherapy*, vol. 127, article 110181, 2020.

[231] D. Du, H. J. Fu, W. W. Ren, X. L. Li, and L. H. Guo, "Psa targeted dual-modality manganese oxide-mesoporous silica nanoparticles for prostate cancer imaging," *Biomedicine & Pharmacotherapy*, vol. 121, article 109614, 2020.

[232] M. Emanet Ciofani, Ö. Şen, and M. Çulha, "Hexagonal boron nitride nanoparticles for prostate cancer treatment," *ACS Applied Nano Materials*, vol. 3, pp. 2364–2372, 2020.

[233] E. Kozenkova, K. Levada, M. V. Efremova et al., "Multifunctional fe3o4-au nanoparticles for the mri diagnosis and potential treatment of liver cancer," *Nanomaterials (Basel)*, vol. 10, p. 1646, 2020.

[234] S. Li, P. E. Saw, C. Lin et al., "Redox-responsive polyprodrug nanoparticles for targeted sirna delivery and synergistic liver cancer therapy," *Biomaterials*, vol. 234, article 119760, 2020.

[235] K. Ishiguro, I. K. Yan, L. Lewis-Tuffin, and T. Patel, "Targeting liver cancer stem cells using engineered biological nanoparticles for the treatment of hepatocellular cancer," *Hepatology Communications*, vol. 4, pp. 298–313, 2020.

[236] J. Luo, T. Gong, and L. Ma, "Chondroitin-modified lipid nanoparticles target the golgi to degrade extracellular matrix for liver cancer management," *Carbohydrate Polymers*, vol. 249, article 116887, 2020.

[237] Y. N. Han, B. Hu, M. Y. Wang et al., "Ph-sensitive tumor-targeted hyperbranched system based on glycogen nanoparticles for liver cancer therapy," *Applied Materials Today*, vol. 18, article 100521, 2020.

[238] M. Suleman and S. Riaz, "In silico study of hyperthermia treatment of liver cancer using core-shell cofe2o4@mnfe2o4 magnetic nanoparticles," *Journal of Magnetism and Magnetic Materials*, vol. 498, article 166143, 2020.

[239] Z. Ding, D. Wang, W. Shi et al., "In vivo targeting of liver cancer with tissue- and nuclei-specific mesoporous silica nanoparticle-based nanocarriers in mice," *International Journal of Nanomedicine*, vol. 15, pp. 8383–8400, 2020.

[240] S. K. Libutti, G. F. Paciotti, L. Myer et al., "Results of a completed phase i clinical trial of cyt-6091: a pegylated colloidal gold-tnf nanomedicine," *Journal of Clinical Oncology*, vol. 27, pp. 3586–3586, 2009.

[241] S. K. Libutti, G. F. Paciotti, A. A. Byrnes et al., "Phase i and pharmacokinetic studies of cyt-6091, a novel pegylated colloidal gold-rhtnf nanomedicine," *Clinical Cancer Research*, vol. 16, pp. 6139–6149, 2010.

[242] G. Batist, K. A. Gelmon, K. N. Chi et al., "Safety, pharmacokinetics, and efficacy of cpx-1 liposome injection in patients with advanced solid tumors," *Clinical Cancer Research*, vol. 15, pp. 692–700, 2009.

[243] L. W. Seymour, "Phase ii studies of polymer-doxorubicin (pk1, fce28068) in the treatment of breast, lung and colorectal cancer," *International Journal of Oncology*, vol. 34, pp. 1629–1636, 2009.

[244] Y. Matsumura, M. Gotoh, K. Muro et al., "Phase i and pharmacokinetic study of mcc-465, a doxorubicin (dxr) encapsulated in peg immunoliposome, in patients with metastatic stomach cancer," *Annals of Oncology*, vol. 15, pp. 517–525, 2004.

[245] J. W. Valle, A. Armstrong, C. Newman et al., "A phase 2 study of sp1049c, doxorubicin in p-glycoprotein-targeting pluronics, in patients with advanced adenocarcinoma of the esophagus and gastroesophageal junction," *Investigational New Drugs*, vol. 29, pp. 1029–1037, 2011.

[246] E. Galanis, S. K. Carlson, N. R. Foster et al., "Phase i trial of a pathotropic retroviral vector expressing a cytocidal cyclin g1 construct (rexin-g) in patients with advanced pancreatic cancer," *Molecular Therapy*, vol. 16, pp. 979–984, 2008.

[247] T. Hamaguchi, K. Kato, H. Yasui et al., "A phase i and pharmacokinetic study of nk105, a paclitaxel-incorporating micellar nanoparticle formulation," *British Journal of Cancer*, vol. 97, pp. 170–176, 2007.

[248] G. Stathopoulos, T. Boulikas, M. Vougiouka, S. Rigatos, and J. Stathopoulos, "Liposomal cisplatin combined with gemcitabine in pretreated advanced pancreatic cancer patients: a phase i-ii study," *Oncology Reports*, vol. 15, 2006.

[249] W. Kim, K. Y. Na, K. H. Lee, H. W. Lee, J. K. Lee, and K. T. Kim, "Selective uptake of epidermal growth factor-conjugated gold nanoparticle (egf-gnp) facilitates non-thermal plasma (ntp)-mediated cell death," *Scientific Reports*, vol. 7, p. 10971, 2017.

[250] S. Irani, Z. Shahmirani, S. M. Atyabi, and S. Mirpoor, "Induction of growth arrest in colorectal cancer cells by cold plasma and gold nanoparticles," *Archives of Medical Science*, vol. 11, pp. 1286–1295, 2015.

[251] A. Dzimitrowicz, A. Bielawska-Pohl, P. Pohl et al., "Application of oil-in-water nanoemulsion carrying size-defined gold nanoparticles synthesized by non-thermal plasma for the human breast cancer cell lines migration and apoptosis," *Plasma Chemistry and Plasma Processing*, vol. 40, pp. 1037–1062, 2020.

[252] P. Jawaid, M. U. Rehman, Q. L. Zhao et al., "Helium-based cold atmospheric plasma-induced reactive oxygen species-mediated apoptotic pathway attenuated by platinum nanoparticles," *Journal of Cellular and Molecular Medicine*, vol. 20, pp. 1737–1748, 2016.

[253] G. Kim, S. R. Park, G. C. Kim, and J. K. Lee, "Targeted cancer treatment using anti-egfr and -tfr antibody-conjugated gold nanoparticles stimulated by nonthermal air plasma," *Plasma Medicine*, vol. 1, pp. 45–54, 2011.

[254] D. Sun, J. McLaughlan, L. Zhang et al., "Atmospheric pressure plasma-synthesized gold nanoparticle/carbon nanotube hybrids for photothermal conversion," *Langmuir*, vol. 35, pp. 4577–4588, 2019.

Hindawi
Oxidative Medicine and Cellular Longevity
Volume 2021, Article ID 3155962, 20 pages
https://doi.org/10.1155/2021/3155962

Review Article

Phytoantioxidant Functionalized Nanoparticles: A Green Approach to Combat Nanoparticle-Induced Oxidative Stress

Acharya Balkrishna,[1,2] Ashwani Kumar,[1] Vedpriya Arya,[1,2] Akansha Rohela,[1] Rachna Verma,[3] Eugenie Nepovimova,[4] Ondrej Krejcar,[5,6] Dinesh Kumar,[7] Naveen Thakur,[8] and Kamil Kuca[4,9]

[1]*Patanjali Herbal Research Department, Patanjali Research Institute, Haridwar 249405, India*
[2]*Department of Allied Sciences, University of Patanjali, Haridwar 249405, India*
[3]*School of Biological and Environmental Sciences, Shoolini University of Biotechnology and Management Sciences, Solan 173229, India*
[4]*Department of Chemistry, Faculty of Science, University of Hradec Kralove, Hradec Kralove 50003, Czech Republic*
[5]*Center for Basic and Applied Science, Faculty of Informatics and Management, University of Hradec Kralove, 50003 Hradec Kralove, Czech Republic*
[6]*Malaysia Japan International Institute of Technology (MJIIT), Universiti Teknologi Malaysia, Jalan Sultan Yahya Petra, Kuala Lumpur 54100, Malaysia*
[7]*School of Bioengineering and Food Technology, Shoolini University of Biotechnology and Management Sciences, Solan 173229, India*
[8]*Department of Physics, Career Point University, Hamirpur 177001, India*
[9]*Biomedical Research Center, University Hospital in Hradec Kralove, Sokolska 581, Hradec Kralove 50005, Czech Republic*

Correspondence should be addressed to Ashwani Kumar; dr.ashwanikumar@prft.co.in, Rachna Verma; rachnac83@gmail.com, and Kamil Kuca; kamil.kuca@uhk.cz

Received 30 July 2021; Revised 19 September 2021; Accepted 4 October 2021; Published 26 October 2021

Academic Editor: Dragica Selakovic

Nanotechnology is gaining significant attention, with numerous biomedical applications. Silver in wound dressings, copper oxide and silver in antibacterial preparations, and zinc oxide nanoparticles as a food and cosmetic ingredient are common examples. However, adverse effects of nanoparticles in humans and the environment from extended exposure at varied concentrations have yet to be established. One of the drawbacks of employing nanoparticles is their tendency to cause oxidative stress, a significant public health concern with life-threatening consequences. Cardiovascular, renal, and respiratory problems and diabetes are among the oxidative stress-related disorders. In this context, phytoantioxidant functionalized nanoparticles could be a novel and effective alternative. In addition to performing their intended function, they can protect against oxidative damage. This review was designed by searching through various websites, books, and articles found in PubMed, Science Direct, and Google Scholar. To begin with, oxidative stress, its related diseases, and the mechanistic basis of oxidative damage caused by nanoparticles are discussed. One of the main mechanisms of action of nanoparticles was unearthed to be oxidative stress, which limits their use in humans. Secondly, the role of phytoantioxidant functionalized nanoparticles in oxidative damage prevention is critically discussed. The parameters for the characterization of nanoparticles were also discussed. The majority of silver, gold, iron, zinc oxide, and copper nanoparticles produced utilizing various plant extracts were active free radical scavengers. This potential is linked to several surface fabricated phytoconstituents, such as flavonoids and phenols. These phytoantioxidant functionalized nanoparticles could be a better alternative to nanoparticles prepared by other existing approaches.

1. Introduction

Nanotechnology is being designated the "next industrial revolution" since it is rapidly developing with the introduction of nanomaterial-based consumer goods [1, 2]. Nanoparticles (10^{-9}m) are small objects that function as a whole unit in their transport and characteristics [3]. Nanoparticles (NPs) have diverse applications in disciplines like agriculture, healthcare, diagnosis, drug delivery, imaging, cosmetics, sunscreens, food, paints, catalysis, biolabeling, sensors, electronics, fiber optics, and other areas [2, 4–7]. Interestingly, most nanoparticles, such as Ag, Au, MgO, CuO, Al, CdS, and TiO_2, are potent antibacterial agents [3, 8–10]. Copper oxide (CuO) NPs are used in antimicrobial products, cosmetics, heat transfer liquids, and semiconductors [11–13]. On the other hand, iron nanoparticles are used in biological material labeling and magnetic separation, drug delivery, and anticancer hyperthermia therapy [14]. Zinc oxide nanoparticles (ZnO NPs) are used in sunscreens, cosmetics, food additives, and packaging purposes [15–17]. Silver nanoparticles (Ag NPs) are popular due to their broad-spectrum antibacterial action [18–20]. Their therapeutic application ranged from silver-impregnated catheters to wound dressings [21, 22]. The silver-Acticoat™ dressing containing Ag NPs is superior to silver nitrate and silver sulfadiazine in wound healing [23, 24]. Ferric oxide (Fe_2O_3) NPs are used as catalysts and in the manufacture of pigments [25]. TiO_2 NPs are believed to be the most valuable materials for cosmetics, food colorants, paper inks, pharmaceuticals, and protecting skin from UV rays [26–29]. Further, they have been used to prevent the spread of many infectious diseases [30, 31]. Furthermore, NPs including SiO_2, TiO_2, Bi_2O_3, Ag_2O, FeO, MnO_2, and Al_2O_3 play important roles in a variety of medicinal applications [32, 33]. In addition, AgS-, CuS-, FeS-, Zn-, and Cu-based metal organic frameworks are frequently utilized in drug delivery and antibacterial formulations [34].

Despite significant advances in nanomedicine, the long-term implications of NP exposure on human health and the environment are unknown [35]. When NPs enter the environment, they affect water, soil, and the air, where they might persist for a longer duration or be gobbled up by living organisms. They may biodegrade or bioaccumulate in the food chain, posing a hazardous risk [36–38]. The membrane injury, inflammatory response, DNA damage, and apoptosis have all been harmful consequences of ZnO NPs in mammalian cells [39–41]. Although Ag NPs are highly toxic to cancer cells, their use is limited since they are also hazardous to normal cells [35]. In continuation, when the toxicity of Ag NPs (10 μg/mL) was investigated in human mesenchymal stem cells, DNA damage, impaired functioning, and cell death were observed [42]. Subsequently, ZnO NPs (300 mg/kg) caused oxidative stress in mice, which resulted in DNA damage [43]. Furthermore, intratracheal instillation of TiO_2 NPs in mice resulted in accumulation of ROS, lipid peroxidation, and decreased antioxidant capacity [44]. Metal-derived NPs (copper, iron, cadmium, and silver) produce reactive oxygen species (ROS), which causes oxidative stress, restricting their wide-ranging application [45–50].

As evidenced by several pieces of research, oxidative stress is the key factor ascribed to the biological potential of nanoparticles [2, 35, 51]. ROS-induced oxidative stress destroys lipids, proteins, and DNA, and long-term exposure leads to neurological disorders, diabetes, rheumatoid arthritis, cancer, cardiovascular problems, and other diseases [52–56]. In the current situation, one interesting possibility for combating nanoparticle-induced oxidative stress could be the phytoantioxidant functionalized nanoparticles synthesized using plant extract-mediated green approach. Since these NPs contain a variety of surface-attached bioactive compounds from plants, they are referred to as phytoantioxidant functionalized NPs. The sonochemical, thermal decomposition, microwave aided, electrochemical, chemical reduction, and green synthesis are some of the chemical and physical methods used to synthesize NPs [57–62]. Unfortunately, many of these technologies employ hazardous chemicals, necessitate much energy, and produce poisonous by-products [63]. Green synthesis, which encompasses synthesis using plants, bacteria, fungus, algae, actinomycetes, and other organisms, is environmentally friendly, cost-effective, biocompatible, and safe [64–70]. Furthermore, phyto-mediated synthesis is preferable to a microbial method, which necessitates time-consuming and expensive downstream processing [71, 72].

Keeping in view the problem of nanoparticle-induced oxidative stress, in this review, we attempted to put some light on the antioxidant potential of phytoantioxidant functionalized NPs. Firstly, we have compiled a brief overview of oxidative stress-associated disorders and oxidative stress-mediated toxicity of nanoparticles. Secondly, a brief overview of green synthesis using plant extracts and the protective role of phytoantioxidant functionalized NPs as a therapeutic for oxidative stress is highlighted along with its mechanistic approaches.

2. Search and Inclusion Criteria

Science Direct, PubMed, and Google Scholar databases have been searched in this review with various keywords like oxidative stress, its related disorders, reactive oxygen and nitrogen species, mechanism of action, the toxicity of nanoparticles, oxidative stress-induced toxicity of nanoparticles, green synthesis, and antioxidant activity of nanoparticles. The literature review took place between May 1, 2021, and July 2, 2021. This review only considered full-length, original, and English-language papers from Web of Science, Scopus-indexed, and peer-reviewed journals.

3. Oxidative Stress and Its Related Disorders: A Brief Overview

Free radicals are strongly reactive atoms or molecules with unpaired electrons in their exterior shell and can be generated when oxygen reacts with specific molecules [73]. Free radicals, such as reactive oxygen species (ROS) and reactive nitrogen species (RNS), are produced continuously throughout cellular metabolism and play an important part in various cell signaling pathways [74–78]. Various endogenous

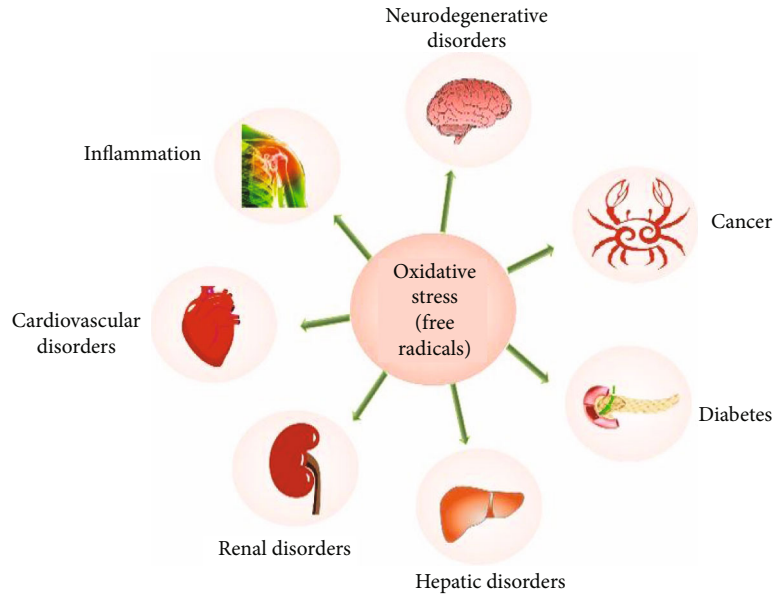

Figure 1: Various indications associated with the generation of oxidative stress.

and external activities generate ROS and RNS, and antioxidant defenses mitigate their harmful effects. Superoxide radicals ($O_2^{\cdot-}$), hydroxyl for ($^{\cdot}OH$), hydrogen peroxide radicals (H_2O_2), and singlet oxygen are generally defined ROS [79–82]. RNS comprises nitric oxide, peroxynitrite ($ONOO^-$), and their reaction products [83].

The protein phosphorylation, transcription factor activation, immunity, apoptosis, and differentiation are all reliant on adequate ROS production within cells, which must be maintained at a minimum level [84]. The ROS generation occurs mainly in the mitochondria, cell membranes, and cytoplasm. Even though these organelles have an inherent potential to scavenge ROS [85], it is noteworthy that this is insufficient to fulfill the cellular demand to eliminate the quantity of ROS generated by mitochondria [86].

The disparities between ROS and RNS generation and antioxidant defenses cause oxidative stress. Furthermore, when the formation of ROS rises, they begin to have adverse effects on essential cellular components (lipids, proteins, and nucleic acids) [77, 78, 87–89]. A substantial body of evidence suggests that oxidative stress has a role in the genesis and overall progress of various diseases, including diabetes; metabolic disorders; atherosclerosis; neurological, cardiovascular, and respiratory disorders; and cancer [90–92]. In Figure 1, several disorders linked to oxidative stress are presented.

Furthermore, as the level of antioxidant enzymes, glutathione peroxidase (GPx), catalase (CAT), and superoxide dismutase (SOD), diminishes with age, the age-related functional losses are attributed to ROS- and RNS-mediated lipid, protein, and DNA damage [93, 94]. Oxidative stress has a role in vascular endothelial dysfunction with age [95]. Several reports (both *in vivo* and *ex vivo*) shred the threads of evidence against oxidative stress-induced atherosclerosis, hypertension, ischemic heart disease, cardiomyopathy, and congestive heart failure [96–99]. Importantly, oxidative stress causes cardiovascular complications in type 2 diabetes (T2D) subjects by promoting prothrombotic reactions [100]. ROS are also associated with cardiac arrest by cardiac hypertrophy development, ischemia-reperfusion injury, and myocyte apoptosis [101–103].

There are reports that asthma and chronic obstructive pulmonary disease (COPD) are linked to ROS-induced oxidative stress [104–106]. Choudhury and MacNee [107] reported increased levels of oxidative stress biomarkers (8-hydroxydeoxyguanosine, protein carbonyl, 3-nitrotyrosine, F2-isoprostanes, and advanced glycation end products) in COPD patients. Subsequently, oxidative stress contributes to chronic kidney disease (CKD) pathogenesis via glomerular damage, renal ischemia, inflammation, and endothelial dysfunction [97, 108, 109]. In CKD patients, polymorphonuclear leukocytes (PMNs) and monocytes are activated, resulting in increased release of nicotinamide adenine dinucleotide phosphate (NADPH) oxidase and myeloperoxidase (MPO), which promotes the formation of ROS [110].

On the other hand, oxidative stress disrupts neuronal and cellular processes and has been related to several neurological illnesses, including amyotrophic lateral sclerosis, depression, amnesia, and Parkinson's and Alzheimer's disease [56, 111, 112]. The lipid membrane is one of the most impacted structures in the brain due to redox imbalance [113]. Moreover, due to higher glucose, insulin blood levels, fatty acids, and impaired glutathione synthesis, diabetes individuals have substantial ROS levels [114]. Increased production of ROS causes a mutation in an oncogene, leading to cancer [115]. ROS disrupt the Akt/PI3K/ERK cell signaling pathway, diminishing proapoptotic proteins while boosting antiapoptotic genes [116, 117]. Subsequently, ROS has been linked to acute liver injury pathogenesis for a long time [118]. Similarly, multiple reports have shown that oxidative stress has a role in the etiology of inflammatory disorders like rheumatoid arthritis [119–121].

4. Oxidative Stress-Mediated Toxicity of Nanoparticles

Nanotechnology has found applications in a range of fields, including the environment, energy, food, and medicine. Nanoparticles are employed in biomedical applications because they have several advantages over bulk materials, including a higher surface-to-volume ratio, improved magnetic characteristics, thermal stability, and improved optical and mechanical properties. Despite the widespread use of NPs stated in Introduction, there is still a lack of ample knowledge about NP-mediated toxicity. However, there are reports that NPs induce toxicity via increasing intracellular ROS levels. Nanoparticle toxicity due to oxidative stress is well documented, restricting their usage in human patients.

In this context, using carboxy-2′,7′-dichlorofluorescein diacetate (H_2DCFDDA) assay, the function of oxidative stress in the toxicity of iron oxide NPs against murine macrophage (J774) cells was examined. It was shown that exposing cells to a higher concentration of NPs (500 μg/mL) enhanced the generation of ROS, resulting in cellular damage and death [122]. Subsequently, when human microvascular endothelial cells were exposed to iron NPs, they showed an increase in permeability, ascribed to ROS generation. Furthermore, when cells are exposed to iron NPs, ROS is proven to be a significant factor in modulating Akt/GSK-3-mediated cell permeability [123].

Ahamed et al. [51] investigated the CuO NP-induced genotoxic reaction in human pulmonary epithelial cells (A549) via the p53 pathway. CuO NPs increased the cell cycle checkpoint protein p53 and the DNA damage repair proteins Rad51 and MSH2. In a dose-dependent manner, CuO NPs also triggered oxidative stress (10, 25, and 50 μg/mL), as evidenced by glutathione, CAT, and SOD depletion and the stimulation of lipid peroxidation. These findings show that CuO NPs exerted genotoxicity in A549 cells, which could be due to oxidative stress. Likewise, using the Alamar blue assay, the cytotoxicity of CuO, silicon oxide, and ferric oxide NPs against human laryngeal epithelial cells (HEp-2) was examined. CuO exhibited cytotoxicity; however, HEp-2 cells were unaffected by silicon oxide or ferric oxide even at high doses (400 μg/cm^2). CuO-induced oxidative stress was suggested by a considerable rise in amount of 8-isoprostanes and the ratio of oxidized glutathione to total glutathione [124]. In human liver cells (HepG2), the apoptotic and genotoxic capacity of ZnO NPs was investigated. Their cellular toxicity was also examined at the molecular level. HepG2 viability was reduced on exposure to ZnO NPs (14-20 μg/mL) for 12 h, and the cell death that occurred was apoptosis. They also triggered DNA damage, as demonstrated by an upsurge in formamidopyrimidine DNA glycosylase- (Fpg-) sensitive regions mediated by oxidative stress. ROS led to a decline in mitochondria membrane capacity and a rise in the Bax/Bcl2 ratio, resulting in a mitochondria-mediated apoptosis pathway [2].

Similarly, the impact of oxidative stress in the toxicity of ZnO NPs against human skin melanoma (A375) cells was studied. ZnO NPs were reported to cause oxidative stress, as evidenced by lipid peroxidation and the depletion of antioxidant enzymes. In cells exposed to the ZnO NPs, DNA damage was seen, which could be mediated by oxidative stress [125]. The occurrence of oxidative damage in lipids and proteins of MRC-5 human lung fibroblasts after exposure to Au NPs was investigated *in vitro* by Li et al. [126]. In addition, Au NP-treated cells produced considerably higher lipid hydroperoxides, indicating lipid peroxidation. Furthermore, oxidative damage was confirmed by verifying malondialdehyde (MDA) protein adducts using western blot study.

The impact of oxidative stress on the cytotoxic and genotoxic potential of Ag NPs was investigated against human lung fibroblasts (IMR-90) and the human glioma (U251) cell lines. The findings revealed mitochondrial malfunction and ROS generation by Ag NPs, which resulted in DNA damage and chromosomal abnormalities. The mitochondrial respiratory chain disruption by Ag NPs is thought to cause the generation of ROS and the cessation of ATP synthesis, which leads to DNA damage [35]. Chairuangkitti et al. [127] evaluated the *in vitro* mechanisms of Ag NP (<100 nm) toxicity in connection to the ROS generation in A549 cells. Surprisingly, both ROS-dependent (cytotoxicity) and ROS-independent (cell cycle arrest) mechanisms are involved in Ag NP toxicity in A549 cells. The oxidative stress-dependent activity of NPs is depicted in Figure 2.

Several investigations using various human cells have added to our understanding of the underlying mechanism of NPs concerning ROS production. To a large extent, ROS formation causes cytotoxicity, genotoxicity, and signaling and inflammatory response activation, revealing the mutagenic and carcinogenic properties of NPs [51, 128, 129]. Increased ROS production is highly linked to the size and shape of NPs [130, 131]. However, because research reports vary, it is difficult to draw broad conclusions about shape and size.

In the event of NP exposure to cells, ROS generation is enhanced and leads to hyperoxidation of cell organelles, disruption of mitochondrial activity, endoplasmic reticulum (ER) stress, and unfolded protein response [129, 132–137]. Mitochondrial and ER stresses have cumulative effects on cell ROS production and apoptotic cell death, referred to as cytotoxicity [35, 132]. Furthermore, NPs in the nucleus cause oxidative base damages (8-oxoguanine), strand breakage, and mutations in DNA, resulting in genotoxicity [138–141]. Furthermore, NPs can mediate oxidative-sensitive activation of signaling cascades such as mitogen-activated protein kinase (MAPK), epidermal growth factor receptor, transcription factor activator protein-1, and nuclear factor-kappa B (NF-κB), as well as activate the inflammatory response, which plays a role in mammalian growth and proliferative and developmental processes [97, 129, 142]. Subsequently, when phagocytes, such as neutrophils and macrophages, fail to phagocytose NPs completely, the NADPH-oxidase enzyme system produces ROS. The stimulation of cell signaling pathways such as MAPK, NF-κB, Akt, and RTK by NP-induced ROS promotes an inflammatory cascade of chemokine and cytokine expression. The majority of the subsequent adverse effects elicited by NPs are due to ROS [129].

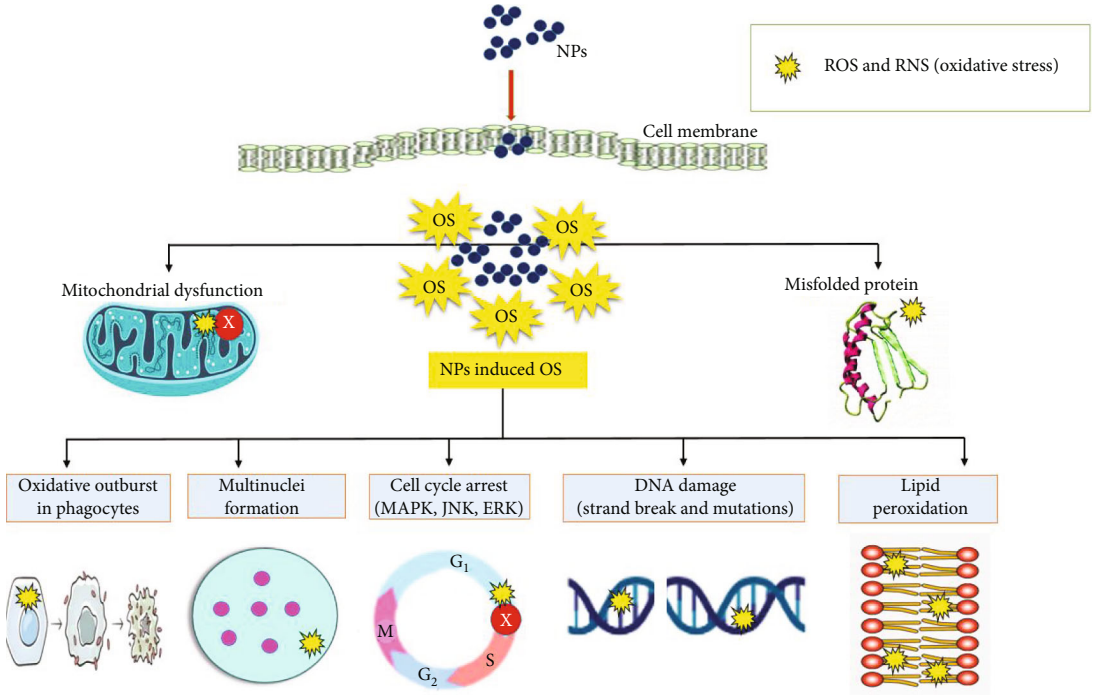

Figure 2: Mechanistic aspects of oxidative stress-mediated nanoparticle-induced toxicity. NPs: nanoparticles; ROS: reactive oxygen species; OS: oxidative stress; RNS: reactive nitrogen species.

For instance, Chen and Schluesener [143] demonstrated that, to the human primary organ system, silver is relatively nontoxic and nonmutagenic. In contrast to antimicrobial metallic NPs (Au, Pt, Cu, Zn, Ti, and so on), silver is recognized to have the most potent antibacterial activity. Ag NPs' powerful antibacterial, antifungal, and antiviral properties are related to their potential to produce H_2O_2, $O_2^{\cdot-}$, $^{\cdot}OH$, and hypochlorous acid (HOCl) singlet oxygen [20, 144–147]. Furthermore, free radicals induced by Ag NPs reduce glutathione to glutathione disulfide that leads to oxidative stress, apoptosis, and stimulation of oxidative signaling pathways [51, 90, 128, 129, 148].

The cytotoxicity, genotoxicity, and inflammatory response of Ag NPs in cells have raised concerns about their unintended human exposure [149]. Ag NPs' cytotoxic, genotoxic, apoptotic, and antiproliferative effects, on the other hand, can be employed to treat glioblastoma [150, 151]. Dakal et al. [152] reported that Ag NP-induced ROS production and increased oxidative stress are linked to antimicrobial effects, with cytotoxic and genotoxic consequences. The most devastating and undeniable issue with using silver or any other nanoparticles in humans is their biosafety and biocompatibility.

5. Green Synthesis of NPs: A Brief Overview

Several methods for the synthesis of NPs have been developed, but their use in biomedical applications is limited due to the use of toxic compounds, the high energy requirements, and the formation of toxic by-products. The choice of a solvent medium, an environmentally friendly reducing agent, and a nontoxic substance for NP stabilization are all important components to consider during the NP preparation process [153]. In this context, green synthesis, which encompasses synthesis through plants, bacteria, fungi, algae, and others, is an effective way for generating NPs [64, 154] as shown in Figure 3(a). The ability of numerous biological entities, such as those indicated above, to generate metal nanoparticles for diverse pharmacological applications has been extensively researched. In general, plant extracts and microorganisms are used in the green, environmentally acceptable synthesis of NPs [65, 66].

Plant-derived NPs overwhelm microorganism-derived NPs, owing to the former's single-step, nonhazardous fabricating process [72]. Furthermore, phyto-mediated synthesis is preferable to microbial synthesis, which requires time-consuming and expensive downstream processing [71]. The plant extract is combined with a metal salt solution in the green synthesis of metal nanoparticles. The electrochemical potential of a metal ion and the pH of the reaction mixture, temperature, concentration, and reaction time are all critical aspects to consider. The phytoconstituents promote metal ion reduction to zero-valent state, followed by nucleation and growth to generate metal NPs [72, 154, 155] as depicted in Figure 3(b).

The plant-mediated synthesis is attributed to protein, phenols, terpenoids, ascorbic acid, and flavonoids that are capable of reducing the ions to nanosize and capping of nanoparticles [156, 157]. This method has several advantages, including energy savings due to the lack of high energy and pressure, use of biological entities that work as both reducing and stabilizing agents, environmental friendliness, lower costs, and the capacity to be employed on a large scale [64, 68, 69, 154]. Several NPs such as TiO_2 using *Azadirachta indica* [9],

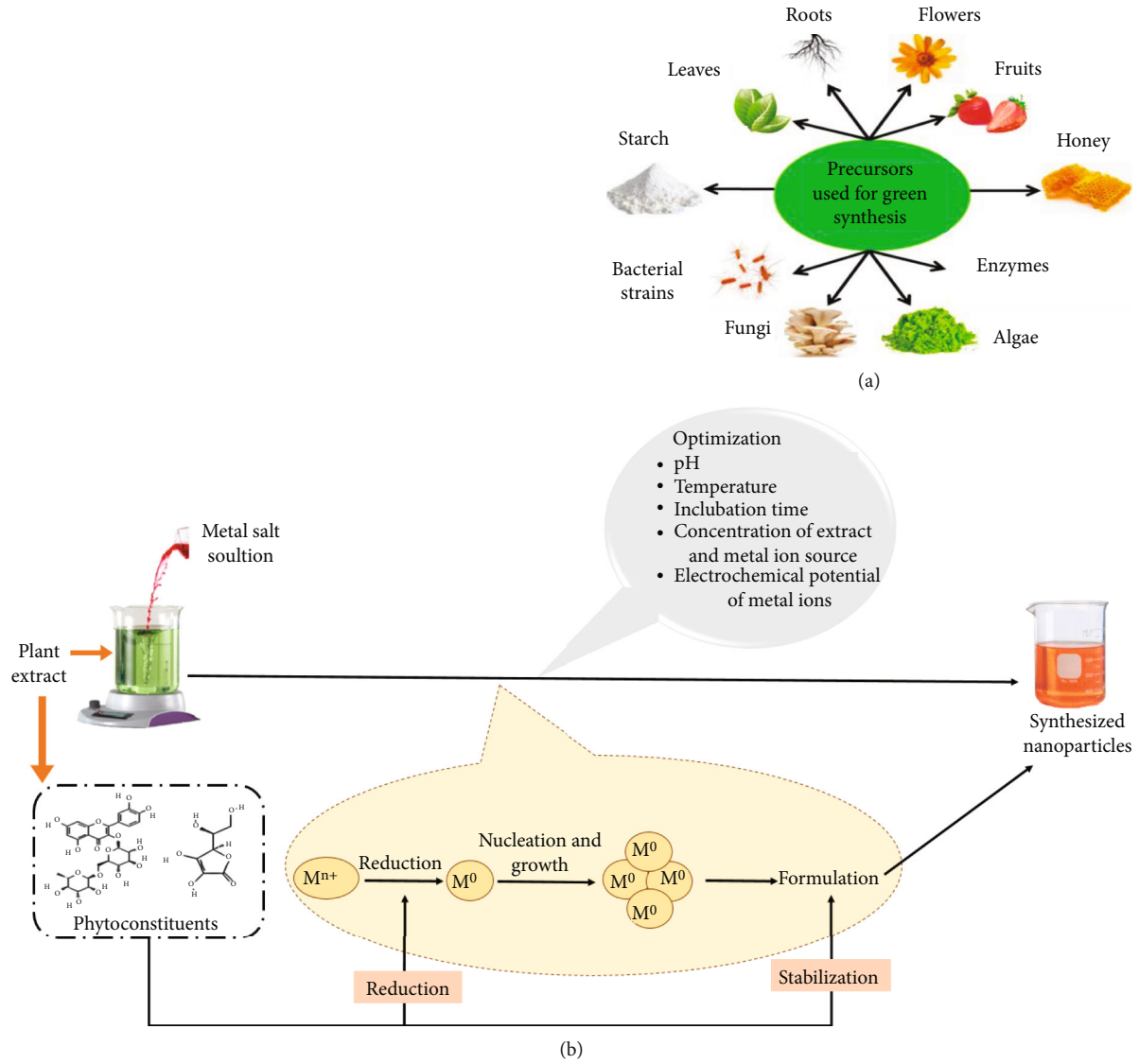

Figure 3: (a) Various precursors used for green synthesis of NPs; (b) mechanistic insight into plant-mediated green synthesis of metallic NPs. Reproduced from Kumar et al. [154] and Bhardwaj et al. [72] under Creative Commons Attribution (CC BY) license (http://creativecommons.org/licenses/by/4.0/).

ZnO using *Ocimum tenuiflorum*[158], CuO using *Ocimum tenuiflorum*[159], and ZnO using *Aloe vera*[160] have been successfully synthesized using the green approach.

6. Antioxidant Potential of Phytoantioxidant Functionalized Nanoparticles

Green synthesis is an innovative method of synthesizing phytoantioxidant functionalized NPs using plant extracts. It is gaining popularity as a result of its cost-effective, environmentally friendly, and large-scale production capabilities. As the importance of green synthesis using plant extracts is already highlighted in Section 5, in Table 1, the antioxidant potential of phytoantioxidant functionalized nanoparticles is shown. *Hibiscus rosa-sinensis* demonstrated excellent ability to synthesize copper NPs at optimal temperatures. These NPs showed good antioxidant potential in ferric-reducing antioxidant power (FRAP) and hydrogen peroxide (H_2O_2) assays [161]. Cu NPs synthesized using *Dioscorea bulbifera* tubers (DBTE) showed 40.81 ± 1.44, 79.06 ± 1.02, and $48.39 \pm 1.46\%$ scavenging against 1,1-diphenyl-2-picryl-hydrazyl (DPPH), nitric oxide (NO), and superoxide radicals ($O_2^{\cdot -}$), respectively; this demonstrated its role in the prevention of oxidative stress, which is a significant factor in the progression of a variety of diseases. The action of DBTE is believed to be due to its substantial ascorbic acid content [162].

The aqueous fruit extract of *Couroupita guianensis* (CG), a promising bioreductant for reducing Au^{3+} ions into their nanoscale analogs, was used to produce gold nanoparticles (Au NPs) in a smaller duration of time. Au NPs have exceptional antioxidant characteristics; DPPH radical scavenging at 100 μg/mL was 70.6%, compared to 96.28% for ascorbic acid. Further, they showed dose-dependent ferric ion

Table 1: Characterization and antioxidant profile of phytoantioxidant functionalized nanoparticles.

Nanoparticle type	Plant (part used)	Reaction time (temp.)	Characterization methods	Size (nm)	Shape	Storage stability	Antioxidant assay and major findings ($IC_{50}\mu g/mL$)	Reference standard in antioxidant assay ($IC_{50}\mu g/mL$)	Data source
Copper	*Hibiscus rosa-sinensis* (leaves)	48 h (RT)	TEM, FT-IR, UV-Vis	NM	NM	n.d.	H_2O_2: 68.5% at 500 $\mu g/mL$ FRAP: OD: 1.2 at 1000 $\mu g/mL$	DNS	[161]
Copper	*Dioscorea bulbifera* (tubers)	5 h (40°C)	TEM, EDX, XRD, DLS, FT-IR, UV-Vis	86-126	Spherical	n.d.	(% at 100 $\mu g/mL$) DPPH: 40.81% NO: 79.06% $O_2^{\cdot-}$: 48.39%	AA (100 $\mu g/mL$) 51.42% 68.37% 14.11%	[162]
Gold	*Couroupita guianensis* (fruits)	1 h (70°C)	TEM, EDX, XRD, DLS, FT-IR, UV-Vis, zeta potential	26	Spherical, triangular, and hexagonal	45 days (RT)	(% and OD at 100 $\mu g/mL$) DPPH: 70.6% $O_2^{\cdot-}$: 89.8% Reducing power: OD: 0.3 $^{\cdot}OH$ (IC_{50}): 36	AA 96.28% 90% OD: >0.7 <20 $\mu g/mL$	[67]
Gold	*Rhus coriaria* (whole plant)	40 min (40°C) followed by 1 h (RT)	UV-Vis, XRD, TEM, FT-IR, zeta potential	15-25	Spherical	n.d.	(% at 800 μM) DPPH: 85.73% ABTS: 96.83%	Glutathione (100%)	[163]
Silver	*Hippophae rhamnoides* (leaves)	24 h (RT)	TEM, UV-Vis, EDX, FT-IR, DLS, zeta potential	10-40	Spherical	1 year	DPPH: >80% at 20 $\mu g/mL$	AA DNS	[164]
Silver	*Costus afer* (leaves)	2 h (90°C)	SEM, TEM, UV-Vis, EDX, FT-IR	20	Spherical	n.d.	DPPH (IC_{50}): <50	Similar to AA	[165]
Silver	*Taraxacum officinale* (leaves)	15 min (RT)	TEM, XRD UV-Vis, FT-IR	5-30	Spherical	4 months (RT)	ABTS (IC_{50}): 45.6 DPPH (IC_{50}): 56.1 NO (IC_{50}): 56.1	AA and catechol (IC_{50}): 40-60	[166]
Silver	*Erythrina suberosa* (leaves)	Overnight (RT)	DLS, TEM, UV-Vis, FT-IR	12-115	Spherical	n.d.	DPPH (IC_{50}): 30.04	BHT (DNS)	[167]
Silver	*Cestrum nocturnum* (leaves)	1 week (RT)	SEM, TEM, XRD, UV-Vis, FT-IR	20	Spherical	n.d.	DPPH: 29.55% H_2O_2: 45.41% $^{\cdot}OH$: 20% $O_2^{\cdot-}$: 8%	AA 24.28% 65.63% 9.47% 32%	[168]
Silver	*Cassia angustifolia* (flowers)	NM (27 ± 1°C)	UV-Vis, SEM, EDX, XRD, FT-IR, DLS, zeta potential	10-80	Spherical	n.d.	DPPH (IC_{50}): 47.24 H_2O_2 (IC_{50}): 78.10 FRAP (IC_{50}): 63.21	AA (IC_{50}) >60 in all tested assays	[169]
Silver	*Camellia sinensis* (leaves), *Allium sativum* (bulb), *Curcuma longa* (rhizome)	2 h (60°C)	SEM, TEM, UV-Vis, EDX, FT-IR	8	Spherical	n.d.	IC_{50} between 5.02 and 22.93 (ABTS, DPPH, $^{\cdot}OH$, $O_2^{\cdot-}$, H_2O_2)	AA and rutoside (IC_{50}) 7.14 ± 1.02 to 14.17 ± 0.24	[170]

Table 1: Continued.

Nanoparticle type	Plant (part used)	Reaction time (temp.)	Characterization methods	Size (nm)	Shape	Storage stability	Antioxidant assay and major findings ($IC_{50}\mu g/mL$)	Reference standard in antioxidant assay ($IC_{50}\mu g/mL$)	Data source
Silver	Spice blend	24 h (NM)	UV-Vis, EDX, SEM, XRD, TEM, FT-IR	6-28	Spherical	n.d.	DPPH (IC_{50}): <31.2 ABTS (IC_{50}): 68.75	Comparable to rutoside	[171]
Silver	*Psidium guajava* (leaves)	30 min (RT)	SEM, TEM, XRD, UV-Vis, EDX, FT-IR, zeta potential	20-35	Spherical	n.d.	DPPH (IC_{50}): 52.53 ABTS (IC_{50}): 55.10	AA (IC_{50}) <40	[172]
Zinc oxide	*Berberis aristata* (leaves)	DNS	SEM, XRD, UV-Vis, FT-IR, EDX, DLS	5-40	Needle-like	n.d.	DPPH (IC_{50}): 3.55	AA (IC_{50}) 1.69	[173]
Silver	*Ananas comosus* (fruit peel)	20-30 min (100°C)	UV-Vis, SEM, EDX, XRD, FT-IR	NM	Spherical	n.d.	(% and OD at 100 $\mu g/mL$) ABTS: 10-20% DPPH: <50% NO: <30% Reducing power: OD < 0.1	BHT (100 $\mu g/mL$) >90% 80% >70% OD > 3.0	[174]
Silver	*Prosopis farcta* (fruits)	25-45 min (50-70°C)	UV-Vis, XRD, TEM	10-15	Spherical	n.d.	DPPH (IC_{50}): 0.70 ± 0.08 FRAP: >25 mmol Fe(II)/mg extract	AA (IC_{50}) (0.26 ± 0.09) NM	[175]
Gold	*Vitex negundo* (leaves)	Overnight (RT)	SEM, TEM, XRD, UV-Vis, FT-IR, EDX	20-70	Spherical	n.d.	DPPH (IC_{50}): 62.18 NO (IC_{50}): 70.45	DNS	[176]
Silver	*Morus alba* (leaves)	10 min (NM)	SEM, TEM, XRD, UV-Vis, EDX, DLS, FT-IR	12-39	Spherical	n.d.	IC_{50} between 25.9 and 97.2 (DPPH, ABTS, $O_2^{\cdot-}$, NO, metal chelating)	AA (IC_{50}) 10-50	[177]
Silver	*Lavandula stoechas* (aerial parts)	30 min (80°C)	UV-Vis, SEM, XRD, TEM, FT-IR	20-50	Spherical	n.d.	(% at 25 mg/mL) DPPH: 75%	AA (25 mg/mL) 100%	[178]
Silver	*Nothapodytes foetida* (leaves)	NM (80°C)	UV-Vis, TEM	20-50	Spherical	n.d.	DPPH (IC_{50}): 22.56 ABTS (IC_{50}): 41.47	Comparable to BHT	[179]
Silver	*Brassica oleracea* (leaves)	10 min (RT)	TEM, EDX, FT-IR, UV-Vis, zeta potential	20	Spherical	n.d.	(% at 200 $\mu g/mL$) DPPH: 80% NO: 80% $O_2^{\cdot-}$: 60-80% $^{\cdot}OH$: 60-80%	AA (200 $\mu g/mL$) >80% in all tested assays	[180]
Silver	*Blighia sapida* (leaves)	2 h (30 ± 2°C)	UV-Vis, FT-IR, SEM	50-70	Spherical	n.d.	(% at 150 $\mu g/mL$) DPPH: 75.42% Reducing power: 53.52%	AA (150 $\mu g/mL$) >80% 70.19%	[181]
Iron	*Asphodelus aestivus* (aerial parts)	20 min (50-60°C)	SEM, TEM, XRD, UV-Vis, FT-IR, EDX, TGA, zeta potential	20-25	NM	n.d.	DPPH (IC_{50}): 3.48	NM	[182]

Table 1: Continued.

Nanoparticle type	Plant (part used)	Reaction time (temp.)	Characterization methods	Size (nm)	Shape	Storage stability	Antioxidant assay and major findings ($IC_{50}\mu g/mL$)	Reference standard in antioxidant assay ($IC_{50}\mu g/mL$)	Data source
Silver	*Atropa acuminata* (leaves)	30 min (60°C)	TEM, XRD, EDX, DLS, zeta potential, UV-Vis, FT-IR	5-20	Spherical	n.d.	DPPH (IC_{50}): 16.08 H_2O_2 (IC_{50}): 25.4 $O_2^{\cdot-}$ (IC_{50}): 21.12	AA (IC_{50}): 27.68 GA (IC_{50}): 28.31 AA (IC_{50}): 30.48	[183]
Titanium dioxide	*Psidium guajava* (leaves)	24 h (RT)	FT-IR, SEM, EDX, XRD	32.58	Spherical	n.d.	(% at 500 μg/mL) DPPH: >85% TAA: >90%	AA (500 μg/mL) >90% <50%	[184]
Titanium dioxide	*Cola nitida* (leaves, pods, seeds, and seed shell)	1 h (RT)	UV-Vis, FT-IR, TEM, XRD, EDX	25-191	Spherical	n.d.	(% at 10-80 μg/mL) DPPH: 32.61-62.06% H_2O_2: 78.45-99.23 %	NM	[185]

Note: n.d.: not determined; NM: not mentioned; DNS: data not shown; AA: ascorbic acid; BHT: butylated hydroxytoluene; GA: gallic acid; IC_{50}: half-maximal inhibitory concentration; %: percent scavenging; RT: room temperature; nm: nanometer; $O_2^{\cdot-}$: superoxide radical; DPPH: DPPH radical scavenging activity; H_2O_2: hydrogen peroxide radical scavenging activity; ABTS: ABTS radical scavenging activity; $^{\cdot}OH$: hydroxyl radical scavenging activity; NO: nitric oxide radical scavenging activity; FRAP: ferric-reducing antioxidant power; UV-Vis: ultraviolet and visible absorption spectroscopy; SEM: scanning electron microscopy; TEM: transmission electron microscopy; FT-IR: Fourier transform infrared spectroscopy; XRD: X-ray diffraction analysis; EDX: energy-dispersive X-ray spectroscopy; DLS: dynamic light scattering; TGA: thermal gravimetric analysis; TAA: total antioxidant activity.

reduction activity and hydroxyl ($^{\cdot}OH$) radical scavenging ability, which is primarily due to the presence of antioxidant residues, such as phenolics from the CG on its surface, which have been recognized, using various analytical techniques [67]. Subsequently, Au NPs were synthesized using *Rhus coriaria*, which is used as a reducing and capping agent. The plant polyphenols may play a role in reducing gold ions, as evident from FT-IR analysis. *In vitro*, antioxidant activity studies showed that DPPH (85.73% at 800 μM) and ABTS activities (96.83% at 800 μM) increased in a dose-dependent manner (25-800 μM) which is related to the adsorption of phytocompounds on the surface of the Au NPs [163].

Hippophae rhamnoides leaves were utilized by Kalaiyarasan et al. [164] for the biosynthesis of silver NPs (Ag NPs). As the sample concentrations (5-25 μg/mL) began to rise, the DPPH radical scavenging abilities increased, indicating that the antioxidant capabilities of the samples are dosage-dependent. The activity of Ag NPs has enhanced by more than tenfold when compared to that of the plant extract alone, which can be attributable to the presence of plant phytochemicals, including flavonoids. Due to these flavonoids and silver ions, antioxidant activity may occur via a single electron transfer mode [186, 187]. Similarly, Ag NPs developed using *Costus after* leaves were more effective DPPH scavengers than the leaf extract alone, and their antioxidant activity was comparable to those of ascorbic acid with IC_{50} value < 50 μg/mL[165]. Ag NPs fabricated using *Taraxacum officinale* leaves demonstrated substantial antioxidant capability against ABTS (IC_{50} 45.6 μg/mL), DPPH (IC_{50} 56.1 μg/mL), and NO (IC_{50} 55.2 μg/mL). Catechol and ascorbic acid were utilized as controls, with IC_{50} 40 to 60 μg/mL [166]. Ag NPs synthesized using *Erythrina suberosa* leaves demonstrated significant antioxidant activity in a DPPH radical scavenging experiment, with IC_{50} 30.04 μg/mL. The BHT was used as a standard. The findings significantly support the use of Ag NPs as natural antioxidants against oxidative stress-linked degenerative disorders [167].

Ag NPs synthesized using *Cestrum nocturnum* leaves, when evaluated for antioxidant activity, were found more active scavengers of DPPH (29.55% at 100 μg/mL) as compared to ascorbic acid at a similar concentration (24.28%). Further, Ag NPs showed 45.41 and 20% scavenging of H_2O_2 and $^{\cdot}OH$ as compared to ascorbic acid (65.63 and 9.47% at 250 μg/mL, respectively). However, negligible activity was reported in the $O_2^{\cdot-}$ scavenging assay [168].

Subsequently, DPPH, H_2O_2, and FRAP assays were used to estimate the antioxidant activity of Ag NPs prepared using *Cassia angustifolia* flowers. Ag NPs were found to have FRAP and DPPH IC_{50} values of 63.21 ± 0.75 and 47.24 ± 0.5 μg/mL, respectively. On the other hand, in the H_2O_2 assay, the IC_{50} value was 78.10 ± 1.2 μg/mL [169]. The H_2O_2 scavenging is well related to the presence of phenolic components in the samples [188]. A compound mixture containing *Camellia sinensis* leaves, *Allium sativum* bulbs, and *Curcuma longa rhizome* mediated Ag NPs which were found highly active scavengers of ABTS, DPPH, $^{\cdot}OH$, $O_2^{\cdot-}$, and H_2O_2 radicals with IC_{50} ranging between 5.02 ± 1.11 and 22.93 ± 0.34 μg/mL in comparison to rutoside and ascorbic acid (IC_{50} between 7.14 ± 1.02 and 14.17 ± 0.24 μg/mL) [170]. Interestingly, Ag NPs synthesized using a spice blend exhibited IC_{50} < 31.25 and 68.75 μg/mL against DPPH and ABTS, respectively, and the findings are comparable to standard rutoside. The different functional groups of spice blends present on the surface of Ag NPs could be responsible for the activity [171]. *Psidium guajava* leaves were utilized by Wang et al. [172] for the successful synthesis of Ag NPs, which were found to be highly active in scavenging free radicals with IC_{50}52.53 ± 0.31 μg/mL (DPPH) and 55.10 ± 0.29 μg/mL (ABTS). In contrast, standard ascorbic acid showed IC_{50} < 40 μg/mL against both DPPH and ABTS radicals. On the other hand, *Berberis aristata* leaf-mediated ZnO NPs, when evaluated for antioxidant activity using DPPH, showed 61.63% scavenging at 5 μg/mL, lower than ascorbic acid (87.76%) at the same concentration [173]. On the other hand, Ag NPs synthesized using *Ananas comosus* fruit peel exhibited a moderate ABTS and DPPH and reduced power and nitric oxide (NO) scavenging activity as compared to standard BHT [174]. The action is due to the involvement of numerous plant functional groups attached to the surface of Ag NPs [189].

The antioxidant activity of Ag NPs fabricated using *Prosopis farcta* (PF) fruits was evaluated using DPPH and FRAP assay. Ag NPs had a scavenging activity of 43 to 63% at doses of 0.2-1 mg/mL; however, the effect was lower (74% at 1 mg/mL) than that of standard ascorbic acid. Ag NPs were also found active with FRAP activity > 25 mmol Fe(II)/mg extract at 1 mg/mL [175]. The primary phytochemicals responsible for the antioxidant capacity are phenolics and flavonoids, abundant in PF [190]. Subsequently, *Vitex negundo* leaf-mediated Au NPs exhibited IC_{50} values of 62.18 and 70.45 μg/mL in DPPH and nitric oxide assays, respectively [176]. Moreover, *Morus alba* leaves were utilized by Das et al. [177] for synthesizing Ag NPs. When compared to ascorbic acid (10-50 μg/mL), antioxidant activity of produced NPs against DPPH, ABTS, superoxide, and nitric oxide was dose-dependent with IC_{50} ranging between 25.9 and 97.2 μg/mL. The lowest IC_{50} (25.9 μg/mL) of Ag NPs was observed in the ABTS assay.

The DPPH radical scavenging activity of *Lavandula stoechas* aerial part-mediated Ag NPs (75% scavenging at 25 mg/mL) is attributed to phytochemical compounds such as phenol and terpenoid flavonoids that are involved in the reduction of Ag^+ to Ag^0[178]. *Nothapodytes foetida* leaf-mediated Ag NPs (100 μg/mL) exhibited strong antioxidant potential with 93.80% inhibition of DPPH and comparatively lower ABTS radical scavenging activity (84.59% at the same conc.); however, results are comparable to standard BHT [179].

Likewise, Ansar et al. [180] utilized *Brassica oleracea* leaves for Ag NP synthesis. Ag NPs revealed a strong antioxidant potential against DPPH, NO, superoxide ($O_2^{\cdot-}$), and hydroxyl radical ($^{\cdot}OH$) with percent scavenging ranged between 60 and 80% at 200 μg/mL as compared to standard ascorbic acid (>80% at 200 μg/mL). The antioxidant capacity of these nanoparticles could be attributed to the abundance of surface fabricated flavonoids and phenolics as capping agents [180]. In another study, Akintola et al. [181]

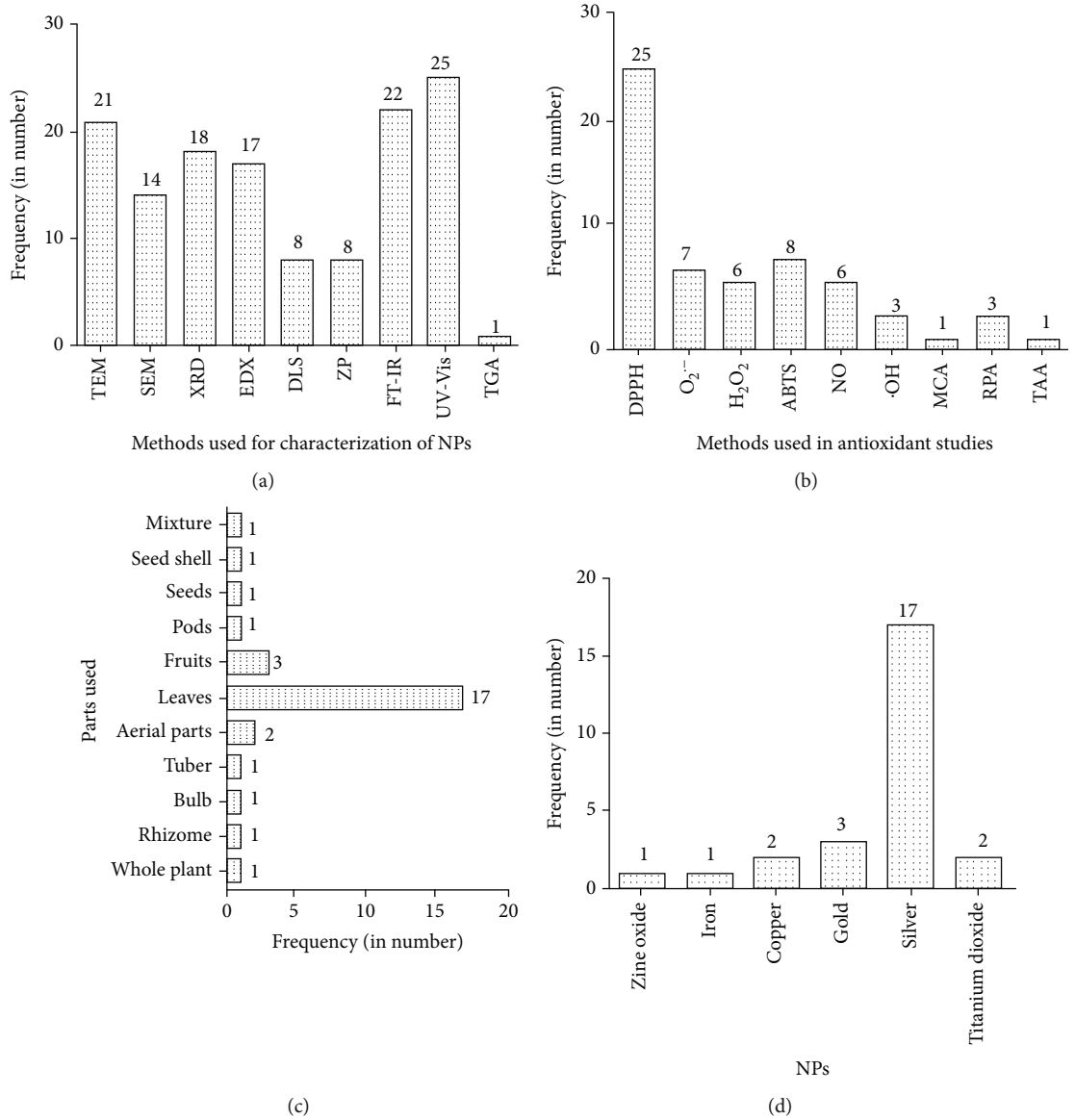

Figure 4: Frequency of methods used for (a) NP characterization, (b) antioxidant studies, (c) plant part used, and (d) types of NPs. Note: $O_2^{\cdot-}$: superoxide radical; DPPH: DPPH radical scavenging activity; H_2O_2: hydrogen peroxide radical scavenging activity; ABTS: ABTS radical scavenging activity; ·OH: hydroxyl radical scavenging activity; NO: nitric oxide radical scavenging activity; FRAP: ferric-reducing antioxidant power; UV-Vis: ultraviolet and visible absorption spectroscopy; SEM: scanning electron microscopy; TEM: transmission electron microscopy; FT-IR: Fourier transform infrared spectroscopy; XRD: X-ray diffraction analysis; EDX: energy-dispersive X-ray spectroscopy; DLS: dynamic light scattering; TGA: thermal gravimetric analysis; TAA: total antioxidant activity.

investigated the antioxidant effects of Ag NPs (synthesized using *Blighia sapida* leaves) using DPPH and reducing power assay. Ag NPs at different concentrations (50, 75, 100, 125, and 150 μg/mL) scavenged DPPH by 58.10, 59.26, 62.33, 71.24, and 75.42%, respectively. These effects, however, are less pronounced than those of ascorbic acid (>80% at 150 μg/mL). Ag NPs had a maximum reduction capability of 53.52% at 150 μg/mL compared to ascorbic acid (70.19%).

Similarly, iron NPs produced using *Asphodelus aestivus* aerial parts scavenged DPPH with IC_{50} 3.48 μg/mL [182]. In addition, Rajput et al. [183] evaluated the antioxidant potential of Ag NPs (*Atropa acuminata* leaf mediated) using DPPH, H_2O_2, and $O_2^{\cdot-}$ assay with IC_{50} 16.08, 25.4, and 21.12 μg/mL, which is lower than standard ascorbic and gallic acid (IC_{50} 27.68-30.48 μg/mL). In the DPPH and total antioxidant activity (TAA) assays, TiO_2 NPs made from *Psidium guajava* leaves displayed strong antioxidant capability, with >85 and >90% scavenging at 500 μg/mL, respectively. When compared to standard ascorbic acid, the action of NPs in TAA is more prominent [184]. On the other hand, different parts (leaves, pods, seeds, and seed shell) of *Cola nitida* (10-80 μg/mL) exhibited 32.61-62.06% scavenging of DPPH. In addition, the scavenging ranged between 78.45 and 99.23% in H_2O_2 assay [185]. The antioxidant activity of phytoantioxidant functionalized NPs is related to the bioactive composition of the plant. The substantial body of

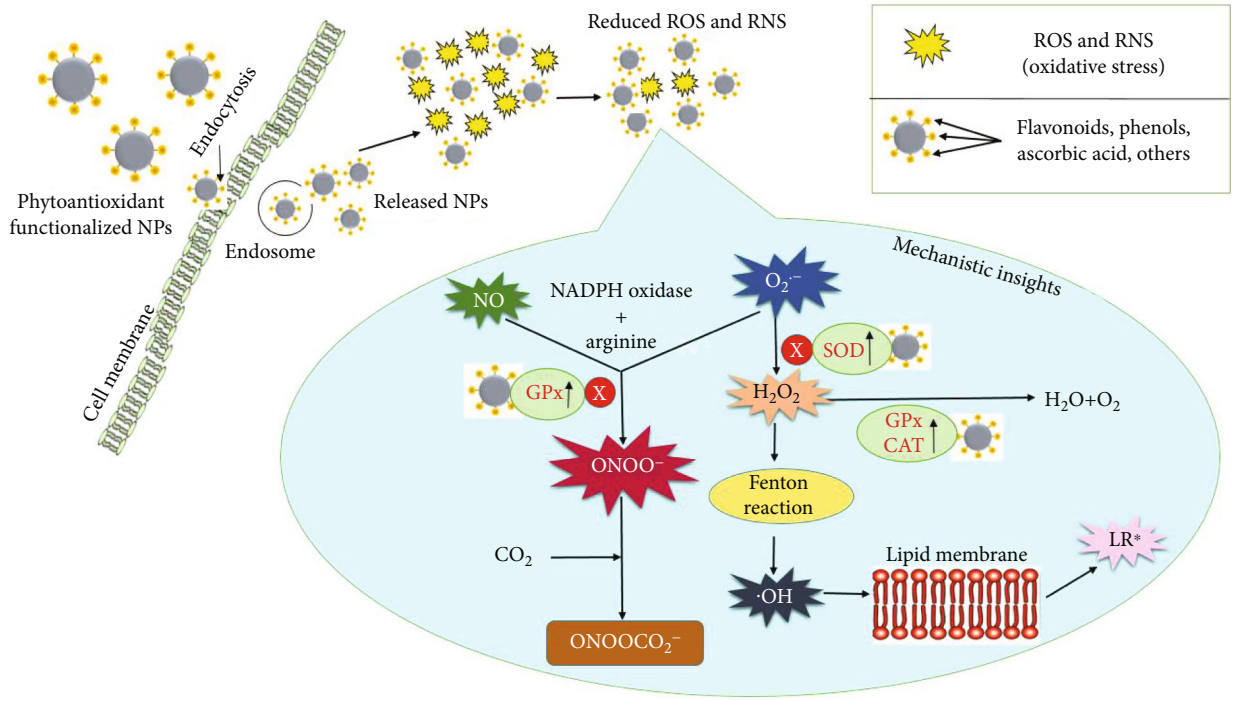

Figure 5: Role of phytoantioxidant functionalized nanoparticles in ameliorating oxidative stress. Note: GPx: glutathione peroxidase; CAT: catalase; $O_2^{\cdot-}$: superoxide radical; H_2O_2: hydrogen peroxide; LR∗: lipid radical; H_2O: water; O_2: oxygen; SOD: superoxide dismutase; ·OH: hydroxyl radical; NO: nitric oxide; CO_2: carbon dioxide; NADPH oxidase: nicotinamide adenine dinucleotide phosphate oxidase; $ONOOCO_2^-$: nitrosoperoxycarbonate; $ONOO^-$: peroxynitrate.

research, including those selected in this study, did not go into extensive depth about plant selection. However, the selection of antioxidant-rich plants is the most important factor in the activity of phytoantioxidant functionalized NPs.

The frequency of methodologies utilized for characterization of NPs, their significance, methods used for assessing antioxidant activity, plant parts used in green synthesis, and choice of NPs were all examined critically. The most commonly used strategy for antioxidant investigations was observed to be DPPH, followed by ABTS, superoxide, nitric oxide, and others. Surprisingly, all of the free radicals were successfully scavenged by the tested NPs. On the other hand, almost all plant parts have been used, but leaves are primarily harvested to synthesize NPs (Figure 4 and Table 1). Ag NPs are frequently employed in practice due to their inclusion in various formulations; the majority of researchers are currently focusing on these NPs, with silver topping the list of studies, followed by gold, copper, iron, and zinc oxide NPs.

The most common approach for measuring surface plasmon resonance and investigating the optical characteristics of produced NPs is UV-visible absorption spectroscopy, followed by FT-IR analysis to identify functional groups corresponding to surface-attached bioactive compounds responsible for reduction and stabilization. In 14, 21, and 18 investigations included in this study ($N = 26$), the shape and size of produced NPs were analyzed using scanning electron microscopy, transmission electron microscopy, and X-ray diffraction analysis. Dynamic light scattering analysis was also used to determine hydrodynamic size and surface charge. Zeta potential measurements were carried out to assess NP stability; a relatively high zeta potential value shows that the surface has a substantial electric charge, demonstrating its stability. The thermal stability of NPs was evaluated using thermal gravimetric analysis (TGA) in a single study (Figure 4 and Table 1). Furthermore, elemental analysis was carried out using energy-dispersive X-ray analysis (EDX), which is used to detect impurities [67, 163, 166, 169, 177, 182, 183].

7. Mechanistic Basis of Oxidative Stress Management by Phytoantioxidant Functionalized NPs

Antioxidant defenses mitigate the detrimental effects of ROS and RNS, which are generated by a variety of endogenous and external mechanisms [88]. NADPH oxidase, lipoxygenase, angiotensin II, and myeloperoxidase (MPO) are all endogenous producers of ROS and RNS [191]. NADPH oxidase produces superoxide radical ($O_2^{\cdot-}$), which in turn is dissociated into the H_2O_2 by SOD [192]. Glutathione peroxidase (GPx), SOD, and CAT aid in the breakdown of free radicals into safe and less active molecules (H_2O_2/alcohol, and O_2) [2, 193–198]. The phytoconstituents upregulate the level of antioxidant enzymes, and SOD is a significant force in radical neutralization [198]. As previously stated, SOD converts $O_2^{\cdot-}$ to H_2O_2, which is then degraded by CAT and GPx into water and oxygen, preventing the formation of ·OH [199, 200]. Glutathione-S-transferase and

glucose-6-phosphate dehydrogenase are two other antioxidant enzymes [200]. The inhibition of ·OH generation contributed to lipid radical (LR∗) inhibition, which is generated due to the interplay between ·OH and lipid membrane [198, 199]. GPx inhibits the peroxynitrite anion produced by numerous interactions, such as when combined with carbon dioxide to make nitrosoperoxycarbonate, which disintegrates over time to form nitrogen dioxide and carbonate radicals [198, 201].

On the other hand, nonenzymatic antioxidants interact with ROS and RNS to stop the free radical chain. In continuation, blood contains α-tocopherol, bilirubin, and β-carotene whereas albumin and uric acid make about 85% of antioxidant defense in plasma [89]. The phytoconstituents on nanoparticle surfaces reduce oxidative stress [72]. In Figure 5, a mechanistic approach to the protective impact of phytoantioxidant functionalized nanoparticles in the regulation of oxidative stress is highlighted.

The abundance of terpenoids, ascorbic acid, flavonoids, phenols, and other bioactive phytoconstituents on the surface of NPs is strongly correlated with their antioxidant activity [178, 180]. The phytoantioxidant functionalized nanoparticles would upregulate the antioxidant enzymes, and nonenzymatic components such as ascorbic acid on the surface of these NPs would also neutralize the adverse effects of free radicals.

8. Conclusion and Perspectives

In conclusion, the evidence of oxidative stress caused by nanoparticle exposure raises concerns about their use in humans. Although the antioxidant potential of phytoantioxidant functionalized NPs is well documented, the majority of the researches have been conducted *in vitro*. The bioactive substances like flavonoids and phenols are correlated to the antioxidant action of these NPs. The stability of nanoparticles is an important aspect, but only three articles have investigated the storage stability of these NPs. Most studies lack a zeta potential measurement, which is an indicator of stability. The data compiled in this review is expected to serve as a roadmap for researchers to fulfill various gaps. Because of their widespread use in a variety of industries, Ag NPs are the most investigated NPs. It is suggested that the plant utilized for green synthesis should be selected carefully, as antioxidant action is linked to phytoconstituents. As an alternative to NPs, phytoantioxidant functionalized NPs could be employed; however, high-quality toxicity studies are necessary. Nanotechnology is rapidly expanding, but research into the nanoparticles' toxicological impacts on human health and the environment is still in its early stages.

Data Availability

All data are included in the manuscript.

Conflicts of Interest

The authors declare no conflict of interest.

Authors' Contributions

A.B. supervised the first draft. A.K. and V.A. wrote the first draft of the manuscript. A.R. and A.K. contributed in figures and in providing literature. R.V., D.K., N.T., E.N., O.K., and K.K. critically reviewed the first draft. A.K. and V.A. improved the first draft. The final submitted version of the manuscript has been seen and approved by all contributors.

Acknowledgments

The authors (A.B., V.A., A.K., and A.R.) are grateful to Revered Swami Ramdev and Patanjali Herbal Research Department colleagues for their support, as well as the Patanjali Research Foundation Trust for providing all essential facilities. This work was supported by the Excellence Project PrF UHK 2011/2021-2022 and MH CZ-DRO (UHHK, 00179906).

Supplementary Materials

Graphical abstract. *(Supplementary Materials)*

References

[1] C. Gerber and H. P. Lang, "How the doors to the nanoworld were opened," *Nature Nanotechnology*, vol. 1, no. 1, pp. 3–5, 2006.

[2] V. Sharma, D. Anderson, and A. Dhawan, "Zinc oxide nanoparticles induce oxidative DNA damage and ROS-triggered mitochondria mediated apoptosis in human liver cells (HepG2)," *Apoptosis*, vol. 17, no. 8, pp. 852–870, 2012.

[3] J. Jeevanandam, A. Barhoum, Y. S. Chan, A. Dufresne, and M. K. Danquah, "Review on nanoparticles and nanostructured materials: history, sources, toxicity and regulations," *Beilstein Journal of Nanotechnology*, vol. 9, no. 1, pp. 1050–1074, 2018.

[4] W. B. Tan, S. Jiang, and Y. Zhang, "Quantum-dot based nanoparticles for targeted silencing of HER2/neu gene via RNA interference," *Biomaterials*, vol. 28, no. 8, pp. 1565–1571, 2007.

[5] K. Y. Yoon, J. Hoon Byeon, J. H. Park, and J. Hwang, "Susceptibility constants of Escherichia coli and Bacillus subtilis to silver and copper nanoparticles," *Science of the Total Environment*, vol. 373, no. 2-3, pp. 572–575, 2007.

[6] J. Kreuter and S. Gelperina, "Use of nanoparticles for cerebral cancer," *Tumori Journal*, vol. 94, no. 2, pp. 271–277, 2008.

[7] H. A. Salam, P. Rajiv, M. Kamaraj, P. Jagadeeswaran, S. Gunalan, and R. Sivaraj, "Plants: green route for nanoparticle synthesis," *International Journal of Biological Sciences*, vol. 1, pp. 85–90, 2012.

[8] A. Kumar, S. Singh, and D. Kumar, "Evaluation of antimicrobial potential of cadmium sulphide nanoparticles against bacterial pathogens," *International Journal of Pharmaceutical Sciences and Research*, vol. 24, pp. 202–207, 2014.

[9] B. K. Thakur, A. Kumar, and D. Kumar, "Green synthesis of titanium dioxide nanoparticles using _Azadirachta indica_ leaf extract and evaluation of their antibacterial activity," *South African Journal of Botany*, vol. 124, pp. 223–227, 2019.

[10] N. Thakur, K. K. Anu, A. Kumar, and A. Kumar, "Effect of (Ag, Zn) co-doping on structural, optical and bactericidal

properties of CuO nanoparticles synthesized by a microwave-assisted method," *Dalton Transactions*, vol. 50, no. 18, pp. 6188–6203, 2021.

[11] H. Chang, C. S. Jwo, C. H. Lo, T. T. Tsung, M. J. Kao, and H. M. Lin, "Rheology of CuO nanoparticle suspension prepared by ASNSS," *Reviews on Advanced Materials Science*, vol. 10, pp. 128–132, 2005.

[12] K. Zhou, R. Wang, B. Xu, and Y. Li, "Synthesis, characterization and catalytic properties of CuO nanocrystals with various shapes," *Nanotechnology*, vol. 17, no. 15, pp. 3939–3943, 2006.

[13] V. Aruoja, H. C. Dubourguier, K. Kasemets, and A. Kahru, "Toxicity of nanoparticles of CuO, ZnO and TiO_2 to microalgae _Pseudokirchneriella subcapitata_," *Science of the Total Environment*, vol. 407, no. 4, pp. 1461–1468, 2009.

[14] D. L. Huber, "Synthesis, properties, and applications of iron nanoparticles," *Small*, vol. 1, no. 5, pp. 482–501, 2005.

[15] K. Gerloff, C. Albrecht, A. W. Boots, I. Forster, and R. P. F. Schins, "Cytotoxicity and oxidative DNA damage by nanoparticles in human intestinal Caco-2 cells," *Nanotoxicology*, vol. 3, no. 4, pp. 355–364, 2009.

[16] T. Jin, D. Sun, J. Y. Su, H. Zhang, and H. J. Sue, "Antimicrobial efficacy of zinc oxide quantum dots against Listeria monocytogenes, Salmonella enteritidis, and Escherichia coli O157:H7," *Journal of Food Science*, vol. 74, no. 1, pp. 46–52, 2009.

[17] K. Schilling, B. Bradford, D. Castelli et al., "Human safety review of nano titanium dioxide and zinc oxide," *Photochemical and Photobiological Sciences*, vol. 9, no. 4, pp. 495–509, 2010.

[18] C. N. Lok, C. M. Ho, R. Chen et al., "Proteomic analysis of the mode of antibacterial action of silver nanoparticles," *Journal of Proteome Research*, vol. 5, no. 4, pp. 916–924, 2006.

[19] S. K. Gogoi, P. Gopinath, A. Paul et al., "Green Fluorescent Protein-ExpressingEscherichiacolias a model system for investigating the antimicrobial activities of silver nanoparticles," *Langmuir*, vol. 22, no. 22, pp. 9322–9328, 2006.

[20] J. S. Kim, E. Kuk, K. N. Yu et al., "Antimicrobial effects of silver nanoparticles," *Nanomedicine*, vol. 3, no. 1, pp. 95–101, 2007.

[21] U. Samuel and J. P. Guggenbichler, "Prevention of catheter-related infections: the potential of a new nano-silver impregnated catheter," *International Journal of Antimicrobial Agents*, vol. 23, pp. 75–78, 2004.

[22] J. Chen, C. M. Han, X. W. Lin, Z. J. Tang, and S. J. Su, "Effect of silver nanoparticle dressing on second degree burn wound," *Zhonghua Wai Ke Za Zhi*, vol. 44, pp. 50–52, 2006.

[23] K. Dunn and V. Edwards-Jones, "The role of Acticoat™ with nanocrystalline silver in the management of burns," *Burns*, vol. 30, pp. S1–S9, 2004.

[24] V. R. Pasupuleti, T. N. V. Prasad, R. A. Shiekh et al., "Biogenic silver nanoparticles using Rhinacanthus nasutus leaf extract: synthesis, spectral analysis, and antimicrobial studies," *International Journal of Nanomedicine*, vol. 8, pp. 3355–3364, 2013.

[25] G. Montes-Hernandez, J. Pironon, and F. Villieras, "Synthesis of a red iron oxide/montmorillonite pigment in a CO_2-rich brine solution," *Journal of Colloid and Interface Science*, vol. 303, no. 2, pp. 472–476, 2006.

[26] M. R. Hoffmann, S. T. Martin, W. Y. Choi, and D. W. Bahnemann, "Environmental applications of semiconductor photocatalysis," *Chemical Reviews*, vol. 95, no. 1, pp. 69–96, 1995.

[27] A. Sinha and S. K. Khare, "Mercury bioaccumulation and simultaneous nanoparticle synthesis by Enterobacter sp. cells," *Bioresource Technology*, vol. 102, no. 5, pp. 4281–4284, 2011.

[28] C. Gélis, S. Girard, A. Mavon, M. Delverdier, N. Paillous, and P. Vicendo, "Assessment of the skin photoprotective capacities of an organo-mineral broad-spectrum sunblock on twoex vivoskin models," *Photodermatology Photoimmunology and Photomedicine*, vol. 19, no. 5, pp. 242–253, 2003.

[29] B. Trouiller, R. Reliene, A. Westbrook, P. Solaimani, and R. H. Schiestl, "Titanium dioxide nanoparticles induce DNA damage and genetic instability in vivo in mice," *Cancer Research*, vol. 69, no. 22, pp. 8784–8789, 2009.

[30] O. Janson, S. Gururaj, S. Pujari-Palmer et al., "Titanium surface modification to enhance antibacterial and bioactive properties while retaining biocompatibility," *Materials Science and Engineering, C*, vol. 96, pp. 272–279, 2019.

[31] C. L. C. Mora, A. Mueller, and A. P. G. Janssen, "Antibacterial medical product and method for producing same," 2018, US Patent 10,143,196.

[32] I. Passagne, M. Morille, M. Rousset, I. Pujalte, and B. L'Azou, "Implication of oxidative stress in size-dependent toxicity of silica nanoparticles in kidney cells," *Toxicology*, vol. 299, no. 2-3, pp. 112–124, 2012.

[33] A. A. Yaqoob, H. Ahmad, T. Parveen et al., "Recent advances in metal decorated nanomaterials and their various biological applications: a review," *Frontiers in Chemistry*, vol. 8, pp. 1–23, 2020.

[34] A. A. Yaqoob, T. Parveen, K. Umar, and M. N. M. Ibrahim, "Role of nanomaterials in the treatment of wastewater: a review," *Water*, vol. 12, pp. 1–30, 2020.

[35] P. V. AshaRani, G. L. K. Mun, M. P. Hande, and S. Valiyaveettil, "Cytotoxicity and genotoxicity of silver nanoparticles in human cells," *ACS Nano*, vol. 24, pp. 279–290, 2009.

[36] B. Nowack and T. D. Bucheli, "Occurrence, behavior and effects of nanoparticles in the environment," *Environmental Pollution*, vol. 150, no. 1, pp. 5–22, 2007.

[37] A. Dhawan and V. Sharma, "Toxicity assessment of nanomaterials: methods and challenges," *Analytical and Bioanalytical Chemistry*, vol. 398, no. 2, pp. 589–605, 2010.

[38] B. A. Jamuna and R. V. Ravishankar, "Environmental risk, human health and toxic effects of nanoparticles," in *Nanomaterials for Environmental Protection*, B. I. Kharisov, O. V. Kharissova, and H. V. Rasika Dias, Eds., pp. 523–535, John Wiley & Sons, New Jersey, 2014.

[39] A. Gojova, B. Guo, R. S. Kota, J. C. Rutledge, I. M. Kennedy, and A. I. Barakat, "Induction of inflammation in vascular endothelial cells by metal oxide nanoparticles: effect of particle composition," *Environmental Health Perspectives*, vol. 115, no. 3, pp. 403–409, 2007.

[40] H. Yang, C. Liu, D. Yang, H. Zhang, and Z. Xi, "Comparative study of cytotoxicity, oxidative stress and genotoxicity induced by four typical nanomaterials: the role of particle size, shape and composition," *Journal of Applied Toxicology*, vol. 29, no. 1, pp. 69–78, 2009.

[41] I. F. Osman, A. Baumgartner, E. Cemeli, J. N. Fletcher, and D. Anderson, "Genotoxicity and cytotoxicity of zinc oxide

and titanium dioxide in HEp-2 cells," *Nanomedicine*, vol. 5, no. 8, pp. 1193–1203, 2010.

[42] S. A. Hackenberg, A. Scherzed, M. Kessler et al., "Silver nanoparticles: evaluation of DNA damage, toxicity and functional impairment in human mesenchymal stem cells," *Toxicology Letters*, vol. 201, no. 1, pp. 27–33, 2011.

[43] V. Sharma, P. Singh, A. K. Pandey, and A. Dhawan, "Induction of oxidative stress, DNA damage and apoptosis in mouse liver after sub-acute oral exposure to zinc oxide nanoparticles," *Mutation Research*, vol. 745, no. 1-2, pp. 84–91, 2012.

[44] Q. Sun, D. Tan, Y. Ze et al., "Pulmotoxicological effects caused by long-term titanium dioxide nanoparticles exposure in mice," *Journal of Hazardous Materials*, vol. 235, pp. 47–53, 2012.

[45] W. MacNee and K. Donaldson, "Mechanism of lung injury caused by PM10 and ultrafine particles with special reference to COPD," *European Respiratory Journal*, vol. 21, no. 40, pp. 47–51, 2003.

[46] H. Y. Jia, Y. Liu, X. J. Zhang et al., "Potential oxidative stress of gold nanoparticles by induced-NO releasing in serum," *Journal of the American Chemical Society*, vol. 131, no. 1, pp. 40-41, 2009.

[47] S. Durocher, A. Rezaee, C. Hamm, C. Rangan, S. Mittler, and B. Mutus, "Disulfide-linked, gold nanoparticle based reagent for detecting small molecular weight thiols," *Journal of the American Chemical Society*, vol. 131, no. 7, pp. 2475–2477, 2009.

[48] C. Kirchner, T. Liedl, S. Kudera et al., "Cytotoxicity of colloidal CdSe and CdSe/ZnS nanoparticles," *Nano Letters*, vol. 5, no. 2, pp. 331–338, 2005.

[49] H. Moriwaki, M. R. Osborne, and D. H. Phillips, "Effects of mixing metal ions on oxidative DNA damage mediated by a Fenton-type reduction," *Toxicology in Vitro*, vol. 22, no. 1, pp. 36–44, 2008.

[50] S. Arora, J. Jain, J. M. Rajwade, and K. M. Paknikar, "Cellular responses induced by silver nanoparticles: _In vitro_ studies," *Toxicology Letters*, vol. 179, no. 2, pp. 93–100, 2008.

[51] M. Ahamed, M. A. Siddiqui, M. J. Akhtar, I. Ahmad, A. B. Pant, and H. A. Alhadlaq, "Genotoxic potential of copper oxide nanoparticles in human lung epithelial cells," *Biochemical and Biophysical Research Communications*, vol. 396, no. 2, pp. 578–583, 2010.

[52] F. He and L. Zuo, "Redox roles of reactive oxygen species in cardiovascular diseases," *International Journal of Molecular Sciences*, vol. 16, no. 11, pp. 27770–27780, 2015.

[53] V. Dias, E. Junn, and M. M. Mouradian, "The role of oxidative stress in Parkinson's disease," *Journal of Parkinson's Disease*, vol. 3, no. 4, pp. 461–491, 2013.

[54] L. Zuo, T. Zhou, B. K. Pannell, A. C. Ziegler, and T. M. Best, "Biological and physiological role of reactive oxygen species-the good, the bad and the ugly," *Acta Physiologica*, vol. 214, no. 3, pp. 329–348, 2015.

[55] B. L. Tan, "Water extract of brewers' rice induces apoptosis in human colorectal cancer cells via activation of caspase-3 and caspase-8 and downregulates the Wnt/β-catenin downstream signaling pathway in brewers' rice-treated rats with azoxymethane-induced colon carcinogenesis," *BMC Complementary Medicine and Therapies*, vol. 15, pp. 1–14, 2015.

[56] Z. Liu, T. Zhou, A. C. Ziegler, P. Dimitrion, and L. Zuo, "Oxidative stress in neurodegenerative diseases: from molecular mechanisms to clinical applications," *Oxidative Medicine and Cellular Longevity*, vol. 2017, Article ID 2525967, 11 pages, 2017.

[57] L. Rodriguez-Sanchez, M. C. Blanco, and M. A. Lopez-Quintela, "Electrochemical synthesis of silver nanoparticles," *The Journal of Physical Chemistry B*, vol. 104, no. 41, pp. 9683–9688, 2000.

[58] F. Mafuné, J. Y. Kohno, Y. Takeda, T. Kondow, and H. Sawabe, "Structure and stability of silver nanoparticles in aqueous solution produced by laser ablation," *The Journal of Physical Chemistry B*, vol. 104, no. 35, pp. 8333–8337, 2000.

[59] M. Salavati-Niasari, F. Davar, M. Mazaheri, and M. Shaterian, "Preparation of cobalt nanoparticles from [bis(salicylidene)-cobalt(II)]-oleylamine complex by thermal decomposition," *Journal of Magnetism and Magnetic Materials*, vol. 320, no. 3-4, pp. 575–578, 2008.

[60] K. Okitsu, M. Ashokkumar, and F. Grieser, "Sonochemical synthesis of gold nanoparticles: effects of ultrasound frequency," *The Journal of Physical Chemistry B*, vol. 109, no. 44, pp. 20673–20675, 2005.

[61] C. Gutiérrez-Wing, R. Esparza, C. Vargas-Hernández, M. E. Fernández García, and M. José-Yacamán, "Microwave-assisted synthesis of gold nanoparticles self-assembled into self-supported superstructures," *Nanoscale*, vol. 4, no. 7, pp. 2281–2287, 2012.

[62] S. Iravani, "Green synthesis of metal nanoparticles using plants," *Green Chemistry*, vol. 13, no. 10, pp. 2638–2650, 2011.

[63] F. Arockiya Aarthi Rajathi, R. Arumugam, S. Saravanan, and P. Anantharaman, "Phytofabrication of gold nanoparticles assisted by leaves of _Suaeda monoica_ and its free radical scavenging property," *Journal of Photochemistry and Photobiology B: Biology*, vol. 135, pp. 75–80, 2014.

[64] A. A. Zahir, I. S. Chauhan, A. Bagavan et al., "Synthesis of nanoparticles using Euphorbia prostrata extract reveals a shift from apoptosis to G0/G1 arrest in Leishmania donovani," *Journal of Nanomedicine and Nanotechnology*, vol. 5, pp. 1–12, 2014.

[65] K. S. Kavitha, S. Baker, D. Rakshith et al., "Plants as green source towards synthesis of nanoparticles," *International Research Journal of Biological Sciences*, vol. 2, pp. 66–76, 2013.

[66] M. S. Akhtar, J. Panwar, and Y. S. Yun, "Biogenic synthesis of metallic nanoparticles by plant extracts," *ACS Sustainable Chemistry and Engineering*, vol. 1, no. 6, pp. 591–602, 2013.

[67] G. Sathishkumar, P. K. Jha, V. Vignesh et al., "Cannonball fruit (Couroupita guianensis, Aubl.) extract mediated synthesis of gold nanoparticles and evaluation of its antioxidant activity," *Journal of Molecular Liquids*, vol. 215, pp. 229–236, 2016.

[68] J. Singh, T. Dutta, K. H. Kim, M. Rawat, P. Samddar, and P. Kumar, "Green synthesis of metals and their oxide nanoparticles: applications for environmental remediation," *Journal of Nanobiotechnology*, vol. 16, pp. 1–24, 2018.

[69] R. Kumar Bachheti, A. Fikadu, A. Bachheti, and A. Husen, "Biogenic fabrication of nanomaterials from flower-based chemical compounds, characterization and their various applications: a review," *Saudi Journal of Biological Sciences*, vol. 27, no. 10, pp. 2551–2562, 2020.

[70] H. Kumar, K. Bhardwaj, D. S. Dhanjal et al., "Fruit extract mediated green synthesis of metallic nanoparticles: a new

avenue in pomology applications," *International Journal of Molecular Sciences*, vol. 21, no. 22, 2020.

[71] K. B. Narayanan and N. Sakthivel, "Green synthesis of biogenic metal nanoparticles by terrestrial and aquatic phototrophic and heterotrophic eukaryotes and biocompatible agents," *Advances in Colloid and Interface Science*, vol. 169, no. 2, pp. 59–79, 2011.

[72] K. Bhardwaj, D. S. Dhanjal, A. Sharma et al., "Conifer-derived metallic nanoparticles: green synthesis and biological applications," *International Journal of Molecular Sciences*, vol. 21, no. 23, pp. 1–22, 2020.

[73] A. Chandrasekaran, M. D. P. S. Idelchik, and J. A. Melendez, "Redox control of senescence and age-related disease," *Redox Biology*, vol. 11, pp. 91–102, 2017.

[74] Y. Liu and J. A. Imlay, "Cell death from antibiotics without the involvement of reactive oxygen species," *Science*, vol. 339, no. 6124, pp. 1210–1213, 2013.

[75] L. A. Sena and N. S. Chandel, "Physiological roles of mitochondrial reactive oxygen species," *Molecular Cell*, vol. 48, no. 2, pp. 158–167, 2012.

[76] G. S. Shadel and T. L. Horvath, "Mitochondrial ROS signaling in organismal homeostasis," *Cell*, vol. 163, no. 3, pp. 560–569, 2015.

[77] M. J. Smallwood, A. Nissim, A. R. Knight, M. Whiteman, R. Haigh, and P. G. Winyard, "Oxidative stress in autoimmune rheumatic diseases," *Free Radical Biology and Medicine*, vol. 125, pp. 3–14, 2018.

[78] M. Karagülle, S. Kardeş, O. Karagülle et al., "Effect of spa therapy with saline balneotherapy on oxidant/antioxidant status in patients with rheumatoid arthritis: a single-blind randomized controlled trial," *International Journal of Biometeorology*, vol. 61, no. 1, pp. 169–180, 2017.

[79] H. Sato, H. Shibata, T. Shimizu et al., "Differential cellular localization of antioxidant enzymes in the trigeminal ganglion," *Neuroscience*, vol. 248, pp. 345–358, 2013.

[80] J. Navarro-Yepes, L. Zavala-Flores, A. Anandhan et al., "Antioxidant gene therapy against neuronal cell death," *Pharmacology and Therapeutics*, vol. 142, no. 2, pp. 206–230, 2014.

[81] I. Keren, Y. Wu, J. Inocencio, L. R. Mulcahy, and K. Lewis, "Killing by bactericidal antibiotics does not depend on reactive oxygen species," *Science*, vol. 339, no. 6124, pp. 1213–1216, 2013.

[82] J. Boonstra and J. A. Post, "Molecular events associated with reactive oxygen species and cell cycle progression in mammalian cells," *Gene*, vol. 337, pp. 1–13, 2004.

[83] S. di Meo, T. T. Reed, P. Venditti, and V. M. Victor, "Role of ROS and RNS sources in physiological and pathological conditions," *Oxidative Medicine and Cellular Longevity*, vol. 2016, Article ID 1245049, 44 pages, 2016.

[84] P. Rajendran, N. Nandakumar, T. Rengarajan et al., "Antioxidants and human diseases," *Clinica Chimica Acta*, vol. 436, pp. 332–347, 2014.

[85] J. M. Hansen, Y. M. Go, and D. P. Jones, "Nuclear and mitochondrial compartmentation of oxidative stress and redox signaling," *Annual Review of Pharmacology and Toxicology*, vol. 46, no. 1, pp. 215–234, 2006.

[86] A. Glasauer and N. S. Chandel, "Targeting antioxidants for cancer therapy," *Biochemical Pharmacology*, vol. 92, no. 1, pp. 90–101, 2014.

[87] V. Lobo, A. Patil, A. Phatak, and N. Chandra, "Free radicals, antioxidants and functional foods: impact on human health," *Pharmacognosy Reviews*, vol. 4, no. 8, pp. 118–126, 2010.

[88] I. Liguori, G. Russo, F. Curcio et al., "Oxidative stress, aging, and diseases," *Clinical Interventions in Aging*, vol. 13, pp. 757–772, 2018.

[89] J. Q. Wu, T. R. Kosten, and X. Y. Zhang, "Free radicals, antioxidant defense systems, and schizophrenia," *Progress in Neuro-Psychopharmacology and Biological Psychiatry*, vol. 46, pp. 200–206, 2013.

[90] K. Rahman, "Studies on free radicals, antioxidants, and co-factors," *Clinical Interventions in Aging*, vol. 2, no. 2, pp. 219–236, 2007.

[91] Y. Taniyama and K. K. Griendling, "Reactive oxygen species in the vasculature," *Hypertension*, vol. 42, no. 6, pp. 1075–1081, 2003.

[92] G. Pizzino, N. Irrera, M. Cucinotta et al., "Oxidative stress: harms and benefits for human health," *Oxidative Medicine and Cellular Longevity*, vol. 2017, Article ID 8416763, 13 pages, 2017.

[93] P. Abete, C. Napoli, G. Santoro et al., "Age-related decrease in cardiac tolerance to oxidative stress," *Journal of Molecular and Cellular Cardiology*, vol. 31, no. 1, pp. 227–236, 1999.

[94] K. B. Beckman and B. N. Ames, "The free radical theory of aging matures," *Physiological Reviews*, vol. 78, no. 2, pp. 547–581, 1998.

[95] A. J. Donato, I. Eskurza, A. E. Silver et al., "Direct evidence of endothelial oxidative stress with aging in Humans," *Circulation Research*, vol. 100, no. 11, pp. 1659–1666, 2007.

[96] T. Bahorun, M. A. Soobrattee, V. Luximon-Ramma, and O. I. Aruoma, "Free radicals and antioxidants in cardiovascular health and disease," *Internet Journal of Medical Update*, vol. 1, pp. 1–17, 2007.

[97] W. Droge, "Free radicals in the physiological control of cell function," *Physiological Reviews*, vol. 82, no. 1, pp. 47–95, 2002.

[98] M. Chatterjee, R. Saluja, S. Kanneganti, S. Chinta, and M. Dikshit, "Biochemical and molecular evaluation of neutrophil NOS in spontaneously hypertensive rats," *Cellular and Molecular Biology*, vol. 53, pp. 84–93, 2007.

[99] A. Ceriello, "Possible role of oxidative stress in the pathogenesis of hypertension," *Diabetes Care*, vol. 31, Supplement 2, pp. S181–S184, 2008.

[100] R. de Cristofaro, B. Rocca, E. Vitacolonna et al., "Lipid and protein oxidation contribute to a prothrombotic state in patients with type 2 diabetes mellitus," *Journal of Thrombosis and Haemostasis*, vol. 1, no. 2, pp. 250–256, 2003.

[101] C. M. Sag, C. X. Santos, and A. M. Shah, "Redox regulation of cardiac hypertrophy," *Journal of Molecular and Cellular Cardiology*, vol. 73, pp. 103–111, 2014.

[102] T. Zhou, E. R. Prather, D. E. Garrison, and L. Zuo, "Interplay between ROS and antioxidants during ischemia-reperfusion injuries in cardiac and skeletal muscle," *International Journal of Molecular Sciences*, vol. 19, pp. 1–20, 2018.

[103] A. Van der Pol, W. H. Van Gilst, A. A. Voors, and P. Van der Meer, "Treating oxidative stress in heart failure: past, present and future," *European Journal of Heart Failure*, vol. 21, pp. 425–435, 2019.

[104] G. Caramori and A. Papi, "Oxidants and asthma," *Thorax*, vol. 59, no. 2, pp. 170–173, 2004.

[105] Y. Hoshino and M. Mishima, "Redox-based therapeutics for lung diseases," *Antioxidants and Redox Signaling*, vol. 10, no. 4, pp. 701–704, 2008.

[106] R. K. Thimmulappa, I. Chattopadhyay, and S. Rajasekaran, "Oxidative stress mechanisms in the pathogenesis of environmental lung diseases," in *Oxidative Stress in Lung Diseases*, pp. 103–137, Springer, Singapore, 2020.

[107] G. Choudhury and W. MacNee, "Role of inflammation and oxidative stress in the pathology of ageing in COPD: potential therapeutic interventions," *Journal of Chronic Obstructive Pulmonary Disease*, vol. 14, no. 1, pp. 122–135, 2017.

[108] J. Galle, "Oxidative stress in chronic renal failure," *Nephrology, Dialysis, Transplantation*, vol. 16, no. 11, pp. 2135–2137, 2001.

[109] S. Balasubramanian, "Progression of chronic kidney disease: mechanisms and interventions in retardation," *Apollo Medicine*, vol. 10, no. 1, pp. 19–28, 2013.

[110] A. Y. Putri and M. Thaha, "Role of oxidative stress on chronic kidney disease progression," *Acta Medica Indonesiana*, vol. 46, no. 3, pp. 244–252, 2014.

[111] B. Halliwell, "Role of free radicals in the neurodegenerative Diseases," *Drugs and Aging*, vol. 18, no. 9, pp. 685–716, 2001.

[112] R. P. Singh, S. Sharad, and S. Kapur, "Free radicals and oxidative stress in neurodegenerative diseases: relevance of dietary antioxidants," *Journal, Indian Academy of Clinical Medicine*, vol. 5, pp. 218–225, 2004.

[113] A. V. Rao and B. Balachandran, "Role of oxidative stress and antioxidants in neurodegenerative diseases," *Nutritional Neuroscience*, vol. 5, no. 5, pp. 291–309, 2002.

[114] S. C. Lee and J. C. Chan, "Evidence for DNA damage as a biological link between diabetes and cancer," *Chinese Medical Journal*, vol. 128, no. 11, pp. 1543–1548, 2015.

[115] Q. Qian, W. Chen, Y. Cao et al., "Targeting reactive oxygen species in cancer via Chinese herbal medicine," *Oxidative Medicine and Cellular Longevity*, vol. 2019, Article ID 9240426, 23 pages, 2019.

[116] M. Redza-Dutordoir and D. A. Averill-Bates, "Activation of apoptosis signalling pathways by reactive oxygen species," *Biochimica et Biophysica Acta*, vol. 1863, no. 12, pp. 2977–2992, 2016.

[117] M. Mehta, D. S. Dhanjal, K. R. Paudel et al., "Cellular signalling pathways mediating the pathogenesis of chronic inflammatory respiratory diseases: an update," *Inflammopharmacology*, vol. 28, no. 4, pp. 795–817, 2020.

[118] A. Ramachandran and H. Jaeschke, "Oxidative stress and acute hepatic injury," *Current Opinion in Toxicology*, vol. 7, pp. 17–21, 2018.

[119] C. M. Quiñonez-Flores, S. A. González-Chávez, D. del Río Nájera, and C. Pacheco-Tena, "Oxidative stress relevance in the pathogenesis of the rheumatoid arthritis: a systematic review," *BioMed Research International*, vol. 2016, Article ID 6097417, 14 pages, 2016.

[120] A. M. M. Attia, F. A. A. Ibrahim, N. A. Abd el-Latif et al., "Therapeutic antioxidant and anti-inflammatory effects of laser acupuncture on patients with rheumatoid arthritis," *Lasers in Surgery and Medicine*, vol. 48, no. 5, pp. 490–497, 2016.

[121] S. Jaswal, H. C. Mehta, A. K. Sood, and J. Kaur, "Antioxidant status in rheumatoid arthritis and role of antioxidant therapy," *Clinica Chimica Acta*, vol. 338, no. 1-2, pp. 123–129, 2003.

[122] S. Naqvi, Naqvi, M. Samim et al., "Concentration-dependent toxicity of iron oxide nanoparticles mediated by increased oxidative stress," *International Journal of Nanomedicine*, vol. 5, no. 1, pp. 983–989, 2010.

[123] P. L. Apopa, Y. Qian, R. Shao et al., "Iron oxide nanoparticles induce human microvascular endothelial cell permeability through reactive oxygen species production and microtubule remodeling," *Particle and Fibre Toxicology*, vol. 6, no. 1, 2009.

[124] B. Fahmy and S. A. Cormier, "Copper oxide nanoparticles induce oxidative stress and cytotoxicity in airway epithelial cells," *Toxicology in Vitro*, vol. 23, no. 7, pp. 1365–1371, 2009.

[125] D. A. Saud Alarifi, S. Alkahtani, A. Verma, M. Ahamed, M. Ahmed, and H. A. Alhadlaq, "Induction of oxidative stress, DNA damage, and apoptosis in a malignant human skin melanoma cell line after exposure to zinc oxide nanoparticles," *International Journal of Nanomedicine*, vol. 8, pp. 983–993, 2013.

[126] J. J. Li, D. Hartono, C. Ong, B. Bay, and L. L. Yung, "Autophagy and oxidative stress associated with gold nanoparticles," *Biomaterials*, vol. 31, no. 23, pp. 5996–6003, 2010.

[127] P. Chairuangkitti, S. Lawanprasert, S. Roytrakul et al., "Silver nanoparticles induce toxicity in A549 cells via ROS-dependent and ROS- independent pathways," *Toxicology in Vitro*, vol. 27, no. 1, pp. 330–338, 2013.

[128] H. J. Johnston, G. Hutchison, F. Christensen, M. Peters, S. Hankin, and S. Stone, "A review of the in vivo and in vitro toxicity of silver and gold particulates: particle attributes and biological mechanisms responsible for the observed toxicity," *Critical Reviews in Toxicology*, vol. 4, pp. 328–346, 2010.

[129] A. Manke, L. Wang, and Y. Rojanasakul, "Mechanisms of nanoparticle-induced oxidative stress and toxicity," *BioMed Research International*, vol. 2013, Article ID 942916, 15 pages, 2013.

[130] T. Huang, J. A. Holden, D. E. Heath, N. M. O'Brien-Simpson, and A. J. O'Connor, "Engineering highly effective antimicrobial selenium nanoparticles through control of particle size," *Nanoscale*, vol. 11, no. 31, pp. 14937–14951, 2019.

[131] S. Cho, B. Lee, W. Park, X. Huang, and D. H. Kim, "Photoperiodic flower mimicking metallic nanoparticles for image-guided medicine applications," *ACS Applied Materials and Interfaces*, vol. 10, no. 33, pp. 27570–27577, 2018.

[132] P. Menu, A. Mayor, R. Zhou et al., "ER stress activates the NLRP3 inflammasome via an UPR-independent pathway," *Cell Death and Disease*, vol. 3, pp. 1–6, 2012.

[133] M. Akter, M. T. Sikder, M. M. Rahman et al., "A systematic review on silver nanoparticles-induced cytotoxicity: Physicochemical properties and perspectives," *Journal of Advanced Research*, vol. 9, pp. 1–16, 2018.

[134] A. R. Lee, S. J. Lee, M. Lee et al., "Editor's highlight: a genome-wide screening of target genes against silver nanoparticles in fission yeast," *Toxicological Sciences*, vol. 161, no. 1, pp. 171–185, 2018.

[135] L. M. Gaetke and C. Kuang, "Copper toxicity, oxidative stress, and antioxidant nutrients," *Toxicology*, vol. 189, no. 1-2, pp. 147–163, 2003.

[136] P. AshaRani, M. P. Hande, and S. Valiyaveettil, "Anti-proliferative activity of silver nanoparticles," *BMC Cell Biology*, vol. 10, no. 1, pp. 1–14, 2009.

[137] R. Zhang, M. J. Piao, K. C. Kim et al., "Endoplasmic reticulum stress signaling is involved in silver nanoparticles- induced

apoptosis," *The International Journal of Biochemistry and Cell Biology*, vol. 44, no. 1, pp. 224–232, 2012.

[138] M. Ahamed, M. Karns, M. Goodson et al., "DNA damage response to different surface chemistry of silver nanoparticles in mammalian cells," *Toxicology and Applied Pharmacology*, vol. 233, no. 3, pp. 404–410, 2008.

[139] R. Foldbjerg, P. Olesen, M. Hougaard, D. A. Dang, H. J. Hoffmann, and H. Autrup, "PVP-coated silver nanoparticles and silver ions induce reactive oxygen species, apoptosis and necrosis in THP-1 monocytes," *Toxicology Letters*, vol. 190, no. 2, pp. 156–162, 2009.

[140] S. Kim, J. E. Choi, J. Choi et al., "Oxidative stress-dependent toxicity of silver nanoparticles in human hepatoma cells," *Toxicology in Vitro*, vol. 23, no. 6, pp. 1076–1084, 2009.

[141] A. Hudecová, B. Kusznierewicz, E. Rundén-Pran et al., "Silver nanoparticles induce premutagenic DNA oxidation that can be prevented by phytochemicals from Gentiana asclepiadea," *Mutagenesis*, vol. 27, no. 6, pp. 759–769, 2012.

[142] K. M. Holmstrom and T. Finkel, "Cellular mechanisms and physiological consequences of redox-dependent signalling," *Nature Reviews Molecular Cell Biology*, vol. 15, no. 6, pp. 411–421, 2014.

[143] X. Chen and H. J. Schluesener, "Nanosilver: a nanoproduct in medical application," *Toxicology and Applied Pharmacology*, vol. 176, pp. 1–12, 2008.

[144] C. Pellieux, A. Dewilde, C. Pierlot, and J. M. Aubry, "[18] Bactericidal and virucidal activities of singlet oxygen generated by thermolysis of naphthalene endoperoxides," *Methods in Enzymology*, vol. 319, pp. 197–207, 2000.

[145] S. H. Kim, H. S. Lee, D. S. Ryu, S. J. Choi, and D. S. Lee, "Antibacterial activity of silver-nanoparticles against Staphylococcus aureus and Escherichia coli," *Korean Journal of Microbiology and Biotechnology*, vol. 39, pp. 77–85, 2011.

[146] D. Wu, W. Fan, A. Kishen, J. L. Gutmann, and B. Fan, "Evaluation of the Antibacterial Efficacy of Silver Nanoparticles against _Enterococcus faecalis_ Biofilm," *Journal of Endodontics*, vol. 40, no. 2, pp. 285–290, 2014.

[147] J. Y. Kim, K. Sungeun, J. Kim, L. Jongchan, and J. Yoon, "The biocidal activity of nano-sized silver particles comparing with silver ion," *Journal of Korean Society of Environmental Engineers*, vol. 27, pp. 771–776, 2005.

[148] I. Fenoglio, I. Corazzari, C. Francia, S. Bodoardo, and B. Fubini, "The oxidation of glutathione by cobalt/tungsten carbide contributes to hard metal-induced oxidative stress," *Free Radical Research*, vol. 42, no. 8, pp. 437–745, 2008.

[149] I. Chopra, "The increasing use of silver-based products as antimicrobial agents: a useful development or a cause for concern," *Journal of Antimicrobial Chemotherapy*, vol. 59, no. 4, pp. 587–590, 2007.

[150] P. Gopinath, S. K. Gogoi, A. Chattopadhyay, and S. S. Ghosh, "Implications of silver nanoparticle induced cell apoptosis forin vitrogene therapy," *Nanotechnolgy*, vol. 19, no. 7, article 075104, 2008.

[151] K. Urbańska, B. Pająk, A. Orzechowski et al., "The effect of silver nanoparticles (AgNPs) on proliferation and apoptosis of in ovo cultured glioblastoma multiforme (GBM) cells," *Nanoscale Research Letters*, vol. 10, pp. 1–11, 2015.

[152] T. C. Dakal, A. Kumar, R. S. Majumdar, and V. Yadav, "Mechanistic basis of antimicrobial actions of silver nanoparticles," *Frontiers in Microbiology*, vol. 7, pp. 1–17, 2016.

[153] B. Baruwati and R. S. Varma, "High value products from waste: grape pomace Extract-A three-in-one package for the synthesis of metal nanoparticles," *ChemSusChem*, vol. 2, no. 11, pp. 1041–1044, 2009.

[154] H. Kumar, K. Bhardwaj, K. Kuča et al., "Flower-based green synthesis of metallic nanoparticles: applications beyond fragrance," *Nanomaterials*, vol. 10, no. 4, p. 766, 2020.

[155] M. Kandiah and K. N. Chandrasekaran, "Green synthesis of silver nanoparticles using Catharanthus roseus flower extracts and the determination of their antioxidant, antimicrobial, and photocatalytic activity," *Journal of Nanotechnology*, vol. 2021, 18 pages, 2021.

[156] P. Kuppusamy, M. Yusoff, G. Maniam, and N. Govindan, "Biosynthesis of metallic nanoparticles using plant derivatives and their new avenues in pharmacological applications - An updated report," *Saudi Pharmaceutical Journal*, vol. 24, no. 4, pp. 473–484, 2016.

[157] S. Jain and M. S. Mehata, "Medicinal plant leaf extract and pure flavonoid mediated green synthesis of silver nanoparticles and their enhanced antibacterial property," *Scientific Reports*, vol. 7, no. 1, p. 15867, 2017.

[158] S. Sharma, K. Kumar, N. Thakur, and M. S. Chauhan, "Ocimum tenuiflorum leaf extract as a green mediator for the synthesis of ZnO nanocapsules inactivating bacterial pathogens," *Chemical Papers*, vol. 74, no. 10, pp. 3431–3444, 2020.

[159] S. Sharma, K. Kumar, N. Thakur, S. Chauhan, and M. S. Chauhan, "Eco-friendly _Ocimum tenuiflorum_ green route synthesis of CuO nanoparticles: Characterizations on photocatalytic and antibacterial activities," *Journal of Environmental Chemical Engineering*, vol. 9, no. 4, p. 105395, 2021.

[160] S. Sharma, K. Kumar, N. Thakur, S. Chauhan, and M. S. Chauhan, "The effect of shape and size of ZnO nanoparticles on their antimicrobial and photocatalytic activities: a green approach," *Bulletin of Materials Science*, vol. 43, no. 1, 2020.

[161] R. Subbaiya and M. M. Selvam, "Green synthesis of copper nanoparticles from Hibicus rosasinensis and their antimicrobial, antioxidant activities," *Research Journal of Pharmaceutical, Biological and Chemical Sciences*, vol. 6, pp. 1183–1190, 2015.

[162] S. Ghosh, P. More, R. Nitnavare et al., "Antidiabetic and antioxidant properties of copper nanoparticles synthesized by medicinal plant Dioscorea bulbifera," *Journal of Nanomedicine and Nanotechnology*, vol. s6, 2015.

[163] H. Shabestarian, M. Homayouni-Tabrizi, M. Soltani et al., "Green synthesis of gold nanoparticles using sumac aqueous extract and their antioxidant activity," *Materials Research*, vol. 20, pp. 264–270, 2017.

[164] T. Kalaiyarasan, V. K. Bharti, and O. P. Chaurasia, "One pot green preparation ofSeabuckthornsilver nanoparticles (SBT@AgNPs) featuring high stability and longevity, antibacterial, antioxidant potential: a nano disinfectant future perspective," *RSC Advances*, vol. 7, no. 81, pp. 51130–51141, 2017.

[165] E. E. Elemike, O. E. Fayemi, A. C. Ekennia, D. C. Onwudiwe, and E. E. Ebenso, "Silver nanoparticles mediated by Costus afer leaf Extract: Synthesis, Antibacterial, Antioxidant and electrochemical properties," *Molecules*, vol. 22, no. 5, p. 701, 2017.

[166] R. G. Saratale, G. Benelli, G. Kumar, D. S. Kim, and G. D. Saratale, "Bio-fabrication of silver nanoparticles using the leaf extract of an ancient herbal medicine, dandelion (Taraxacum officinale), evaluation of their antioxidant, anticancer

potential, and antimicrobial activity against phytopathogens," *Environmental Science and Pollution Research*, vol. 25, no. 11, pp. 10392–10406, 2018.

[167] Y. K. Mohanta, S. K. Panda, R. Jayabalan, N. Sharma, A. K. Bastia, and T. K. Mohanta, "Antimicrobial, antioxidant and cytotoxic activity of silver nanoparticles synthesized by leaf extract of Erythrina suberosa (Roxb.)," *Frontiers in Molecular Biosciences*, vol. 4, 2017.

[168] A. K. Keshari, R. Srivastava, P. Singh, V. B. Yadav, and G. Nath, "Antioxidant and antibacterial activity of silver nanoparticles synthesized by _Cestrum nocturnum_," *Journal of Ayurveda and Integrative Medicine*, vol. 11, no. 1, pp. 37–44, 2020.

[169] D. Bharathi and V. Bhuvaneshwari, "Evaluation of the cytotoxic and antioxidant activity of phyto-synthesized silver nanoparticles using Cassia angustifolia flowers," *BioNanoScience*, vol. 9, no. 1, pp. 155–163, 2019.

[170] D. A. Selvan, D. Mahendiran, R. S. Kumar, and A. K. Rahiman, "Garlic, green tea and turmeric extracts-mediated green synthesis of silver nanoparticles: Phytochemical, antioxidant and _in vitro_ cytotoxicity studies," *Journal of Photochemistry and Photobiology B: Biology*, vol. 180, pp. 243–252, 2018.

[171] G. A. Otunola and A. J. Afolayan, "In vitroantibacterial, antioxidant and toxicity profile of silver nanoparticles green-synthesized and characterized from aqueous extract of a spice blend formulation," *Biotechnology and Biotechnological Equipment*, vol. 32, no. 3, pp. 724–733, 2018.

[172] L. Wang, Y. Wu, J. Xie, S. Wu, and Z. Wu, "Characterization, antioxidant and antimicrobial activities of green synthesized silver nanoparticles from Psidium guajava L. leaf aqueous extracts," *Materials Science and Engineering: C*, vol. 86, 2018.

[173] H. Chandra, D. Patel, P. Kumari, J. S. Jangwan, and S. Yadav, "Phyto-mediated synthesis of zinc oxide nanoparticles of _Berberis aristata_ : Characterization, antioxidant activity and antibacterial activity with special reference to urinary tract pathogens," *Materials Science and Engineering C-Materials for Biological Applications*, vol. 102, pp. 212–220, 2019.

[174] G. Das, J. K. Patra, T. Debnath, A. Ansari, and H. S. Shin, "Investigation of antioxidant, antibacterial, antidiabetic, and cytotoxicity potential of silver nanoparticles synthesized using the outer peel extract of Ananas comosus (L.)," *PloS One*, vol. 14, no. 8, p. e0220950, 2019.

[175] S. Salari, S. E. Bahabadi, A. Samzadeh-Kermani, and F. Yosefzaei, "In-vitro evaluation of antioxidant and antibacterial potential of GreenSynthesized silver nanoparticles using Prosopis farcta fruit extract," *Iranian Journal of Pharmaceutical Research*, vol. 18, no. 1, pp. 430–455, 2019.

[176] S. Veena, T. Devasena, S. S. M. Sathak, M. Yasasve, and L. A. Vishal, "Green synthesis of gold nanoparticles from Vitex negundo leaf extract: characterization and in vitro evaluation of antioxidant-antibacterial activity," *Journal of Cluster Science*, vol. 30, no. 6, pp. 1591–1597, 2019.

[177] D. Das, R. Ghosh, and P. Mandal, "Biogenic synthesis of silver nanoparticles using S1 genotype of Morus alba leaf extract: characterization, antimicrobial and antioxidant potential assessment," *SN Applied Sciences*, vol. 1, no. 5, pp. 1–16, 2019.

[178] R. Mahmoudi, S. Aghaei, Z. Salehpour et al., "Antibacterial and antioxidant properties of phyto-synthesized silver nanoparticles usingLavandula stoechasextract," *Applied Organometallic Chemistry*, vol. 34, no. 2, 2020.

[179] K. D. Datkhile, S. R. Patil, P. P. Durgavale, M. N. Patil, N. J. Jagdale, and V. N. Deshmukh, "Studies on antioxidant and antimicrobial potential of biogenic silver nanoparticles synthesized using Nothapodytes foetida leaf extract (Wight) Sleumer," *Biomedical and Pharmacology Journal*, vol. 13, no. 1, pp. 441–448, 2020.

[180] S. Ansar, H. Tabassum, N. S. Aladwan et al., "Eco friendly silver nanoparticles synthesis by _Brassica oleracea_ and its antibacterial, anticancer and antioxidant properties," *Scientific Reports*, vol. 10, no. 1, pp. 1–12, 2020.

[181] A. O. Akintola, B. D. Kehinde, P. B. Ayoola et al., "Antioxidant properties of silver nanoparticles biosynthesized from methanolic leaf extract ofBlighia sapida," *In IOP Conference Series: Materials Science and Engineering*, vol. 805, 2020.

[182] B. S. Tuzun, T. Fafal, P. Tastan et al., "Structural characterization, antioxidant and cytotoxic effects of iron nanoparticles synthesized using Asphodelus aestivus Brot. aqueous extract," *Green Processing and Synthesis*, vol. 9, no. 1, pp. 153–163, 2020.

[183] S. Rajput, D. Kumar, and V. Agrawal, "Green synthesis of silver nanoparticles using Indian Belladonna extract and their potential antioxidant, anti-inflammatory, anticancer and larvicidal activities," *Plant Cell Reports*, vol. 39, no. 7, pp. 921–939, 2020.

[184] T. Santhoshkumar, A. A. Rahuman, C. Jayaseelan et al., "Green synthesis of titanium dioxide nanoparticles using _Psidium guajava_ extract and its antibacterial and antioxidant properties," *Asian Pacific Journal of Tropical Medicine*, vol. 7, no. 12, pp. 968–976, 2014.

[185] P. O. Akinola, A. Lateef, T. B. Asafa, L. S. Beukes, A. S. Hakeem, and H. M. Irshad, "Multifunctional titanium dioxide nanoparticles biofabricated via phytosynthetic route using extracts of _Cola nitida_ : antimicrobial, dye degradation, antioxidant and anticoagulant activities," *Heliyon*, vol. 6, no. 8, p. e04610, 2020.

[186] N. K. Upadhyay, M. S. Y. Kumar, and A. Gupta, "Antioxidant, cytoprotective and antibacterial effects of Sea buckthorn (_Hippophae rhamnoides_ L.) leaves," *Food and Chemical Toxicology*, vol. 48, no. 12, pp. 3443–3448, 2010.

[187] G. Clarke, K. N. Ting, C. Wiart, and J. Fry, "High correlation of 2, 2-diphenyl-1-picrylhydrazyl (DPPH) radical scavenging, ferric reducing activity potential and total phenolics content indicates redundancy in use of all three assays to screen for antioxidant activity of extracts of plants from the Malaysian rainforest," *Antioxidants*, vol. 2, 2013.

[188] S. A. Gaddam, V. S. Kotakadi, D. S. Gopal, Y. S. Rao, and A. V. Reddy, "Efficient and robust biofabrication of silver nanoparticles by Cassia alata leaf extract and their antimicrobial activity," *Journal of Nanostructure in Chemistry*, vol. 4, no. 1, 2014.

[189] A. A. Adedapo, F. O. Jimoh, A. J. Afolayan, and P. J. Masika, "Antioxidant activities and phenolic contents of the methanol extracts of the stems of Acokanthera oppositifolia and Adenia gummifera," *BMC Complementary and Alternative Medicine*, vol. 8, no. 1, 2008.

[190] S. Saumya and P. Basha, "Antioxidant effect of Lagerstroemia speciosa Pers (Banaba) leaf extract in streptozotocin-induced diabetic mice," *Indian Journal of Experimental Biology*, vol. 49, no. 2, pp. 125–131, 2011.

[191] D. Salisbury and U. Bronas, "Reactive oxygen and nitrogen species: impact on endothelial dysfunction," *Nursing Research*, vol. 64, no. 1, pp. 53–66, 2015.

[192] M. Genestra, "Oxyl radicals, redox-sensitive signalling cascades and antioxidants," *Cell Signal*, vol. 19, no. 9, pp. 1807–1819, 2007.

[193] R. Dhalaria, R. Verma, D. Kumar et al., "Bioactive compounds of edible fruits with their anti-aging properties: a comprehensive review to prolong human life," *Antioxidants*, vol. 9, no. 11, pp. 1123–1138, 2020.

[194] D. M. Nagmoti, D. K. Khatri, P. R. Juvekar, and A. R. Juvekar, "Antioxidant activity free radical-scavenging potential of Pithecellobium dulce Benth. seed extracts," *Free radical and Antioxidant*, vol. 2, no. 2, pp. 37–43, 2012.

[195] F. Boora, E. Chirisa, and S. Mukanganyama, "Evaluation of nitrite radical scavenging properties of selected Zimbabwean plant extracts and their phytoconstituents," *Journal of Food Processing*, vol. 2014, 7 pages, 2014.

[196] H. S. Tehrani and A. A. Moosavi-Movahedi, "Catalase and its mysteries," *Progress in Biophysics and Molecular Biology*, vol. 140, pp. 5–12, 2018.

[197] M. Rakotoarisoa, B. Angelov, S. Espinoza, K. Khakurel, T. Bizien, and A. Angelova, "Cubic liquid crystalline nanostructures involving catalase and curcumin: BioSAXS study and catalase peroxidatic function after cubosomal nanoparticle treatment of differentiated SH-SY5Y cells," *Molecules*, vol. 24, no. 17, pp. 1–21, 2019.

[198] A. Balkrishna, A. Rohela, A. Kumar et al., "Mechanistic insight into antimicrobial and antioxidant potential of Jasminum species: a herbal approach for disease management," *Plants*, vol. 10, no. 6, pp. 1–25, 2021.

[199] E. D. Wills, "Effects of lipid peroxidation on membrane-bound enzymes of the endoplasmic reticulum," *Biochemical Journal*, vol. 123, pp. 983–991, 1971.

[200] E. Birben, U. M. Sahiner, C. Sackesen, S. Erzurum, and O. Kalayci, "Oxidative stress and antioxidant defense," *World Allergy Organization Journal*, vol. 5, no. 1, pp. 9–19, 2012.

[201] C. Szabó, H. Ischiropoulos, and R. Radi, "Peroxynitrite: biochemistry, pathophysiology and development of therapeutics," *Nature Reviews Drug Discovery*, vol. 6, no. 8, pp. 662–680, 2007.

Hindawi
Oxidative Medicine and Cellular Longevity
Volume 2021, Article ID 8511576, 11 pages
https://doi.org/10.1155/2021/8511576

Research Article

Anticancer, Enhanced Antibacterial, and Free Radical Scavenging Potential of Fucoidan- (*Fucus vesiculosus* Source) Mediated Silver Nanoparticles

S. Rajeshkumar,[1] **Eman F. Aboelfetoh**,[2] **Sri Renukadevi Balusamy**,[3] **Daoud Ali**,[4] **Mohammed H. A. Almarzoug**,[4] **Jule Leta Tesfaye**,[5,6] **and Ramaswamy Krishnaraj**[5,7]

[1]*Department of Pharmacology, Saveetha Dental College and Hospital, SIMATS, Chennai, 600077 Tamil Nadu, India*
[2]*Chemistry Department, Faculty of Science, Tanta University, Tanta 31527, Egypt*
[3]*Department of Food Science and Biotechnology, Sejong University, Gwangjin-gu, Seoul 05006, Republic of Korea*
[4]*Department of Zoology, College of Science, King Saud University, PO Box 2455, Riyadh 11451, Saudi Arabia*
[5]*Centre for Excellence-Indigenous Knowledge, Innovative Technology Transfer and Entrepreneurship, Dambi Dollo University, Ethiopia*
[6]*Department of Physics, College of Natural and Computational Science, Dambi Dollo University, Ethiopia*
[7]*Department of Mechanical Engineering, Dambi Dollo University, Ethiopia*

Correspondence should be addressed to Ramaswamy Krishnaraj; prof.dr.krishnaraj@dadu.edu.et

Received 16 July 2021; Revised 5 August 2021; Accepted 26 August 2021; Published 30 September 2021

Academic Editor: Dragica Selakovic

The present research displays the green synthesis of stable silver nanoparticles (AgNPs). The aqueous solution of Fucoidan from *Fucus vesiculosus* source (brown marine algae) is used as a reducing and capping agent. UV-Vis spectroscopy, XRD, FT-IR, SEM, EDX, and TEM with selected area electron diffraction are used to characterize the synthesized silver nanoparticles (AgNPs). The synthesized AgNPs exhibit a surface plasmon resonance at 430 nm after 24 h. The characterization results showed that AgNPs are crystalline in nature and exhibit mostly spherical shapes with an average diameter of 4-45 nm. Silver nanoparticles showed effective antibacterial activity against representative pathogens of bacteria. The activities of commercial antibiotics were enhanced by impregnation with the synthesized AgNPs. It also shows good fungicidal and anticancer activity against liver and lung cell lines and shows significant antioxidant efficacy (84%) at 10 μg/ml AgNP concentration against DPPH. The utilization of environmentally synthesized AgNPs offers numerous benefits of ecofriendliness and compatibility for biomedical applications.

1. Introduction

The noble metal nanoparticles have gained great interest in a number of studies due to their potential applications in medical, optical, electronic devices, and water treatment. The most prominent challenge is how to control their sizes and shapes. For this purpose, a large number of reports have been published for the synthesis of metal nanoparticles of diverse structures [1]. The silver nanoparticles have become a comprehensive research point owing to their broad range of applications as disinfectant agents, catalyst, biosensor, and water treatment [2]. Various approaches were made for synthesis of AgNPs such as chemical reduction, electrochemical techniques, photochemical reduction, sonochemical, microwave, and radiation-assisted process [3]. Among these methods, the chemical reduction method is the most frequently used but remains costly and employs risky substances, such as organic solvents and harmful reducing agents, e.g., sodium borohydride, hydrazine, and N,N-dimethyl formamide. Furthermore, surface passivation and capping agents are generally added to the reaction system to avoid aggregates formation of the nanoparticles [3]. The state-of-the-art studies have focused on the green synthesis approaches to avoid utilization of highly toxic materials.

(a) (b)

Figure 1: Fucoidan- (*F. vesiculosus*) mediated AgNPs. (a) Initial reaction and (b) after 24 h final color change reaction.

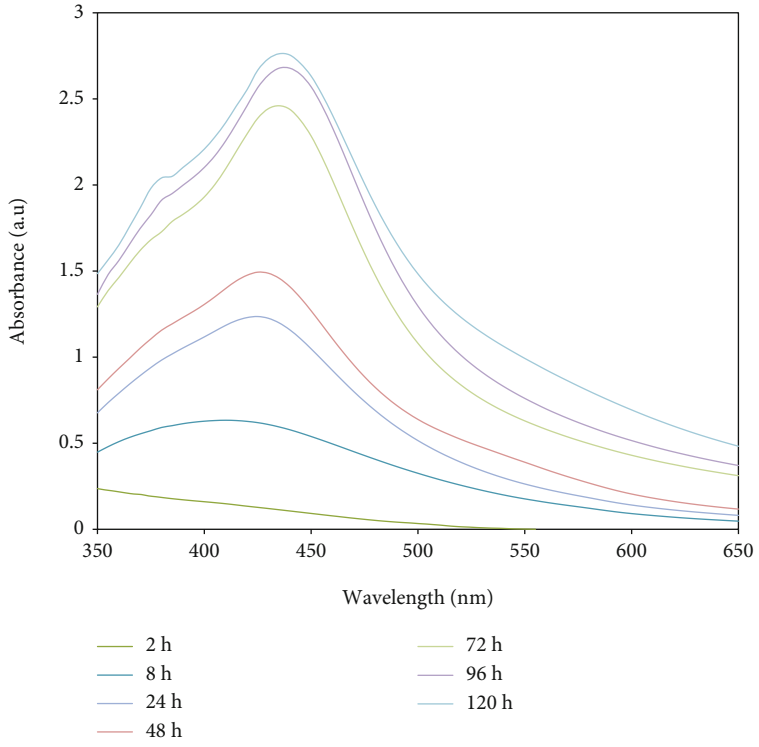

Figure 2: UV-Vis spectra of fucoidan-stabilized AgNPs at different time intervals. *X*-axis indicates the wavelength in nm and *Y*-axis indicates the absorbance of nanoparticles.

These approaches emphasize on the utilization of eco-friendly, cost-effective, and biocompatible reducing agents for the synthesis of AgNPs, which gives the synthesized AgNPs sufficient stability in the strong electrolytic and pH conditions for therapeutic application [4]. Various biological organisms have emerged as simple and viable substitutes to obtain AgNPs such as bacteria, yeast, fungi, algae, and plants [4–7]. Polysaccharides acquired from marine algae include fucoidan, alginate, ascophyllan, agar, and carrageenan as phycocolloids have been used for decades in medicine and pharmacy [8–15]. Fucoidan (sulfated fucan) is one of nonstarch polysaccharide which is soluble in water. It has complicated chemical structure and found in brown sugars such as galactose, xylose, and mannose. Fucoidan is derived from marine brown algae, containing large quantities of L-fucose and sulfated including *Fucus vesiculosus* [15–20]. Due to the wide spectrum of activity of fucoidan in biological systems including antitumor,

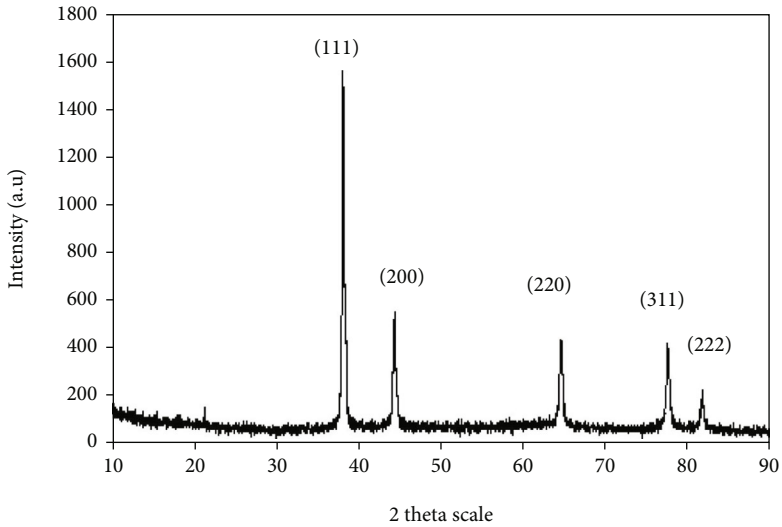

Figure 3: XRD pattern of the synthesized AgNPs. *X*-axis shows the 2-theta scale, and *Y*-axis indicates the intensity of the silver nanoparticles.

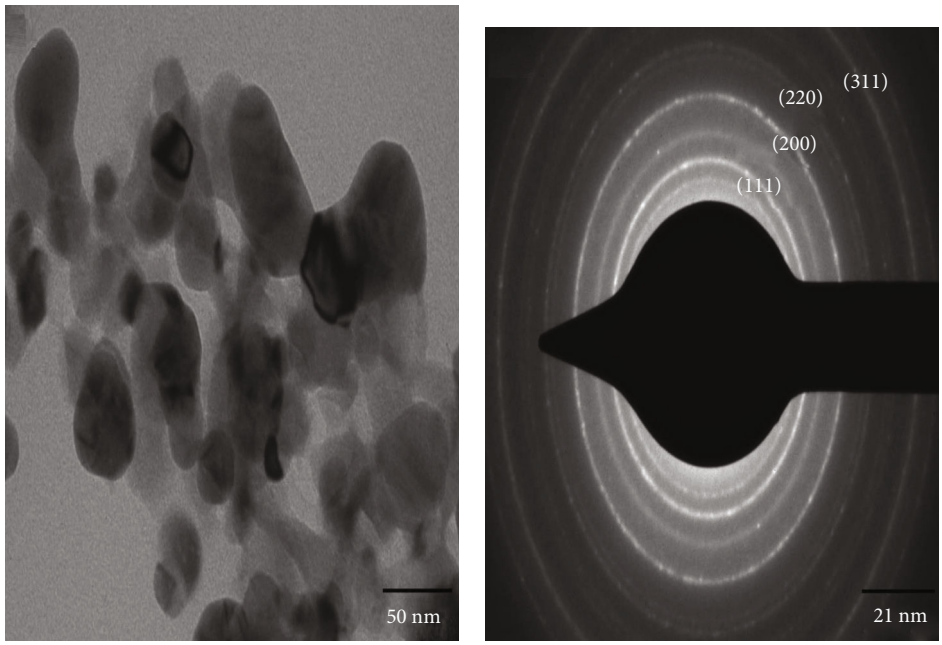

Figure 4: (a) TEM micrograph of AgNPs and (b) SAED pattern.

immunomodulatory, antibacterial, antiviral, anti-inflammatory, anticoagulant, and antithrombotic effects [20–25], the aim of the present study is to synthesize AgNPs using the commercially available fucoidan source of *Fucus vesiculosus* (Fv-fucoidan) as a reducing and capping agent and to explore the potential antimicrobial, antioxidant, and anticancer activities of the synthesized AgNPs.

2. Materials and Methods

Fucoidan from *Fucus vesiculosus* source (brown marine algae) and silver nitrate was purchased from Sigma Aldrich, India, and the standard antibiotics and media were purchased from HiMedia laboratories, Mumbai, India. The bacterial strains used in the present study were obtained from Micro Labs, Tamil Nadu, India (*Bacillus* sp., *Serratia pnematodiphila*, *Streptococcus* sp., and *Klebsiella pneumoniae*), and Micro Labs, Chandigarh, India (*Bacillus subtilis* and *Klebsiella planticola*).

2.1. Synthesis and Characterization of AgNPs. Colloidal AgNPs were synthesized by reducing the silver nitrate in an aqueous solution of fucoidan from *Fucus vesiculosus* source (brown marine algae). Briefly, fucoidan-stabilized

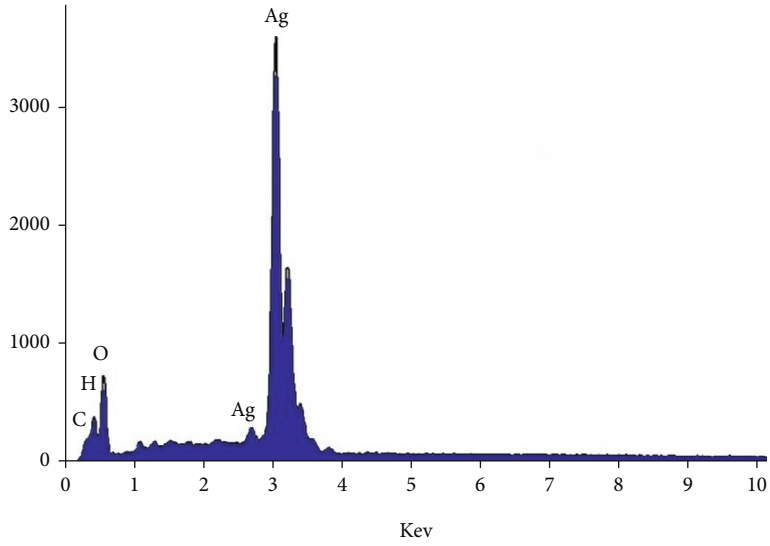

Figure 5: EDX spectrum of the synthesized AgNPs.

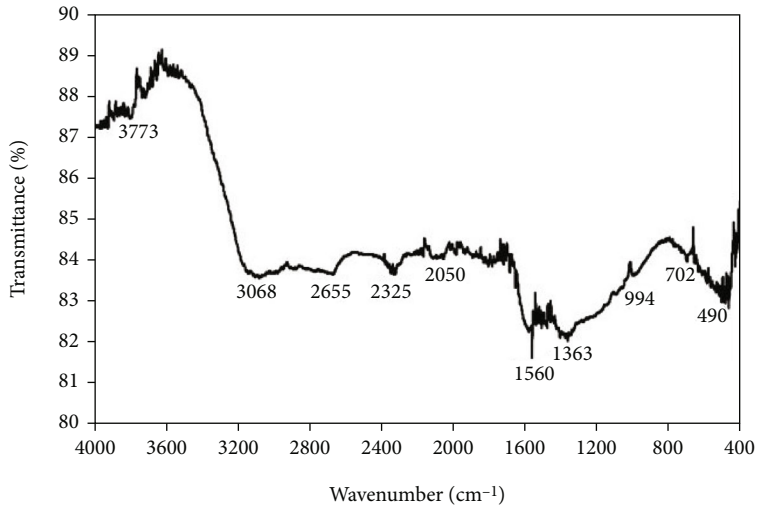

Figure 6: FT-IR spectrum of AgNPs synthesized using Fv-fucoidan, *X*-axis shows the wavenumber in cm^{-1}, and *Y*-axis indicates the transmittance of the silver nanoparticles.

AgNPs were synthesized by mixing aqueous solutions of fucoidan (10 ml) and silver nitrate (100 ml, 1 mM) in an Erlenmeyer flask at room temperature. The flask was kept in the orbital shaker at 300 rpm to homogenize the resulting solution for 20 min. The reduction of Ag+ to AgNPs was regularly checked by the UV-visible spectra. The analysis was done using UV-visible spectrophotometer (Perkin Elmer) in the wavelength range 350–650 nm.

The synthesized AgNPs were purified using deionized water with continuous centrifugation, collected, and dried in hot air oven at 80°C for 2 hours. The dried AgNPs were characterized by various techniques. The crystalline nature was studied by XRD (Bruker, Karlsruhe, Germany), and the functional groups responsible for reduction of silver ions and stabilization of the formed AgNPs were studied by Fourier transform infrared (FT-IR) spectroscopy (Perkin Elmer). To examine the size and shape of AgNPs, the transmission electron microscope (TEM) (Hitachi S-4500) and scanning electron microscope (SEM) (Philip model CM 200) were used. The elemental analysis was determined by energy-dispersive X-ray spectroscopy (EDS) attached to the SEM [26–28].

2.2. Antibacterial Assessment. The antibacterial activity of fucoidan-stabilized AgNPs was examined against six bacterial strains (*Bacillus* sp., *Serratia pnematodiphila*, *Streptococcus* sp., *Klebsiella pneumoniae*, *Bacillus subtilis*, and *Klebsiella planticola*). The standard antibiotic disks were purchased from HiMedia laboratories (Mumbai, India). Two different diffusion methods were applied [27–30] to assess the antibacterial activity.

2.3. Agar Well Diffusion Method. The antibacterial activity of the synthesized AgNPs were explored against Gram-

Table 1: Antibacterial activity of fucoidan-stabilized AgNPs.

AgNPs conc.	25 μl	50 μl	75 μl
Bacterial isolates		Zone of inhibition (mm)	
Bacillus subtilis	09.03 ± 0.033	10.17 ± 0.088	11.17 ± 0.088
Bacillus sp.	09.27 ± 0.146	09.97 ± 0.033	11.03 ± 0.033
K. planticola	09.07 ± 0.120	10.07 ± 0.120	11.77 ± 0.394
K. pneumoniae	10.23 ± 0.186	11.00 ± 0.000	15.53 ± 0.318
Serratia nematodiphila	10.20 ± 0.116	11.00 ± 0.000	14.00 ± 0.000
Streptococcus sp.	09.06 ± 0.177	09.67 ± 0.334	10.23 ± 0.234

Table 2: Antibacterial activity of diverse antibiotics and AgNPs impregnated with diverse antibiotics (blend).

Bacterial isolates	*Bacillus subtilis*		*Bacillus* sp.		*K. planticola*		*K. pneumoniae*		*Serratia nematodiphila*		*Streptococcus* sp.	
	Zone of inhibition (mm)											
Antibiotics	Ab	Blend	Ab	Blend	Ab	Blend	Ab	Blend	Ab	Blend	Ab	Blend
Tetracycline	15	18	18	21	21	25	29	31	13	12	15	18
Novobiocin	15	15	16	18	18	23	18	20	0	6	15	17
Gentamicin	11	14	18	23	19	24	25	29	17	21	19	20
Kanamycin	18	20	19	20	21	28	21	30	19	19	18	20
Streptomycin	15	19	15	20	16	20	16	22	13	14	16	20
Penicillin	0	5	0	8	20	19	36	38	0	6	0	8
Chloramphenicol	25	28	21	25	32	38	34	37	27	30	24	21
Ampicillin	0	11	8	11	20	23	38	43	15	22	0	9
Ciprofloxacin	27	22	27	25	34	39	31	33	40	41	27	25

negative (*Serratia pnematodiphila*, *Klebsiella pneumonia*, and *Klebsiella planticola*) and Gram-positive (*Streptococcus* sp., *Bacillus subtilis*, and *Bacillus* sp.) bacteria by adopting the agar well diffusion method [10]. Roughly, 20 ml of sterilized and cooled Mueller-Hinton agar medium was filled with sterile Petri dishes and permitted to solidify at room temperature. The overnight growth test organisms were spread over the agar medium by a sterile cotton swab for each test, and then, the wells were made using a sterile polystyrene tip. Diverse concentrations of AgNPs (25, 50, and 75 μl) were added to the wells. The AgNP-inoculated plates were incubated for 24 h at 37°C. After that, the inhibition zone around the well was calculated and recorded. The tests were done in triplicates [31–34].

2.4. Disk Diffusion Method. Disk diffusion method was used to evaluate the in vitro enhanced antibacterial activity of diverse antibiotics (ampicillin, tetracycline, novobiocin, penicillin, kanamycin, gentamicin, chloramphenicol, streptomycin, and ciprofloxacin) against the clinical isolates of bacteria (such as *B. subtilis*, *Bacillus* sp., *S. nematodiphila*, *K. planticola*, *K. pneumoniae*, and *Streptococcus* sp.). To determine the mutual effect, each standard antibiotic disks was further impregnated with 25 μl of the freshly prepared AgNPs. The Petri dishes containing 20 ml Mueller-Hinton agar (MHA) were swabbed with 24 h culture of bacterial strains. Standard sterile antibiotic disks are known as positive control, and

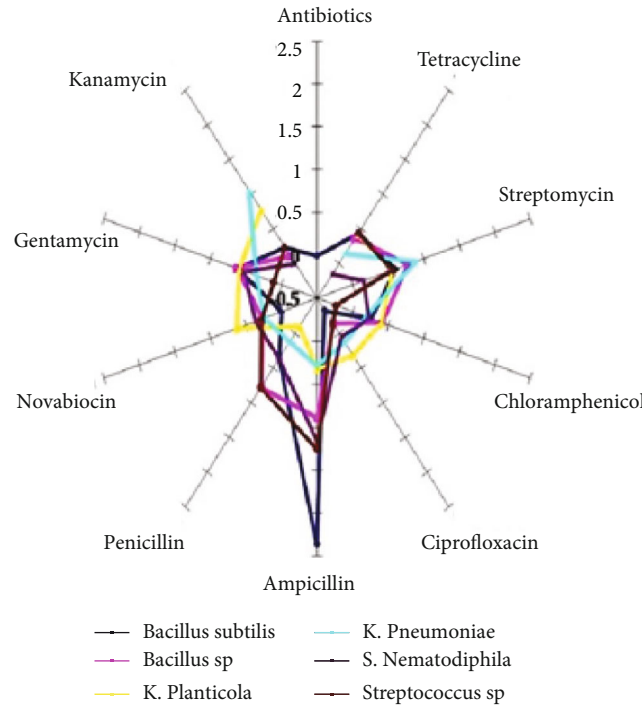

Figure 7: Increased fold area of fucoidan-stabilized AgNPs for enhanced antibacterial activity.

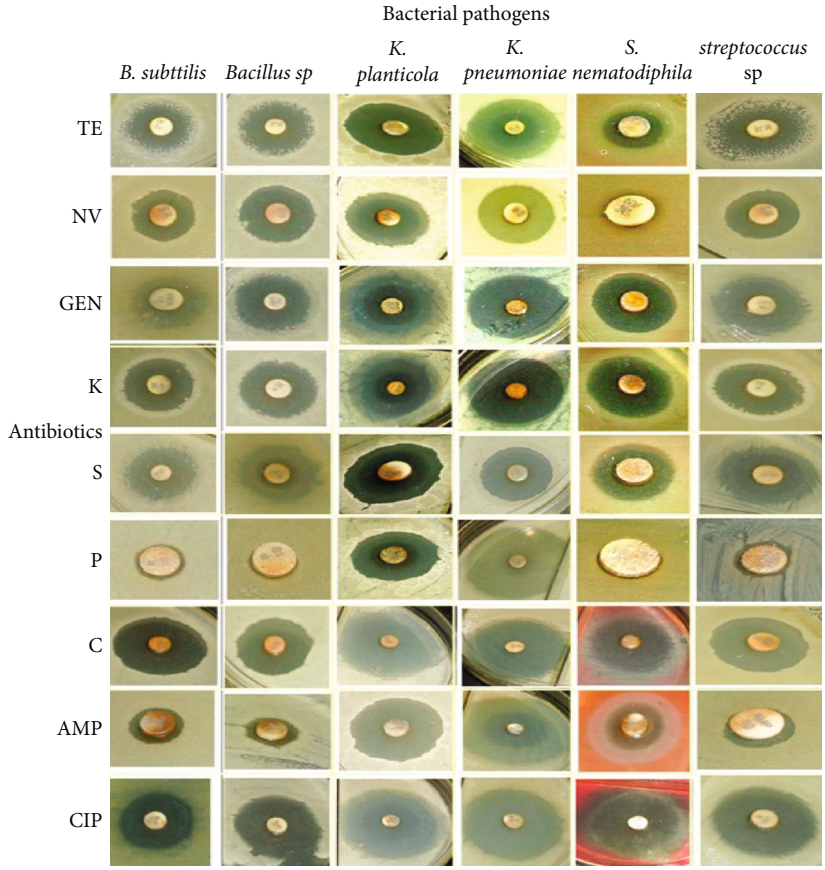

Figure 8: Enhanced antibacterial activity of the synthesized AgNPs impregnated with diverse antibiotics in the *Y*-axis the antibiotics such as TE (tetracycline), NV (novamycin), GEN (gentamycin), K (kanamycin), S (streptomycin), P (penicillin), C (cephalexin), AMP (ampicillin), CIP (ciprofloxacin) against the bacterial strains in *X*-axis *B. subtilis*, *Bacillus* sp., *K. planticola*, *K. pneumoniae*, *S. pnematodiphila*, and *Streptococcus* sp.

antibiotics disks impregnated with AgNPs were placed onto the MHA medium inoculated with pathogenic bacterial isolates. The inoculated plates were then incubated at room temperature for 24 h. After the incubation, the zone of inhibition was measured, and the assays were performed in triplicates. The enhancement in the fold area in the zone of inhibition was evaluated by calculating the mean surface area of the inhibition zone generated by an antibiotic (a) and AgNPs impregnated with an antibiotic (b). The fold increase area was calculated by the following equation.

$$\frac{\left(b^2 - a^2\right)}{a^2}, \tag{1}$$

where a refers to the inhibition zones for antibiotic alone and b refers to the AgNPs impregnated with antibiotic, respectively [11].

2.5. Antifungal Susceptibility by the Well Diffusion Method. Several pathogenic impacts of fungi have been stated in plants and animals, as well as humans. The opportunistic infections are caused by fungi such as *Aspergillus niger*, *Aspergillus fumigatus*, *Candida* sp., and *Aspergillus flavus*. Inoculum suspensions were prepared by scratching the surface of the colonies via an antiseptic needle, and the fungal spores were blended with 10 ml sterilized distilled water. Each fungal suspension was swabbed consistently using sterile cotton swabs on sterilized Potato Dextrose Agar (PDA) plates. With the help of a sterilized polystyrene tip, about 3 wells (5 mm diameter) were prepared. Diverse concentrations of AgNPs solution (50 μl, 100 μl, and 150 μl) were added to each well on all plates. Then, the plates were incubated at 37°C for 48-78 h. A clear inhibition zone around the wells was detected. For each organism, the inhibition zone diameter was measured (in millimeter).

2.6. Anticancer Activity of AgNPs against HepG2 and A549 Cell Lines

2.6.1. Cell Viability Test. The in vitro cytotoxic effect of the synthesized AgNPs on HepG2 and A549 cell lines were evaluated by MTT assay [11]. Briefly, the cell lines were plated separately in 96 well plates (1 × 104 cells/well) and incubated for 24 h at 37°C in 5% CO_2. Afterwards, the cells were washed twofold with 100 μl of serum-free medium and starved for 1 h in CO_2 incubator. Subsequently, the cells were treated with various concentrations of AgNPs in the range of 1-100 μg/ml and again warmed at 37°C in CO_2 incubator. After 24 h incubation, MTT (0.05 mg/ml) was added in every well and again incubated for 4 h. The MTT-

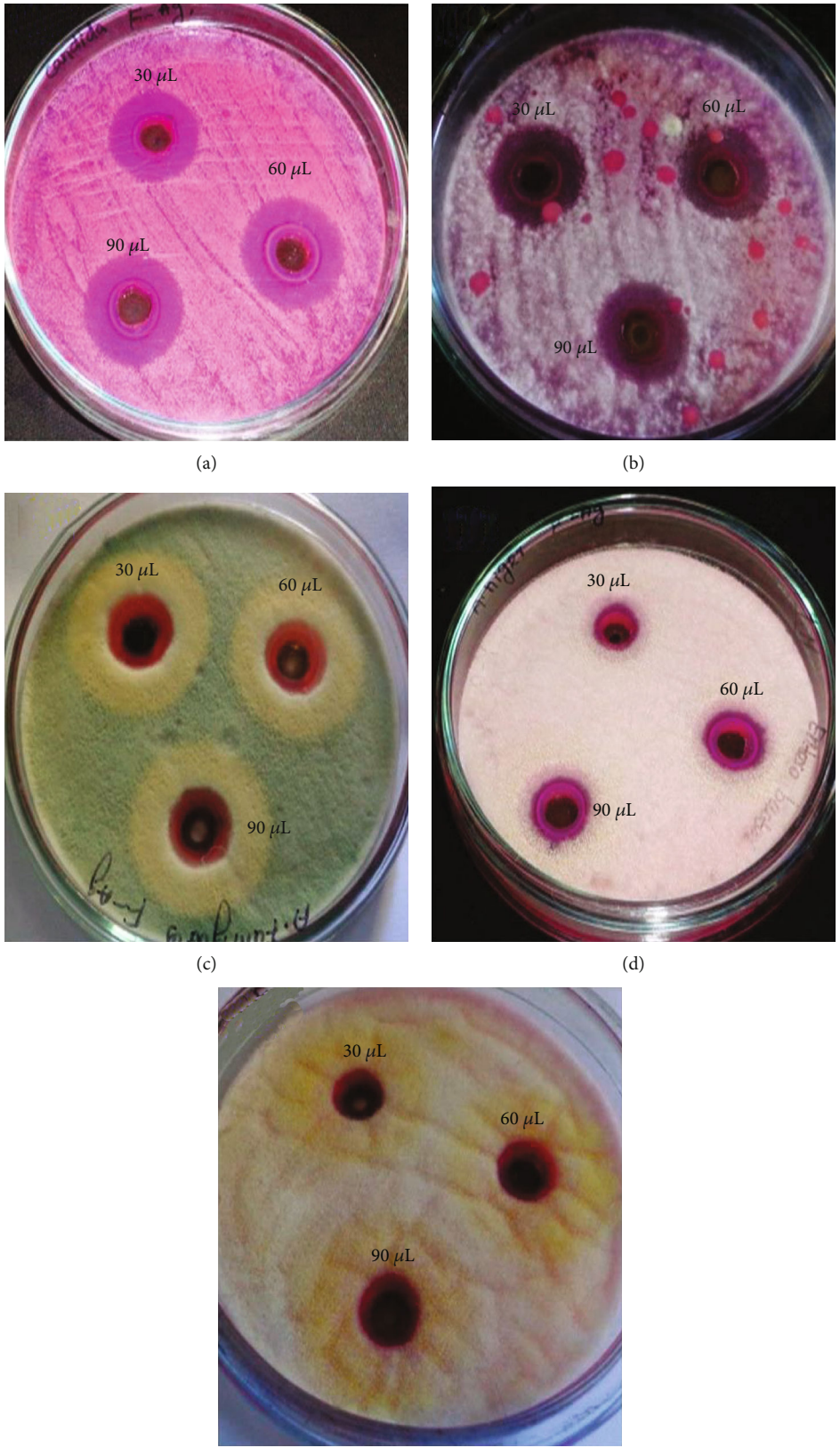

Figure 9: Fungicidal activity of the synthesized AgNPs against the selected fungi. (a) *C. albicans*, (b) *Fusarium* sp., (c) *A. fumigatus*, (d) *A. niger*, and (e) *A. flavus*.

containing medium was thrown away and washed with 200 μl phosphate buffer saline solutions. Then, the crystals were dissolved by adding 100 μl of DMSO and mixed well. The appearance of purple blue formazan dye was measured in a microplate reader (570 nm). The cytotoxicity of AgNPs is analyzed using the GraphPad Prism 5 software.

2.7. Antioxidant Activity of AgNPs (DPPH Radical Scavenging Activity). The formation of free radicals or the deficient removal of reactive oxygen species can develop oxidative damage to biomolecules. These damage leads to numerous sicknesses for human, such as tumor, atherosclerosis, diabetes, maturing, and other degenerative disorders [12]. DPPH (2,2-diphenyl-2-picrylhydrazyl) is a stable free radical that accepts an electron or hydrogen radical from the antioxidant compound and gets reduced to a stable diamagnetic molecule. The reduction of DPPH is associated with color change from pink to yellow. The scavenging ability of DPPH free radicals by fucoidan extract-mediated AgNPs and vitamin C was used as standard as mentioned in the previous study [13]. The percentage of inhibition was calculated by utilizing the following equation:

$$\%\text{Inhibition} = \left(\frac{\text{absorbance of control} - \text{absorbance of test sample}}{\text{absorbance of control}}\right) \times 100. \quad (2)$$

3. Results and Discussion

3.1. Visual Inspection and UV-Visible Spectroscopy of AgNPs. The formation of AgNPs by aqueous solution of fucoidan at room temperature was affirmed by visual examination. As appeared in Figure 1, the color of the reaction mixture change from yellow to brown which shows the generation of silver nanoparticles, due to the reduction of Ag ions into AgNPs through the active molecules present in the fucoidan extract. This color is credited due to the excitation of surface plasmon spectra (SPR). Moreover, the formation of AgNPs was followed by measuring the UV-visible absorbance at various time intervals in the range of 350–650 nm (Figure 2).

3.2. X-Ray Diffraction Analysis. The crystalline nature of AgNPs was confirmed by XRD (Figure 3). The diffraction patterns showed four distinct peaks at $2\theta = 38.15°, 44.30°, 64.53°$, and $76.96°$. These peaks can be indexed to the (111), (200), (220), and (311) reflection planes which predicts the face centered cubic structure (fcc) of AgNPs in agreement with the previous study.

3.3. Transmission Electron Microscopy. The TEM image of AgNPs showed monodisperse nanoparticles with spherical shape in the size ranges from 4 to 45 nm (Figure 4(a)). Moreover, the crystalline nature of the nanoparticles is evidenced by the selected area electron diffraction (SAED) patterns with bright circular spots matching to (111), (200), (220), and (311) planes. The SAED pattern results stay in concordant good agreement with the previous study [14].

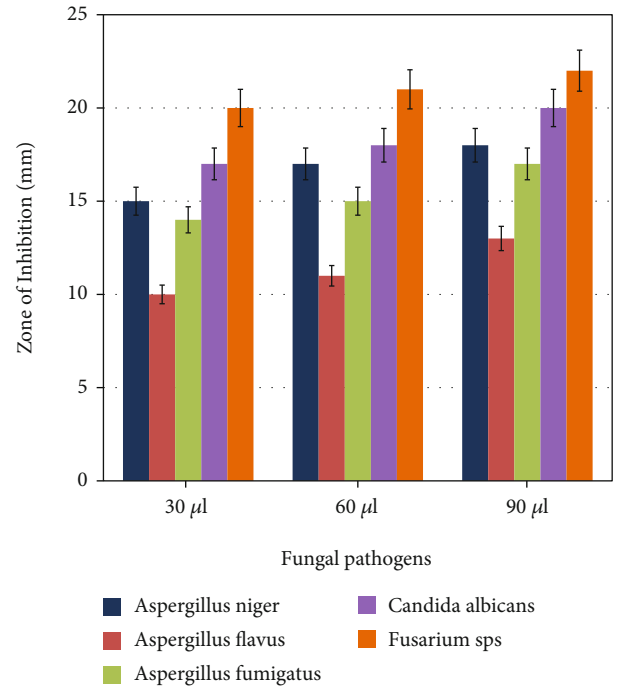

Figure 10: The fungicidal activity of AgNPs against different fungal pathogens. *X*-axis indicates the different concentration of silver nanoparticles, and *Y*-axis indicates the zone of inhibition in mm

3.4. Energy-Dispersive X-Rays (EDX). The elemental outline of the synthesized AgNPs (Figure 5) showed higher proportion of silver at 3 keV. Mostly, metallic silver nanoparticles display distinctive optical absorption peak almost at 3 keV due to their surface plasmon resonance.

3.5. Fourier Transform Infrared Spectroscopy. The inorganic biomolecules in the fucoidans responsible for the synthesis of silver nanoparticles were analyzed by using the FT-IR analysis (Figure 6). Silver nanoparticle-synthesized Fv-fucoidan had the absorption band at 3068 cm^{-1}, showing C-H stretching groups of aromatics, and the low absorption band shows at 2655 and 2325 cm^{-1}, indicating the presence of O-H stretching carboxylic groups. The band at 1560 cm^{-1} corresponds to amides of N-H bending group, 1363 cm^{-1} shows aliphatic nitro groups, and 994 cm^{-1} shows =C-H bending of alkenes groups. The small bands at 702 and 490 cm^{-1} indicate the presence of alkyl halides.

3.6. Antibacterial Activities of Fucoidan-Mediated Silver Nanoparticles. The result demonstrated that AgNPs display great bactericidal action against Gram-negative and Gram-positive microscopic organisms. The Gram-negative bacteria (*K. planticola*, *K. pneumoniae*, and *Serratia nematodiphila*) indicated bigger inhibition zones than the Gram-positive bacteria (*Bacillus Subtilis*, *Bacillus* sp., and *Streptococcus* sp.) (Table 1).

This might be due to the variety in the composition of their cell walls [14, 15]. The bactericidal action increases by increasing the AgNP concentration. Interestingly, the combination of AgNPs and diverse antibiotics demonstrated a synergistic impact. It was observed that AgNPs impregnated

Table 3: Anticancer activity of AgNPs against liver (HepG2) and lung (A549) cancer cell lines.

	AgNPs conc. (μg)	1	10	25	50	100
HepG2	% cell viability (treatment)	90.48	74.23	59.25	47.56	32.22
	% cell viability (cyclophosphamide)	87.81	73.40	23.21	1.93	1.48
A549	% cell viability (treatment)	98.27	89.26	75.20	68.25	50.14
	% cell viability (cyclophosphamide)	85.57	68.64	37.90	19.30	5.40

with novobiocin and penicillin disks showed a great inhibition zone (Table 2 and Figures 7 and 8) compared to the novobiocin and penicillin antibiotic-treated *S. nematodiphila* (6 mm), penicillin-treated *B. subtilis* (5 mm), *Bacillus* sp. (8 mm), and *Streptococcus* sp. (8 mm), and ampicillin-treated *B. subtilis* (11 mm) and *Streptococcus* sp. (9 mm).

3.7. Antifungal Activity of Fucoidan-Mediated Silver Nanoparticles. The synthesized AgNPs showed excellent fungicidal activity against all chosen clinical isolates (Figures 9 and 10). The inhibition zone increases in a specific order ranging from *Fusarium* sp. (22.43 ± 0.296) > *C. albicans* (20.07 ± 0.067) > *A. niger* (17.87 ± 0.241) > *A. fumigatus* (17.50 ± 0.501) > *A. flavus* (12.97 ± 0.261). The minimal fungicidal action was noted against *A. flavus*.

3.8. Anticancer Activity of AgNPs against Liver and Lung Cancer Cell Lines. The liver and lung cancers are the most common cancers causing a lot of death globally. The results of anticancer action imply the high cytotoxic activity of the synthesized AgNPs against the tumor cells (HepG2 and A549) when compared with the standard cyclophosphamide. The cytotoxic effect of fucoidan-mediated silver nanoparticles was higher in A549 cell line than HepG2. As the concentration of AgNPs increases, the cytotoxicity also increases as predicted in Table 3.

3.9. DPPH Radical Scavenging Activity. The free radical scavenging activity by the DPPH (2,2-diphenyl-2-picrylhydrazyl) method showed higher activity in the green synthesized AgNPs when compared with fucoidan and vitamin C (standard). The antioxidant activity of AgNPs displayed significant dosage-dependent inhibition (Figure 11). The maximum inhibition percentage of AgNPs at 10 μg/ml concentration was recorded to be 84% for DPPH scavenging.

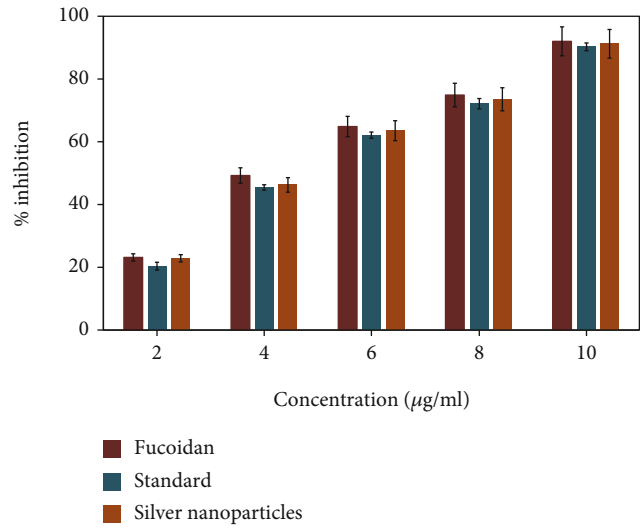

Figure 11: DPPH radical scavenging activity of fucoidan, fucoidan-stabilized AgNPs, and vitamin C as standard *X*-axis indicates the different concentrations of silver nanoparticles and *Y*-axis indicates the percentage of inhibition.

4. Discussion

Noble metals are known to exhibit unique optical properties due to the excitation of SPR. A distinctive surface plasmon resonance (SPR) band was observed at 430 nm after 24 h which is characteristic for AgNPs. As the incubation time was increased, the absorbance of SPR band increased too without band shift. This clearly reflects the development of AgNPs. The stability of the formed AgNPs was evidenced by measuring its UV-Vis absorbance after two months where no alteration in absorbance or shapes of bands was recognized. In the XRD results, the intensity of these peaks (111), (200), (220), and (311) reflects the high degree of crystalline nature of the AgNPs [11].

The EDX spectrum additionally shows that the weak signals for oxygen, nitrogen, and carbon were observed. This could be due to the biochemical molecules of Fv-fucoidan responsible for AgNP synthesis and stabilization [14]. In concurrence with previous studies, the AgNPs impregnated with antibiotics showed fine antibacterial action when compared with AgNPs and antibiotics separately [16, 17]. These are essential results to prompt a diminishment in the amount of medications important to treat illnesses, subsequently reducing side effects and improvement of antibacterial action against drug-resistant bacterial strains.

Despite the fact that it is more pathogenic, it also has more noteworthy harmfulness and produces mycotoxins. Moreover, the increase in AgNPs concentration reduces the antifungal action in a dose-dependent manner [35]. The cytotoxic effect of AgNPs is due to the physicochemical interaction of silver atoms with the functional groups of intracellular proteins, as well as with the phosphate group's nitrogen bases in DNA [2]. Some of the approved chemotherapeutic agents were identified to cause side effects. Accordingly, there is an imperative need to create alternative drugs against these deadly diseases. Thus, the green synthesized AgNPs from fucoidan extract act as a powerful free radical scavenger and thus establish their therapeutic importance [11, 35].

5. Conclusion

In the current study, we have recognized an ecofriendly, cost-effective, and facile method for the synthesizing AgNPs using fucoidan extract from *Fucus vesiculosus* source (brown marine algae) at ambient temperature as an effective green reducing and stabilizing agent. The spectroscopic characterization methods display the formation of stable, crystalline, and spherical shape of AgNPs with size ranges from 4 to 45 nm. The synthesized AgNPs show good antimicrobial activity against the selected six pathogenic microorganisms. They also showed a synergistic effect on the antimicrobial activity of the standard antibiotics. Moreover, AgNPs inhibit the cell viability of liver cancer cells lines (HepG2) and lung cancer cell lines (A549). In vitro antioxidant assays illustrated that AgNPs have the potential scavenging activity against DPPH. The conventional chemical methods for synthesizing nanoparticles are costly and time consuming and pose a great threat when disposed in environment, and contact with these chemically synthesized nanoparticles might result in major diseases like skin cancer and lung cancer. Therefore, this green synthesis approach appears to be an ecofriendly alternative to the conventional chemical methods and stands as an effective alternative drug that can be used for biomedical applications in the future.

Data Availability

The authors confirm that the data supporting the findings of this study are available within the article.

Conflicts of Interest

The authors declare no conflicts of interest.

Authors' Contributions

This work was carried out in collaboration among all authors. Author 1 designed the study and performed the research. Author 2 wrote the first draft of the manuscript. Authors 3 and 4 managed the statistical analysis of the study, analyses, and revision. Author 5 managed the literature searches and manuscript revision. All authors read and approved the final manuscript.

Acknowledgments

This work was funded by the Researchers Supporting Project (RSP-2021/165), King Saud University, Riyadh, Saudi Arabia.

References

[1] P. J. Rivero, J. Goicoechea, A. Urrutia, and F. J. Arregui, "Effect of both protective and reducing agents in the synthesis of multicolor silver nanoparticles," *Nanoscale Research Letters*, vol. 8, no. 1, pp. 1–9, 2013.

[2] A. Haider and I. K. Kang, "Preparation of silver nanoparticles and their industrial and biomedical applications: a comprehensive review," *Advances in Materials Science and Engineering*, vol. 2015, Article ID 165257, 16 pages, 2015.

[3] N. L. Pacioni, C. D. Borsarelli, V. Rey, and A. V. Veglia, "Synthetic routes for the preparation of silver nanoparticles," in *Silver nanoparticle applications*, pp. 13–46, Springer, Cham, 2015.

[4] S. Ahmed, M. Ahmad, B. L. Swami, and S. Ikram, "A review on plants extract mediated synthesis of silver nanoparticles for antimicrobial applications: a green expertise," *Journal of Advanced Research*, vol. 7, no. 1, pp. 17–28, 2016.

[5] J. G. Fernandez, M. A. Fernandez-Baldo, E. Berni et al., "Production of silver nanoparticles using yeasts and evaluation of their antifungal activity against phytopathogenic fungi," *Process Biochemistry*, vol. 51, no. 9, pp. 1306–1313, 2016.

[6] B. Xue, D. He, S. Gao, D. Wang, K. Yokoyama, and L. Wang, "Biosynthesis of silver nanoparticles by the fungus Arthroderma fulvum and its antifungal activity against genera of Candida, Aspergillus and Fusarium," *International Journal of Nanomedicine*, vol. 11, p. 1899, 2016.

[7] T. N. J. I. Edison, R. Atchudan, C. Kamal, and Y. R. Lee, "Caulerpa racemosa: a marine green alga for eco-friendly synthesis of silver nanoparticles and its catalytic degradation of methylene blue," *Bioprocess and Biosystems Engineering*, vol. 39, no. 9, pp. 1401–1408, 2016.

[8] S. Mohsin, R. Mahadevan, A. S. Sumayya, and G. M. Kurup, "Bifunctional effect of fucoidan from Padina tetrastromatica against human pathogenic microbes and free radicals," *Journal of Medicinal Herbs and Ethnomedicine*, vol. 2, pp. 1–10, 2016.

[9] T. C. Y. Leung, C. K. Wong, and Y. Xie, "Green synthesis of silver nanoparticles using biopolymers, carboxymethylated-curdlan and fucoidan," *Materials Chemistry and Physics*, vol. 121, no. 3, pp. 402–405, 2010.

[10] M. Balouiri, M. Sadiki, and S. K. Ibnsouda, "Methods for _in vitro_ evaluating antimicrobial activity: A review," *Journal of pharmaceutical analysis*, vol. 6, no. 2, pp. 71–79, 2016.

[11] S. Rajeshkumar, C. Malarkodi, M. Vanaja, and G. Annadurai, "Anticancer and enhanced antimicrobial activity of biosynthesizd silver nanoparticles against clinical pathogens," *Journal of Molecular Structure*, vol. 1116, pp. 165–173, 2016.

[12] B. Halliwell, "Reactive species and antioxidants. Redox biology is a fundamental theme of aerobic life," *Plant Physiology*, vol. 141, no. 2, pp. 312–322, 2006.

[13] J. P. Abraham, B. Plourde, L. Vallez, J. Stark, and K. R. Diller, "Estimating the time and temperature relationship for causation of deep-partial thickness skin burns," *Burns*, vol. 41, no. 8, pp. 1741–1747, 2015.

[14] S. Shrivastava, T. Bera, A. Roy, G. Singh, P. Ramachandrarao, and D. Dash, "Characterization of enhanced antibacterial effects of novel silver nanoparticles," *Nanotechnology*, vol. 18, no. 22, p. 225103, 2007.

[15] M. R. Shah, S. Ali, M. Ateeq et al., "Morphological analysis of the antimicrobial action of silver and gold nanoparticles stabilized with ceftriaxone on Escherichia coli using atomic force microscopy," *New Journal of Chemistry*, vol. 38, no. 11, pp. 5633–5640, 2014.

[16] I. Akpinar, M. Unal, and T. Sar, "Potential antifungal effects of silver nanoparticles (AgNPs) of different sizes against phytopathogenic fusarium oxysporum f. sp. radicis-lycopersici (FORL) strains," *SN Applied Sciences*, vol. 3, no. 4, pp. 1–9, 2021.

[17] S. Jebril, R. Khanfir Ben Jenana, and C. Dridi, "Green synthesis of silver nanoparticles using _Melia azedarach_ leaf extract and their antifungal activities: _In vitro_ and _in vivo_," *Materials Chemistry and Physics*, vol. 248, p. 122898, 2020.

[18] S. V. Kumar, T. R. Sri, N. Prakash, and E. Muthusankar, "Preparation and evaluation of silver nanoparticles embedded in Muntingia calabura leaf extract to cure White Piedra," *Journal of Pharmaceutical Innovation*, vol. 135, pp. 1–12, 2021.

[19] S. Hari, "Biosynthesis of nanoparticles from microorganisms," *Research Journal of Pharmacy and Technology*, vol. 13, no. 4, pp. 2024–2028, 2020.

[20] A. Sidhu, A. Bala, H. Singh, R. Ahuja, and A. Kumar, "Development of MgO-sepoilite nanocomposites against phytopathogenic fungi of rice (Oryzae sativa): a green approach," *ACS Omega*, vol. 5, no. 23, pp. 13557–13565, 2020.

[21] M. Gośliński, D. Nowak, and L. Kłębukowska, "Antioxidant properties and antimicrobial activity of manuka honey versus Polish honeys," *Journal of Food Science and Technology*, vol. 57, no. 4, pp. 1269–1277, 2020.

[22] S. Walia, S. Mukhia, V. Bhatt, R. Kumar, and R. Kumar, "Variability in chemical composition and antimicrobial activity of Tagetes minuta L. essential oil collected from different locations of Himalaya," *Industrial Crops and Products*, vol. 150, article 112449, 2020.

[23] R. Kalarani, M. Sankarganesh, G. V. Kumar, and M. Kalanithi, "Synthesis, spectral, DFT calculation, sensor, antimicrobial and DNA binding studies of Co(II), Cu(II) and Zn(II) metal complexes with 2-amino benzimidazole Schiff base," *Journal of Molecular Structure*, vol. 1206, p. 127725, 2020.

[24] S. A. Akintelu, B. Yao, and A. S. Folorunso, "Green synthesis, characterization, and antibacterial investigation of synthesized gold nanoparticles (AuNPs) from Garcinia kola pulp extract," *Plasmonics*, vol. 16, no. 1, pp. 157–165, 2021.

[25] D. Bismarck, A. Dusold, A. Heusinger, and E. Müller, "Antifungal in vitro activity of essential oils against clinical isolates of Malassezia pachydermatis from canine ears: a report from a practice laboratory," *Complementary medicine research*, vol. 27, no. 3, pp. 143–154, 2020.

[26] A. S. Márquez-Rodríguez, S. Nevárez-Baca, J. C. Lerma-Hernández et al., "In vitro antibacterial activity of Hibiscus sabdariffa L. phenolic extract and its in situ application on shelf-life of beef meat," *Foods*, vol. 9, no. 8, 2020.

[27] A. Habib, M. A. Iqbal, H. N. Bhatti, A. Kamal, and S. Kamal, "Synthesis of alkyl/aryl linked binuclear silver(I)- _N_ -Heterocyclic carbene complexes and evaluation of their antimicrobial, hemolytic and thrombolytic potential," *Inorganic Chemistry Communications*, vol. 111, p. 107670, 2020.

[28] A. Salama, M. Hasanin, and P. Hesemann, "Synthesis and antimicrobial properties of new chitosan derivatives containing guanidinium groups," *Carbohydrate Polymers*, vol. 241, p. 116363, 2020.

[29] A. A. Menazea and N. S. Awwad, "Antibacterial activity of TiO_2 doped ZnO composite synthesized via laser ablation route for antimicrobial application," *Journal of Materials Research and Technology*, vol. 9, no. 4, pp. 9434–9441, 2020.

[30] J. Jin, T. T. H. Nguyen, S. Humayun et al., "Characteristics of sourdough bread fermented with _Pediococcus pentosaceus_ and _Saccharomyces cerevisiae_ and its bio-preservative effect against _Aspergillus flavus_," *Food Chemistry*, vol. 345, p. 128787, 2021.

[31] A. Günsel, A. T. Bilgiçli, C. Kandemir, R. Sancak, G. Arabaci, and M. Nilüfer Yarasir, "Comparison of novel tetra-substituted phthalocyanines with their quaternized derivatives: antioxidant and antibacterial properties," *Synthetic Metals*, vol. 260, p. 116288, 2020.

[32] L. Tesfaye Jule, K. Ramaswamy, N. Nagaprasad, V. Shanmugam, and V. Vignesh, "Design and analysis of serial drilled hole in composite material," *Materials Today: Proceedings*, vol. 45, no. 6, pp. 5759–5763, 2021.

[33] L. T. Jule, R. Krishnaraj, B. Bekele, A. Saka, and N. Nagaprasad, "Experimental investigation on the impacts of annealing temperatures on titanium dioxide nanoparticles structure, size and optical properties synthesized through sol-gel methods," *Materials Today Proceeding*, vol. 45, no. 6, pp. 5752–5758, 2021.

[34] N. Nagaprasad, B. Stalin, V. Vignesh, M. Ravichandran, N. Rajini, and O. Ismail, "Applicability of cellulosic-based Polyalthia longigolia seed filler reinforced vinyl ester biocomposites on tribological performance," *Polymer Composites*, vol. 42, no. 2, pp. 791–804, 2021.

[35] K. C. Hembram, R. Kumar, L. Kandha, P. K. Parhi, C. N. Kundu, and B. K. Bindhani, "Therapeutic prospective of plant-induced silver nanoparticles: application as antimicrobial and anticancer agent," *Artificial Cells, Nanomedicine, and Biotechnology*, vol. 46, supplement 3, pp. S38–S51, 2018.

Hindawi
Oxidative Medicine and Cellular Longevity
Volume 2021, Article ID 7995223, 14 pages
https://doi.org/10.1155/2021/7995223

Review Article

An Update Report on the Biosafety and Potential Toxicity of Fullerene-Based Nanomaterials toward Aquatic Animals

Nemi Malhotra,[1] **Gilbert Audira**,[2,3] **Agnes L. Castillo**,[4] **Petrus Siregar**,[2,3] **Johnsy Margotte S. Ruallo**,[5] **Marri Jmelou Roldan**,[6] **Jung-Ren Chen**,[7] **Jiann-Shing Lee**,[8] **Tzong-Rong Ger**,[1,9] **and Chung-Der Hsiao**[2,3,9,10]

[1]*Department of Biomedical Engineering, Chung Yuan Christian University, Chung-Li 320314, Taiwan*
[2]*Department of Chemistry, Chung Yuan Christian University, Chung-Li 320314, Taiwan*
[3]*Department of Bioscience Technology, Chung Yuan Christian University, Chung-Li 320314, Taiwan*
[4]*Faculty of Pharmacy, The Graduate School and Research Center for the Natural and Applied Sciences, University of Santo Tomas, Manila 1008, Philippines*
[5]*The Graduate School, University of Santo Tomas, Manila 1015, Philippines*
[6]*Faculty of Pharmacy and Graduate School, University of Santo Tomas, Manila 1008, Philippines*
[7]*Department of Biological Science & Technology, College of Medicine, I-Shou University, Kaohsiung 82445, Taiwan*
[8]*Department of Applied Physics, National Pingtung University, Pingtung 900391, Taiwan*
[9]*Center for Nanotechnology, Chung Yuan Christian University, Chung-Li 320314, Taiwan*
[10]*Research Center for Aquatic Toxicology and Pharmacology, Chung Yuan Christian University, Chung-Li 320314, Taiwan*

Correspondence should be addressed to Jiann-Shing Lee; jslee@mail.nptu.edu.tw, Tzong-Rong Ger; sunbow@cycu.edu.tw, and Chung-Der Hsiao; cdhsiao@cycu.edu.tw

Received 30 May 2021; Accepted 26 June 2021; Published 19 July 2021

Academic Editor: Dragica Selakovic

Fullerene molecules are composed of carbon in the form of a hollow sphere, tube, or ellipsoid. Since their discovery in 1985, they have gained a lot of attention in many science fields. The unique carbon cage structure of fullerene provides immense scope for derivatization, rendering potential for various industrial applications. Thus, the prospective applications of fullerenes have led to assorted fullerene derivatives. In addition, their unique chemical structure also eases them to be synthesized through various kinds of conjugating techniques, where fullerene can be located either on the backbone or the branch chain. In this review, we have compiled the toxicity and biosafety aspects of fullerene in aquatic organisms since the frequent use of fullerene is likely to come in contact and interact with the aquatic environment and aquatic organisms. According to the current understanding, waterborne exposure to fullerene-based nanomaterials indeed triggers toxicities at cellular, organic, molecular, and neurobehavioral levels.

1. Introduction and Application of Fullerene

1.1. Introduction of Fullerene. Carbon is known to be found in two allotropes, namely, diamond and graphite. In 1985, Kroto, Curl, and Smalley discovered another allotropic form of carbon, which was fullerene. Because of the discovery and their pioneering efforts, they received the Nobel Prize in 1996 [1]. Fullerenes are regarded as three-dimensional analogs of benzene and composed of carbon atoms that are joined by single and double bonds. Together with fused rings of five to seven carbon atoms, these bonds form a closed or partially closed mesh. Carbon atoms in a fullerene molecule can be found in a variety of sizes and shapes, including hollow spheres, ellipsoids, and tubes [2, 3]. The discovered fullerenes consist of various n numbers of carbon atoms, which obeyed a specific rule.

C_{60}, one of the most well-known and abundant forms of fullerenes, is composed of $n = 60$ carbon atoms, which are arranged in a spherical cage structure of about 7 Å in diameter.

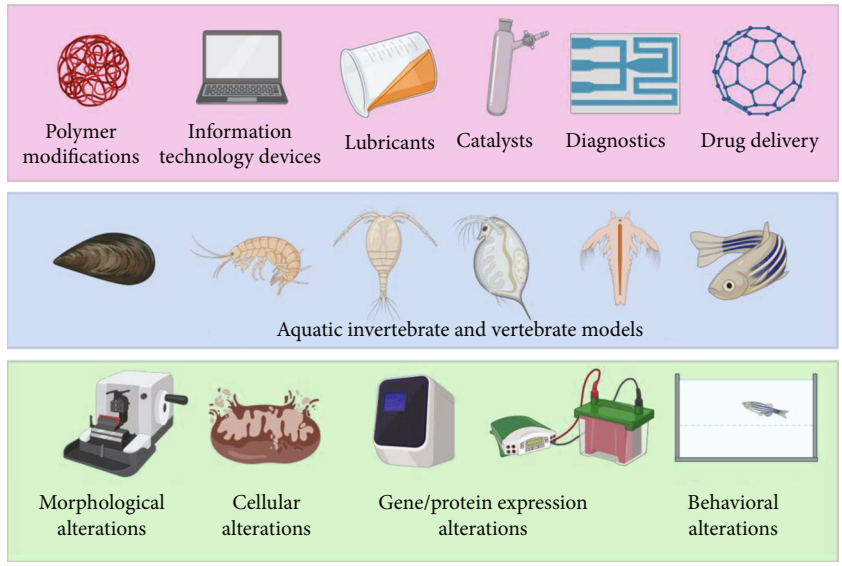

Figure 1: Summary of applications, animal models, and methods of fullerene toxicity assessment in aquatic species. The industrial and biomedical applications of fullerene were compiled in the upper panel (pink color). The invertebrate and vertebrate animal models used to perform fullerene toxicity assessment were compiled in the middle panel (blue color). The various methods used to detect fullerene-induced changes at either morphological, cellular, gene/protein expressional, or behavioral levels were summarized in the bottom panel (green color).

Furthermore, to honor the inventor of geodesic domes in the 1960s, it also goes by the name of buckminsterfullerene [2]. Informally, C_{60} fullerenes are also known as buckyballs since their shape resembles a soccer ball shape. In C_{60} fullerenes, there are two types of C-C bonds with distinct lengths: C_5-C_5 single bonds in the pentagons and C_5-C_6 double bonds in the hexagons with 1.45 Å and 1.40 Å in distance, respectively [4]. The C_{60} has a low specific gravity relative to the diamond (1.65 compared to 3.51). Chemically, the molecule is very stable owing to the fact that destruction of the cages requires temperatures above 1000°C [4, 5]. In addition, besides C_{60}, other fullerenes can consist of numerous carbon atoms, ranging from 30 to 980, creating various structures with different characteristics and applications.

1.2. Applications of Fullerene. These new forms of carbon's distinctive physical and chemical properties have taken numerous scientists to propose several technological applications. Nowadays, C_{60} molecules have attracted a lot of attention since they have a high electron affinity and antioxidant and radical scavenging properties, which can absorb many free radicals responsible for aging the skins and grafting surfactants or hydrophilic polymers in aqueous environments [6–8]. Fullerenes can be integrated into shafts and frames for strengthening composite materials with very thin-walled, lightweight, robust carbon structures that make them currently be applied in cosmetic products and sporting goods industries [9]. Recently, several investigations suggested that a lot of the proposed fullerenes are applicable in many areas, including information technology devices, lubricants, catalysts, diagnostics, pharmaceuticals, polymer modifications, energy applications, and environmental fields [2, 3, 6, 10]. Furthermore, the unique cage structure of fullerenes, coupled with their immense scope for derivatization, opens up the potential of fullerenes to be a therapeutic agent. In addition, it has also been extensively used in many biomedical applications, including MRI contrast agents, X-ray imaging contrast agents, anti-HIV drugs, targeted drug delivery systems, and photodynamic therapy [11–13]. Therefore, the production and usage of fullerenes are expected to escalate in the future. However, most fullerenes are nonbiodegradable molecules whose potential toxicity has not been thoroughly investigated so far. The increased demand for fullerenes and their mass production have raised biosafety and environmental concerns. *In vivo* toxicity testing provides intact systems for the prediction of biological responses. Aquatic invertebrates and vertebrates provide cost, labor, and time-effective platforms for these studies. These *in vivo* study models provide results on many cellular, anatomical, and physiological characteristics. Moreover, their small size, speedy development, and short life cycle make them attractive for evaluating nanomaterial's toxicological effects. Various methods of toxicity assessments have been developed at different levels of these *in vivo* model systems, such as morphological alterations assessed under a microscope, cellular alterations, gene/-protein expression alteration, biochemical analysis, and behavior alterations. The applications of fullerene, aquatic invertebrate, and vertebrate model systems used to assess the toxicity and methods of toxicity analysis of fullerene are compiled in Figure 1.

2. Types and Chemical Composition of Fullerene

2.1. Types of Fullerenes. Fullerenes occur in nature and have a similar structure to graphite, except that they may contain pentagonal rings [14]. Small quantities of fullerene in the form of C_{60}, C_{70}, C_{76}, and C_{84} might be found hidden in

carbon soot [15]. In 2010, by using Spitzer infrared telescope, NASA also found C_{60} and C_{70} in a cloud of cosmic dust surrounding a star [16]. Generally, the synthesis of these fullerenes starts by forming fullerene-rich soot. The original process generates an electric arc between two graphite rods in an inert atmosphere resulting in a vaporized carbon that is subsequently cooled into sooty residue [1, 17]. In addition, laser ablation of graphite targets or laser pyrolysis of aromatic hydrocarbons can also form carbon soot [17]. By contrast, combustion is the most effective method to produce commercial fullerenes in high-temperature, low-pressure premixed flat flames [18]. Later, through these chemical processes, a solid mixture of various fullerenes and other carbons is formed. Afterward, by using suitable organic solvents, small amounts of fullerenes are extracted from the soot and separated by liquid chromatography [17].

The closed buckyballs and cylindrical carbon nanotubes are two major fullerene classes with distinct properties and applications, although some hybrid structures also exist besides these families, including carbon nanobuds. These classes have unique properties due to their carbon atom arrangement. Each carbon atom in the closed fullerenes, especially C_{60}, bonds to three others and is sp^2 hybridized. These delocalized electrons on the surface of a three-dimensional structure stabilize the spheroid structure of C_{60} by resonance [19]. Distorted buckyballs with $n = 24$, 28, 32, 36, and 50 were also obtained, but they are predicted to be unstable. Other relatively common clusters with $n = 70$, 72, 74, 76, 80, 82, and 84 exist but are less abundant in the experimentally produced carbon soot [20]. A general rule is observed that the chemical reactivity significantly decreases with the increasing size of the fullerene molecule. The closed buckyballs, in contrast to graphite, are not electrically conductive. Due to their spherical shape, buckyballs are well known as suitable lubricants. Moreover, buckyballs might be useful in medicine deliveries in the future because of their unique and hollow cage. On the other hand, cylindrical fullerenes, another major family of fullerenes, are known as carbon nanotubes or buckytubes. Every nanotube is a single molecule consisting of millions of carbon atoms. Generally, this molecule's width is only a few nanometers; however, the length ranges from less than a micrometer to several millimeters [21]. Most of the time, the nanotubes have closed ends; however, it is also possible to be open-ended. Carbon nanotubes exhibit higher tensile strength, flexibility, elasticity, and high thermal conductivity [22, 23]. They are often utilized to reinforce composite materials with improved mechanical, electrical, and thermal properties. In addition, these nanotubes may act electrically as either a metal or a semiconductor depending on the hexagonal units' orientation in the tube wall with the tube axis [24].

2.2. Chemical Composition of Fullerene. Since every fullerene possesses abundant cyclohexanes, they are very aromatic and have stable and inert carbon bonds. The insolubility in aqueous media and poor miscibility of fullerenes limit the biological applications, and its strong tendency to form self-aggregate also leads to phase separation problems [25, 26]. Since pristine fullerenes and carbon nanotubes lack hydrogen atoms or other groups on their surface, they cannot undergo substitution reactions. Because of this reason, they need to carry out surface modification in order to promote the functionalization on their surface [26]. It is worth noting that fullerenes are the only known allotropic carbons that are soluble in common organic solvents (for example, toluene) despite a limited solubility in most solvents [4, 26–28]. Once fullerenes are dissolved in organic solvents, various chemical reactions tend to proceed in solution, and thus, numerous fullerene derivatives are formed. In producing these derivatives, fullerenes can undergo various chemical reactions, e.g., oxidation, reduction, nucleophilic substitutions, halogenations, hydrogenations, radical additions, transition-metal-complex formations, and regioselective functionalization reactions [2]. By attaching active groups to their surface and modifying their basic properties to be adjusted to specific functions, the increment in fullerenes reactivity has been demonstrated.

Functionalized buckyballs are primarily divided into two classes: endohedral and exohedral fullerenes. Exohedral fullerenes are formed with substituents outside their cages, while endohedral fullerenes are formed with trapped atomes or molecules inside their cages [27]. These endohedral and exohedral derivatives have been shown to exhibit attractive photonic, electronic, superconducting, lubrication, biomedical, and magnetic properties due to their unique structures [25]. Similar studies have shown that the carbon nanotubes require chemical modifications by attaching the functional groups to improve the compatibility, processing, and solubility with host materials in the engineering of multifunctional materials [29, 30]. Accordingly, the chemical modifications maintain the interesting pristine fullerenes electrochemical, chemical, and physical properties and make them more applicable and reactive for many applications [31].

3. Interaction of Fullerene with Aquatic Invertebrates in reference to Bioavailability, Toxicity, and Biosafety

The invertebrates are among the target groups for nanoparticle (NP) ecotoxicity due to their highly developed cellular internalization processes, such as phagocytosis and endocytosis, of nano- and microscale particles that are essential for physiological functions (cellular immunity and intracellular digestion). The biologic, ecologic, and toxicologic characteristics of invertebrates render them a suitable model to detect chemicals and pollutants in typical habitats, primarily via bioaccumulation potential. In addition, invertebrates also offer an advantage to evaluate the individual effect of exposure to the tested chemicals. Assumptions have also been made that the invertebrate model can be used to predict the effects of some toxicants at population and community levels. Thus, they can early indicate the ecosystem function and structure's deterioration or restoration [32]. We are going to discuss the effects of fullerene in aquatic invertebrate organisms in the current section.

First, the chronic toxicity of fullerene C_{60} was tested on *Chironomus riparius*, also known as the harlequin fly, and

hypothesized that higher food concentration could reduce the toxic response. This 10-day test was performed by using *Urtica* sp. as food in two different concentrations, which were 0.5 and 0.8%. The test was conducted in sediment that contained fullerene with masses of 0.36 to 0.55 mg/cm^2. The results demonstrated that at 0.5% food treatment, a significant difference in growth-related endpoints was found, whereas little effect was observed for the higher food concentrations than the control group. Furthermore, although they found agglomerates of fullerene in the gut, the microvilli were damaged. Taken together, this finding demonstrated the fullerene's potential toxicity to *C. riparius* in terms of morphological changes and larval growth inhibition [33]. Next, a similar study on the chronic effects of C_{60} on different life stages of *C. riparius* in 10-day growth (larvae) and 42-day (adult midges) emergence tests was conducted. The results showed a decrease in body length at a concentration of 0.0025-20 mg/kg C_{60}, but effects disappeared at higher concentrations. The study stated that small fullerene agglomerates more significantly affected *C. riparius* than the large ones, as shown with high doses of C_{60}. Further, a bell-shaped dose-response relationship was observed in the C_{60} exposure results, which might be caused by the relative growth pattern. This dose-response relationship makes ecological risk assessment of C_{60} more difficult since several effects occur at low concentrations [34].

Several prior studies had assessed the toxicity of C_{60} in *Mytilus*. First, the toxicity of C_{60} at 1, 5, and 10 μg/ml concentrations was investigated in marine bivalve *Mytilus*. From the results, the C_{60} expressed no significant effect in lysosomal membrane stability, which indicated an absence of a major toxicity effect. However, C_{60} suspension led to the release of lysozyme and extracellular oxyradical and nitric oxide production in a concentration-dependent manner. Therefore, the results supported the speculation about the bivalve immune system as a key target of NPs [35]. Forward, in a similar study with *Mytilus* sp., a marine mussel, they were exposed for three days to either 0.10-1 mg/l of C_{60} and 32-100 μg/l of polycyclic aromatic hydrocarbon (PAH) fluoranthene or the combination of both compounds. The observed results depicted a concentration-dependent increase in DNA strand breaks caused by C_{60} and fluoranthene individually; however, their combined exposure enhanced the level of DNA strand breaks together with a twofold increment in total glutathione (GSH) content, indicating oxidative stress. The work concluded the generation of toxic response and damage with additive effects. Afterward, the research group suggested further analysis of C_{60} and fluoranthene alone or in combination for a longer duration to establish concrete toxicity results [36]. Further, *Mytilus galloprovincialis Lam.* were also exposed to C_{60} at 0.01, 0.1, and 1 mg/l concentration for 72 h. Later, the accumulation of C_{60} in the digestive gland was demonstrated to induce dephosphorylation of mTOR with no oxidative stress for cellular distribution of C_{60} at 0.01 mg/l concentration. The study suggested that mussels' most affected functions were related to the organization of the cytoskeleton, energy metabolism, and lysosomal activity [36, 37]. Lastly, in another report on *Mytilus galloprovincialis*, the mussels were exposed to C_{60} (0.01, 0.1, and 1 mg/l), B[a]P (5, 50, and 100 μg/l), and B[a]P (5, 50, and 100 μg/l) in combination with C_{60} (1 mg/l). Afterward, the uptake of each treatment group was measured by a different set of chromatography techniques. The study supports the hypothesis of an interaction between these two compounds and demonstrated an antagonistic relationship at the genotoxic and proteome expression level. However, as this effect is observed on a single concentration, the research group further suggested that other dosage concentrations should also be investigated [37, 38].

Further, ecotoxicities of several fullerenes (C_{60}, C_{70}, and C_{60}-phenyl-C_{61}-butyric acid methyl ester (PCBM)) on *Lumbriculus variegatus* (California blackworm), a benthic organism, were assessed. The results indicated that 25 to 150 mg/kg of C_{60} reduce the population growth of *L. variegatus*, even though no effect on the organism's growth or weight was observed after treated with 25 mg/kg of C_{70} [38, 39]. Similarly, in another study, 10 and 50 mg/kg dry mass of C_{60} were exposed to *L. variegatus* for 28 days. Later, it was found that the survival rate or reproduction of *L. variegatus* was not affected by C_{60}. However, the impairment of feeding activity observed in the study indicated the C_{60}'s disruptive effect on worm feeding. In addition, electron and light microscopy also detected C_{60} agglomerates in fecal pellets, and they were not absorbed in gut epithelial cells. This study also reported that through feeding and egestion, fullerene transfer from sediment-to-sediment surface occurred in *L. variegatus*. This phenomenon might increase the bioavailability of C_{60} to epibenthic organisms and facilitate the C_{60} transfer in the food web [39, 40].

The acute toxicity of C_{60} was also assessed on *Daphnia magna*, *Hyalella Azteca*, and *Copepods*. The 21-day exposure of C_{60} in different concentrations (2.5 and 5 ppm) generated a significant delay in molting and a reduction in offspring production, producing impacts at a population level [40, 41]. Further toxicity tests were performed in *Daphnia magna* and *Moina macrocopa* with 4 h/d sunlight exposure, testing the photo-toxicity of fullerene by the environmental level of ultraviolet light. The neonates were exposed acutely to aqu/nC_{60} filtered through 0.2 μm (0, 0.462, 0.925, 1.85, 3.70, and 7.40 mg/l) and filtered through 0.45 μm (0, 0.703, 1.40, 2.81, 5.62, and 11.2 mg/l) at 21 ± 1°C, and observations were recorded at 24, 48, 72, and 96 hours. From the results, antioxidant enzyme activities were observed to be increased by coexposure to C_{60} aqueous suspensions and sunlight. The results demonstrated that fullerene led to oxidative damage to *D. magna*, aggravated by natural sunlight [41, 42]. Next, in another study, C_{60} NPs were prepared at different concentrations by sonication (0.5, 1, 2, 3, 4, 5, 6, 7, 8, 9, and 10 ppm) and ultrafiltration (40, 180, 260, 350, 440, 510, 700, and 880 ppb) before exposure to *Artemia salina* for 1, 6, 12, 24, 36, 48, and 96 h for acute toxicity testing. The results showed that sonicated C_{60} caused varied mortalities in different chosen stages of this brine shrimp at 15-24 h, 24-48 h, 72-96 h, 6 to 7 days old, and adult. In contrast, filtered solution showed increased mortality with increased C_{60} NP concentrations [42, 43]. Next, a prior study analyzed the antioxidant and oxidative damage responses in the several regions of *Lophiotoma acuta* (marbled turrid) and a bacterium (feeding on

mucus produced by *L. acuta*) after C_{60} exposure for 24 h. After 1.0 mg of C_{60}/l was administered, low levels of antioxidant capacity and lipid peroxidation were displayed in the anterior region of *L. acuta*, indicating that complex interactions between estuarine organisms and associated bacteria could be compromised by nanomaterials, which is C_{60} in this case. This finding highlights the importance of proper evaluation of C_{60} usage, considering the ecological consequences [43, 44]. Next, C_{60} was tested in *Daphnia magna* for 48 h acute toxicity tests. From the results, C_{60} increased the mortality rate with an increased concentration of C_{60} and caused even more severe toxicity effects at lower C_{60} concentrations [44, 45]. Similarly, the amount of C_{60} stored in the body at a particular time due to the exposure of C_{60} was also evaluated on *Daphnia*. After being treated with 1 mg/l of C_{60}, C_{60} was taken with a body burden of 413 μg/g wet weight. C_{60} was observed to be accumulated significantly in the gut of *Daphnia*. Moreover, gut impairments, reduced digestion and filtration rates, and inhibited several digestive enzymes, such as β-galactosidase, trypsin, cellulose, and amylase, were shown after the exposure. The research work provides evidence for limitation in energy acquisition and increases in oxidative damage in *Daphnia* that might be associated with the C_{60} bioaccumulation, which causes immobility and mortality later [45, 46]. In another similar study with the same animal model, the toxicity of C_{60} in artificial freshwater was investigated. After 2 mg/l of fullerene solution was administered for 24 hours, the wet weight of the organism's wet mass was 4.5 ± 0.7 g/kg. However, after depuration for 24 and 48 h in clean water, 46% and 74% of accumulated fullerene, respectively, were eliminated. Also, large aggregates of fullerenes were found in the gut of *Daphnids*. Taken together, the study suggested that *D. magna* might have contributed to carrying fullerene from one trophic level to another because of their significant uptake of fullerene and relatively slow depuration [46, 47]. Further, another behavior study in *D. magna* also discovered that chronic exposure of nC_{60} (21 days) in different concentrations (0.1 or 1 mg/l) yielded a reduction in their feeding ability, hopping, and heartbeat frequencies. Later, the transcriptome analysis depicted this phenomenon which is possibly due to alterations in some underlying physiological functions, including protein degradation, reproduction, energy metabolism, and cell structure repair [37, 38]. Similarly, C_{60} and PCBM (is a solubilized version of the C60) were not found to be acutely toxic when tested at 5, 10, 25, and 50 mg/l for 21 days, while C_{70} had significant acute toxic effects. However, C_{60}, C_{70}, and PCBM depicted heart rate elevation over time [47, 48]. In addition, another study demonstrated that accumulated C_{60} in *D. magna* could be transferred to zebrafish through dietary exposure and accumulated mostly in the intestines; however, no magnification was found [48, 49].

Taken together, we envisage that when exposed to *Daphnia magna*, the suspended C_{60} nanoparticles revealed protection against short-term UV and fluoranthene photo-induced toxicity, although it caused cellular damage. The cellular components, such as microvilli, mitochondria, and basal unfolding, are protected by C_{60}, which evidenced by transmission electron microscopy in organisms after being shortly exposed to UV and fluoranthene photo-toxicity, while longer exposure time (21 days) of C_{60} at low concentration led to significant cellular damage in the alimentary canal of *Daphnia magna* [49, 50]. Further, when C_{60} was analyzed in *Perinereis gualpensis* (a Polychaete species), there were no oxidative damage, GSH (glutathione), and GCL (glutamate cysteine ligase) observed in all tested concentrations, even though after 2 and 7 days, the antioxidant capacity was found to be elevated in the treated group, suggesting a possibility for fullerene acting as an antioxidant [50, 51]. The summary of the toxicity of fullerene-based nanomaterial to aquatic invertebrates is described in Table 1.

4. Interaction of Fullerene with Aquatic Vertebrates in reference to Bioavailability, Toxicity, and Biosafety

Identification of nanomaterial toxicity is challenging since the potential usage of nanomaterial exposes them to the environment and eventually harms human health. The assessment of cytotoxicity of nanomaterials is important to understand the actual interaction and interpretation in a biological organism. The quality of NPs depends on the dispersion medium used for their suspension, which may add to their cytotoxicity potential. The main concern of fullerene testing is to identify the associated risk factors. In addition, the defined conditions of laboratories play a large part in understanding the toxicology profile. The comprehension of nanomaterial interaction inside the biological body is essential to understand all aspects of cells, organs, and blood systems. The vertebrate system plays a significant part in providing cheap, easy, and time-efficient animal models to assess toxicity rapidly. In a prior study, fullerenes (100-500 ppb of C_{60} and C_{70} and 500-5000 ppb of $C_{60}(OH)_{24}$) were administered 24-96 hours of postfertilization (hpf) zebrafish embryo. The results showed that while C_{60} alone led to apoptotic and necrotic cell death, both C_{60} and C_{70} were demonstrated to cause mortality, malformations, and pericardial edema in the embryos. On the other hand, even though $C_{60}(OH)_{24}$ exposure increased embryonic cellular death, it did not lead to apoptosis. Therefore, the study suggested less toxicity of $C_{60}(OH)_{24}$ compared to C_{60} [52]. Furthermore, in a similar study in the embryonic zebrafish model conducted by Henry et al., the depletion of C_{60} from exposure medium and embryonic zebrafish uptake was evaluated [53]. Later, it was found that around 90% of C_{60} could be recovered from zebrafish embryo extracts. The toxicological assay revealed that sorption to test vials caused the loss. After 6 hours, this absorption already resulted a decrease of exposure solution to less than 50% of the initial dose. The embryo uptake of C_{60} increased throughout the 12 h exposure. The study suggested that it is necessary to measure the time course of the C_{60} dose to determine the range of concentrations to which the organism will be exposed. Furthermore, in a prior experiment done by Zhu et al., the *Danio rerio* embryo was exposed to nC_{60} to analyze the developmental toxicity in a 96 h exposure [54]. The results demonstrated that 1.5 mg/l of nC_{60} delayed the development of the zebrafish embryo

Table 1: Fullerene-based nanomaterial toxicity in aquatic invertebrates.

Fullerene	Model organism	Dosage and time	Toxic effect	LC50	Reference
C_{60}	*Chironomus riparius*	10 g wet artificial sediment and 40 ml C_{60}, food source 0.5 and 0.8% *Urtica* sp. 10 days	Morphological changes and inhibiting larval growth. Agglomeration in gut and damage of microvilli.	NA	[33]
C_{60}	*Chironomus riparius*	Artificial sediment 0.0004-80 mg/kg dry weight 10 days and 42 days	C_{60} resulted in a bell-shaped dose-response relationship in view of the relative growth patterns.	NA	[34]
C_{60}	*Mytilus galloprovincialis Lam.*	1, 5, and 10 ppm 30 minutes to 4 hours	Concentration-dependent lysozyme release, extracellular oxyradical, and nitric oxide production.	NA	[35]
C_{60}	*Mytilus galloprovincialis Lam.*	0.01, 0.1, and 1 ppm 72 h	C_{60} accumulated in the digestive gland-induced dephosphorylation of mTOR.	NA	[36, 37]
C_{60} and fluoranthene alone and combination	*Mytilus sp.*	0.10–1 ppm 32–100 ppb 3 days	C_{60} and fluoranthene evoke toxic responses and genetic damage. The combined exposure produced enhanced damage with additive rather than synergistic effects.	NA	[36, 51]
C_{60}, C_{70}, and C_{60}-PCBM	*Lumbriculus variegatus*	0, 10, 25, 100, 150 ppm 28 days	C_{60} can affect the population growth of *L. variegatus* but C_{60}-PCBM and C_{70} effects are lower in comparison.	NA	[38, 39]
C_{60}	*Lumbriculus variegatus*	10 and 50 ppm 28 days	Impairment of feeding activity and C_{60} aggregate presence in feces.	NA	[39, 40]
C_{60}	*Daphnia magna, Hyalella azteca, copepods*	30 ppm 5 days 7 ppm 48-96 h 0, 3.75, 7.5, 15, and 22.5 ppm 96 h	C_{60} 21-day *Daphnia* exposure resulted in a significant delay in molting and reduced offspring production at 2.5 and 5 ppm.	NA	[40, 41]
C_{60}	*Daphnia magna* and *Moina macrocopa*	4 hr/d sunlight C_{60} filtered 0.2 μm (0, 0.462, 0.925, 1.85, 3.70, and 7.40 ppm) and 0.45 μm (0, 0.703, 1.40, 2.81, 5.62, and 11.2 ppm) 24, 48, 72, and 96 h	Fullerene leads to oxidative damage to *D. magna* and it was aggravated by natural sunlight.	0.2 μm—96 h LC50—5.95 ppm 0.45 μm—96 h LC50; >11.2 ppm (outdoor) 0.2 μm—96 h LC50 1.35 ppm 0.45 μm—96 h LC50 1.58 ppm (outdoor)	[41, 42]
C_{60}	*Artemia salina*	Filtered C_{60} 40, 180, 260, 350, 440, 510, 700, and 880 ppb Sonicated C_{60} 0.5, 1, 2, 3, 4, 5, 6, 7, 8, 9, and 10 ppm for 1, 6, 12, 24, 36, 48, and 96 h	Exposure to sonicated nanoparticles shows varied mortalities in different stages of *A. salina*, whereas filtered solutions showed increased mortality with the increase in concentration.	Sonicated $C_{60,}$ the adult LC50 value was 3.17 ppm, whereas it was 617 ppb for the filtered solution.	[42, 43]

Table 1: Continued.

Fullerene	Model organism	Dosage and time	Toxic effect	LC50	Reference
C_{60}	*Laeonereis acuta*	0.01, 0.10, or 1.00 ppm 24 h	*L.acuta* anterior region presented lower antioxidant capacity and lipid peroxidation after exposure to 1.0 mg C_{60}/l.	NA	[43, 44]
C_{60}	*Daphnia magna*	Filtered C_{60} 40, 180, 260, 350, 440, 510, 700, and 880 ppb Sonicated C_{60} 0.2, 0.45, 0.9, 2.25, 4.5, 5.4, 7.2, and 9 ppm 48 h	C_{60} caused an increase in mortality with an increase in concentration and higher levels of toxicity at lower concentrations.	Filtered C_{60} 460 ppb Sonicated C_{60} 7.9 ppm	[44, 45]
C_{60}	*Daphnia magna*	1, 5, 10, 20, and 40 ppm 72 h	C_{60} exposure restricted-energy acquisition and induced oxidative damage, which might be the mechanisms underlying the observed acute toxicity of C_{60} to daphnia.	16.3 ± 0.8 ppm	[45, 46]
C_{60}	*Daphnia magna*	Accumulation 0, 0.2, 2, 7, 15, 30, and 50 ppm 24 h Depuration 48 h	*D. magna* may play a role as a carrier of fullerenes from one trophic level to another.	NA	[46, 47]
C_{60}	*Daphnia magna*	Short term 22 ppm and long term 1 ppm 10 and 21 days	C_{60} protected cellular components in organisms exposed to UV and fluoranthene photo-toxicity in short-term exposure, whereas long-term exposure (21 days) of low-level C_{60} caused significant cellular damage in *Daphnia magna* alimentary canal.	NA	[49, 50]
C_{60}	*Perinereis gualpensis*	200 g 14 days	The data indicated an absence of toxic responses mediated by oxidative stress in estuarine worms exposed to C_{60} mixed in sediments.	NA	[50, 51]

NA: not available.

and larvae, reduced the hatching and survival rates, and caused pericardial edema, whereas 50 mg/l of fullerol hydroxylated C_{60} derivative did not affect the zebrafish embryos. The study also showed that the addition of an antioxidant (glutathione) mitigated the toxicity, suggesting the developmental toxicities are regulated by a free radical-induced mechanism or another form of oxidative stress. Furthermore, in the following study reported by Henry et al., C_{60} in two different forms (C_{60}-water) and tetrahydrofuran (THF-C_{60}) were exposed to larval zebrafish to assess the changes in survival and gene expression [55]. The results demonstrated that the zebrafish larval survivability was compromised in THF-C_{60} and THF-water. However, this phenomenon was not observed in the C_{60}-water treatment group. In addition, in terms of gene expression, the biggest difference was displayed in the THF-C_{60} group. The research indicated that toxic effects found in this study might be associated with the products of THF degradation rather than C_{60}. Additionally, this also may explain the C_{60} toxicity found in other findings.

In another *in vivo* study conducted by Sarasamma et al. [56], waterborne C_{60} was exposed to adult zebrafish for 12 days at 1 and 2 ppm concentrations, respectively, and fish's behavioral alterations were measured by phenomics approach. The results showed the alteration in fish's locomotor activity, response to a novel environment, aggression level, shoal formation, and color preference. Moreover, the fish also displayed dysregulation in the circadian rhythm locomotor activity. The corroboratory biochemical test results showed the induction of oxidative stress and DNA damage, followed by a significant reduction in antioxidative capacity and ATP level. The research group concluded low concentration of C_{60}-induced multiple behavioral abnormalities in adult zebrafish. Similarly, in another prior study also conducted by Sarasamma et al. [57], the potential adverse effects of fullerene C_{70} exposure were assessed on adult zebrafish. Two different doses, 0.5 ppm and 1.5 ppm, were exposed to adult zebrafish for two weeks. Similar to C_{60} results, the results showed abnormalities in locomotion, explorative behavior, aggressiveness level, conspecific social interaction behavior, shoal formation, anxiety elevation, and circadian rhythm locomotor activity. Also, biochemical marker tests revealed a significant increase in superoxide dismutase (SOD), reactive oxygen species (ROS), cortisol, Hif 1-α, ssDNA, TNF-α, and IL-1 in brain and muscle tissue, concluding several and similar toxic effects in altering the neurobehavior parameters of zebrafish after exposed to fullerene-based nanomaterials [57]. Taken together, the studies performed on *Danio rerio* in the embryos and adult stages indicate the importance of concentration range and exposure time in assessing the toxicity effect of fullerene over vertebrate model since different toxicological effects are observed in different studies under different concentrations and tests performed. To establish a concrete result of the toxicological effect of fullerene, it is necessary to accumulate more data on different parameters.

Next, in a previous study done by Oberdörster, when 0.5 ppm of uncoated nC_{60} was exposed to largemouth bass, *Micropterus salmoides*, for 48 hours, it resulted in significant lipid peroxidation in the brain [58]. In addition, GSH was observed to be marginally decreased in the fish's gills with an increase in water clarity. Further, in another experiment on *Anabas testudineus*, a freshwater fish, C_{60} was demonstrated to induce toxicity, specifically on reproductive parameters, after being exposed for 60 days at 5 mg/l and 10 mg/l. The results showed a reduction in gonadal steroidogenesis with a decrease in steroidogenic enzymes, 3β- and 17β-hydroxysteroid dehydrogenase. Furthermore, a significant decrement was also observed in the serum testosterone and estradiol in male and female fish, respectively, in concentration- and time-dependent manners. Thus, the study suggested stress induced by administration of C_{60} leads to reproductive toxicity in *Anabas testudineus* [59]. In a similar study protocol on *Anabas testudineus*, the toxic effect of C_{60} was evaluated on their behavior and hematology levels at 5 and 10 mg/l for 96 h and 60 days. The decline in acetylcholinesterase (AChE) enzyme activity in brain tissue showed prominent changes in fish behavior. Furthermore, the hematological parameter showed a significant reduction in blood cells with increased alanine and aspartate aminotransferase in serum. The results concluded that the sublethal concentration of C_{60} generates toxicity by affecting the normal physiology of *A. testudineus*, which might affect the ecosystem's health status [59, 60].

Forward, in another prior study by Sumi and Chitra and Blickley and McClellan-Green., the role of C_{60} was evaluated on the role of the brain antioxidant system of cichlid fish, *Pseudetroplus maculatus* [60, 61]. In their study, 0.1 mg/l of C_{60} was administered to the fish for 96 hours. The results demonstrated no significant alterations in terms of the brain weight, whereas the notable reduction in antioxidant enzymes (like catalase, SOD, and GSH) and a significant increase in hydrogen peroxide and lipid peroxidation were found after 48 h C_{60} treatment. Also, acetylcholinesterase (AChE), a marker enzyme for the brain, showed a significant reduction after exposure to C_{60} at the end of 48-96 h. Thus, the work showed that the administration of C_{60} has adverse effects on the fish brain. The aqueous suspensions of C_{60} aggregates were studied on marine teleost *Fundulus heteroclitus* of an embryo, larvae, and adult stages. In natural seawater, the aggregates of C_{60} are mixed and precipitated in bottom water after 24 hours, resulting in very low mortality. No median lethal doses could be calculated at a concentration below 10 mg/l. In addition, even though the C_{60} aggregates were attached to chorion, no effect in the development of the embryos on hatching success was observed. With higher exposure levels, the movement of C_{60} from chorion into the embryo tended to increase together with a dose-dependent increase in GSH and a decrease in lipid peroxidation (LPO) [61]. Further, the C_{60} exposed to *Cyprinus carpio* (common carp) demonstrated no effect on viability, whereas hampered growth occurred after 3 h of exposure to several concentrations of C_{60}, which were 0.1, 1, and 10 mg/l. Also, higher antioxidant competence to peroxyl radicals was observed in this fullerene than in other reactive colonies [62, 63].

On the contrary, another study exposed three different chemical toxins, which were 6-hydroxydopamine, gentamicin, and cisplatinum, to a whole animal system in order to

investigate the fullerenes' ability to protect the animal from the toxins. This model is useful to predict the toxicity and efficacy of this fullerene in mammals. When water-soluble fullerenes in both positive and negative charges were exposed to the zebrafish embryos at 1 and 500 μM for 24-120 hpf, the results indicated that the fullerenes could give protection against the toxins, which can induce apoptotic cell death in a vertebrate. Furthermore, this work suggested that the relative potential for these compounds' pharmacologic use varies significantly with respect to stability [63, 64]. Hence, more studies on different parameters of concentration, time, environmental factors, and vertebrate model are necessary to understand the toxic as well as beneficial properties of fullerene nanomaterials. We have compiled the results of different toxicity studies in Table 2.

5. Biodistribution and Fate of Fullerene after Ingestion by Aquatic Organisms

The biodistribution of fullerene on ingestion by aquatic organisms has been seldom addressed in the literature. Moreover, the concentration of fullerenes in many environmental matrices is still unknown, while quantification methods are under development [33, 65, 66]. However, NPs within cells may cause alterations in the cytoskeletal network [67, 68]. Waissi-Leinonen and colleagues depicted the agglomeration of fullerene C_{60} in the gut area and damaged the microvilli of *C. riparius* [33]. Furthermore, in another study by Sforzini et al. and Barranger et al., C_{60} was reported to be distributed in mussel digestive gland cells [36, 37]. In addition, the inhibition of mTOR might also be involved in pathophysiological perturbation induced by nanoparticle accumulation. Further, they stated that autophagic induction by fullerene C_{60} might reflect the degradation of unrecognized materials attempted by lysosomes. These materials might be identified by cells as damaged intracellular proteins and membranes or pathogens. The statement was made based on observations, where C_{60} accumulation in the lysosomal-vacuolar system of the epithelial cells is in the major digestive gland. Overall, the report suggested that dysregulation of mTOR 1 and 2 might inhibit the growth and reproduction of cells and organisms. Also, in a study, Pakarinen et al. and Oberdörster et al. reported that fullerene concentration in feces of *L. variegatus* was high in comparison to the bulk sediments [39, 40]. The study suggested that high fullerene concentration in the form of pellets might partially stem from worm's consumption and absorption of some sediment fraction for nutritional purposes, whereas the fullerenes and other particles are excreted. Further, Tao et.al and Rouse et al. exposed *D. magna* to 0, 0.01, 0.02, 0.04, 0.06, and 1.0 mg/l for seven days and the results showed an increment in body burden of C_{60} along with a higher dose and bigger particle size [69, 70]. Thus, the various papers and results suggest that more research is needed to understand the risks that fullerene may pose in sediments and organisms' bodies in different doses and concentrations under specific environmental conditions. Therefore, the limited information in the fullerene biodistribution is an important topic for future research.

6. Discussion Based on Current Understanding

The manufacturing of fullerenes to fit in for a specific task demands changes in their surface chemistries and properties. With the improvement according to demand, the fullerenes acquire novel physicochemical properties to be assessed for potential toxicological behavior compared to the natural ones. The impact of fullerenes via direct contact with water containing the amount of fullerene through skin and inhalation and via an indirect consumption of aquatic organisms exposure might pose a serious threat to human health in the long run [65, 67, 71, 72]. Until now, the real effects associated with the interaction of fullerenes with the aquatic organisms are still lacking and remain challenging to analyze in the absence of relevant data.

The methods to evaluate the toxicity of fullerenes are evolving in recent years. The current understanding of the toxicity of fullerene must acknowledge that data compilation limitation serves as a barrier to understanding the interaction of fullerene inside the organism's body to interpret the results firmly. In reviewing the emerging environmental problem, it is highlighted that all significant effects on environmental fate, transport, and bioavailability of cocontaminants play a crucial part in understanding fullerene's toxicology.

The toxicity of fullerenes is, to date, poorly understood and contradictory in some cases. However, experimentation on fullerene toxicity testing has demonstrated that fullerene is toxic in some forms. Studies have shown that ROS and free radical production are among the main mechanisms of nanotoxicity; in turn, they might lead to inflammation, oxidative stress, and consequent damage to proteins, membranes, and DNA [69, 73]. In a study, Oberdörster showed that fullerenes caused damage in fish brains [58]. Also, Fortner et al. and Howard demonstrated that fullerenes killed water fleas and showed bactericidal properties [66, 71]. Furthermore, Sayes et al. and Daughton stated that toxicity is a sensitive function of surface derivatization [68, 72], while Rouse et al. and Nel et al. reported that the extent of aggregation, emulsion bases, and different solvents are important variables in the formation of aggregates [70, 73].

The studies discussed here with fullerene toxicity response on invertebrate and vertebrate models depicted contradictory results. Although fullerene C_{60} has been shown to cause mortality, ROS production, aggregation, and lipid peroxidation on a large basis, some studies have reported conflicting results. Waissi-Leinonen et al. demonstrated the effect of C_{60} in relative growth patterns of *C. riparius* in a bell-shaped dose-response manner [34]. Rajasree et al. and Marques et al. showed that exposure of sonicated C_{60} resulted in varied mortality in different stages of *A. salina*, whereas the filtered solution of C_{60} upon exposure revealed increasing mortality with an increase in concentration [42, 43]. Similarly, Blickley and McClellan-Green and Letts et al. also suggested the nontoxic effect of water-stirred suspensions of C_{60} at a concentration up to 10 mg/l in *H. heteroclitus* at different life stages [61, 62].

Next, in another study, Tervonen et al. and Wang et al. mentioned the role of *D. magna* in carrying fullerene from one trophic level to another [46, 47]. Similarly, Pakarinen

Table 2: Fullerene-based nanomaterial toxicity in aquatic vertebrates.

Fullerene	Model organisms	Dosage and time	Toxic effect	LC50	Reference
C_{60}, C_{70}, $C_{60}(OH)_{24}$	*Danio rerio* (embryo)	100 and 500 ppb for C_{60} and C_{70} and 500 to 5000 ppb for $C_{60}(OH)_{24}$	Exposure to C_{60} induced both necrotic and apoptotic cell deaths in the embryo, while $C_{60}(OH)_{24}$ induced an increase in embryonic cellular death. Results obtained suggest $C_{60}(OH)_{24}$ is significantly less toxic than C_{60}.	C_{60}/C_{70}—200 ppb $C_{60}(OH)_{24}$—4000 ppb	[52]
C_{60}	*Danio rerio* (embryo)	100, 200, and 400 ppb 2, 6, 12 h	Concentrations of C_{60} decreased to levels not associated with mortality, <50 μg/l, 100% mortality results when the embryos were exposed to concentrations from 250 to 130 ppb.	130 ppb	[53]
nC_{60}, fullerol	*Danio rerio* (embryos)	nC_{60}—1.5 ppm $C_{60}(OH)_{16-18}$—50 ppm 96 hpf	nC_{60} at 1.5 ppm delayed the zebrafish embryo and larval development, decreased the survival and hatching rates, and caused pericardial edema, whereas fullerol hydroxylated C_{60} derivative at 50 ppm did not exert to the zebrafish embryos.	NA	[54]
Water-soluble fullerenes (1-12)	*Danio rerio* (embryos)	1, 10, 100, and 250 μM for 24 hours	Positively charged water-soluble fullerenes tend to exhibit greater toxicity than negatively charged fullerenes with similar structures; toxicity varies considerably among negatively charged fullerenes from very low to moderate, depending on structural features.	Cationic fullerenes—120 μM Anionic fullerenes—500 μM	[63, 64]
C_{60}	*Danio rerio* (adult)	1 and 2 ppm for 1 day	C_{60} exposure to adult zebrafish at low concentration induces multiple behavioral abnormalities.	NA	[56]
C_{70}	*Danio rerio* (adult)	0.5 and 1.5 ppm for 2 weeks	Toxicity and the alterations were observed in several neurobehavior parameters after zebrafish exposure to environmentally relevant amounts of C_{70}.	NA	[57]
nC_{60}	*Micropterus salmoides* (juveniles)	0.5 ppm and 1 ppm for 48 h	Increase in lipid peroxidation in the brains at 0.5 ppm and marginal depletion of glutathione (GSH) in the gills.	NA	[58]
C_{60}	*Anabas testudineus*	5 and 10 ppm for 60 days	Stress induced by fullerene C_{60} exposure provoked reproductive toxicity in the fish, *Anabas testudineus*.	96 h LC50—50 ppm	[59, 64]
C_{60}	*Anabas testudineus*	5 and 10 ppm for 96 h and 60 days	Sublethal concentrations of fullerene C_{60} have a toxic impact on fish *A. testudineus* by affecting normal physiology.	96 h LC50—50 ppm	[59, 60]

Table 2: Continued.

Fullerene	Model organisms	Dosage and time	Toxic effect	LC50	Reference
C_{60}	*Pseudetroplus maculatus*	0.1 ppm for 96 h	Decrease in SOD, CAT, GSH reductase, AChE. Increase in hydrogen peroxide and lipid peroxidation.	NA	[60, 61]
C_{60}	*Fundulus heteroclitus*	0, 1, 2.5, and 10 ppm for 96 h	Water-stirred suspensions of nC_{60} are not toxic to embryonic, larval, or adult stages of *F. heteroclitus* at concentrations up to 10 ppm.	NA	[61, 62]
C_{60}	*Cyprinus carpio*	0.1, 1, and 10 ppm for 48 h	The results indicated that C_{60} affects bacterial communities that live in mucus secretions of common carp.	NA	[62, 63]

NA: not available.

et al. and Oberdörster et al. demonstrated the fullerenes transfer process from sediment to sediment surface by *L. variegatus* through feeding and egestion [39, 40]. This observation indicated that this transfer might potentially increase the fullerenes' bioavailability to epibenthic organisms, which might be more sensitive to the exposures and might further assist the transfer process in the food chain. Beuerle et al. and Sumi and Chitra stated that positively charged fullerene exhibited greater toxicity in the vertebrate model compared to negatively charged fullerene, which showed a dependency behavior on the structural features [63, 64].

7. Conclusions of Future Directions

Taken together, the toxicity of fullerenes to aquatic animals was clearly demonstrated. Since it has great medical implication potentials, it should be studied further in the future. We propose that techniques such as behavioral assay by phenomics, tissue distribution analysis by MASS spectrum, or isotope labeling for *in vivo* tracking should be used to study fullerene-induced toxicity in aquatic animals (i.e., specific biomarkers study, biodistribution, and interaction within an organism's body) to accumulate relevant data required to achieve a clear picture about fullerene-induced toxicity.

Data Availability

Data is available upon request to authors.

Disclosure

This paper has been submitted as a preprint in Research Square in the below link: https://www.preprints.org/manuscript/202009.0376/v1.

Conflicts of Interest

The authors declare no conflicts of interest.

Authors' Contributions

N.M. and C.-D.H. are responsible for the conceptualization. T.-R.G., J-S.L., and C.-D.H. are responsible for the funding acquisition. T.-R.G., J-S.L., and C.-D.H. are responsible for the investigation. C.-D.H. is responsible for the project administration. A.L.C., G.A., P.S., J.M.S.R., and M.J.R. are responsible for the resources. T.-R.G. and C.-D.H. are responsible for the supervision. N.M. and C.-D.H. are responsible for the visualization. N.M., T.-R.G., J.-S.L., J.-R.C., and C.-D.H are responsible for writing the original draft. All authors have read and agreed to the published version of the manuscript. Nemi Malhotra and Gilbert Audira are equal contribution authors.

Acknowledgments

This study was funded by the grants sponsored by the Ministry of Science and Technology (MOST107-2622-B-033-001-CC2, MOST108-2622-B-033-001-CC2, and MOST108-2313-B-033-001-MY3 to C.-D.H., MOST109-2112-M153-002 to J.-S.L., and MOST108-2221-E033-017-MY3 to T.-R.G.).

References

[1] H. Kroto, J. R. Heath, S. C. O'Brien, R. F. Curl, and R. E. Smalley, "C_{60}: buckminsterfullerene," *Nature*, vol. 318, no. 6042, pp. 162-163, 1985.

[2] P. Bhakta and B. Barthunia, "Fullerene and its applications: a review," *Journal of Indian Academy of Oral Medicine and Radiology*, vol. 32, no. 2, p. 159, 2020.

[3] R. Bakry, R. M. Vallant, M. Najam-ul-Haq et al., "Medicinal applications of fullerenes," *International Journal of Nanomedicine*, vol. 2, no. 4, pp. 639–649, 2007.

[4] S. Thakral and R. Mehta, "Fullerenes: an introduction and overview of their biological properties," *Indian Journal of Pharmaceutical Sciences*, vol. 68, no. 1, p. 13, 2006.

[5] V. Georgakilas, J. A. Perman, J. Tucek, and R. Zboril, "Broad family of carbon nanoallotropes: classification, chemistry, and applications of fullerenes, carbon dots, nanotubes, graphene, nanodiamonds, and combined superstructures," *Chemical Reviews*, vol. 115, no. 11, pp. 4744–4822, 2015.

[6] K. Aschberger, H. J. Johnston, V. Stone et al., "Review of fullerene toxicity and exposure - appraisal of a human health risk assessment, based on open literature," *Regulatory Toxicology and Pharmacology*, vol. 58, no. 3, pp. 455–473, 2010.

[7] P. J. Krusic, E. Wasserman, P. N. Keizer, J. R. Morton, and K. F. Preston, "Radical reactions of C60," *Science*, vol. 254, no. 5035, pp. 1183–1185, 1991.

[8] J. Tam, J. Liu, and Z. Yao, "Effect of microstructure on the antioxidant properties of fullerene polymer solutions," *RSC Advances*, vol. 3, no. 14, pp. 4622–4627, 2013.

[9] P. Prasanthi, G. S. Rao, and B. U. Gowd, "Mechanical behavior of fullerene reinforced fiber composites with interface defects through homogenization approach and finite element method," *International Journal of Advanced Science and Technology*, vol. 78, pp. 67–82, 2015.

[10] F. Giacalone and N. Martin, "Fullerene polymers: synthesis and properties," *Chemical Reviews*, vol. 106, no. 12, pp. 5136–5190, 2006.

[11] Y.-Y. Huang, S. K. Sharma, R. Yin, T. Agrawal, L. Y. Chiang, and M. R. Hamblin, "Functionalized fullerenes in photodynamic therapy," *Journal of Biomedical Nanotechnology*, vol. 10, no. 9, pp. 1918–1936, 2014.

[12] G. Lalwani and B. Sitharaman, "Multifunctional fullerene-and metallofullerene-based nanobiomaterials," *Nano Life*, vol. 3, no. 3, p. 1342003, 2013.

[13] H. Kazemzadeh and M. Mozafari, "Fullerene-based delivery systems," *Drug Discovery Today*, vol. 24, no. 3, pp. 898–905, 2019.

[14] P. R. Buseck, S. J. Tsipursky, and R. Hettich, "Fullerenes from the geological environment," *Science*, vol. 257, no. 5067, pp. 215–217, 1992.

[15] F. Mollaamin, T. T. Pham, D. M. T. Dang, M. Monajjemi, and C. M. Dang, "Modelling and Controlling of ion transport rate efficiency in Proton exchange membrane (PEMFC), alkaline (AFC), direct methanol (DMFC), phosphoric acid (PAFC), direct forming acid (DFAFC) and direct carbon (DCFC) fuel cells," *Biointerface Research in Applied Chemistry*, vol. 9, no. 4, pp. 4050–4059, 2019.

[16] J. Cami, J. Bernard-Salas, E. Peeters, and S. E. Malek, "Detection of C60 and C70 in a young planetary nebula," *Science*, vol. 329, no. 5996, pp. 1180–1182, 2010.

[17] A. Nimibofa, E. A. Newton, A. Y. Cyprain, and W. Donbebe, "Fullerenes: synthesis and applications," *Journal of Materials Science*, vol. 7, pp. 22–33, 2018.

[18] R. Taylor, "Lecture Notes on Fullerene Chemistry," in *A Handbook for Chemists*, pp. 1–288, World Scientific, 1999.

[19] R. Haddon, L. Brus, and K. Raghavachari, "Rehybridization and π-orbital alignment: the key to the existence of spheroidal carbon clusters," *Chemical Physics Letters*, vol. 131, no. 3, pp. 165–169, 1986.

[20] I. Obodovskiy, "Radiation," in *Fundamentals, applications, risks, and safety*, Elsevier, 2019.

[21] S. Sweeney, D. Berhanu, S. K. Misra, A. J. Thorley, E. Valsami-Jones, and T. D. Tetley, "Multi-walled carbon nanotube length as a critical determinant of bioreactivity with primary human pulmonary alveolar cells," *Carbon*, vol. 78, pp. 26–37, 2014.

[22] N. Anzar, R. Hasan, M. Tyagi, N. Yadav, and J. Narang, "Carbon nanotube - A review on Synthesis, Properties and plethora of applications in the field of biomedical science," *Sensors International*, vol. 1, 2020.

[23] A. S. Wu and T.-W. Chou, "Carbon nanotube fibers for advanced composites," *Materials Today*, vol. 15, no. 7-8, pp. 302–310, 2012.

[24] N. Saifuddin, A. Raziah, and A. Junizah, "Carbon nanotubes: a review on structure and their interaction with proteins," *Journal of Chemistry*, vol. 2013, Article ID 676815, 18 pages, 2013.

[25] Y. Kanbur and Z. Küçükyavuz, "Synthesis and characterization of surface modified fullerene," *Fullerenes, Nanotubes, and Carbon Nanostructures*, vol. 20, no. 2, pp. 119–126, 2012.

[26] R. Taylor and D. R. Walton, "The chemistry of fullerenes," *Nature*, vol. 363, no. 6431, pp. 685–693, 1993.

[27] K. N. Semenov, N. A. Charykov, V. A. Keskinov, A. K. Piartman, A. A. Blokhin, and A. A. Kopyrin, "Solubility of light fullerenes in organic solvents," *Journal of Chemical & Engineering Data*, vol. 55, no. 1, pp. 13–36, 2010.

[28] L. Y. Chiang, R. B. Upasani, and J. W. Swirczewski, "Versatile nitronium chemistry for C60 fullerene functionalization," *Journal of the American Chemical Society*, vol. 114, no. 26, pp. 10154–10157, 1992.

[29] Z. Špitalský, L. Matějka, M. Šlouf et al., "Modification of carbon nanotubes and its effect on properties of carbon nanotube/epoxy nanocomposites," *Polymer Composites*, vol. 30, no. 10, pp. 1378–1387, 2009.

[30] V. N. Khabashesku and M. X. Pulikkathara, "Chemical modification of carbon nanotubes," *Mendeleev Communications*, vol. 16, no. 2, pp. 61–66, 2006.

[31] M. Maggini, G. Scorrano, and M. Prato, "Addition of azomethine ylides to C60: synthesis, characterization, and functionalization of fullerene pyrrolidines," *Journal of the American Chemical Society*, vol. 115, no. 21, pp. 9798-9799, 1993.

[32] L. Lagadic and T. Caquet, "Invertebrates in testing of environmental chemicals: are they alternatives?," *Environmental Health Perspectives*, vol. 106, suppl 2, pp. 593–611, 1998.

[33] G. C. Waissi-Leinonen, E. J. Petersen, K. Pakarinen, J. Akkanen, M. T. Leppänen, and J. V. K. Kukkonen, "Toxicity of fullerene (C60) to sediment-dwelling invertebrate Chironomus riparius larvae," *Environmental Toxicology and Chemistry*, vol. 31, no. 9, pp. 2108–2116, 2012.

[34] G. C. Waissi-Leinonen, I. Nybom, K. Pakarinen, J. Akkanen, M. T. Leppänen, and J. V. K. Kukkonen, "Fullerenes(nC_{60}) affect the growth and development of the sediment-dwelling invertebrate Chironomus riparius larvae," *Environmental Pollution*, vol. 206, pp. 17–23, 2015.

[35] L. Canesi, C. Ciacci, D. Vallotto, G. Gallo, A. Marcomini, and G. Pojana, "In vitro effects of suspensions of selected nanoparticles (C60 fullerene, TiO_2, SiO_2) on Mytilus hemocytes," *Aquatic Toxicology*, vol. 96, no. 2, pp. 151–158, 2010.

[36] S. Sforzini, C. Oliveri, A. Barranger et al., "Effects of fullerene C60 in blue mussels: role of mTOR in autophagy related cellular/tissue alterations," *Chemosphere*, vol. 246, p. 125707, 2020.

[37] A. Barranger, L. M. Langan, V. Sharma et al., "Antagonistic interactions between benzo [a] pyrene and fullerene (C60) in toxicological response of marine mussels," *Nanomaterials*, vol. 9, no. 7, p. 987, 2019.

[38] S. Ponte, E. A. Moore, C. T. Border, C. W. Babbitt, and A. C. Tyler, "Fullerene toxicity in the benthos with implications for freshwater ecosystem services," *Science of the Total Environment*, vol. 687, pp. 451–459, 2019.

[39] K. Pakarinen, E. J. Petersen, M. T. Leppänen, J. Akkanen, and J. V. K. Kukkonen, "Adverse effects of fullerenes (nC_{60}) spiked to sediments on Lumbriculus variegatus (Oligochaeta)," *Environmental Pollution*, vol. 159, no. 12, pp. 3750–3756, 2011.

[40] E. Oberdörster, S. Zhu, T. M. Blickley, P. McClellan-Green, and M. L. Haasch, "Ecotoxicology of carbon-based engineered nanoparticles: effects of fullerene (C_{60}) on aquatic organisms," *Carbon*, vol. 44, no. 6, pp. 1112–1120, 2006.

[41] K. H. Ji, J. K. Kim, and K. H. Choi, "Sunlight enhances toxicity of fullerene (C60) to freshwater invertebrates Daphnia magna and Moina macrocopa," *Journal of Health Sciences*, vol. 51, no. 1, pp. 35–45, 2014.

[42] S. R. R. Rajasree, V. G. Kumar, L. S. Abraham, and N. Manoharan, "Assessment on the toxicity of engineered nanoparticles on the lifestages of marine aquatic invertebrate Artemia salina," *International Journal of Nanoscience*, vol. 10, pp. 1153–1159, 2011.

[43] B. F. Marques, L. F. Cordeiro, L. W. Kist et al., "Toxicological effects induced by the nanomaterials fullerene and nanosilver in the polychaeta Laeonereis acuta (Nereididae) and in the bacteria communities living at their surface," *Marine Environmental Research*, vol. 89, pp. 53–62, 2013.

[44] S. B. Lovern and R. Klaper, "Daphnia magna mortality when exposed to titanium dioxide and fullerene (C60) nanoparticles," *Environmental Toxicology and Chemistry*, vol. 25, no. 4, pp. 1132–1137, 2006.

[45] X. Lv, B. Huang, X. Zhu et al., "Mechanisms underlying the acute toxicity of fullerene to Daphnia magna: energy acquisition restriction and oxidative stress," *Water Research*, vol. 123, pp. 696–703, 2017.

[46] K. Tervonen, G. Waissi, E. J. Petersen, J. Akkanen, and J. V. Kukkonen, "Analysis of fullerene-C60 and kinetic measurements for its accumulation and depuration in Daphnia magna," *Environmental Toxicology and Chemistry*, vol. 29, no. 5, pp. 1072–1078, 2010.

[47] P. Wang, B. Huang, Z. Chen et al., "Behavioural and chronic toxicity of fullerene to Daphnia magna: mechanisms revealed by transcriptomic analysis," *Environmental Pollution*, vol. 255, p. 113181, 2019.

[48] E. A. Moore, C. W. Babbitt, S. J. Connelly, A. C. Tyler, and G. Rogalskyj, "Cascading ecological impacts of fullerenes in

freshwater ecosystems," *Environmental Toxicology and Chemistry*, vol. 38, no. 8, pp. 1714–1723, 2019.

[49] X. Yang, R. Edelmann, and J. Oris, "Suspended C_{60} nanoparticles protect against short-term UV and fluoranthene photoinduced toxicity, but cause long-term cellular damage in *Daphnia magna*," *Aquatic Toxicology*, vol. 100, no. 2, pp. 202–210, 2010.

[50] M. Díaz-Jaramillo, J. Ribas, A. M. da Rocha et al., "Antioxidant responses in the polychaetePerinereis gualpensis(Nereididae) exposed to the carbon nanomaterial fullerene (C60)," *Chemistry and Ecology*, vol. 27, no. 1, pp. 43–48, 2011.

[51] S. N. al-Subiai, V. M. Arlt, P. E. Frickers et al., "Merging nano-genotoxicology with eco-genotoxicology: An integrated approach to determine interactive genotoxic and sub-lethal toxic effects of C_{60} fullerenes and fluoranthene in marine mussels, *Mytilus* sp.," *Mutation Research/Genetic Toxicology and Environmental Mutagenesis*, vol. 745, no. 1-2, pp. 92–103, 2012.

[52] C. Y. Usenko, S. L. Harper, and R. L. Tanguay, "In vivo evaluation of carbon fullerene toxicity using embryonic zebrafish," *Carbon*, vol. 45, no. 9, pp. 1891–1898, 2007.

[53] T. B. Henry, E. J. Petersen, and R. N. Compton, "Aqueous fullerene aggregates (nC_{60}) generate minimal reactive oxygen species and are of low toxicity in fish: a revision of previous reports," *Current Opinion in Biotechnology*, vol. 22, no. 4, pp. 533–537, 2011.

[54] X. Zhu, L. Zhu, Y. Li, Z. Duan, W. Chen, and P. J. J. Alvarez, "Developmental toxicity in zebrafish (Danio rerio) embryos after exposure to manufactured nanomaterials: buckminsterfullerene aggregates (nC60) and fullerol," *Environmental Toxicology and Chemistry*, vol. 26, no. 5, pp. 976–979, 2007.

[55] T. B. Henry, F. M. Menn, J. T. Fleming, J. Wilgus, R. N. Compton, and G. S. Sayler, "Attributing effects of aqueous C60 nanoaggregates to tetrahydrofuran decomposition products in larval zebrafish by assessment of gene expression," *Environmental Health Perspectives*, vol. 115, no. 7, pp. 1059–1065, 2007.

[56] S. Sarasamma, G. Audira, S. Juniardi et al., "Evaluation of the effects of carbon 60 nanoparticle exposure to adult zebrafish: a behavioral and biochemical approach to elucidate the mechanism of toxicity," *International Journal of Molecular Sciences*, vol. 19, no. 12, p. 3853, 2018.

[57] S. Sarasamma, G. Audira, P. Samikannu et al., "Behavioral impairments and oxidative stress in the brain, muscle, and gill caused by chronic exposure of C70 nanoparticles on adult zebrafish," *International Journal of Molecular Sciences*, vol. 20, no. 22, p. 5795, 2019.

[58] E. Oberdörster, "Manufactured nanomaterials (fullerenes, C60) induce oxidative stress in the brain of juvenile largemouth bass," *Environmental Health Perspectives*, vol. 112, no. 10, pp. 1058–1062, 2004.

[59] N. Sumi and K. Chitra, "Impact of fullerene C 60 on behavioral and hematological changes in the freshwater fish, Anabas testudineus (Bloch, 1792)," *Applied Nanoscience*, vol. 9, no. 8, pp. 2147–2167, 2019.

[60] N. Sumi and K. Chitra, "Fullerene (C60) induced alteration in the brain antioxidant system of the cichlid fish, Pseudetroplus maculatus (Bloch, 1795)," *Journal of Global Biosciences*, vol. 6, no. 4, pp. 4908–4917, 2017.

[61] T. M. Blickley and P. McClellan-Green, "Toxicity of aqueous fullerene in adult and larval Fundulus heteroclitus," *Environmental Toxicology and Chemisty*, vol. 27, no. 9, pp. 1964–1971, 2008.

[62] R. E. Letts, T. C. B. Pereira, M. R. Bogo, and J. M. Monserrat, "Biologic responses of bacteria communities living at the mucus secretion of common carp (Cyprinus carpio) after exposure to the carbon nanomaterial fullerene (C 60)," *Archives of Environmental Contamination and Toxicology*, vol. 61, no. 2, pp. 311–317, 2011.

[63] F. Beuerle, P. Witte, U. Hartnagel, R. Lebovitz, C. Parng, and A. Hirsch, "Cytoprotective activities of water-soluble fullerenes in zebrafish models," *Journal of Experimental Nanoscience*, vol. 2, no. 3, pp. 147–170, 2007.

[64] N. Sumi and K. C. Chitra, "Possible role of C 60 fullerene in the induction of reproductive toxicity in the freshwater fish, Anabas testudineus (Bloch, 1792)," *Environmental Science and Pollution Research*, vol. 27, no. 16, pp. 19603–19615, 2020.

[65] C. W. Isaacson, M. Kleber, and J. A. Field, "Quantitative analysis of fullerene nanomaterials in environmental systems: a critical review," *Environmental Science & Technology*, vol. 43, no. 17, pp. 6463–6474, 2009.

[66] J. Fortner, D. Y. Lyon, C. M. Sayes et al., "C60 in water: nanocrystal formation and microbial response," *Environmental Science & Technology*, vol. 39, no. 11, pp. 4307–4316, 2005.

[67] O. Ispanixtlahuatl-Meráz, R. P. Schins, and Y. I. Chirino, "Cell type specific cytoskeleton disruption induced by engineered nanoparticles," *Environmental Science: Nano*, vol. 5, no. 2, pp. 228–245, 2018.

[68] C. M. Sayes, J. D. Fortner, W. Guo et al., "The differential cytotoxicity of water-soluble fullerenes," *Nano Letters*, vol. 4, no. 10, pp. 1881–1887, 2004.

[69] X. Tao, Y. He, B. Zhang, Y. Chen, and J. B. Hughes, "Effects of stable aqueous fullerene nanocrystal (nC_{60}) on Daphnia magna: evaluation of hop frequency and accumulations under different conditions," *Journal of Environmental Sciences*, vol. 23, no. 2, pp. 322–329, 2011.

[70] J. G. Rouse, J. Yang, A. R. Barron, and N. A. Monteiro-Riviere, "Fullerene-based amino acid nanoparticle interactions with human epidermal keratinocytes," *Toxicology In Vitro*, vol. 20, no. 8, pp. 1313–1320, 2006.

[71] C. Howard, "Small particles–big problems," *International Laboratory News*, vol. 34, no. 2, pp. 28-29, 2004.

[72] C. G. Daughton, "Non-regulated water contaminants: emerging research," *Environmental Impact Assessment Review*, vol. 24, no. 7-8, pp. 711–732, 2004.

[73] A. Nel, T. Xia, L. Mädler, and N. Li, "Toxic potential of materials at the nanolevel," *Science*, vol. 311, no. 5761, pp. 622–627, 2006.